Phytochemical, Anti-cancer, Anti-inflammatory and Neuroprotective Studies on compounds isolated from Malaysian plants: *Aquilaria malaccensis* and *Hopea dryobalanoides*

A thesis presented by

Siti Aisya binti Saud Gany

in fulfilment of the requirement for the degree of

Doctor of Philosophy

2020

Strathclyde Institute of Pharmacy and Biomedical Sciences

University of Strathclyde

This thesis is the result of the author's original research. It has been composed by the author and has not been previously submitted for examination which has led to the award of a degree.

Signed:

Date:

ACKNOWLEDGEMENTS

First and foremost, I would like to express my grateful thanks to Allah s.w.t for blessing me and giving me the strength to complete my PhD study.

My deepest thanks go to my parents, Saud Gany and Siti Jamilah for their unconditional love, support and prayers during my study.

I would also like to express my sincere appreciation and immense gratitude to my supervisor, Dr. Valerie A. Ferro, for her continued support, patience, moral uplifting and guidance throughout this study. I really appreciated your support. My thanks also extend to my second supervisor, Mrs Louise Young, for guiding me throughout my PhD and her kind words of encouragement during the various phases of developing this work.

My sincere thanks extend to Prof Alexander I. Gray and Prof. John O. Igoli for their valuable time, knowledge and support with the phytochemical analysis, to Miss Grainne Abbott for her help in the biological assays, to Dr. Rothwelle Tate for supervising the molecular biology part of my thesis.

I would also like to thank my colleagues for their support and friendship which helped me to finish my work smoothly and made my life easy and comfortable in Glasgow.

TABLE OF CONTENTS

LIST OF FIGURES

LIST OF TABLES

LIST OF APPENDICES

LIST OF ABBREVATIONS

·OH	Hydroxyl radical
1D NMR	One-dimensional NMR
$^1O_2$	Singlet oxygen
2D NMR	Two-dimensional NMR
2DG	2-deoxyglucose
2DG6P	2-deoxyglucose-6-phosphate
2-h PG	2-hour plasma glucose
6PDG	6-phosphodeoxygluconate
7-aca	7-methoxy acacetin
A2780	Human ovarian cancer cell line
A549	Adenocarcinoma human alveolar basal epithelial cells
Acetone-D_6	Deuterated acetone
acetyl-CoA	Acetyl-coenzyme A
ACh	Acetylcholine
AChE	Acetylcholinesterase
AD	Alzheimer's disease
AE	*A.malaccensis* ethyl acetate extract
AH	*A.malaccensis* hexane extract
AIFs	Apoptosis-initiating factors
ALS	Amyotrophic lateral sclerosis
AM	*A.malaccensis* methanol extract
AP-1	Activator protein-1
APAF-1	Apoptotic protease activating factor 1
APOE	Apolipoprotein E
APP	Amyloid precursor protein
AR	Androgen receptor
ARUK	Alzheimer's Research UK
ATP	Adenosine triphosphate
Aβ	Beta amyloid

BAK	B-cell lymphoma 2 antagonist/killer
Bala	Balanocarpol
BAX	B-cell lymphoma 2-associated protein X
BCL-2	B-cell lymphoma 2
BIRC3	Baculoviral IAP Repeat Containing 3
BSA	Bovine serum albumin
BTK	Bruton tyrosine kinase
CAT	Catalase
CC	Column chromatography
$CDCl_3$	Deuterated chloroform
cDNA	Complementary DNA
CMV	Cytomegalovirus
CNS	Central nervous system
CoA	Coenzyme A
COSY	Correlation spectroscopy
COX	Cyclooxygenase
CPT	Camptothecin
CRUK	Cancer research uk
Cys-Gly	Cystine-glycine
D	Doublet
DCF	2', 7'–dichlorofluorescein
DCFDA	2',7'–dichlorofluorescein diacetate
Dd	Doublet of doublet
DEGs	Differentially expressed genes
dH2O	Deionised water
DMSO	Dimethyl sulfoxide
DMSO-d_6	Deuterated DMSO
DNases	Deoxyribonucleases
DPPH	2,2-Diphenyl-1-picrylhydrazyl
DPPH●	DPPH free radical
DTT	Dithiothreitol
EA	Ethyl acetate

EAA	Excitatory amino acid
ECM	Extracellular matrix
EGCG	Epigallocatechin-3-gallate
EOAD	Early onset AD
ESI	Electrospray ionisation
ETC	Electron transport chain
F6P	Fructose-6-phosphate
FADH2	Flavin adenine dinucleotide
FBS	Foetal bovine Serum
FCCP	Carbonyl cyanide-4-(trifluoromethoxy)phenylhydrazone
FDA	Food and Drug Administration
FN	Fibronectin
FRIM	Forest research institute Malaysia
G6PDH	Glucose-6-phosphate dehydrogenase
GLUT1	Glucose transporters 1
GO	Gene ontology
GpX	Glutathione peroxidase
GSH	Reduced glutathione
GSR	Glutathione reductase
GSSG	Oxidised glutathione
H_2O_2	Hydrogen peroxide
HBSS	Hanks' balanced salt solution
HD	Huntington's disease
HE	*H. dryobalanoides* ethyl acetate extract
HepG2	Human hepatic cells
Hex	Hexane
HH	*H. dryobalanoides* hexane extract
HIF-1	Topoisomerase I
HK2	Hexokinase 2
HL-60	Human leukemia cell line

HM	*H. dryobalanoides* methanol extract
HMBC	Heteronuclear multiple bond coherence
HOCl	Hypochlorous acid
HPLC	High performance liquid chromatography
HPV	Human papillomavirus
HSQC	Heteronuclear single quantum coherence
Hz	Hertz
IC_{50}	The half maximal inhibitory concentration
IĸB	Inhibitor of kappa B
IKK	Iĸb kinase
Il1b	Interleukin 1 beta gene
IL1β	Interleukin 1 beta
IL6	Interleukin-6 gene
IL6	Interleukin-6
J	Coupling constant
JAK	Janus kinase
JNK	C-jun N-terminal kinase
kD	Kilodaltons
KEGG	Kyoto Encyclopedia of Genes and Genomes
LC-MS	Liquid chromatography–mass spectrometry
LDH	Lactate dehydrogenase
LDHA	Lactate dehydrogenase A
LOAD	Late-onset AD
LOX	Lipoxygenase
LPS	Lipopolysaccharide
m	Multiplets value
MAPK	Mitogen activated protein kinase
MCF-7	Human breast cancer cell line with estrogen, progesterone and glucocorticoid receptors
MCL-1	Myeloid cell leukemia-1
MDA-MB-231	Triple-negative breast cancer cell line
Meoh	Methanol

MMP9	Matrix metallopeptidase 9
MOMP	Outer mitochondrial membrane
MPT	Mitochondrial protein translation
MtCK1	Mitochondrial creatine kinase 1
MULT	Multiplets
NAD+	Nicotinamide adenine dinucleotide
NADH	Nicotinamide adenine dinucleotide
NADPH	Nicotinamide adenine dinucleotide phosphate
NAMPT	Nicotinamide phosphoribosyltransferase
NCTC cells	Human skin cell line
NF-κB	Nuclear factor–κb
NMDA	N-methyl-D-aspartic acid
NMR	Nuclear magnetic resonance
NO	Nitric oxide
NOESY	Nuclear overhauster effect spectroscopy
NOX	NADPH oxidase
O_2^-	Superoxide
OD	Optical density
OXPHOS	Oxidation phosphorylation pathway
p38MAPK	P38 mitogen-activated protein kinases
PARP	Poly (ADP-ribose) polymerase
PBS	Phosphate-buffered saline
PCA	Principal components analysis
PCR	Polymerase chain reaction
PD	Parkinson’s disease
PD-1	Programmed death 1
PDK1	Pyruvate dehydrogenase kinase
PFKM	Phosphofructokinase
PGE_2	Prostaglandin E2
PI3K	Phosphatidylinositol-3-Kinase
PMA	Phorbol-12-myristate-13-acetate
PNT2A	Prostate epithelial cells

PPP	Pentose phosphate pathway
PRXs	Peroxiredoxins
PUFA	Polyunsaturated fatty acids
Q/A	Mixture of quercitrin and afzelin
QC	Quality control
RA	Rheumatoid arthritis
RIN	Rna integrity number
RNA	Ribonucleic acid
RNA-Seq	RNA sequencing
RNases	Ribonucleases
ROS	Reactive oxygen species
RPM	Rotation per minute
RPMI-1640	Roswell Park Memorial Institute-1640
RQI	RNA quality indicator
S	Singlet
SEC	Size-exclusion chromatography
SIRT1	Sirtuin 1
SK1	Sphingosine kinase 1
SMAC	Second mitochondria-derived activator of caspases
SOCS3	Cytokine signalling 3
SOD	Superoxide dismutase
STAT	Signal transducer and activator of transcription
TAMs	Tumour-associated macrophages
TBPH	Tert-butyl hydroperoxide
TCA cycle	Tricarboxylic acid cycle
TCA cycle	Tricarboxylic acid cycle
TGF-β	Transforming growth factor beta
THP-1	Human monocytic cell line
TLC	Thin layer chromatography
TLR4	Toll like receptor 4
TME	Tumour microenvironment
TMRE	Tetramethylrhodamine, ethyl ester

TNF-α	Tumor necrosis factor-alpha gene
TNF-α	Tumor necrosis factor-alpha
TRAIL)	TNF-related apoptosis-inducing ligand
TRX	Thioredoxin
U2OS	Human osteosarcoma
u-PA	Plasminogen activator
VCAM-1	Vascular cell adhesion molecule-1
VLC	Vacuum liquid chromatography
ZR-75-1	Human caucasian breast carcinoma
ΔΨM	Mitochondria membrane potential

MATERIALS AND REAGENTS

MATERIAL/REAGENT	SUPPLIER
µ-SLIDE 8 WELL CHAMBER SLIDE	Ibidi, UK
0.2µM FILTER	Sigma Aldrich, UK
20-ML GLASS VIAL	VWR, UK
75CM^2 CELL CULTURE FLASKS	Sigma Aldrich, UK
96-WELL CELL CULTURE PLATES	Sigma Aldrich, UK
96-WELL HALF AREA PLATE (BLACK)	Grenier Bio-One, UK
96-WELL HALF AREA PLATE (CLEAR)	Grenier Bio-One, UK
A2780	ATCC
ACETONE-D$_6$	Sigma Aldrich, UK
ACETONITRILE	Sigma Aldrich, UK
ACETYLCHOLINE	Sigma Aldrich, UK
ACETYLCHOLINE CHLORIDE	Sigma Aldrich, UK
ACETYLCHOLINESTERASE	Sigma Aldrich, UK
ALAMARBLUE™ CELL VIABILITY REAGENT	Invitrogen, UK
AMPLEX® RED	Sigma Aldrich, UK
ANTI-BUMPING GRANULES	BDH, UK
BOVINE SERUM ALBUMIN	Sigma Aldrich, UK
BSA	Sigma Aldrich, UK
CASPASE-GLO 3/7	Promega
CDCL$_3$	Sigma Aldrich, UK
CELLULOSE EXTRACTION THIMBLES (SINGLE THICKNESS)	VWR, UK
CHOLINE OXIDASE	Sigma Aldrich, UK
CYTOSELECTTM 24-WELL CELL INVASION ASSAY	CELL BIOLABS, UK
CYTOSELECTTM 24-WELL CELL MIGRATION ASSAY	CELL BIOLABS, UK
CYTOSELECTTM 48-WELL CELL ADHESION FIBRONECTIN-COATED	CELL BIOLABS, UK

DCFH-DA DYE	Sigma Aldrich, UK
DMEM	Invitrogen, UK
DMSO	Sigma Aldrich, UK
DMSO-D_6	Sigma Aldrich, UK
DPPH	Sigma Aldrich, UK
EPIFLUORESCENT INVERTED MICROSCOPE ECLIPSE TE300	NIKON, JAPAN
ETHANOL	Sigma Aldrich, UK
ETHYL ACETATE (HPLC GRADE)	Sigma Aldrich, UK
EXACTIVE (ORBITRAP) MASS SPECTROMETER	Thermo Fisher Scientific, Bremen, Germany
EXPERION™ RNA STDSENS ANALYSIS KIT	Bio-Rad, UK
FCCP	Sigma Aldrich, UK
FOETAL BOVINE SERUM	Biosera, UK
GSH-GLO™	Promega, UK
HBSS	Thermo Fisher, UK
HEPES	Sigma Aldrich, UK
HEPG2	ATCC
HEXANE (HPLC GRADE)	Fisher Chemicals
HORSERADISH PEROXIDASE	Sigma Aldrich, UK
HPLC VIALS	
HPLC-GRADE ACETONITRILE	Merck, UK
HPLC-GRADE WATER	Merck, UK
HUMAN UNCOATED ELISA KITS TNF-A, IL-1B, IL-6	Invitrogen, UK
L-GLUTAMINE	LifeTech, Paisley, UK
LPS O111:B4 *E. COLI*	Sigma Aldrich, UK
LPS	Sigma-Aldrich
METHANOL (HPLC GRADE)	VWR, UK
MICROSCOPE	Olympus, Japan
MONARCH® TOTAL RNA MINIPREP KIT	NEB, UK

NANODROP™ SPECTROPHOTOMETER (2000C)	Thermo Fisher Scientific, UK
NMR TUBES (5 X 178 MM)	VWR, UK
PARAFFIN WAX	Sigma Aldrich, UK
PBS	Thermo Fisher Scientific, UK
PENICILLAN/STREPTOMYCIN	Life Technologies, UK
PMA	Sigma-Aldrich, UK
RPMI-1640	Thermo Fisher Scientific, UK
SPECTRAMAX M5 PLATE READER	Molecular Devices, Sunnyvale, CA, USA
STAUROSPORINE	Sigma-Aldrich, UK
SULPHURIC ACID	Sigma-Aldrich, UK
TERT-BUTYL HYDROPEROXIDE	Sigma Aldrich, UK
TETRO CDNA SYNTHESIS KIT	Bioline, UK
THERMO CALMIX SOLUTION	Thermo Fisher Scientific, Bremen, German
THP-1	ATCC
TLC GRADE SILICA [SILICA GEL 60H]	Merck, UK
TMRE	Thermo Fisher Scientific, UK
TRIPLE EXPRESS	Life Technologies, UK
TRIS-HCL	Sigma Aldrich, UK
TRITON X	Sigma Aldrich, UK
U2OS	ATCC
ZIC-PHILIC COLUMN	HiChrom (Reading, UK)
ZR-75-1	ATCC

ABSTRACT

Natural products have been used for medicinal purposes for centuries and remain the main source of new drugs to treat diseases due to their biological activities such as anticancer, anti-inflammatory and neuroprotective effects. This thesis aimed to : 1) isolate bioactive compounds from two Malaysian plants which are: *Aquilaria malaccensis* and *Hopea dryobalanoides* using column chromatography and characterised them by nuclear magnetic resonance (NMR); 2) assess the anti-cancer activity of the isolated compounds through various *in vitro* assays and metabolomics profiling; 3) investigate the anti-inflammatory properties of the compounds by inhibition of the pro-inflammatory cytokines (tumour necrosis factor-α (TNF-α), interleukin-1β (IL-1β) and interleukin-6 (IL-6)) levels in response to lipopolysaccharide (LPS) stimulation in macrophage cells and identify the effects of the compound treatments on the gene expression against the inflammatory response caused by LPS-stimulated macrophage cells; 4) examine the protective effects of the compounds against oxidative stress induced in neuron cells.

1) Plants extracts, investigated phytochemically, resulted in the isolation of 7-methoxy acacetin (7-aca) from the hexane extract of *A. malaccensis* twigs for the first time, a mixture of two compounds quercitrin and afzelin (Q/A) from the methanol extract of *A. malaccensis* twigs and two compounds named balanocarpol (bala) and heimiol A from the ethyl acetate extract of *H. dryobalanoides* bark. There are limited reports on the biological activity of 7-aca, however a similar compound called acacetin (aca) has been reported to have a range of bioactivates including anti-cancer, anti-inflammatory

and protective effects. Therefore, aca was purchased commercially for comparison purposes.

2) Cytotoxicity screening of 7-aca, aca, Q/A and bala resulted in decreased viability of A2780 (ovarian) and ZR-75-1 (breast) cells in a concentration dependant manner. 7-Aca exhibited a more potent cytotoxicity against A2780 and ZR-75-1 cells (IC_{50}= 7.9µM and 8.5µM, respectively) compared to aca (IC_{50}= 19.5µM and 17.5µM, respectively). Heimiol A did not show toxic effects against both cancer cells even at the highest concentration (150µM). All compounds showed selective toxicity toward the cancers cells, as they did not cause toxicity against normal PNT2A (prostate) cells. Further investigation behind the cytotoxic effect of the compounds revealed that 7-aca, aca, Q/A and bala caused the production of ROS, depletion of mitochondria membrane potential (ΔΨM) and an increase in caspase-3/7 levels in A2780 and ZR-75-1 cells. Many studies have reported that an excessive increase in ROS in cancer cells disrupts the mitochondrial membrane thus causing the loss of ΔΨM that leads to activation of effectors such as caspase-3, which eventually result in apoptotic cell death. Moreover, 7-aca showed the strongest anti-metastatic effects through the inhibition of adhesion of cancer cells to the ECM protein fibronectin as well as inhibiting the migration and invasion of A2780 and ZR-75-1 cells by approximately 50-70%. The overall results revealed that 7-aca showed a stronger anti-cancer effects towards both cancer cells compared to aca and bala. Due to the more potent activity shown by 7-aca, A2780 and ZR-75-1 cells treated with 7-aca was chosen for metabolite analysis of cell lysates and aca was used as comparison. Several biomarker metabolites were decreased significantly ($P<0.05$) by the compounds, including ATP and NAD+ in the oxidative phosphorylation (OXPHOS) pathway and glucose-6-phosphate dehydrogenase,

glutathione disulphide and NADPH in the pentose phosphate pathway (PPP). 7-Aca showed to cause greater reduction in all these metabolites compared to aca. These findings showed promising results for the compounds to be used as anti-cancer agents.

3) Anti-inflammatory assessment of 7-aca, aca and bala demonstrated the ability of these compounds to inhibit production of the pro-inflammatory cytokines TNF-α, IL-1β and IL-6 by LPS-stimulated THP-1 macrophage cells. Bala at 10μM showed the strongest inhibition of TNF-α, IL-1β and IL-6 by 75%, 68% and 67%, respectively. 7-aca and aca showed similar activity by causing approximately 40-50% inhibition of all the cytokines. Due to the potent activity shown by bala, this compound was selected to carry out a retrospective investigation into any gene changes. RNA-sequencing analysis on RNA isolated from THP-1 macrophage cells treated with LPS or combination treatment of LPS and bala (LPS/bala) revealed that 27 genes associated with the cytokine-cytokine interaction pathway including *TNF-α* and *IL-6* were down-regulated by LPS/Bala treatment compared to LPS treatment alone. Furthermore, another two significant ($P<0.05$) pathways were also affected; the TNF-α and JAK-STAT signalling pathways. The genes associated with these pathways were shown to be significantly ($P<0.05$) down-regulated by LPS/bala treatment compared to LPS treatment alone.

4) 7-aca, aca and bala significantly ($P<0.01$) protected SH-SY5Y cells (neuroblastoma) from ROS generated by tert-butyl hydroperoxide (TBPH). Furthermore, these compounds showed their protective effects from TBPH-induced toxicity/oxidative stress through an increase in $\Delta\Psi M$ and decrease in caspase 3/7 levels in SH-SY5Y cells. Glutathione (GSH) levels were significantly ($P<0.01$) increased by all compounds which confirmed their potential antioxidant activity. Bala showed to be

the most potent antioxidant by increasing GSH level by 66.1%, decrease ROS level by 69% and inhibiting DPPH radical (IC_{50} = 6.2 μM). 7-Aca and aca showed similar antioxidant activity and neuroprotective effect.

These findings suggest that compounds from *A. malaccensis* and *H. dryobalanoides* can provide excellent sources of natural raw material to isolate bioactive agents. In addition, the data also showed that the compounds isolated could possibly be used as anti-cancer, anti-inflammatory and neuroprotective agents in the future, based on the positive results obtained from the *in vitro* assays in this study.

Chapter 1. General introduction

1.1 Review of cancer and neurodegenerative disease

Although cancer and neurodegenerative disease are two distinct pathological disorders, they are two of the most clinically problematic classes of disease impacting on the world's aging populations (Du and Pertsemlidis, 2011). In 2018, the top two diseases affecting women were cancer and dementia-related disease in England and Wales (ARUK, 2018). Cancer is characterised by the disruption of cell regulation mechanisms that leads to uncontrolled cell growth, spreading to other parts of the body and invading local tissues, whereas conversely, in neurodegenerative disorders, such as Alzheimer's disease (AD), it is associated with increased neuronal death, either caused by, or concomitant with, beta amyloid (Aβ) and tau deposition (Behrens *et al.*, 2009). However, there are studies that have demonstrated evidence indicating that these two types of disease could share common mechanisms such as mutations in a variety of genes involved in regulation of the cell cycle, DNA repair pathways, protein turnover, oxidative stress, and autophagy which have been implicated in both of these diseases (Morris *et al.*, 2010). For example, increased expression of amyloid precursor protein (APP) has been associated with AD with evidence showing that APP is concentrated at neuronal synapses and is the primary component of AD-associated amyloid plaques following proteolysis (Rovelet-Lecrux *et al.*, 2006, LaFerla *et al.*, 2007, Theuns *et al.*, 2006). APP has also been reported to have significant correlation with cancer cell proliferation (Pandey *et al.*, 2016) and have been shown to be over-expressed in various cancers, including oral cavity, esophageal, pancreatic, neuroendocrine, thyroid, colorectal and breast cancers (Krause *et al.*, 2008, Arvidsson *et al.*, 2008, Hansel *et al.*, 2003, Ko *et al.*, 2004, Wu *et al.*, 2020).

1.2 Cancer

Cancer is a world-wide issue and remains the leading cause of death in the UK with more than a quarter (28%) of all deaths occurring in 2017. According to Cancer Research UK (CRUK) in 2015-2017, 165,000 people died from cancer in the UK with 367, 000 new cases in the same year (CRUK, 2017b). Cancer initiation and progression can be caused by many factors such as an uncontrolled cell mass that rapidly proliferates and results in the production of genetic instabilities and alterations that accumulate within cells and spread to surrounding tissues. These genetic instabilities include mutations in DNA repair genes (p21, p22, p27, p51, p53 and tool box for DNA), tumour suppressor genes (p53, NF1, NF2, RB and biological breaks), oncogenes or biological accelerators (MYC, RAF, Bcl-2, RAS) and genes involved in cell growth metabolism (Iqbal *et al.*, 2017). External factors such as radiation, chemicals, environmental pollutants and microorganisms, as well as internal factors such as genetic predisposition, hormonal and metabolic disorders can contribute to cancer development. Lifestyle factors such as cigarette smoking, diet and alcohol also contribute to cancer. In the UK, it has been reported that the highest cancer cases are due to tobacco followed by an unhealthy diet (Figure 1.1). Lung cancer is the most frequent cancer and the leading cause of cancer death among males in the UK, followed by prostate and bowel cancer. Among females, lung cancer is also the most commonly diagnosed cancer and the leading cause of cancer death, followed by breast and bowel cancer (CRUK, 2017b). In 2017, the global death number caused by cancer exceeded 9 million; the total number of global deaths due to cancer in males were higher (5,390,260) than that of females (4,063,665). People over the age of 50 years have a higher risk of developing cancer compared to people under the age of 15 years

which accounted for less than 1% of total number of incidence and death rates (Bray *et al.*, 2018). Globally, more than 90% of the total deaths is accounted for by people over 50 years who died with oesophageal, stomach, lung, uterine, colon and rectal, prostate, gallbladder, and biliary tract, as well as bladder cancers (Lin *et al.*, 2019a).

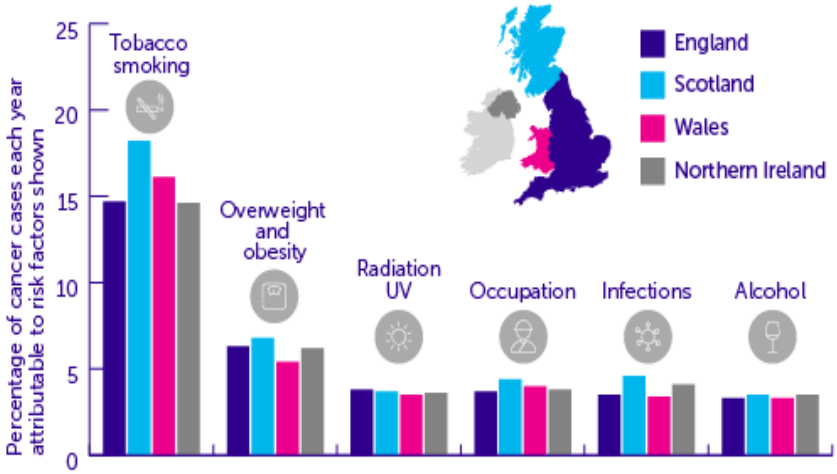

Figure 1.1 Cancer cases attribute to risk factors in the UK (CRUK, 2020)

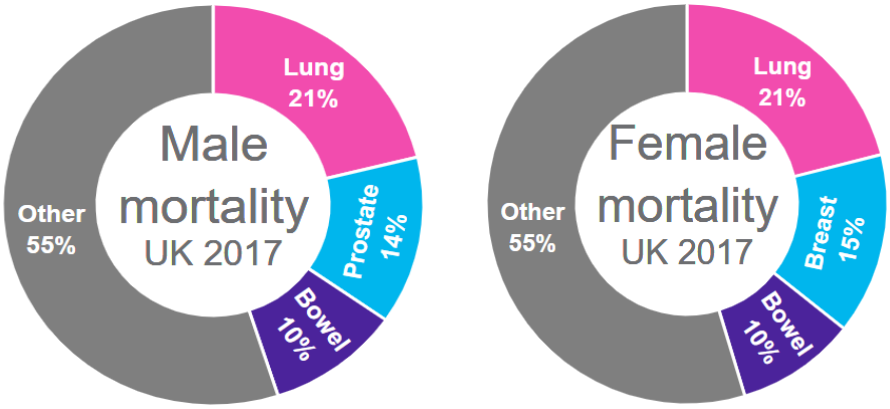

Figure 1.2 Three most common causes of cancer death in males and females in the UK (CRUK, 2017) .

1.2.1 Apoptosis

According to a study by Hanahan and Weinberg, emerging cancer cells need to acquire eight biological capabilities (the hallmarks of cancer) in order to compromise normal cellular function and cause overgrowth of cells. The eight distinct hallmarks consist of sustaining proliferative signalling, evading growth suppressors, resisting cell death, enabling replicative immortality, inducing angiogenesis, activating invasion and metastasis, deregulating cellular energetics and metabolism, and avoiding immune destruction (Hanahan and Weinberg, 2017). One of the most important hallmarks of cancer is the ability of cancer cells to evade apoptosis. Apoptosis, also known as cellular suicide, is programmed in every single cell in the body. Under normal physiological conditions when a cell detects DNA damage, it has the capability to activate apoptosis to eliminate the mutated cells from the population. Cell suicide starts off from a series of cellular events that leads to the activation of a family of cysteine proteases called caspases. There are two routes to apoptosis: extrinsic and intrinsic pathways. Both pathways cause the activation of initiator caspases (caspase-2, -8, -9, or -10) which then leads to the cleavage and activation of executioner caspases (e.g. caspase-3 or -7) that carry out mass proteolysis and consequently, cell death.

In the extrinsic pathway, apoptosis is initiated by caspase-8 and -10 triggered by death ligand binding to a death receptor such as tumour necrosis factor (TNF) receptors, and TNF-related apoptosis-inducing ligand (TRAIL). The TNF receptor family is a large family consisting of more than 20 proteins that shares similar cysteine-rich extracellular domains and have a cytoplasmic domain (also called “death domain”) of about 80 amino acids which is essential for transmitting the death signal from the cell's surface to intracellular signalling pathways (Fulda and Debatin, 2006). Whereas in the

intrinsic pathway (also called the mitochondrial pathway of apoptosis), permeabilisation of the outer mitochondrial membrane (MOMP) is involved in the caspase activation. Cytotoxic or stress stimuli such as DNA damage and viral infection activates pro-apoptotic B-cell lymphoma 2 (BCL-2) family members such as multi-BH domain proteins (e.g. BAX [BCL2-associated protein X] and BAK [BCL2 antagonist/killer], which share BH1-BH3 domains) that will form oligomers in the outer mitochondria membrane that leads to the release of cytochrome c, second mitochondria-derived activator of caspases (SMAC)/ DIABLO, Omi/HtrA2, apoptosis-initiating factors (AIFs) and endonuclease G to the mitochondrial intermembrane space (Fernald and Kurokawa, 2013, Saelens *et al.*, 2004). Cytochrome C in the cytosol drives the cells into apoptosis by binding to apoptotic protease activating factor 1 (APAF-1) that will assemble into a structure called an apoptosome (Cain *et al.*, 2000). Initiator caspase-9 is then activated by forming a caspase-9-activating complex. Then, caspase-3 is recruited to the apoptosome, where it is activated by the resident caspase-9 through proteolytic cleavage of caspase-3 (Bratton *et al.*, 2001). Activation of caspase-3 then triggers many of the cellular and biochemical events of apoptosis.

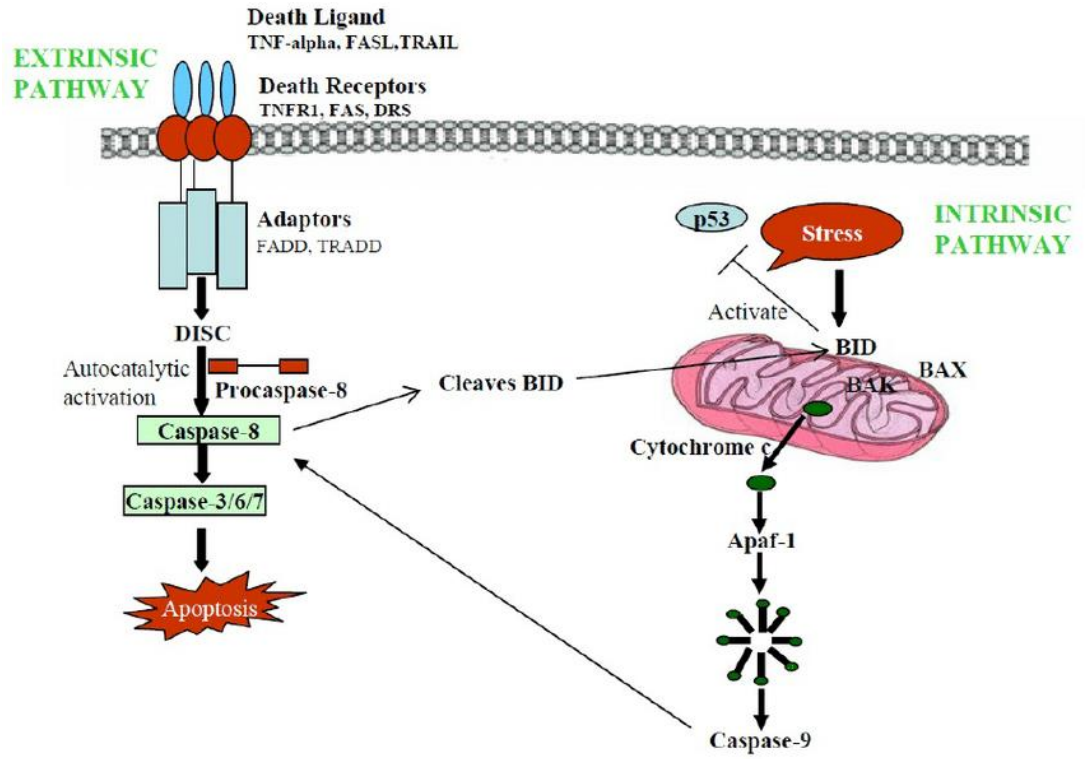

Figure 1.3 Extrinsic and intrinsic pathways of apoptosis (Rampal *et al.*, 2020).

Cancer cells evade apoptosis by deregulating the intrinsic apoptosis pathway. Overexpression of anti-apoptotic BCL-2 proteins has been observed in cancers cells (Yip and Reed, 2008, Adams and Cory, 2007). Amplification of anti-apoptotic BCL-2 has been observed in lung cancer, haematological malignancies, as well as solid bone tumours (Tonon *et al.*, 2005, Soini *et al.*, 1998). Increase of myeloid cell leukemia-1 (MCL-1) expression has also been detected in many cancers and is associated with the progression and promotion of tumourigenesis (Goodwin *et al.*, 2015, Kendall *et al.*, 2007, Allen *et al.*, 2011). Pro-apoptotic BH3 proteins have also been observed to be widely affected in cancer cells. Anti-apoptotic BCL-2 family proteins prevent the activation of BAX and BAK by binding to BH3-only proteins (Vo and Letai, 2010, Letai *et al.*, 2002, Cheng *et al.*, 2001, Manoochehri *et al.*, 2014). In normal cells, p53

is an important nuclear transcription factor that regulates the expression of a variety of genes that triggers apoptosis, growth arrest, or senescence due to various cellular stresses. In cancer cells, the loss of p53 tumour suppressor results in the downregulation of pro-apoptotic BH3-only proteins such as PUMA, BID, APAF-1, and NOXA (Oda *et al.*, 2000, Yu *et al.*, 2001, Fortin *et al.*, 2001).

1.2.2 ROS homeostasis in cancer

The electron transport chain (ETC) is the central system of mitochondrial adenosine triphosphate (ATP) production; essential for cancer growth. Nicotinamide adenine dinucleotide (NADH) or flavin adenine dinucleotide (FADH2) (generated from substrates in the tricarboxylic acid (TCA) cycle) donates its electrons to four protein complexes (I, II, III and IV) of the mitochondrial ETC in a coordinated manner. The electron travels from complexes I and II via complex III to complex IV. During this movement, energy is generated with the help of electron carriers, ubiquinone and cytochrome c by pumping protons to the intermembrane space from the matrix of the mitochondria. The continuous pumping of protons creates a positively charged intermembrane and a negatively charged matrix. Then the protons re-enter the matrix through the ATPase synthase complex which generates ATP from ADP and inorganic phosphate that provides the cell with its fundamental energy substrate (Rohlena *et al.*, 2011).

Due to the extensive electron flow in and out of the mitochondria matrix, the ETC is the major source of reactive oxygen species (ROS). ROS homeostasis is a key component for cancer cell survival. Mitochondria consume approximately 80% of molecular oxygen and 1% of it is used to produce superoxide (O_2^-) (Quinlan *et al.*, 2012, Handy and Loscalzo, 2012) which is released from mitochondrial complexes I,

II and III into the mitochondrial matrix (Kowaltowski *et al.*, 2009, Brand, 2010, Lemarie and Grimm, 2011, Lemarie *et al.*, 2011, Murphy, 2009). Studies have investigated that cancer cells show persistently high levels of ROS such as hydrogen peroxide (H_2O_2), O_2^-, hypochlorous acid (HOCl), singlet oxygen ($^1O_2$) and hydroxyl radical (·OH). Increased levels of ROS in cancer are due to a high metabolic rate in mitochondrial, endoplasmic reticulum, and cell membranes (Kumari *et al.*, 2018). However, excessive ROS levels beyond the optimal range can induce oxidative damage and cell death, therefore regulation of the concentration of ROS is crucial to be maintained so that it does not reach cytotoxic levels incompatible with cancer cell growth. High levels of ROS in cancer is balanced with high levels of antioxidant enzymes such as superoxide dismutases (SODs), peroxiredoxins (PRXs), glutathione peroxidases (GPXs), and catalase (CAT) to maintain intracellular balance mechanisms (Wood *et al.*, 2003, Cox *et al.*, 2009). Accumulation of O_2^- is rapidly converted to H_2O_2 by SODs and H_2O_2 is converted to H_2O by many antioxidants such as PRXs, GPXs and CAT (Schieber and Chandel, 2014, Rhee *et al.*, 2012). These antioxidant enzymes are present in many cellular compartments and their high abundance makes them ideal H_2O_2 scavengers. PRXs detoxify H_2O_2 by being an oxygen acceptor and oxidised PRXs is then reduced by thioredoxin (TRX) (Rhee *et al.*, 2012, Berndt *et al.*, 2007). In the cytosol and the mitochondria, GPXs convert to H_2O_2 at the expense of glutathione (GSH) which is reduced to glutathione disulphide (GSSG). NADPH then donates an electron to reduce oxidised GSSG back to GSH by glutathione reductase (Reczek and Chandel, 2017).

High levels of ROS and high levels of antioxidant defence in cancer cells makes it more sensitive to apoptosis by disruption of the cancer cellular redox balance by either increasing or decreasing ROS levels (Trachootham *et al.*, 2009). Excessive damage caused by increased ROS levels will result in cytochrome C release from mitochondria which causes caspase-3 activation that eventually results in apoptotic death (Simon *et al.*, 2000). Inhibition of ECT complex I has been proven to increase or decrease ROS production depending on which binding site is inhibited (flavin or ubiquinone) (Forkink *et al.*, 2015, Chen *et al.*, 2003, Rohlena *et al.*, 2011, Orr *et al.*, 2013). Other molecular pathways that generate ROS such as activating Akt and changes in phosphorylation of Bcl-2 could result in the activation of the caspase-dependent apoptotic pathway (Aggarwal *et al.*, 2019). Apoptotic death through disruption of redox homeostasis in cancer can also be achieved by blocking antioxidant activity which decreases the cancer's ability to balance oxidative insult caused by high levels of ROS. For example, studies have shown that the depletion of GSH, an antioxidant enzyme, will interrupt the GSH/GSSG redox status in cancer cells which leads to an increase in ROS generation, which accelerates mitochondrial damage and induces apoptosis (Zhao *et al.*, 2012, Armstrong *et al.*, 2002, Honda *et al.*, 2004). Table 1.1 shows drugs that target redox systems for the treatment of cancer.

Table 1.1 Drugs targeting redox systems for the treatment of cancer

Drug	Cancer	Target	Reference
Auranofin	Lung, Ovarian	Inhibition of thioredoxin reductase	(Fan *et al.*, 2014) (Marzano *et al.*, 2007)
Motexafin gadolinium	Lung	Inhibition of thioredoxin reductase	(Magda and Miller, 2006)
Arsenic trioxide	Acute promyelocytic leukaemia, Lung, Hodgkin Lymphoma (HL) and Non-Hodgkin Lymphoma	Mitochondria, Trx-1/-2, GSH	(Zheng *et al.*, 2015) (Bhalla *et al.*, 2008)
Doxorubicin	Breast, bladder, lymphoma, and acute lymphocytic leukemia and more	Reduce GSH, SOD, and catalase Promote ROS production	(Gorini *et al.*, 2018)
Topotecan	Lung Ovarian	Topoisomerase I (HIF-1)	(Choi *et al.*, 2009, Onnis *et al.*, 2009)
Bortezomib	Multiple myeloma and mantle cell lymphoma.	Proteasome inhibitor	(Dolloff *et al.*, 2015)

1.2.3 Warburg effect

Altered metabolism and active glycolytic pathways and its regulators have strongly been linked to apoptosis resistance in cancers. One of the major ATP sources for cancer cells is fermentation of glucose via the aerobic glycolysis pathway in the cytosol which is also called the Warburg effect. With adequate oxygen levels, normal cells extract energy from glucose through the oxidation phosphorylation (OXPHOS) pathway in the ETC of the inner mitochondrial membrane. In the OXPHOS pathway, 36/38 ATP is generated, which is higher when compared to the glycolysis pathway that only yields 2 ATP. Normal cells only undergo glycolysis when there is insufficient

oxygen levels (Marbaniang and Kma, 2018). However, despite the availability of oxygen, cancer cells prefer to use aerobic glycolysis as the main source of ATP production. With or without the presence of oxygen, 85% of pyruvate is reduced to lactate via lactate dehydrogenase (LDH) through the aerobic glycolysis pathway. With the presence of oxygen, 5% pyruvate is oxidised to yield acetyl-coenzyme A (acetyl-CoA) then acetyl-CoA is oxidised completely to CO_2 and H_2O in the mitochondria via the TCA cycle. This causes the generation of high energy molecules such as NADPH or FADH2 which are reduced by ETC in the inner mitochondria through the OXPHOS pathway and creates energy in the form of ATP (Yu *et al.,* 2017).

Even though cancer cells prefer aerobic glycolysis for energy metabolism, the majority of tumour cells demonstrate normal mitochondrial function and OXPHOS pathway is still essential for proliferation of cancer cells (Fu *et al.,* 2017). It has been suggested by many studies that some cancer cells still retain OXPHOS and mitochondrial activity for cancer growth and survival (Hirpara *et al.*, Farge *et al.*, 2017, Griguer *et al.*, 2005). Several studies indicate that OXPHOS may be upregulated in breast cancer, classical Hodgkin lymphoma and large B-cell lymphoma (Whitaker-Menezes *et al.,* 2011, Jones *et al.,* 2016, Birkenmeier *et al.,* 2016, Caro *et al.,* 2012). Mitochondrial dysfunction and OXPHOS have been investigated to contribute to metastasis of cancer cells which is one of the main causes of cancer patients' death. Metastasis is the migration of cancer cells through blood and lymphatic vessels and colonisation of different tissues (Denisenko *et al.,* 2019). The loss of tumour suppressor gene RB1 induces mitochondrial protein translation (MPT) and OXPHOS which promotes metastasis (Zacksenhaus *et al.*, 2017). Another study also showed that breast cancer cells use both OXPHOS and glycolysis-dependent metabolic strategies to achieve their broad

metastatic potential, whereas lung metastatic cells relied on glutamine uptake and OXPHOS to metastasise (Dupuy *et al.*, 2015). The ability of cancer cells to switch between glycolysis and OXPHOS to resist cell death make both aerobic glycolysis and OXPHOS function an ideal anticancer therapeutic approach (Kumari *et al.*, 2018).

Targeting various critical enzymes that are involved in the glycolysis and OXPHOS processes could be a useful approach for cancer therapies. For example, inhibiting enzymes that are responsible for the glycolytic breakdown of glucose such as glucose transporters 1 (GLUT1), hexokinase 2 (HK2), phosphofructokinase (PFKM), lactate dehydrogenase A (LDHA), and pyruvate dehydrogenase kinase (PDK1) will inhibit glycolysis causing ATP depletion, cell cycle inhibition and ultimately cell death (Zhao *et al.*, 2013b). Studies have shown that weakening the activity of complex I and complex III in the mitochondria will cause inhibition of OXPHOS that will result in the dysfunction of mitochondria, decrease in ATP production and increase in ROS production (Sun *et al.*, 2014, Hahm *et al.*, 2011, Cheng *et al.*, 2019). Table 1.2 shows some FDA-approved agents targeting the mitochondrial aerobic metabolism (OXPHOS) of cancer cells which results in apoptosis. However these drugs do not just act on mitochondrial pathways.

Table 1.2 Effects of FDA approved antitumor agents on cancer cells in *in vitro* and preclinical studies (Aminzadeh-Gohari *et al.*, 2020)

Type of cancer	Agents	Target
Gastrointestinal	Cisplatin	OXPHOS uncoupling Increase state 2,3 % respiration
Colon	Doxorubicin	Modulation OXPHOS genes
Neuroblastoma	Sorafenib	Destabilization of complex I Decrease respiration
Breast	Tamoxifen	Decrease complex I activity
	Metformin	Decrease respiration, complex I activity and ATP
Prostate	Deferiprone	Decrease respiration and ATP
Oral squamous cell	Cannabinoids	Decrease respiration and ATP
Colorectal adenocarcinoma	Indomethacin	Decrease complex I activity and ATP
Liver	Valproate	Decrease respiration and ATP

1.2.4 Inflammation and cancer

Inflammation is a feature of the biological response to harmful stimuli/agents such as pathogens, damaged cells, or irritants. There are two major types of inflammation: acute, which usually features a fast-onset, lasting from minutes to days, depending on the extent of injury, a self-limiting "classical" response reflecting the body's response to infection or injury with neutrophils as the major cell type involved (Raghavendra *et al.*, 2015); and chronic, characterised by a slow, long-term inflammation lasting for prolonged periods of several months to years due to persistent inflammatory stimuli, involving cells of the adaptive immune system such as macrophages, monocytes and lymphocytes (Anderson, 2013). Uncontrolled acute inflammation may become chronic, contributing to a variety of chronic inflammatory diseases (Zhou *et al.*, 2016). There is much evidence to suggest that chronic inflammation plays an important role in the development of diseases including

diabetes, atherosclerosis, rheumatoid arthritis, obesity and neurodegeneration (Goldberg and Dixit, 2015, Schultze *et al.*, 2015). Rheumatoid arthritis (RA) is a chronic, systemic, inflammatory disorder. The two immune systems and their interactions are intimately involved in the development of RA (Guo *et al.*, 2018). Macrophages are important immune cells that are involved in both initiation and resolution of inflammation. They are of critical importance in RA, where they generate cytokines that enhance inflammation and contribute to destruction of cartilage and bone (Udalova *et al.*, 2016). Nonsteroidal anti-inflammatory drugs (NSAIDs) and Corticosteroids are usually used as the first medication to treat inflammation diseases including RA. Medications, considered to be fast-acting, are NSAIDs including acetylsalicylate (Aspirin), naproxen (Naprosyn), ibuprofen (Advil and Motrin), and etodolac (Lodine) (Bullock *et al.*, 2018). Corticosteroids are a more potent anti-inflammatory medication than NSAIDs, but they come with greater side effects (Barnes, 2006).

It has been reported numerous of times that inflammation is involved in all stages of carcinogenesis, from tumour initiation to progression and metastasis of established tumours (Mantovani, 2010, Conway *et al.*, 2016, Atri *et al.*, 2018). Table ***1.3*** shows a list of chronic inflammatory diseases that are associated with the development of cancer. Macrophages are key mediators in the link between inflammation and cancer (Qian and Pollard, 2010b, Biswas and Mantovani, 2010, Mantovani *et al.*, 2013, Wynn *et al.*, 2013). Macrophages originate from bone marrow and reach body tissues by infiltrating through blood vessels in order to act as guards against various kinds of damage and their numbers increase immensely in inflammation, autoimmunity diseases, and cancers (Corliss *et al.*, 2016). Although macrophages provide the first

line of defence in protecting the host from infections, inappropriate or prolonged activation can result in damage to the host, immune dysregulation, and disease (Lewis and Pollard, 2006).

Table 1.3 List of chronic inflammatory disorders associated with cancer

Associated inflammatory stimuli	**Cancer**	**Reference**
Inflammatory bowel diseases ulcerative colitis and Crohn's diseases	Colorectal cancer/colitis-associated cancer	(Jess *et al.*, 2006)
Liver fluke and primary sclerosing cholangitis	Cholangiocarcinoma	(Zabron *et al.*, 2013)
Chronic gastritis *Helicobacter Pylori*	Gastric cancer	(Yoshida *et al.*, 2014)
Inflammation caused by asbestos, infections, smoking, and silica	Lung cancer	(Vainio and Boffetta, 1994)
Escherichia coli infection of prostate	Prostate cancer	(Krieger John *et al.*, 2000)
Infection with hepatitis virus B and hepatitis virus C	Hepatocellular carcinoma	(Bartosch, 2010)
UV irradiation-associated skin inflammation	Melanoma	(D'Orazio *et al.*, 2013)
Endometriosis	Endometrial carcinoma	(Modugno *et al.*, 2005)
Gall bladder stone-associated chronic cholecystitis	Gall bladder carcinoma	(Espinoza *et al.*, 2016)
Barrett's esophagitis	Oesophageal cancer	(O'Sullivan *et al.*, 2014)
Inflammation caused by Human papillomavirus	Ovarian cancer	(Xie *et al.*, 2017)
Cytomegalovirus	Brain, breast, colon, cervical and prostate	(Wick and Platten, 2014, Richardson *et al.*, 2015, Han *et al.*, 1997, Harkins *et al.*, 2002, Samanta *et al.*, 2003)

In the past, cancer research focused on the tumour cell itself. In recent years, however, investigations of the tumour microenvironment (TME) and its essential function in supporting malignancy has become more and more important, especially with regard to new immunotherapies (Quail and Joyce, 2013). Among the diverse cell types of the TME, macrophages are the most abundant non–tumour cell type in most cancers (Noy and Pollard, 2014).These tumour-associated macrophages (TAMs) can compose up to 50% of the solid tumour mass (Mills *et al.*, 2016, Solinas *et al.*, 2009). Cytokines, which is also referred as interleukins, chemokines, or growth factors, are small secreted proteins (<40 kDa), which are produced by nearly every cell to regulate and influence immune response (Takeuchi and Akira, 2010). The release of pro-inflammatory cytokines will lead to activation of immune cells such as macrophages and production as well as the release of further cytokines (Kany *et al.*, 2019). When the macrophages is activated, they will secrete pro-inflammatory cytokines IL-1, IL-6 and TNF-α and effector molecules (including reactive nitrogen intermediates) and express chemokines such as CXCL9 and CXCL0 (Biswas and Mantovani, 2010). These molecules exert and amplify antimicrobial and tumoricidal activities. However, prolonged activation of macrophages can cause overproduction and inappropriate release of these molecules, which results in chronic inflammation and extensive DNA damage that potentially could lead to cancer (Qian and Pollard, 2010b). Secretion of pro-inflammatory cytokines such as TNF-α, IL-6 and IL-1 by immunocompetent cells or tumour cells in the TME may take part in the development and progression of cancer and may affect the prognosis (Zielińska *et al.*, 2018). For example, patients with inflammatory bowel disease including ulcerative colitis and Crohn's disease have an

increased risk of developing neoplasia (Gupta *et al.*, 2007) owing to the production of TNF-α, IL-6, and IL-1beta (IL-1β) by TAMs (Popivanova *et al.*, 2008, Ning *et al.*, 2015, Wang *et al.*, 2014d). Another study demonstrated that IL-1β secreted by macrophages stimulates an auto-amplification loop, which results in enhanced expression of IL-1β and cyclooxygenase (COX)-2 by both macrophages and breast cancer cells which contributes to the proliferation of malignant cells (Hou *et al.*, 2011). Amplification of the pro-inflammatory response in the TME has been reported to be associated with several inflammatory pathways such as nuclear factor–κB (NF-κB) signalling pathway that is initiated by macrophages (Maeda *et al.*, 2005, Luedde *et al.*, 2007, Karin and Greten, 2005, Greten *et al.*, 2004). For example, a study demonstrated that significant activation of the NF-κB signalling pathway by LPS-treated macrophages induced the expression of pro-inflammatory cytokines, such as TNF-α, IL-6, IL-1β and IL-8 in gastric cancer cells, which led to chronic inflammation and tumour cell proliferation (Zhou *et al.*, 2018). NF-κB is involved in pathogenesis of various chronic inflammatory disorders and has emerged as a central regulator of TAM function (Farahmand *et al.*, 2017, Poh and Ernst, 2018). NF-κB activation is critical for macrophage responses to microbial/inflammatory stimuli, including toll-like receptor (TLR) ligands, TNF-α, and IL-1β.

1.2.5 Current therapeutic anti-cancer agents

Until now, conventional treatments are used for cancer such as chemotherapy and radiotherapy and surgical removal of the accumulated biomass of cancer. The mode of treatment used is dependent on the type of cancer or the stage of the cancer. For example, if the patient is diagnosed with breast cancer at an early stage, it is more likely for the patient to undergo surgery than chemotherapy (CRUK, 2017a). In

England, 92.8 % of patients diagnosed with Stage 1 breast cancer during 2013-2014 had surgery to remove their primary tumour and 70.5 % patients diagnosed with Stage 3 received chemotherapy as part of their treatment (CRUK, 2017a). The initial treatment for Stage 1 ovarian cancer 95.4% patients had surgery to remove the ovaries or fallopian tubes. Patients also then undergo chemotherapy to ensure that there will not be a reoccurrence. At Stage 2-4 of ovarian cancer 70-80% undergo chemotherapy (CRUK, 2017c). Chemotherapy is the best treatment for cure, control, and minimisation of the cancer by killing the cancer cells. Table 1.4 shows recently Food and Drug Administration (FDA)-approved chemotherapy agents. However, they also can cause damage to healthy cells that results in side effects and recurrence of the cancer which threatens the patients' welfare (Mansano-Schlosser and Ceolim, 2012). Cisplatin is a well know anti-cancer chemotherapy drug that is very effective in treating cancer such as lung, breast and ovarian cancer. However, cisplatin has been linked to various toxic side effects in patients such as nausea, vomiting nephrotoxicity, cardiotoxicity, hepatotoxicity and neurotoxicity (Aldossary, 2019). Other current treatments for cancer therapy linked with several side effects are shown in Table 1.5. Therefore, therapeutic strategies that selectively target a cancer gene or its metabolites while doing less damage to normal cells and causes lesser adverse effects are very valuable. Natural products and plants have been receiving a lot of attention from researchers in the past 30 years for the discovery of novel cancer preventive and therapeutic agents.

Table 1.4 Recent FDA-approved chemotherapy agents with a specific target site.

Drug	Type of cancer	Target	References
Balversa	Bladder	FGFR3 or FGFR2 receptors	(de Almeida Carvalho *et al.*, 2019)
Piqray	Breast	PI3K/AKT/mTOR pathway	(Ando *et al.*, 2019)
Atezolizumab and Nab-Paclitaxel	Advanced triple negative breast cancer	Programmed death 1 (PD-1) and PD-L1 receptor	(Schmid *et al.*, 2018)
Pembrolizumab	Lung, Head and neck squamous cell carcinoma, Hodgkin lymphoma, Urothelial carcinoma, Gastic and gastroesophageal carcinoma	PD-1 receptor	(Dang *et al.*, 2016)
Polatuzumab vedotin	Melanoma	D79b-targeted antibody-drug conjugate delivering monomethyl auristatin E (MMAE), a microtubule inhibiton	(Deeks, 2019)
Zanubrutinib	Mantle cell lymphoma (blood cancer)	Bruton tyrosine kinase (BTK), a B-cell receptor	(Tam *et al.*, 2019)
Darolutamide	Prostate	Androgen receptor (AR)	(Bastos and Antonarakis, 2019)
Selinexor	Gastric, Multiple myeloma	Exportin-1 (XPO1	(Subhash *et al.*, 2018)

Table 1.5 Summary of the side effects associated with some anti-cancer drugs (Dicato, 2013).

Anti-cancer drug	Mode of action	Clinical use	Side effects
Paclitaxel	Antimicrotubule: stabilizer	Breast, ovarian, cervical, endometrial, sarcomas	Hypersensitivity, peripheral neuropathy, bradycardia and hypotension
Docetaxel	Antimicrotubule: stabilizer	Breast, ovarian, cervical, endometrial, sarcomas	Hypersensitivity, fluid retention, peripheral neuropathy, alopecia, rash/pruritus, nail changes, arthralgia/myalgia
Ixabepilone	Antimicrotubule: stabilizer	Breast, lung, prostate, endometrial, ovarian	Myelosuppression, hypersensitivity, peripheral neuropathy
Eribulin	Antimicrotubule: stabilizer	Breast and liposarcoma	QT prolongation, myelosuppression, peripheral neuropathy
Vinorelbine	Antimicrotubule: stabilizer	Non-small cell lung and breast	Acute dyspnea and severe bronchospasm, constipation/ileus neuropath, chest pain
Doxorubicin/epirubicin	Anthracyclines	Ovarian, breast, endometrial, Kaposi's sarcoma, lymphoma, and acute lymphocytic leukemia	Cardiotoxicity: acute, chronic, and delayed, hyperuricemia (rare)
5-fluorouracil/capecitabine	Antimetabolite	Colon, esophageal, stomach, pancreatic, breast, cervical	Cardiotoxicity (acute myocardial infarction, angina, dysrhythmias, cardiac arrest, cardiac failure, and ECG changes), hyperbilirubinemia,
Gemcitabine	Antimetabolite	Breast, ovarian, non-small cell lung, pancreatic, bladder	Elevated liver, enzymes, haemolytic uremic syndrome, pulmonary toxicity, acute dyspnea and severe pulmonary

			toxicities, fever/ flu like symptoms, vascular toxicity
Methotrexate	Antimetabolite	breast, leukemia, lung, lymphoma,osteosarcoma.	Hepatotoxicity, pulmonary toxicity, neurological toxicity
Cyclophosphamide	Alkylating agent	lymphomas, leukaemias, myeloma, lung, breast	Cardiac toxicity, haemorrhagic cystitis, interstitial fibrosis, fluid retention and dilutional hyponatremia
Carboplatin	Alkylating agent	Breast, ovarian, lung	Myelosuppression, hypersensitivity, nephrotoxicity

1.2.6 Natural products and cancer

Natural products comprise of any chemical compound or substance that is produced from living organisms. Drug discovery from natural products has played an important role over 40 years in the development of therapeutic agents towards combating cancer, either in their naturally occurring forms such as plant secondary metabolites and their derivatives or their synthetically modified forms (Kinghorn *et al.*, 2009). Compared to conventional synthetic drug discovery approaches, drug discovery and development from plant-based compounds is inexpensive and less time-consuming (Rayan *et al.*, 2017). Anticancer plant-derived agents are categorised into four main classes of compound (Elrayess and Nageh, 2019). These are:

1. **Vinca alkaloids**

   Vinca alkaloids include vinblastine, vincristine, vindesine, and vinorelbine originally isolated from the Madagascan periwinkle, *Catharanthus roseus* G. Don. (Apocynaceae). These compounds were the first natural product-based cytotoxic drugs to be used clinically. They act as anti-microtubule and anti-mitotic agents to cause cytotoxic affects against various cancers such as haematological malignancies, sarcomas, breast cancer, and lung cancer. Vinca alkaloids are now produced synthetically which has led to development of active semi-synthetic analogues (Moudi *et al.*, 2013).

2. **Epipodophyllotoxins**

   Epipodophyllotoxins are semisynthetic derivatives of podophyllotoxin isolated from the Mayapple plant *Podophyllum* species (Podophyllaceae) that possess anti-tumour activity caused by very potent toxicity. They are phase-specific cytotoxic drugs that affect the late S and early G2 phases of the cell cycle by

causing breaks in DNA strands by interacting with DNA topoisomerase II (Cragg and Newman, 2005).

3. **Taxanes**

   Taxol (also known as Paclitaxel®) was first isolated from the bark of Pacific yew tree *Taxus brevifolia* and later found in other parts of the tree such as needles and seeds and other Taxus species (Nikolic *et al.*, 2011, Sreekanth *et al.*, 2009). In 1992, the US FDA approved paclitaxel for the treatment of advanced ovarian cancer then it was used to treat other types of cancer such as breast cancer, colorectal cancer, and squamous cell carcinoma of the bladder by acting as a microtubule-stabilising drug (Zhu and Chen, 2019).

4. **Camptothecins**

   Camptothecin (CPT) was first isolated from the stem wood of Chinese *Camptotheca acuminate*. The mechanism of action involves cell cycle arrest at both S and G2 phases, which causes cytotoxicity. CPT also inhibits DNA and RNA (including ribosomal RNA) synthesis and induces DNA damage (Li *et al.*, 2017).

1.3 Neurodegenerative disease

Neurodegenerative diseases such as Alzheimer's disease(AD), Parkinson's disease (PD), Huntington's disease (HD) and amyotrophic lateral sclerosis (ALS) are characterised by excessive neuronal cell death (Rager, 2015). These diseases mostly affect the elderly population and has become a great burden on society in terms of disability, high economic cost and personal suffering (Pitchai *et al.*, 2019). Dementia is a disorder that causes the loss of brain function, including memory loss and difficulties with thinking, problem-solving, or communication (Duong *et al.*, 2017).

There were an estimated 46.8 million people worldwide living with dementia in 2015 and it is estimated that it will almost double every 20 years with a projected 75 million in 2030 and 131.5 million in 2050 (Figure 1.4) (ADI, 2015).

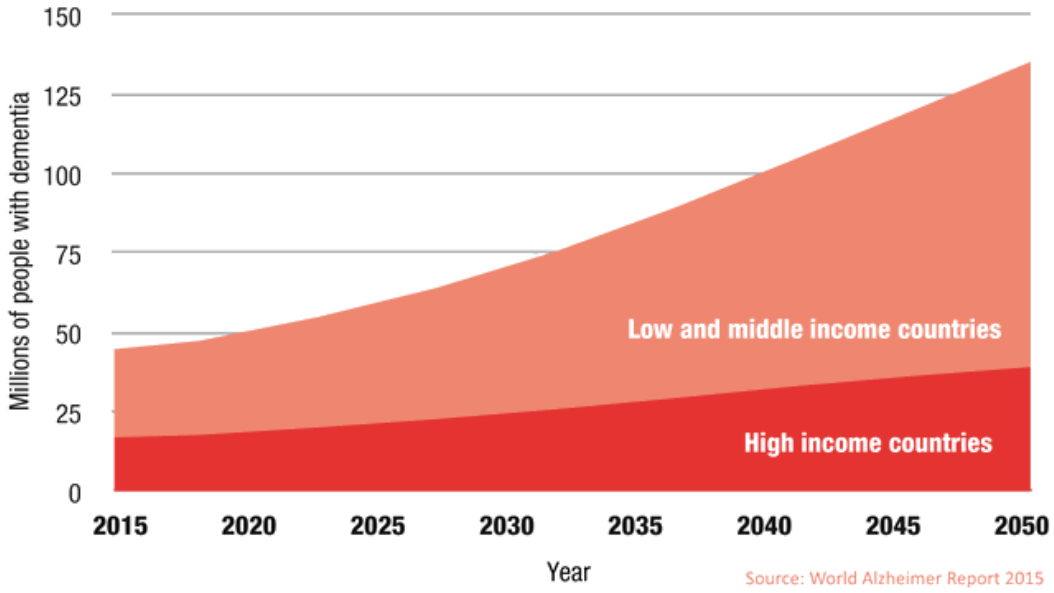

Figure 1.4 Number of people with dementia in low, middle and high income countries (in millions)

In 2014 there were 850,000 people estimated living with dementia in the UK and it is expected to increase to up to 35% by 2025 (estimated 1 million) and 146% by 2050 (estimated 2 million) (Figure 1.5)(ARUK, 2014). Increase in age is one of the risk factors of dementia and due to the longer life expectancy of women compared to men, women have a higher chance of being affected by dementia than men (Figure 1.6)(ARUK, 2014). In 2017, dementia has become the number one cause of death for women (16% dementia related death) in contrast to other top four leading causes of death; ischaemic heart diseases, cerebrovascular diseases, chronic lower respiratory diseases and lung cancer. For men, dementia is the second leading cause of death (8.7%)(ARUK, 2018).

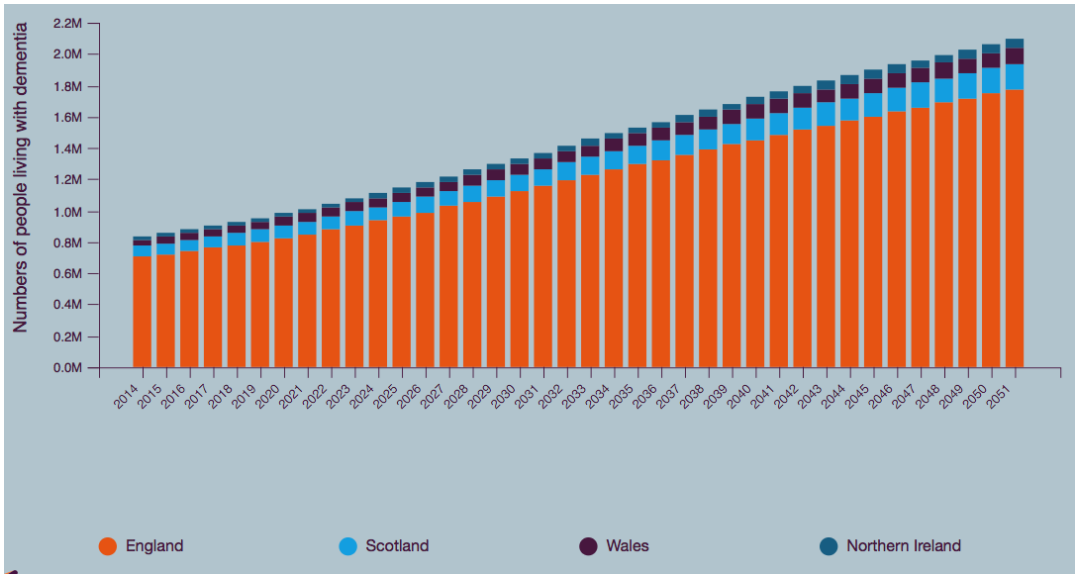

Figure 1.5 Projections of dementia prevalence in the UK from 2014-2051 (ARUK, 2014)

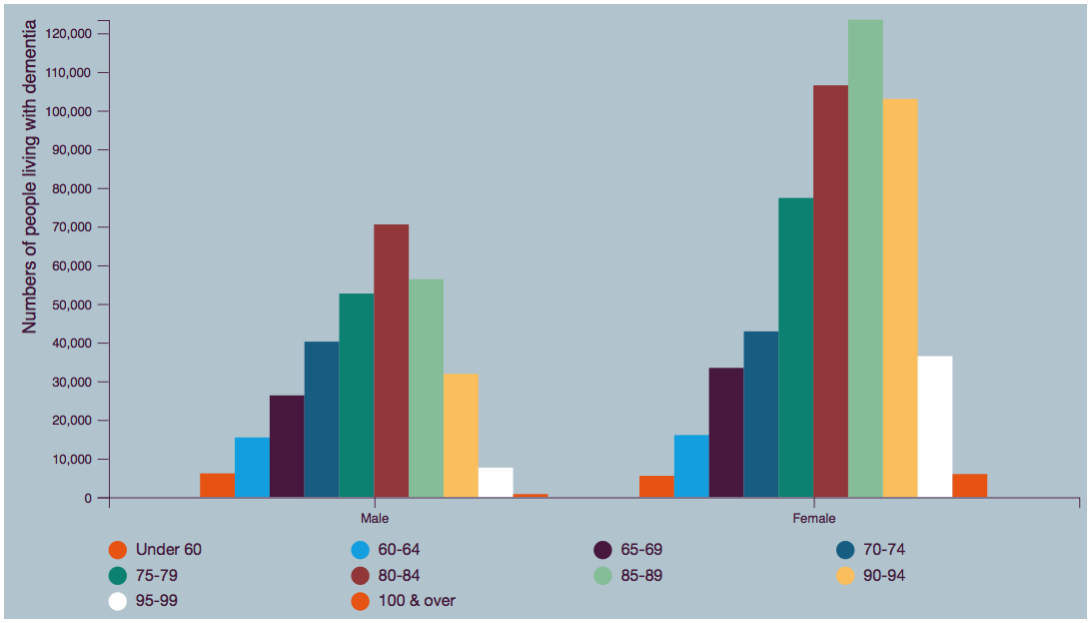

Figure 1.6 Estimated number of men and women living with dementia by age group (ARUK, 2014)

1.3.1 Alzheimer's disease (AD)

AD is the major form of dementia in the elderly and possibly contributes to 60–70% of cases (WHO, 2019). It is mostly thought to be a disease in aging, with 90% of diagnoses present in those aged 65 years and older (Herrup, 2015). The disease was

named after a German psychiatrist and neuropathologist, Alois Alzheimer, in 1906 when he gave an exceptional lecture for the first time regarding the description of a form of dementia. He described his findings based on a patient called Auguste D, a 50-year-old woman from Frankfurt who had shown progressive cognitive impairment, focal symptoms, hallucinations, delusions, and psychosocial incompetence. When an autopsy was carried out on the same patient, amyloid plaques, neurofibrillary tangles and vascular anomalies were observed (Hippius and Neundörfer, 2003). This disease affects the brain areas that are responsible for learning and memory capabilities beginning in the entorhinal cortex and hippocampus then spreading to the temporal, parietal, and finally the frontal brain lobes (Jahn, 2013). Therefore, AD patients will usually experience memory loss, mild cognitive impairment and loss in judgement. A number of factors including genetic, environment exposure and lifestyle choices has been proposed to increase AD risk.

a. Genetic factors

Gene mutations in the APP and presenilin (PSEN) 1 and 2 genes, results in the synthesis of Aβ peptide. Mass production of Aβ peptides such as size 40 amino acids (Aβ40) and size 42 amino acid (Aβ42) causes neuronal cell death. These gene mutations occur in familial early onset AD (EOAD). In late-onset AD (LOAD), Apolipoprotein E (APOE) is the major genetic risk factor. Individuals carrying the ε4 allele are at increased risk of AD compared with those carrying the more common ε3 allele. This gene is commonly inherited and displays variable binding to the amyloid ß-protein fragment (Bu, 2009, Reitz and Mayeux, 2014). Animal model studies have demonstrated that aggregation and deposition of Aβ were detected in mice that express apoE4 or apoE3 (Tai *et al.*, 2013). Another study has demonstrated that Aβ peptides

can interfere with the normal function of apoE in brain lipid metabolism and thus contribute to AD pathogenesis (Hone *et al.*, 2005).

b. Environmental exposure

Exposure to environmental agents including pesticides, metals and microbial toxins have been recognised as possible risk factors for AD. Many studies have reported that exposure of aluminium in drinks in elderly subjects (65 years and older) is associated with an increased risk of dementia and AD (Rondeau *et al.*, 2009, Walton, 2014). Aluminium dust inhalation is also associated with increased risk of AD (Peters *et al.*, 2013). The most recent meta-analysis that was carried out involving 10,567 participants (eight cohort- and case-controlled studies) conducted prior to 2015 concluded that individuals exposed to aluminium were 71% more likely to develop AD (Wang *et al.*, 2016b). Effects of aluminium exposure have been reported based on *in vivo* experiments obtained from humans and animals and shown the presence of oxidative stress, mitochondrial dysfunction, microglial activation and functional dysregulation of microglia (Morris and Berk, 2016). There is little evidence of dementia risk by other metals such as arsenic (Dani, 2010), copper and iron (Shen *et al.*, 2014, Loef and Walach, 2012).

c. Lifestyle

Most lifestyle factors that are linked to the development and AD are modifiable such as smoking, and diet. Smoking results in the generation of free radicals, and thus causes the increase of oxidative stress. It also affects the immune system by promoting pro-inflammatory production which leads to phagocytes activation. In addition, smoking may lead to cerebrovascular diseases, which increase the risk of AD (Traber

et al., 2000, Durazzo *et al.*, 2014). Many studies have discovered that intake of saturated or trans fats is associated with AD (Laitinen *et al.*, 2006, Luchsinger *et al.*, 2002). A number of well-controlled studies of cognitive decline have found that high saturated fat intake increases the rate of decline in cognitive abilities with age (Beydoun *et al.*, 2007, Devore *et al.*, 2009, Eskelinen *et al.*, 2008, Okereke *et al.*, 2012). Increased saturated fat intake has been linked to cardiovascular disease and type 2 diabetes (Briggs *et al.*, 2017), therefore it is also associated with increased risk of AD (Santos *et al.*, 2017). A murine study showed high-fat diets and cholesterol were able to increase the deposition of Aβ peptides (Nizari *et al.*, 2016). High cholesterol in total plasma in human patients showed a 57% higher risk of developing AD (Solomon *et al.*, 2009, Anstey *et al.*, 2017).

1.3.2 Neuronal cell death

Neuronal cell death, specifically, apoptosis also known as programmed cell death, has been proven to be a distinctive attribute for both acute and chronic neurologic disease (Yuan and Yankner, 2000). There are two pathways involved in apoptosis: 1) the death receptor pathway (extrinsic), where the neuron cell membrane is activated by death signals which eventually leads to cell death; 2) the mitochondrial pathway (intrinsic), where pro-apoptotic molecules (response to cell death signals) cause mitochondria to release pro-apoptotic factors such as cytochrome c, apoptosis-inducing factor (AIF), Smac (second mitochondria-derived activator of caspase)/DIABLO (direct inhibitor of apoptosis protein (IAP)-binding protein with low PI), Omi/HtrA2 or endonuclease G from the mitochondrial intermembrane space (Hengartner, 2000, Fulda and Debatin, 2006). Several reported genetic and environmental factors that modulate apoptosis in

neurodegenerative diseases such as Alzheimer's, Parkinson's, Huntington's and amyotrophic lateral sclerosis are shown in Table 1.6.

Table 1.6 Factors that modulate apoptosis in neurodegenerative disorders (Mattson, 2000).

Disease	Genetic factor	Environmental factor
Alzheimer's	APP, presenilin mutations, ApoE	Head trauma, brain haemorrhage and ischaemia, calorie intake, aluminium, and viral infections
Parkinson's	α-synuclein, parkin mutations, LRRK2mutations	Head trauma, toxins, calorie intake
Huntington's	Expended HD gene defect containing a polymorphic trinucleotide CAG	-
Amyotrophic lateral sclerosis	Cu/Zn-SOD mutations	Toxins (insecticide and pesticide) exposure, electrical injury

The apoptotic pathway involved in neurodegenerative disease is similar to that discussed in section 1.2.1. Briefly, the principal molecular players that are involved in the apoptotic programme such as: apoptosis-inducing or death receptors (e.g. Apo-1/Fas), Apaf-1 and other AIFs; the release of cytochrome c from the mitochondria into the cytoplasm leads to formation of a cytoplasmic complex which results in the activation of initiator caspases (8, 9 and 10). The initiator caspases then activate downstream effector caspases (3, 6 and 7) and Bcl-2 family members (BAX, BID, BAD, BAK, BCL-xS) that enhance apoptosis.

1.3.3 Reduction of acetylcholine (ACh) level

Decreased cholinergic neurons in the brain and the loss of neurotransmission are the major causes of the decline in cognitive function in patients with AD. Cholinergic neurons are nerve cells within the nucleus basalis and the septal diagonal band complex that secretes the neurotransmitter acetylcholine (ACh) which plays a key role in learning and memory (Colangelo *et al.*, 2019, Auld *et al.*, 2002). The reduction of activity in cholinergic neurons due to deficiency in the production of ACh in the brains of AD patients was first proposed in 1982, which is also known as the cholinergic hypothesis of AD (Bartus *et al.*, 1982). One therapeutic approach to enhance cholinergic neurotransmission is to increase the availability of ACh by inhibiting acetylcholinesterase (AChE), the enzyme that degrades acetylcholine in the synaptic cleft (Figure 1.7). AChE is a cholinergic enzyme primarily found at postsynaptic neuromuscular junctions that breaks down or inactivates ACh into acetate and choline in the synaptic cleft (Colović *et al.*, 2013). The function of AChE is to terminate neuronal transmission and signalling between synapses to prevent ACh dispersal and activation of nearby receptors (Rotundo, 2009).

Cholinergic receptors function in signal transduction of the somatic and autonomic nervous system and these receptors are activated by the ligand ACh. These receptors subdivide into nicotinic and muscarinic receptors (Tiwari *et al.*, 2013). However, it is largely unknown whether the effect of ACh is mediated by nicotinic ACh receptors (nAChRs), muscarinic receptors, or both. Studies involving cholinergic lesions and local administration of cholinergic antagonists indicate that both nAChRs and muscarinic receptors located in the hippocampus are of particular importance for learning and memory processes (Ishibashi *et al.*, 2014). AChE inhibitors aim to

decrease the rate of decomposition of ACh at synapses in the brain thereby raising the potential for increased levels of excitatory amino acid (EAA) transmission and improved cognitive function (Giacobini, 2004, Lane *et al.*, 2006). This strategy has proved moderately successful, yielding potent reversible AChE inhibitors such as tacrine which was the first of the AChE inhibitors approved for AD treatment in 1993 (Tumiatti *et al.*, 2010).

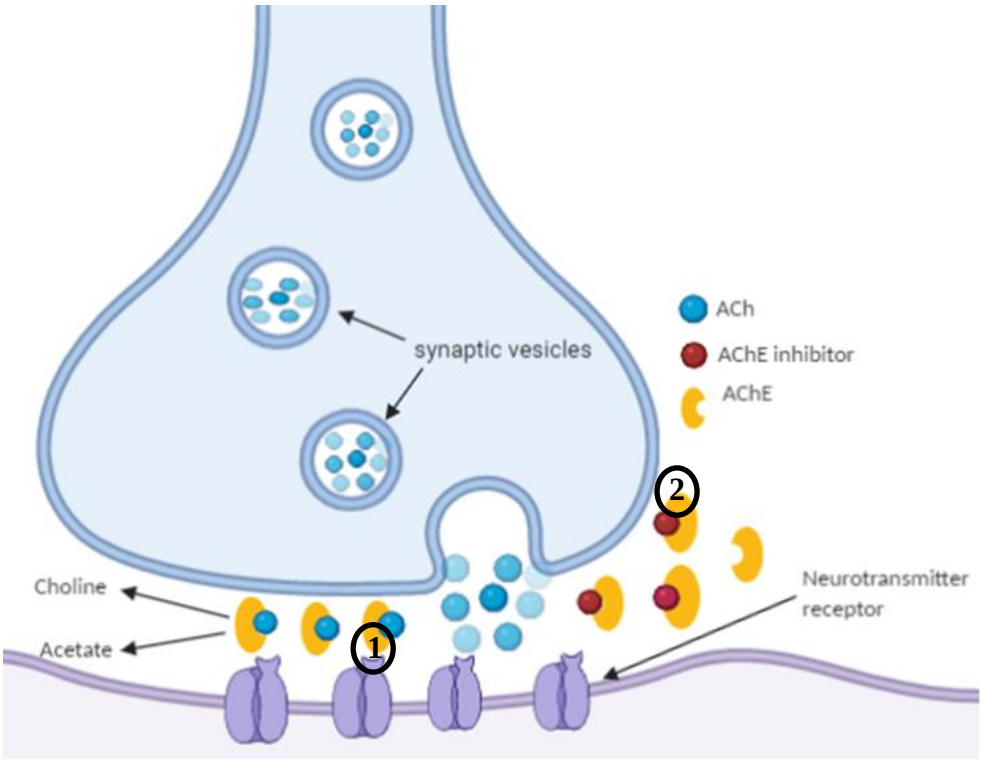

Figure 1.7 Schematic representation of the ACh release course and cholinergic hypothesis of AD. (1) AChE catalyses the breakdown of ACh into choline and acetate. (2) AChE inhibitors inhibit AChE from breaking down to ACh, increasing both the level and duration of the neurotransmitter action in the synapse.

Abbreviations: ACh, acetylcholine; AChE, acetylcholinesterase.

1.3.4 Oxidative stress

The importance of increased oxidative stress in the central nervous system (CNS) has consistently been proven to facilitate the pathogenesis of AD. The imbalance that occurs between the level of free radicals and their products, with antioxidant defence mechanism in the body, results in oxidative stress. This imbalance can occur due to an increase in free radical production or a decrease in antioxidant defences (Gandhi and Abramov, 2012). Free radicals or ROS in the body can be generated as by-products through aerobic respiration and during metabolism. This causes cumulative oxidative stress that induces cellular damage, impairment of the DNA repair system and mitochondrial dysfunction. These are the key factors that speed up the aging process, thus increasing the risk of development of neurodegenerative disorders (Patten *et al.*, 2010, Kim *et al.*, Kim *et al.*, 2015a, Gandhi and Abramov, 2012).

Free radicals exist in different forms and these harmful radicals are capable of being removed by antioxidant enzymes that are naturally generated in the body, while dietary antioxidants help in assisting the body in neutralising free radicals (Minioti and Georgiou, 2010). The CNS is vulnerable to free radical and oxidative damage due to the brain's high oxygen consumption (approximately 20% of the organism's total oxygen intake) compared to other tissues which leads to higher amounts of ROS to be generated from the leakage of electrons from the mitochondrial ETC (Gandhi and Abramov, 2012). The brain's abundant lipid content such as polyunsaturated fatty acids (PUFA) makes it vulnerable to free radical attack because of the weak double bonds present in the membrane which allows non-enzymatic oxidation and fragmentation during lipid peroxidation to occur easily and form a mass of toxic products (Nowak, 2013). Insufficient amounts of enzymatic antioxidants (e.g.,

superoxide dismutase, catalase) increases the high risk of free radical attack as well (Aksenova *et al.*, 2005, Obuobi *et al.*, 2016). Many synthetic antioxidants have shown toxic and mutagenic effects, which have shifted attention towards naturally occurring antioxidants.

Due to a high oxygen requirement, natural antioxidant is crucial to maintain ROS homeostasis in the brain. Antioxidants are natural compounds that protect cells by neutralising unstable molecules (free radicals) which cause cell damage (Birben *et al.*, 2012). Consumption of dietary or exogenous antioxidants that are capable of trapping oxygen include vitamin C, ascorbyl palmitate, citric acid, vitamin A, beta-carotene and selenium (Marković, 2016, Leopoldini *et al.*, 2011). Other than dietary intake, the body is dependent on several endogenous defence mechanisms such as GSH and ascorbic acid to help protect against free radical-induced cell damage (Sidoryk-Wegrzynowicz *et al.*, 2011). GSH is the most abundant endogenous antioxidant in the brain and AD-related increase in oxidative stress has been attributed to decreased levels GSH (Saharan and Mandal, 2014). If the body's natural antioxidants are not able to neutralise excess free radicals, a diet that is rich in antioxidants needs to be reinforced (Li *et al.*, 2008). Studies have suggested there are associations between the consumption of an antioxidant rich diet (such as fruits and vegetables) and the prevention of neurodegenerative diseases. The investigation of antioxidant properties of natural products has grown considerably to demonstrate that it could be one of the major causes of prevention of AD.

1.3.5 Mitochondrial dysfunction

Mitochondrial anomalies including increase in free radical causing oxidative stress from the respiratory chain and accumulation of injured mitochondria are one of the

main features of the aging process (Amigo *et al.*, 2016, Chistiakov *et al.*, 2014). Neurons are completely dependent on mitochondria OXPHOS for energy supplies. Neural presynaptic and postsynaptic terminals require the constant presence of mitochondria to produce high demands of ATP and buffer Ca2+-ion concentration in order to maintain neurotransmission (Shankar and Walsh, 2009, Gazit *et al.*, 2016, Verstreken *et al.*, 2005). Thus, mitochondrial dysfunction may reduce the production of ATP and altered Ca2+ homeostasis which contribute to the progression of AD (Huang *et al.*, 2016a). A decrease of enzymes that are involved in mitochondrial ATP production such as complex IV cytochrome c oxidase, pyruvate dehydrogenase complex, mitochondrial isocitrate dehydrogenase, α-ketoglutarate dehydrogenase, and ATP synthase complex were found in AD patient's brains (Maurer *et al.*, 2000, Cardoso *et al.*, 2004, Gibson and Shi, 2010, Wojsiat *et al.*, 2015).

Mitochondria dysfunction is linked to AD pathogenesis due it being the major source of ROS. Increased oxidative stress and ROS damage by a faulty ETC in AD brains results in DNA, lipid, and protein damage (Bonda *et al.*, 2014, Wang *et al.*, 2014c). Many studies have shown a strong connection between oxidative stress and mitochondrial dysfunction. These studies were carried out by analysing samples taken from different AD experimental models and AD patients. A study by (Du *et al.*, 2010) revealed that accumulation of Aβ peptide in synaptic mitochondria in the brain's of mice overexpressing human APP/Aβ led to deficits in mitochondrial function shown by increased mitochondrial permeability transition, mitochondrial respiratory function damage, decrease in cytochrome c oxidase activity and oxidative stress. Data from 5xFAD mice showed that synaptosomal mitochondrial dysfunction with elevated oxidative stress levels are early phenomena shown in AD brain pathology in an Aβ-

accumulated environment (Wang *et al.*, 2016a). Decreased mitochondrial complex IV activity (cytochrome c oxidase) has been detected in platelets from AD patients (Fisar *et al.*, 2016, Valla *et al.*, 2006). A study showed that in peripheral blood lymphocytes from AD and mild cognitive impairment patients, ATP synthase activity is compromised, thus causes reduction in ATP levels, decreased basal mitochondrial ΔΨM levels and also significant impairment of total OXPHOS capacity (Tramutola *et al.*, 2018, Leuner *et al.*, 2012). Thus, drugs that improve mitochondria function, scavenge excessive ROS, or enhance the autophagic flux may have the potential to treat neurodegenerative diseases. Table 1.7 shows a list of compounds that target free radicals and mitochondria in experimental models of AD.

Table 1.7 Compounds that target free radicals and mitochondria in experimental models of AD (Cenini and Voos, 2019).

Compounds	Activity	Experimental AD model
Vitamin E	Increases ΔΨM ROS scavenger Reduction of lipid peroxidation	*In vitro* glutamate-injured astrocytes *In vivo* aged old mice
Selenium	Inhibition of ROS production and oxidative damage Reduction of mitochondrial membrane depolarisation	*In vitro* Aβ42-CFP-overexpressed HEK293 cell line
Vitamin C	Maintenance of mitochondrial integrity through reduction of oxidative damage	*In vitro* Aβ1-42 peptide-treated human cortical neurons
Coenzyme Q10	Attenuation of decreased oxidative phosphorylation efficiency and of increased H_2O_2 production Reduction of mitochondrial accumulation of Aβ peptide Prevention of Aβ peptide-induced mPTP opening Protection against dissipation of ΔΨM Beneficial effect of mitochondrial ETC	Isolated mitochondria from Aβ1-40 peptide treated diabetic Goto–Kakizaki aged rats *In vitro* Aβ25-35 peptide-treated HUVEC cell line *In vitro* Aβ1-42 peptide-treated M17 cell line *In vivo* TgP301S mice
Mitoquinone (MitoQ)	Prevention of increased ROS production, loss of ΔΨM, decreased GSH/GSSG ratio, increased MDA and 3-NT Regulation of mitochondrial fusion, fission, and matrix genes Protection of mitochondrial structure Amelioration of ATP production, cyclooxygenase (COX) activity, and depletion of the cardiolipin	*In vitro* Aβ22-35 peptide-treated mouse cortical neurons and N2a cell line *In vivo* 3xTg-AD and Tg2576 mice *In vivo* human Aβ-overexpressed *C. elegans* SkQ1
SkQ1	Preservation of mitochondrial structure Improvement of mitochondrial biogenesis Increase of COX activity Inhibition of ROS production Reduction of mtDNA deletion	I*n vivo* OXYS rats

Melatonin	Restoration of: respiration rate, RCC proteins expression, ΔΨM, ROS production, ATP levels Prevention of decreased mitochondrial volume Improvement of mitochondrial biogenesis factors expression and mtDNA/nuDNA ratio Amelioration of mitochondrial membrane fluidity and mitochondrial structure Stabilisation of cardiolipin and mPTP Decrease of mitochondrial Ca2+ levels	Isolated mitochondria from APPswe and APP/PSEN1 mice *In vitro* APPswe-overexpressed HEK293 cell line *In vitro* Aβ22-35 peptide-treated cultured rat hippocampal neurons *In vitro* Aβ peptide-treated NARP cybrids cell line *In vivo* OXYS rats *In vivo* injection of Aβ1-42 peptide in rats hippocampus *In vivo* APP/PSEN1 mice
MitoApo or Apocynin	Protection against oxidative stress-induced cell death Reduction of superoxide production Prevention of mitochondrial H_2O_2 production	*In vitro* 6-OHDA-treated LUHMES cell line *In vitro* Aβ1-42 oligomers-treated mouse hippocampal neuro
α-Lipoic acid (LA)	Decrease of oxidative stress and apoptotic markers Preservation of COX assembly Elevation of ATP levels, Krebs cycle dehydrogenase, complex I, and COX activities	*In vitro* AD fibroblasts *In vivo* aged rats *In vitro* Aβ1-42 peptide-treated differentiated SH-SY5Y cell line *In vivo* ApoE4 Tg mice
Rapamycin	Prevention the loss of ΔΨM Stimulation of mitophagy/autophagy	*In vitro* Aβ1-42 peptide-treated PC12 cell line

1.3.6 Current therapeutic agents for AD

Currently there are five prescription drugs that are approved by the FDA for their symptomatic treatment that help to reduce or stabilise cognitive symptoms experienced by AD patients by affecting certain chemicals (such as ACh) involved in carrying messages among the brain's nerve cells. Donepezil (Aricept), galantamine (Razadyne), rivastigmine (Exelon) and tacrine (Cognex) are the four approved AChE inhibitors. Many studies have supported the effectiveness of these drugs as a potent cholinesterase inhibitor treatment. They are prescribed to improve the patient's reason, memory, attention, language and the ability to perform simple tasks (Cacabelos, 2007, Atri *et al.*, 2013, Birks, 2006). Memantine (Namenda) is the first anti-Alzheimer drug that modulates N-methyl-D-aspartic acid (NMDA) receptors (antagonist-type) that is approved by the FDA to treat moderate to severe AD. A clinical study and *post hoc* analyses investigated treatment with memantine and cholinesterase inhibitor as a combination therapy in moderate-to-severe AD that produced consistent benefits that appeared to increase over time, and that are beyond those of cholinesterase inhibitor treatment alone (Gauthier and Molinuevo, 2012). These approved drugs are known to be well-tolerated. However, there are a few reported cases of the adverse effects of these drugs during clinical trials. Some patients that consumed Memantine, Donepezil and Rivastigmine experienced nausea, vomiting, headaches and diarrhoea during the trials (Bullock *et al.*, 2005, Tariot *et al.*, 2004, Dunn *et al.*, 2000). Tacrine has previously been demonstrated to causes hepatoxicity *in vivo* and in clinical trials (Watkins *et al.*, 1994, Yip *et al.*, 2018, Lou *et al.*, 2015).

1.3.7 Natural product and neuroprotection

For thousands of years natural products have historically played a very important role in the world's health care and have often been the sole means for the prevention or treating of diseases due to their complex chemical multiple-target molecules found mainly in plants and microorganisms (Bagli *et al.,* 2016). Oxidative stress has been pointed out as one of the leading causes of brain aging which lead to neurodegenerative diseases. Therefore, consumption or administration of antioxidants is a beneficial strategy recommended for preventing brain aging and several brain age-related diseases (Fiorella *et al.,* 2017). Polyphenols have been extensively studied regarding their antioxidant activities. Many studies have suggested a strong association between polyphenol consumption (particularly the ones from red wine or green tea) and reduced prevalence of various neurodegenerative diseases (Lorenzo *et al.*, 2019, Mandel *et al.*, 2006, Mani *et al.*, 2018, Gray *et al.,* 2018, Caruana *et al.,* 2016). The most relevant example of polyphenolic compound is resveratrol. Resveratrol can activate sirtuin 1 (SIRT1) which protects the neuron cells or in the hippocampus from oxidative stress and cytotoxicity caused by Aβ peptide and alpha-synuclein (Albani *et al.*, 2009, Khan *et al.*, 2012, Li *et al.,* 2014a). Resveratrol also restores intracellular antioxidant enzymes such as GSH, catalase and SODs levels in a cell culture model (Konyalioglu *et al.*, 2013, Gaballah *et al.,* 2016). Table 1.8 shows other compounds isolated from plants used for the treatment of AD.

Table 1.8 Compounds isolated from plants used for AD treatment

Compound isolated	Plant	Activity	References
Physostigmine (alkaloid)	Calabar bean, the seeds of *Physostigma venensosum* Balf	Potent, short-acting and reversible AChE inhibitor Improves cognitive functions *in vivo* and in both normal and AD patients	(Bitzinger *et al.*, 2019, Kamal *et al.*, 2000)
Galantamine (alkaloid)	Amaryllidaceae family	Reversible AChE inhibitor	(Lilienfeld, 2002)
Huperzine A (quinolizidine alkaloid)	Club moss *Huperzia serrata* (Thumb) Trevis	Reversible AChE inhibitor Protection against ROS and Aβ	(Tun and Herzon, 2012)
Curcumin	Turmeric plant *Curcuma longa L.* (Zingiberaceae)	Increases ATP levels and COX activity Positive effects on ΔΨM and respiratory control ratio Reduction of ROS production and mitochondria-mediated apoptosis Restoration of complex I, II, COX levels and activities	(Hagl *et al.*, 2014, Chang *et al.*, 2014, Sood *et al.*, 2011)
Resveratrol (3,4',5-trihydroxystilbene)	Vitaceae family, grapes, berries, and peanuts	Attenuation of ROS accumulation, ΔΨM and mitochondria-mediated apoptosis Increase of COX levels Stimulation of mitophagy/autophagy	(Deng and Mi, 2016, Porquet *et al.*, 2014, Wang *et al.*, 2018a)
Quercetin	Fruits, vegetables, and grains	Restoration of ΔΨM, ROS production, and ATP levels, and normal mitochondrial morphology Increased MnSOD activity	(Wang *et al.*, 2014a, Sharma *et al.*, 2016, Jiang *et al.*, 2016, Godoy *et al.*, 2017)

		Prevention of mitochondria-mediated apoptosis	
N-Acetyl-cysteine (NAC)	*Gingko biloba*	Decreases oxidative stress and apoptotic markers Preservation of COX assembly Stabilisation of ΔΨM and ATP production Reduction of ROS/RNS production Increases mitochondrial APE1 levels Enhancement of complex I, III, COX activities Improvement of oxygen consumption Up-regulation of mitochondrial DNA Blocks mitochondria-mediated apoptosis	(Rhein *et al.*, 2010, Eckert *et al.*, 2005, Tian *et al.*, 2013)
Wogonin	*Scutellaria baicalensis*	Rescues the ΔΨM loss Attenuation of mitochondria-mediated apoptosis Inhibits APP processing in the β-secretase pathway	(Huang *et al.*, 2017b)
Epigallocatechin-3-gallate (EGCG)	Green tea such as *Camellia sinensis* L. Ktze	Attenuation of ROS accumulation Increase of MnSOD level Restoration of altered MMO, ATP levels, and mitochondria respiratory rates	(Zhang *et al.*, 2017b, Biasibetti *et al.*, 2013, Dragicevic *et al.*, 2011)

1.4 Plants as a natural product for drug discovery

One of the best sources to identify hits and develop leads for drug discovery is products from natural origin. However, drug discovery in natural products is a lengthy process coupled with difficulties in obtaining sufficient samples for isolation and low-yields of active compounds. Nevertheless, due to vast biodiversity, there are still a lot of interest in natural products as a source of new drugs. From 1981 to 2006, 1184 new chemical entities were reported and 60% were derived from or based on natural products. Twenty-five percent of all prescription medications are made using the various types of secondary metabolites from living organisms, mainly plants (Butler, 2004, Mishra and Tiwari, 2011). Tropical rainforests have been called the 'world's largest pharmacy', because about 70% of the drugs used today are models of natural products and Malaysia is covered with forest by more than 50% (Jantan *et al.*, 2015). Traditional Chinese Medicine (TCM) and the Indian Ayurveda are popular alternative medicine used in Malaysia. *Aquilaria* sp. (agarwood) has been a part of Ayurvedic and TCM for centuries (Hashim *et al.*, 2016).

1.5 *Aquilaria* sp. and its uses

There are more than 30 species of *Aquilaria* sp. (Thymelaeaceae) distributed mainly around Asian countries such as Indonesia, Malaysia, China, India, Philippines, Cambodia, Vietnam, Laos, Thailand, Papua New Guinea, and Singapore. There are 5 indigenous species found in rainforests of Malaysia such as *A. malaccensis, A. microcarppa, A hirta, A hirta,* A. *beccariana* and *A. rostrate* (Mohamad Ali *et al.*, 2008). The wood of *Aquilaria* trees produces a secondary metabolite called agarwood also known as gaharu in Malaysia and Indonesia which is a resinous heartwood that acts as a defence response when the bark is injured caused by wind, lighting, gnawing

by ants or insects, or by microbial infection (Kristanti *et al.*, 2018). The natural process of agarwood takes over decades to completely develop. Therefore, to speed up the process, the bark of the tree is burned, cut or inoculated deliberately with fungi such as *Fusarium* sp in order to produce agarwood (Li *et al.*, 2014b, Gao *et al.*, 2014, Ueda *et al.*, 2006, Yang *et al.*, 2014a). This high value resinous heartwood has commercially been used in traditional medicine for digestive, sedative and antiemetic treatment. In China, topical application of *Aquilaria* leaves helps to treat injuries such as fractures and bruises (Zhou *et al.*, 2008). Burning of the dark wood of *Aquilaria* tree emits a pleasant smell due to the presence of resin. Therefore it is used as incense for religious ceremonies, for perfume as well as a source of aromatic and therapeutic oils (Zuhaidi, 2016, Mat, 2012).

1.5.1 *Aquilaria malaccensis*, Lam

Aquilaria malaccensis (synonymous *A. agallocha* Roxb) has a wide distribution and has been found in 10 countries in South Asia and South East Asia, namely Bangladesh, Bhutan, India, Indonesia, Malaysia, Myanmar, the Philippines, Singapore and Thailand (Naef, 2011, Oldfield *et al.*, 1998). Despite this wide distribution, *Aquilaria* sp often occur in low density and can be found throughout primary and secondary forests, mainly in plains, but also on hillsides and ridges at altitudes between 0 to 1000m above sea level (Swee and Chua, 2008). It is the main source of agarwood in Malaysia and considered one of the most exploited species in Malaysia due to its high economic value (Faizal *et al.*, 2017). *A. malaccensis* is an evergreen tree that can grow up to 18-40 m in height with an average trunk of 40 cm in diameter. Before the production of resin, the wood is typically white, lightweight and low in density and after resin production, the resin rich wood becomes dark, heavy and hard. *A.*

malaccensis tress reach maturity after 7 – 9 years by starting to produce flowers and seeds. Medium sized trees can produce up to 1.5kg of seeds. The branches of the *A. malaccensis* tree produces yellowish green or white flowers (Adelina *et al.*, 2004) as well as green and egg-shaped fruits (Elias *et al.*, 2017, Adelina *et al.*, 2004)

1.5.2 Previously reported scientific research on *A. malaccensis*

The *Aquilaria* genus has been investigated for their biological effects and phytochemical characteristics. This plant is rich in a variety of different classes of natural products, but the most significant bioactive compounds of these plants are sesquiterpenes and chromones, alkaloids, flavonoids, benzophenones, diterpenoids, triterpenoids and lignin compounds. Agarwood resins contain essential oils which give out a special aroma that is used for making perfumes. These perfumery ingredients in agarwood oil contain a complex mixture of secondary metabolites such as sesquiterpenes and chromones (Ismail *et al.*, 2014). Sesquiterpenes such as agarofuran, eudesmanes, agarospiran and prezizane have been previously isolated from *A. malaccensis* (Kristanti *et al.*, 2018, Wang *et al.*, 2018d, Kalra and Kaushik, 2017). Agarwood essential oil has previously been tested for anti-cancer activity against cancer cell lines such as breast, pancreatic and colorectal carcinoma cells (Dahham *et al.*, 2016c, Abbas *et al.*, 2014, Dahham *et al.*, 2016b, Hashim *et al.*, 2014). Agarwood hydrosol obtained from hydrodistillation of *A. malaccensis* showed anti-attachment and cytotoxic effects on Calu-3 lung cancer cells (Hussein *et al.*, 2019).

Other than the bark, compounds with active biological effects have also been previously isolated from *A. malaccensis* leaves, stems and seeds. 4'-hydroxyacetanilide or acetaminophen is a synthetic drug that is commonly used to treat fever, migraine and other types of illness that was originally obtained from a leaf

extract of *A. malaccencis* (Afiffudden *et al.,* 2015). The earliest publication found on agarwood pharmacological activities reported that an alcohol extract of *A. malaccensis* stem bark and stem showed mild cardiotonic activity and anti-cancer effects against Eagle's carcinoma of the nasopharynx (Gunasekera *et al.*, 1981). Other studies showed an oil extract of *A. malaccensis* stembark (clean and infected part) caused cytotoxic activity (IC_{50} :44 µg/ml) against HCT116 cells (human colon cancer cells) (Ibrahim *et al.*, 2011). Furthermore, a study by Korinek *et al.* (2016) reported that a phorbol ester compound called aquimavitalin, isolated from the ethanolic extract of *A. malaccensis* seeds, showed antiallergic activities by exhibiting a strong inhibitory effect in A23187- and antigen-induced degranulation assays (IC_{50}: 1.7 and 11 nM, respectively) (Korinek *et al.*, 2016). Another study isolated four new phorbol esters **(1−4)** and two known phorbol esters (**5** and **6**) (Table 1.9 and Figure 1.8). Compound **1** (IC_{50} 2.7 µM), **5** (IC_{50} 0.8 µM), and **6** (IC_{50} 2.1 µM) showed potent anti-inflammatory activity by exhibiting inhibitory activity on N-formyl-L-methionyl-L-leucyl-L-phenylalanine (fMLF)/cytochalasin B (CB)-induced elastase release by human neutrophils. All the compounds were also evaluated for their cytotoxic properties against HepG2 (hepatoma), MDA-MB-23 (breast), and A549 (lung) cancer cells, but did not show any activity (Wagh *et al.*, 2017).

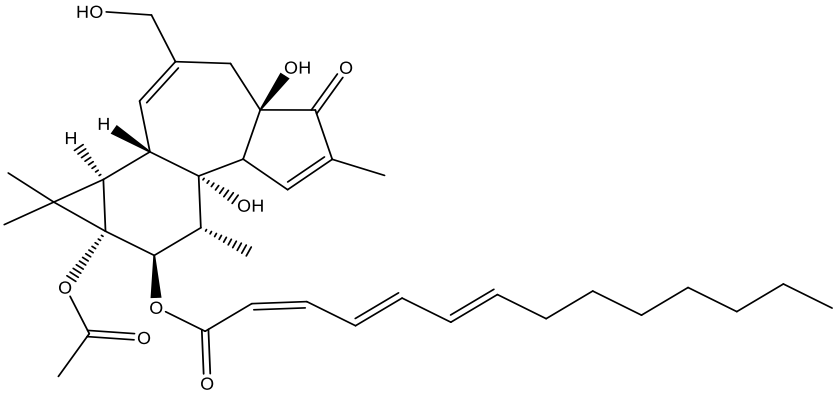

Figure 1.9 Chemical structure of aquimavitalin

Table 1.9 Phorbol esters isolated from *A. malaccensis* seeds

Compound	**Name**
1	12-O-(2′E,4′E)-6-oxohexa-2′,4′-dienoylphorbol-13-acetate.
2	12-deoxy-13-O-acetylphorbol-20-(9′Z)-octadecenoate.
3	12-O-(2′E,4′E)-6′,7′-(erythro)-dihydroxytetradeca-2′,4′-dienoylphorbol-13-acetate.
4	12-O-(2′E,4′E)-6′,7′-(threo)-dihydroxytetradeca-2′,4′-dienoylphorbol-13-acetate.
5	12-O-deoxyphorbol 13-decanoate
6	Mellerin A

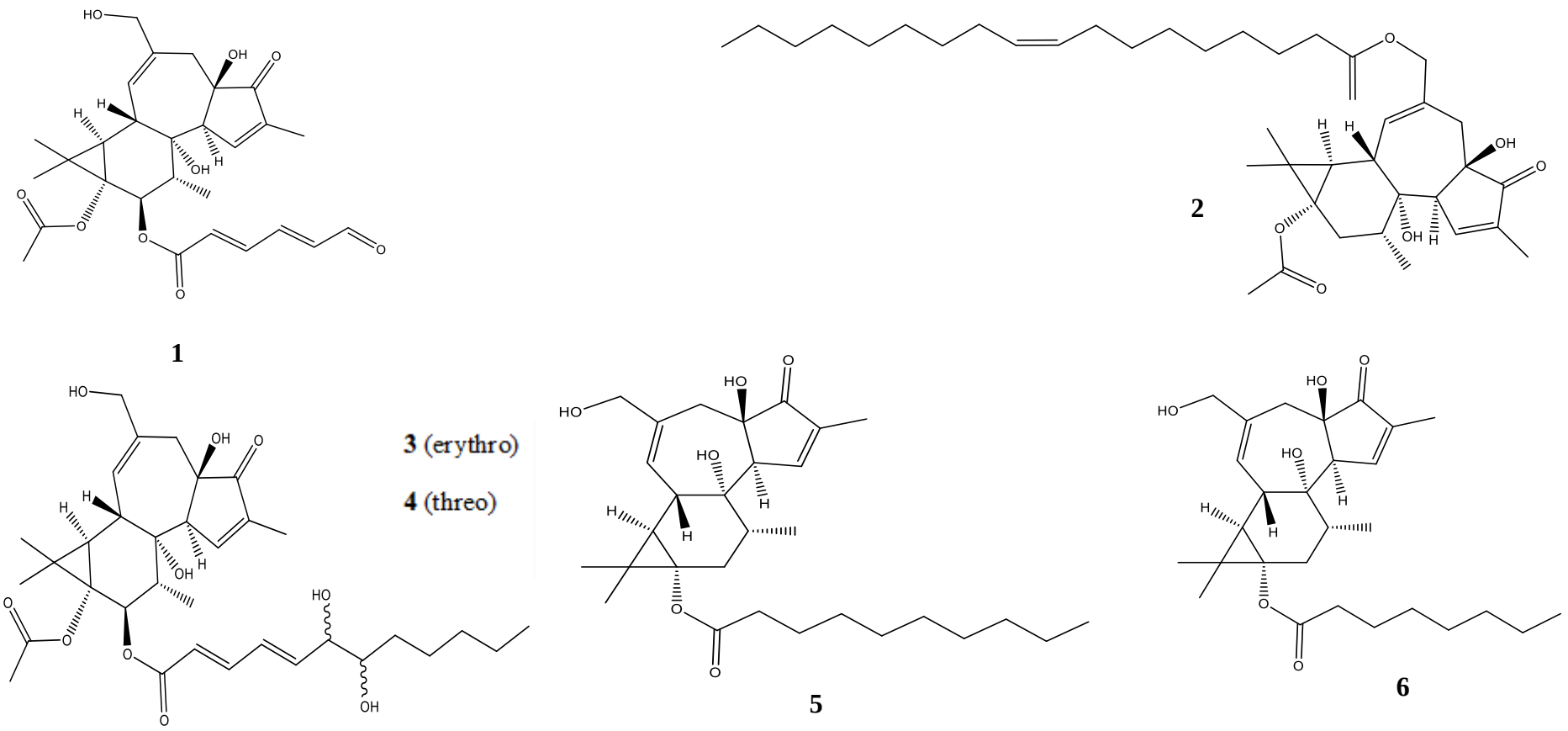

Figure 1.8 Chemical structure of phorbol esters **1-6** isolated from *A. malaccensis* seeds.

1.6 *Hopea* sp. and its uses

Hopea Roxb. is reported to be the largest genus with at least a 100 species in the plant family Dipterocarpaceae. Dipterocarpaceae is a well-known family of rainforest trees that comprises more than 500 species, widely distributed in the evergreen forests and rainforest of Indochina, upto the northern Malayan peninsula and it is also the most economically and ecologically dominant genera (Hamilton, 2018, Lee *et al.*, 1997). It was proposed that dipterocarps trees originate from the Eurasian plate and migrated to the Far East including South Asia and Africa. The bulk of tropical hardwoods came from dipterocarps since the early 70s traded in the international and domestic markets (Larsen, 1998). Resin produced from the bark of *Dipterocarpus*, *Hopea* and *Shorea sp*. are used for lighting and sealing boats, and as a base for paints, as well as varnishes (Dyrmose *et al.*, 2017). *Hopea* species named *Hopea odorata* Roxb. have been used as medicinal plants in Khok Pho District (Pattani Province) of Thailand and North Andaman Islands of India (Wiyakrutta *et al.*, 2004, Prasad *et al.*, 2008). The stem bark of this species is known to be rich in tannins, has been used for treating paralysis, haemorrhoids, diarrhoea, gum inflammation, urinary incontinence and neck pains (Chuakul, 2005, Yang *et al.*, 2013).

1.6.1 Previously reported scientific research on the *Hopea* genus

The *Hopea* genus from the family Dipterocarpaceae has been known to produce oligostilbenoid compounds such as resveratrol oligomers. These oligomers include stilbene dimers, trimers, tetramers, hexamers, heptamers and octamers that are composed of a diverse assemblage of two or more resveratrol monomers by an oxidation process. Some of these compounds exert biological activities, such as

antibacterial, antiviral, and cytotoxic effects (Sahidin *et al.*, 2005, Cichewicz and Kouzi, 2002). Compounds isolated from *H. dryobalanoides* are shown in Figure 1.9.

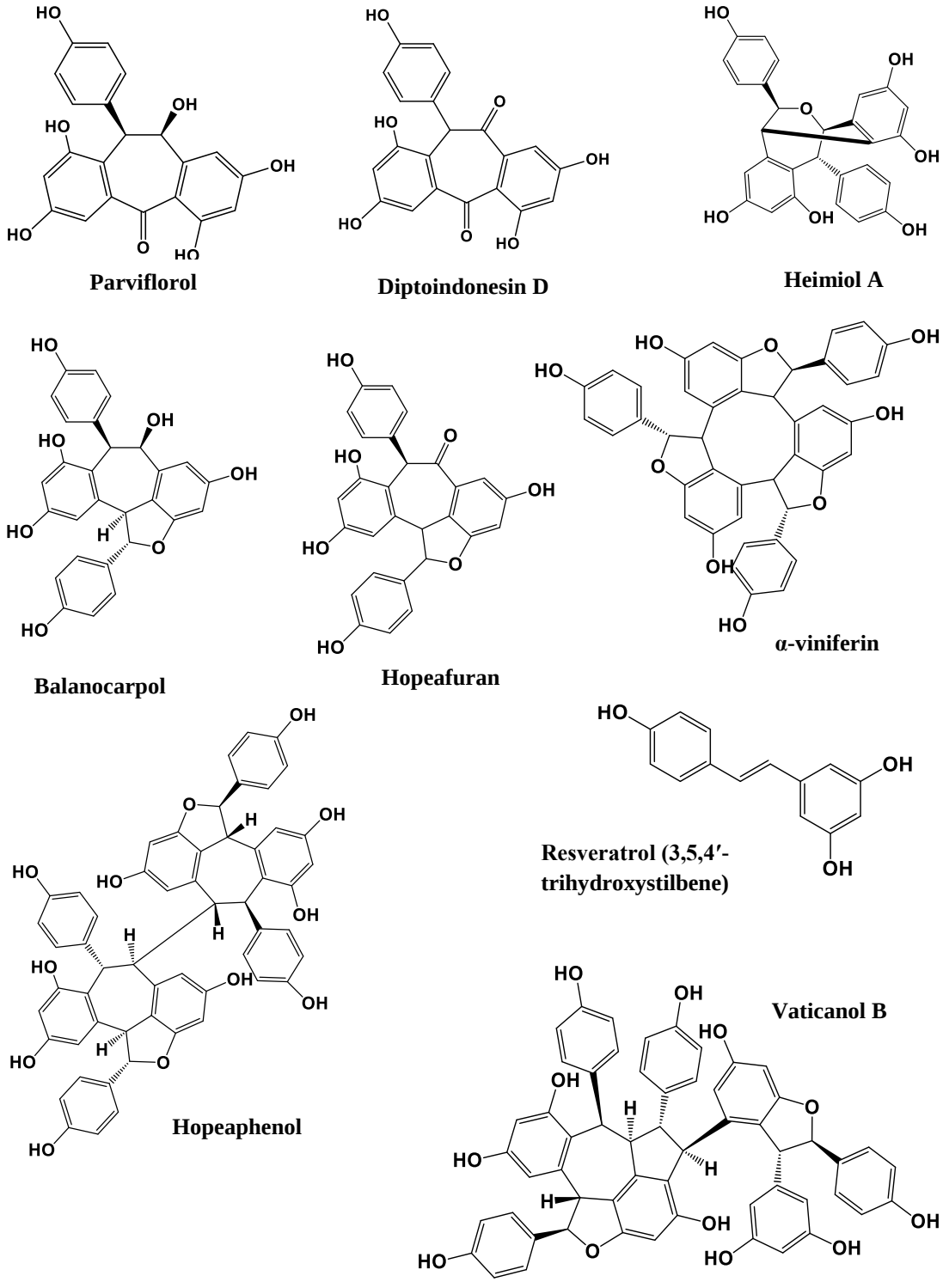

Figure 1.9 Compounds previously isolated from *H. dryobalanoides*

One of the first compounds that was isolated from *Hopea* sp. was a resveratrol tetramer called hopeaphenol which was elucidated using X-ray crystallography a few years later (Coggon *et al.*, 1965, Coggon *et al.*, 1970). Since then, other researchers managed to isolate the same compound from other *Hopea* sp. such as *H. dryobalanoides, H .malibato* and *H. parviflora* (Sahidin *et al.*, 2005, Dai *et al.*, 1998, Tanaka *et al.*, 2000). Hopeaphenol was reported to be very active against several cancer cell lines including human epidermoid nasopharynx carcinoma, A549 and breast cancer (MCF-7) (Ohyama *et al.*, 1999). Hopeaphenol also exhibited potent cytotoxic effects against P-388 murine leukaemia cells (IC_{50}=5.2µM), colon cancer cells SW480 (IC_{50}=28.6 µM) and leukaemia HL60 cells (IC_{50}=21.3 µM) (Muhtadi *et al.*, 2006, Ito *et al.*, 2003). Another study showed that hopeaphenol exhibited its anticancer effects by causing arrest at the G1 phase of the cell cycle in SK-MEL-28 melanoma cells (Moriyama *et al.*, 2016). Other than that the compound also showed DPPH, superoxide and hydrogen peroxide scavenging activity (Subramanian *et al.*, 2015). α-viniferin is also a resveratrol trimer which was first isolated from wine grapes (*Vitis vinifera*) and used as an antifungal agent (Langcake and Pryce, 1977). Subsequently, α -viniferin has been isolated from *H. dryobalanoides* (Sahidin *et al.*, 2005). Similar to other resveratrol oligomers, α -viniferin showed very potent growth inhibitory effects on various cancer cell such as HL-60, MCF-7, HepG2, A549, P-388 cells and human colon cancer (HCT-116, HT-29, Caco-2) (Wibowo *et al.*, 2011, Gonzalez-Sarrias *et al.*, 2011). α-viniferin also showed significant anti-inflammatory activity in several studies. In one study, α-viniferin suppressed the expression of proinflammatory genes *iNOS* and *COX-2* in LPS-stimulated BV2 microglial cells (Dilshara *et al.*, 2014). This was also seen in another study whereby α-viniferin attenuated mRNA levels of iNOS in inhibited

interferon (IFN)-gamma-stimulated RAW 264.7 macrophages (Chung *et al.*, 2010). It was reported that α-viniferin inhibited anti-cholinesterase activity, which has been targeted for treatment of neurodegenerative diseases such as AD (Sung *et al.*, 2002, Yan *et al.*, 2012).

1.7 Research aims

Various *Aquilaria sp.*, *Hopea sp.* and the compounds isolated from the plants have been proven to have many biological activities. Hence, the current research aims to investigate the potential anti-cancer, neuroprotective and anti-inflammatory activities of *A. malaccensis* and *H. dryobalanoides* extracts with a focus on their isolated compounds that could be potentially responsible for their activities. These aims will be achieved by exploring various research aspects which are discussed and explained in Chapters 2-5..

Chapter 2 focuses on the phytochemical investigation of the plant materials and the characterisation of the isolated compounds that will be used in subsequent chapters.

Chapter 3 focuses on the potential anti-cancer activity of the plant extracts and isolated compounds by using various enzymatic assays to obtain data that supports the aim.

In Chapter 4, anti-inflammatory studies on the isolated compounds and RNA sequencing (RNA-Seq) was carried out on differentiated human monocytic THP-1 cells.

Chapter 5 investigates the potential neuroprotective effects isolated compounds on neuroblastoma SHSY-5Y cells. Lastly, chapter 6 summarises the findings, conclusion and future work.

Chapter 2. Phytochemical investigation of *A. malaccensis* and *H. dryobalanoides*

2.1. Introduction

Since ancient times, natural products exclusively from plants have served as the most successful source of medicines (Veeresham, 2012). The earliest record on the use of natural products was from Mesopotamia (2600 B.C.) which showed that oils from *Cupressus sempervirens* (Cypress) and *Commiphora* species (myrrh) were used to treat coughs, colds and inflammation, and are still being used today (Dias *et al.*, 2012). Egyptian and Chinese natural products have played prominent roles in ancient traditional medicine systems. A great deal of knowledge on Ancient Egyptian medicine dates back from 1550 BC from the Edwin Smith Papyrus, the Ebers Papyrus and the Kahun Papyrus that consist of a huge number of drugs derived from plant crude extracts (Abou El-Soud, 2010). The Chinese Materia Medica has been extensively documented over the centuries, with the first record dating from about 1100 B.C. named Wu Shi Er Bing Fang (52 prescriptions), followed by works such as the Shennong Herbal (~100 B.C.; 365 drugs), and the Tang Herbal (659 A.D.; 850 drugs) (Cragg Gordon and Newman David, 2005). Many famous drugs which to date are still being used in hospitals or sold by big pharmaceutical companies are plant-based. For example, aspirin (acetylsalicylic acid) (Figure 2.1), well-known for its anti-inflammatory properties, is derived from salicin, a glycoside, which was isolated from the bark of the willow tree *Salix alba L.* (Montinari *et al.*, 2018). Morphine, first reported in 1803, was isolated from *Papaver somniferum* L. (opium poppy). Then in the 1870s, it was found that boiling crude morphine (isolated from *P. somniferum*) in acetic anhydride yield diacetylmorphine (heroin) that can be readily converted to codeine which until now is used to treat pain, coughing, and diarrhoea (Dias *et al.*,

2012). Even though new drug discovery methods are being developed, natural products have been the most productive source for clinical trials and contributed to the development of drugs (Butler, 2004). Natural products continue to be a major source of bioactive agents due to their large-scale structural diversity compared to synthetic compounds. The major benefit of natural products is that plant-based metabolites can avoid the side effects of synthetic drugs (Lahlou, 2013). Many synthetic drugs have been reported to cause major side effects such as paracetamol which is a well-known antipyretic drugs that causes liver poisoning and ibuprofen causes nephrotoxicity (Tanne, 2006, Mann *et al.*, 1993) .

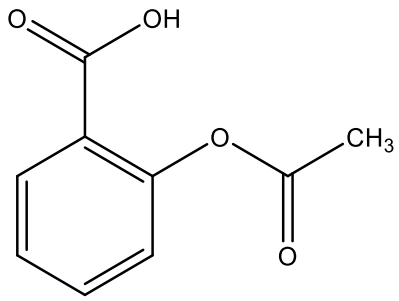

Figure 2.1 Chemical structure of aspirin

Phytochemicals or "plant chemicals" are biologically active secondary metabolites present in plants which also play a part in giving colour, aroma, and flavour and provide protection for the plant from infection and predators (Sharif *et al.*, 2018, Kumar, 2019). Many secondary metabolites in both plant extracts and purified compounds isolated from plant-based natural products have been explored to have potential anti-cancer, anti-inflammatory and anti-oxidative properties. The main

active plant classes which have been identified and extracted from plants for these properties include flavonoids, alkaloids, tannins, terpenoids and sterols (Salih *et al.*, 2014, Seca and Pinto, 2018).

2.1.1. Flavonoids

Flavonoids are a group of secondary metabolites that can be found in fruits, flowers, vegetables and herbs. The general structure of a flavonoid as shown in Figure 2.2 is made up of a fifteen-carbon skeleton consisting of two benzene rings (A and B) and a heterocyclic pyrane ring (C). They can be divided into 6 different classes: flavones, flavanols, flavanones, flavanonols, isoflavones and flavan-3-ols (Kumar and Pandey, 2013). Flavonoids are responsible for influencing the transport of the plant hormone (auxin), the flavonoid pigment provides the yellow colour of flowers and leaves and act as a defence system from microbes and insects (Samanta *et al.*, 2011).

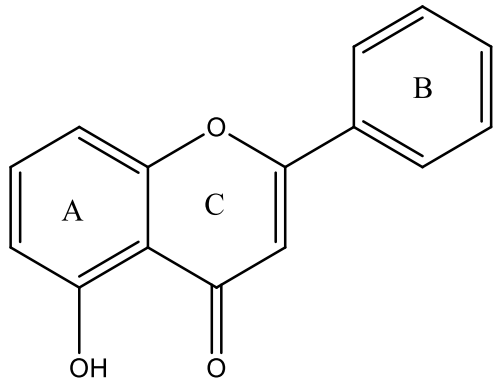

Figure 2.2 Generic structure of flavonoids

Flavonoids have been shown to be promising anti-cancer agents with several cancer related mechanisms such as the ability to block cell cycle resulting in the inhibition of cell growth and proliferation, inducing apoptosis and differentiation (Raffa *et al.*, 2017). Quercetin is the most abundant flavonoid that is found widely in plants such as

bark, flowers, seeds of tomatoes, apples, berries, grapes, onions, tea leaves, vegetables, capers, shallots, and nuts. It has been investigated for its anti-cancer, anti-inflammatory and anti-oxidant properties for many years (Li *et al.*, 2016). Quercetin has been reported to exhibit an apoptotic effect on several cancer cell lines including MCF-7, HL-60 (leukemia) and HepG2 (liver) (Nguyen *et al.*, 2017a, Zhao *et al.*, 2014, Yuan *et al.*, 2012). Several studies have reported that quercetin exhibited anti-inflammatory activity by inhibiting LPS-induced TNF-α, IL-8, IL-1α, COX and lipoxygenase (LOX), Src- and Syk-mediated phosphatidylinositol-3-Kinase (PI3K)-(p85) tyrosine phosphorylation and Toll Like Receptor 4 (TLR4) production in different cell lines (Manjeet and Ghosh, 1999, Geraets *et al.*, 2007, Bureau *et al.*, 2008, Endale *et al.*, 2013, Lee *et al.*, 2010b, Kim *et al.*, 1998). Quercetin can also alleviate oxidative damage by reducing ROS levels in cell lines (Zhu *et al.*, 2017a) (Zerin *et al.*, 2013, Hu *et al.*, 2015a).

Figure 2.3 shows other flavonoids isolated from plants that have been intensively researched on their anti-cancer (Imran *et al.*, 2019, Yan *et al.*, 2017, Tuorkey, 2016), anti-inflammatory (Kadioglu *et al.*, 2015, Soares *et al.*, 2006, Aziz *et al.*, 2018) and anti-oxidant (Wang *et al.*, 2018b, Jung, 2014, Romanova *et al.*, 2001) properties.

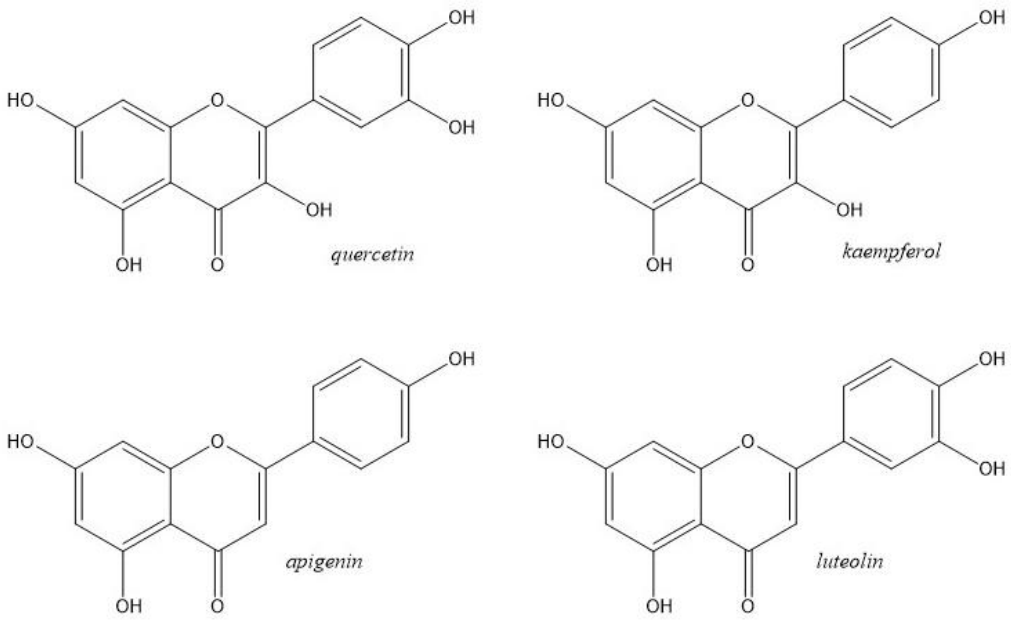

Figure 2.3 Chemical structure of quercetin, kaempferol, apigenin and luteolin

2.1.2. Alkaloids

Alkaloids are organic compounds that occur naturally in plants and fungi as secondary metabolites that possess a wide range of activites (Hussain *et al.*, 2018). The general chemical structure of the compounds contains the presence of at least one nitrogen. Other than that, alkaloids also contain carbon, hydrogen and usually oxygen. A German pharmacist named Wilhelm Meissner was the first to introduce the term "alkaloid" which is also traditionally defined based on their bitter taste, basicity, plant origin, and physiological actions (Eguchi *et al.*, 2019).

An alkaloid compound, taxol (also known as Paclitaxel®) was first isolated from the bark of the Pacific yew tree *Taxus brevifolia* and later found in other parts of the trees such as needles and seeds and other *Taxus* species (Nikolic *et al.*, 2011, Sreekanth *et al.*, 2009). This compound is sold under the trademark Taxol® and has become the

most successful anti-cancer agent. In 1992, the FDA approved paclitaxel for the treatment of advanced ovarian cancer, then it was used to treat other types of cancer such as breast cancer, colorectal cancer, and squamous cell carcinoma of the bladder (Zhu and Chen, 2019). Berberine, an isoquinoline alkaloid that possesses a broad spectrum of pharmacological activities including anti-inflammatory, anti-oxidant and anti-cancer (Neag *et al.*, 2018). This compound can be found widely distributed in natural herbs such as *Hydrastis canadensis*, *Cortex phellodendri* and *Rhizoma coptidis* (Shamsizadeh *et al.*, 2017). Other than having the ability to cause apoptosis through cell cycle arrest and affect mitochondria membrane potential, it is also able to suppress pro-inflammatory cytokines and ROS production while increasing antioxidant enzyme activity (Eissa *et al.*, 2018, Li *et al.*, 2014c).

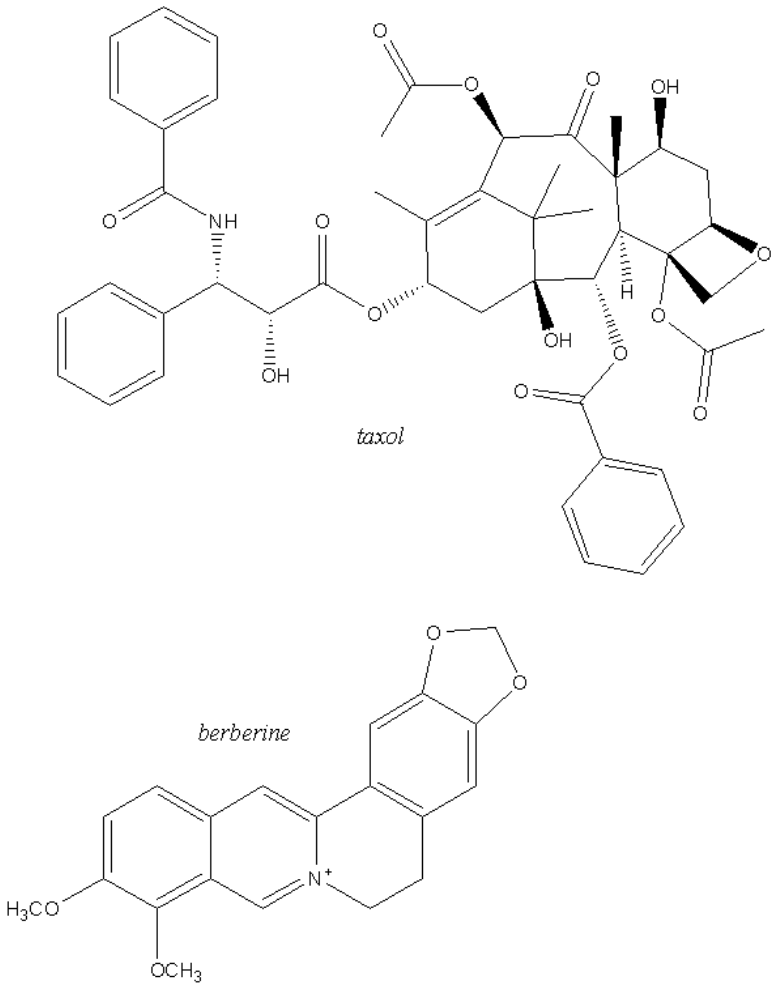

Figure 2.4 Chemical structure of taxol and berberine

2.1.3. Terpene and terpenoids

Terpenes/terpenoids consists of isoprene units which constitute one of the biggest classes of secondary metabolites found in natural products. This is due to the chemical diversity that can arise from the isoprene units which can be assembled to each other in thousands of ways (Jiang *et al.*, 2016). Terpenoids are terpenes that contain different functional groups and oxidised methyl groups modified at various positions. Depending on their carbon units, terpenoids can be divided into monoterpenes, sesquiterpenes, diterpenes, sesterpenes, and triterpenes (Perveen, 2018). Many

terpenoids isolated from natural products have been investigated as potential anti-cancer and anti-inflammatory agents (Salminen *et al.*, 2008). Lupeol, betulinic acid and betulin are pentacyclic triterpenoids, which are found in many natural products. Lupeol is commonly found in fruits and vegetables, e.g. olives, figs, mangoes, strawberries, red grapes and in medicinal plants (Saleem, 2009). Betulinic acid is a product of betulin oxidation and both can be found abundantly in the outer bark of birches (Betula, Betulaceae) (Hordyjewska *et al.*, 2019). Lupeol and betulinic acid possess potential anti-inflammatory properties by decreasing the generation of pro-inflammatory cytokines in LPS-treated macrophages/microglial and lupeol was also able to decrease type II cytokine levels in a bronchial asthma mouse model (Fernandez *et al.*, 2001, Vasconcelos *et al.*, 2008, Li *et al.*, 2018). Lupeol, betulinic acid and betulin were reported to be able to suppress cell viability and migration as well as induce cellular apoptosis through ROS and via a mitochondria pathway in many cell lines (Zhao *et al.*, 2018, Wang *et al.*, 2018e, He *et al.*, 2018).

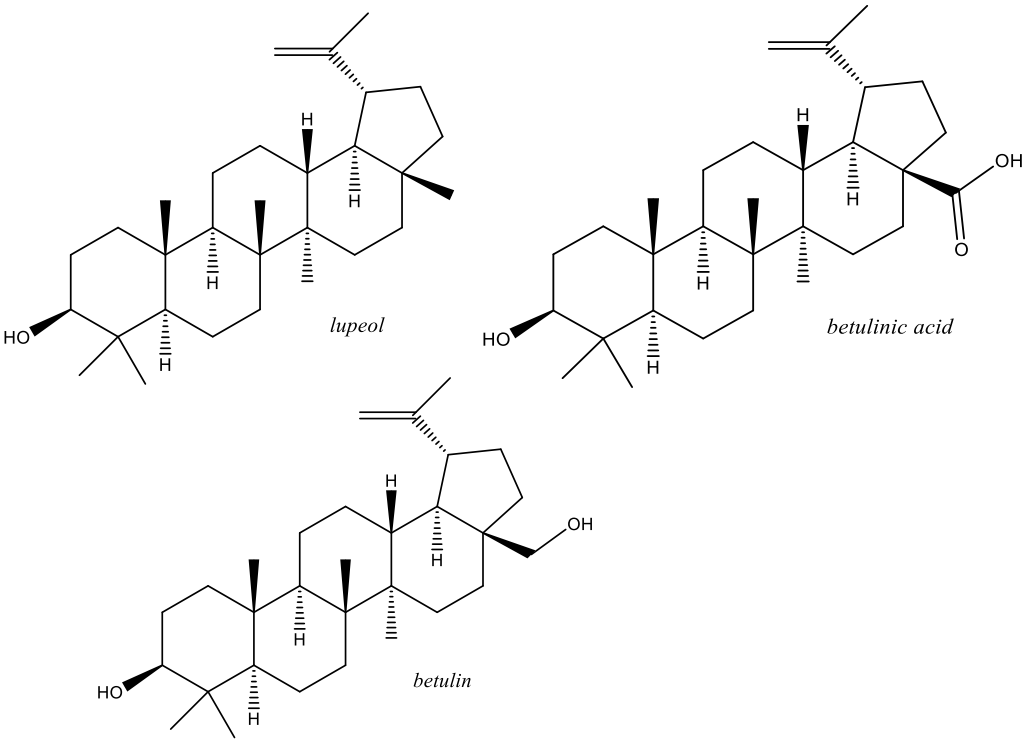

Figure 2.5 Chemical structure of lupeol, betulinic acid and betulin

2.1.4. Plant collection and extraction methods

The concentration and the type of chemical metabolites produced by plants may vary in different seasons. One of the main factors that could affect metabolite production is stress caused by environmental changes and place of growth (Isah, 2019). Therefore, it may be difficult to isolate the same compounds from the same plant species that have been collected in different seasons or regions. Phytochemicals are distinctive to definite plants and parts of plants. Due to the abundant amount of chlorophyll contained in the leaves, more time and solvent are needed to extract the chlorophyll out completely in order to isolate other secondary metabolites that may present in the leaves. Therefore, other parts such as bark and twigs are more preferred and easier to work on.

After collection of plant materials, they are air dried to remove all moisture and ground to obtain a homogenous powdered sample. The powdered sample is then subjected to extraction processes using various methods, such as maceration, heating under reflux, or Soxhlet extraction to extract desired compounds. Different solvents systems can be used for the extraction process depending on the type of compounds desired. For example, hexane is usually used to remove chlorophyll pigment and to extract non-polar components. Hydrophilic compounds are usually extracted using polar solvents such as methanol, ethanol or ethyl acetate and for the extraction of lipophilic compounds, less polar solvents are used such as dichloromethane (Amaro *et al.*, 2015, Sasidharan *et al.*, 2011). A rotary evaporator is used to concentrate the extracts by evaporating them at 40°C under reduced pressure until solvent free before proceeding to separation and purification using various chromatographic techniques.

2.1.5. Chromatographic techniques for compound isolation

Several chromatographic techniques have been developed through the years for the separation of mixtures of compounds present in plant extracts and to further purify the isolated compounds. Some of the techniques include thin layer chromatography (TLC), gel filtration chromatography (GFC) and column chromatography (CC).

2.1.5.1. Thin layer chromatography (TLC)

The first reported TLC application was by Stahl (Malins, 1965). The advantage of TLC is that it is quick and sensitive. This technique of chromatography is used to determine the number of components in the extracts or mixtures, to prepare the appropriate conditions for CC and to detect similar fractions from CC (Marston, 2011).

TLC is carried out by dissolving the extracts, fractions or pure compounds in an appropriate solvent such as chloroform for non-polar samples and ethanol or methanol for polar samples. Using a capillary tube, the samples are spotted on an appropriate TLC plate (usually silica gel pre-coated on aluminium sheets) approximately 1.5 cm from the bottom edge. Spots are applied as bands to facilitate movement and accurate observation, but the bands must be kept as narrow as possible to reduce overlaps. A small volume of the mobile phase (solvent combinations of e.g. hexane/ethyl acetate or ethyl acetate/methanol) is transferred into a TLC tank before placing the sample-loaded TLC plate for separation. In addition, a piece of filter paper is placed in the chamber to help create an atmosphere saturated with the mobile phase. Plates after separation are dried and examined under UV light using short (λ = 254 nm) and long wavelength (λ = 366 nm). Then the plates are sprayed with anisaldehyde-sulphuric acid reagent and heated with a hot air gun until colour develops. Different solvent systems can be used until a desirable resolution between the spots is obtained. Rf values are then determined as the ratio of distance travelled by each spot to the distance travelled by the mobile phase. Fractions from CC can be examined by TLC and fractions showing similar TLC profiles are pooled into one fraction.

2.1.5.2. Gel filtration chromatography (GFC)

Gel filtration chromatography (GFC) or size exclusion chromatography is a form of liquid chromatography which separates compounds according to their molecular size (Stanton, 2004). The process employs a cross-linked dextran-based resin, Sephadex® LH20, suspended in an aqueous buffer solution and packed into a chromatographic column. The Sephadex® slurry is prepared in methanol and packed in a glass column then kept overnight. The sample to be fractionated is dissolved in methanol and applied

onto the top of the column. Once the sample has diffused into the column, a cotton plug is inserted to prevent the escape of the gel into the solvent above the column bed. The column is eluted using appropriate solvents such as methanol and 5-10 ml fractions are collected in glass vials.

2.1.5.3. Column chromatography (CC)

Among the separation methods, column chromatography (CC) is the easiest to carry out, it has good stability and separates both polar and non-polar compounds which can result in the isolation of a single compound. Compounds with different weights and polarities will move down the column at different rates and therefore, CC separates compounds based on differential adsorption to the adsorbent to yield fractions and pure compounds. This technique is commonly applied to plant mixtures for several reasons. One of the reasons is that this technique is commonly used because there are various sizes of chromatography columns which allows small to large scale separation using different quantities of extracts or starting material (Coskun, 2016).

2.1.6. Spectroscopic techniques

2.1.6.1. Nuclear Magnetic Resonance (NMR)

NMR techniques are used to identify the type of compounds present in a mixture or fraction and to elucidate the structure of a compound by identifying the types and number of carbon, hydrogen and other atoms in a compound (Jackman, 1969). NMR spectroscopy works by recording the interaction of radiofrequency electromagnetic radiations with the nuclei of molecules placed in a strong magnetic field. The common atoms that are detected by NMR spectroscopy are hydrogen (^{1}H) and carbon (^{13}C). The spectra for these atoms are normally recorded on one axis and are known as one-dimensional NMR (1D NMR). In ^{1}H NMR, the chemical shifts and integration indicate

the kind and number of each type of proton present in the molecule while ^{13}C NMR indicates the number and kind of carbons in the molecule. The chemical shifts are in delta (δ) as parts per million (ppm). In 1D NMR, a J-coupling is calculated for coupled (d, t, q, dd) and it gives information about relative bond distances, angles and connectivity of the atoms.

A more advanced structural elucidation technique such as two-dimensional NMR (2D NMR) is usually carried out for more complex molecules and for accurate assignments of proton and carbon chemical shifts. These techniques include Correlation Spectroscopy (COSY) that shows ^{1}H-^{1}H connectivity that are plotted on both axes with a contour plot along the diagonal of the square graph. Heteronuclear Single Quantum Coherence (HSQC) determines the connectivity between carbon atoms and their attached hydrogen atoms while Heteronuclear Multiple Bond Coherence (HMBC) gives the connectivity between carbon atoms and their neighbouring hydrogen atoms. Nuclear Overhauser Enhancement Spectroscopy (NOESY) records all the proton correlations occurring through space in a molecule. The protons detected by NOESY are close to each other in space, but they are not bonded to adjacent or linked carbon atoms.

2.2. Aims and objectives

The aim of this chapter is to report and discuss the isolation and characterisation of the phytochemical constituents of *A. malaccensis* twigs and *H. dryobalanoides* bark which will be achieved by several objectives:

1. Collection of plant material.

2. Processing the plant material by washing, drying and grinding them into powder.
3. Subjecting the powdered plant materials to Soxhlet extraction.
4. Analysing the extracts by NMR.
5. Isolating major compounds from the plant crude extracts using several chromatography techniques.
6. Structural elucidation of the isolates using ^{1}H and ^{13}C and 2D NMR techniques.

2.3. Methods

2.3.1. Plant collection and processing

Twigs of *A. malaccensis* and bark of *H. dryobalanoides* were collected from the Forest Research Institute Malaysia (FRIM), Kuala Lumpur Malaysia in June 2014. The plant materials were washed to remove dirt and air-dried to minimise degradation and contamination. The plants were authenticated by Kafi M.J at FRIM where voucher specimens (F/3056.2010 and F/2120.2010) were deposited for future reference.

Figure 2.6 *A. malaccensis* (left) and *H. dryobalanoides* (right) leaves and twigs.

2.3.2. Plant grinding and powdering

Dried twigs and bark were cut into small pieces and ground into a fine powder using an electrical grinder. This is to ease extraction by Soxhlet apparatus.

2.3.3. Extraction

The powdered plant materials were packed in a cellulose extraction thimble and subjected to successive extraction for 8 h per day over 5 days for each solvent starting with hexane, ethyl acetate and then methanol. Extraction flasks containing anti-bumping granules were used to prevent solvents from bumping when the flask was heated. The extracts were evaporated at 40°C under vacuum using a rotary evaporator. The paste like extracts were transferred to pre-weighed flasks and left in a fume hood to dry for a few days in order to ensure a solvent-free extract. The solvent-free extracts were then weighed and kept until further use. The percentage yield was calculated using the following formula:

$$\% \text{ Yield} = \frac{\text{Weight of crude extract (g)}}{\text{Weight of plant material used (g)}} \times 100$$

2.3.4. NMR of samples

Samples were dissolved in suitable deuterated NMR solvents ($CDCl_3$ or acetone-*d*6) approximately 0.6ml in 5 mm NMR tubes. One dimensional ^{1}H and ^{13}C NMR (^{13}C and Dept-q 135) experiments were carried out first for characterisation of the extracts and fractions and selection of pure compound fractions. Spectra obtained were processed using MestReNova software 12.0.4 (Willcott, 2009). 2D experiments such as COSY, HSQC, NOESY and HMBC were carried out to assign proton and carbon chemical shifts and to determine the relative stereochemistry of the compounds. The spectra of known compounds were also compared with published data. Structures of identified compounds were then drawn using ChemDraw Professional software, Version 17.1.0.105.

2.3.5. Column chromatography

The initial activity screening on the solvent extracts of the plants showed that hexane extract of *A. malaccensis*, and the ethyl acetate extract of *H. dryobalanoides* to be the most active, therefore, only these extracts were subjected to separation and fractionation separately using open CC. The chromatography technique was performed on silica gel 60 (mesh size 0.063-0.200mm). An open glass column (55 x 3 cm) was packed with 50g of silica gel 60 saturated with 100% hexane solvent. Any trapped air bubbles were removed by tapping. Then, the pre-adsorbed extract was added to the top of the column and followed by inserting a cotton plug to prevent disturbance of the loaded material by the elution solvent system. Elution was carried

out isocratically or using a gradient by adding 100% hexane, and then the gradient elution was continued. The polarity was increased by 5% each time (300 ml of each solvent system) using ethyl acetate until it reached 100% ethyl acetate. The last solvent system was 5% (v/v) methanol in ethyl acetate – higher methanol percentages can dissolve the silica gel. Samples/fractions were collected every 15ml in a 30ml glass vial.

2.3.6. High Resolution Liquid Chromatography Mass spectrometry (HR-LCMS)

All isolated compounds were prepared at a concentration of 1mg/ml in methanol. A blank solvent was also prepared. The experiment was carried out using the Thermo Finnigan Exactive Orbitrap Mass Spectrometer in both positive and negative ionisation switching mode. Solvent A (0.1%, v/v, formic acid in H_2O) and solvent B (0.1%, v/v, formic acid in acetone) was prepared for the experiment. A silica C-18 HPLC column, size 75.0 x 3.0 mm^2, particle size 5µM and pore size 100°A was used. Each sample were eluted at a flow rate of 300 µl/min using a linear gradient of 10% B to 100% B for 30 mins, followed by isocratic elution at 100% B for 5 min and a linear gradient of 100% B to 10% B for 1 min, after which the column was further re-equilibrated with the same solvent system for another 9 min. The pressure and temperature were monitored to be within the normal range of 37-70 bars and 22 °C, respectively, for the instrument to operate smoothly. LC-MS data was recorded using Xcalibur version 2.2.

2.4. Results

2.4.1. Solvent Extraction and Yield

Crude extracts were obtained using Soxhlet extraction of the ground *A. malaccensis* twigs and *H. dryobalanoides* bark (1 kg) in each solvent starting with hexane, ethyl acetate and methanol. The yields are shown in Table 2.1.

Table 2.1 Percentage of yield of each plant extract (1kg) using various solvents

Solvent system	Amount extracted (g)	% Yield
***A.malaccensis* twigs**		
Hexane	7.9	0.79
Ethyl acetate	10.3	1.03
Methanol	15.4	1.54
***H. dryobalanoides* bark**		
Hexane	0.9	0.09
Ethyl acetate	8.8	0.88
Methanol	10.5	1.05

2.4.2. Characterisation of crude extract samples by NMR

All crude extracts obtained were analysed using NMR (Figure 2.7 to Figure 2.12) to identify the type of compounds present in the extracts. Table 2.2 shows a summary of the type of compounds in each extract.

Table 2.2 Main constituents present in plant crude extracts

Solvent	**Constituents**
***A. malaccensis* twigs**	
Hexane (AH)	Mixture of glycerides, fatty compounds, unsaturated fatty acids, 7-methoxy acacetin
Ethyl acetate (AE)	Unsaturated fatty acids
Methanol (AM)	Mixtures of more than two sugars possibly dissacharides
***H. dryobalanoides* bark**	
Hexane (HH)	Tritepenes possibly sitosterol or stigmasterol and fats
Ethyl acetate (HE)	Balanocarpol, heimiol A and mixture of fatty acids
Methanol (HM)	Mixture of sugars

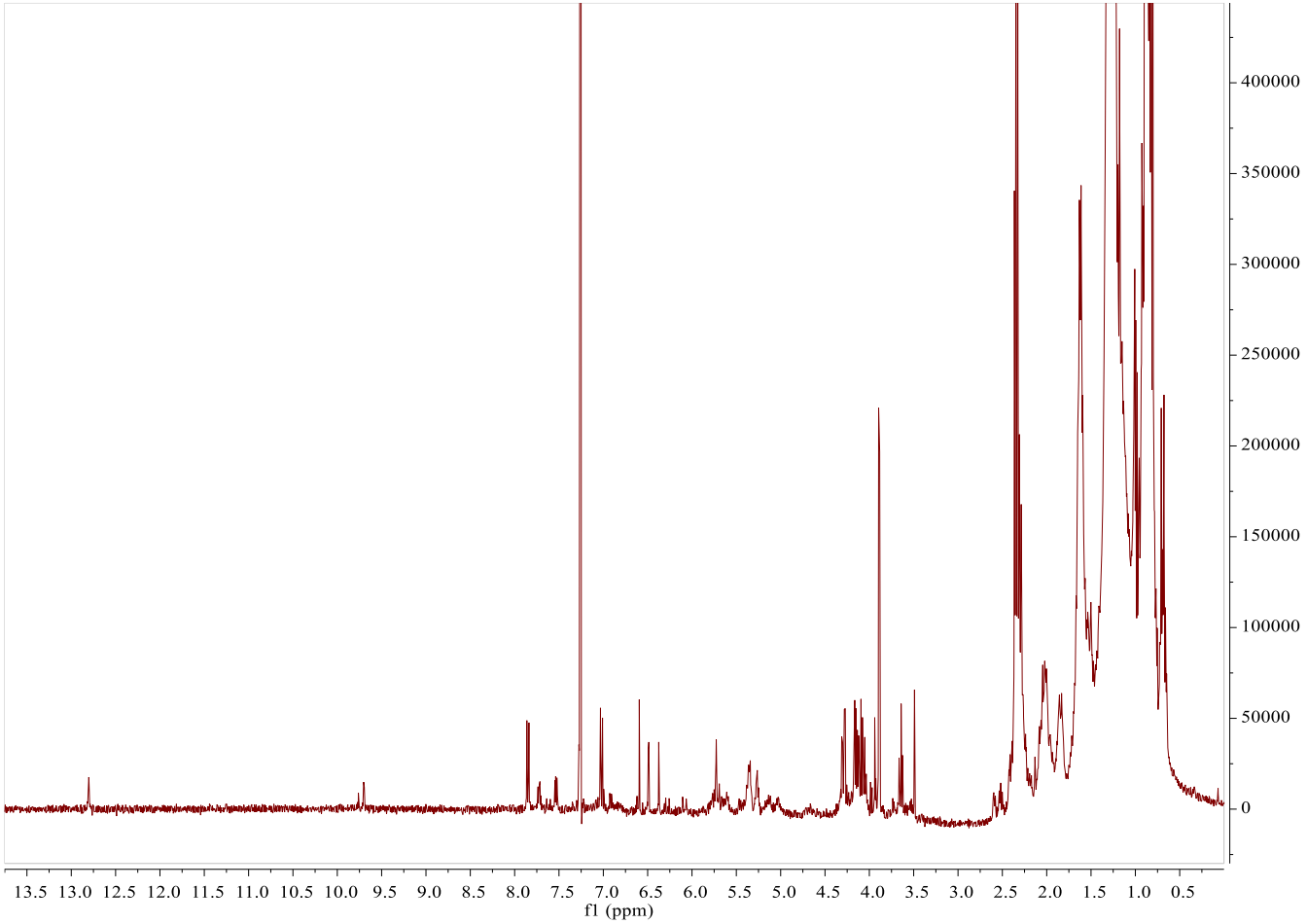

Figure 2.7 ^{1}H NMR spectrum (400 MHz) of *A. malaccensis* hexane extract in $CDCl_3$.

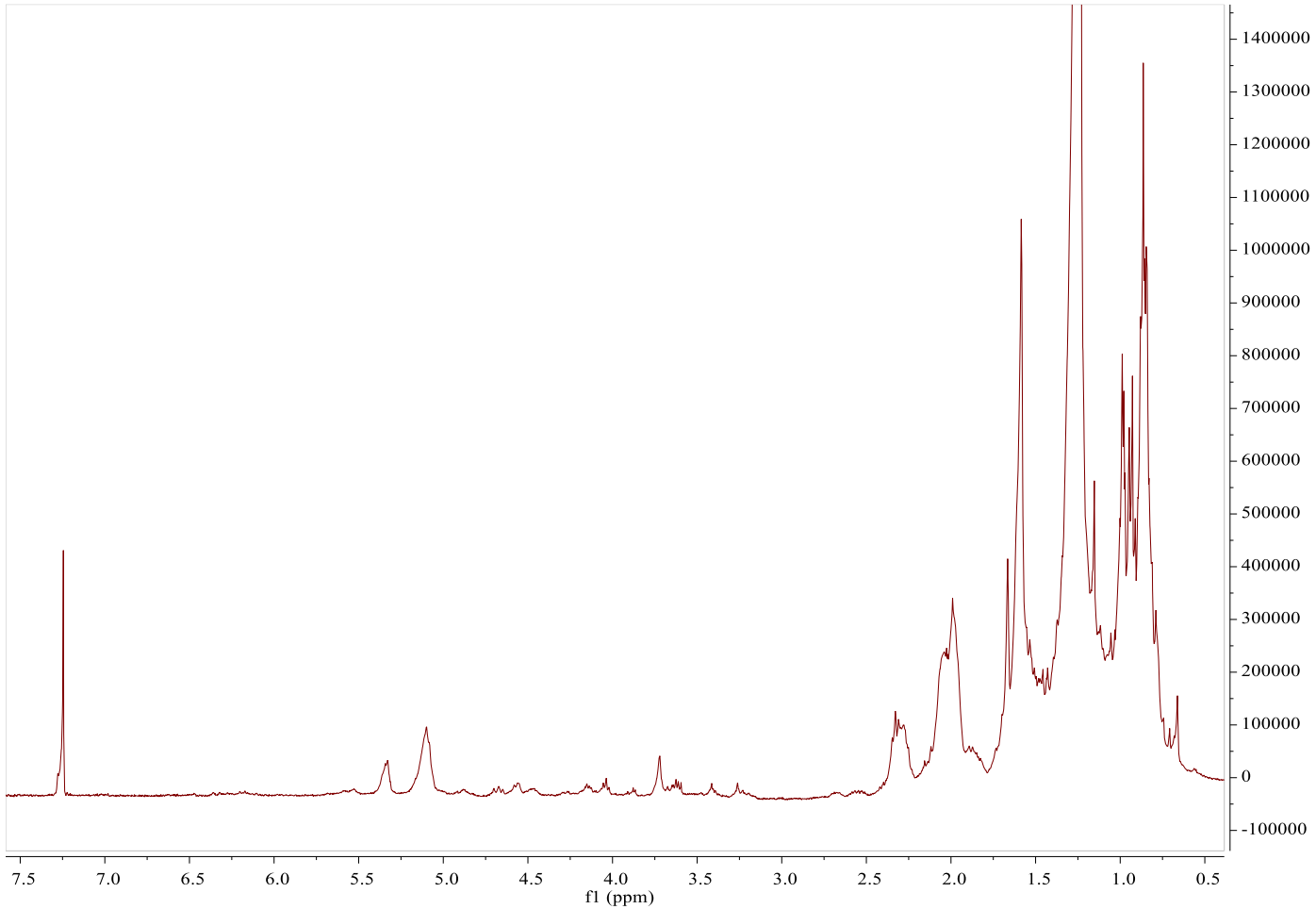

Figure 2.8 ^{1}H NMR spectrum (400 MHz) of *A. malaccensis* ethyl acetate extract in $CDCl_3$.

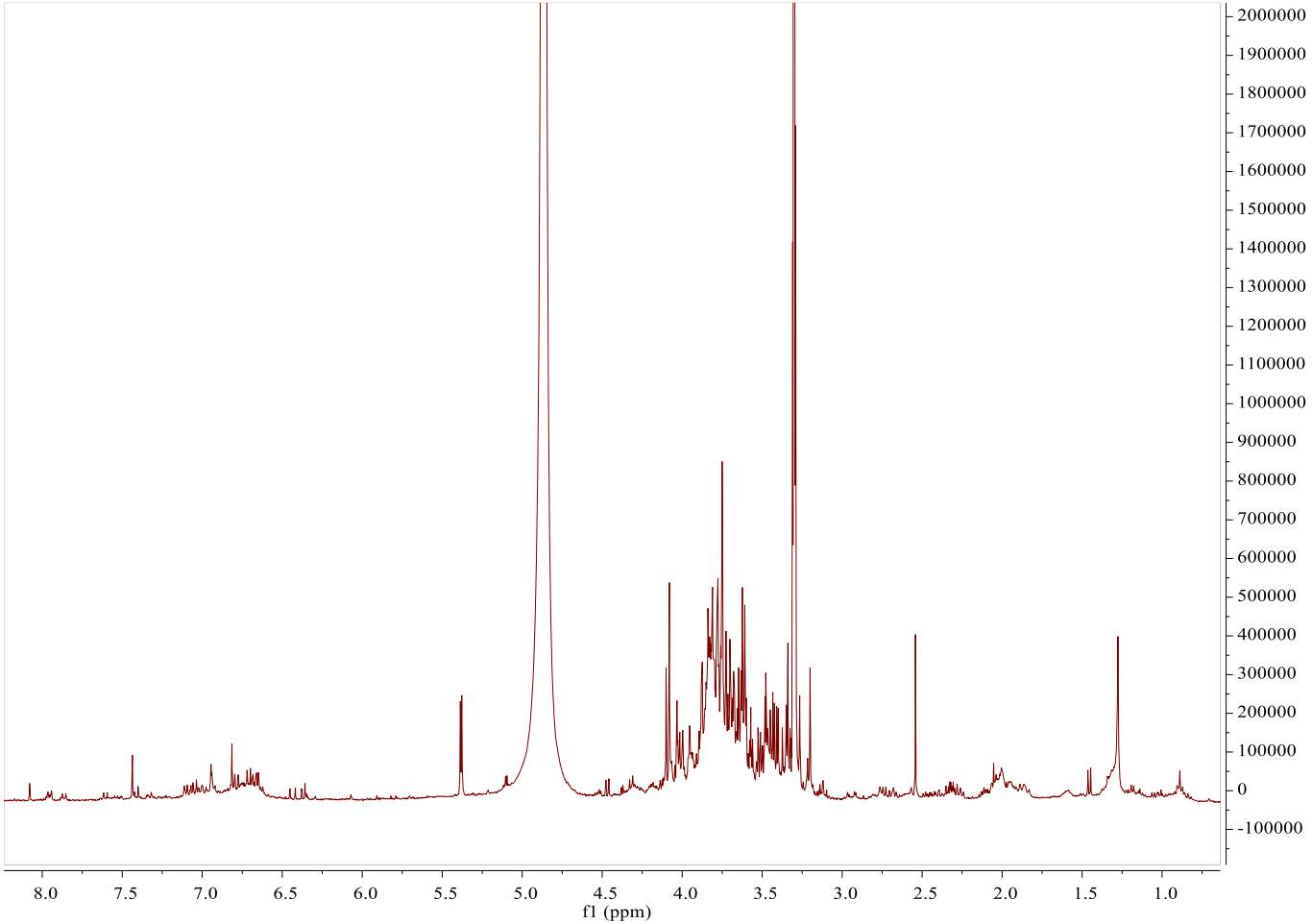

Figure 2.9 ^{1}H NMR spectrum (400 MHz) of *A. malaccensis* methanol extract in $CDCl_3$.

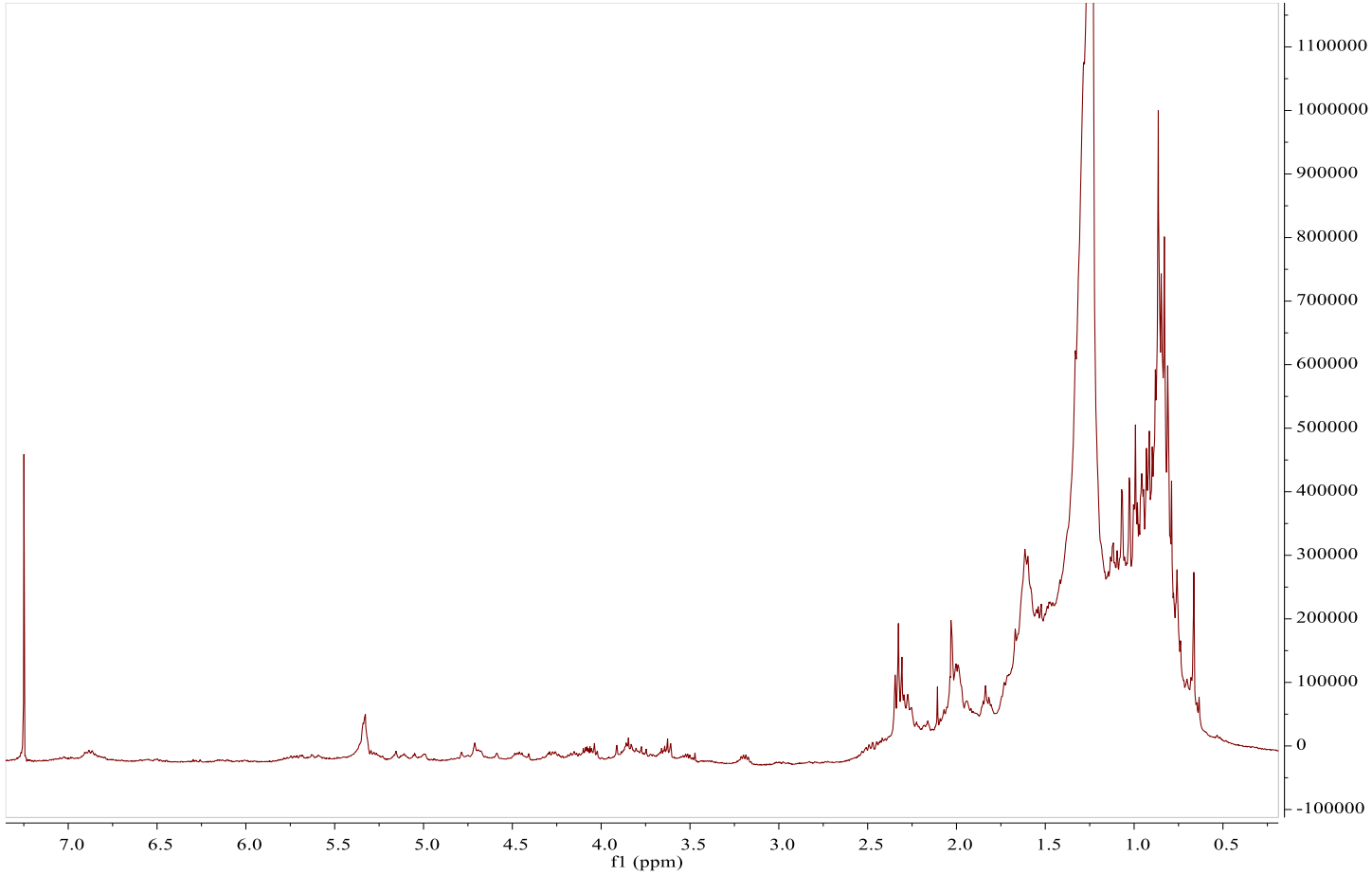

Figure 2.10 ^{1}H NMR spectrum (400 MHz) of *H. dryobalanoides* hexane extracts in $CDCl_3$.

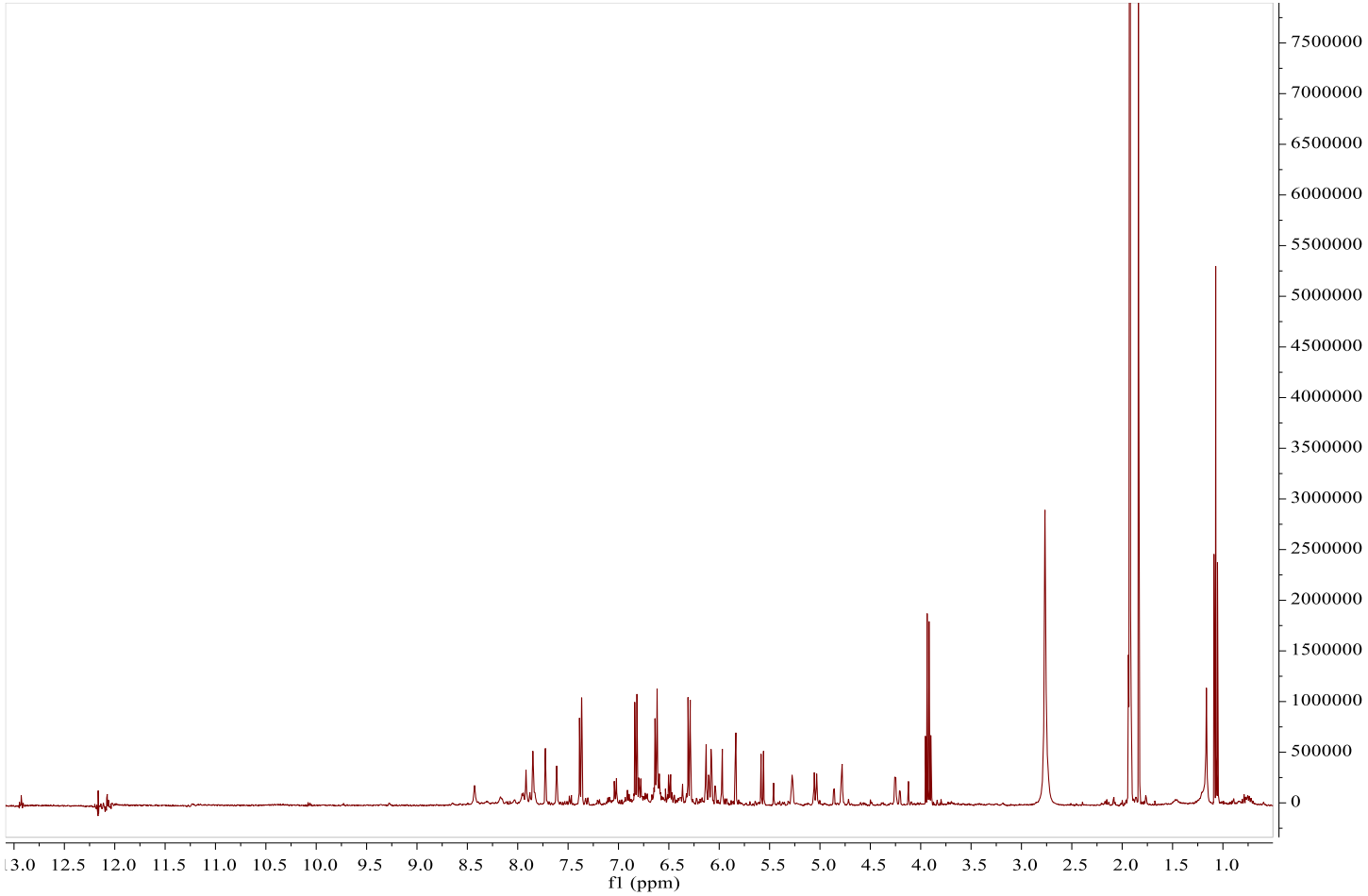

Figure 2.11 ^{1}H NMR spectrum (400 MHz) of *H. dryobalanoides* ethyl acetate extract in acetone-d6.

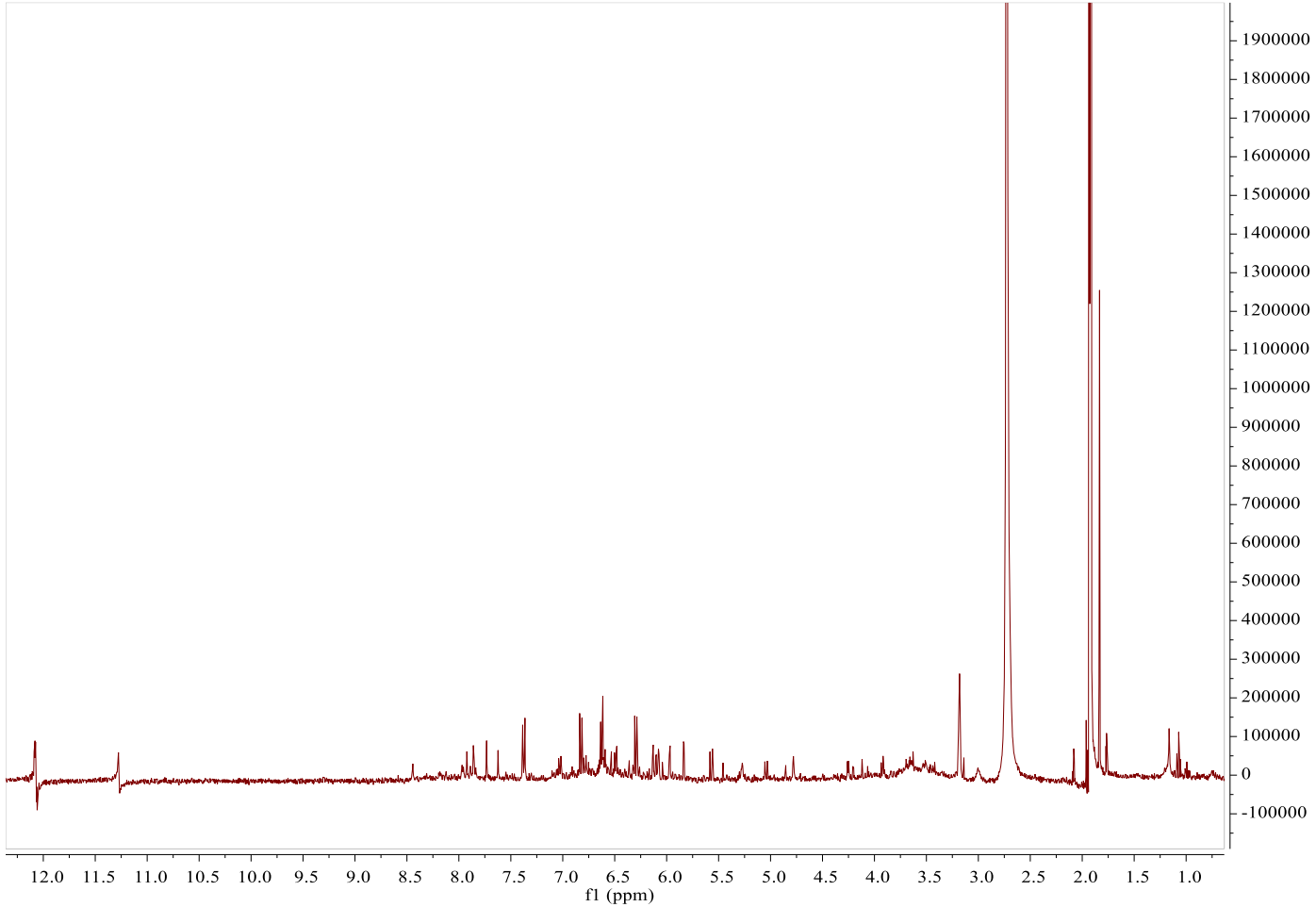

Figure 2.12 ^{1}H NMR spectrum (400 MHz) of *H. dryobalanoides* methanol extracts in acetone-d6.

2.4.3. Isolation and characterisation of compounds

2.4.3.1. Characterisation of fraction AH 17-18 as 7-methoxy acacetin (7-aca)

All the extracts of *A. malaccensis* were subjected to ^{1}H NMR experiments. The proton NMR of the hexane extract showed the presence of aromatic rings between the region δ_H6.40 to 7.89 ppm. Separation was carried out using a silica gel column eluting gradient wise with hexane and ethyl acetate. Fraction ABH 17-18 eluted with 9:1 (hexane: ethyl acetate) yielded a light-yellow powder which gave a yellowish spot on TLC after spraying with anisaldehyde sulphuric acid reagent. The LCMS-HRESI (positive mode) gave a $[M+H]^+$ ion at m/z 299.0912 (calc for $C_{17}H_{15}O_5$) suggesting a molecular formula of $C_{17}H_{14}O_5$ (Figure 2.13).

The proton spectrum (Figure 2.14) in $CDCl_3$ showed the presence of a highly deshielded H-bonded proton at 12.81 ppm indicating the 5-OH of a flavone moiety. It also showed two aromatic proton signals at 7.84 (2H, d, J = 8.9 Hz, H-2'/6') and 7.02 (2H, d, J = 8.9 Hz, H-3'/5') confirming the presence of a parasubstituted ring B of a flavonoid moiety. The spectrum also showed signals at 6.58 (1H, s H-3), 6.37 (1H, d, J = 2.2 Hz, H-6), 6.48 (1H, d, J = 2.2 Hz, H-8) and two methoxy groups at 3.88 (3H, s) and 3.89 (3H, s) ppm. The carbon spectrum (Figure 2.15) showed the presence of 17 carbon atoms made up of one carbonyl at δ_C 182.5 ppm, seven quaternary carbons (including five phenolic carbons at 157.7, 162.6, 162.5, 164.1, 164.8), seven aromatic CH carbons (92.7, 98.1, 104.4, 128.1, 114.5, 128.1, 114.5) and two methoxy carbons. The structure was elucidated by examining its 2D (^{1}H-^{1}H COSY, ^{1}H-^{13}C, HSQC and HMBC) NMR spetra and confirmed by comparison with literature reports (Krishna *et al.*, 2015). The chemical shifts for the protons and carbon atoms in the compound are given in Table 2.3.

Table 2.3 ^{1}H and ^{13}C NMR chemical shift assignments for 7-aca.

	7-methoxy acacetin (chloroform-d)		7-methoxy acacetin (chloroform-d) (Krishna *et al.*, 2015)	
	δ H ppm (*J*, Hz)	δ C ppm	δ H ppm (*J*, Hz)	δ C ppm
1	-	-	-	
2	-	164.1	-	165.4
3	6.58 *s*	104.4	6.58 *s*	104.2
4	-	182.5	-	182.3
5	-	157.7	-	157.7
6	6.37 *d* (2.2)	98.1	6.38 *d* (2)	98.0
7	-	164.8	-	164.0
8	6.48 *d* (2.2)	92.7	6.5 *d* (2)	92.6
9	-	162.6	-	162.6
10	-	105.6	-	105.6
1’	-	123.6	-	123.6
2’, 6’	7.84 *d* (8.9)	128.1	7.86 *d* (9)	128.1
3’, 5’	7.02 *d* (8.9)	114.5	7.04 *d* (9)	114.5
4’	-	162.5	-	162.5
7-OCH_3	3.89 *s*	55.8	3.90 *s*	55.8
4-OCH_3	3.88 *s*	55.5	3.89 *s*	55.5
5-OH	12.81 s	-	12.82	

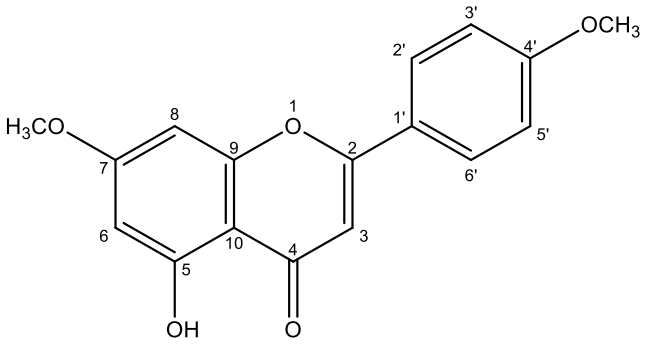

Figure 2.13 Structure of 7-aca

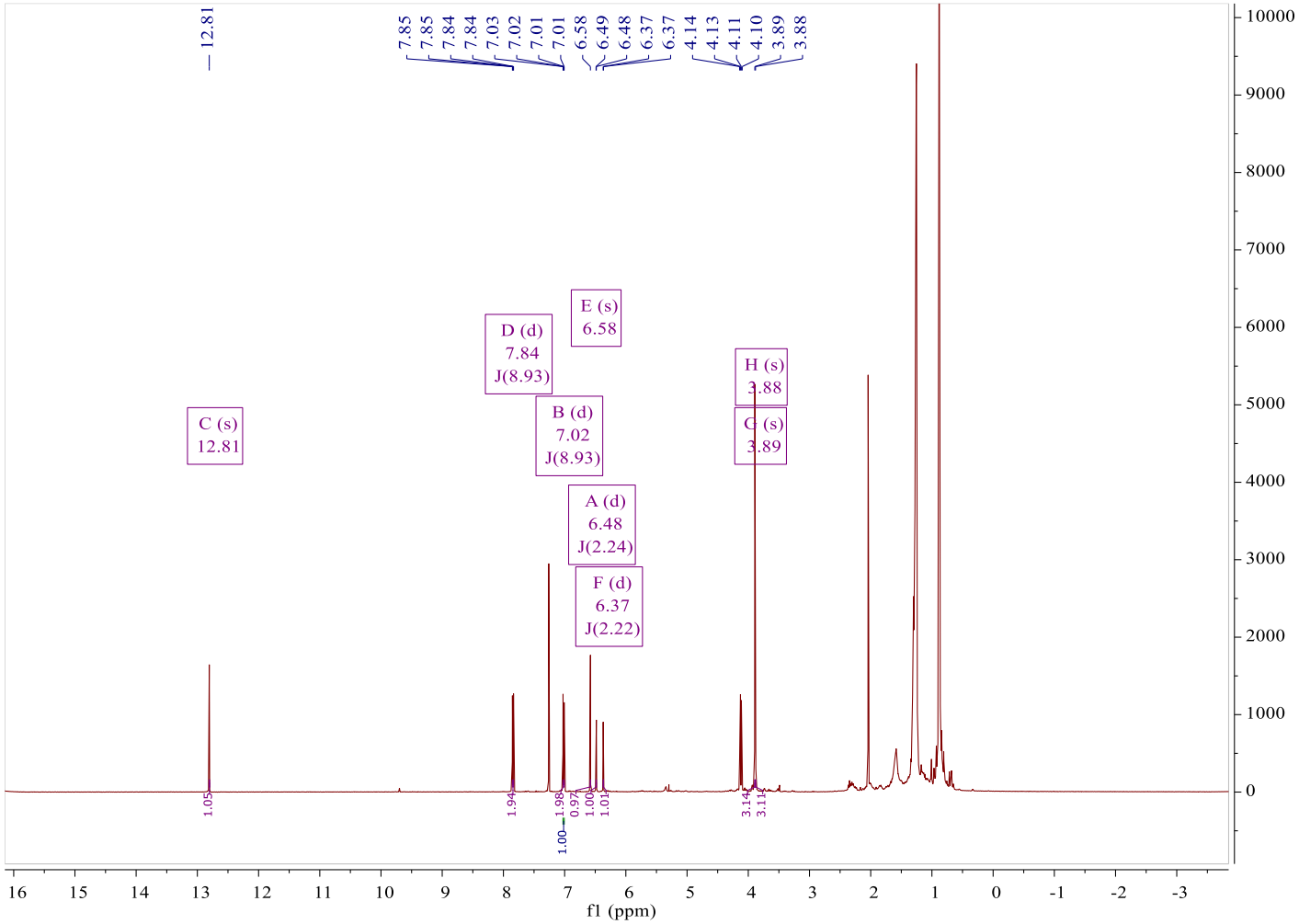

Figure 2.14 ^{1}H NMR spectrum (400 MHz) of 7-aca in $CDCl_3$.

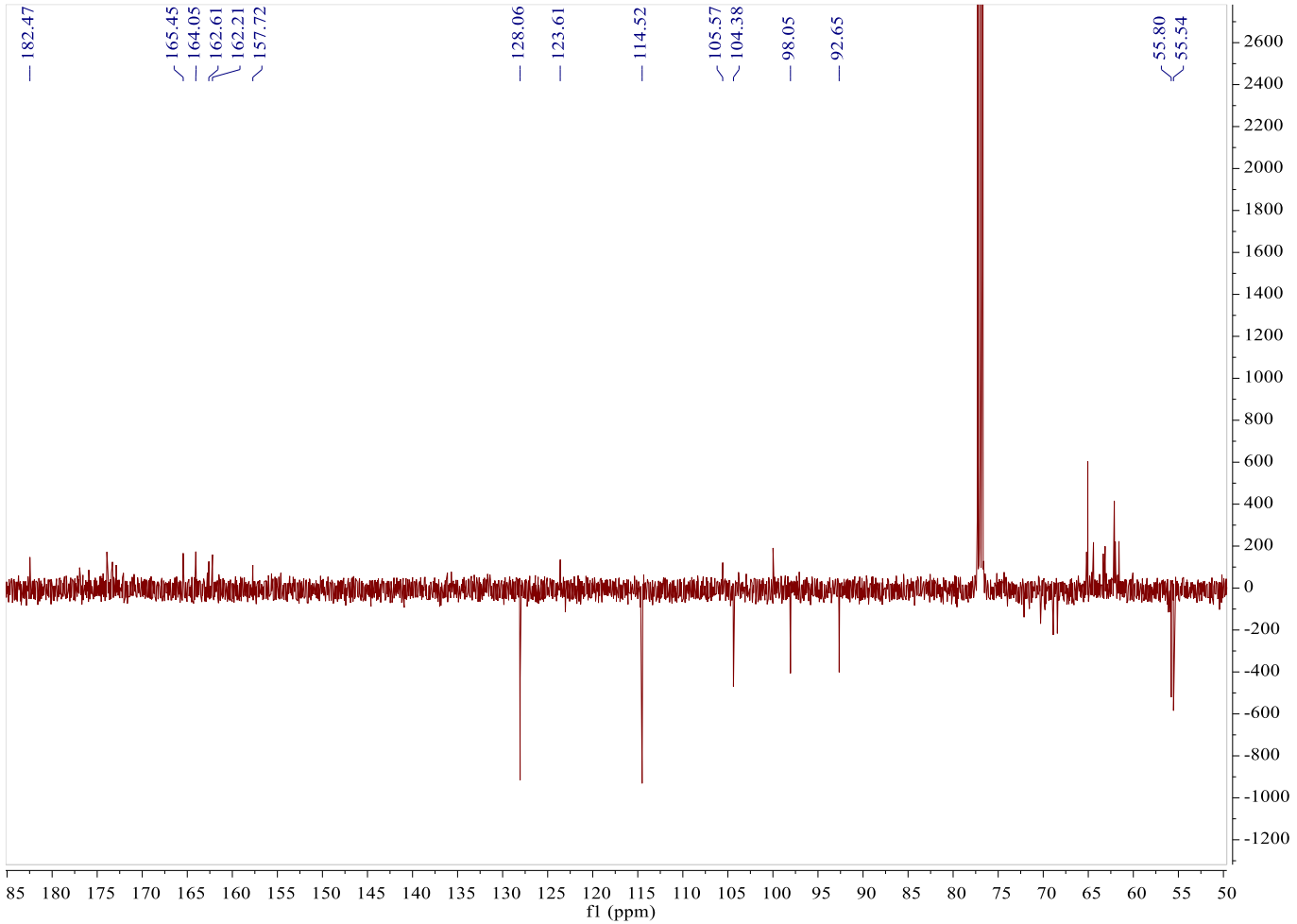

Figure 2.15 ^{13}C NMR NMR spectrum (400 MHz) of 7-aca in $CDCl_3$

2.4.3.2. Characterisation of AM-3-9-10 as a mixture of quercitrin and afzelin (Q/A).

The fraction AM-3 9-10 was obtained as a dark brown powder. The LCMS-HRESI (negative mode) gave two molecular ions at m/z 447.0937 $[M-H]^-$ (calc for $C_{21}H_{19}O_{11}$) suggesting a molecular formula of $C_{21}H_{20}O_{11}$ and at m/z 433.1133 $[M+H]^+$ (calc for $C_{21}H_{21}O_{10}$) suggesting a molecular formula of $C_{21}H_{20}O_{10}$ (Figure 2.16). Thus, the fraction could be a mixture of similar compounds or analogues. This was confirmed from the proton spectrum (Figure 2.17) of the fraction which showed two H-bonded hydroxyl protons at δ_H 12.74 and 12.73 corresponding to their 5-OH protons. The compounds must be flavones as indicated by two meta-coupled protons at 6.28 (*J* = 2.4 Hz, H-6) and 6.48 (*J* = 2.5 Hz, H-8) ppm arising from the H-6 and H-8 of the flavone ring A. The protons of ring B for the compounds were observed as a mixture of two AA′BB′ coupled doublets at 7.87 (2H, d, *J* = 8.6 Hz, H-2'/6') and 7.04 (2H, d, *J* = 8.7 Hz, H-3'/5') and a set of ABX protons at 7.01 (1H, d, *J* = 8.3 Hz, H-5'), 7.41 (1H, dd, *J* = 8.4, 2.1 Hz, H-6') and 7.52 (1H, d, *J* = 2.1 Hz, H-2'). The absence of a proton singlet for H-3 implies the compounds were both substituted at C-3 and this could be the position of attachment of the sugar moiety observed in the spectrum. The presence of a sugar moiety in the compounds was confirmed by two anomeric proton signals at 5.53 and 5.56 ppm and the sugar moieties must be of a rhamnose type indicated by the presence of two methyl doublets at 0.92 and 0.93 ppm.

The carbon spectrum (Figure 2.18) showed the number of carbon signals expected for each of the compounds, although some signals were overlapped. Comparison of their chemical shifts to literature reports (Lee *et al.*, 2014a) confirmed the compounds and they were isolated as a 2:1 ratio of quecitrin to afzelin mixture. Due to the limited

amount of Q/A that was isolated, separation of the two compounds were not carried out.

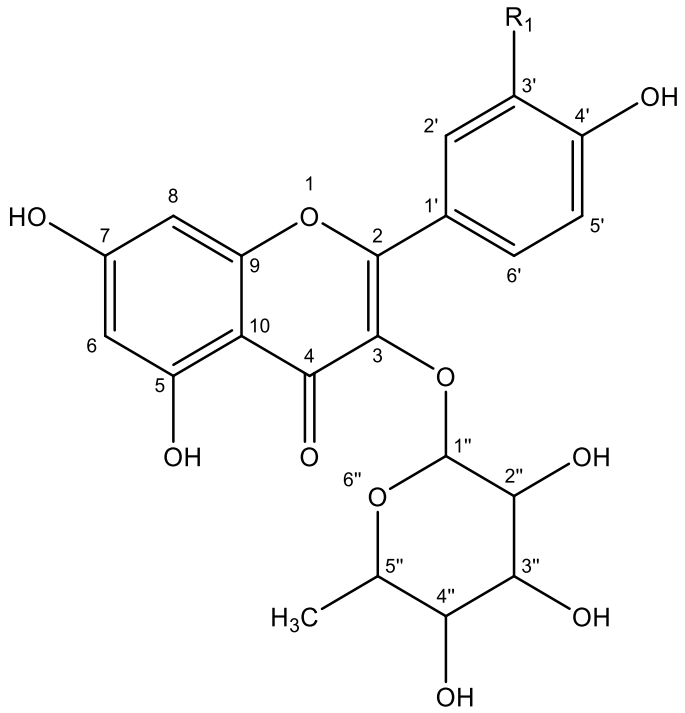

Quercitrin R_1 =OH
Afzelin R_1= H

Figure 2.16 Structure of quercitrin and afzelin (Q/A)

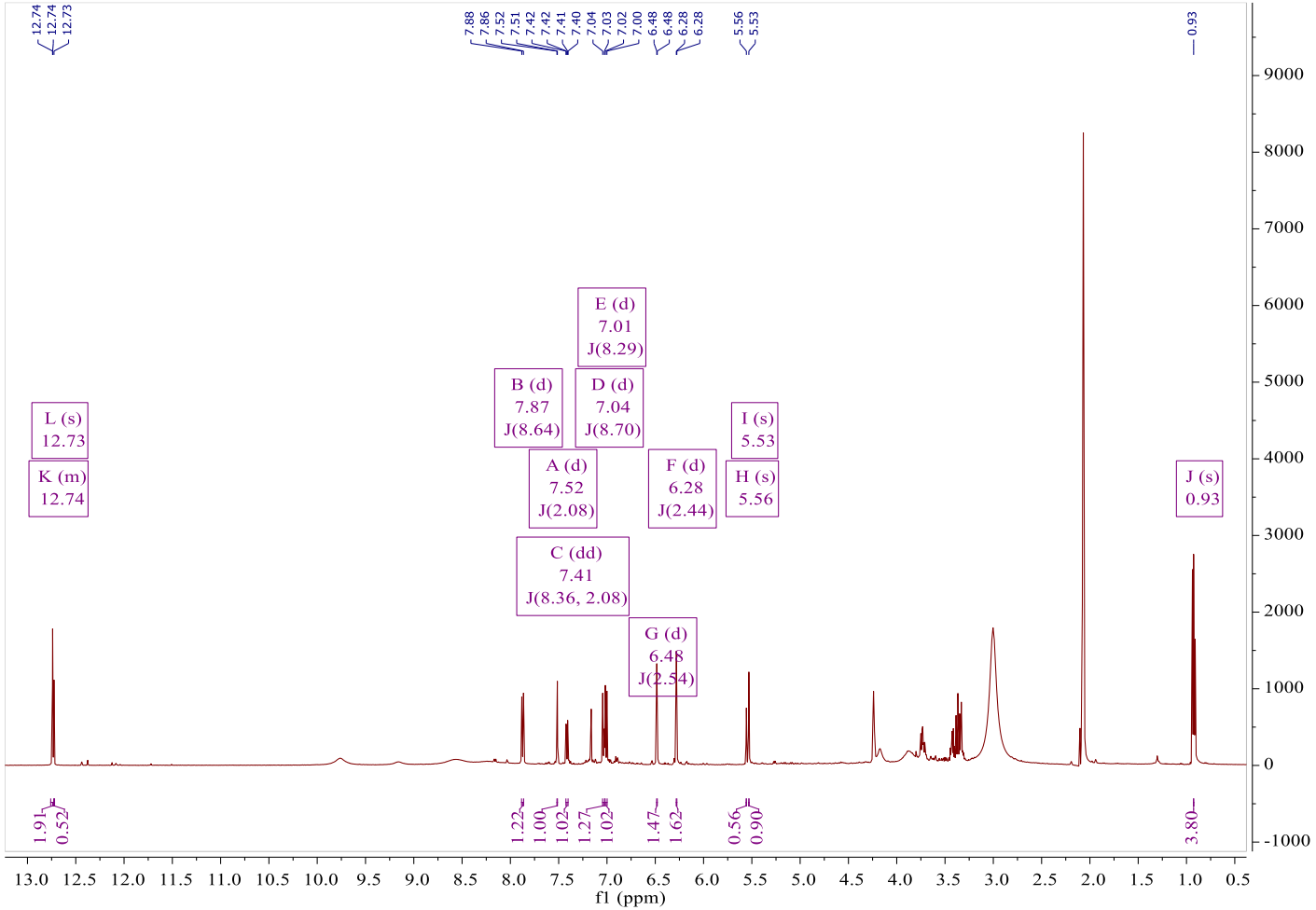

Figure 2.17 ^{1}H NMR spectrum (400 MHz) of the mixture of Q/A in acetone-d6.

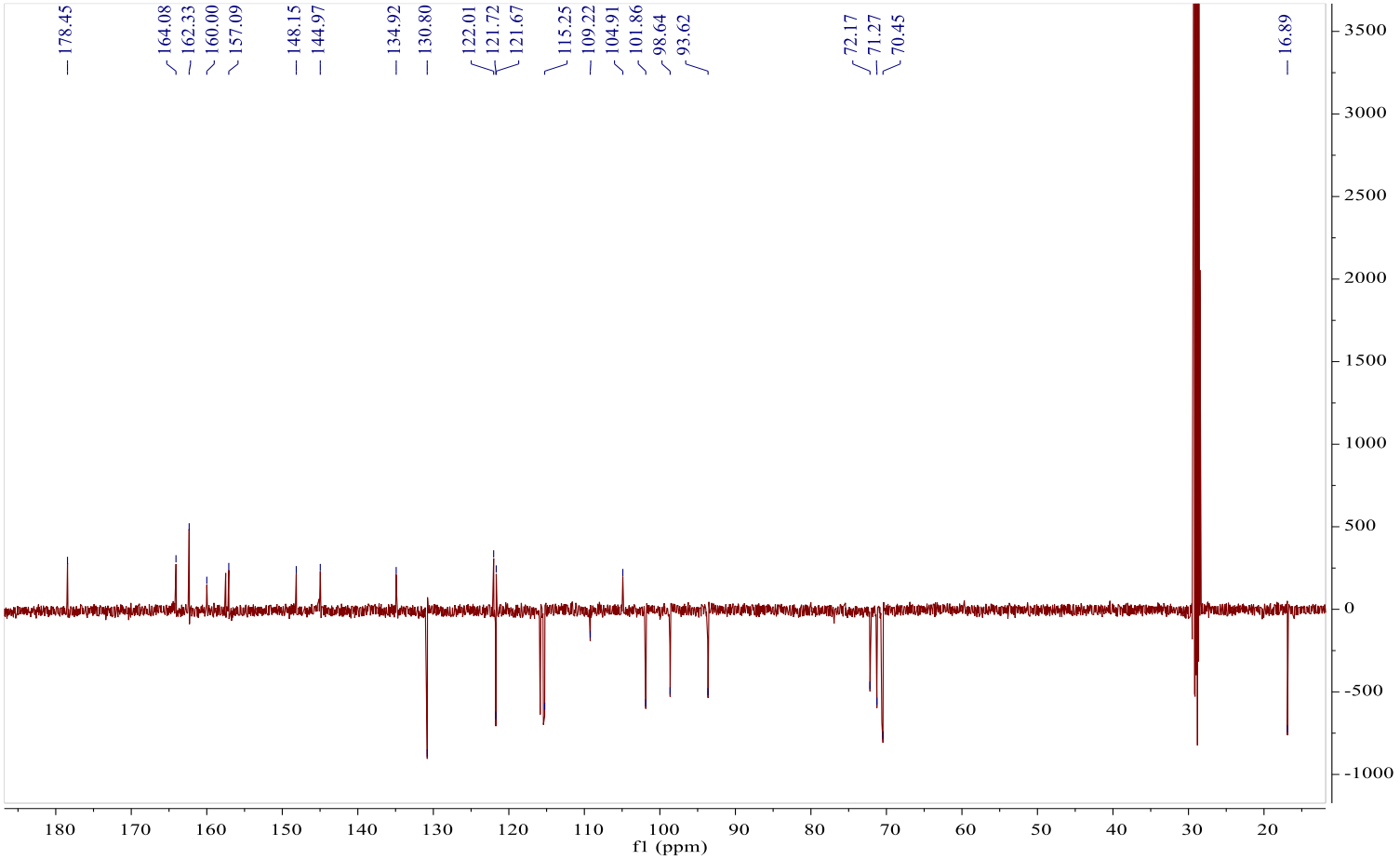

Figure 2.18 ^{13}C NMR spectrum (400 MHz) the mixture of Q/A in acetone-d6

2.4.3.3. Characterisation of HE 63-73 as balanocarpol (bala)

Fraction HE 63-73 was obtained as a pale-yellow powder. The LCMS-HRESI (positive mode) gave a $[M+H]^+$ ion at m/z 471.1441 (calc for $C_{28}H_{23}O_7$) suggesting a molecular formula of $C_{28}H_{22}O_7$ (Figure 2.19)

The ^1H NMR spectrum (Figure 2.20) in acetone-*d6* showed eight sets of aromatic signals made up of four ortho-coupled doublets at δ_H 6.77 (2H, d, *J* = 8.5 Hz, H-2/6) and 6.44 (2H, d, *J* = 8.6 Hz, H-3/5) ppm and at 7.52 (2H, d, *J* = 8.5 Hz, H-2'/6') and 6.97 (2H, d, *J* = 8.5 Hz, H-3'/5') ppm. The spectrum also showed four meta-coupled doublets at 5.98 (1H, d, J = 2.1 Hz, H-12) and 6.12 (1H, d, *J* = 2.0 Hz, H-14) ppm and at 6.28 (1H, d, *J* = 2.4, H-12') and 6.23(1H, d, *J* = 2.3, H-14') ppm. Signals for four aliphatic protons were observed at 5.72 (1H, d, *J* = 9.5 Hz, H-7') and 5.18 (d, *J* = 9.5 Hz, H-8'), each integrated for 1H and were characteristic for trans-coupled protons. There were signals for two cis-coupled protons at 4.92 (1H, br s, H-7) and 5.42 (1H, d, H-8) ppm.

The carbon spectrum (Figure 2.21) gave 28 signals made up of 24 aromatic and four aliphatic carbons. The aromatic carbons were made up of six phenolic, 12 CH and six quaternary carbons. While the aliphatic carbons were made up of two oxygen bearing and two non-oxygen bearing carbons. This structure was elucidated from its 2D (COSY, HMBC and HSQC) spectra and confirmed using literature reports (Atun *et al.*, 2006). The chemical shifts for the protons and carbon atoms in the compound are given in Table 2.4.

Table 2.4 ^{1}H and ^{13}C NMR chemical shift assignments for bala.

No.	Bala (acetone-d_6)		Bala (acetone-*d*6) (Atun *et al.*, 2006)	
	δ H ppm (*J*, Hz)	δ C ppm	δ H ppm (*J*, Hz)	δ C ppm
1	-	132.6	-	133.5
2,6	6.77 *d* (8.5)	130.7	6.75 *d* (8.3)	131.5
3,5	6.44 *d* (8.6)	113.3	6.42 *d* (8.3)	114.2
4	-	154.9	-	155.8
7	4.92 *br s*	49.4	4.90 *br s*	50.3
8	5.42 *d*	72.3	5.40 *br s*	73.2
9	-	139.9	-	140.8
10	-	112.9	-	113.8
11	-	158.8	-	159.7
12	5.98 *d* (2.1)	94.4	6.20 *br s*	95.1
13	-	158.3	-	159.2
14	6.12 *d* (1.8)	103.6	6.26 *d* (2.0)	104.4
1’	-	132.8	-	133.7
2’,6’	7.52 *d* (8.5)	129.6	7.50 *d* (8.3)	130.5
3’,5’	6.97 *d* (8.5)	115.6	6.95 *d* (8.3)	116.4
4’	-	157.7	-	158.6
7’	5.72 *d* (9.5)	92.6	5.69 *d* (9.3)	93.5
8’	5.18 *d* (9.5)	51.5	5.16 *br d* (9.3)	52.3
OH				
9’	-	142.0	-	142.8
10’	-	119.6	-	120.4
11’	-	156.5	-	157.4
12’	6.28 *d* (2.4)	101.1	6.09 *br s*	102.0
13’	-	156.0	-	156.9
14’	6.23 *d* (2.3)	105.9	5.96 *d* (2.3)	106.8

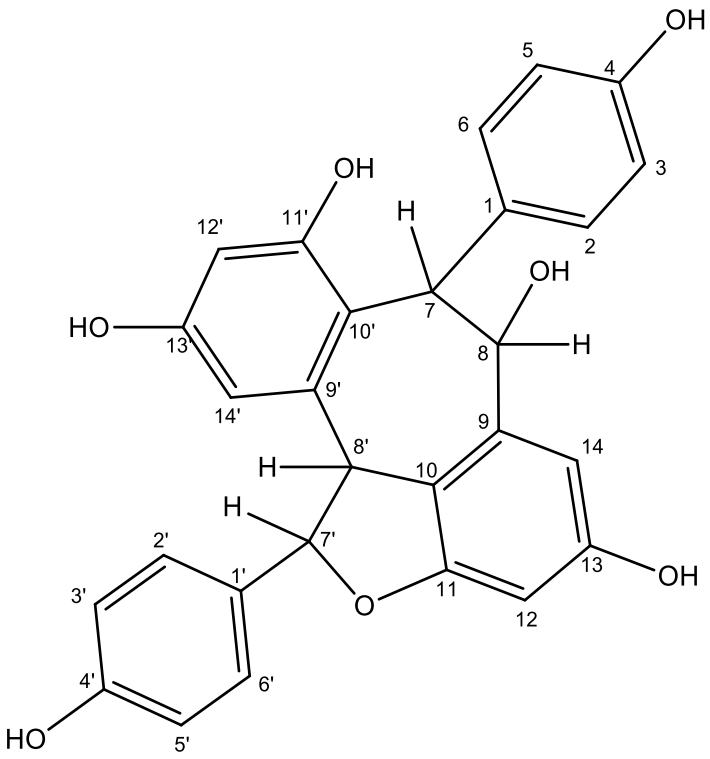

Figure 2.19 Structure of bala.

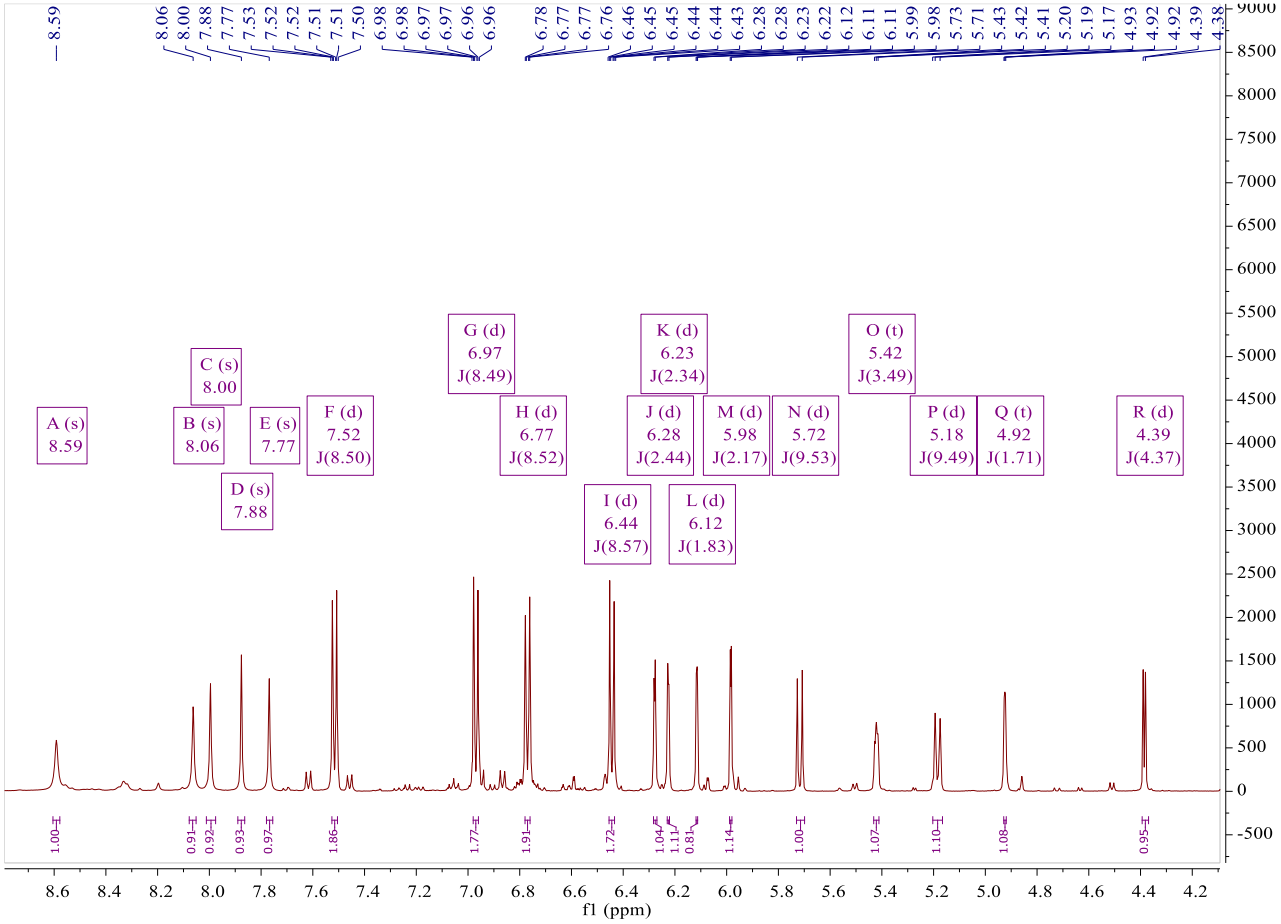

Figure 2.20 ^{1}H NMR spectrum (400 MHz) of bala in acetone-d6.

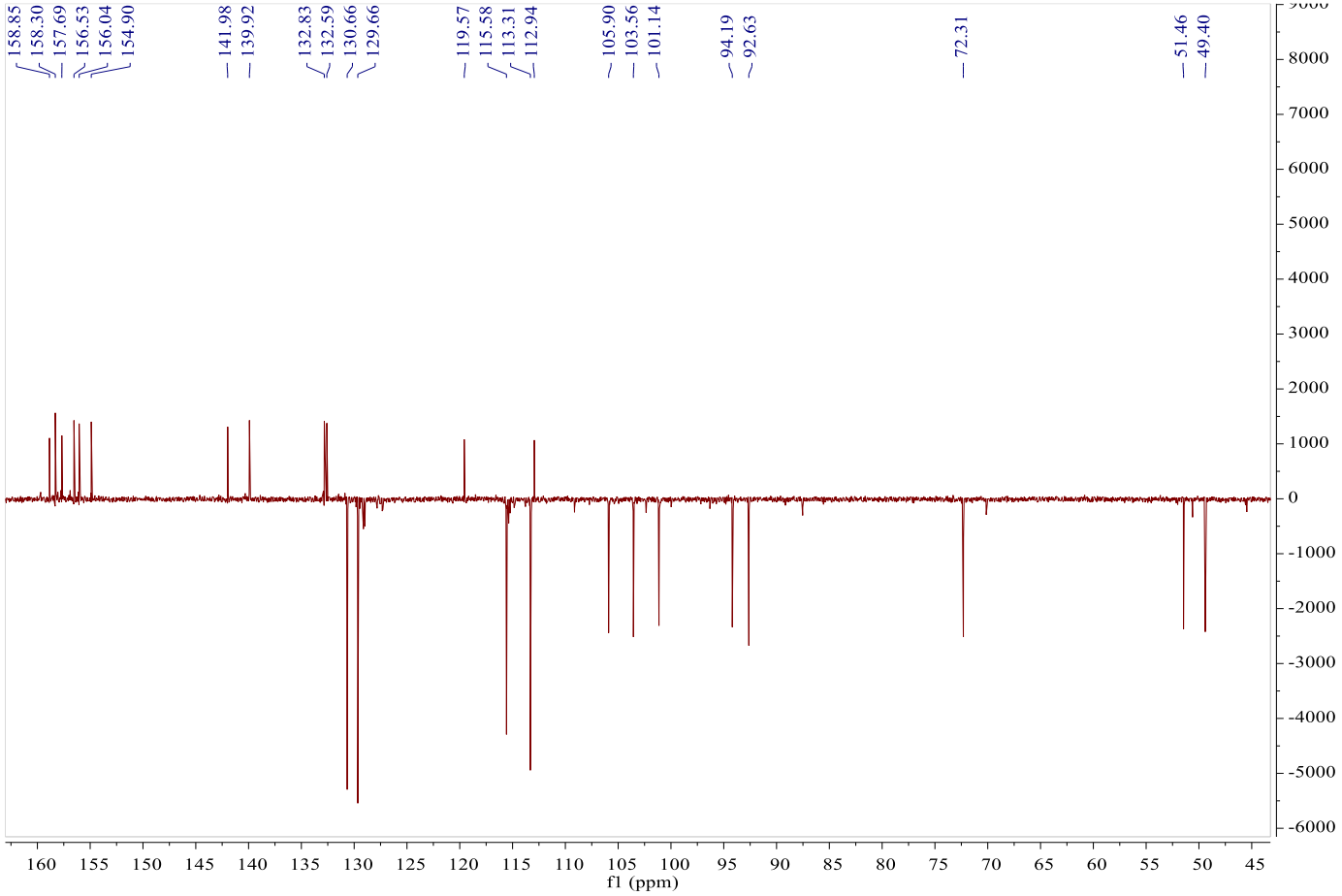

Figure 2.21 ^{13}C NMR NMR spectrum (400 MHz) bala in acetone-d6

2.4.3.4. Characterisation of HE 74-100 as heimiol A

Fraction HE 74-100 was also obtained as a pale-yellow powder. The LCMS-HRESI (negative mode) gave a $[M-H]^-$ ion at m/z 469.1298 (calc for $C_{28}H_{21}O_7$) suggesting a molecular formula of $C_{28}H_{22}O_7$ (Figure 2.22).

The ^1H NMR spectrum (Figure 2.23) in acetone-*d*6 was similar to that of bala and it also showed eight sets of aromatic doublets made up of four ortho-coupled protons at δ_H 6.62 (2H, d, *J* = 8.5 Hz, H-3/5) and 6.91 (2H, d, *J* = 8.5 Hz, H-2/6) ppm and at 6.73 (2H, d, *J* = 8.4 Hz, H-3'/5') and 7.16 (2H, d, *J* = 8.6 Hz, H-2'/6') ppm. The spectrum also showed four meta-coupled doublets at 6.42 (1H, d, *J* = 2.4 Hz, H-10) and 6.17 (1H, d, *J* = 2.4 Hz, H-12) ppm and at 6.49 (1H, d, *J* = 2.2, H-10') and 6.23 (1H, d, *J* = 2.0, H-12') ppm. Signals of four aliphatic protons were observed at 4.25 (1H, d, *J* = H-8), 4.33 (1H, d, *J* =,3.3 H-7'), 4.98 (1H, d, *J* = 3.3, H-8') and 5.59 (1H, s, H-7).

The carbon spectrum (Figure 2.24) also showed 28 signals made up of 24 aromatic and four aliphatic carbons. The aromatic carbons were made up of six phenolic, 12 CH and six quaternary aromatic carbons. While the aliphatic carbon was made up of two oxygen bearing and two non-oxygen bearing carbons.

Proton H-7 in heimiol A was observed to be more deshielded than in bala hence it must be attached to an oxygen bearing carbon. This is confirmed by the chemical shift observed for C-7 in heimiol A at 81.5 ppm compared to bala observed at 49.2 ppm. A similar observation was made for C-8' in heimiol A (δ_C 81.4) and in bala at 51.8 ppm, hence there must be an oxygen link between C-7 and C-8' in heimiol A. The absence of a hydroxyl group at C-8 in heimiol A compared to bala is confirmed by the chemical shift for C-8 in heimiol A observed at 46.9 ppm while in bala C-8 was observed at 72.3

ppm. This implies a different aliphatic ring pattern in beimiol A and the structure was deduced based on correlations observed in its 2D (COSY, HMBC and HSQC) spectra and confirmed using literature reports (Atun *et al.*, 2006). The chemical shifts for the protons and carbon atoms in the compound are given in Table 2.5.

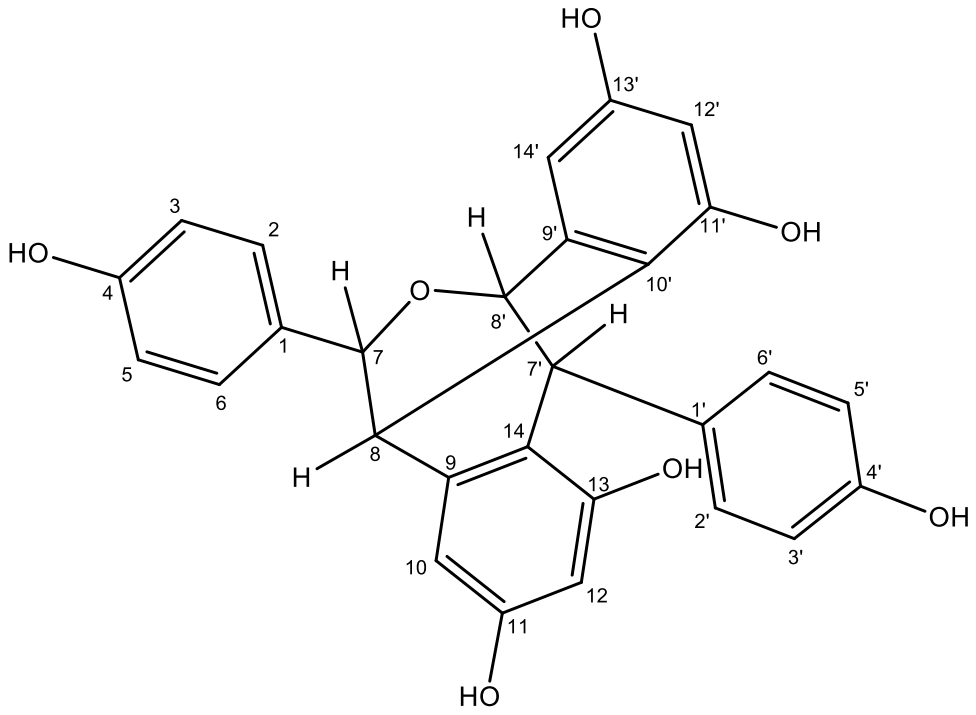

Figure 2.22 Structure of heimiol A

Table 2.5 ^{1}H and ^{13}C NMR chemical shift assignments for heimiol A

No.	Heimiol A (Experimental; acetone-d_6)		Heimiol A (Atun *et al.*, 2006); acetone-*d*6	
	δ H ppm (*J*, Hz)	δ C ppm	δ H ppm (*J*, Hz)	δ C ppm
1	-	136.8	-	136.8
2,6	6.91 (d, 8.5)	127.9	6.90 (d, 8.5)	127.9
3,5	6.62 (d, 8.5)	115.3	6.69 (d, 8.5)	116.4
4	-	157.1	-	157.2
7	5.59 (s)	81.5	5.57 (br s)	81.5
8	4.25 (s)	46.9	4.27 (br s)	46.9
9	-	147.4	-	147.4
10	6.42 (d, 2.4)	107.3	6.41 (d, 2.6)	107.4
11	-	157.4	-	157.4
12	6.17 (d, 2.4)	102.1	6.16 (d, 2.6)	102.0
13	-	154.7	-	154.6
14	-	116.5	-	116.0
1’	-	136.9	-	136.9
2’,6’	7.16 (d, 8.5)	130.0	7.14 (d, 8.4)	130.0
3’,5’	6.73 (d, 8.6)	115.4	6.72 (d, 8.4)	115.5
4’	-	157.2	-	157.2
7’	4.33 (d, 3.3)	50.9	4.32 (d, 3.3)	50.9
8’	4.98 (d, 3.3)	81.4	4.97 (d,3.3)	81.4
9’	-	142.6	-	142.6
10’	6.49 (d, 2.2)	104.7	6.48 (d, 2.2)	104.8
11’	-	158.1	-	158.1
12’	6.23 (d, 2.2)	102.3	6.21 (d, 2.2)	102.1
13’	-	156.2	-	156.2
14’	-	117.0	-	117.0

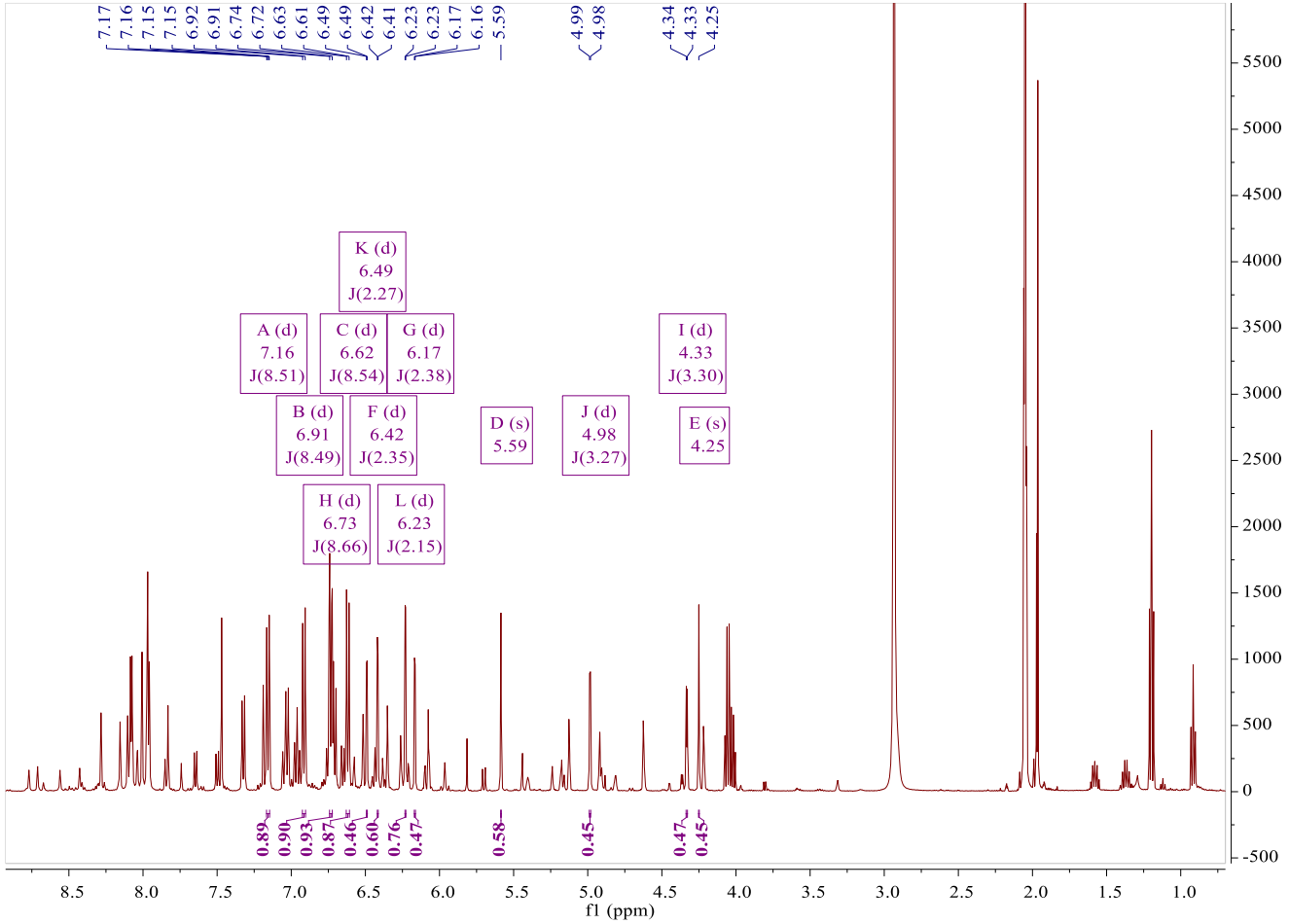

Figure 2.23 ^{1}H NMR spectrum (400 MHz) of heimiol A in acetone-d6.

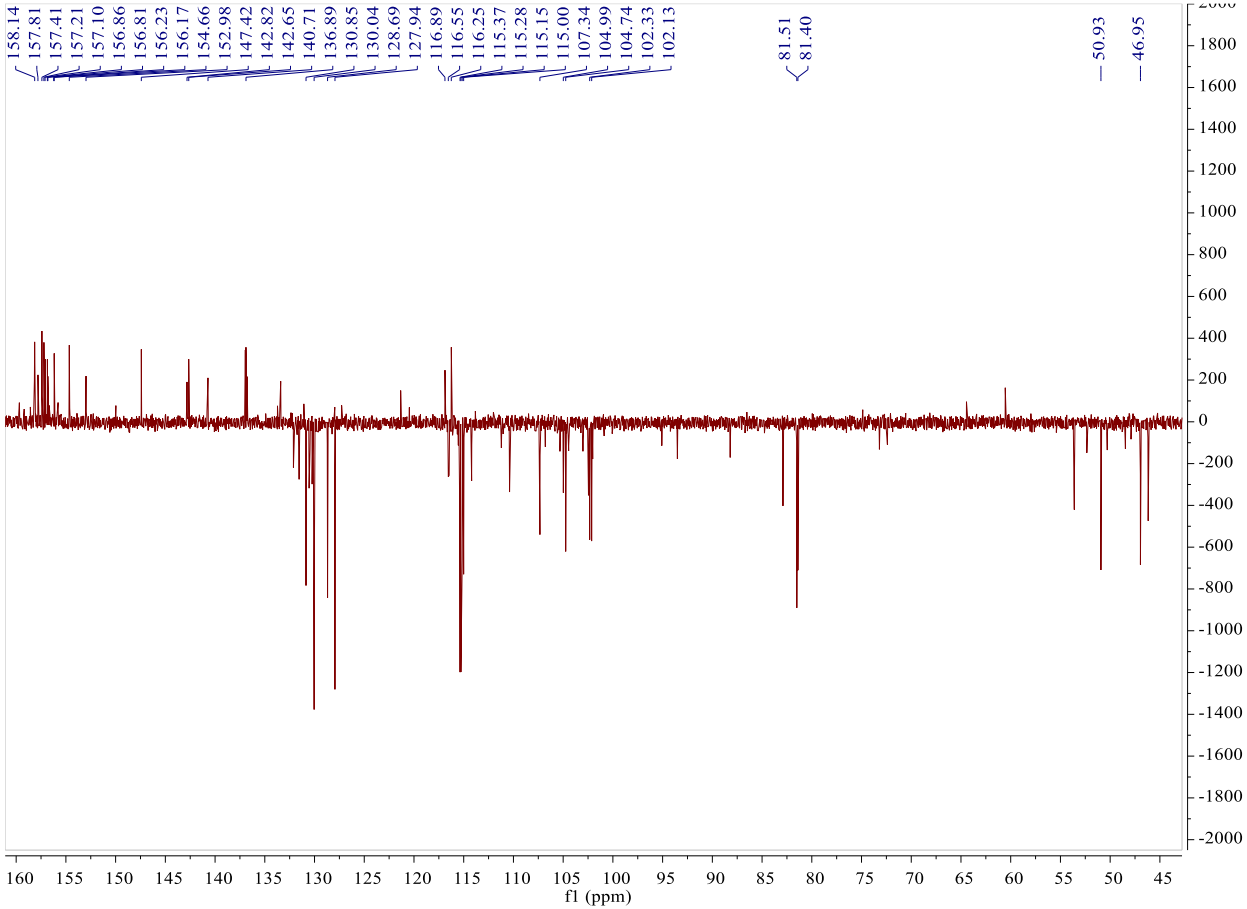

Figure 2.24 ^{13}C NMR spectrum (400 MHz) of heimiol A in acetone-d6

2.4.4. Summary of phytochemical screening carried out on *A. malaccensis* and *H. dryobalanoides*

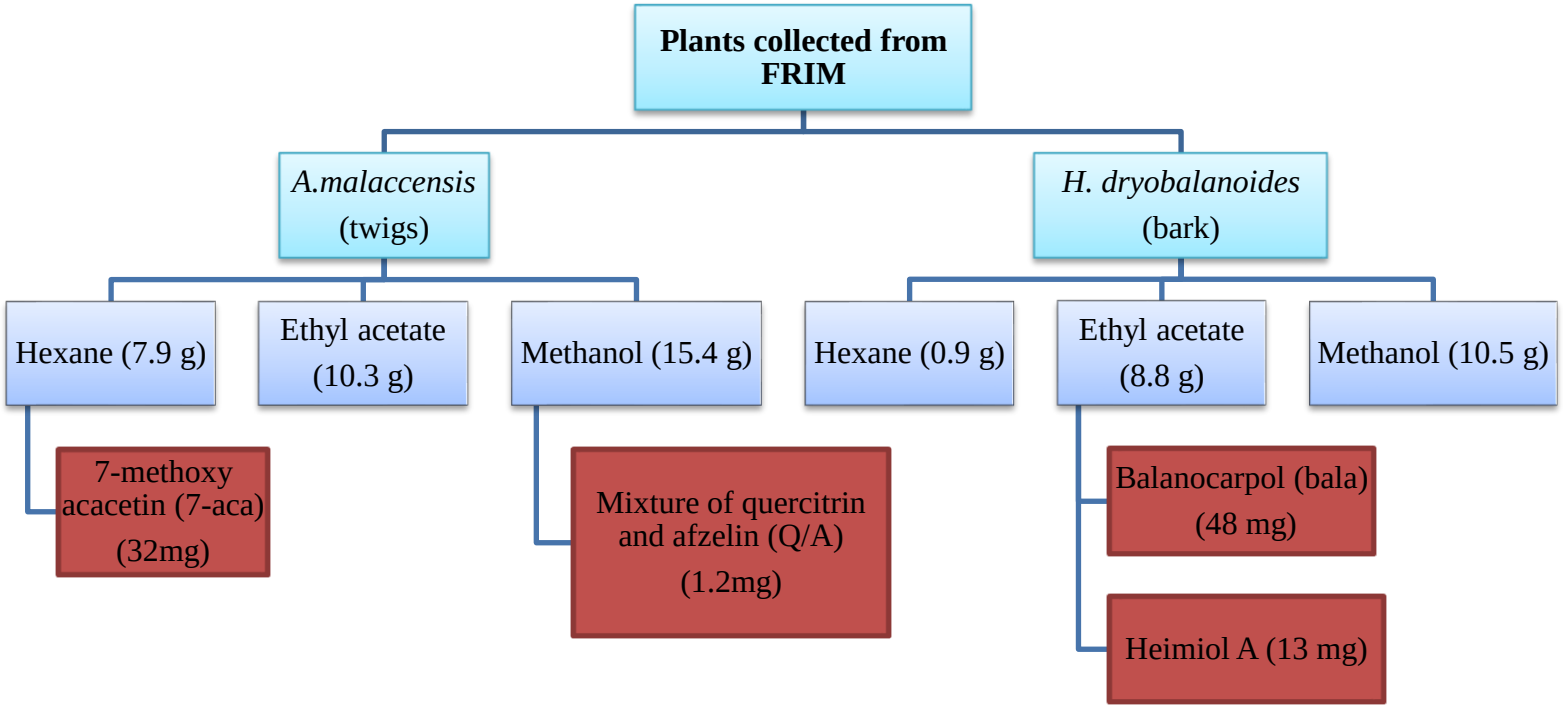

2.5. Discussion and conclusion

A. malaccensis and *H. dryobalanoides* are both well-known in Malaysia for producing resins used for several purposes such as giving flavour to curry or in making varnishes and cements. *Aquilaria* sp. leaves are taken orally for their medicinal use and *Hopea sp*. are only known to be used topically as medicine. In this study, *A. malaccensis* twigs and *H. dryobalanoides* bark were ground into powdered form before subjecting them to solvent extraction with hexane, ethyl acetate and then methanol using a Soxhlet apparatus. The Soxhlet extraction process was run continuously using three solvents with increasing polarity in order to extract the highest amount of bioactive compound(s) from the plant materials. Compared to other extraction methods, Soxhlet extraction method uses the least amount of solvent and requires less time therefore it was most preferred. However, this method requires continuous extraction with high temperatures which may cause degradation of volatile and heat-sensitive compounds (Zhang *et al.*, 2018). The extraction process for both plant materials start off with a non-polar solvent hexane, followed by ethyl acetate a slightly polar solvent then finishes with a more polar solvent methanol.

NMR spectra of the *A. malaccensis* hexane extract (AH) showed the presence of unsaturated fatty acids and fatty compounds which are expected to be extracted by hexane as compounds with fatty acid chains are hydrophobic. The NMR spectrum of the hexane extract also showed the presence of highly deshielded protons around 12.8 ppm which indicates that the extract contained flavonoid type compounds. The ethyl acetate extract of the plant showed the presence of more unsaturated fatty acids, whereas the methanol extract contained mixtures of sugars possibly some

disaccharides which are polar compounds and are usually extracted by polar solvents such as methanol.

Due to the bioactive effects of hexane and methanol extracts *A. malaccensis* that will be discussed in Chapter 3 they were subjected to CC for the isolation of their potential active compounds. CC of the AH extract yielded 7-methoxy acacetin (7-aca) also known as apigenin-4',7-dimethyl ether, 5-hydroxy-7, 4'-dimethoxyflavon, 4',7-dimethoxy-5-hydroxyflavone; 4',7-O-dimethylapigenin and 4',7-dimethoxyapigenin. This was the major component in AH extract (32 mg). The compound is a dimethoxyflavone that closely resembles a well-known natural flavone called acacetin (aca) with a methoxy substitution instead of hydroxy at C-7. Aca has gained a lot of attention due to its diverse pharmacological activities such as anti-inflammatory, neuroprotective, cardioprotective, anti-ageing and antimicrobial properties (Carballo-Villalobos *et al.*, 2014, Bu *et al.*, 2019, Wu *et al.*, 2018, Cha *et al.*, 2014). It is most well-known for its anticancer activity by promoting apoptosis in many cancer cells such as prostate cancer (Kim *et al.*, 2013), breast cancer (Ren *et al.*, 2018), lung cancer (Punia *et al.*, 2017) and liver cancer cells (Zeng *et al.*, 2017). Aca was first isolated from the leaves of *Robinia pseuducacia* Linn by A.G. Perkin (Robinson and Venkataraman, 1926). The compound can be found in plant pigments, vascular plants, and it is responsible for many of natural colours (Cody, 1988). Since then aca has been isolated from many other plants such as *Calea urticifolia*, *Ziziphora clinopodioides* and *A. sinensis* (Chaurasiya *et al.*, 2016, Yang *et al.*, 2014b, Feng and Yang, 2012). Aca has never been isolated from *A. malaccensis*, however, it has been recently identified through phytochemical screening, GC-MS, and LC/Q-TOF-MS in the plant (Eissa *et al.*, 2020). The first isolation of 7-aca is unknown, however, the earliest

publication found on the detection of the compound is in 1983 by Wollenweber and Mann who identified apigenin-7,4'-dimethyl (synonym of 7-aca) from *Cistus psilosepalus* and *C. salvifolius* as minor constituents (Wollenweber and Mann, 1984). The compound has also been isolated from the ariel parts of *Hyptis capitate* (Almtorp *et al.,* 1991) *Combretum zeyheri* leaves (Mangoyi *et al.,* 2015), *A. agallocha* leaves and *A. sinensis* stems (Liu *et al.,* 2018a, Wang *et al.,* 2015a). This is an initial report on the isolation of this compound from *A. malaccensis* stems for the first time. There are only a few publications to date on the pharmacological activity of 7-aca. The compound has been previously reported to possess nitrite scavenging activity and a weak cytotoxicity effect on HepG2 liver cancer cells (Yang *et al.,* 2018) and it was reported to have anti-fungal properties against *Candida albicans* (Mangoyi *et al.,* 2015). No other published anti-cancer properties of 7-aca has been reported so far.

Next, CC on the methanolic extract of *A. malaccensis* (AM) yielded a mixture of quercitrin and afzelin (Q/A). This is the first time both compounds were isolated from *Aquilaria sp*. Quercitrin was the major compound in the mixture which is also known as quercentin-3-*O*-rhamnoside. It is formed from the flavonoid quercetin substituted by a deoxy sugar rhamnose at position C-3 via a glycosidic linkage. Quercetin is a well-known compound in natural products as it is the most abundant natural flavonoid and it is found in high concentration in many vegetables, fruits and medicinal plants such as *Ginkgo biloba*, *Hypericum perforatum*, *Sambucus canadensis* and *A. sinesis* (Hakkinen *et al.,* 1999, Williamson and Manach, 2005, Anand David *et al.,* 2016, Yang *et al.,* 2018). The name quercetin was coined in 1857 from quercetum (after Quercus, i.e., oak) (Fischer *et al.,* 1997) and since then the pharmacological importance of quercetin as a potent bioactive metabolite has been investigated

intensively (Anand David *et al.*, 2016, Li *et al.*, 2016, Alrawaiq and Abdullah, 2014). The first isolation of quercetin and quecitrin is unknown, but the earliest publication on both compounds was by Heinrich Hlasiwetz who investigated both compounds from 1825–1875 (Soukup, 2019). Similar to quercetin, quercitrin can also be found in many fruits, vegetables and plants such as *Zanthoxylum Bungeanum* Maxim Leaves (He *et al.*, 2016), *Blepharocalyx salicifolius* (Siqueira *et al.*, 2011), *Solidago chilensis* leaves (Barros *et al.*, 2016) and *Euphorbia hirta* (Kadiyala *et al.*, 2016). However, compared to quercetin, there are not as many publications on the pharmacological activities of quercitrin. Quercitrin was reported to exhibit leishmanicidal activity (Siqueira *et al.*, 2011), anti-snake venom activity against *Naja najavenom* induced toxicity (Kadiyala *et al.*, 2016), antioxidant activity and antimelanogenic activities (Hong *et al.*, 2013).

Afzelin, also known as kaempferol-3-rhamnoside or apigenin-3-*O*-rhamnoside, was the minor compound in the mixture with quercitrin. It is derived from the natural flavone kaempferol substituted by an alpha-L-rhamnosyl residue at position C-3 via a glycosidic linkage. Kaempferol can be found widely distributed in fruits and green leafy vegetables such as spinach and kale, and herbs such as dill, chives, and tarragon (Dabeek and Marra, 2019). It has also been isolated from *A. sinesis* leaves (Yang *et al.*, 2018), *A. agallocha* flowers (Chen *et al.*, 2019a) and *A. subintegra* stems (Bahrani *et al.*, 2014). Similarly to quercetin, kaempferol has also been investigated for many pharmacological activities such as anti-inflammatory activity, antioxidant and mostly as a potent anticancer agent (Chen and Chen, 2013, Wang *et al.*, 2018b, Kadioglu *et al.*, 2015). Its glycoside derivative, afzelin, has previously been isolated from *Cornus macrophylla* leaves (Lee *et al.*, 2014a), *Zanthoxylum Bungeanum* Maxim leaves (He

et al., 2016). *Solidago chilensis* leaves (Barros *et al.*, 2016) and *Hymenostegia afzelii* bark and leaves (Awantu *et al.*, 2011). This is the first-time afzelin has been isolated from *A. malaccen*sis twigs. Afzelin has also been getting some interest in natural product drug discovery. It has been reported that the compound possesses anti-bacterial activity (Lee *et al.*, 2014b), as well as α-glucosidase and α-amylase inhibitory activity (Torres-Naranjo *et al.*, 2016). Furthermore, afzelin showed inhibition towards UVB (ultraviolet)-induced cell death through inhibition of an apoptotic signalling pathway and inhibition of pro-inflammatory mediator through interference of p38 kinase pathway (Shin *et al.*, 2013). Afzelin also showed anti-cancer activity against other cancer cell lines such as LNCaP (prostate) (Halimah *et al.*, 2015), MCF-7 (breast) (Diantini *et al.*, 2012a) and CNE-1 (nasopharyngeal) (Huang *et al.*, 2017a).

NMR spectra of *H. dryobalanoides* hexane extract (HH) showed the presence of a tritepene that could possibly be sitosterol or stigmasterol and with some fatty mixtures. Due to the low amount of HH extract obtained (0.9 g), no further fractionation by CC was carried out to investigate the compounds and biological testing. Next, in the NMR spectra of *H. dryobalanoides* ethyl acetate extract (HE), bala was detected as the major compound in the extract, with heimiol A as the minor component and some traces of fats. Whereas, methanol extract of the plant only showed mixtures of sugars. HE was later subjected to CC in order to isolate the compounds detected in the plant extract.

Bala was the first compound to be isolated from the ethyl acetate extract, followed by heimiol A; both classified as resveratrol oligomers which are formed by the polymerisation of two resveratrol monomers (known as resveratrol dimers) by an oxidation reaction (Lins *et al.*, 1982, Xue *et al.*, 2014). Bala is formed by fusion of cis- and trans-isomers of resveratrol (Lim *et al.*, 2012). Resveratrol (3,4′,5-

trihydroxystilbene) is a well-known active metabolite that can be identified in two isomeric forms, cis- and trans-resveratrol and both forms are made up of two phenol rings linked to each other by an ethylene bridge (Figure 2.25). Trans-resveratrol is the dominant and more well-documented due to its health benefits in grapes and wine. Cis-resveratrol is a lesser known companion as it is detected at a much lower quantity in natural products compared to the trans-isomer (Anisimova *et al.*, 2011, Cvejic *et al.*, 2010). Resveratrol can be classified as a polyphenol or stilbene (a type of natural phenol) and was first isolated from the roots of white hellebore, *Veratrum grandiflorum O. Loes* (Takaoka, 1939*).* Since then resveratrol has been detected in more than 70 plants and is especially high in quantity in grape skins and seeds (Mukherjee *et al.*, 2010). Numerous studies have demonstrated potent activities that resveratrol possesses. The metabolite was reported to have a high antioxidant potential through radical scavenging and metal ion chelation abilities (Gülçin, 2010, Rossi *et al.*, 2013, Iuga *et al.*, 2012). Studies have shown that compounds containing OH-groups (such as polyphenols) at position 4', 3 and 5 could be the source of antioxidant activity of the compound (Szekeres *et al.*, 2010, Stivala *et al.*, 2001). Resveratrol was also reported to have a potent anti-inflammatory effect by reducing the production and expression of inflammatory factors (de Sá Coutinho *et al.*, 2018). Furthermore, resveratrol exhibits its protective effects through its anti-inflammatory, anti-oxidant properties and also by improving mitochondria function (Csiszar, 2011, Lee *et al.*, 2007b). Resveratrol is known to be a double-edged sword because treatment with a low dose or high dose of the compound will result in different biological effects. For example, a low resveratrol dose (0.1–1.0 μg/ml) causes increase in cell proliferation and high doses (10.0–100.0 μg/ml) induce apoptosis and decreases mitotic activity on

human tumours and endothelial cells (Szende *et al.*, 2000). Another study showed that, treatment of a low resveratrol dose (1 and 10 μmol/L) causes the proliferation of HT-29 colon cancer cells and a high resveratrol dose (50 or 100 μmol/L) causes apoptosis to the cancer cells (San Hipolito-Luengo *et al.*, 2017).

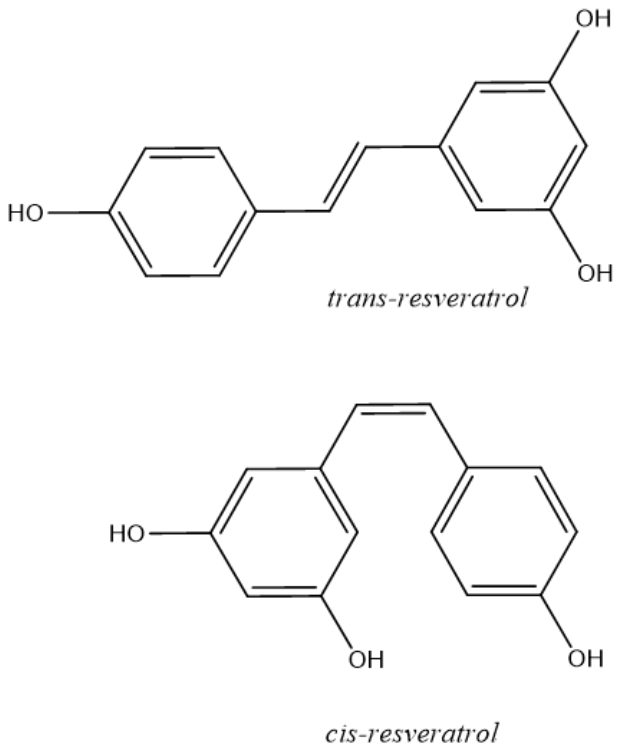

Figure 2.25 Structure of trans and cis resveratrol

Resveratrol oligomers are fungal detoxification products of resveratrol metabolism in plants. Bala was first isolated from *Balanocarpus zeylanicus* and *H. jucunda* (Diyasena *et al.*, 1985) then the compound was found in many Dipterocarpaceae species such as *H. mengarawan* (Atun *et al.*, 2006), *H. odorata* (Atun *et al.*, 2012), *H. dryobalanoides* (Sahidin *et al.*, 2005). Heimiol A was first isolated from *Neobalanocarpus heimii* (Weber *et al.*, 2001) then later the compound was isolated from other Dipterocarpaceae species such as *H. mengarawan* (Atun *et al.*, 2006) *H. dryobalanoides* (Sahidin *et al.*,

2005). Similar to resveratrol, many resveratrol oligomers have been reported to exhibit many biological effects such as antibacterial, antifungal, anticancer, anti-HIV, and antioxidant activities (Cichewicz and Kouzi, 2002). Even though there are many publications on the isolation of bala and heimiol A, there are only a few publications on the biological effects of bala and even fewer on heimiol A. Bala was reported to inhibit novel sphingosine kinase 1 (SK1) by affecting SK1 expression, growth and survival of breast cancer cells MCF-7 (Lim *et al.*, 2012). Bala exhibited stronger hydroxyl radical scavenging activity compared to heimiol A (Atun, 2006) On the anticancer activity of the compounds, bala showed a cytotoxic effect towards HeLa-S3, Raji and P-388 leukaemia cancer cells, however, heimiol A was shown to be inactive against all three cancer cells (Atun *et al.*, 2008, Sahidin *et al.*, 2005). It was also suggested that the cytotoxic effect of bala could be due to the presence of a cycloheptadiene ring in the structure (Sahidin *et al.*, 2005).

In conclusion, 7-aca, quercitrin and afzelin have been isolated from *A. malaccensis* for the first time. Aca is well known for its various biological activities including anticancer. Therefore, potential anti-cancer activity for aca will be compared to its derivative, 7-aca and discussed in depth in Chapter 3. Even though, bala and heimiol A have been isolated from plants many times, their biological effects have not been intensively studied. Therefore, the compounds will be investigated for their potential anticancer effect in Chapter 3, anti-inflammatory effect in Chapter 4 and neuroprotective studies in Chapter 5.

Chapter 3 Investigation of the potential anti-cancer properties of *A. malaccensis* and *H. dryobalanoides* extracts and their compounds.

3.1 Introduction

Many plants have been used as a source of anti-cancer agents because they contain a broad spectrum of secondary metabolites. Some of the anticancer agents that have been used for cancer treatment are paclitaxel (Taxol), vincristine and vinblastine. These chemotherapy agents were derived from plants and are still being used in hospitals to treat cancer patients as the main treatment or as a combination therapy (Greenwell and Rahman, 2015). Plant-derived drugs with anti-cancer activity are more desirable as they are more tolerated by patients and generally are chosen to be non-toxic to normal cells (Shah *et al.*, 2013). Researchers have investigated the anti-cancer activities of *Aquilaria* sp. and *Hopea* sp. and both species have proven to possess cytotoxic effects towards various cancer cells (Dahham *et al.*, 2016b, Hashim *et al.*, 2018, Dahham *et al.*, 2015, Nguyen *et al.*, 2017b, Paul *et al.*, 2016). Phytochemical investigation on both plants has shown them to be rich in polyphenolic compounds (Chen *et al.*, 2012, Chen *et al.*, 2019a, Cheng *et al.*, 2013, Qi *et al.*, 2009, Sasikumar *et al.*, 2019, Atun *et al.*, 2012), which are a class of secondary metabolites that are well known to have anti-cancer properties (Chahar *et al.*, 2011, Abdelkader *et al.*, 2017). The screening of bioactive compounds involves a large number of assays that allow assessment of the therapeutic potential of biological extracts or molecules. Some of the means by which anti-cancer agents achieve therapeutic effects are through preliminary testing such as the cytotoxicity assay and further testing on the mechanism behind the cytotoxicity of the compounds, as described below.

3.1.1 Cell viability

Assays that assess cell viability are widely adopted in preliminarily screening to identify those extracts or compounds with anti-cancer activity. For example, the sulforhodamine B assay is a preferred high-throughput assay used for toxicity screening of compounds currently used by the National Cancer Institute in the USA in their *in vitro* anticancer-drug discovery programme (van Tonder *et al.*, 2015). Other popular cell viability assays used in small-scale assessment of cancer cell viability after exposure to investigational compounds include resazurin reduction using alamarBlue® reagent. This method is used for the identification of potentially active extracts or compounds in primary screening which facilitates selection to undergo further investigations. Viable cells maintain a reducing environment in the cytosol of the cell. Resazurin, the main active ingredient in alamarBlue®, is water-soluble, stable in culture medium, is non-toxic and permeable through cell membranes (Rampersad, 2012). Resazurin is an oxidation–reduction sensitive dye that changes colour/fluorescence properties to its reduced form resorufin by living cells. Only viable cells that are metabolically active generate a fluorescent signal in the medium. On the other hand, non-viable cells are unable to carry out the conversion from resazurin to resorufin and therefore the medium remains coloured blue and shows no fluorescence (Bowling *et al.*, 2012).

3.1.2 DCFDA / H2DCFDA - Cellular Reactive Oxygen Species Detection Assay

Cell permeant reagent 2'-7'dichlorofluorescin diacetate (DCFH-DA) is a fluorogenic dye that measures ROS activity such as production of hydroxyl and peroxyl free radicals. When DCFH-DA enters cells, the dye is deacetylated by cellular esterases to a non- fluorescent compound (Wojtala *et al.*, 2014). It is then oxidised by ROS into 2'-

7'dichlorofluorescein (DCF), which can be monitored by several fluorescence-based techniques (e.g. spectroscopy, confocal microscopy, flow cytometry) (Kalyanaraman *et al.*, 2012). In the presence of ROS, yellow DCF shows intense fluorescence, while in the absence of ROS no fluorescence is detected.

3.1.3 TMRE assay

Tetramethylrhodamine, ethyl ester (TMRE) is a fluorescent dye that is readily sequestered by active mitochondria, allowing for fluorescence or imaging analysis to assess for apoptosis or mitochondrial depolarization in living cells (Scaduto and Grotyohann, 1999). TMRE dye stains the cells and emits a red fluorescence which can be detected by flow cytometry or fluorescence microscopy. The level of TMRE fluorescence in stained cells can be used to determine whether mitochondria in a cell have high or low ΔΨM (Crowley *et al.*, 2016). Lower levels of TMRE fluorescence resulting from a potent mitochondrial uncoupler such as FCCP reflect the depolarisation of ΔΨM (Joshi and Bakowska, 2011).

3.1.4 Caspase-3/7

In cancer treatment, apoptosis is a well-recognised cell death mechanism through which cytotoxic agents kill tumour cells and the members of the caspase family play a central role in coordinating the stereotypical events that occur during apoptosis (Huang *et al.*, 2011). Effector caspases (caspase-3 and caspase-7) cleave the target proteins that eventually leads to the death of the cell. Caspase-3 and caspase-7 are structurally similar to one another, however caspase-3 mediates DNA fragmentation and morphologic changes associated with apoptosis, whereas caspase-7 plays little role in these processes. In contrast, caspase-7 appears to have an essential role in the loss of cellular viability, although the combined role of both caspases is crucial in this area

(Lakhani *et al.*, 2006). Therefore, caspase- 3/7 measurement is used as an indicator of apoptosis. Caspase-Glo 3/7 assay reagent was used for caspase detection in treated cells *in vitro*. The reagent provides a pro-luminescent caspase-3/7 substrate, which contains the tetrapeptide sequence DEVD, in combination with luciferase and a cell-lysing agent. The addition of the Caspase-Glo 3/7 reagent directly to the assay well results in cell lysis, followed by caspase cleavage of the DEVD substrate, and the generation of luminescence. The amount of luminescence as displayed on the readout is proportional to the amount of caspase activity in the sample (Payne *et al.*, 2013).

3.1.5 Cell adhesion, migration and invasion

Metastasis is the process by which cancer cells spread from the primary tumour site to surrounding tissues and to distant organs (Jiang *et al.*, 2015). It involves numerous factors including the degradation of the extracellular matrix (ECM), tumour angiogenesis and defects in programmed cell death such as apoptosis, autophagy and necrosis (Su *et al.*, 2015). The ECM is an essential component of the tumour microenvironment, cancer cell proliferation and invasion. The ECM basement membrane is primarily composed of laminin, collagen type IV, entactin, and proteoglycans. In addition, stromal cells, adipocytes, and immune cells produce many ECM proteins such as bone sialoprotein, osteopontin, osteonectin, osteocalcin, fibronectin and vitronectin (Cho *et al.*, 2015, Jena and Janjanam, 2018). Other than that, migration and invasion by cancer cells are required for metastasis to occur at new sites (Keleg *et al.*, 2003). Migration and invasion are two key properties of cancer progression and represent an important drug target in the development of new therapeutics for cancer treatment (Martin *et al.*, 2013).

The CytoSelect™ cell adhesion, cell migration and cell invasion assay kit were used to investigate the anti-metastatic properties of the samples. The cell adhesion kit utilizes a fibronectin-coated well plate where the adherent cells are captured. Next, unbound cells are removed with consecutive washes. Finally, the adherent cells are lysed and subsequently detected with CyQuant® GR Dye. The Cell Migration Assay Kit contains a polycarbonate membrane chamber that serves as a barrier to discriminate migratory cells from nonmigratory cells. Migratory cells are able to extend protrusions towards chemoattractants (via actin cytoskeleton reorganization) and ultimately pass through the pores of the polycarbonate membrane. These migratory cells are then dissociated from the membrane and subsequently detected with CyQuant® GR Dy. The Cell Invasion Assay Kit contains polycarbonate membrane inserts which is coated with a uniform layer of dried basement membrane matrix solution. This basement membrane layer serves as a barrier to discriminate invasive cells from non-invasive cells. Invasive cells are able to degrade the matrix proteins in the layer, and ultimately pass through the pores of the polycarbonate membrane. Finally, the invaded cells are dissociated from the membrane and subsequently detected with CyQuant® GR Dye (Invitrogen).

3.1.6 Metabolomics

Metabolomics is a powerful tool used to study endogenous small molecules (referred to as metabolites) in biological systems such as biofluids, organisms, organs, tissues or cells focusing on characterising, understanding and measuring the chemical processing of metabolites and evaluating the changes in metabolites in response to treatment, pathophysiological stimuli or genetic modification (Deidda *et al.*, 2015). Basically, metabolomics plays an essential role in identification of key biomarkers for

diagnosis and therapeutic evaluation in different disease states, including cancer (Vermeersch and Styczynski, 2013, Dettmer *et al.*, 2007). Moreover, drug metabolism investigations have become an essential part of pharmaceutical development, toxicity studies and clinical trials (Guengerich, 2001).

Cell culture models have been used extensively to study the molecular mechanism of disease progression, response, and resistance to therapeutics. Within a living cell, metabolomics enables the investigation and detection of endogenous biochemical reaction products, elucidating information on the particular metabolic pathways and demonstrating the connections among different pathways that operate within a living cell (Wang *et al.*, 2011). Cell metabolomics relies on four sequential phases: (a) reliable preparation and extraction of samples, (b) appropriate detection methods in order to perform metabolomic profiling of samples such as NMR or mass spectrometry (c) pattern recognition approaches (e.g. MzMine, MzMatch) and bioinformatics data analysis (e.g. SIMCA-P), (d) metabolite identification resulting in putative biomarkers and molecular targets (Zhang *et al.*, 2013).

3.2 Aims and objectives

This chapter aims to evaluate the anti-cancer potential of *A. malaccensis* and *H. dryobalanoides* extracts and isolated compounds. The objectives were:

1. To test the cytotoxic effects of the plant extracts and the isolated compounds on a panel of cancer cells: A2780 (ovarian), HepG2 (liver), U2OS (bone) and ZR-75-1 (breast) cells as well as to ensure that tested samples are non-cytotoxic to normal cells PNT2A (prostate).

2. To test the ability of the extracts and isolated compounds to generate or inhibit ROS using the DCFH-DA assay in cancer cells.
3. To test the ability of the extracts and isolated compounds to reduce ΔΨM using TMRE dye in cancer cells.
4. To test possible apoptotic effects of the extracts and isolated compounds by measuring the production of caspase- 3/7 level in cancer cells.
5. To investigate the possible opposing effect of selected isolated compounds on the adhesion, migration and invasion of cancer cells.
6. To characterise the metabolic profiles of cancer cells in response to their exposure to selected isolated compounds.

3.3 Methods

3.3.1 Maintenance of different types of cells

All cell culture work was carried out in a cell culture hood. A2780, PNT2A and ZR75 were cultured in RPMI-1640 culture media. HepG2 and U2OS were cultured in DMEM culture media. Both culture media were supplemented with 10% (v/v) Foetal Bovine Serum (FBS), 1% (v/v) penicillin-streptomycin and 1% (v/v) L-glutamine.

3.3.1.1 Thawing of cells

Cells in 1.5ml cryovials were retrieved from liquid nitrogen storage and immediately thawed by placing the cryovials into a water bath heated to 37°C. In a cell culture hood, cells were then transferred from the cryovials into a 25cm^2 cell culture flask containing 5 ml of appropriate medium (pre-warmed at 37°C) to allow dilution of the cryoprotector DMSO. The cells were then incubated and grown until they reached 70-80% confluency in a humidified incubator at 37°C with 5% CO_2.

3.3.1.2 Passaging and splitting of cells

After the cells had reached 70-80% confluency, they were then passaged and split by first discarding the cell culture medium in the flask. Cells were washed twice with sterile Hanks' Balanced Salt Solution (HBSS) before being exposed to 3 ml ($25cm^2$ flask) or 5ml ($75cm^2$ flask) of TripLE Express for 5-7 min in the incubator. Then, 7ml ($25cm^2$ flask) or 10ml ($75cm^2$ flask) of the appropriate cell culture medium was added to the flask to deactivate the trypsin. The cells were transferred into a centrifuge tube and centrifuged for 2 min at 1000 RPM. The supernatant was removed, and the cell pellet was resuspended in culture media and then counted using a haemocytometer under a light microscope. After cell counting, cell suspensions were either seeded into a fresh cell culture flask or in cell culture plates for subsequent experiments calculated based on desired cell density.

3.3.2 Cytotoxicity of plant crude extracts and compounds on different cell lines

All samples were evaluated in an *in vitro* cytotoxicity test using alamarBlue®. A2780 (7.5×10^3 cells/well), HepG2, PNT2A, U20S and ZR-75-1 (3×10^3 cells/well) were seeded in flat bottomed 96-well plates and incubated for 24 h or 48 h in a humidified incubator at 37°C with 5% CO_2 prior to adding the samples.

Samples were prepared by dissolving them in 100% DMSO to make a stock concentration of 10mM (compounds) or 10mg/ml (extracts) then diluted using cell culture medium to make the highest concentration of 30 µM (compounds) or 30 µg/ml (extracts) in the assay plate. Selected samples were further diluted as follows: 0.01, 0.03, 0.1, 0.3, 1, 3, 10 and 30 µM or µg/ml and added to the assay plate. The positive control consisted of cells treated with 0.1% (v/v) Triton X (cytotoxic agent) only and the negative control consisted of untreated cells. Vehicle control (DMSO) was also

carried out in the concentration range (1%-0.01%) in which no effect was seen on cell viability. After cells were treated with compounds or Triton X for 24 or 48 h, cells were incubated with 10% (v/v) alamarBlue® at 37°C for 4-5 h, then the plate was read in a SpectraMax M5 plate reader using Softmax Pro software, at a fluorescence excitation wavelength of Ex560nm/Em590nm. The results were expressed as a mean ± standard error of the mean (SEM) of triplicate readings. Viable cells following treatments were calculated as a percentage of the untreated control cells as follows:

$$\%\ cell\ viabiliy = \frac{samples\ reading}{control\ reading} \times 100$$

GraphPad Prism for Windows (version 8.00, GraphPad Software, San Diego, CA, USA) was used to fit concentration–response curves and obtain mean inhibitory concentration (IC50) values. Data were normalized to the untreated control response so that all IC50 curves begin with a plateau around 100% and are assumed to fall to 0%. The data was fitted using the following equation:-

Fifty=(Top+Baseline)/2

Y=Bottom + (Top-Bottom)/(1+10^((LogIC50-X)*HillSlope + log((Top-Bottom) / (Fifty-Bottom)-1))

Where Y is the % for the maximum value observed, X is the inhibitor concentration while Top was set to be 100% (untreated control value) and Bottom was set to zero (approximate value of negative control following treatment with 0.1% Triton).

Data was analysed statistically using One-Way ANOVA with Bonferroni multiple comparison test (GraphPad Prism software). A significance level of $p < 0.05$ was adopted.

3.3.3 Estimation of Intracellular ROS levels using a DCFH-DA probe

Intracellular ROS levels of A2780 and ZR-75-1 cells were determined using a microplate assay and a fluorescence microscopy assay. For the microplate assay, confluent cells were trypsinised and seeded at a density of 5×10^4 cells/well (A2780) and 2.5×10^4 cells/well (ZR-75-1) in culture media in a 96-well half area black plate with clear bottom. The plate was incubated for 24 h in a humidified incubator at 37°C with 5% CO_2. A stock concentration of 10mM DCFH-DA was prepared with DMSO, then later a working concentration of 10µM DCFH-DA was prepared in phenol red-free HBSS. The tubes were wrapped with aluminium foil and stored at -20°C for further use. The next day, all media were removed from the wells and the cells were washed once with 50 µl phenol red-free HBSS (all HBSS used in this experiment contained 10%, v/v, FBS). Then, 50µl of test samples and positive control were added to appropriate wells. All samples were prepared in phenol red-free HBSS: 30 µM (7-aca and aca), 150µM (bala and heimiol A) or 30 µg/ml (Q/A and extracts) in the assay plate. 7-Aca, aca and Q/A were further diluted (1:10) as follows: 0.01, 0.03, 0.1, 0.3, 1, 3, 10 and 30 µM or µg/ml. Bala was further diluted 1:2 as follows: 1.2, 2.3, 4.7, 9.4, 18.7, 37.5, 75 and 150 µM. The positive control consisted of 100µM tert-Butyl hydroperoxide (TBPH) prepared in HBSS. Plates were then incubated for 1.5 h with test samples or TBPH in a humidified incubator at 37°C with 5% CO_2. After the incubation period, all tests samples and TBPH were removed from the wells and washed once with 50µl of phenol red-free HBSS before adding 50µl of 10µM of

DCFH-DA to all wells except for blank wells which contained 50µl of phenol red-free HBSS. Plates were incubated for 30 min in a humidified incubator at 37°C with 5% CO_2. After the 30 min incubation, the DCFH-DA was removed, and the cells were washed twice with 50 µl phenol red-free HBSS. Then, 50µl of phenol red free HBSS was added to the plates before being measured on a SpectraMax M5 plate reader using Softmax Pro at a maximum excitation and emission spectra of 485 and 535 nm, respectively.

3.3.4 TMRE assay for mitochondrial membrane depolarization (ΔψM)

Loss of ΔψM in cells were evaluated by staining with TMRE. This assay was carried out using microplate and fluorescence microscopy assays. For the microplate assay, confluent cells were trypsinised and seeded at a density of 5 x 10^4 cells/well (A2780) and 2.5 x 10^4 cells/well (ZR-75-1) in culture media in a 96-well half area black plate with clear bottom. The plate was incubated for 24 h in a humidified incubator at 37°C with 5% CO_2. A 10mM stock concentration of TMRE and carbonyl cyanide-4-(trifluoromethoxy)phenylhydrazone (FCCP) a positive control was prepared in DMSO. Later TMRE and FCCP were diluted to their working concentration with phenol red-free HBSS (all HBSS used in this experiment contained 10%, v/v, FBS).

The next day, all media were removed from the wells and the cells were washed once with 50 µl phenol red-free HBSS. Then, 50µl of test samples or 20µM FCCP was added to the wells and incubated for 30 min (FCCP) or 3 h (test samples) in a humidified incubator at 37°C with 5% CO_2. All samples were prepared in phenol red-free HBSS and diluted to make a concentration of 0.01, 0.03, 0.1, 0.3, 1, 3, 10 and 30 µM or µg/ml (7-aca, aca and Q/A) and 1.2, 2.3, 4.7, 9.4, 18.7, 37.5, 75 and 150 µM (bala and heimiol A).

After the incubation, all test samples and FCCP were removed before washing the cells once with 50 µl phenol red-free HBSS. A 200nM working concentration of TMRE was prepared and added to all wells except for blank wells. Plates were incubated for 30 min in a humidified incubator at 37°C with 5% CO_2. Then, the TMRE was removed and the cells were washed twice with 50 µl phenol red-free HBSS. Phenol red-free HBSS was added to all wells and plates were read immediately on SpectraMax M5 plate reader using Softmax Pro at the maximum excitation and emission spectra of 549 and 575 nm.

3.3.5 Measurement of Caspase- 3/7 levels

A Caspase-Glo 3/7 assay was performed according to the manufacturer's protocol. Confluent cells were trypsinised and seeded in clear bottom white-walled 96 well half area plates at a density of 5 x 10^4 cells/well (A2780) and 2.5 x 10^4 cells/well (ZR-75-1). The plate containing cells was incubated for 24 h in a humidified incubator at 37°C with 5% CO_2. All test samples were prepared in RPMI-1640 media to 30 µM (7-aca and aca), 150 µM (bala) or 30 µg/ml (Q/A and extracts) in the assay plate. The negative control (cells with medium only) and positive control (staurosporine) were also included. Staurosporine was dissolved in DMSO to make a stock concentration of 1 mM, then further diluted to a range of concentrations from 10µM to 0.07µM.

After 24 h incubation, 50 µl of test samples and negative control were added to appropriate wells, then incubated for 6, 12 or 24 h in a humidified incubator at 37°C with 5% CO_2. The next day, the plates containing cells were removed from the incubator and allowed to equilibrate to room temperature for 30 min. A total of 100 µl of Caspase-Glo reagent was added to each well, and the plate gently mixed on a plate shaker at 300–500 rpm for 30 sec. The plate was then incubated at room temperature

for 2 h. The luminescence of each sample was measured on a Spectramax M5 microplate reader with parameters of 1 min lag time and 0.5 sec/well-read time.

3.3.6 Cell Adhesion assay

A CytoSelect^{TM} 48-Well Cell Adhesion Fibronectin-Coated, Colorimetric Format assay kit was used to evaluate cellular adhesion. The Fibronectin Adhesion plate was warmed to room temperature for 10 min in a cell culture hood. Cell suspensions were prepared containing 1.0 x 10^6 cells/ml in serum free RPMI-1640 containing 0.5% (w/v) bovine serum albumin (BSA), 2mM $CaCl_2$ and 2mM $MgCl_2$. Test samples were directly added to the cell suspension. Then, 150µl of the cell suspension containing test samples was added to the inside of each fibronectin-coated wells and incubated for 90 min in a humidified incubator at 37°C with 5% CO_2. Cell suspension without test samples were added in the BSA-coated wells as a negative control and placed in a cell culture incubator for 90 min. After incubation, the medium was carefully discarded from each well before being gently washed 4 times with 250ul PBS. A total of 200µl of Cell Stain Solution was then added to each well for 10 min, discarded, and the wells were gently washed 5 times with 500µl deionized water. Wells were air dried and then 200µl extraction solution was added per well and placed on an orbital shaker for 10 min. A total of 150µl from each extracted sample was added to a 96 well microtitre plate and measured at 560nm in a SpectraMax M5 plate reader using Softmax Pro.

3.3.7 Cell migration assay

A CytoSelect^{TM} 24-well Cell migration Assay, 8µm, Colorimetric kit was used to assay the migratory properties of cells. The migration plate was warmed to room temperature for 10 min in a cell culture hood. Cell suspensions of A2780 and ZR-75-1 were prepared containing 1.0 x 10^6 cells/ml in serum free RPMI-1640 containing

0.5% (w/v) BSA, 2mM CaCl2, 2mM MgCl2. Test samples were directly added to cell suspension. Firstly, 500 µl of RPPMI-1640 containing 10% (v/v) FBS was added to the lower well of the migration plate. Then, 300 µl of cell suspension containing test sample was added to cell culture inserts (8µm pore size) and incubated for 24 h. The insert was discarded, and the interior of the inserts were carefully swabbed with a wet cotton-tipped bud to remove non-migratory cells. The inserts were then transferred with forceps to a clean well containing 300µl of Cell Stain Solution and incubated for 10 min at room temperature. Using forceps, the inserts were gently dipped and washed several times in a beaker of water and allowed to air dry. The inserts were then transferred again to a clean well containing 200µl of Extraction Solution per well and incubated for 10 min at room temperature on an orbital shaker. Each extracted sample (100µl) was added to a 96 well microtitre plate and measured at 560nm on a SpectraMax M5 plate reader using Softmax Pro software.

3.3.8 Cell invasion assay

A CytoSelectTM 24-well Cell Invasion Assay, Basement Membrane, Colorimetric kit was used to assay the invasive properties of cells. The invasion chamber plate was warmed to room temperature for 10 min in a cell culture hood. The basement membrane layer of the cell culture inserts was rehydrated by adding 300 µl of serum-free RPMI1640 to the inner compartment for 1 h and incubated at room temperature. Cell suspensions of A2780 and ZR-75-1 were prepared containing 1.0 x 106 cells/ml in serum free RPMI-1640 containing 0.5% (w/v) BSA, 2mM CaCl2, 2mM MgCl2. Test samples were directly added to cell suspension. Firstly, 500 µl of RPPMI-1640 containing 10% (v/v) FBS was added to the lower well of the invasion plate. Then, 300 µl of cell suspension containing test sample was added to the cell culture inserts

and incubated for 24 h in a humidified incubator at 37°C with 5% CO2. After incubation, media in the insert were discarded and the interior of the inserts were carefully swabbed with wet cotton-tipped buds to remove non-migratory cells. The inserts were then transferred with forceps to a clean well containing 300µl of Cell Stain Solution and incubated for 10 min at room temperature. Using forceps, the inserts were gently dipped and washed several times in a beaker of water and allowed to air dry. The inserts were then transferred again to a clean well containing 200µl of Extraction Solution per well and incubated for 10 min at room temperature on an orbital shaker. 100µl of each extracted sample was added to a 96 well microtiter plate and measured at 560nm on a SpectraMax M5 plate reader using Softmax Pro software.

3.3.9 Cell extraction for metabolomic analysis

Confluent cells were trypsinised and seeded at 4.5 x 10^5 cells/well for 48 h in 6-well plates before treatment with the compounds. The cells were treated with test compounds at concentrations of 30 µM or just RPMI-1640 (control) for another 48 h. Every extraction condition was prepared in five biological replicates. After the treatment, the medium was aspirated, and the cells were washed with 3 ml of phosphate-buffered saline (PBS) twice at 37 °C before lysis. Then the cells were extracted with ice cold methanol:acetonitrile:water (50:30:20) (1 ml per 2 × 10^6 cells) to prepare cell lysates. The cells were scraped, and cell lysates mixed on a Thermo mixer at 1440 rpm for 12 min at 4 °C, before being centrifuged at 13, 500 RPM for 15 min at 0 °C. The supernatants were collected and transferred into autosampler vials for liquid chromatography–mass spectrometry (LC-MS) analysis or stored at -80°C until further use. A pooled quality control (QC) sample was prepared by taking equal aliquots from each of the samples and mixing them together and placing them into a

HPLC vial. The pooled QC sample and authentic standard metabolite mixtures were injected in each analysis run in order to ensure the stability and reproducibility of the analytical method.

3.3.10 Liquid chromatography-mass spectrometry conditions

3.3.10.1 Chromatographic conditions for ZIC-pHILIC column

A ZIC-pHILIC column (L150 × I.D. 4.6 mm, 5μm, polymeric bead support) supplied by HiChrom was used to study the effects of 7-aca and aca on A2780 and ZR-75-1 cell metabolomes. The aqueous mobile phase (solvent A) for ZIC-pHILIC was made up of 20mM ammonium carbonate buffer in HPLC-grade water (A) and the organic phase (solvent B) consisted of HPLC grade acetonitrile. All mobile phase solutions were freshly prepared and were stored at room temperature for up to 72 h. Firstly, the system was purged with 100% of mobile phase B for 5 min at a flow rate of 5ml/min then followed by mobile phase A at the same flow rate and time. The column was then eluted with solvent A:solvent B ratio at a linear gradient starting with 20:80 at 0 min, 80:20 at 30 min with a flow rate of 0.3 ml/min, followed by washing with 95:5 at 35 min and then re-equilibration with 20:80 at 45 min. To avoid degradation, the samples were kept in a vial tray at a constant temperature of 4℃. The MS was operated in a positive/negative polarity switching mode.

3.3.10.2 Accela HPLC-ESI-Exactive Orbitrap

LC-MS was carried out on an Accela HPLC system coupled to an Exactive (Orbitrap) mass spectrometer. The temperature of the ion transfer capillary was 275 °C while the nitrogen sheath and auxiliary gas flow rates were maintained at 50 and 17 ml/min. The electrospray ionisation (ESI) interface was operated in a positive/negative dual polarity mode. The spray voltage was 4.5 kV for positive mode and 4.0 kV for negative

mode. Full scan data was obtained in the mass-to-charge ratio (m/z) range of 75 to 1200 for both ionisation modes. Mass calibration was performed for both positive and negative ESI polarities before analysis using the standard Thermo Calmix solution with additional coverage of the lower mass range with signals at m/z 83.0604 (2×ACN+H) for the positive and m/z 91.0037 (2×$HCOO^-$) for the negative modes. The resulting data were recorded using the XCalibur 2.1.0 software package (Watson *et al.*, 2013).

3.3.11 Data Extraction and Statistical Analysis

3.3.11.1 LC-MS data processing by MZMatch software

The data were extracted using MZMatch software (http://mzmatch.sourceforge.net/). A macro-enabled Excel Ideom file was used to filter, compare and identify the metabolites (http://mzmatch.sourceforge.net/ideom.php). Library searches were also used for identification and carried out against accurate mass data of the metabolites in the Human Metabolome Data Base, lipid maps and Kyoto Encyclopedia of Genes and Genomes (KEGG). All metabolites were within 3 ppm of their exact masses. Metaboanalyst 3.0 (Xia *et al.*, 2015) , a web-based metabolomic data processing tool, was employed for univariate analysis. Microsoft Excel and paired t-tests were used to perform univariate comparisons between treated and control cells and differences were considered significant at $P<0.05$. SIMCA-P software v.14.0 (Wu *et al.*, 2010) was used for visualisation and multivariate analysis of the metabolite data by fitting n PCA-X and OPLS-DA. Data were log2-transformed and then Pareto scaled, where the responses for each variable were centred by subtracting the mean value and then dividing by the square root of its standard deviation (van den Berg *et al.*, 2006). The relative standard deviation (RSD) of each metabolite was also calculated based on the

reading of the pooled sample that was run throughout the sequence and metabolites with RSD higher than 30% were excluded. PCA was initially used for data visualisation and to explore how variables clustered based on their metabolic composition regardless of their grouping. With OPLS-DA, the supervised model, the discrimination between groups was applied by neglecting the systemic variations (Kirwan *et al.*, 2012). OPLS-DA models were validated based on multiple correlation coefficient (R2) and cross-validated R2 (Q2) as diagnostic tools in cross-validation and permutation test. Where, R2 reflects the percentage of variation explained by the model, while Q2 indicates the percentage of variation in response to cross validation (Kirwan *et al.*, 2012). The model was also validated using cross validation ANOVA (CV-ANOVA).

3.4 Results

3.4.1 AlamarBlue® assay

Cytotoxic effects of *A. malaccensis* and *H. dryobalanoides* extracts at a concentration of 30µg/ml were tested against 4 cancer cells A2780, HepG2, U2OS and ZR-75-1 and 1 normal cells PNT2A as shown in Figure 3.1. After 24 h incubation, hexane extract of *A. malaccensis* (AH) was shown to be the most active cytotoxic compound against A2780 and ZR-75-1 by reducing the percentage of cell viability to approximately 50%. The extract also showed a reduction in the percentage of cell viability for U2OS cells. The methanol extract for *A. malaccensis* (AM) and *H. dryobalanoides* (HE) only showed moderate cytotoxic effects against A2780 and ZR-75-1 cells (60-70% cell viability). None of the plant extracts were cytotoxic against PNT2A cells. Thus, A2780 and ZR-75-1 cells were selected to test the cytotoxicity of isolated compounds. Firstly, 30µM of 7-aca, aca, bala, heimiol A and 30µg/ml of Q/A mixture were tested against

the selected cancer cells for 24 h and 48 h (Figure 3.2). Although the cell viability decreased by 10-15% from 24 h to 48 h, statistically, it was not significant ($P<0.05$). 7-aca was shown to be the most potent compound against both cell lines by reducing the cell viability of A2780 and ZR-75-1 to <40%. The second most active compound was aca followed by Q/A. 7-Aca, aca and Q/A also showed dose-dependent activity at a range of 0.01 - 30µM or µg/ml (Figure 3.3 and Figure 3.4). Aca exhibited a weaker cytotoxic effect (A2780 IC_{50}=19.5 µM, ZR-75-1 IC_{50} =17.5µM) compared to 7-aca (A2780 IC_{50}= 7.9µM, ZR-75-1 IC_{50}= 8.5 µM) against both cell lines. Bala and heimiol A did not have any effect at 30 µM on both cancer cell lines (Figure 3.2). Therefore, bala and heimiol A were tested at a higher concentration range of 2.3µM to 300µM; only bala exhibited its cytotoxic effects in a concentration dependent manner giving an IC_{50} of 64.1µM against A2780 cells and IC_{50} of 134.4 µM against ZR-75-1. All compounds were not cytotoxic against the normal PNT2A cell line, except for bala at the highest concentration tested (300µM) which reduced cell viability to approximately 80% (Figure 3.5). Therefore, the highest concentration that was used for subsequent experiments was 150µM.

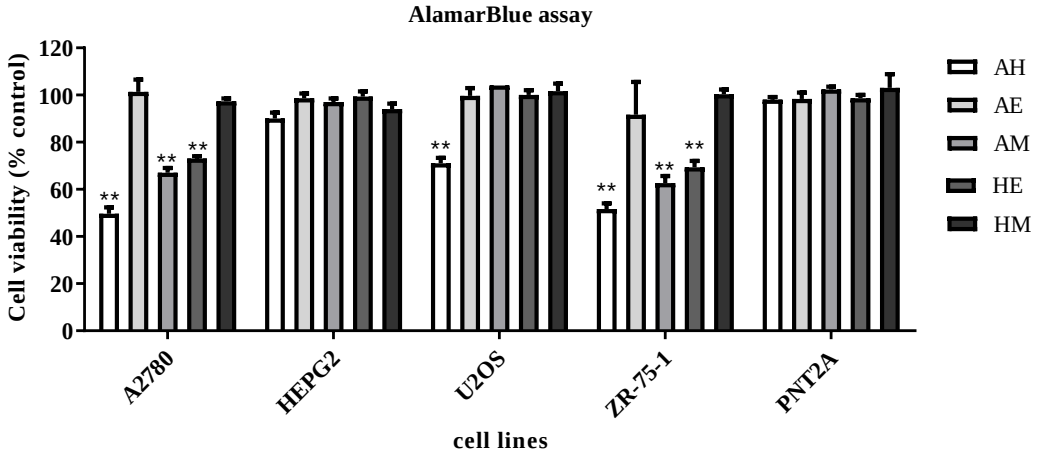

Figure 3.1 Examination of cell viability after 24 h treatment with *A. malaccensis* and *H. dryobalanoides* extracts on different cell lines. Data was analysed using One-Way ANOVA with Bonferroni multiple comparison test. Data represents mean ± SEM, n=3. **P<0.01 represents significant decrease in cell viability vs untreated cells (control). AH; *A. malaccensis* hexane, AE; *A. malaccensis* ethyl acetate, AM; *A. malaccensis* methanol, HE; *H. drybalanoides* ethyl acetate, HM; *H. drybalanoides* methanol.

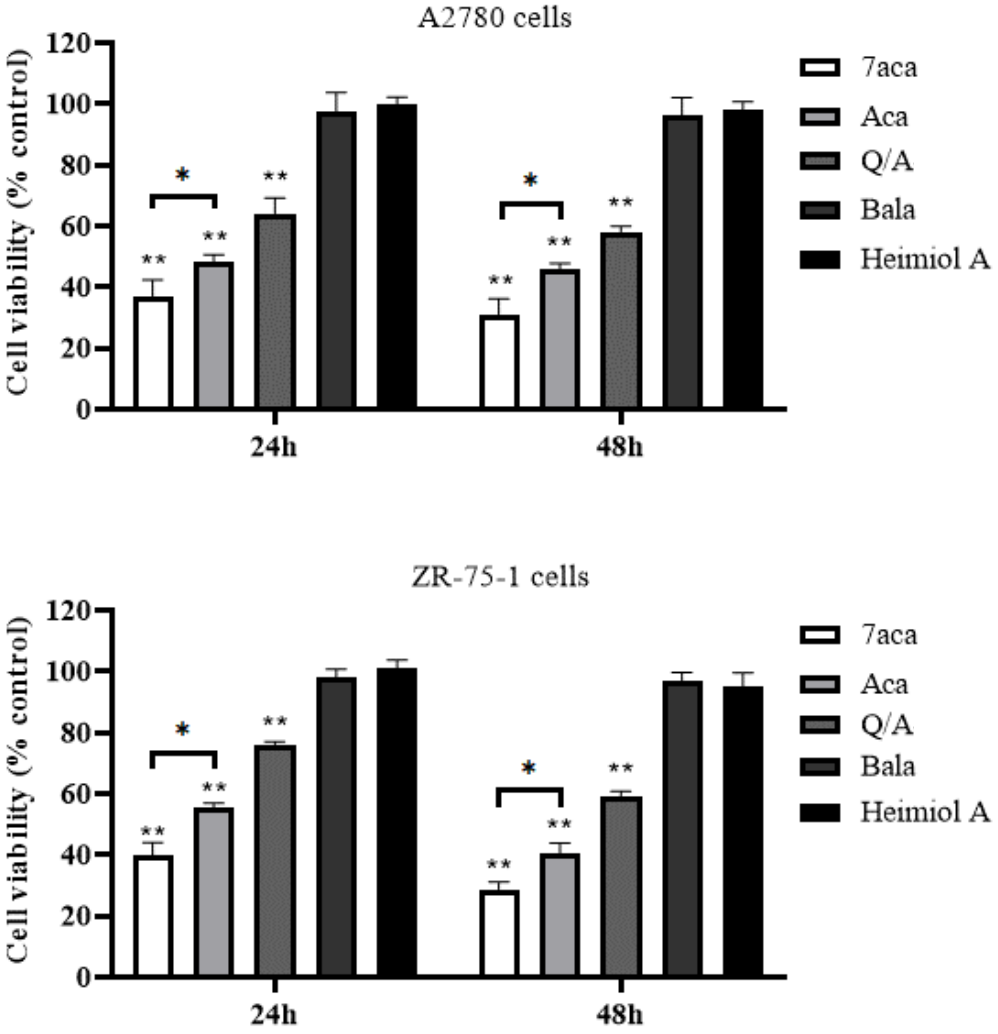

Figure 3.2 Examination of cell viability after 24 h or 48 h treatment with isolated compounds on A2780 and ZR-75-1. 7-aca, aca, bala and heimiol A was tested at 30µM and Q/A tested at 30µg/ml. Data was analysed using One-Way ANOVA with Bonferroni multiple comparison test. Data represents mean ± SEM, n=3. **P<0.01 and *P<0.05 represents significant decrease in cell viability vs untreated cells (control).

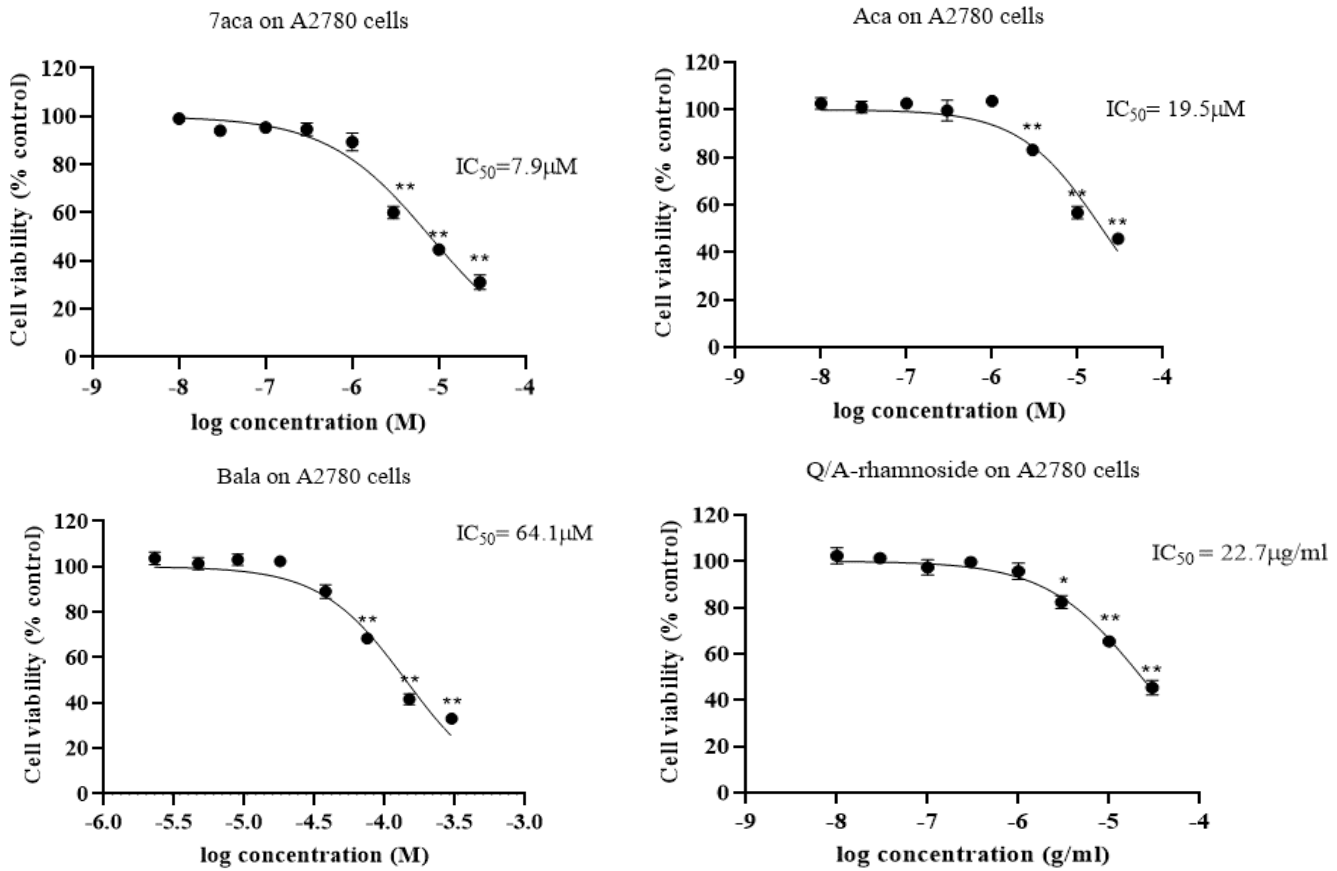

Figure 3.3 Examination of cell viability 48 h treatment with 7-aca, aca, Q/A and bala on A2780 cells. 7-aca and aca were tested at the concentration of 30-0.01µM, Q/A at 30-0.01µg/ml and bala at 300-2.3µM. Data was analysed using One-Way ANOVA with Bonferroni multiple comparison test. Data represents mean ± SEM, n=3. **P<0.01 represents a significant decrease in cell viability vs untreated cells (control).

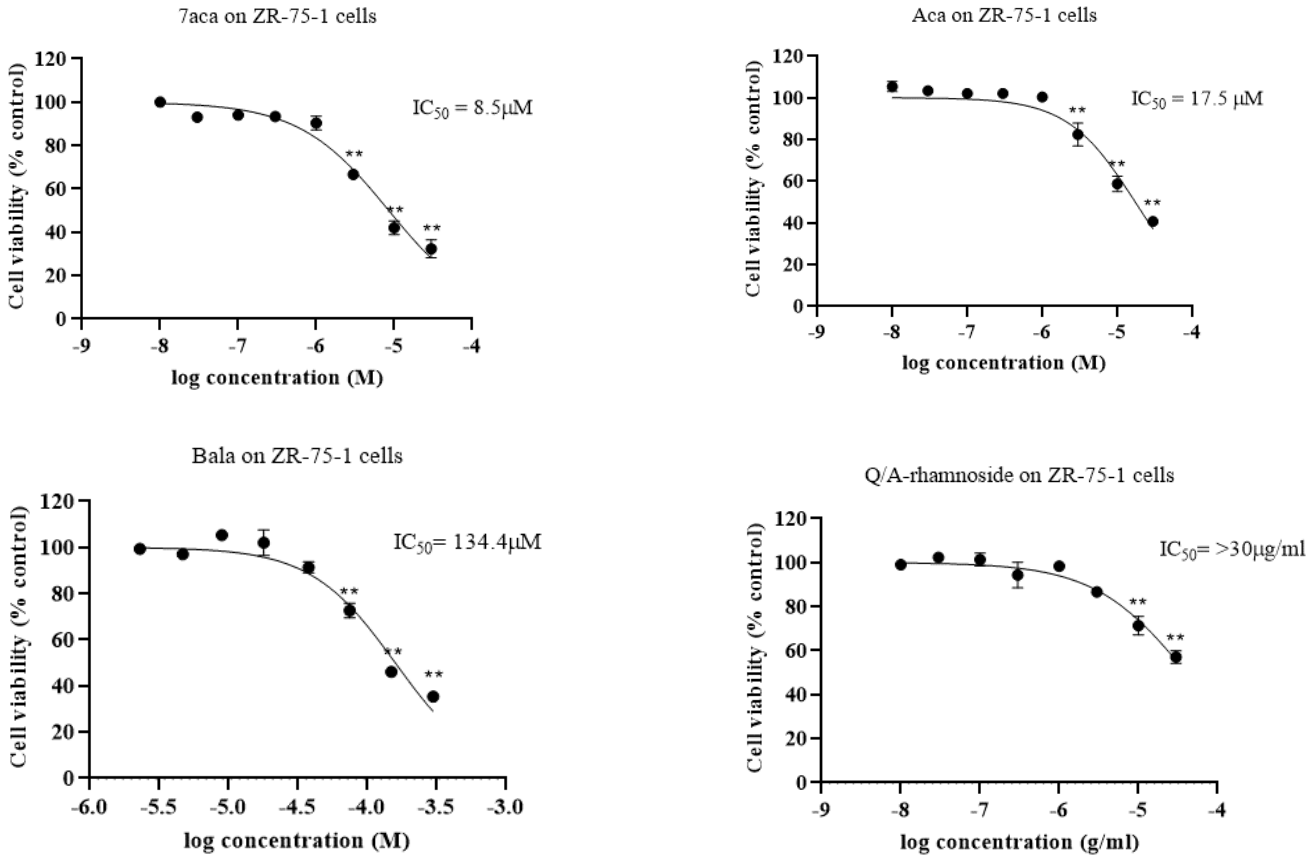

Figure 3.4 Examination of cell viability 48 h treatment with 7-aca, aca, Q/A and bala on ZR-75-1 cell. 7-aca and aca were tested at the concentration of 30-0.01µM, Q/A at 30-0.01µg/ml and bala at 300-2.3µM. Data was analysed using One-Way ANOVA with Bonferroni multiple comparison test. Data represents mean ± SEM, n=3. **P<0.01 represents significant decrease in cell viability vs untreated cells (control).

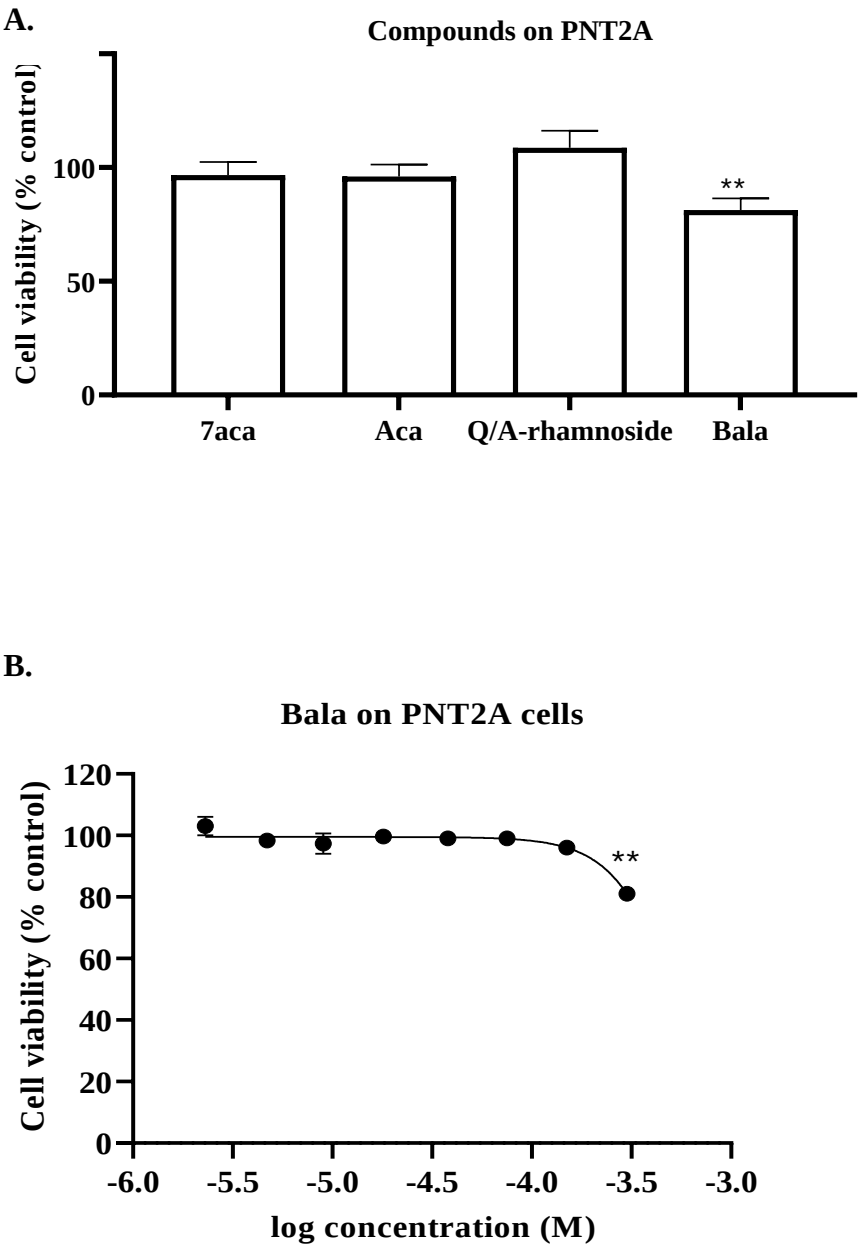

Figure 3.5 A) Examination of cell viability 48 h treatment with 7-aca, aca, Q/A and bala on PNT2A cell. A) 7-aca and aca were tested at the concentration of 30 µM, Q/A at 30 µg/ml and bala at 300 µM. B) Bala were tested at the concentration of 300-2.3 µM. Data was analysed using One-Way ANOVA with Bonferroni multiple comparison test. Data represents mean ± SEM, n=3. **P<0.01 represents significant decrease in cell viability vs untreated cells (control).

3.4.2 DCFH-DA assay

The DCFH-DA assay was carried out with DCFH-DA dye to assess the ability of the extracts and isolated compounds to produce ROS. Increase in dye fluorescence emission is correlated with increased production of ROS. The fluorescence intensity results were compared to the control which had only cells and DCFH-DA to obtain the percentage of DCF fluorescence intensity. For the positive control, cells were stimulated using 100 μM TBPH. AH, AM, HE and isolated compounds showed significant ($P<0.01$) increase in DCF fluorescence compared to the control for both cell lines. Heimiol A did not show any effects on both cell lines as shown in Figure 3.7. All samples except heimiol A increased ROS by more than 3-fold in comparison with the control in both cell lines and the result was statistically significant ($P < 0.01$). 7-Aca was shown to be the most potent ROS generator by increasing ROS 5.3-fold at 30μM in A2780 cells and 4.1-fold in ZR-75-1 cells when compared to the control. 7-Aca was also shown to be significantly ($P<0.05$) more active compared to aca which caused increased ROS in A2780 and ZR-75 cells by 3.9-fold and 3.3-fold, respectively.

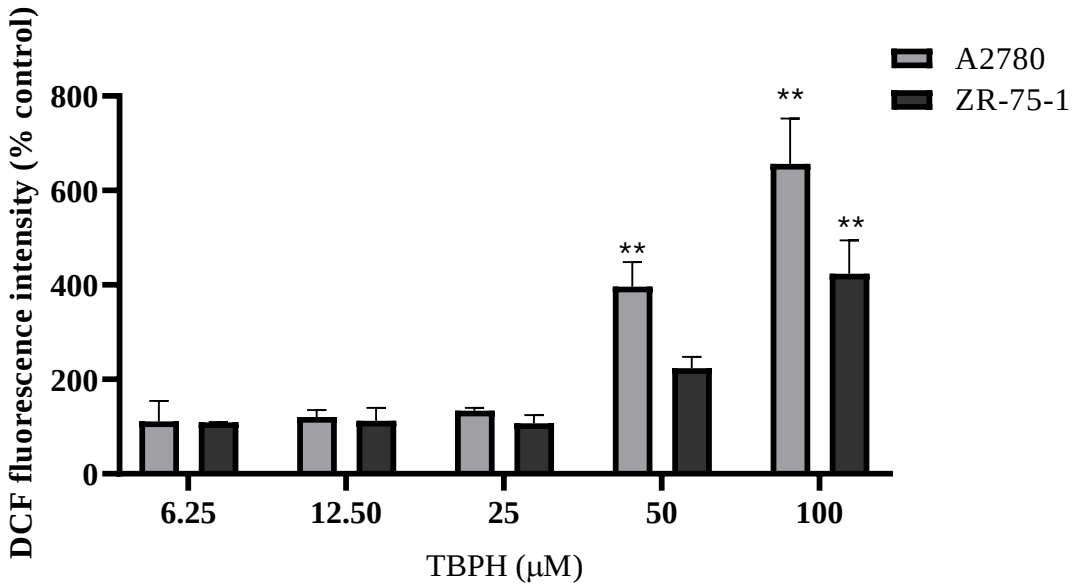

Figure 3.6 ROS production using DCFH-DA solution in A2780 and ZR-75-1 cells after various concentrations of TBHP stimulation for 1.5 h. Data was analysed using One-Way ANOVA with Bonferroni multiple comparison test. Data represents mean ± SEM, n=3. **P<0.01 represents a significant increase in ROS generation vs untreated cells (control).

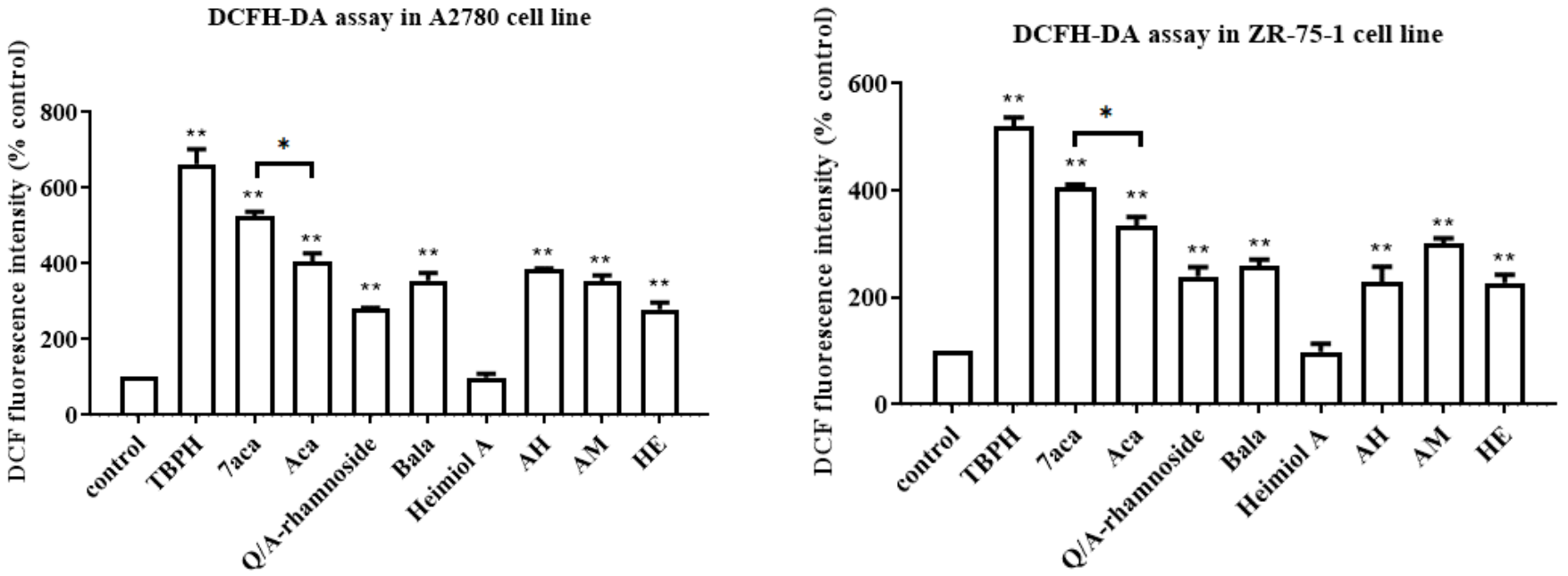

Figure 3.7 ROS measurement using DCFH-DA solution in A2780 and ZR-75-1 cells after stimulation with test samples or 100 µM TBPH for 1.5 h. 7-aca and aca were tested at 30µM. Q/A and plant extracts were tested at 30µg/ml. Bala and heimiol A were tested at 150 µM. Data was analysed using One-Way ANOVA with Bonferroni multiple comparison test. **P<0.01 and *P<0.05 represents significant increase in ROS generation vs untreated cells (control).

3.4.3 TMRE assay

Loss of ΔΨM of A2780 and ZR-75-1 was measured after treatment with all isolated compounds including aca and selected plant extracts using TMRE dye. Reduction in TMRE fluorescence indicated cells were losing their mitochondrial membrane integrity. Figure 3.8 shows the ability of FCCP (positive control) at a range of concentrations to eliminate ΔΨM and TMRE staining. All plant extracts and compounds except for heimiol A showed comparable results to those for the control when tested at 30 μg/ml for extracts and Q/A, 30 μM for 7-aca and aca, 150 μM for bala in A2780 and ZR-75-1 cells (Figure 3.11). Exposure to 30 μM of 7-aca resulted in 70% loss of ΔΨM in A2780 and ZR-75-1 cells which was significantly ($P<0.05$) more potent than aca. Incubation with 7-aca, aca, Q/A and bala resulted in a concentration-dependent decrease in ΔΨM for both cell lines (**Error! Reference s ource not found.** and **Error! Reference source not found.**). At the highest concentration of 150μM, bala showed a weak effect on decreasing the ΔΨM of ZR-75-1 cells (**Error! Reference source not found.**). Q/A also showed a weak effect on d ecreasing the ΔΨM of ZR-75-1 cells as well as A2780.

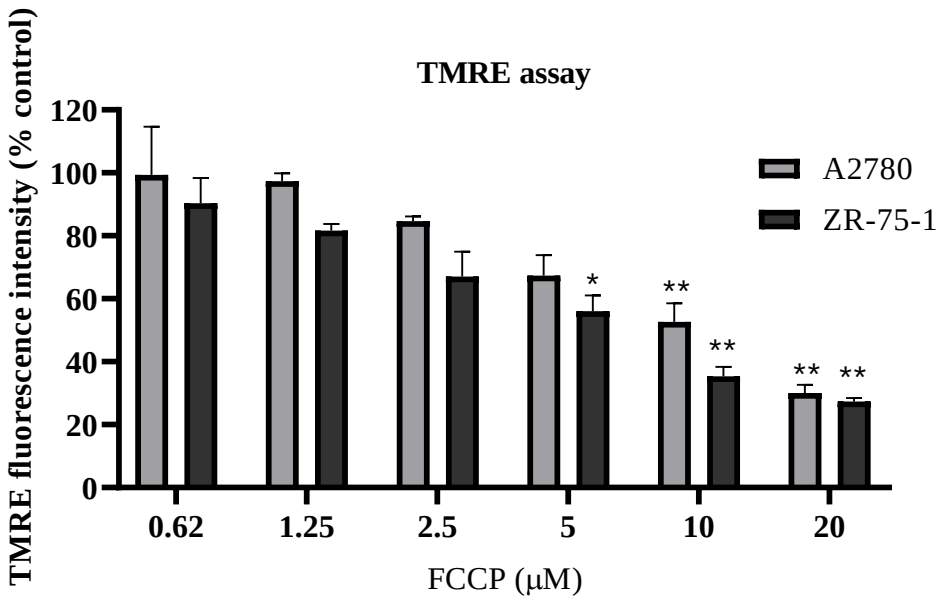

Figure 3.8 ΔΨM measurement using TMRE in A2780 and ZR-75-1 cells after stimulation with FCCP (30min). Fluorescence intensity was measured using a fluorescence microplate reader. Data was analysed using One-Way ANOVA with Bonferroni multiple comparison test. Data represents mean ± SEM, n=3. **P<0.01 and *P<0.05 represents a significant decrease in ΔΨM vs untreated cells (control).

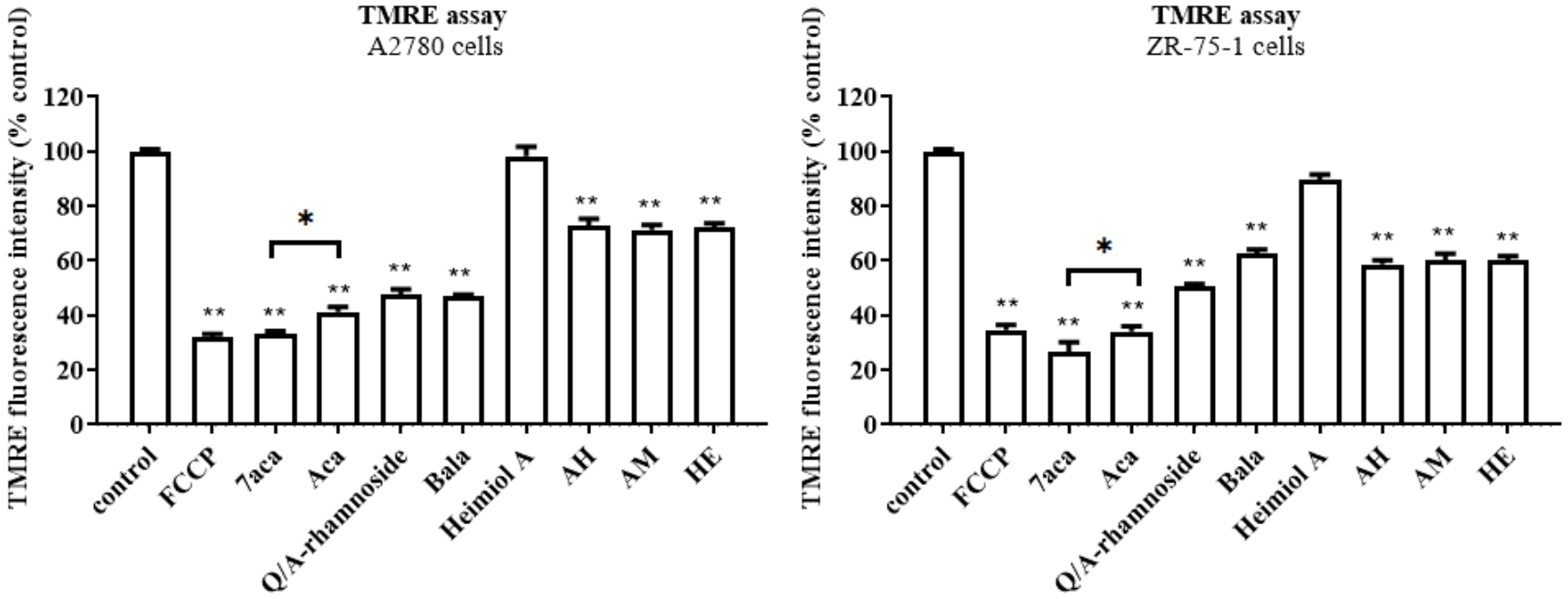

Figure 3.9 ΔΨM measurement using TMRE in A2780 and ZR-75-1 cells after stimulation with test samples (12 h) or FCCP (30min). 7-aca and aca were tested at the concentration of 30µM. Q/A and plant extracts were tested at 30µg/ml. Bala and heimiol A was tested at 150 µM. Data was analysed using One-Way ANOVA with Bonferroni multiple comparison test.**P<0.01 and *P<0.05 represents significant decrease in ΔΨM vs untreated cells (control).

3.4.4 Caspase-Glo 3/7 assay

To examine if 7-aca, aca, Q/A, bala and the plant extracts induced an apoptotic signalling pathway in A2780 and ZR-75-1 cells, caspase-3/7 levels were measured at 6,12 and 24 h after treatment by measuring the luminescent signal (RFU) produced by caspase cleavage of the substrate. Staurosporine was used as a positive control, as this drug is known to induce apoptosis in cancer cells. Staurosporine induced caspase-3/7 in A2780 and ZR-75-1 cells in 6 h in a concentration-dependent manner (10-0.07 μM) (Figure 3.10). Caspase-3/7 levels were not elevated for all compounds in treated cells over the period of 6 h (Figure 3.11). At 12 h, caspase-3/7 increased dramatically for all the compounds in both cell lines. The highest increment in RFU was seen by treatment of 7-aca (30μM) in both cell lines. The compounds increased caspase-3/7 levels 5 to 7-fold after 12 h. By 24 h, all compounds induced production of caspase-3/7 by at least 7 to 9-fold. There was a significant difference ($P<0.05$) between the caspase levels induced by 7-aca and aca for both cell lines in 12 and 24 h.

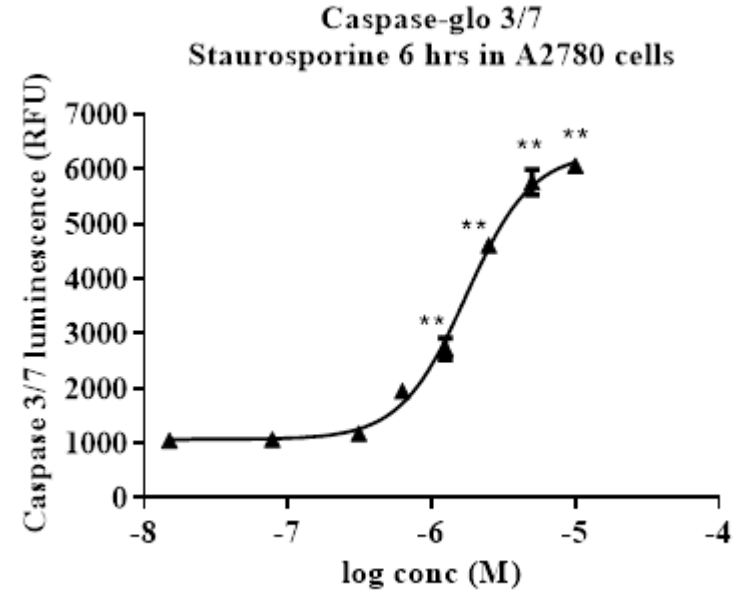

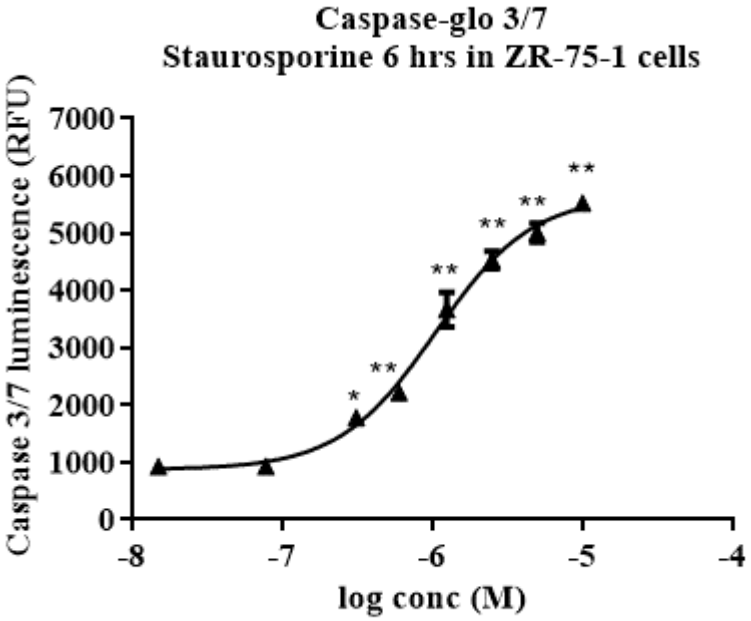

Figure 3.10 Caspase-3/7 activation evaluation in A2780 and ZR-75-1 cells treated with 10-0.07 μM Staurosporine for 6 h. Data was analysed using One-Way ANOVA with Bonferroni multiple comparison test. Data represents mean ± SEM, n=3. **P<0.01 and *P<0.05 represents a significant increase in caspase activity vs untreated cells (control).

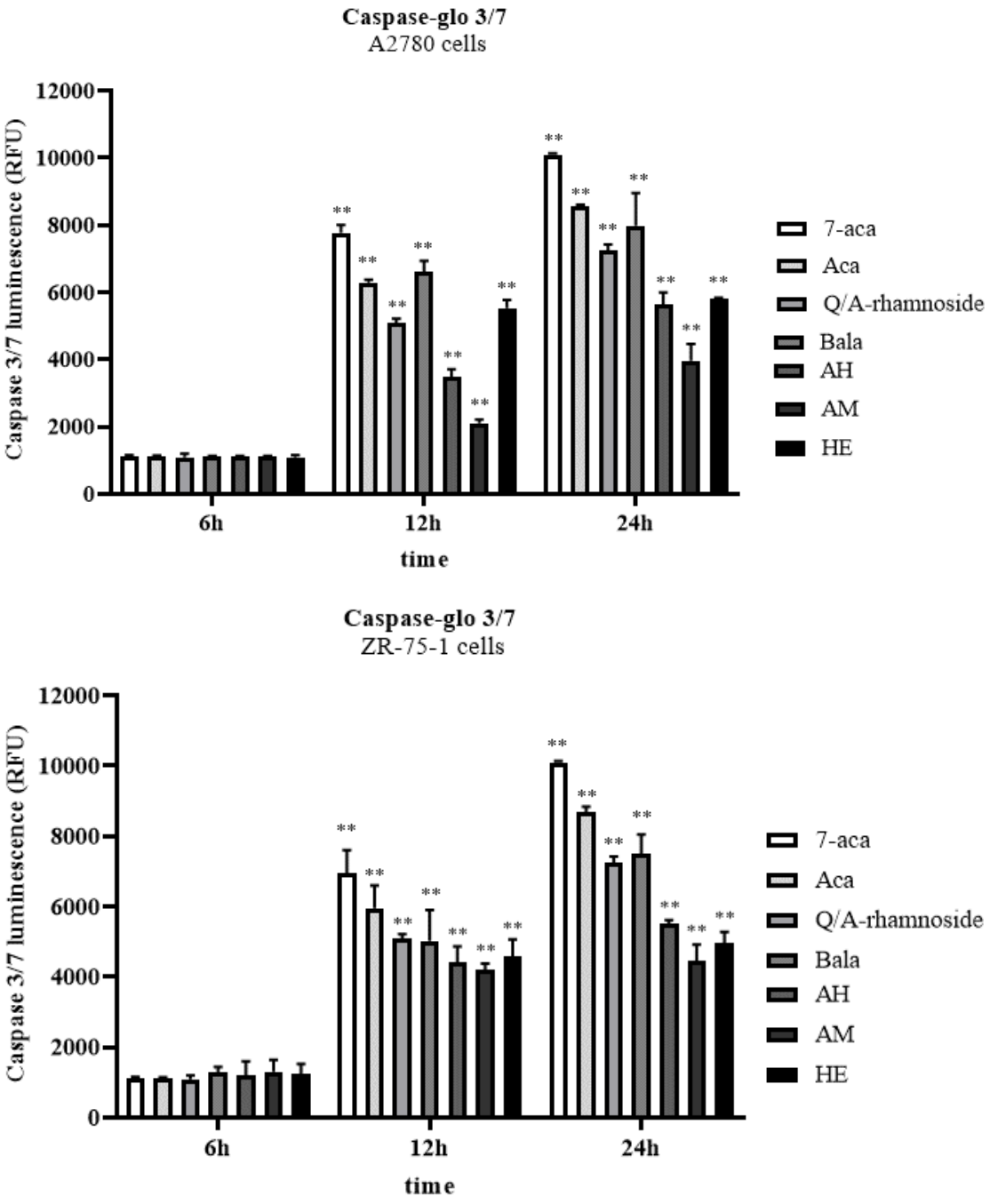

Figure 3.11 Caspase-3/7 activation evaluation in A2780 and ZR-75-1 cells treated with 7-aca and aca at 30 µM, Q/A at 30 µg/ml and bala at 150µM for 6,12 and 24 h. Data was analysed using One-Way ANOVA with Bonferroni multiple comparison test. **P<0.01 and *P<0.05 represents significant increase in caspase activity vs untreated cells (control). AH; *A. malaccensis* hexane, AM; *A. malaccensis* methanol, HE; *H. drybalanoides* ethyl acetate.

3.4.5 Cell adhesion, migration and invasion

The cell adhesion assay revealed that adhesion of A2780 and ZR-75-1 cells to fibronectin-coated wells was significantly ($P<0.01$) reduced under the treatment of 7-aca, aca, and bala in comparison to untreated cells (Figure 3.12). 7-Aca (1µM) was shown to be the most active by reducing cell adhesion by approximately 70.3% in A2780 cells and 61.7% in ZR-75-1 cells followed by aca (1µM) which reduced cell adhesion by 63% in A2780 cells and 46% in ZR-75-1 cells. Exposing A2780 and ZR-75-1 cells to bala at a concentration of 30µM inhibited cell adhesion significantly ($P<0.01$) by approximately 50.7% and 30%, respectively. To study the anti-migratory effects of test compounds, a cell migration assay was carried out using a Cytoselect^{TM} 24-well Cell Migration Assay. Compound treatment significantly ($P<0.01$) reduced the migration of cells relative to that of untreated controls (Figure 3.13). Treatment of A2780 and ZR-75-1 cells to 7-aca (1µM) significantly ($P<0.01$) reduced cell migration by 56.7 and 42.3%, respectively. This was followed by aca which inhibited cell migration by 40.7% for A2780 and 32.3% for ZR-75-1. There was also a significant ($P<0.05$) inhibitory effect of bala on cell migration of A2780 and ZR-75-1 cells.

To analyse the ability of A2780 and ZR-75-1 cells to invade the surrounding ECM, an invasion assay was performed using a Cytoselect^{TM} 24-well Cell Invasion Assay. The invasiveness of A2780 and ZR-75-1 cells under the treatment of 7-aca, aca and bala significantly ($P<0.01$) reduced invasion compared to untreated cells (Figure 3.14). Treatment of both cells with 7-aca reduced the percentage of invading cells by approximately 50% and aca reduced cell invasion by approximately 40%.

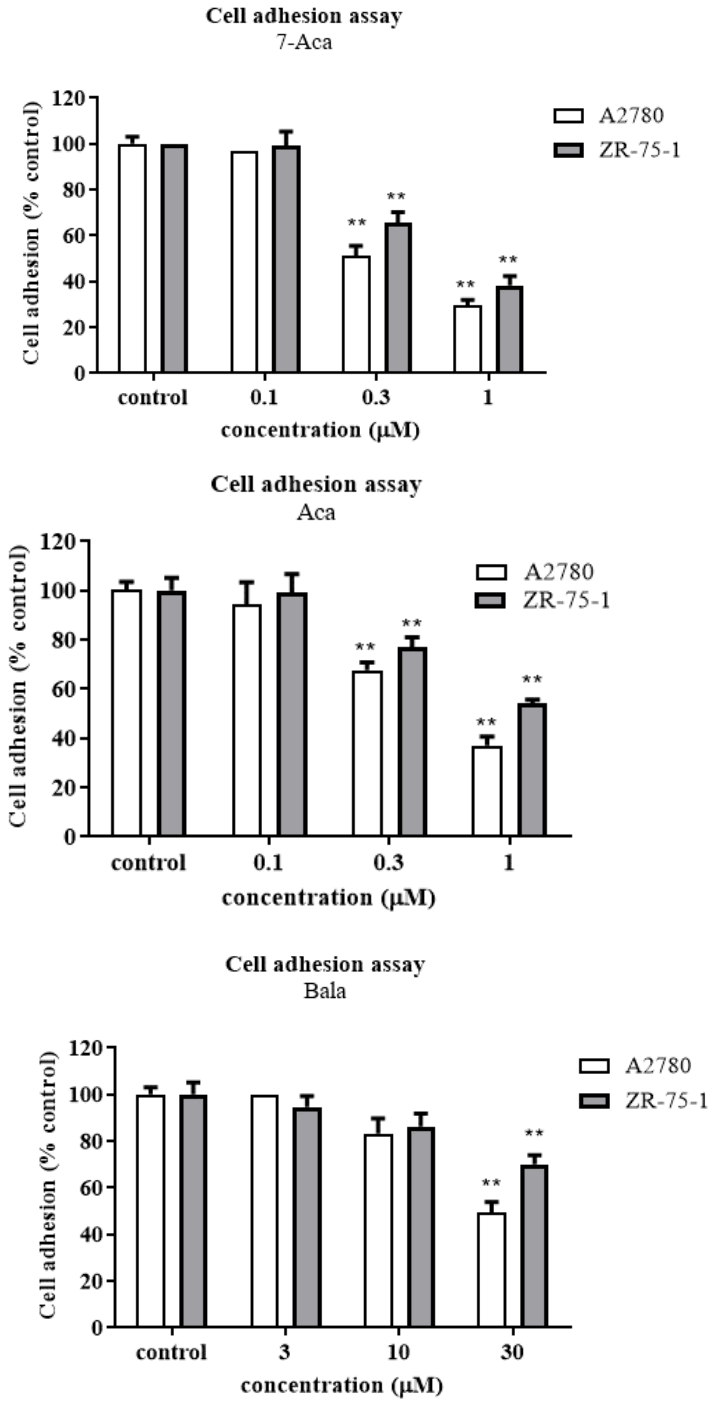

Figure 3.12 Effect of 7-aca, aca and bala on the cell adhesion of A2780 and ZR-75-1 cells over 24 h. Data was analysed using One-Way ANOVA with Bonferroni multiple comparison test. **P<0.01 represents significant decrease in cell adhesion vs untreated cells (control).

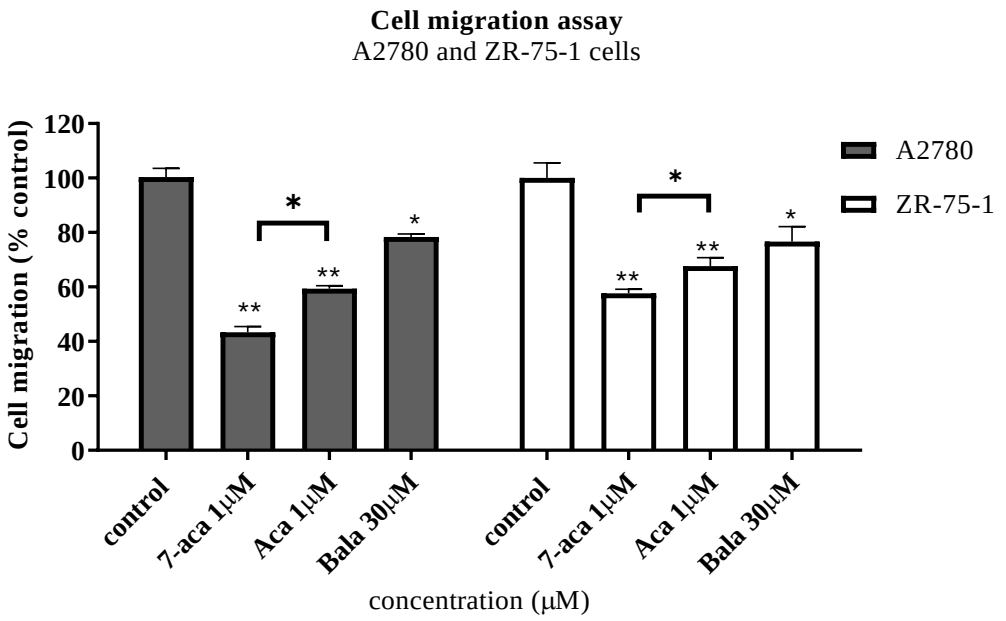

Figure 3.13 Effect of 7-aca and aca at 1μM and bala at 30μM on the cell migration of A2780 and ZR-75-1 cells over 24 h. Data was analysed using One-Way ANOVA with Bonferroni multiple comparison test. **P<0.01 and *P<0.05 represents significant decrease in cell adhesion vs untreated cells (control).

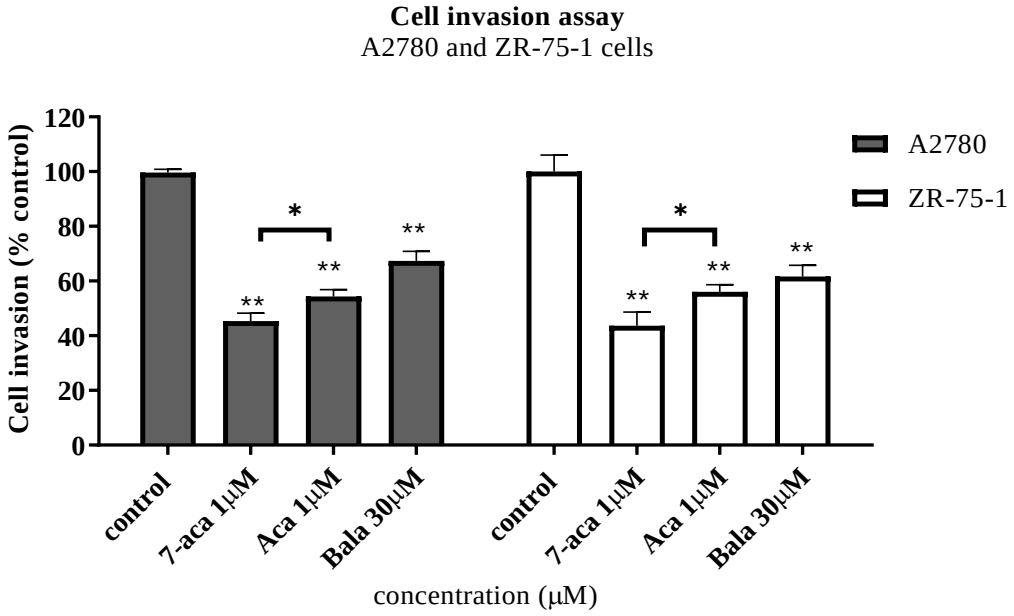

Figure 3.14 Effect of 7-aca and aca at 1 μM and bala at 30μM on the cell invasion of A2780 and ZR-75-1 cells over 24 h. Data was analysed using One-Way ANOVA with Bonferroni multiple comparison test. **P<0.01 and *P<0.05 represents significant decrease in cell adhesion vs untreated cells (control).

3.4.6 Metabolomics study

From the previous experiments 7-aca and its commercial counterpart aca were shown to be the most active compounds. Therefore, only these two compounds were chosen for a LC-MS based metabolomics study in order to gain a better understanding of the mechanism of the compounds' anti-cancer activity in the A2780 and ZR-75-1 cell lines. It also allows differences in the levels of metabolites induced by treatment with the two similar compounds to be observed. Multivariate analysis techniques such as PCA and OPLS-DA models were used in this study. To measure the precision of the instrument, pooled samples (P1, P2, P3 and P4) were injected four times during the course of the run and from the PCA scores plot the pooled samples were shown to be clustered close together in the middle of the plot which indicated that the LC-MS system is stable throughout the entire analytical run (Figure 3.15*)*. A clear separation was also seen of treated cells and their respective untreated controls indicating unique metabolite profiles for the treated and control cells on a PCA scores plot. The model parameters and validation of the PCA plot suggested a good model (R2X (cum) = 0.873; Q2 (cum) = 0.777). Next, OPLS-DA was used to understand the differences between treatments and to identify the biomarkers that distinguish one treatment from another. The OPLS-DA model showed a clear clustering pattern for each treated cell line and untreated cells (Figure 3.16). The CV-ANOVA of the model (A) P = 2.48E-05 and model (B) P = 1.55E-05 indicated that the model is valid. There was also a very clear separation between the 7-aca treatment and aca treatment in both cell lines as showed in the OPLS-DA model. OPLS-DA has been widely used in the metabolomics field, and it is now the method of choice for multivariate linear models for classification (i.e. classifying new objects into one of the classes) and class

discrimination (i.e. separating two classes and investigate the reasons for the class separation), such as biomarker discovery and lower and higher concentrations of metabolites.

Table 3.1 and Table 3.2 demonstrated clear differences in metabolic levels between 7-aca and aca in A2780 and ZR-75-1 cells, thereby confirming distinct metabolic profiles for each treatment. 7-aca and aca significantly ($P<0.05$) affected pathways associated with cancer metabolism, including the tricarboxylic acid (TCA) cycle, OXPHOS and the pentose phosphate pathway (PPP) for A2780 and ZR-75-1 cells. The majority of the levels of metabolites such as ATP/ADP and NADH/NAD were lowered after treatment of 7-aca and aca in both cell lines. However, most metabolites were reduced more in 7-aca-treated cells compared to aca-treated cells. Furthermore, a clear significant ($P<0.05$) decrease was noted in the levels of metabolites involved in the TCA/glycolysis pathway such as acetyl-COA, D-glucose 1-phosphate, D-fructose 6-phosphate and oxalosuccinate for 7-aca treatment in both cells, but aca showed a weaker effect on the same metabolites. In the pentose phosphate pathway (PPP), metabolites such as D-Glucose 6-phosphate (G6PD) and D-Sedoheptulose 7-phosphate were decreased significantly ($P<0.05$) by 7-aca and aca in both cell lines.

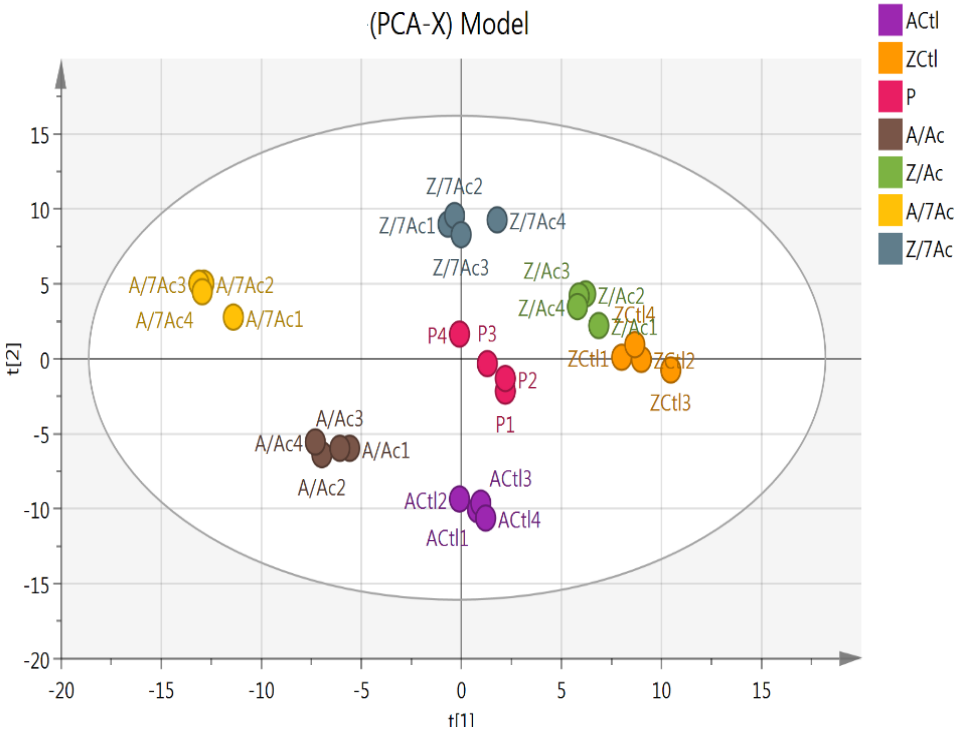

Figure 3.15 Represent Principal components analysis (PCA) plots. PCA scores plot generated from PCA using LC-MS normalized data of cells after exposure to 7-aca, aca and controls of A2780 and ZR-75-1 cell lines. The groups: ACtl, control of A2780; ZCtl, control of ZR-75-1; A/Ac, A2780 after treatment with aca; Z/Ac, ZR-75-1 after treatment with aca; A/7Ac, A2780 after treatment with 7-aca; Z/7Ac, ZR-75-1 after treatment with 7-aca. P1, P2, P3 and P4 represent the pooled sample frequently runs throughout the experiment.

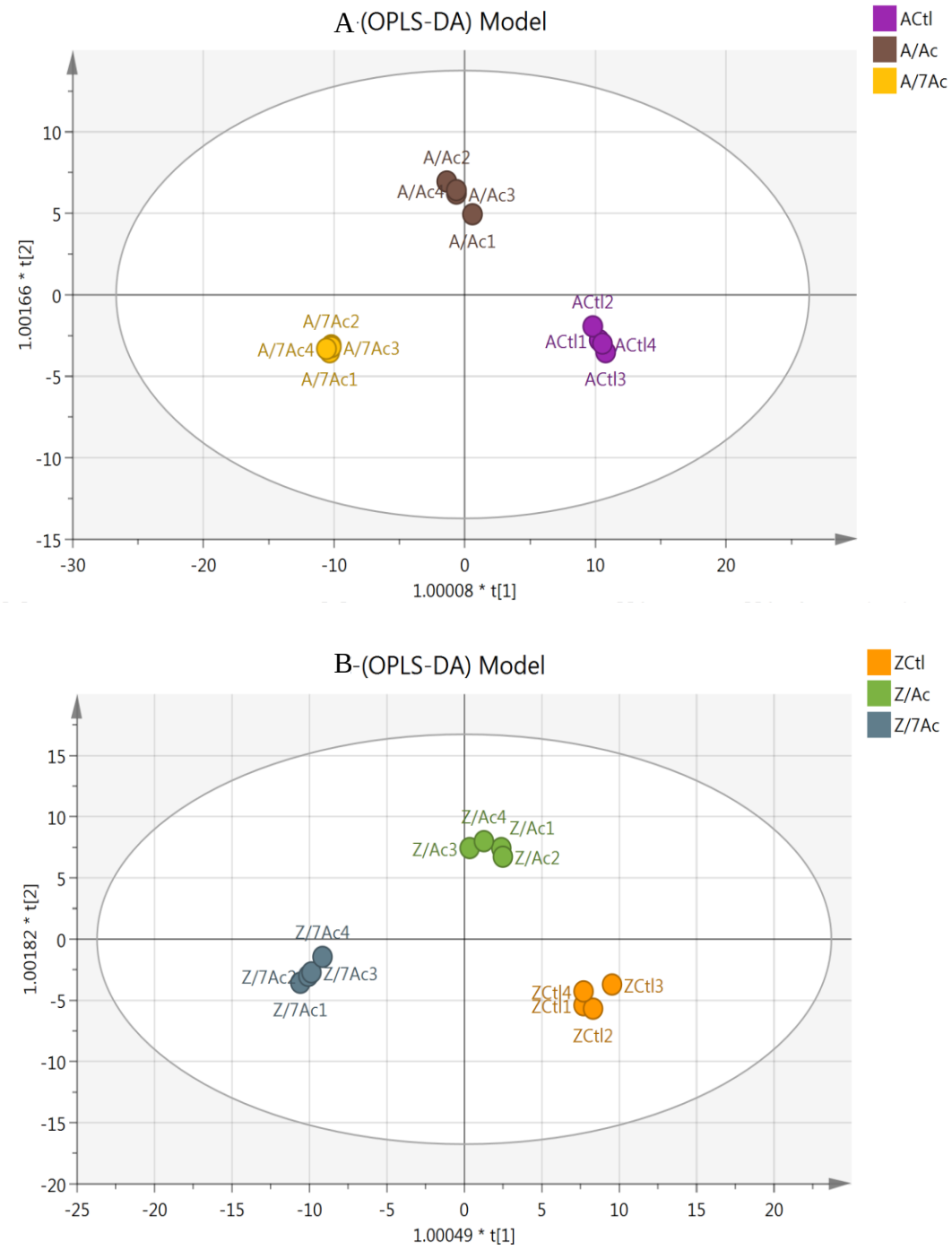

Figure 3.16 OPLS-DA score plots OPLS-DA scores plot generated from OPLS-DA using LC-MS normalized data of cells after exposure to A) 7-aca, aca and control of A2780 cells. B) 7-aca, aca and control of ZR-75-1 cells. The groups: ACtl, control of A2780; ZCtl, control of ZR-75-1; A/Ac, A2780 after treatment with aca; Z/Ac, ZR-75-1 after treatment with aca; A/7Ac, A2780 after treatment with 7-aca; Z/7Ac, ZR-75-1 after treatment with 7-aca.

Table 3.1 Significantly changed metabolites within A2780 cells treated with 30 µM aca and 7-aca in comparison with untreated controls

Mass A2780	**RT**	**Metabolites**	**Aca**		**7-aca**	
			Ratio	P-value	Ratio	P-value
Arginine and proline metabolism						
246.13	14.38	N2-(D-1-Carboxyethyl)-L-arginine	0.263	0.000	0.132	0.000
175.09	16.39	L-Citrulline	0.461	0.000	0.370	0.000
211.03	15.98	Phosphocreatine	0.584	0.000	0.602	0.000
290.12	17.46	N-(L-Arginino) succinate	0.764	0.018	0.120	0.001
113.04	14.85	1-Pyrroline-2-carboxylate	0.395	0.001	0.570	0.012
103.06	14.96	4-Aminobutanoate	0.871	0.075	1.333	0.005
174.11	27.27	D-Arginine	0.713	0.000	0.647	0.000
Glycolysis/ TCA cycle						
767.11	14.41	CoA	0.948	ns	0.567	0.000
190.01	17.49	Oxalosuccinate	0.835	0.000	0.222	0.000
185.99	18.14	3-Phosphoglycerate	0.876	ns	0.027	0.000
260.03	17.69	D-Glucose 1-phosphate	0.807	0.008	0.143	0.000
809.12	12.96	Acetyl-CoA	0.804	ns	0.246	0.009
260.03	3.66	D-Fructose 6-phosphate	0.848	0.000	0.180	0.000
OXPHOS/Pentose phosphate pathway						
177.94	15.96	Pyrophosphate	0.441	0.000	0.252	0.000
665.12	13.61	NADH	0.728	0.004	0.256	0.000
663.10	14.45	NAD+	0.737	ns	0.416	0.002
97.97	15.41	Orthophosphate	1.861	ns	1.639	0.007
506.99	17.57	ATP	0.536	0.005	0.167	0.000
427.02	14.45	ADP	0.757	0.004	0.449	0.000
260.03	17.00	D-Glucose 6-phosphate	0.440	0.000	0.278	0.000
290.04	17.14	D-Sedoheptulose 7-phosphate	0.575	0.003	0.215	0.000
230.01	16.98	D-Xylulose 5-phosphate	0.895	0.841	0.590	0.000
Gluthahione/Glutamate metabolism						
178.04	14.96	Cys-Gly	0.442	0.000	0.451	0.000
259.04	16.05	D-Glucosamine 6-phosphate	0.549	0.000	0.396	0.000
301.05	15.95	N-Acetyl-D-glucosamine 6-phosphate	0.523	0.000	0.658	0.000
612.15	18.20	Glutathione disulfide	0.628	0.006	0.177	0.001
745.09	18.30	NADPH	0.671	0.007	0.420	0.001
743.07	17.56	NADP+	0.630	0.008	0.565	0.000
Pyrimidine metabolism						
403.01	18.15	CDP	0.582	0.010	0.141	0.000

324.03	17.36	3'-UMP	0.683	0.001	0.281	0.000
323.05	18.12	3'-CMP	0.683	0.001	0.129	0.000
227.09	15.97	Deoxycytidine	0.693	0.001	0.735	0.000
111.04	10.5	Cytosine	0.696	0.008	0.539	0.001
324.03	20.54	Pseudouridine 5'-phosphate	0.734	0.003	0.674	0.002
483.96	19.18	UTP	0.839	ns	0.685	0.002
403.01	19.72	CDP	0.866	ns	0.615	0.007
244.06	12.30	Pseudouridine	1.398	0.003	1.626	0.005
176.04	17.92	N-Carbamoyl-L-aspartate	0.476	0.000	0.017	0.000
89.04	15.76	beta-Alanine	0.412	0.000	0.360	0.000
114.04	13.10	5,6-Dihydrouracil	0.236	0.000	0.189	0.000
112.02	12.44	Uracil	0.673	0.001	0.726	ns
404.00	15.97	UDP	0.495	0.000	0.509	0.000
Alanine metabolism						
89.04	15.13	L-Alanine	0.491	0.003	0.614	0.001
226.10	16.11	Carnosine	1.258	0.011	1.526	0.001
Fructose/mannose/ galactose metabolism						
589.08	18.65	GDP-L-fucose	0.670	0.000	0.462	0.000
182.07	14.35	Mannitol	0.951	ns	0.692	0.005
605.07	19.3	GDP-mannose	0.836	0.001	0.462	0.000
180.06	13.93	D-Fructose	1.313	0.075	2.496	0.000
180.06	17.80	D-Galactose	1.224	ns	3.817	0.000
Glycine/serine metabolism						
103.06	12.39	N,N-Dimethylglycine	0.940	0.005	0.931	ns
117.05	16.30	Guanidinoacetate	1.246	ns	1.430	0.002
103.09	21.63	Choline	1.444	ns	2.338	0.000
105.04	16.36	L-Serine	2.392	0.002	2.678	0.000
Miscellaneous						
222.06	17.72	Cystathionine	0.443	0.000	0.149	0.000
109.01	15.49	Hypotaurine	0.377	0.000	0.311	0.000
227.04	18.010	5-(2'-Carboxyethyl)-4,6-dihydroxypicolinate	0.940	ns	0.060	0.000
109.05	42.43	2-Aminophenol	1.484	0.006	1.237	ns
204.08	11.89	L-Tryptophan	2.641	0.000	2.468	0.000
197.06	21.83	3,4-Dihydroxy-L-phenylalanine	0.372	0.000	0.122	0.000
137.0	42.41	Tyramine	1.388	ns	1.779	0.001
153.07	42.38	Dopamine	1.455	ns	1.513	0.001
103.06	11.73	L-3-Amino-isobutanoate	0.940	0.006	0.925	0.004
179.05	15.53	Hippurate	1.149	0.000	1.277	0.009
851.17	10.55	Pentanoyl-CoA	1.006	ns	3.026	0.000
110.04	13.02	Imidazole-4-acetaldehyde	0.450	0.000	0.453	0.000
111.07	44.01	1H-Imidazole-4-ethanamine	0.966	ns	0.888	0.043

283.04	15.97	N2-Acetyl-L-aminoadipyl-delta-phosphate	0.565	0.000	0.579	0.000

RT:min; Aca: Aca treated A2780; 7-aca: 7-aca treated A2780; ns: non-significant. * Matched to retention time of standard.

Table 3.2 Significantly changed metabolites within ZR-75-1 cells treated with 30 μM aca and 7-aca in comparison with untreated controls.

Mass	**RT**	**Metabolites**	**Aca**		**7-aca**	
			Ratio	*P*-value	Ratio	*P*-value
Arginine and proline metabolism						
175.09	16.39	L-Citrulline	0.672	0.001	0.525	0.000
211.03	15.98	Phosphocreatine	0.525	0.000	0.238	0.000
290.12	17.46	N-(L-Arginino) succinate	1.490	0.008	0.818	ns
113.04	9.26	1-Pyrroline-2-carboxylate	0.815	ns	0.597	0.000
174.11	27.27	D-Arginine	1.375	0.003	1.623	0.001
103.06	15.84	4-Aminobutanoate	0.955	0.108	0.833	0.003
Glycolysis/ TCA cycle						
190.01	17.49	Oxalosuccinate	0.914	ns	0.472	0.000
767.44	14.41	CoA	1.003	ns	0.270	ns
185.99	18.14	3-Phosphoglycerate	0.931	ns	0.411	0.000
809.12	12.96	Acetyl-CoA	0.868	0.000	0.485	0.000
260.03	17.69	D-Glucose 1-phosphate	0.977	ns	0.546	0.000
260.03	3.66	D-Fructose 6-phosphate	0.823	ns	0.630	0.013
OXPHOS/Pentose phosphate pathway						
177.94	15.96	Pyrophosphate	0.817	ns	0.207	0.007
665.12	13.61	NADH	0.374	0.000	0.174	0.000
663.10	14.45	NAD+	0.633	0.000	0.323	0.000
97.976	15.41	Orthophosphate	1.878	0.000	1.227	ns
427.02	16.00	ADP	0.686	0.008	0.227	0.000
506.99	17.57	ATP	0.644	0.000	0.200	0.000
260.03	17.00	D-Glucose 6-phosphate	0.654	0.000	0.488	0.003
290.04	17.14	D-Sedoheptulose 7-phosphate	0.678	0.001	0.033	0.000
230.01	16.98	D-Xylulose 5-phosphate	0.584	ns	0.305	0.000
Glutamate/glutathione metabolism						
745.09	18.30	NADPH	0.756	0.005	0.629	0.001
743.07	17.56	NADP+	0.426	0.004	0.255	0.002
178.04	14.96	Cys-Gly	0.534	0.002	0.222	0.013

259.04	16.05	D-Glucosamine 6-phosphate	0.648	0.000	0.448	0.000
301.05	15.95	N-Acetyl-D-glucosamine 6-phosphate	0.711	0.000	0.347	0.002
612.15	18.20	Glutathione disulfide	0.630	0.001	0.456	0.030
Pyrimidine metabolism						
483.96	19.18	UTP	2.502	0.000	2.051	0.000
244.06	12.30	Pseudouridine	1.971	0.000	2.156	0.000
324.03	19.14	Pseudouridine 5'-phosphate	2.467	0.000	1.190	ns
227.09	14.65	Deoxycytidine	0.696	0.001	0.690	0.000
111.04	10.54	Cytosine	0.730	0.004	0.573	0.004
324.03	17.36	3'-UMP	1.139	ns	0.460	0.000
324.03	20.54	Pseudouridine 5'-phosphate	0.789	0.043	0.736	0.004
323.05	18.12	3'-CMP	0.928	ns	0.227	0.000
403.01	18.15	CDP	1.067	ns	0.297	0.000
176.04	17.99	N-Carbamoyl-L-aspartate	0.774	ns	0.120	0.000
89.04	15.76	beta-Alanine	0.987	ns	0.860	0.033
112.02	12.44	Uracil	0.762	0.007	0.648	0.005
114.04	13.10	5,6-Dihydrouracil	0.779	ns	0.433	0.004
404.00	15.97	UDP	0.759	0.009	1.121	ns
Fructose/mannose/ galactose metabolism						
589.08	18.65	GDP-L-fucose	0.875	ns	0.501	0.000
244.03	14.29	L-Fuculose 1-phosphate	1.922	0.015	2.891	0.002
182.07	14.35	Mannitol	0.617	0.004	1.117	ns
605.07	19.32	GDP-mannose	0.692	0.006	0.483	0.000
180.06	15.01	D-Mannose	207.392	0.000	428.201	0.000
180.06	13.93	D-Fructose	1.750	0.001	2.950	0.000
180.06	17.80	D-Galactose	0.955	ns	2.943	0.000
254.10	13.85	3-beta-D-Galactosyl-sn-glycerol	0.538	0.001	0.409	0.000
Glycine/serine metabolism						
103.09	14.94	Choline	0.380	0.007	0.260	0.000
105.04	16.36	L-Serine	2.045	0.000	2.926	0.007
Miscellaneous						
536.04	17.27	UDP-D-xylose	1.430	ns	0.204	0.001
222.06	17.72	Cystathionine	1.691	0.000	0.930	ns
189.04	42.45	Kynurenate	1.462	0.002	3.191	0.000
109.05	7.52	2-Aminophenol	1.867	0.014	1.617	0.007
204.08	11.89	L-Tryptophan	1.291	0.022	0.958	ns
306.97	42.12	Iodotyrosine	1.583	0.019	1.692	0.010
137.08	42.41	Tyramine	1.517	0.001	1.522	0.006
153.07	42.38	Dopamine	1.239	0.023	1.155	ns
181.07	13.43	L-Tyrosine	1.384	0.020	0.905	ns

103.06	11.73	L-3-Amino-isobutanoate	0.823	0.001	0.753	0.000
179.05	42.64	Hippurate	1.084	ns	1.373	0.005
192.02	19.42	5-Dehydro-4-deoxy-D-glucarate	1.317	0.000	1.274	0.002
255.99	20.54	L-Ascorbate 6-phosphate	0.704	0.009	0.719	0.006
219.11	8.90	Pantothenate	1.927	0.001	3.293	0.000
84.02	8.48	3-Butynoate	0.259	0.000	0.124	0.000
168.01	4.35	Butanoylphosphate	1.538	0.013	1.596	0.010
210.07	14.49	Sedoheptulose	0.987	ns	0.233	0.000

RT:min; Aca: aca treated ZR-75-1; 7-aca: 7-aca treated ZR-75-1; ns: non-significant.

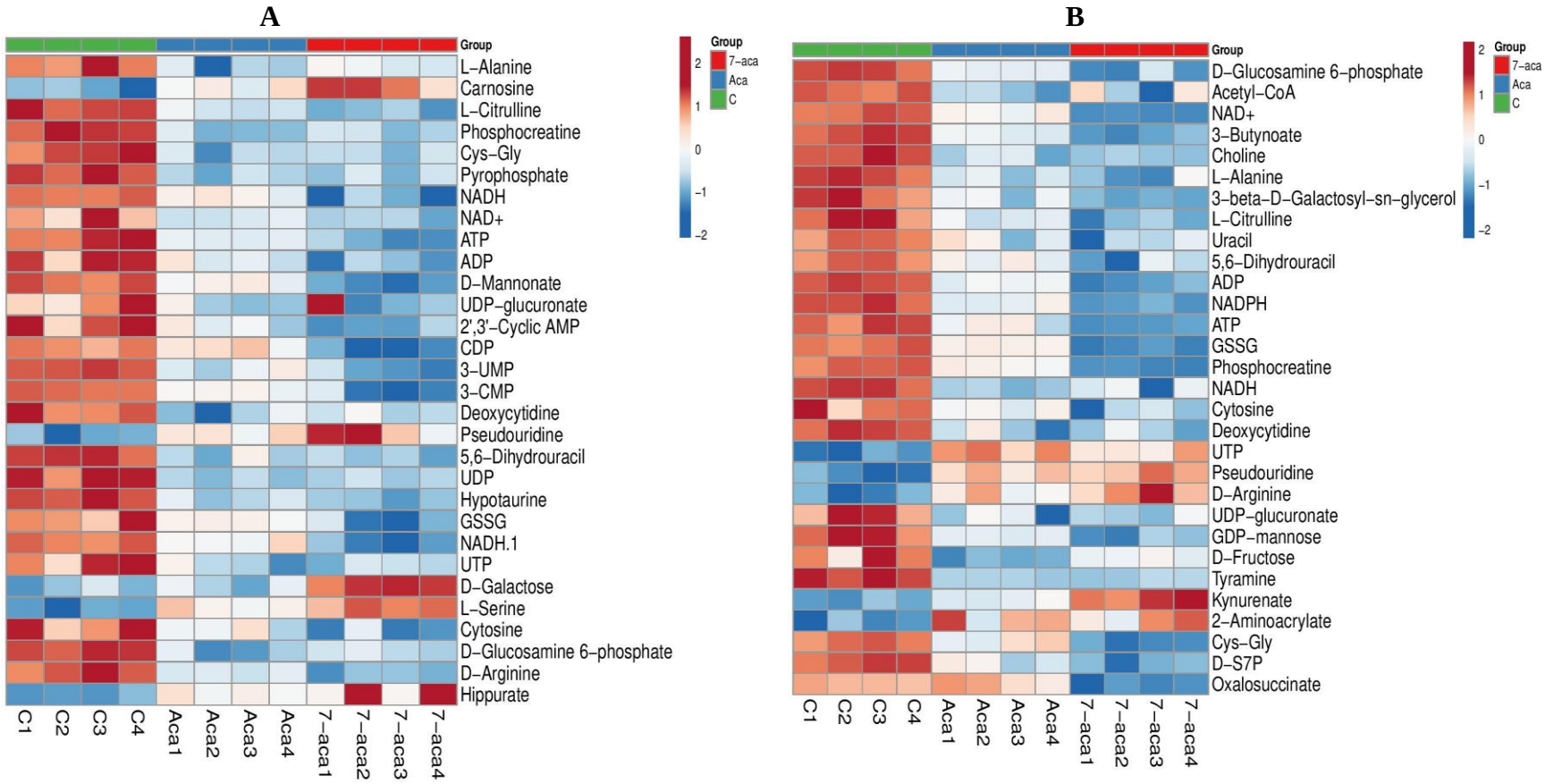

Figure 3.17 Heatmap showing alterations of the top 30 most significant putative metabolites A) between control, 7-aca and aca in A2780 cells and B) between control, 7-aca and aca in ZR-75-1 cells. Row: represents the metabolite; Column: represents the samples; The colour key specifies the metabolite intensity: lowest: dark blue; highest: dark red. The data are displayed on a log2 scale.

3.5 Discussion

Natural products can exhibit anticancer activity through inhibition of multiple cellular pathways. The main objective of this chapter was to investigate *A. malaccensis* and *H. dryobalanoides* plant extracts and their isolated compounds for their potential anticancer properties. The assays chosen were suitable for primary high-throughput screening.

3.5.1 Cytotoxic effects and caspase-3/7 activation

An alamarBlue® assay was chosen as the primary screen to investigate the anticancer activity of *A. malaccensis* and *H. dryobalanoides* plant extracts by examining the *in vitro* cytotoxicity of the extracts on a panel of cancer cell lines. Various human-derived cancer cells were chosen including A2780, ZR75, HepG2 and U2OS. Besides the cytotoxic potency and the pharmacological target, the other most important key feature of an anticancer drug is the ability to selectively kill cancer cells without affecting normal cells (Lopez-Lazaro, 2015, López-Lázaro, 2015, Calderón-Montaño *et al.*, 2014). Therefore, normal PNT2A cells were chosen to test the selectivity of the samples.

Solvent crude extracts of *A. malaccensis* twigs and *H. dryobalanoides* bark showed no cytotoxic activity against PNT2A cells, however, was selective towards the cancer cells especially A2780 and ZR-75-1 cells. AH, AM and HE extracts at 30µg/ml showed significant ($P<0.01$) cytotoxicity against the ovarian and breast cancer cells. This is the first report of the activity of *A. malaccensis* on both cells, but other *Aquilaria sp* extracts of fruits and stem bark had shown cytotoxic effects against breast cancer (MCF-7 and T47-D) and ovarian cancer (A2780 and SKOV-3) (Dahham *et al.*, 2016a, Yunos *et al.*, 2017). *H. dryobalanoides* and other *Hopea* sp were reported to

contain compounds that exhibit potent cytotoxicity against breast cancer cells, however there are no reports on ovarian cancer cells (Paul *et al.*, 2016, Lim *et al.*, 2012). Due to the activity shown by AH, AM and HE, these extracts were selected for phytochemical investigation to isolate compounds that could potentially be responsible for their activities.

As described in Chapter 2, 7-aca and a mixture of two compounds Q/A were isolated from AH and AM, respectively. Two compounds, bala and heimiol A, were isolated from HE. These compounds were subjected to cytotoxicity screening against A2780 and ZR-75-1 cells. The well-known anti-cancer agent acacetin (aca) was purchased in order to compare it to a similar compound isolated in this study (7-aca). As shown in the results, 7-aca, aca and Q/A showed toxic effects towards the cancer cells. 7-Aca was shown to be the more potent compared to aca as well as Q/A and bala against A2780 and ZR-75-1 with an IC_{50} of 7.9µM and 8.5 µM, respectively. There are no current reports on the cytotoxic activity of 7-aca against breast, ovarian or any other type of cancer. Aca had previously been reported to be cytotoxic towards breast cancer MCF-7 cell with an IC_{50} of 26.4 µM, which is slightly higher compared to this study (IC_{50} =17.5µM) (Shim *et al.,* 2007). Aca also showed growth inhibition towards OVCAR-3 and A2780 cells (Liu *et al.*, 2011).

The mechanistic details of the cytotoxic effects of the active compounds and plant extracts were then investigated for their ability to induce apoptosis in A2780 and ZR-75-1 cells. Both cell lines treated with isolated compounds and selected plant extracts displayed a significant ($P<0.01$) increase in the activity of caspase-3/7 when compared to the untreated cells. 7-aca, the major compound in AH extracts caused the highest level of caspase-3/7 expression compared to other isolated compounds. Therefore, 7-

aca could possibly be responsible for the activity shown by AH extract. 7-Aca also showed to cause a significant ($P<0.05$) higher increased of caspase-3/7 level compared to aca in both cells. Caspase-3 and caspase-7 are both activated universally during apoptosis. Previous data reported that treatment of aca caused cell death towards MCF-7 cells through increase of apoptotic mediators caspase 7 (Shim *et al.*, 2007). Therefore, this could suggest that 7-aca initiate apoptosis through the increase of caspase 3/7. Furthermore, the same study demonstrated the increase of an 85 kDa cleavage form of Poly (ADP-ribose) polymerase (PARP) resulting from the treatment of breast cancer cells with aca. PARP is an early apoptosis marker generated by the caspase-3/7 activation cascade (Chaitanya *et al.*, 2010).

In this study, Q/A (mixture of quercitrin and afzelin) showed moderate cytotoxic effects and caspase activation against both cells. Quercitrin is made up of a compound called quercetin with a rhamnose sugar attached to the C-3. So far there are no publications on the cytotoxic effects of quercitrin against breast and ovarian cancer cells. On the other hand, quercetin has many reports on its ability to induce apoptotic cell death by the activation of the executioner caspases-3/7 (Manouchehri *et al.*, 2016, Zhou *et al.*, 2015, Gao *et al.*, 2012, Teekaraman *et al.*, 2019). Moreover, treatment of MCF-7 and MDA-MB-231 breast cancer cell lines with quercetin induced apoptosis by causing G1 phase arrest and via the suppression of p38 mitogen-activated protein kinases (p38MAPK), phospho-JAK1 and phospho-STAT3 (Liao *et al.*, 2015, Ranganathan *et al.*, 2015, Seo *et al.*, 2016). Afzelin was reported to inhibit the proliferation of MCF-7 cells with an IC_{50} value of 227 μM. In the same study, the compound also triggered cell death intrinsically via the upregulation of caspase-9 and caspase-3 and activation of PARP (Diantini *et al.*, 2012b). The same apoptotic effect

was seen on prostate cancer cells after treatment with afzelin (IC_{50} =218 µM) (Halimah *et al.*, 2015). These published reports suggested that the cytotoxic effect exhibited by Q/A on A2780 and ZR-75-1 cells could be due to the increase in caspase 3/7 level that leads to apoptotic cell death.

At 30µM, bala did not show any effects towards the cells. However, by increasing the concentration to 300µM, significant ($P<0.01$) cytotoxic effects were seen. Bala is made up of two resveratrol monomers and resveratrol has been recorded many times for its dual activity. At a low concentration (5 µM) resveratrol increases cell proliferation or acts as an antioxidant which protects cells from DNA damage, while at higher concentrations (usually >50 µM) it induces apoptosis in various cancer cells (Kuršvietienė *et al.*, 2016, Stervbo *et al.*, 2007). This probably explains the findings of the current study, whereby a higher concentration of bala treatment was needed to cause cytotoxicity towards the cancer cells. It was reported that resveratrol causes 50% cell inhibition at 60.3 µM (A2780 cells) and 74.11 µM (ZR-75-1 cells) (Engelke *et al.*, 2016, Venkatadri *et al.*, 2016, Murias *et al.*, 2008). In this study, bala showed a higher IC_{50} value of 122.5µM and 220.4 µM on A2780 and ZR-75-1 cells, respectively. Bala also caused the activation of caspases-3/7 in A2780 and ZR-75-1 cells which could suggest that cytotoxicity caused by bala involved the caspase-3/7-dependent pathway. Resveratrol was reported to inhibit cancer cell proliferation and induce apoptosis through caspase-3 activation (Alkhalaf *et al.*, 2008, Liu *et al.*, 2018b, Mirzapur *et al.*, 2018).

Impaired apoptosis is one of the hallmarks of cancer. Caspase-3 is known to be the major executioner caspase that degrades multiple cellular proteins and causes morphological changes and DNA fragmentation in cells during apoptosis. ZR-75-1

was reported to express a very low or a complete lack of caspase-3 protein expression (Yang *et al.*, 2007). Inactive caspase was also seen in A2780 cells before the treatment of cisplatin (Shaulov-Rotem *et al.*, 2015, Singh *et al.*, 2013). Caspase-3 defects were suggested to be one of the mechanisms for chemoresistance and cancer cell survival (McIlwain *et al.*, 2013). Therefore, the findings in this study indicate that the tested compounds possibly stimulate breast and ovarian cancer cell death via apoptosis and that this process is mediated, at least in part by the activation of caspases-3/7.

3.5.2 ROS production, and reduction in mitochondrion permeability

ROS is regarded as a double-edged sword and a slight change in ROS homeostasis in cancer cells will cause cell death. Low levels of ROS can promote cell proliferation and invasion, whereas high levels of ROS cause oxidative damage to proteins, lipids, RNA and DNA which results in cell apoptosis (Georgieva *et al.*, 2017, Meng *et al.*, 2018). Most chemotherapeutics use this as a target by increasing intracellular levels of ROS which can affect the redox-homeostasis of cancer cells. Another distinct feature of apoptosis is the disruption of active mitochondria that leads to changes in the ΔΨM (Ricci *et al.*, 2004). Thus, ΔΨM has been used to measure cell health, as ΔΨM is usually compromised during stress responses and a good indicator of ongoing cell death. In this study, plant extracts (AH, AM and HE) and compounds (7-aca, aca, Q/A and bala) were subjected to the measurement of intracellular ROS using DCFH-DA dye and monitoring changes in ΔΨM using TMRE dye to further investigate the possible mechanism behind the apoptotic cell death caused by the tested samples in A2780 and ZR-75-1 cells.

The results in this study revealed that all three isolated compounds, including aca as well as the selected plant extracts significantly induced the intracellular production of

ROS. 7-Aca has been shown to be a more significant ($P<0.05$) potent ROS generator by increasing ROS 5.3-fold at 30µM in A2780 cells and 4.1-fold in ZR-75-1 cells compared to aca, however showed weaker activity when compared to TBPH, a known ROS generator. Aca caused the increased ROS 3.9-fold and 3.3-fold in A2780 and ZR-75 cells, respectively. Furthermore, both compounds caused significant loss of ΔΨM in both cell lines whereby 7-aca showed a significant ($P<0.05$) greater ΔΨM loss compared to aca. Exposing 7-aca to cells resulted in a 66% and 73% of decrease of ΔΨM which is significantly ($P<0.05$) more potent than aca with a 51% and 60% decrease on ΔΨM in A2780 and ZR-75-1 cells, respectively. These results are in agreement with the literature whereby aca-induced apoptosis in MCF-7 cells was due to ROS generation and a decrease in ΔΨM (Shim *et al.*, 2007). In the same study, pre-treatment of aca, reduced levels of mitochondrial apoptogenic factors cytochrome c and AIF in cytosolic fractions which causes caspase-independent cell death (Cregan *et al.*, 2004, Garrido *et al.*, 2006). Other than that, aca also showed an apoptotic effect by caspase activation, ROS generation and mitochondria-mediated death signalling on human AGS gastric carcinoma cell lines and chronic lymphocytic leukemia (CLL) B-lymphocytes, lung cancer A549 cells and human T cell leukemia Jurkat cells (Pan *et al.*, 2005, Salimi *et al.*, 2016) (Hsu *et al.*, 2004, Watanabe *et al.*, 2012).

The apoptotic cell death via the mitochondrial pathway of bala has not been previously reported. In this study, bala caused an increase in ROS production by 3-fold in A2780 and 2-fold in ZR-75-1 cells. Furthermore, at a concentration of 150µM bala caused loss of ΔΨM by 40-50% for both cells. Several studies have reported an increase in ROS production and loss of ΔΨM induced by resveratrol in cancer cells such as ovarian cancer, breast cancer, colon cancer, lung cancer and pancreatic cancer where

caspase-3-dependent apoptotic death took place (Filomeni *et al.*, 2007, Lang *et al.*, 2015, (Blanquer-Rosselló *et al.*, 2017, Yousef *et al.*, 2017, Cheng *et al.*, 2018). It has been well established that the loss of ΔΨM occurs during early stages of apoptosis where caspase activation further induces permeabilisation of the mitochondrial membrane. Depolarisation of mitochondria plays a vital role in triggering cell death and activation of apoptosis. Cell death is triggered through the release of apoptotic proteins to the cytoplasm from the disturbed and disrupted mitochondrial membrane (Ferreira *et al.*, 2012). Therefore, the results obtained in this study suggest that 7-aca, aca, Q/A and bala support apoptotic cell death of A2780 and ZR-75-1 cells through the disruption of the cancer cells' ROS homeostasis and the depolarisation of ΔΨM.

3.5.3 Adhesion, migration and invasion

From these preliminary findings, all isolated compounds except for heimiol A showed moderate to strong activity. Therefore, they were chosen to investigate the effect on anti-adhesion properties of A2780 and ZR-75-1 cells. Due to an insufficient amount, Q/A was not tested for its anti-metastatic properties. In order to exclude the cytotoxic effect of the compounds (7-aca, aca and bala) from its effects on cell adhesion, migration and invasion, compound concentrations that were non-toxic to the cells were used for subsequent experiments.

This study demonstrated that the 7-aca, bala and purchased aca causes significant anti-metastatic properties against A2780 and ZR-75-1 cell lines. Adhesion assays depend on the ability of integrin receptors on the cell surface to interact with ECM proteins on a coated plate. A very important process of cancer cell invasion and migration is the ability of the cancer cells to degrade ECM (Fares *et al.*, 2020). Fibronectin, an ECM glycoprotein, plays important roles in the various stages of wound healing, with its

main function being cellular adhesion (To and Midwood, 2011). In the breast tumour, fibronectin accumulates as the tumour develops, which causes an increase in tissue stiffness which promotes proliferation and increases tumour cell aggressiveness (Bayer *et al.*, 2019, Insua-Rodríguez and Oskarsson, 2016). Fibronectin has been found to be in abundance in ovarian tumour-associated stroma and it is well-documented to have high importance in the migration, invasion, and metastasis of ovarian cancer (Ricciardelli and Rodgers, 2006, Ajeti *et al.*, 2017, Kenny *et al.*, 2008, Mitra *et al.*, 2011, Yousif, 2014). Therefore, in this study, fibronectin coated plates were chosen as an adhesive substrate to address the ability of tested samples to block A2780 and ZR-75-1 cell adhesion. All compounds significantly ($P< 0.01$) reduced A2780 cell adhesion, with 7-aca (1 µM) showed to be more potent compared to aca by decreasing cell adhesion by 70%. Aca (1 µM) decreased cell adhesion by 60% and bala (30µM) by 50%. At the same concentration, 7-aca also inhibited cell adhesion of ZR-75-1 cells significantly ($P< 0.01$) by 60%, aca by 40% and bala by 20%. These results correlate well with those found by (Shen *et al.*, 2010) who showed aca at 1-10µM inhibited adhesion, invasion and migration abilities of human prostate cancer DU145 cells by reducing matrix metalloproteinases (MMP-2 and MMP-9). The MMP family consist of enzymes that are associated with adhesion molecules on the cell surface during cell migration and invasion by enabling the degradation of ECM by tumour cells. Therefore, these enzyme help to facilitate the movement of cancer cells (Jabłońska-Trypuć *et al.*, 2016). Other studies have also reported anti-metastatic activity of other flavonoids including quercetin and kaempferol by reducing the protein level of MMP-2/MMP-9 in various cancer cells such as SCC4 oral cancer, HCCLM3 cells, MDA-MB-231, OVCAR-3 cells (Lu *et al.*, 2018, Lai *et al.*, 2013, Lin *et al.*,

2013, Li *et al.*, 2015, Luo *et al.*, 2008). Ten oligomers of resveratrol at a dose of 10 μM including resveratrol trimers (cis- and trans-gnetin H, suffruticosol A-C, cis- and trans-suffruticosol D and dimers (cis- and trans-ε-viniferin) significantly affected the migration and invasion of MDA-MB-231 cells. However the anti-metastatic mechanism of these compounds was not determined (Gao and He, 2017). The current work also demonstrated that 7-aca showed stronger inhibitory effects on migration and invasion of A2780 and ZR-75-1 compared to aca and bala as explained in section 3.4.5. The mechanism behind the anti-migration and invasion activity of 7-aca is unknown. However, a study carried out by (Chien *et al.*, 2011) suggested that treatment of aca on lung cancer A549 showed anti-migration and anti-invasion effects due to inhibition on the binding abilities of NF-κB and activator protein-1 (AP-1). In the same study it was also found that the treatment inhibited the activation of p38α MAPK which concurrently reduced activities of MMP-2/9 and urokinase-type plasminogen activator (u-PA). Similarly, resveratrol has been reported to cause inhibition of migration and invasion of breast and ovarian cancer cells (Liu *et al.*, 2018b, Sun *et al.*, 2019, Tang *et al.*, 2008, Baribeau *et al.*, 2014). The compound was able to exert its anti-metastatic effects on human breast cancer MCF-7 cells by causing downregulation of phosphatidylinositol 3-kinase (PI3K)/Akt and Wnt/β-catenin signalling pathways (Tsai *et al.*, 2013). In view of these previous findings, there are many possible mechanisms for the anti-metastatic effect of 7-aca and bala on A2780 and ZR-75-1 cells. Based on the data from the current work, 7-aca showed to be a more potent anti-metastatic compound compared to aca. Therefore, 7-aca could be a promising compound to treat breast and ovarian cancer by inhibiting cell migration and invasion as a result of reduced or inhibited attachment to ECM proteins (such as fibronectin).

3.5.4 Metabolomics

From previous experiments, 7-aca and aca showed the most potent activity. Therefore, for the first time these two compounds were chosen to determine their effects on the metabolic output of A2780 and ZR-75-1 cancer cell lines. The altered metabolites in both cells encompassed several pathways including those of amino acid, energy, and carbohydrate metabolism. The overall impression is that treatment of 7-aca and aca showed different responses of intracellular metabolites in both cells as seen in the OPLS-DA model which clearly showed the separation between both treatments and control groups.

The pathways most affected in both cell lines by 7-aca and aca treatment were those involved in amino acid metabolism, but pathways involved in carbohydrate, energy and nucleotide metabolism were also altered. The arginine and proline pathway metabolites such as phosphocreatine, L-citrulline, D-arginine, N-(L-arginino) succinate, 1-pyrroline-2-carboxylate and 4-aminobutanoate were altered in A2780 and ZR-75-1 cells. This study showed that phosphocreatine was significantly decreased in both cell types after treatment with both compounds; with 7-aca showing greater effect than aca. It has been reported that phosphocreatine is important for metabolism, growth and fuelling metastatic survival of tumours such as breast and colon cancer cells (Sullivan and Christofk, 2015, Kurmi *et al.*, 2018, Loo *et al.*, 2015). The phosphocreatine energy shuttle is facilitated by mitochondrial creatine kinase 1 (MtCK1) and phosphocreatine can be quickly converted to ATP and creatine when energy levels are low in metabolically active cancer cells (Wallimann *et al.*, 2011).

From this study, the metabolic profile of the treatment of both cells with 7-aca and aca showed an impact on the OXPHOS pathway in both cell lines. It is common

knowledge that cancer cells typically switch from cellular respiration to glycolysis for their metabolic needs, which is also known as the Warburg effect. However, some cancer cells still show a dependence on OXPHOS for their ATP needs (Viale *et al.*, 2014, Viale *et al.*, 2015) It has been reported that estrogen receptor positive (ER+) breast cancer cells such as ZR-75-1 cells possess higher OXPHOS levels to sustain their energy metabolic needs (Lucantoni *et al.*, 2018), whereas, A2780 has been suggested to use both glycolysis and OXPHOS pathways, with a slightly higher preference for using the glycolysis pathway for energy metabolism (Dar *et al.*, 2017). In this study, ATP/ADP were found to be reduced in both cell lines after treatments with 7-aca and aca. 7-aca treatment showed lower levels of ATP/ADP for both cells in comparison with aca treatment. ATP is involved in different cell death mechanisms including apoptosis, autophagy and necrosis. In apoptosis, ATP is depleted due to mitochondrial disruption which then causes activation of the apoptotic biochemical cascade (Martin *et al.*, 2000). Studies have reported that the depletion ATP caused by inhibiting the mitochondria OXPHOS pathway was found to induce apoptosis (Cheng *et al.*, 2019, Izyumov *et al.*, 2004).

Furthermore, both compounds also caused the depletion of levels of NAD^+ and NADH in both cell lines. 7-aca treatment showed lower levels of NAD+ and NADH for both cell types in comparison with aca treatment. Cancer cells require the continuous replenishment of NADH which supports their proliferation and survival of fast-dividing cancer cells. NAD+ serves as an electron donor for the OXPHOS complexes to produce ATP (O'Mahony *et al.*, 2012). It has been reported that depletion of ATP and NAD+ leads to suppression of tumor cell growth and induction of apoptosis (Alaee *et al.*, 2017, Tan *et al.*, 2015, Komatsu *et al.*, 2000). Therefore, in this study, apoptotic

cell death caused by the treatment of 7-aca and aca in A2780 and ZR-75-1 cells could be due to the depletion of ATP and NAD+ levels. Moreover, high levels of nicotinamide phosphoribosyltransferase (NAMPT), the enzyme that catalyses NAD+ biosynthesis, is frequently observed in several types of malignant tumours, including, colorectal, ovarian, breast, gastric, thyroid, prostate cancers, gliomas, and malignant lymphomas (Yaku *et al.*, 2018). Inhibition of NAMPT also causes depletion of NAD+ synthesis and this is being used in clinical trials as the therapeutic target for cancer treatment (Sampath *et al.*, 2015, Lewis *et al.*, 2019).

Inhibited glycolysis/TCA cycle activity was seen in A2780 and ZR-75-1 cells treated with 7-aca as indicated by lower levels of fructose-6-phosphate (F6P), acetyl-CoA, 3-phosphoglycerate and oxalosuccinate. However, for aca-treated cells, the glycolysis/TCA cycle was only slightly affected. Furthermore, both cells showed reduction of D-glucose-6-phosphate (G6PD) and D-sedoheptulose 7-phosphate in the pentose phosphate pathway (PPP) after treatment with 7-aca and aca. PPP is a major biochemical pathway that generates antioxidant NADPH in order to counteract the high level of ROS in cancer cells. G6PD is the key enzyme in the PPP and has been found to be highly elevated in several types of cancer such as breast cancer, oesophageal carcinoma, renal cancer (Wang *et al.*, 2015b, Batai *et al.*, 2018, Ringnér *et al.*, 2011, Györffy *et al.*, 2010). G6PD expression causes an increase in NADPH that supports biosynthesis and antioxidant defence (glutathione) through PPP, which is a favourable condition for the survival of tumour cells. Therefore, many studies have reported that G6PD inhibition causes the build-up of ROS through the disruption of the NADPH/NADP+ ratio (Fang *et al.*, 2016, Gao *et al.*, 2009, Cheng *et al.*, 2004, Ho *et al.*, 2000).

Both compounds showed alteration of glutathione disulphide (GSSG) and NADPH levels in A2780 and ZR-75-1 cells. 7-aca treatment showed a greater decrease in GSSG and NADPH levels for both cells in comparison with aca treatment. It is known that cancer cells have an increase in the antioxidant defence system to balance the high ROS level in order to maintain cell homeostasis (Weinberg *et al.*, 2019). It was reported that untreated ovarian cancer cells such as A2780 and OVCAR3 and breast cancer cells such as ZR-75-1 and MCF-7 cells show elevated GSH levels, which is correlated with the resistance of these cells to the induction of apoptosis (Pan *et al.*, 2018, Sarkhosh-Inanlou *et al.*, 2020, Syed Alwi *et al.*, 2012, Jabłońska-Trypuć *et al.*, 2020, Malla *et al.*, 2020). GSH, a natural antioxidant, is oxidised to GSSG when it reacts with H_2O_2 in the presence of glutathione peroxidase (GpX), an enzyme that facilitates the inactivation of H_2O_2. Thus, the decrease in the levels of GSSG observed in this study could potentially be due to the decrease of the antioxidant defence system of the cancer cells, particularly GSH. Many studies have reported that GSH depletion in ovarian and breast cancer cells caused by treatment with anti-cancer drugs has caused ROS generation and depletion of mitochondrial function and caspase-3/7 activation which ultimately results in cell death (Miran *et al.*, 2018, Hong *et al.*, 2015, Mukherjee *et al.*, 2015, Syng-ai *et al.*, 2004, Filomeni *et al.*, 2007). Furthermore, 7-aca and aca caused decrease in other metabolites that are involved in glutathione metabolism such as cystine-glycine (Cys-Gly). Possible mechanisms of action causing elevation of ROS after treatment of 7-aca and aca in A2780 and ZR-75-1 cells are shown in Figure 3.18.

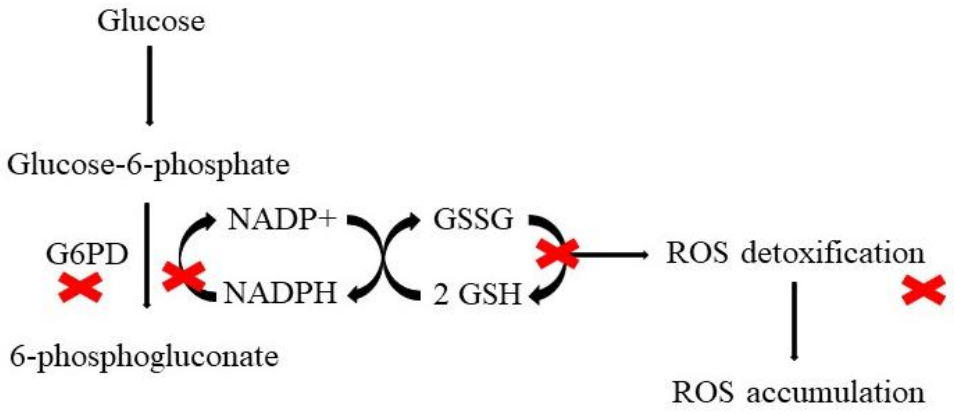

Figure 3.18 Possible pro-oxidant mechanism of action of 7-aca and aca on A2780 and ZR-75-1 cells.

To conclude, from the findings obtained in this chapter, compounds isolated from plant extracts AH, AE and HE could have contributed apoptotic cell death effects on A2780 and ZR-75-1 cells. The compounds 7-aca, Q/A and bala caused an increase in intracellular ROS and disruption of ΔΨM which is suggested to be the major contribution of apoptosis initiation in both cancer cell lines. Furthermore, non-cytotoxic concentrations of 7-aca and bala showed anti-metastatic activity by inhibiting adhesion, migration and invasion of both cancer lines. Metabolomic studies on 7-aca and aca suggested that the accumulation of ROS levels could be due to the disruption of the GSSG/GSH ratio. Moreover, the depletion of ATP/ADP and NAD+/NADH levels suggested the inhibition of mitochondria OXPHOS activity. Based on the results, 7-aca shower a stronger anti-cancer activity compared to aca in both cells. The glycolytic/ TCA activity of both cancer cells was strongly inhibited by 7-aca treatment, but was only slightly affected with the treatment of aca.

Chapter 4. Anti-inflammatory activity of isolated compounds

4.1.Introduction

The project findings in Chapters 3 suggested that 7-aca, Q/A and bala possess anti-cancer activity towards A2780 and ZR-75-1 cells. All isolated compounds showed potent cytotoxic effects, apoptotic effects by increases in caspase-3/7 levels as well as increases in intracellular ROS levels and disruption of ΔΨM of the cancer cell lines. Furthermore, the isolated compounds also showed anti-metastatic effects by inhibition of cell adhesion, migration, and invasion. A metabolomics study of 7-aca showed that the accumulation of ROS could be due to the disruption of the GSSG/GSH ratio. Moreover, the depletion of ATP/ADP and NAD+/NADH levels suggested the inhibition of mitochondria OXPHOS activity. Following on from the above findings, it was thought pertinent to investigate whether the isolated compounds could potentially possess anti-inflammatory properties. Inflammation is an immune system's response by cells or vascular tissues to remove injurious stimuli such as pathogens, damaged cells, irritants, toxic compounds, or irradiation and cause the initiation of the healing process (Chen *et al.*, 2017). However, prolonged inflammation, also known as chronic inflammation, causes and advances many common diseases such as diabetes, cardiovascular disease, arthritis, bowel diseases and cancer (Libby, 2007).

Macrophages are the first line of defence in the immune system that plays a vital role in maintenance of tissue homeostasis, and the protection of our bodies from foreign substances (Chen *et al.*, 2019b). Two major polarisation states have been described for macrophages: M1 macrophages polarisation can be induced by bacterial cell wall components (such as LPS) and interferon-γ (IFN-γ) and produce pro-inflammatory cytokines like TNF-α, IL-1β, IL-6 and IL-12; M2 macrophage polarisation can be

induced by different stimuli: IL-4 and/or IL-13, immune complexes and toll-like receptors, IL-1 receptor ligands or IL-10. In cancer, macrophages that are recruited to the tumour microenvironment (TME) are termed tumour-associated macrophages (TAM) which are well known to affect tumour growth, tumour angiogenesis, immune regulation, metastasis, and chemoresistance (Lin *et al.*, 2019b). TAMs are recruited to the tumour in response to an inflammatory TME and secretes pro-inflammatory cytokine such as IL-6, TNF, and IFNγ which further supports inflammation. This step is thought to be crucial to sustain chronic inflammation in the TME, creating a mutagenic milieu and thereby supporting tumour initiation and promotion (Qian and Pollard, 2010a, Pollard, 2004, Noy and Pollard, 2014). Chronic inflammation generates malignancy through the prolonged exposure of pro-inflammatory cytokines and activation of several signalling pathways. Several cytokines have been implicated in carcinogenesis, due to its participation in chronic inflammatory diseases and tumour growth including TNF-α and IL-6 (Landskron *et al.*, 2014). TNF-α induced tumour initiation and tumour promotion are mediated by the activation of NF-κB that is critical for TNF-α-induced tumour promotion (Wu and Zhou, 2010b). Whereas IL-6 involves the activation of Janus kinase (JAK) which leads to the activation of transcription factor signal transducer and activator of transcription 3 (STAT3) (Heinrich *et al.*, 2003). STAT3 is known to play an important role in promoting tumorigenesis of diverse human cancers that involves cancer cell proliferation, differentiation, invasion, inflammation, and immune function (Wang and Sun, 2014).

Therefore, this chapter aims to assess the anti-inflammatory activity of the compounds 7-aca, aca, Q/A and bala by determining the expression of pro-inflammatory cytokines in LPS-stimulated THP-1 macrophage cells using enzyme-linked immunosorbent

assay (ELISA). Furthermore, in order to investigate the inflammatory signalling pathway that is affected due to compound treatments, gene expression evaluation using RNA sequencing (RNA-Seq) was also carried out. These assays are introduced and described below:

4.1.1.Enzyme-linked immunosorbent assay (ELISA)

ELISA is a popular routine method used for detecting and quantifying cytokines, peptides, proteins, antibodies, and hormones for samples such as cell supernatants, serum blood or urine (Alhajj and Farhana, 2020). In this study, an indirect sandwich ELISA was used to detect levels of cytokines in cell supernatant. There are four basic steps involved in an indirect sandwich ELISA: 1) Capturing analyte from sample with capture antibody/primary antibody that is coated onto the wells of the plate, (2) detecting captured analyte with detection antibody/secondary antibody, (3) detection amplification with streptavidin that has been conjugated with an enzyme such as horseradish peroxidase (HRP) and (4) substrate addition and signal measurement via optical density (OD) with a microplate reader (Chiswick *et al.*, 2012).

4.1.2. RNA sequencing (RNA-Seq)

RNA-Seq is an advanced technology that enables deep investigation of samples of interest via transcriptome-wide profiling of gene expression. RNA-Seq uses next-generation sequencing (NGS) technologies to examine the quantity and presence of RNA in a biological sample at a given moment (Hwang *et al.*, 2018). Analysis using RNA-Seq involves six important steps: (1) The initial step involves extraction of RNA samples from biological material, (2) converting RNA to complementary DNA (cDNA), then sequencing using high-throughput platform, (3) a genome or a transcriptome is mapped from the generated sequenced cDNA, (4) the next step

involves the estimation of expression levels of each gene or isoform, (5) normalisation of mapped data is carried out using statistical and machine learning techniques to identify differentially expressed genes (DEGs) following treatment and (6) the data is evaluated using a biological context.

4.2. Aims and objectives

This chapter aims to investigate the anti-inflammatory effects of compounds on THP-1 derived-macrophages cells induced by LPS. This was achieved by:

1. Measuring the viability of THP-1 monocytes and PMA-differentiated THP-1 macrophages after exposure to the compounds.
2. Determining the pro-inflammatory cytokines (TNF-α, IL-1β, and IL-6) levels in response to the compounds in the presence and absence of LPS.
3. Isolating total RNA from LPS stimulated THP-1 derived-macrophages cells treated with selected compounds.
4. Carrying out a transcriptome-wide gene expression analysis of selected groups using RNA-Seq.
5. Conducting a bioinformatics analysis of the RNA-Seq DEG to try to understand the effects of selected compounds on LPS stimulated THP-1 derived-macrophages cells.

4.3.Materials and methods

4.3.1.Cell culture and differentiation of THP-1 cells

The THP-1 human cell line was maintained at a 1×10^5 cells/ml seeding density in Roswell Park Memorial Institute (RPMI) 1640 containing 10% (*v*/*v*) FBS, 2 mmol/L L-glutamine and 100 IU/100 μg/ml penicillin/streptomycin. Cells were sub-cultured using fresh media every 2–4 days and maintained in an incubator (37 °C, 5% CO_2, 100% humidity). THP-1 cells were differentiated using at a final concentration of 60 ng/ml phorbol 12-myristate 13-acetate (PMA) and incubated for 48 h. THP-1 differentiated cells were rested for a further 24 h by removing the PMA-containing media and adding fresh media. Cells were checked under a light microscope for the evidence of differentiation. Differentiated THP-1 macrophages were used for following experiments.

4.3.2. Cell viability

THP-1 cells were seeded at a density of 1×10^5 cells/well in 96-well plates and incubated for 24 h at 37 °C in a humidified atmosphere of 5% CO_2. An alamarBlue® cell viability assay was carried out as per Section 3.3.2.

Following differentiation, the cells were pre-treated with selected concentrations of 7-aca, aca, bala and Q/A for 6 h and then incubated with or without LPS (1 μg/ml) for an additional 24 h. Conditioned medium was collected and frozen until required for ELISA ($n = 3$).

4.3.3. ELISA

Human Uncoated ELISA kits were performed according to the manufacturer's instructions to quantify the release of inflammatory cytokines (TNF-α, IL-1β and IL-

6). The reaction was stopped using acid solution (1 M sulphuric acid). The plates were read using a SpectraMax M5 plate reader at 560 nm and the absorbance values were corrected by subtracting readings taken at 570 nm.

Standard calibration curves were plotted by fitting the OD data of TNF-α, IL-1β and IL-6 to 4-parameter logistic (4-PL) regression curves. Each of these standards were prepared in triplicate at each of the concentrations in the ranges recommended by the manufacturer. The regression analysis also computes the R2 value which gives an indication of how best the fitted curve agrees with the data. The concentrations of TNF-α, IL-1β and IL-6 induced by each of the samples assayed (with and without LPS) were calculated and expressed as ratios of the mean cytokine level induced by LPS (positive control), assayed in triplicate (n=3). The resulting data were then analysed with GraphPad Prism 8 to obtain bar graphs whose statistical significances were tested at 95% confidence level relative to the mean positive control LPS.

4.3.4. Sample preparation for RNA extraction

THP-1 cells were plated in 6-well plates at a concentration of 1×10^5 cells/well with PMA (60 ng/ml) and incubated for 48 h. THP-1 differentiated cells were rested for a further 24 h by removing the PMA-containing media and adding fresh media. Then, the cells were incubated with selected compounds for 6 h then further treated with or without LPS (1 μg/ml) for an additional 24 h.

4.3.5. RNA extraction

Total RNA from PMA-differentiated THP-1 cells was isolated using a Monarch® Total RNA Miniprep Kit. Media in the 6-well plates were removed and washed with sterilised PBS before adding 300μl RNA lysis buffer to each well. Then the lysed cell samples were processed as per the Monarch® Total RNA Miniprep Kit protocol. Total

RNA was eluted from the spin column with 50 µl of nuclease-free water and stored at -80°C until required.

4.3.6. RNA quality and integrity

The concentrations of the extracted RNA were measured using a NanoDrop ND-2000C spectrophotometer. The RNA integrity was assessed using a Bio-Rad Experion™ automated electrophoresis system and Experion StdSens RNA Analysis; the procedure was carried out per the manufacturer's protocol.

4.3.7. RNA sequencing

Six RNA samples (two controls, two LPS-treated and two LPS/bala-treated) were selected for RNA-Seq analysis. The selection of samples was based on the RNA integrity scores obtained from the Bio-Rad Experion™ StdSens Analysis Kit. Samples were submitted to BGI-Tech (Shenzhen, China) to perform the RNA-Seq using their DNBseq platform, averagely generating about 26.29 M reads per sample.

4.3.8.Pathway enrichment analysis

Cytoscape Software (version 3.3.0, (Shannon *et al.*, 2003)), a software for complex network analysis and visualisation was used with ClueGO plugin (version 2.2.4, (Lotia *et al.*, 2013)) that has the ability to relate a group of genes to a particular biological activity, was used to analyse the RNA-Seq DEG list results received from BGI. The ClueGo plugin is a visualising tool that is capable of relating a group of genes to their functions, displaying a cluster network of results. The following parameters (Table 4.1) were applied with the ClueGo plugin:

Table 4.1 Parameters applied with the ClueGo plugin on Cytoscape.

Parameter	**ClueGo Setting**
Statistical test	Two-sided hypergeometric option with Benjamini-Hochberg correction
Pathway	Significant KEGG (Kyoto Encyclopedia of Genes and Genomes) pathway enrichment ($P < 0.05$)
Kappa score	3
GO Term/Pathway selection	(3/4%)

Pathview web (Luo and Brouwer, 2013) was also used to identify the enrichment of KEGG pathways by the DEGs list obtained. The genes that showed at least two-fold changes were only considered in this analysis. Pathway Selection option was set to auto to identify the most significantly enriched pathway.

4.4.Results

4.4.1. Cytotoxicity of compounds against PMA-Differentiated THP-1 Cells

Cytotoxicity testing using alamarBlue® cell viability assay was carried out on 7-aca, aca, bala, and Q/A prior to performing the ELISA in THP-1 cells after differentiation with PMA. Cytotoxicity assays were carried out to ensure the compounds were not cytotoxic to the cells prior to carrying out the anti-inflammatory assays. At the concentration of 30µM and 10µM of 7-aca, aca and bala (30µM) showed decreased cell viability and Q/A showed no cytotoxic effect on the cells. Therefore, the two highest non-toxic concentrations of the compounds were used to analyse the cytokine production by ELISA.

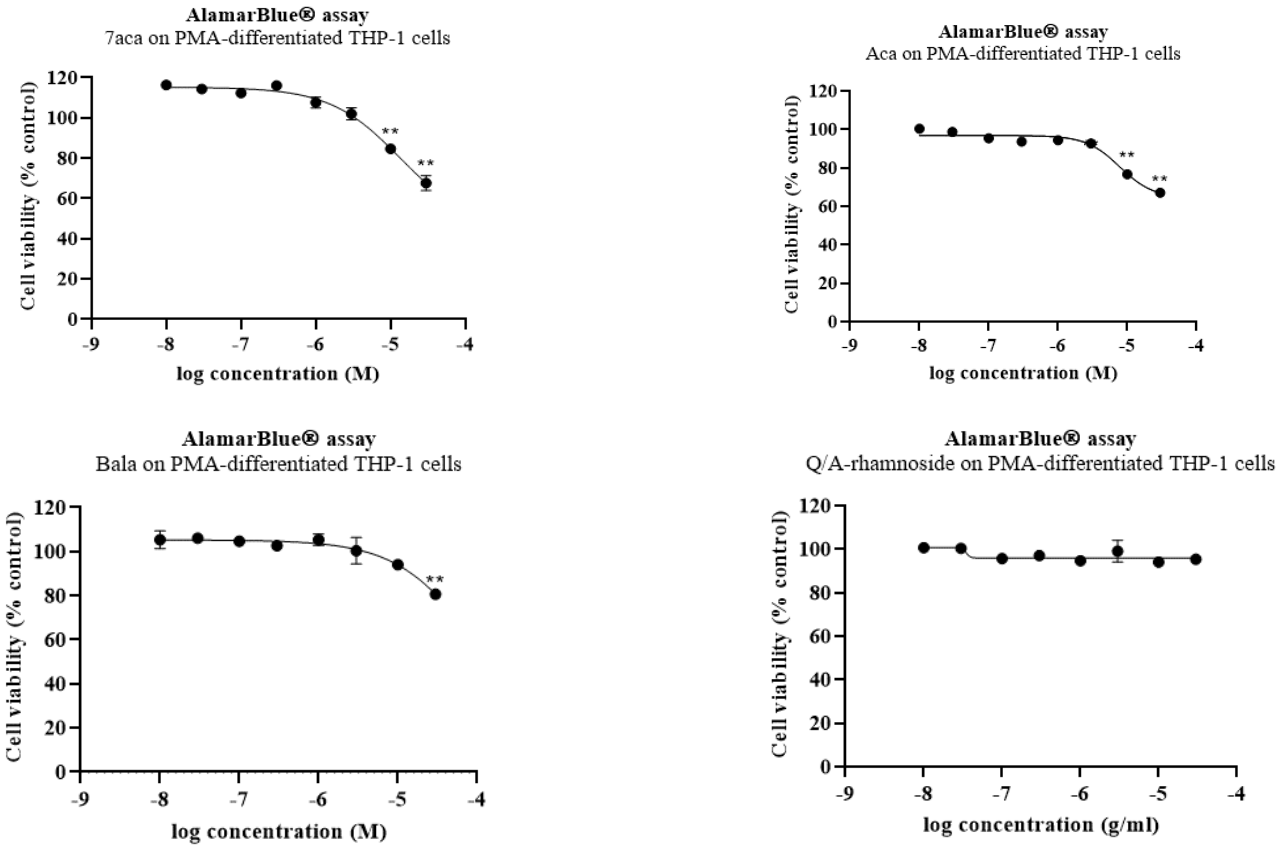

Figure 4.1 Cytotoxic effect of compounds PMA-differentiated THP-1 cells. Data was analysed using One-Way ANOVA with Bonferroni multiple comparison test. Data represents mean ± SEM, n=3. **P<0.01 represents significant decrease in cell viability vs untreated cells (control). The relative IC50 of the graph is the concentration corresponding to a response midway between the estimates of the lower and upper plateaus (no constrains settings was applied for the *Bottom* and *Top* parameters).

4.4.2. Effect of compounds on pro-inflammatory TNF-α cytokine production

As shown in Figure 4.2, the concentrations of TNF-α in THP-1-derived macrophages exhibited a significant (P< 0.01) decrease in the release of the pro-inflammatory TNF-α cytokine in response to the treatment of 7-aca, aca, and bala when compared with LPS alone. At 10µM, bala showed the most activity by reducing 75% of TNF-α produced compared to LPS treatment, whilst at 3µM 7-aca and aca showed similar effect by reducing 43.8% and 49.5% of TNF-α, respectively. Control cells and cells treated with compounds only showed a background level release of cytokine.

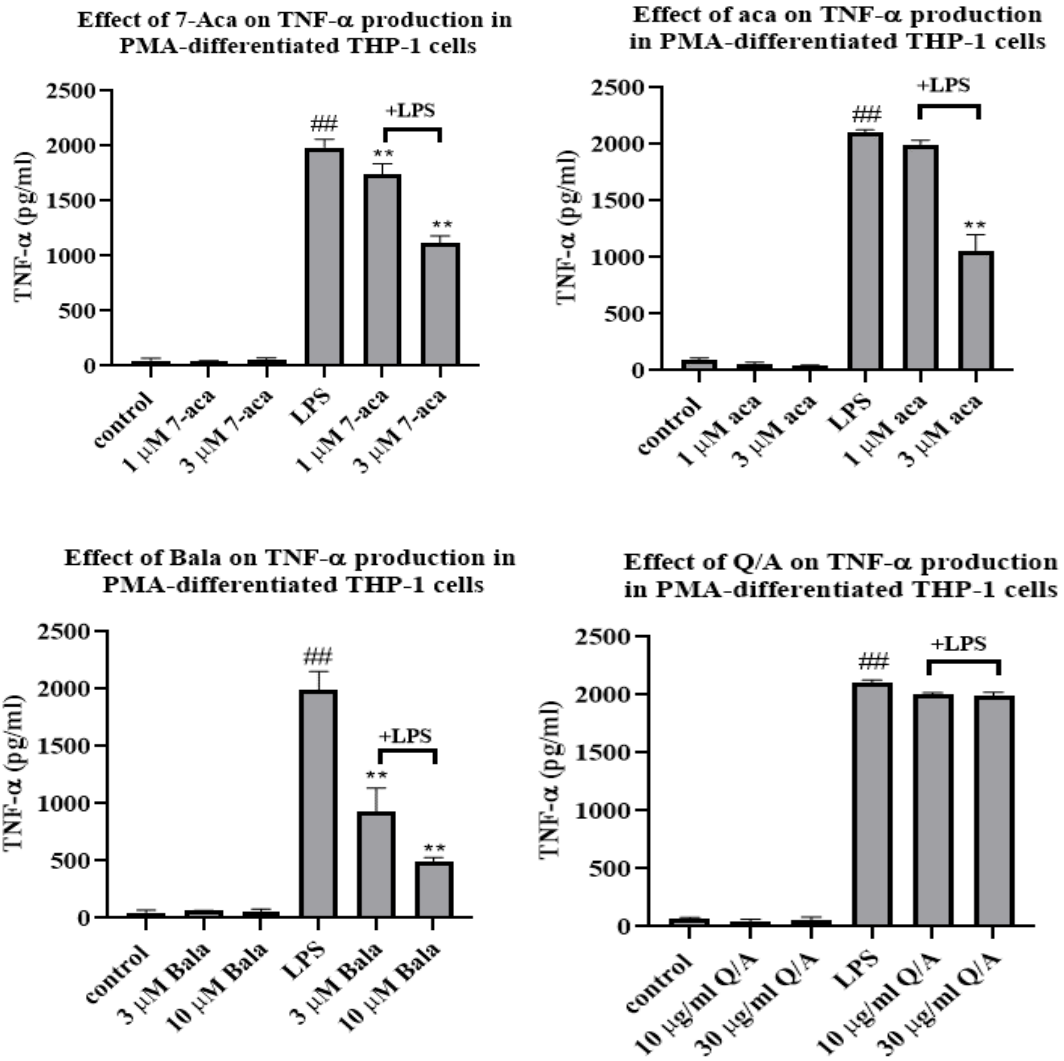

Figure 4.2 Effect of 7-aca, aca, bala, and Q/A on the production of TNF-α cytokine in the presence and absence of LPS (1 µg/ml) on PMA-differentiated THP-1 cells (n = 3). **: (P< 0.01) vs LPS alone. ## :(P < 0.01) vs control.

4.4.3.Effect of compounds on pro-inflammatory IL-1β cytokine production

The production of IL-1β was assessed using selected concentrations of 7-aca, aca, bala and Q/A. The release of IL-1β level was decreased by 7-aca, aca and bala in the presence of LPS (1μg/mL) when compared with LPS alone. At 10μM bala exhibited the strongest activity compared to the other compounds by supressing 68% of IL-1β production caused by LPS treatment, whilst 7-aca and aca (3μM) reduced IL-1β to 50.2% and 48.9%, respectively. In addition, no effect was observed for cells treated with all the compounds alone when compared with the negative control cells.

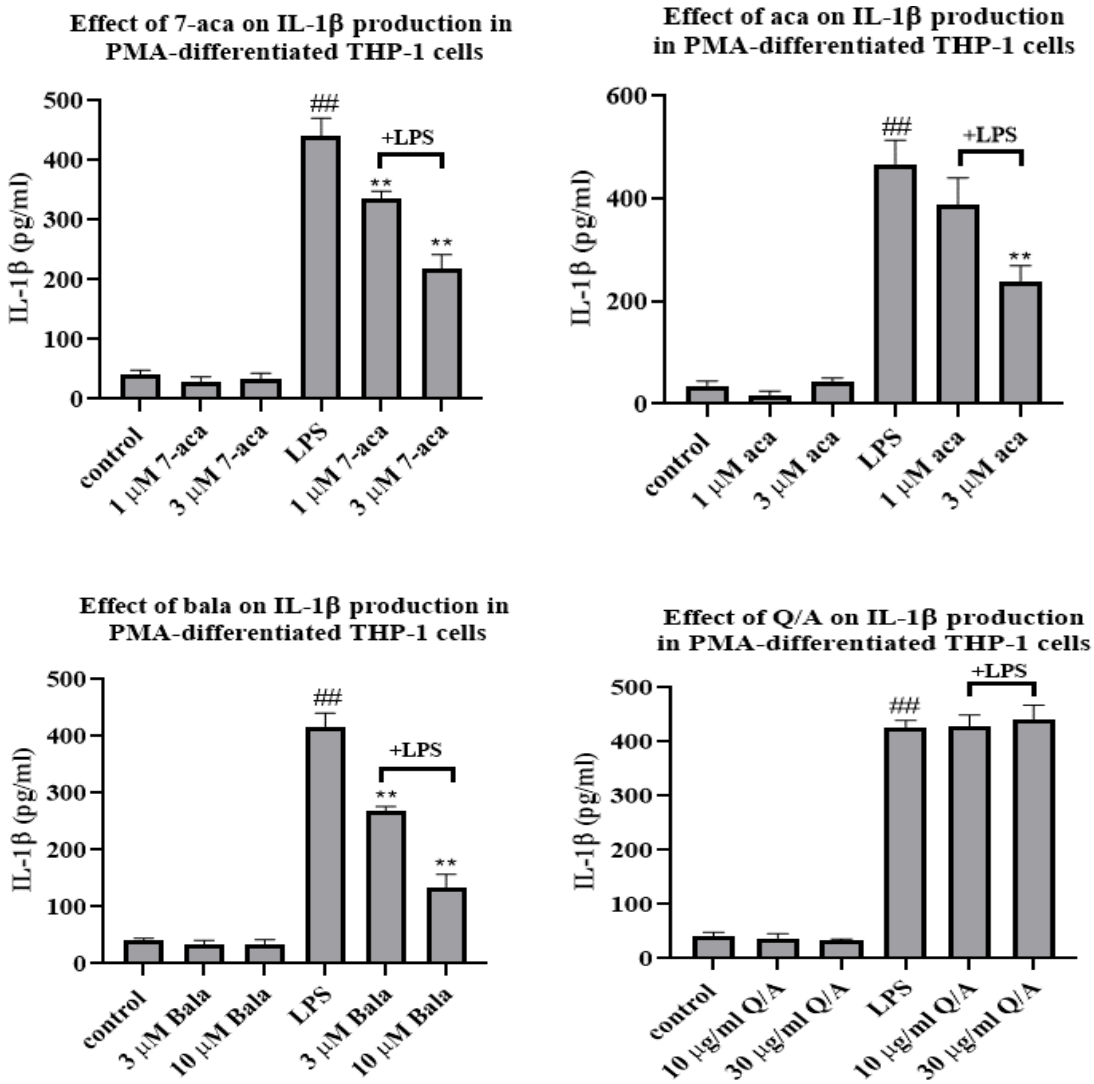

Figure 4.3 Effect of 7-aca, aca, bala and Q/A on the production of IL-1β cytokine in the presence and absence of LPS (1 μg/ml) on PMA-differentiated THP-1 cells (n = 3). **: ($P < 0.01$) vs LPS alone. ## :($P < 0.01$) vs control.

4.4.4. Effect of compounds on pro-inflammatory IL-6 cytokine production

In agreement with the observed decrease in the release of the pro-inflammatory cytokines above, IL-6 also showed a decrease in production in response to treatment with 7-aca, aca and bala with the presence of LPS when compared to LPS treatment alone. At 10µM, bala exhibited the strongest activity compared to the other compounds by supressing 67.28% IL-6 production caused by LPS treatment, whilst 7-aca and aca (3µM) reduced IL-6 to 54.7% and 50.8%, respectively. Although 30µg/ml of Q/A showed a decrease in IL-6 levels, the results did not reach statistical significance with 1 µg/mL LPS alone.

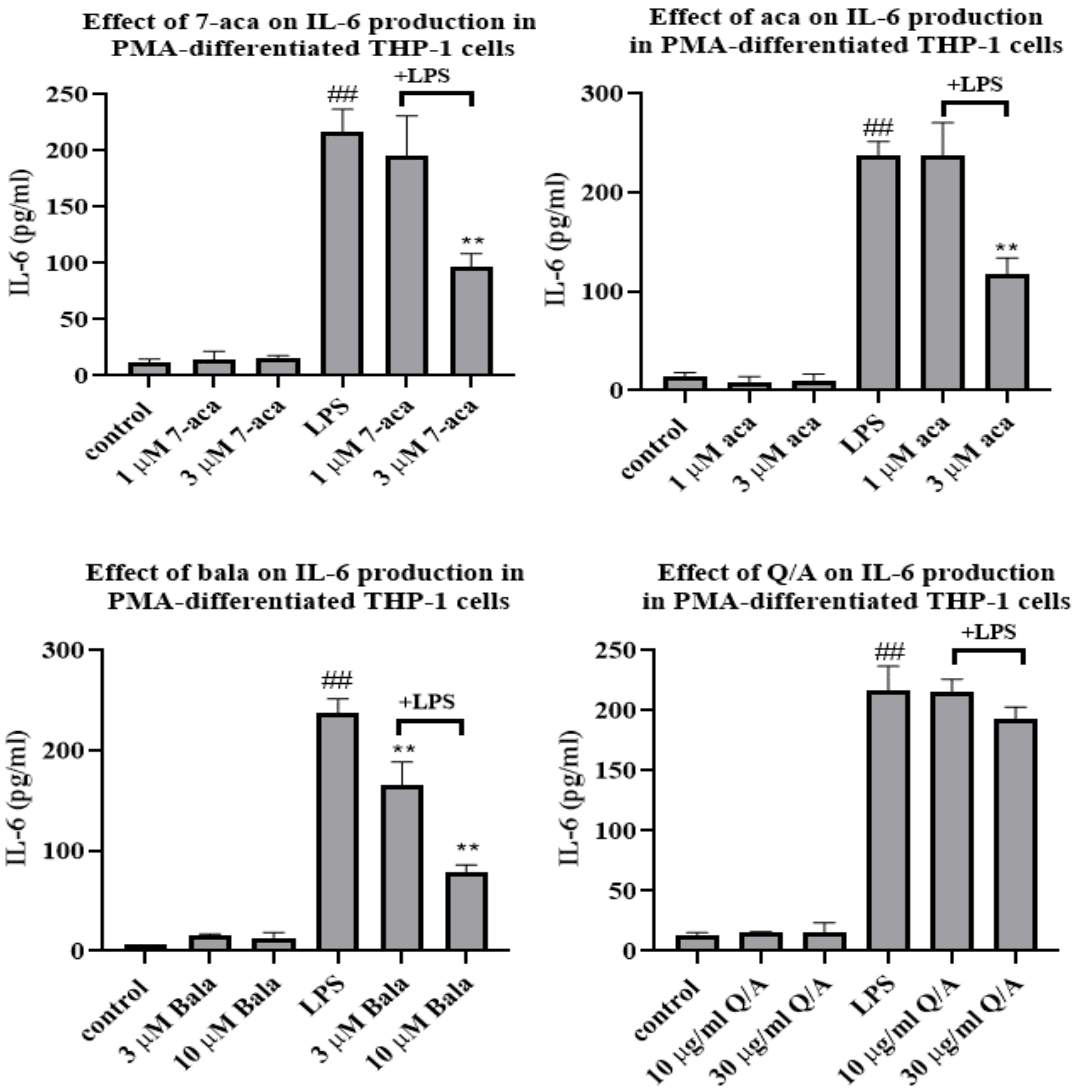

Figure 4.4 Effect of 7-aca, aca, bala and Q/A on the production of IL-6 cytokine in the presence and absence of LPS (1 μg/ml) on PMA-differentiated THP-1 cells (n = 3). **: ($P < 0.01$) vs LPS alone. ## :($P< 0.01$) vs control.

4.4.5.RNA extraction and quality control

4.4.5.1.Nanodrop analysis

Based on the ELISA results, bala at the concentration of 10 µM was chosen for RNA-seq analysis. RNA samples were extracted from THP-1 macrophage cells after treatment with LPS, combination treatment of LPS and bala (LPS/bala), and untreated cells. The extracted RNA samples were then analysed using a Nanodrop 2000c spectrophotometer to quantify and assess the quality and purity of the isolated RNA. The group of samples used in this study consisted of control, LPS, and LPS/bala. Each group had a total of 6 individual RNA samples. The summary of these findings is shown in Table 4.2. The RNA purity was assessed by the absorbance ratio at 260nm and 280nm (optimum RNA purity has a ratio close to 2). In addition, the quality of RNA was also assessed by the ratio of 260/230, where a ratio of approximately 2 is ideal. Therefore, the obtained results for all 18 RNA samples were considered as acceptable for these studies.

Table 4.2 A summary of the RNA extraction results from THP-1 cells (see Appendix 3 for Nanodrop traces)

Group	Sample name	RNA conc. (ng/µl)	A260/A280	A260/A230
Controls	Control 1A	266.2	2.06	2.12
	Control 1B	250.2	2.06	2.09
	Control 1C	216.6	2.09	2.38
	Control 2A	324.0	2.09	2.33
	Control 2B	267.4	2.09	1.85
	Control 2C	465.4	2.08	1.92
LPS treatment	LPS 1A	229.0	2.10	2.04
	LPS 1B	191.3	2.10	1.92
	LPS 1C	215.2	2.09	2.02
	LPS 2A	269.1	2.09	2.15
	LPS 2B	453.0	2.07	1.85
	LPS 2C	471.6	2.07	1.85
LPS/bala treatment	LPS/bala 1A	318.4	2.08	1.92
	LPS/bala 1B	355.1	2.08	1.90
	LPS/bala 1C	427.9	2.07	1.81
	LPS/bala 2A	319.7	2.06	1.99
	LPS/bala 2B	297.0	2.05	1.89
	LPS/bala 2C	333.5	2.09	1.85

4.4.5.2.Experion™ RNA StdSens Analysis

An Experion™ RNA StdSens kit was used in addition to the Nanodrop due to its ability to assess total RNA and mRNA integrity, purity, and concentration. The samples' RNA quality and integrity can be examined through an RNA quality indicator (RQI) or RNA Integrity Number (RIN) determination in automated electrophoresis systems. In this study, the RQI value which can range from 1 (completely degraded RNA) to 10 (highly intact RNA) was used to assess the integrity of the samples with the Bio-Rad Experion^{TM} system. This method is similar to the RIN standard developed by Agilent for their similar BioAnalyzer systems (Denisov *et al.*, 2008). For optimum RNA-Seq analysis, RQI is preferred to be 7 or greater.

The Experion™ RNA StdSens kit also determines the samples' RNA integrity by measuring the intact levels of ribosomal RNA (rRNA) which makes up >80% of total RNA samples, with the majority of that comprised by the 28S and 18S rRNA. 28S rRNA is at least twice the size of 18S rRNA. Therefore, 28S to 18S ratio of 2 is accepted for intact RNA, a ratio of greater than 1 is also acceptable. A virtual gel was produced by Experion™ RNA StdSens kit for all 18 RNA samples (Figure 4.5). As seen in Figure 4.5A, an error was made with sample C2C, but then was repeated in Figure 4.5B and was shown to be acceptable. The BGI RNA-Seq service requires submitted samples to have RQI values of ≥7 in order to perform RNA-Seq analysis as degraded samples may compromise the quality of the data obtained. All the isolated RNA samples had RQI values ranging from 9.3 to 10, and their 28S/18S ratios were in the range of 1.52-1.82 as shown in Table 4.3. Three RNA samples from each group were then pooled together to make 1 sample (n=1) and another three samples from

each group was pooled together to make n=2. The total RNA samples that was sent to BGI for RNA sequencing was 6 (2 samples for each group).

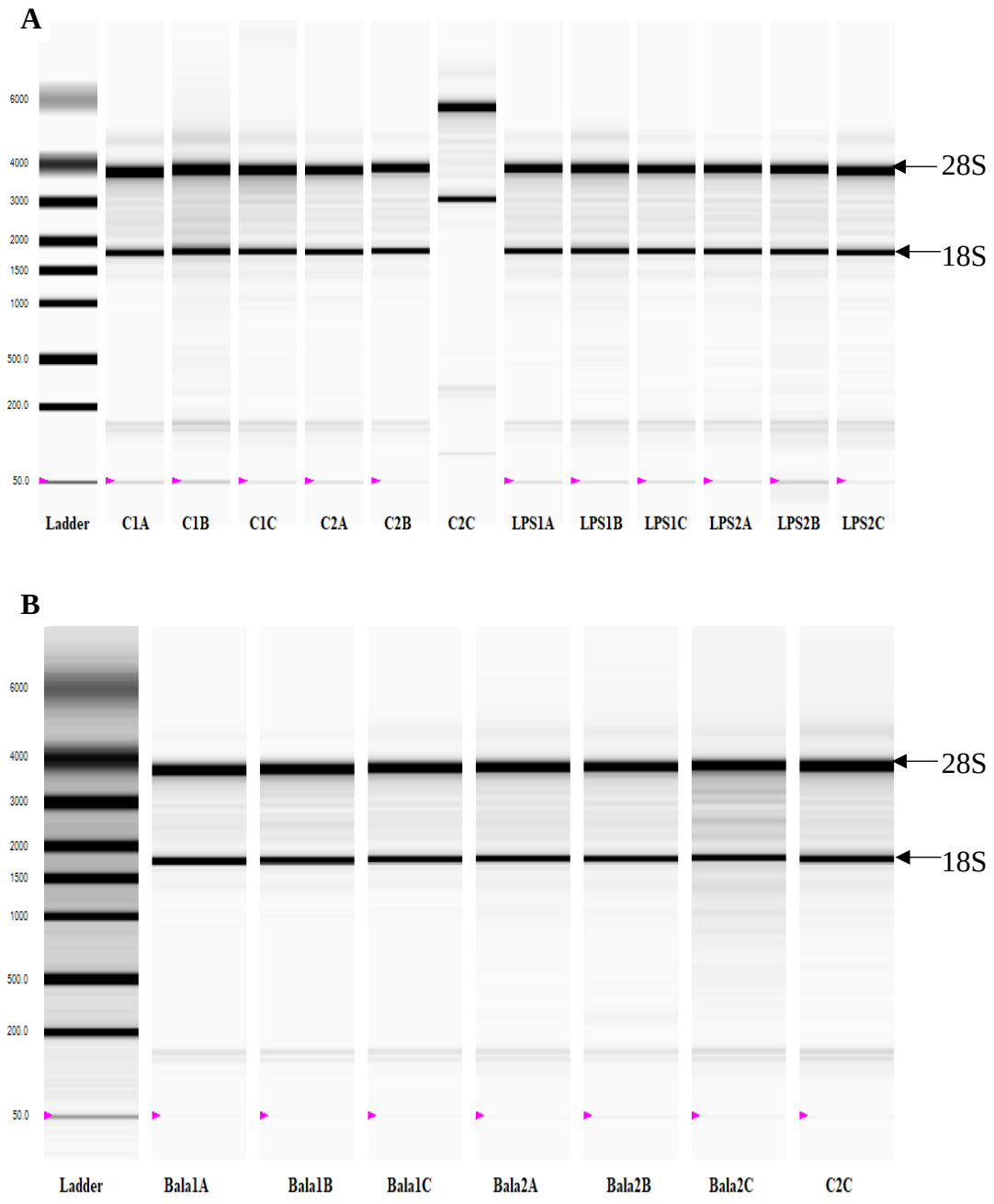

Figure 4.5 Virtual gel produced by Experion™ RNA StdSens kit for all RNA samples. Shown are separations of the RNA ladder, A) 12 samples and B) 7 samples on a single chip. Pink triangles in the virtual gel indicate the position of the spike-in marker for calibration. The Ladder lane shows the migration pattern of the RNA ladder standard (ranging from 50 – 6000 nucleotides).

Table 4.3 Ratio of 28S:18S and RQI values for all RNA samples.

Group	Sample name	Ratio (28S/18S)	RQI
Control 1	Control 1A	1.73	10
	Control 1B	1.52	9.7
	Control 1C	1.71	9.9
Control 2	Control 2A	1.71	9.9
	Control 2B	1.57	9.8
	Control 2C	1.71	9.8
LPS 1	LPS 1A	1.6	9.8
	LPS 1B	1.61	9.6
	LPS 1C	1.59	9.8
LPS 2	LPS 2A	1.67	9.8
	LPS 2B	1.62	9.5
	LPS 2C	1.75	9.8
LPS/bala 1	LPS/bala 1A	1.82	10.0
	LPS/bala 1B	1.78	10.0
	LPS/bala 1C	1.81	10.0
LPS/bala 2	LPS/bala 2A	1.82	9.9
	LPS/bala 2B	1.75	9.8
	LPS/bala 2C	1.81	9.3

4.4.5.3.RNA-Seq analysis

The purpose of the RNA-Seq analysis was to obtain an overview of the effects on PMA-differentiated THP-1 macrophages after treatment with LPS and combination treatment of LPS/bala. This information was obtained to act as guidance for future work and the next steps involved in this project. BGI were able to successfully perform the RNA-Seq analysis on all RNA samples. A total of 3 test groups (2 replicates each groups) were conducted, resulting in approximately 26 million clean reads for all groups. A summary of the alignment statistics is shown in Table 4.4.

Table 4.4 Alignment statistics for the six RNA samples, provided by BGI.

Group	Replicates no.	Total Clean Reads	Total Mapping Ratio	Uniquely Mapping Ratio
Control	Control 1	26,285,786	94.74%	77.81%
	Control 2	26,288,641	94.76%	78.47%
LPS	LPS 1	26,277,290	93.56%	76.92%
	LPS 2	26,273,907	93.81%	77.14%
LPS/bala	LPS/bala 1	26,289,049	93.57%	75.95%
	LPS/bala 2	26,296,725	94.39%	76.93%

4.4.5.4.Correlations between samples

In this study, Pearson correlation coefficients were calculated to measure the correlation between the six samples in terms of the expressed genes and these coefficients were reflected in the form of heat maps. All the samples underwent hierarchical clustering by the expression level of all genes. The analysis provides an

overview of all the variation between samples showing a correlation value. Values closer to 1 show a high correlation between samples and similar. The X and Y axes represent each sample. The colour represents the correlation coefficient (the darker the colour, the higher the correlation, the lighter the colour, the lower the correlation). As shown in Figure 4.6, the Pearson value seen was close to 1 when replicates in a group were compared to one another. Hence, there was a high correlation between the replicates in each group. In comparison to the control group, the LPS/bala group showed a coefficient value of 0.901-0.903 and the LPS group showed a coefficient value of 0.813-0.879. This indicates the LPS/bala treated group was more similar to the control than the LPS treated group. Furthermore, the comparisons of the LPS vs LPS/bala groups showed a coefficient value of 0.899-0.942. Another thing that should be noted is that although high correlation was seen between the LPS replicates, they showed a slightly different correlation value when compared to other group replicates. For example, LPS 1 showed a value of 0.942 when compared to LPS/bala 1, however LPS 2 showed a lower value of 0.905 when compared to LPS/bala 1. The difference between LPS replicates (Treatment 1) was also seen in the PCA plots (Figure 4.7). PCA plots are used to visualise grouping among replicates and aid in identifying technical or biological outliers. It may well be that the difference that is seen between the two replicates in Treatment 1 is not due to the (small) differences in RNA quality between the samples but an unfortunate consequence of differences in either their treatment or RNA-seq processing (or both) but this is very unlikely. Replication of the with higher N numbers would allow for identification of experimental outliers. Nevertheless, the LPS group still showed low correlations with the Control group and

the LPS/bala group. The differences between each group indicate the effects of LPS and LPS/bala on gene expression.

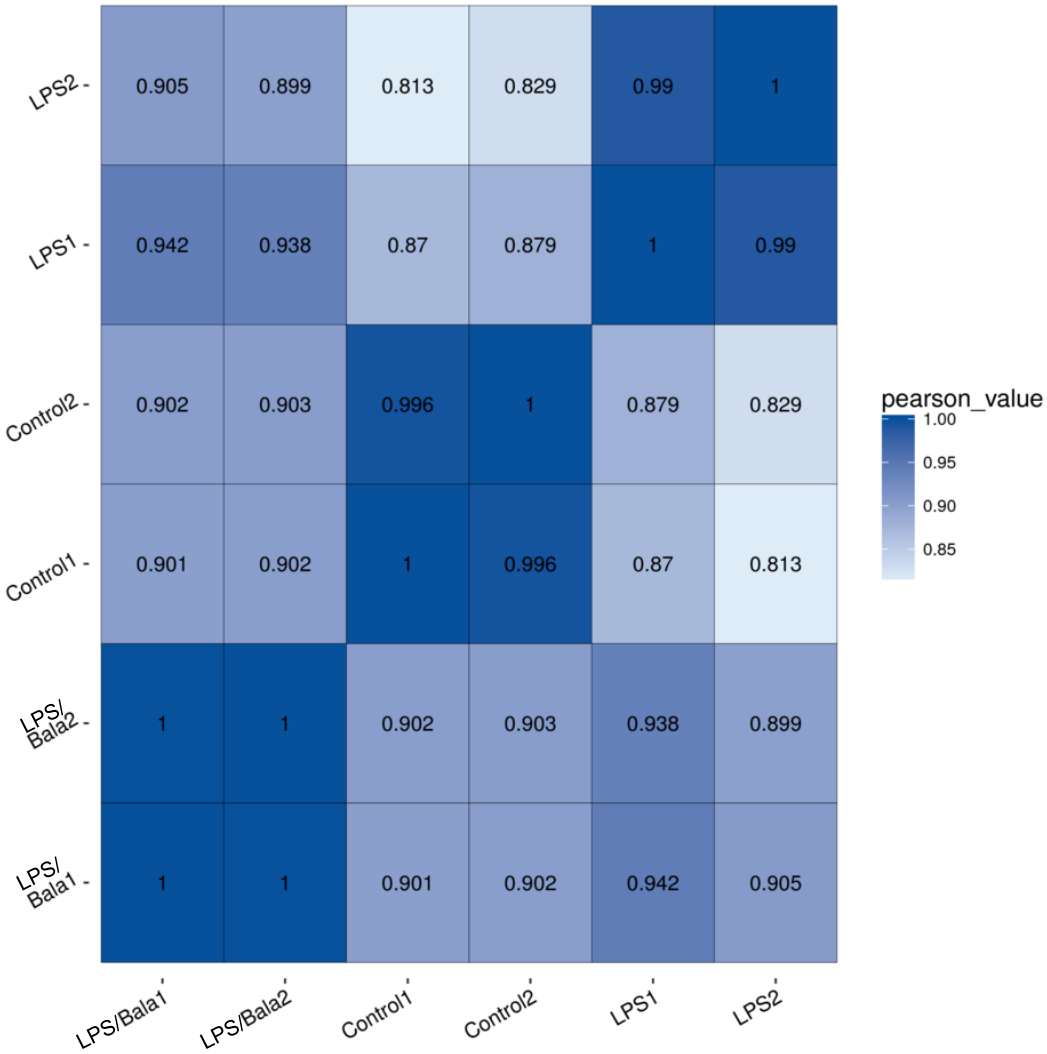

Figure 4.6 Heatmap correlation for all six samples that were RNA sequenced provided by BGI-Tech. If one sample is highly similar with another one, the correlation value between them is very close to 1.

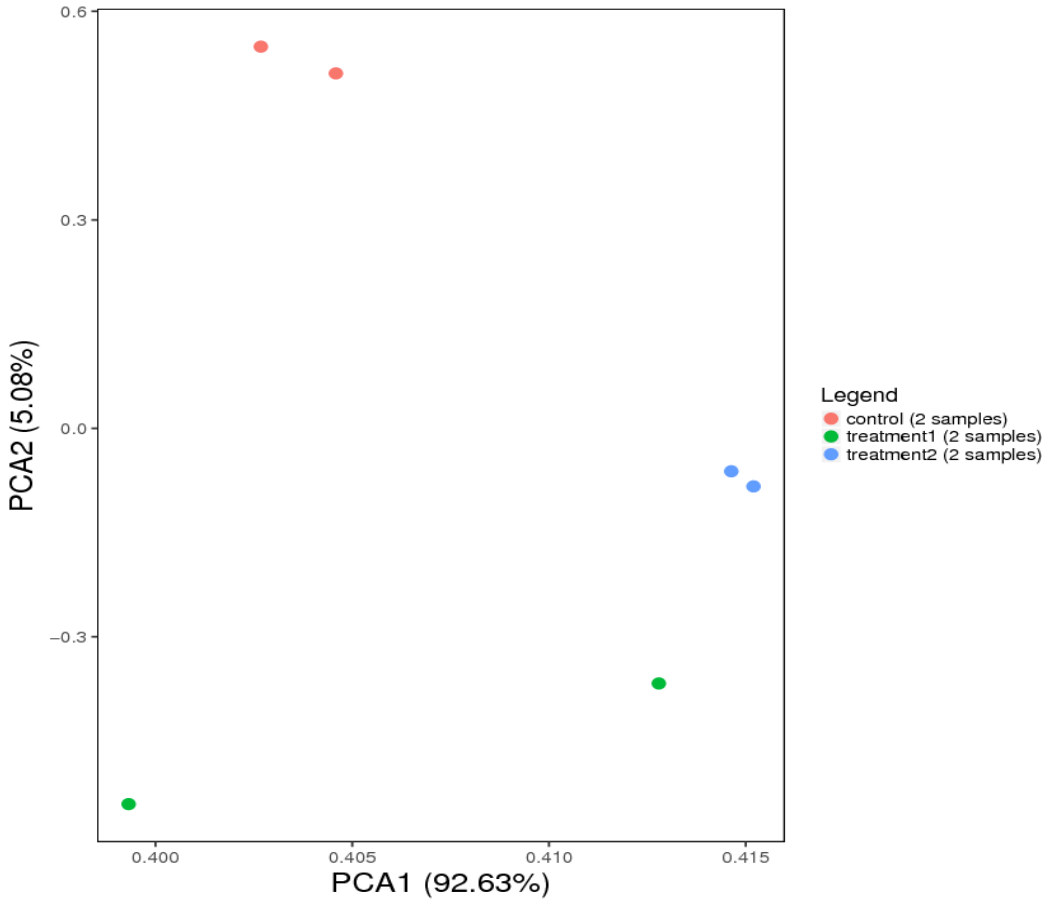

Figure 4.7 PCA plot displaying all six samples along PCA1 and PCA2, which describe 5.08% and 92.63% of the variability, respectively, within the expression data set. Control: untreated cells, treatment 1: LPS replicates, treatment 2: LPS/bala replicates

4.4.5.5. DEGs

A summary of DEGs between the Control, LPS and LPS/bala groups is given in Figure 4.9. When comparing LPS group with Control group, there were higher number of up-regulated genes (1173 genes) than down-regulated genes (675 genes). However, LPS/bala treatment caused a decrease in the number of up-regulated genes (690 genes) with a slightly higher number of down-regulated genes (742 genes) when compared to the control. Furthermore, when LPS/bala is compared to LPS, more genes were down-regulated (697 genes) than up-regulated (115 genes). The scatter plot in Figure 4.9 shows the magnitude and distribution of fold changes of DEGs in control vs LPS, control vs LPS/bala and LPS vs LPS/bala.

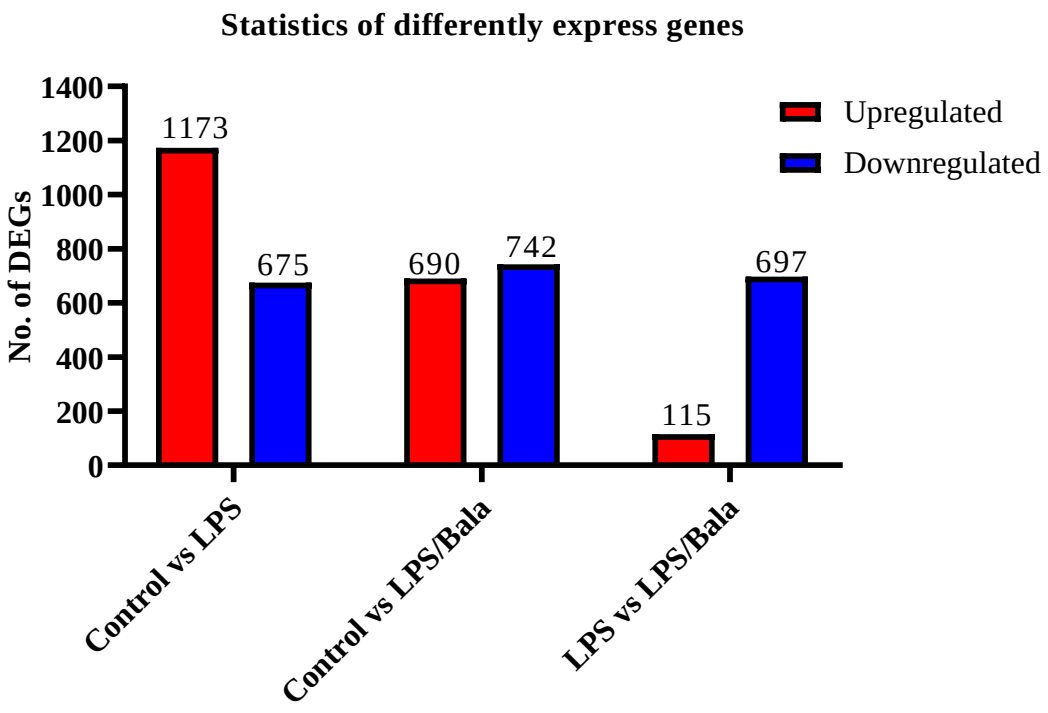

Figure 4.8 Summary of DEGs. Log2FC of Control vs LPS, Control vs LPS/bala and LPS vs LPS/bala was compared (log2FC ≥ 1 for up-regulated genes and log2FC ≤ -1 for down-regulated genes). False discover rate (FDR) ≤ 0.001. FC means fold-change.

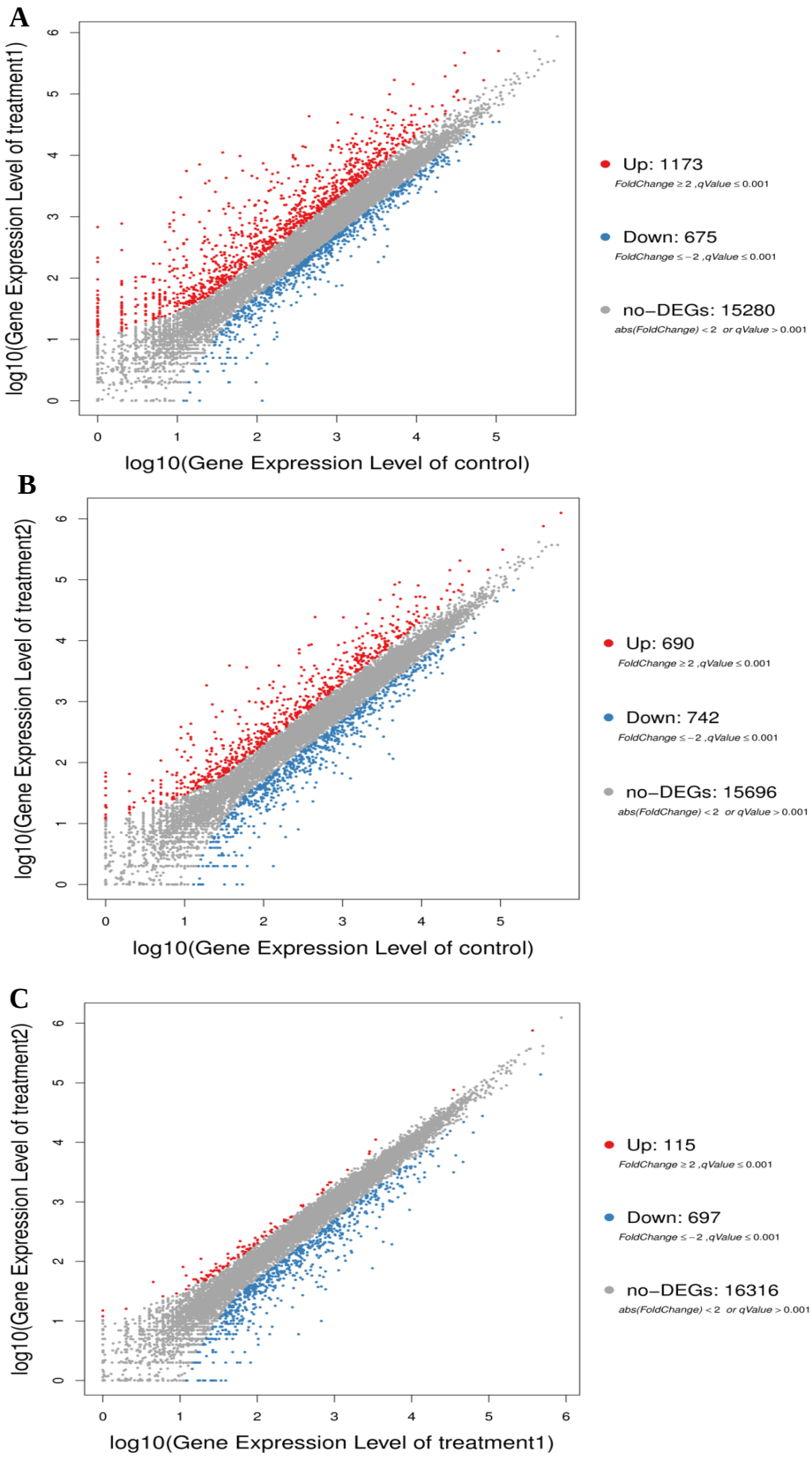

Figure 4.9 Scatter plot of DEGs: A) control vs LPS; B) control vs LPS/bala and C) LPS vs LPS/bala.

4.4.5.6.Pathway enrichment analysis

Deep analysis of the RNA-Seq data provided by BGI was carried out using Cytoscape software with a ClueGo plugin. Only significant ($P<0.05$) affected gene ontologies (GO) from the KEGG pathways were selected. The genes that showed at least two-fold change in comparison from one group to another were only considered in this analysis.

A summary of the ClueGo results is shown in Figure 4.10-Figure 4.12 and Table 4.5-Table 4.7. When comparing the control group with the LPS group, there were 43 significant GO terms associated with up-regulated genes and no significant GO terms associated with down-regulated genes. On the other hand, comparison of control vs LPS/bala showed 20 GO terms associated with up-regulated genes and 7 GO terms were associated with down-regulated genes. LPS/bala were compared to LPS produced only 1 GO terms associated with up-regulated genes, and 36 significant GO terms were affected by down-regulated genes.

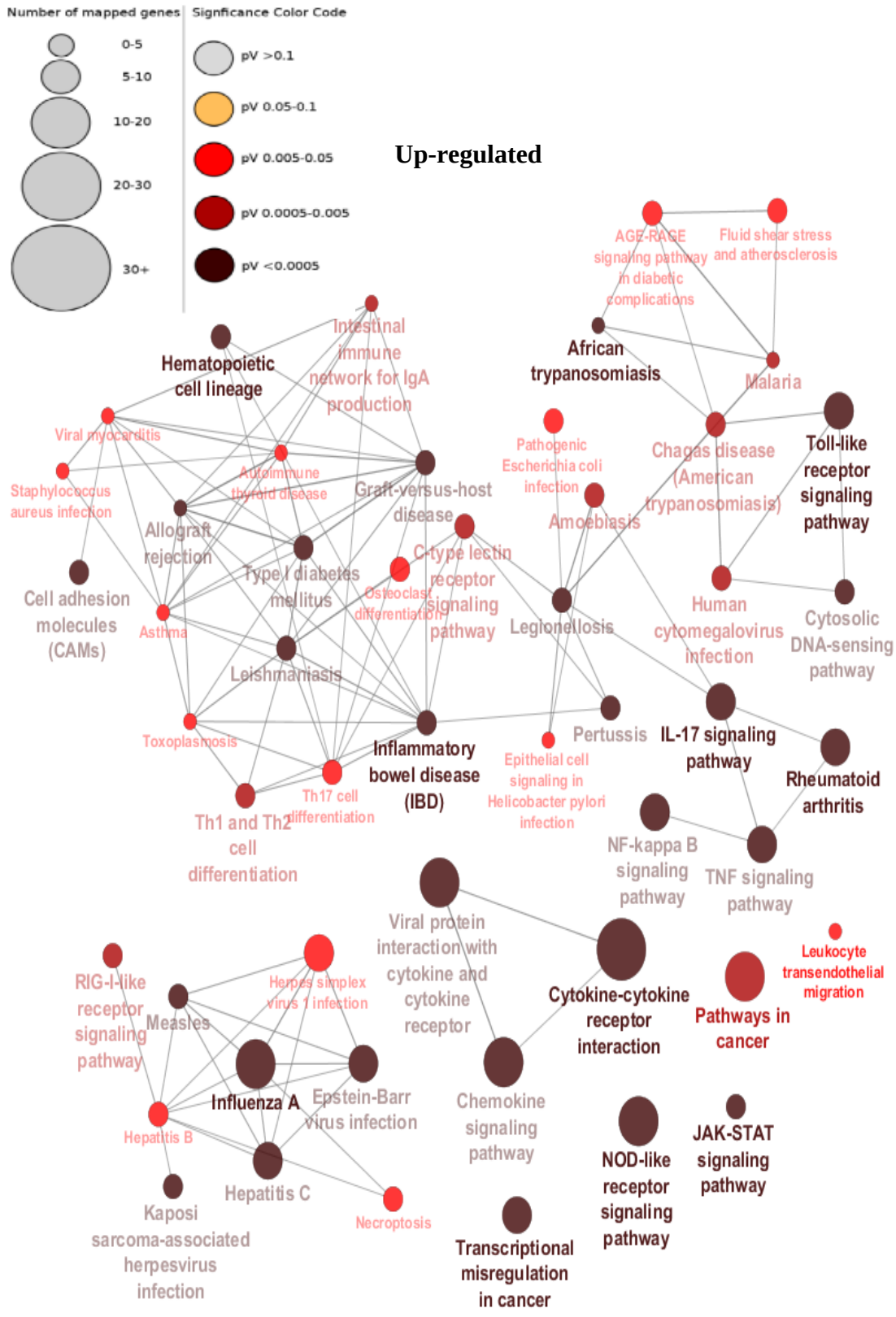

Figure 4.10 Cluster results obtained from Cytoscape GlueGO using DEGs in the control vs LPS. Results represents GO terms enriched with up-regulated DEGs (log2FC ≥ 1). Size of the circles is directly related to the number of genes in each GO, the circle's colour is linked to the significance of the affected pathway.

Table 4.5 List of significant genes linked with particular gene ontologies when comparing control vs LPS. The table shows the genes associated with those KEGG pathways listed.

KEGG pathway	%	No. of genes	List of genes
Up-regulated			
Cytokine-cytokine receptor interaction	15.99	47.00	*ACKR4, CCL1, CCL17, CCL2, CCL20, CCL3, CCL3L1, CCL3L3, CCL4, CCL4L1, CCL4L2, CCL5, CCL7, CCR7, CRLF2, CSF2, CSF3, CXCL1, CXCL10, CXCL11, CXCL12, CXCL13, CXCL2, CXCL3, CXCL5, CXCL6, CXCL8, CXCL9, FAS, β2B, IL15RA, IL18R1, IL1A, IL1R2, IL23A, IL2RA, IL33, IL36G, IL36RN, IL6, IL7, LTA, TNF, TNFSF10, TNFSF13B, TNFSF8, TSLP*
Viral protein interaction with cytokine and cytokine receptor	31.00	31.00	*ACKR4, CCL1, CCL17, CCL2, CCL20, CCL3, CCL3L1, CCL3L3, CCL4, CCL4L1, CCL4L2, CCL5, CCL7, CCR7, CXCL1, CXCL10, CXCL11, CXCL12, CXCL13, CXCL2, CXCL3, CXCL5, CXCL6, CXCL8, CXCL9, IL18R1, IL2RA, IL6, LTA, TNF, TNFSF10*
Chemokine signalling pathway	14.29	27.00	[*CCL1, CCL17, CCL2, CCL20, CCL3, CCL3L1, CCL3L3, CCL4, CCL4L1, CCL4L2, CCL5, CCL7, CCR7, CXCL1, CXCL10, CXCL11, CXCL12, CXCL13, CXCL2, CXCL3, CXCL5, CXCL6, CXCL8, CXCL9, HCK, ITK, NCF1*]
Rheumatoid arthritis	23.66	22.00	[*CCL2, CCL20, CCL3, CCL3L1, CCL3L3, CCL5, CD80, CSF2, CXCL1, CXCL12, CXCL2, CXCL3, CXCL5, CXCL6, CXCL8, HLA-DPB1, IL1A, IL23A, IL6, MMP3, TNF, TNFSF13B*]
TNF signalling pathway	19.64	22.00	[*BIRC3, CCL2, CCL20, CCL5, CSF2, CXCL1, CXCL10, CXCL2, CXCL3, CXCL5, CXCL6, EDN1, FAS, IL1β, IL18R1, IL6, LTA, MMP9, NOD2, PTGS2, TNF, TNFAIP3, TRAF1, VCAM1*]
IL-17 signalling pathway	20.21	19.00	[*CCL17, CCL2, CCL20, CCL7, CSF2, CSF3, CXCL1, CXCL10, CXCL2, CXCL3, CXCL5, CXCL6, CXCL8, IL6, MMP3, PTGS2, S100A8, TNF, TNFAIP3*]
NF-kappa B signalling pathway	16.67	18.00	[*BCL2A1, BIRC3, CCL4, CCL4L1, CCL4L2, CXCL1, CXCL12, CXCL2, CXCL3, CXCL8, DDX58, LTA, MMP9, NFKBIA, NFKBIZ,*

			PTGS2, TNF, TNFAIP3, TNFSF13B, TRAF1,VCAM1]
Toll-like receptor signalling pathway	15.38	16.00	*[CCL3, CCL3L1, CCL3L3, CCL4, CCL4L1, CCL4L2, CCL5, CD80, CXCL10, CXCL11, CXCL8, CXCL9, IL12B, IL6, TLR3, TNF*]
Influenza A	9.41	16.00	[*CCL2, CCL5, CXCL10, CXCL8, DDX58, FAS, HLA-DPB1, IFIH1, IL12B, IL1A, IL33, IL6, RSAD2, TLR3, TNF, TNFSF10*]
NOD-like receptor signalling pathway	8.84	16.00	[*AIM2, BIRC3, CCL2, CCL5, CXCL1, CXCL2, CXCL3, CXCL8, GBP1, GBP2, GBP4, GBP7, IL6, NOD2, TNF, TNFAIP3*]
Transcriptional misregulation in cancer	8.06	15.00	[*BCL2A1, BIRC3, CSF2, CXCL8, ETV7, GZMB, IGFBP3, IL1R2, IL6, KDM6A, MMP3, NFKBIZ, PAX5, PLAT, RUNX1T1*]
Human cytomegalovirus infection	6.22	14.00	[*CCL2, CCL3, CCL3L1, CCL3L3, CCL4, CCL4L1, CCL4L2, CCL5, CXCL12, CXCL8, FAS, IL6, PTGS2, TNF*]
JAK-STAT signalling pathway	6.79	13.00	[*CRLF2, CSF2, CSF3, IL12B, IL15RA, IL23A, IL2RA, IL6, IL7, STAT1, STAT3, STAT4, TSLP*]
Hematopoietic cell lineage	11.11	11.00	[*CD38, CSF2, CSF3, HLA-DPB1, IL1A, IL1R2, IL2RA, IL6, IL7, ITGA1, TNF*]
Chagas disease	9.80	10.00	[*CCL2, CCL3, CCL3L1, CCL3L3, CCL5, CXCL8, FAS, IL12B, IL6, TNF*]
Amoebiasis	9.80	10.00	[*CSF2, CXCL1, CXCL2, CXCL3, CXCL8, IL12B, IL1R2, IL6, SERPINB4, TNF*]
Kaposi sarcoma	5.38	10.00	[*CSF2, CXCL1, CXCL2, CXCL3, CXCL8, FAS, HCK, IL6, PTGS2, TLR3*]
Cytosolic DNA-sensing pathway	14.29	9.00	[*AIM2, CCL4, CCL4L1, CCL4L2, CCL5, CXCL10, DDX58, IL33, IL6*]
Inflammatory bowel disease (IBD)	13.85	9.00	[*HLA-DPB1, IL12B, IL18R1, IL1A, IL23A, IL6, NOD2, STAT4, TNF*]
Pertussis	11.84	9.00	[*CXCL5, CXCL6, CXCL8, IL12B, IL1A, IL23A, IL6, IRF8, TNF]*
Measles	6.52	9.00	[*DDX58, FAS, IFIH1, IL12B, IL1A, IL2RA, IL6, SLAMF1, TNFAIP3*]
Necroptosis	5.56	9.00	[*BIRC3, FAS, IL1A, IL33, STAT4, TLR3, TNF, TNFAIP3, TNFSF10*]
Type I diabetes mellitus	18.60	8.00	[*CD80, FAS, GZMB, HLA-DPB1, IL12B, IL1A, LTA, TNF*]
Atherosclerosis	5.76	8.00	[*CCL2, EDN1, IL1A, IL1R2, NCF1, PLAT, TNF, VCAM1*]

Hepatitis C	5.16	8.00	[*CXCL10, DDX58, FAS, IFIT1, IFIT1B, RSAD2, TLR3, TNF*]
Hepatitis B	4.94	8.00	[*CXCL8, DDX58, FAS, IFIH1, IL6, STAT4, TLR3, TNF*]
Graft-versus-host disease	17.07	7.00	[*CD80, FAS, GZMB, HLA-DPB1, IL1A, IL6, TNF*]
Legionellosis	12.28	7.00	[*CXCL1, CXCL2, CXCL3, CXCL8, IL12B, IL6, TNF*]
RIG-I-like receptor signalling pathway	10.00	7.00	[*CXCL10, CXCL8, DDX58, IFIH1, IL12B, ISG15, TNF*]
AGE-RAGE signalling pathway	7.00	7.00	[*CCL2, CXCL8, EDN1, IL1A, IL6, TNF, VCAM1*]
African trypanosomiasis	16.22	6.00	[*FAS, IDO1, IL12B, IL6, TNF, VCAM1*]
Allograft rejection	15.79	6.00	[*CD80, FAS, GZMB, HLA-DPB1, IL12B, TNF*]
Intestinal immune network for IgA production	12.24	6.00	[*CD80, CXCL12, HLA-DPB1, IL15RA, IL6, TNFSF13B*]
Malaria	12.00	6.00	[*CCL2, CSF3, CXCL8, IL6, TNF, VCAM1*]
Epithelial cell signalling	8.57	6.00	[*CCL5, CXCL1, CXCL2, CXCL3, CXCL8, TJP1*]
Leishmaniasis	7.79	6.00	[*HLA-DPB1, IL12B, IL1A, NCF1, PTGS2, TNF*]
C-type lectin receptor signalling pathway	5.77	6.00	[*CCL17, IL12B, IL23A, IL6, PTGS2, TNF*]
Apoptosis	4.41	6.00	[*BCL2A1, BIRC3, FAS, GZMB, TNF, TNFSF10*]
Th1 and Th2 cell differentiation	5.43	5.00	[*DLL4, HLA-DPB1, IL12B, IL2RA, STAT4*]
Th17 cell differentiation	4.67	5.00	[*HLA-DPB1, IL23A, IL2RA, IL6, IRF4*]
Autoimmune thyroid disease	7.55	4.00	[*CD80, FAS, GZMB, HLA-DPB1*]
Asthma	9.68	3.00	[*HLA-DPB1, PRG2, TNF*]
Prion diseases	8.57	3.00	[*CCL5, IL1A, IL6*]

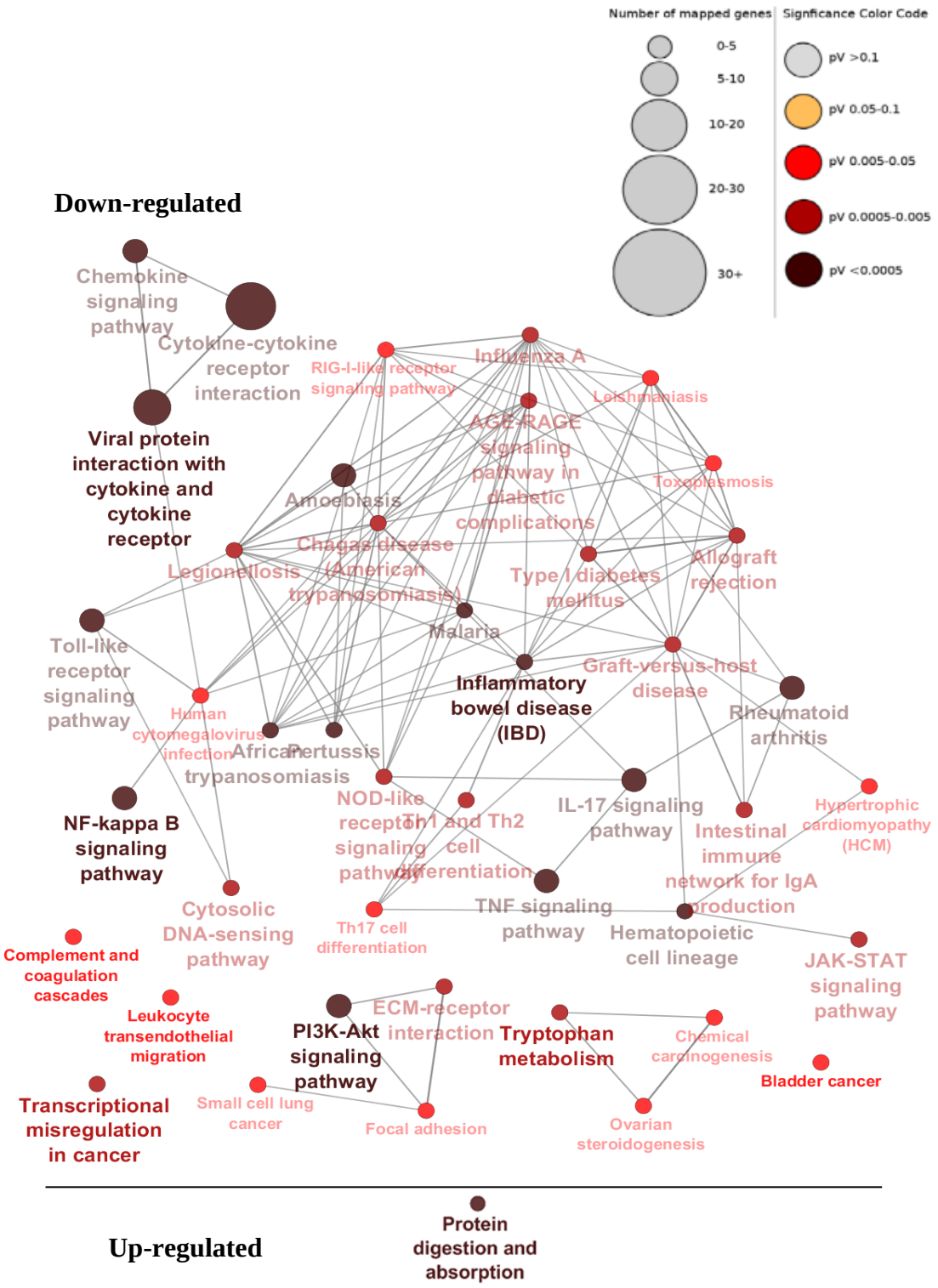

Figure 4.11 Cluster results obtained from Cytoscape GlueGO using DEGs in the LPS vs LPS/bala. Results represents GO terms enriched with down-regulated (log2FC ≤ -1) and up-regulated DEGs (log2FC ≥ 1). Size of the circles is directly related to the number of genes in each GO, the circle's colour is linked to the significance of the affected pathway.

Table 4.6 List of significant genes linked with particular gene ontologies when comparing LPS vs LPS/bala. The table shows the percentage of genes associated with those KEGG pathways listed.

KEGG pathway	%	No. of genes	List of genes
Down-regulated			
Cytokine-cytokine receptor interaction	8.16	27.00	[*ACKR3, ACKR4, CCL1, CCL2, CCL7, CCL8, CNTFR, CSF2, CSF3, CXCL11, CXCL13, CXCL5, CXCL9, CXCR5, IL12B, IL18R1, IL2RA, IL36G, IL36RN, IL6, INHBA, LTA, TNF, TNFSF10, TNFSF13B, TNFSF8, XCR1*]
Viral protein interaction with cytokine and cytokine receptor	17.00	17.00	[*ACKR3, ACKR4, CCL1, CCL2, CCL7, CCL8, CXCL11, CXCL13, CXCL5, CXCL9, CXCR5, IL18R1, IL2RA, IL6, LTA, TNF, XCR1*]
PI3K-Akt signalling pathway	4.24	15.00	[*C8orf44-SGK3, COL4A1, COL4A2, CSF3, FGF2, FLT1, IBSP, IGF2, IL2RA, IL6, ITGA1, ITGB8, LPAR3, NR4A1, THBS1*]
NF-kappa B signalling pathway	13.67	14.00	[*BIRC3, CXCL1, CXCL12, CXCL2, CXCL3, CXCL8, DDX58, LTA, MMP9, NFKBIA, NFKBIZ, TNF, TNFAIP3, TNFSF13B*]
TNF signalling pathway	8.93	12.00	[*BIRC3, CCL2, CSF2, CXCL5, IL18R1, IL6, LTA, MMP9, PTGS2, SOCS3, TNF, VCAM1*]
Chemokine signalling pathway	5.82	11.00	[*CCL1, CCL2, CCL7, CCL8, CXCL11, CXCL13, CXCL5, CXCL9, CXCR5, ITK, XCR1*]
IL-17 signalling pathway	10.64	10.00	[*CCL2, CCL7, CSF2, CSF3, CXCL5, IL6, MMP1, MMP13, PTGS2, TNF*]
Rheumatoid arthritis	9.68	9.00	[*CCL2, CD80, CSF2, CXCL5, FLT1, HLA-DPA1, IL6, MMP1, TNF*]
Pertussis	10.53	8.00	[*C4A, C4B, CXCL5, IL12B, IL6, IRF8, NOS2, TNF*]
Hematopoietic cell lineage	8.08	8.00	[*CD5, CSF2, CSF3, HLA-DPA1, IL2RA, IL6, ITGA1, TNF*]
Amoebiasis	7.84	8.00	[*COL4A1, COL4A2, CSF2, IL12B, IL6, NOS2, SERPINB4, TNF*]
JAK-STAT signalling pathway	4.94	8.00	[*CNTFR, CSF2, CSF3, IL12B, IL2RA, IL6, SOCS3, STAT3, STAT4*]
Inflammatory bowel disease (IBD)	10.77	7.00	[*GATA3, HLA-DPA1, IL12B, IL18R1, IL6, STAT4, TNF*]

Toll-like receptor signalling pathway	6.73	7.00	[*CD80, CXCL11, CXCL9, IL12B, IL6, TLR8, TNF*]
Malaria	12.00	6.00	[*CCL2, CSF3, IL6, THBS1, TNF, VCAM1*]
ECM-receptor interaction	6.82	6.00	[*COL4A1, COL4A2, IBSP, ITGA1, ITGB8, THBS1*]
Th1 and Th2 cell differentiation	6.52	6.00	[*DLL4, GATA3, HLA-DPA1, IL12B, IL2RA, STAT4*]
AGE-RAGE signalling pathway in diabetic complications	6.00	6.00	[*CCL2, COL4A1, COL4A2, IL6, TNF, VCAM1*]
African trypanosomiasis	13.51	5.00	[*IDO1, IL12B, IL6, TNF, VCAM1*]
Type I diabetes mellitus	11.63	5.00	[*CD80, HLA-DPA1, IL12B, LTA, TNF*]
Leishmaniasis	6.49	5.00	[*HLA-DPA1, IL12B, NOS2, PTGS2, TNF*]
Complement and coagulation cascades	5.88	5.00	[*C4A, C4B, CFH, F2RL3, SERPINB2*]
Hypertrophic cardiomyopathy (HCM)	5.56	5.00	[*CACNA2D3, IL6, ITGA1, ITGB8, TNF*]
Chagas disease (American trypanosomiasis)	4.90	5.00	[*CCL2, IL12B, IL6, NOS2, TNF*]
Th17 cell differentiation	4.67	5.00	[*GATA3, HLA-DPA1, IL2RA, IL6, IRF4*]
Allograft rejection	10.53	4.00	[*CD80, HLA-DPA1, IL12B, TNF*]
Graft-versus-host disease	9.76	4.00	[*CD80, HLA-DPA1, IL6, TNF*]
Tryptophan metabolism	9.52	4.00	[*CYP1A1, CYP1B1, IDO1, KMO]*
Chemical carcinogenesis	4.88	4.00	[*CYP1A1, CYP1B1, GSTM5, PTGS2*]
Small cell lung cancer	4.35	4.00	[*COL4A1, COL4A2, NOS2, PTGS2*]
Staphylococcus aureus infection	4.17	4.00	[*C4A, C4B, CFH, HLA-DPA1*]
Dilated cardiomyopathy (DCM)	4.17	4.00	[*CACNA2D3, ITGA1, ITGB8, TNF*]
Protein digestion and absorption	4.21	4.00	[*COL11A1, COL2A1, COL9A1, PGA5*]
Intestinal immune network for IgA production	6.12	3.00	[*CD80, HLA-DPA1, IL6*]

Ovarian steroidogenesis	5.88	3.00	[*CYP1A1, CYP1B1, PTGS2*]
Legionellosis	5.26	3.00	[*IL12B, IL6, TNF*]
Up-regulated			
Protein digestion and absorption	4.21	4.00	[*COL11A1, COL2A1, COL9A1, PGA5*]

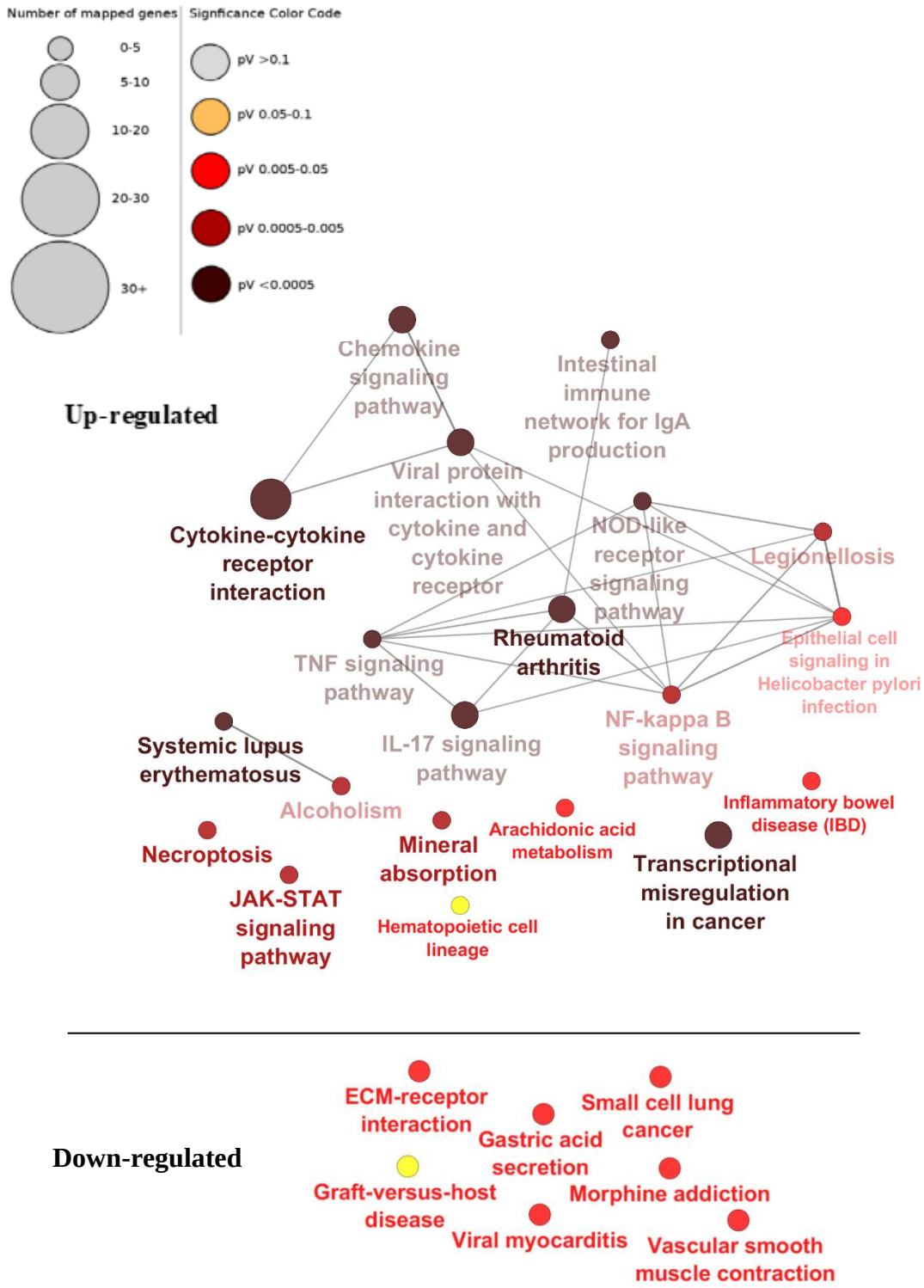

Figure 4.12 Cluster results obtained from Cytoscape GlueGO using DEGs in the control vs LPS/bala. Results represents GO terms enriched with down-regulated (log2FC ≤ -1) and up-regulated DEGs (log2FC ≥ 1). Size of the circles is directly related to the number of genes in each GO, the circle's colour is linked to the significance of the affected pathway.

Table 4.7 List of significant genes linked with particular gene ontology when comparing control vs LPS/bala. The table shows the percentage of genes associated with those KEGG pathways listed.

KEGG pathway	%	No. of genes	List of genes
Up-regulated			
Cytokine-cytokine receptor interaction	6.80	22.00	[*CCL17, CCR7, CRLF2, CSF2, CSF3, CXCL1, CXCL11, CXCL12, CXCL13, CXCL2, CXCL3, CXCL6, IL6, IL15RA, IL23A, IL32, IL36RN, TNF, TNFSF10, TNFSF13B, TNFSF8, TSLP*]
Rheumatoid arthritis	11.83	11.00	[*CD80, CSF2, CXCL1, CXCL12, CXCL2, CXCL3, CXCL6, HLA-DQA1, IL23A, MMP3, TNFSF13B*]
Chemokine signalling pathway	5.82	11.00	[*CCL17, CCR7, CXCL1, CXCL11, CXCL12, CXCL13, CXCL2, CXCL3, CXCL6, HCK, ITK*]
IL-17 signalling pathway	10.64	10.00	[*CCL17, CSF2, CSF3, CXCL1, CXCL2, CXCL3, CXCL6, MMP3, S100A8, S100A9*]
Viral protein interaction with cytokine and cytokine receptor	10.00	10.00	[*CCL17, CCR7, CXCL1, CXCL11, CXCL12, CXCL13, CXCL2, CXCL3, CXCL6, TNFSF10*]
Transcriptional misregulation in cancer	5.38	10.00	[*BIRC3, CSF2, ETV7, H3C10, H3C14, H3C15, MMP3, NFKBIZ, PAX5, PLAT*]
TNF signalling pathway	8.04	9.00	[*BIRC3, CSF2, CXCL1, CXCL2, CXCL3, CXCL6, EDN1, MMP9, NOD2, PTGS2*]
Systemic lupus erythematosus	6.77	9.00	[*CD80, H2AC13, H2AC7, H2BC18, H2BC5, H3C10, H3C14, H3C15, HLA-DQA1*]
NOD-like receptor signalling pathway	4.97	9.00	[*BIRC3, CASP1, CXCL1, CXCL2, CXCL3, GBP1, GBP2, GBP4, NOD2*]
Necroptosis	4.94	8.00	[*BIRC3, CASP1, H2AC13, H2AC7, PLA2G4B, STAT4, TLR3, TNFSF10*]
Alcoholism	4.35	8.00	[*ADORA2A, H2AC13, H2AC7, H2BC18, H2BC5, H3C10, H3C14, H3C15*]
JAK-STAT signalling pathway	4.32	8.00	[*CRLF2, CSF2, CSF3, IL15RA, IL23A, STAT3, STAT4, TSLP*]
NF-kappa B signalling pathway	5.88	7.00	[*BIRC3, CXCL1, CXCL12, CXCL2, CXCL3, MMP9, TNFSF13B*]

Intestinal immune network for IgA production	10.20	5.00	[*CD80, CXCL12, HLA-DQA1, IL15RA, TNFSF13B*]
Legionellosis	7.02	4.00	[*CASP1, CXCL1, CXCL2, CXCL3*]
Mineral absorption	6.90	4.00	[*MT1E, MT1F, MT1G, MT1X*]
Inflammatory bowel disease (IBD)	6.15	4.00	[*HLA-DQA1, IL23A, NOD2, STAT4*]
Hematopoietic cell lineage	4.04	4.00	[*CD38, CSF2, CSF3, HLA-DQA1*]
Arachidonic acid metabolism	4.76	3.00	[*CYP2J2, PLA2G4B, PTGES*]
Epithelial cell signalling in Helicobacter pylori infection	4.29	3.00	[*CXCL1, CXCL2, CXCL3*]
Down-regulated			
Vascular smooth muscle contraction	4.55	6.00	[*ADCY8, CALCRL, EDNRA, KCNMA1, KCNMB1, PRKG1*]
ECM-receptor interaction	4.55	4.00	[*COL4A1, IBSP, ITGA9, LAMC3*]
Morphine addiction	4.40	4.00	[*ADCY8, GABRA4, GABRB2, PDE7B*]
Small cell lung cancer	4.35	4.00	[*COL4A1, LAMC3, NOS2, RXRG*]
Graft-versus-host disease	7.32	3.00	[*KIR2DL3, KLRC1, PRF1*]
Viral myocarditis	5.00	3.00	[*CAV1, CXADR, PRF1*]
Gastric acid secretion	4.00	3.00	[*ADCY8, KCNJ1, KCNQ1*]

After analysing the results using the Cytoscape ClueGo plugin, it was shown that the cytokine-cytokine receptor interaction pathway was the most significantly ($P<0.05$) affected with highest number of associated genes among the three comparisons (Control vs LPS, control vs LPS/bala, LPS vs LPS/bala). The log2 fold change of the DEGs associated with the cytokine-cytokine receptor interaction pathway for all three groups is presented in a heatmap shown in Figure 4.13. All expressed genes associated with the cytokine pathway showed to be up-regulated in Control vs LPS group and were down-regulated in LPS vs LPS/bala group.

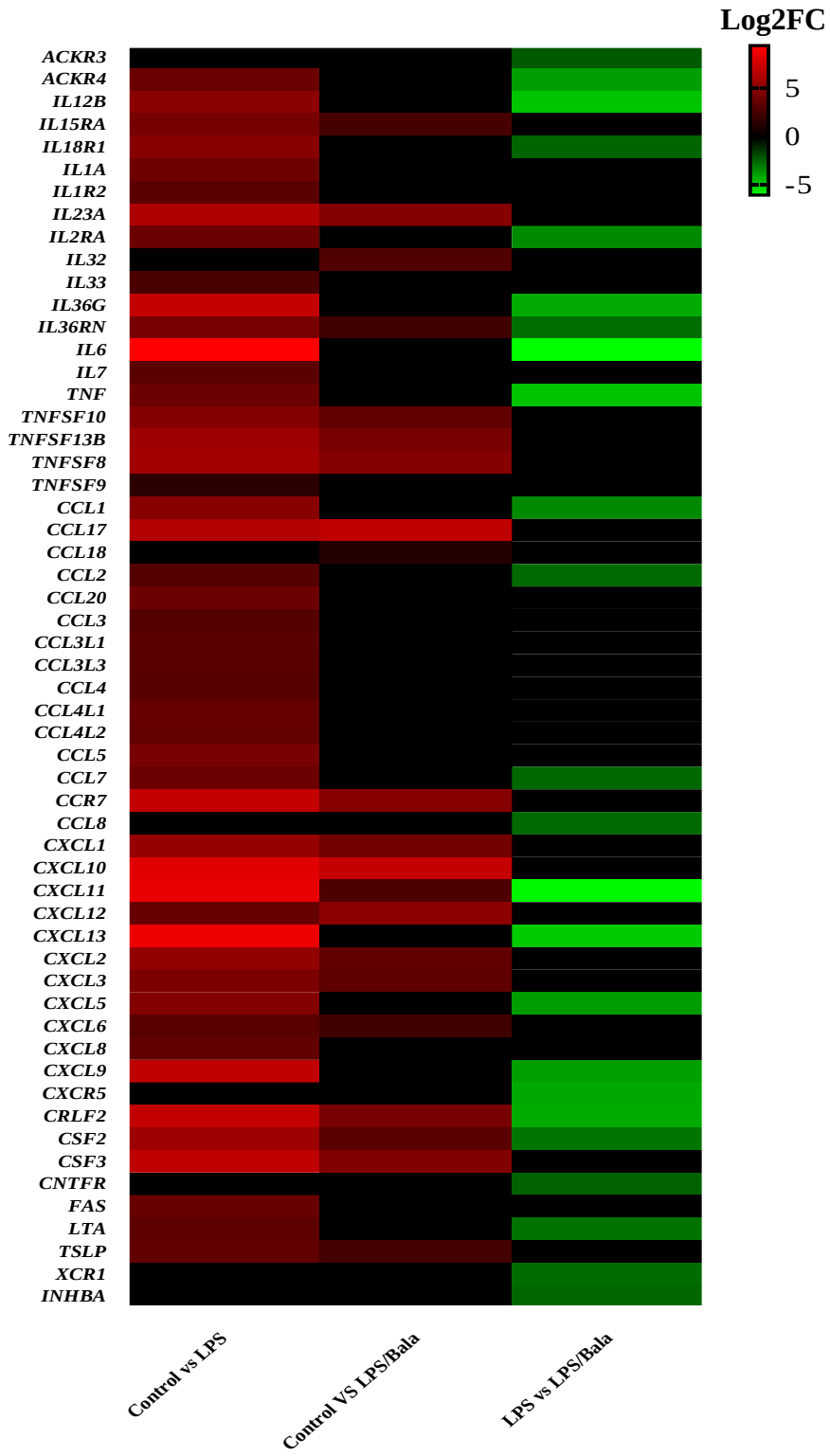

Figure 4.13 Heatmap showing the Log2 ratio of genes associated with the cytokine-cytokine receptor interaction pathway among the three comparisons using GraphPad Prism 8. Red represents up-regulated genes; Green represents down-regulated genes; Black represents no change.

4.4.5.7. Pathview significant analysis

KEGG pathway analysis using PathView demonstrated that treatment of the THP-1 cells with these compounds resulted in DEGs which (P<0.05) significantly enriched two key immune pathways; the TNF signalling pathway and the JAK/STAT signalling pathway. Figure 4.15 and Figure 4.16 shows the TNF signalling pathway for control vs LPS and LPS vs LPS/bala treatment groups, respectively. In the TNF signalling pathway, for the group treated with LPS, the 5 most up-regulated genes were *BIRC3* (baculoviral IAP Repeat Containing 3), *MMP9* (matrix metallopeptidase 9), *PTGS2* (prostaglandin-endoperoxide synthase 2) and *TNF-α* that were up-regulated by more than 4-fold and *IL-6* was up-regulated by 6-fold (Figure 4.14). When comparing the LPS/bala treated group to control, the same genes were either up-regulated by less than 3-fold or no change at all (*TNF-α* and *IL-6*). These genes were also showed to be down-regulated in the group treated with LPS/bala when compare to the LPS treatment alone with down-regulation of IL-6 by more than 5-fold.

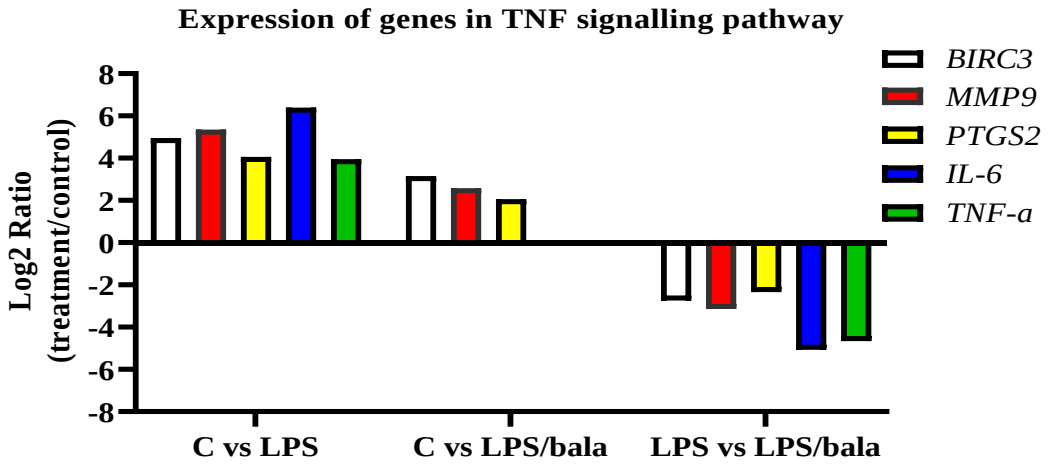

Figure 4.14 A bar chart showing the Log2 ratio of the top five genes expressed among the three comparisons: Control (C) vs LPS, Control (C) vs LPS/bala and LPS vs LPS/bala. LPS and LPS/bala treatment has statistically ($P < 0.05$) up-regulated all genes expression when compared to control. LPS/bala treatment statistically ($P < 0.05$) down-regulated gene expression when compared to LPS alone.

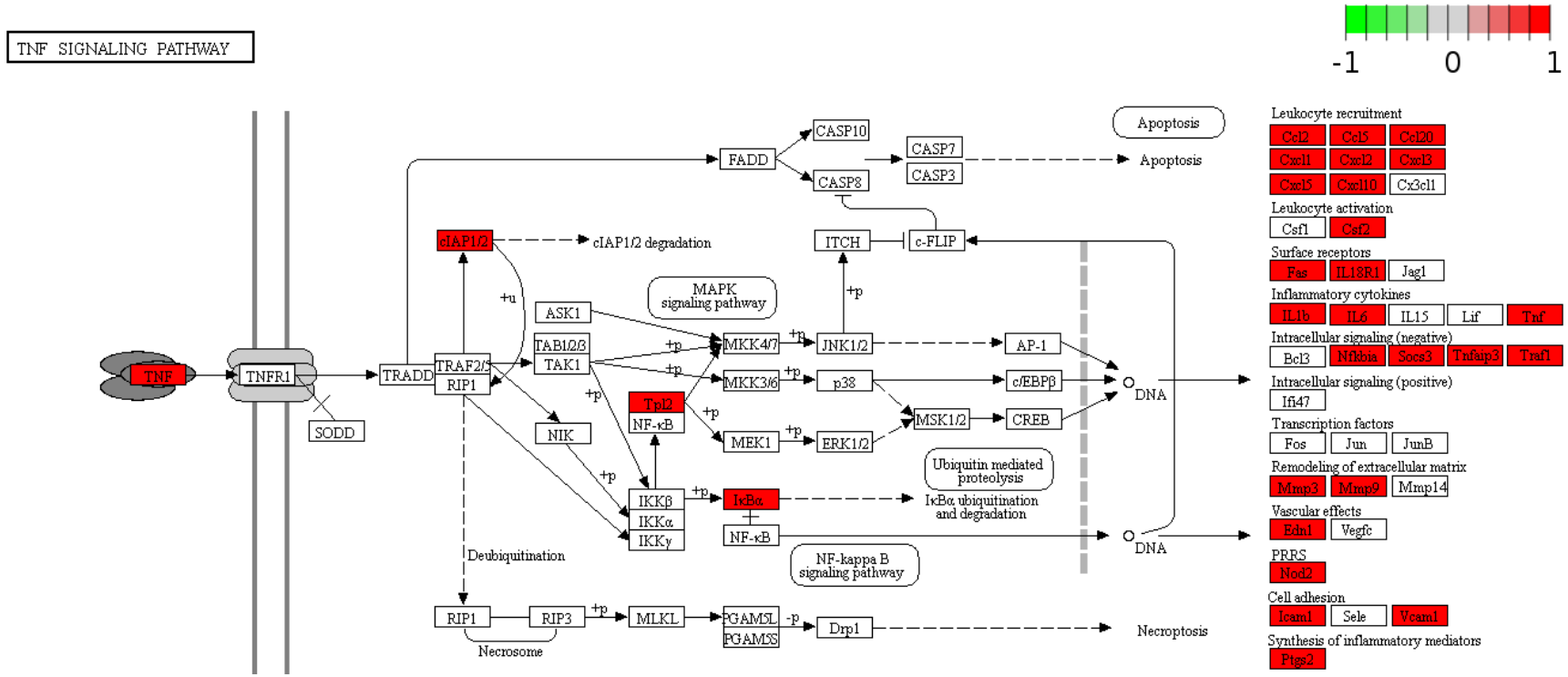

Figure 4.15 DEGs enriched KEGG map of TNF signalling pathway rendered by Pathview for control vs LPS group. Target genes in the pathway are depicted by boxes while arrows depict signalling routes. The coloured scale corresponds to log2-fold changes. Red colour indicates statistically significant increase in expression (P<0.05). No colour corresponds to no changes.

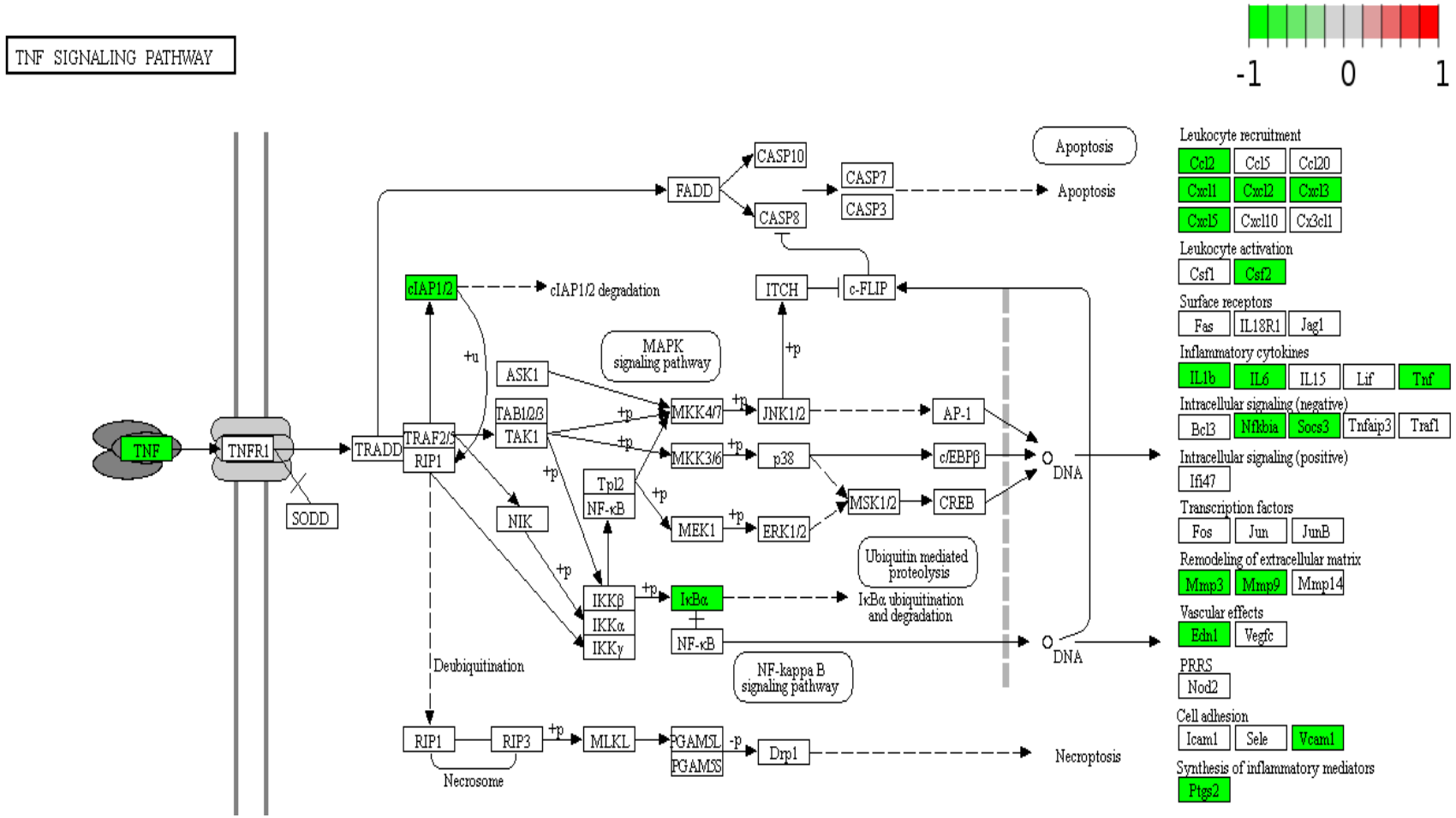

Figure 4.16 DEGs enriched KEGG map of the TNF signalling pathway rendered by Pathview for the LPS vs LPS/bala group. Target genes in the pathway are depicted by boxes while arrows depict signalling routes. The coloured scale corresponds to log2-fold changes. Green indicates a statistically significant (P<0.05) decrease in expression. No colour corresponds to no changes.

Figure 4.18 and Figure 4.19 show the JAK/STAT signalling pathway for the control vs LPS and LPS vs LPS/bala treatment groups, respectively. In the JAK/STAT signalling pathway, for the group treated with LPS, the three most up-regulated genes were *STAT1*, *STAT3,* and *STAT4* (Figure 4.17) by LPS treatment and these genes are known to be closely related to the pathway. LPS and LPS/bala treatment statistically ($P<0.05$) up-regulated expression of *STAT1* by 2-fold, *STAT3* by 4-fold and 2-fold, respectively, and *STAT4* genes by 5-fold and 3-fold, respectively, when compared to the control. LPS/bala treatment statistically ($P<0.05$) down-regulated *STAT3* (3-fold) and *STAT4* (3-fold) gene expression.

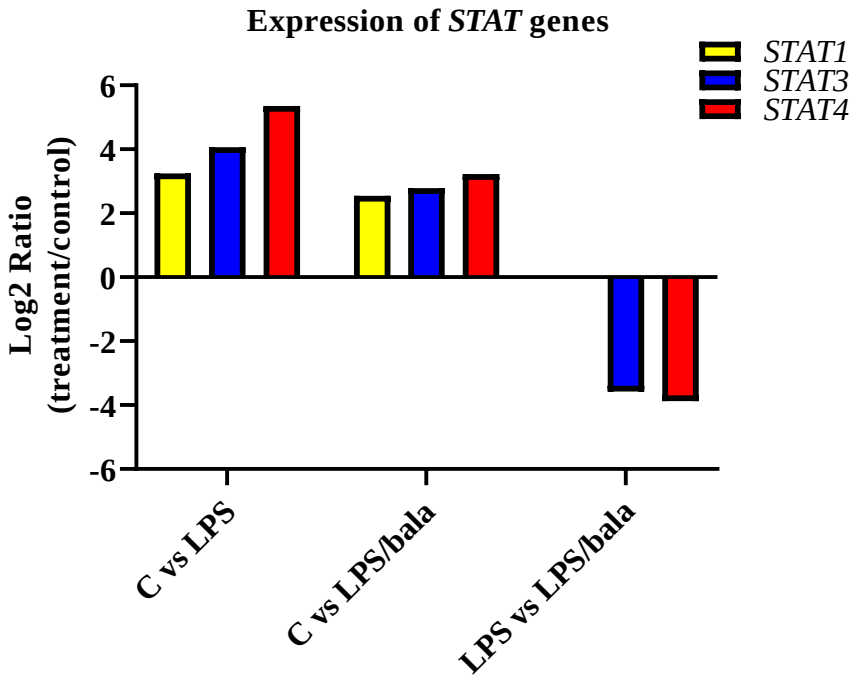

Figure 4.17 A bar chart showing the Log2 ratio of *STAT1, STAT3* and *STAT4* gene expression among the three comparisons. LPS and LPS/bala treatment has statistically ($P < 0.05$) up-regulated all STAT genes expression when compared to control. LPS/bala treatment statistically ($P < 0.05$) down-regulated *STAT3* and *STAT4* gene expression when compared to LPS alone.

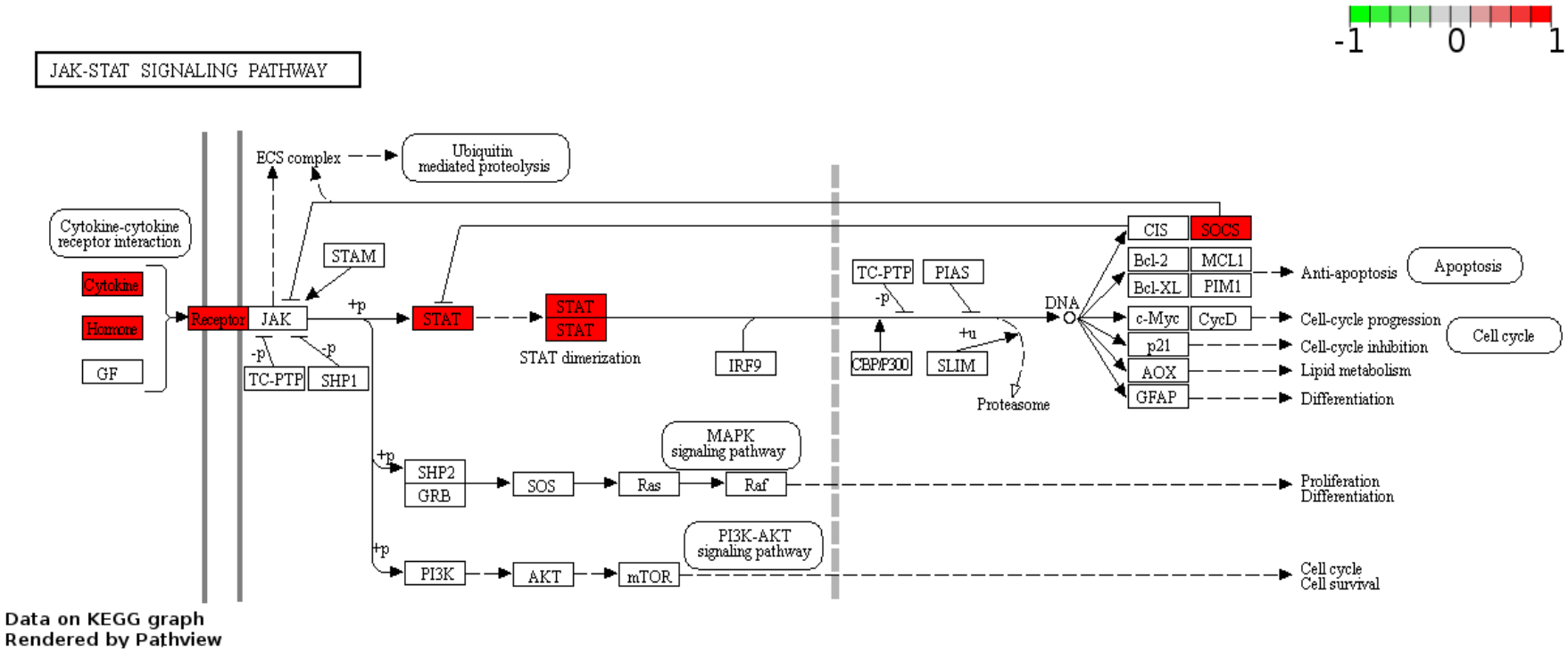

Figure 4.18 DEGs enriched KEGG map of JAK/STAT signalling pathway rendered by Pathview for control vs LPS. Target genes in the pathway are depicted by boxes while arrows depict signalling routes. The coloured scale corresponds to log2-fold changes. Red colour indicates statistically significant ($P<0.05$) increase in expression. No colour corresponds to no changes.

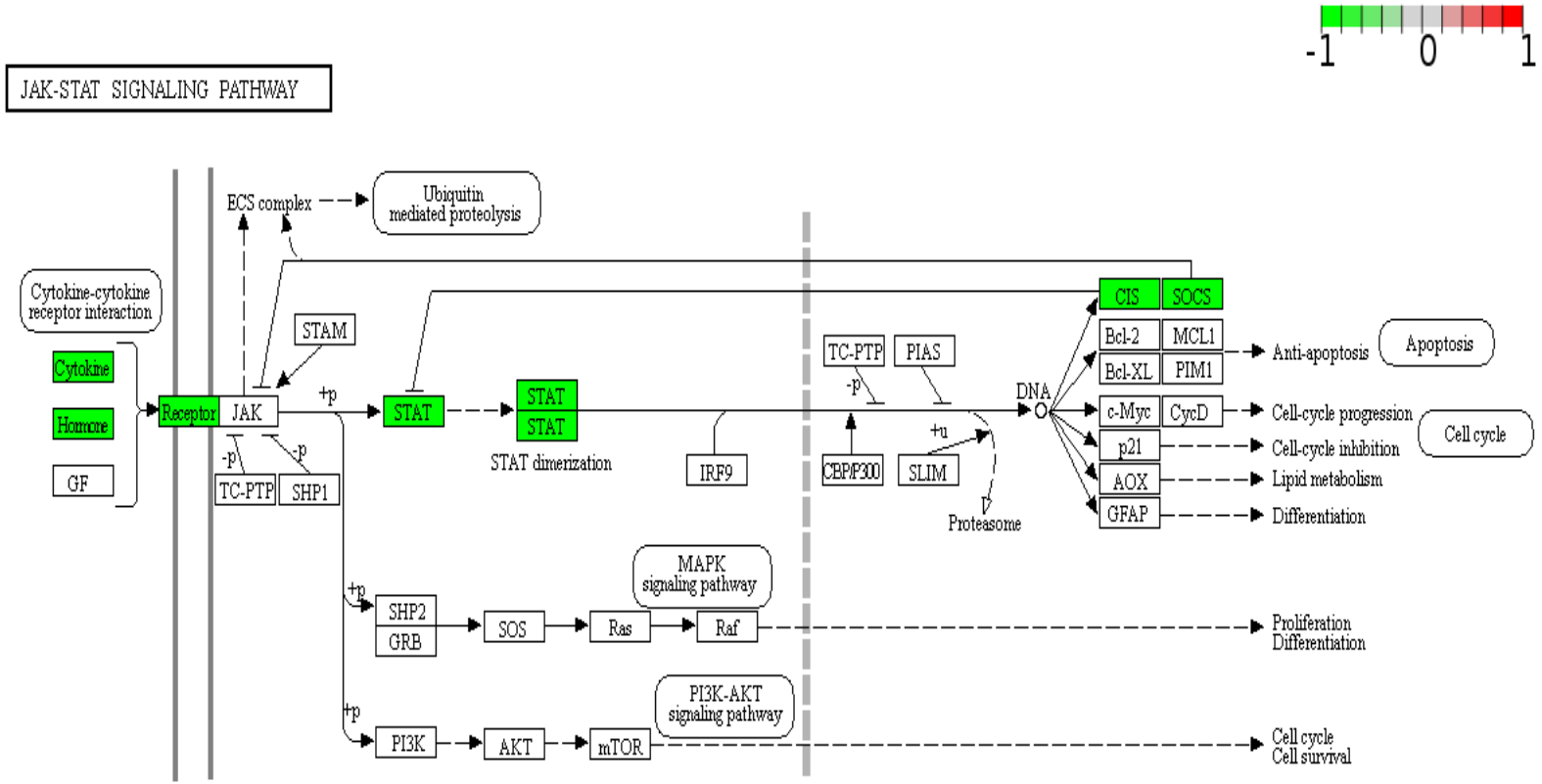

Figure 4.19 DEGs enriched KEGG map of JAK/STAT signalling pathway rendered by Pathview for LPS vs LPS/bala group. Target genes in the pathway are depicted by boxes while arrows depict signalling routes. The coloured scale corresponds to log2-fold changes. Green colour indicates statistically significant ($P<0.05$) decrease in expression. No colour corresponds to no changes

4.5.Discussion and conclusion

Macrophages are a type of innate immune cells that are known to be part of the body's major defence system and are thought to play a major role in inflammatory diseases including cancer cell growth (Williams *et al.*, 2016, Quail and Joyce, 2013, Song *et al.*, 2017). When the body is invaded by microorganisms such as bacteria, viruses, fungi, and protozoa, macrophages act as phagocytic cells and cause destruction of the organisms (Parameswaran and Patial, 2010). Furthermore, these microorganisms can cause the activation of macrophages which will lead to the secretion of a wide variety of products, including pro-inflammatory cytokines, such as IL-1β, IL-6, and TNF-α (Kumar, 2019). However, prolonged activation of macrophages by invading microorganisms can lead to excessive production of inflammatory cytokines also known as a "cytokine storm" which can contribute to chronic inflammatory diseases (Tisoncik *et al.*, 2012). Chronic inflammation is critically involved in chronic diseases such as asthma, autoimmune diseases, atherosclerosis, AD, coeliac disease, cancer, inflammatory bowel diseases (IBDs), rheumatoid arthritis (RA), and diabetes (Libby, 2007).

4.5.1. Cytotoxicity on PMA-differentiated THP-1 cells

To investigate the anti-inflammatory effects of 7-aca, aca, bala and Q/A in this study, PMA-differentiated THP-1 macrophages were used. Firstly, cytotoxicity assays were carried out to ensure the compounds were not cytotoxic to the cells prior to carrying out the anti-inflammatory assays. The cytotoxicity assays showed that the THP-1 macrophage cells' viability was significantly ($P<0.01$) decreased by more than 25% when exposed to 7-aca and aca at the two highest concentrations (30 and 10 µM), while bala caused a significant ($P<0.01$) decrease of 22 % of cell viability at 30µM.

No significant cell lysis was observed at 3μM or below for 7-aca and aca and 10μM or below for bala. No significant cell lysis was observed on cells treated with Q/A at all concentrations. Therefore, non-toxic concentrations of the compounds were used to determine the anti-inflammatory effect of the compounds.

4.5.2. Measurement of pro-inflammatory cytokine levels using ELISA

Macrophages that enter the tumour environment, also known as TAM, have long been known to promote cancer, partly through their ability to secrete angiogenic, metastatic, and growth factors. Macrophages can be polarised into two major states: the classically activated type 1 (M1) and the alternatively activated type 2 (M2). Classical activation of macrophages occurs following injury or infection (Genin *et al.*, 2015). *In vitro*, macrophages are polarised into M1 using bacterial cell wall components (such as LPS), IFN-γ, or TNF-α and the THP-1 monocyte-derived macrophage cell line has been reported to be very sensitive to LPS (Yang *et al.*, 2016a, Aparna Sudhakaran *et al.*, 2013, Genin *et al.*, 2015). M1 macrophages are characterised by the production of pro-inflammatory cytokines like TNF-α, IL-1β, IL-6, and IL-12 (Genin *et al.*, 2015). In this current study, treatment with all compounds in the absence of LPS sustained basal TNF-α, IL-1β, and IL-6 levels and showed no significant difference with their respective control samples (cells not treated with compounds or LPS). Treatment with LPS alone resulted in the most enhanced TNF-α, IL-1β, and IL-6 production, framing an M1-like pattern. However, high levels of these pro-inflammatory cytokines induced by LPS were greatly reduced by 3μM of 7-aca, aca and 10 μM of bala. Interestingly, the production of all cytokines was not significantly decreased by Q/A in the combination treatment with LPS.

Proinflammatory innate cytokines including IL-1β, TNF-α, and IL-6 are crucial to resolve acute inflammations. However, high levels of innate cytokines, as apparent in chronic inflammation, may promote tumour development through activation of many signalling pathways (Qu *et al.*, 2018, Kim and Choi, 2015, Huang *et al.*, 2016b). A study demonstrated that IL-1β contributes to immunosuppression in the TME of mammary tumours and blocking IL-1β enhances antitumor cell immunity which leads to tumour regression (Kaplanov *et al.*, 2019). Upregulation of TNF-α activates hepatocyte NF-kB in adjacent endothelial and inflammatory cells which causes hepatitis and hepatocellular carcinoma progression in Mdr2-knockout mice (Pikarsky *et al.*, 2004).

Currently there are no published reports on the anti-inflammatory activities of 7-aca. However, aca has been previously reported to have anti-inflammatory effects by inhibiting the elevation of pro-inflammatory cytokines such as TNF-α and IL-6 in macrophage RAW 246.7 cells (Liou *et al.*, 2017). Aca has also shown inhibition on other inflammatory mediators such as nitric oxide (NO) and cyclooxygenase-2 (COX-2) in LPS activated RAW 264.7 cells (Pan *et al.*, 2006). Other than that, aca has been reported to reduced pro-inflammatory cytokines in cells associated with disorders including fibroblast-like synoviocytes cells (rheumatoid arthritis), human umbilical vein endothelial cells (cancer metastasis) and bronchoalveolar lavage fluid of mice (sepsis-induced lung injury), microglia BV2 cells (brain disorders) (Chen *et al.*, 2015, Tanigawa *et al.*, 2013, Sun *et al.*, 2018, Ha *et al.*, 2012).

This is also the first report on bala as a possible anti-inflammatory agent. On the other hand, resveratrol monomer (bala is made up of two resveratrol monomers) has been reported to attenuate LPS-induced expression of NO, prostaglandin E2 (PGE2), COX-

2, TNF-α, IL-6, and IL-1β in macrophages cells such as RAW 264.7 and U-937cells (Zong *et al.*, 2012, Yang *et al.*, 2014c, Walker *et al.*, 2014, Song *et al.*, 2016). In this study, bala was found to be significantly ($P<0.01$) the most active in inhibiting all three pro-inflammatory cytokines compared to 7-aca and aca. Therefore, bala was chosen for RNA sequencing analysis to examine its mechanism of action on expression of genes and affected pathways in THP-1 cells caused by the treatment of LPS alone or combination treatment of LPS and bala. RNA seq can also help to investigate whether there is some evidence at gene expression level supporting the findings on the ELISA assay.

4.5.3. RNA seq

RNA-Seq transcriptome analysis is an experimental tool that reveals the presence and quantity of RNAs in a biological sample under a particular condition (Wang, Gerstein and Snyder, 2009). Given its high-throughput capability, RNA-seq has been widely used for gene discovery, to determine the molecular mechanisms of action, helps to improve disease diagnosis, and enhance the discovery of new effective therapeutic agents (Costa *et al.*, 2013). Therefore, this technique was used in this study in order to examine the transcriptome of the THP-1 cells following the treatment of LPS and combination treatment of LPS and bala. The aim is to find out information on the anti-inflammatory action of bala on LPS-activated macrophages. These cells play a vital role in the production of cytokines that can lead to chronic inflammatory diseases. Isolating high quality intact RNA is crucial when carrying out quantitative deep molecular analysis such as RNA-Seq. The isolated RNA samples in this study showed RQIs of 9-10, which are indicative of very intact RNA samples.

ELISA studies revealed that the combination treatment of LPS/bala lead to inhibition of pro-inflammatory cytokines TNF-α, IL-1β, and IL-6 on and this was supported by RNA-seq findings of the down-regulation of *TNF-α* and *IL-6* genes. However, *IL-1β* gene expression was not seen to be significantly ($P>0.05$) altered by LPS treatment or LPS/bala treatment. The main finding of the RNA-Seq analysis from the use of Cytoscape ClueGo was that the most significantly ($P<0.05$) enriched pathway for all groups (control vs LPS, control vs LPS/bala and LPS vs LPS/bala) were the cytokine-cytokine receptor interaction pathway with the highest number of associated genes from the DEG list. In this study, the treatment of LPS and LPS/bala on THP-1 macrophage cells caused up-regulation of 47 and 22 genes associated with the cytokine-cytokine receptor interaction pathway, respectively, when compared to the control group. However, when the LPS/bala treatment was compared to the LPS treatment, down-regulation of 27 genes associated with the cytokine-cytokine receptor interaction pathway were observed. Secretion of cytokines from activated M1 macrophages has been suggested to be mainly controlled by the activation and nuclear translocation of the transcription factor nuclear factor kappa-light-chain enhancer of B-cells (NF-κB) (Reynoso *et al.*, 2017). Previous studies have reported that LPS polarises macrophage to M1-type through activation of a series of pathways including the MyD88-dependent Toll-like receptor (TLR) pathway (Riddell *et al.*, 2010, Liu *et al.*, 2017b, Ma *et al.*, 2018). These lead to the activation of downstream inhibitory-κB Kinase (IKK), which in turn phosphorylate the NF-κB inhibitor alpha (IκBα), leading to ubiquitin-dependent IκBα degradation and NF-κB activation (Liu *et al.*, 2017b). NF-κB activation causes the production of a large number of inflammatory genes including pro-inflammatory cytokines (TNF-α, IL-1β, and IL-6) and chemokines

(Lawrence, 2009). LPS/TLR4 signalling can also cause the activation of the downstream mitogen-activated protein kinase (MAPK) pathways that leads to the induction of another transcription factor activator protein-1 (AP-1) which also has a role in the expression of proinflammatory cytokines (Lu *et al.*, 2008). Therefore, the addition of bala with LPS in the treatment of THP-1 macrophage cells could alter the impact and effect of these pathways through the reduced expression of a number of key cytokines observed in in this study.

Pathview software was used to visualise the KEGG pathway that was significantly ($P<0.05$) enriched and affected by the treatments on THP-1 cell gene expression. The TNF signalling pathway was found to be one of the affected pathways by LPS and LPS/bala treatments. TNF signalling pathway acts through two receptors, TNFR1 (TNF Receptor-1) and TNFR2 (TNF Receptor-2). Activation of both receptors is responsible for a large number of inflammatory responses classically attributed to the secretion of TNF-α (Parameswaran and Patial, 2010). TNF-α plays an important role in the immune system as it is the earliest endogenous mediator of an inflammatory reaction (Baud and Karin, 2001). It has been reported that overproduction of inflammatory cytokines such as IL-4, IL-6, IL-8, and TNF-α could promote proliferation, metastasis/invasion and recurrence of cancer, leading to poor prognosis and increased mortality (Stoimenov and Helleday, 2009, Szlosarek *et al.*, 2006, Bachelot *et al.*, 2003, Foguer *et al.*, 2016). TNF-α has also been previously linked to many signalling pathways that helps to promote inflammation which supports tumour growth and progression. Signalling pathways and transcription factors activated by TNF-α are considered the key to invasion and metastasis in cancer cells and one of the factors that it relies on is NF-κB signalling pathway activation (Tang *et al.*, 2017). It

was observed that LPS treatment caused the upregulation of genes associated with the TNF signalling pathway such as *TNF-α*, *BIRC3*, *MMP3*, *PTGS2* and *IL-6* compared to the control. However, LPS/bala treatment caused the downregulation of these same genes when compared to LPS treatment. TNF-α has been reported to promote progression of cancers such as oral, ovarian, and breast cancer through NF-κB signalling pathway activation which protects cells and tissues from apoptosis (Wu and Zhou, 2010a, Hwang *et al.*, 2012, Lu *et al.*, 2014). Another study showed that co-culture of activated macrophages with ovarian and breast epithelial cancer cell lines led to TNF-α-dependent activation of JNK and NF-κB pathways in tumour cells (Hagemann *et al.*, 2005). Activation of NF-κB signalling due to TNF-α helps tumour cells to escape TNF-α induced cytotoxicity (Mantovani, 2010, Ben-Neriah and Karin, 2011, Wang *et al.*, 2009). *BIRC3* has been previously linked to the activation of the TNF-α/NF-κB signalling pathway (Simon *et al.*, 2007, Edilova *et al.*, 2018, Yamato *et al.*, 2015). A previous study showed that the *BIRC3* gene were expressed in TNF-α induced NF-κB activation of beta cells (Tan *et al.*, 2013). *MMP9* can be induced by TNF-α and LPS and it is one of the target genes of NF-κB (Tsai *et al.*, 2014). In mouse macrophage cells, LPS induced production of MMP9 and inhibition of NF-κB represses LPS-stimulated MMP9 activity (Rhee *et al.*, 2007, Lappas *et al.*, 2003). Furthermore, it was reported that treatment with olive oil extracts and individual compounds prevented the stimulation of MMP-9 expression and secretion in TNF-α due to impaired NF-κB signalling in THP-1 monocytic cells (Dell'Agli *et al.*, 2010). *PTGS2* gene (also known as *COX-2*) codes for the COX-2 enzyme which can be induced in response to growth factors, stresses or pro-inflammatory stimuli through the activation of the NF-κB signalling pathway (Chiu and Lin, 2008, Carothers *et al.*,

2010, Endale *et al.*, 2017). Several studies have shown that, treatment with NSAIDs or other compounds *in vivo* or *in vitro* inhibits the expression *COX-2* gene or COX-2 enzyme through the suppression of NF-κB pathway (Bhui *et al.*, 2009, Lai *et al.*, 2007, Yuan *et al.*, 2000, Wang *et al.*, 2014b, Cerella *et al.*, 2010). The NF-κB family is a critical signalling pathway that regulates the transcription of numerous pro-inflammatory cytokines (TNF-α, IL-1β, IL-6), nitrogen intermediates and COX-2 during inflammation (Hayden and Ghosh, 2008, Tripathi and Aggarwal, 2006). Therefore, based on these findings, the NF-κB signalling pathway could play a role in the mechanism of action of LPS and LPS/bala treatment in this study. Anti-TNF therapy has led to major progress not only for patients with cancer but also for patients with other chronic inflammatory diseases, such as Crohn's disease, ulcerative colitis, psoriasis, psoriatic arthritis, ankylosing spondylitis and juvenile RA (Monaco *et al*., 2015). Tumor necrosis factor (TNF)-α antagonists, such as infliximab (IFX) and certolizumab pegol (CZP) have been widely used for the treatment of RA (Ma and Xu, 2013).

IL-6 is a multifunctional cytokine that has a major role in acute-phase inflammatory responses (Chaudhry *et al.*, 2013). Binding of IL-6 to the IL-6 receptor activates the JAK family members such as JAK1 and JAK2 which leads to the activation of transcription factors of the STAT family (Čokić *et al.*, 2015). It has been reported that the activation of NF-κB ensures subsequent JAK/STAT3 activation through the expression of IL-6 in several cell lines including macrophages and some cancer cell lines (McFarland *et al.*, 2013, Wongchana and Palaga, 2012, Yoon *et al.*, 2012, Basu *et al.*, 2017). In this study, the mechanism of action of LPS treatment of THP-1 macrophages appears to involve the JAK/STAT signalling pathways as *STAT1, STAT3*

and *STAT4* genes all showed an upregulation by 2-fold, 4-fold, and 5-fold, respectively (Figure 4.17). Treatment with the LPS/bala combination showed the downregulation of *STAT3* and *STAT4* by 3-fold. This is of interest as many studies have shown the link between JAK/STAT pathway and the signal transduction of invasive and metastatic phenotypes of many cancer cells including colon, breast, ovarian, and prostate (Gordziel *et al.*, 2013, Masjedi *et al.*, 2018, Browning *et al.*, 2018, Tam *et al.*, 2007). It has been previously reported that activated THP-1 macrophages induce the upregulation of CD59 in an IL-6R/STAT3-dependent manner in pancreatic cancer that has acted to promote tumour growth and progression (Zhang *et al.*, 2019). Another study demonstrated that the increased macrophage secretion of IL-6 in the TME exerts an amplifying effect on the inflammation response, thus promoting the occurrence and development of hepatocellular carcinoma via STAT3 signalling (Kong *et al.*, 2016). Furthermore, it has been reported that TAMs-derived IL-6 promotes resistance of solid tumours to chemotherapy by inducing anti-apoptotic programmes. For example, a study has demonstrated that IL-6 secreted by macrophages through inhibition of the Hedgehog pathway could support breast cancer cells to maintain or promote their proliferation and invasive potential (Xu *et al.*, 2019). In colorectal cancer, TAMs-derived IL-6 activates the STAT3 pathway to block the tumour suppressor miR-204-5p expression which will promote chemotherapy resistance by increasing anti-apoptotic protein RAB22A and BCL2 expression in cancer cells (Yin *et al.*, 2017, Zhu *et al.*, 2017b). Another report demonstrated that STAT3 and STAT6 cooperate in macrophages and enhance tumour progression in a cathepsin-dependent manner and genetic deletion of *STAT3* and *STAT6* impaired tumour development and invasion *in vivo* (Yan *et al.*, 2016).

This is the first report of an anti-inflammatory mechanism of action of bala, however, the resveratrol monomer has been investigated intensively as an NF-κB signal transduction inhibitor (Li *et al.*, 2013, Liu *et al.*, 2017a, Tino *et al.*, 2016). In carcinogen-induced brain endothelial cells, resveratrol prevents disruption of the blood brain barrier during neuroinflammation by inhibiting MMP-9 and COX-2 through depletion of NF-κB activity (Annabi *et al.*, 2012). Furthermore, resveratrol down-regulated the expression of IL-6 in LPS-stimulated RAW264.7 cells and these actions were mediated by suppressing the phosphorylation of STAT-1 and -3 (Ma *et al.*, 2015). This finding is similar to what is seen in this study, whereby bala caused the suppression of IL-6 and *STAT* 3 gene in LPS-treated THP-1 macrophage cells. Although 7-aca and aca were not analysed with RNA-Seq in this study, many reports have shown that anti-inflammatory activity of aca occurs through inhibition of several signalling pathways such as NF-κB, MAPK and STAT. Aca treatment inhibited the expression of NF-κB p65 and IκB-α phosphorylation in lung tissues of mice with sepsis and RAW264.7 cells (Sun *et al.*, 2018). Another study demonstrated that aca caused the down-regulation of inflammatory iNOS and COX-2 gene expression in LPS stimulated-RAW264.7 cells by inhibiting the activation of NF-κB and interfering with the activation PI3K/Akt/IKK and MAPK (Pan *et al.*, 2006). Aca has also previously demonstrated inhibition of STAT3 activation by preventing tyrosine phosphorylation in cancer cells (Bhat *et al.*, 2013).

In conclusion, ELISA and RNA-Seq findings using THP-1 macrophage cells showed that 7-aca and bala used in this project could be promising anti-inflammatory agents. Both compounds showed significant inhibition of pro-inflammatory cytokines TNF-α, IL-1β, and IL-6 induced by LPS in THP-1 macrophage cells. This indicated that the

compounds could impact on chronic inflammatory diseases which has been known to contribute to cancer progression. One of the main findings in the RNA-seq study is that treatment of LPS/bala appears to affect the TNF-α/NF-κB signalling pathway and IL-6/JAK/STAT3 signalling pathway by down-regulating a number of the genes associated with them.

Chapter 5. Neuroprotective effect of isolated compounds

5.1. Introduction

In Chapter 3, 7-aca, aca and bala were shown to be cytotoxic to A2780 and ZR-75-1 cells. In Chapter 4, it was demonstrated that the compounds also possessed anti-inflammatory activity by inhibiting the production of pro-inflammatory cytokines such as TNF-α, IL-1β and IL-6 in THP-1 macrophages. Therefore, it was thought to be pertinent to further investigate the protective activity of 7-aca, aca and bala. Chronic inflammation and oxidative stress is a major cause of age-related diseases and cancer (Khansari *et al.*, 2009). In fact, ROS is known to be the activator of many inflammatory pathways. For example, ROS is able to drive modification of IκB proteins, such as phosphorylation by a serine kinase, IKK, which leads to its degradation, thus freeing NF-κB that can then translocate to the nucleus where, either alone or in combination with other transcription factors, it induces expression of several genes that express inflammatory proteins (Chatterjee, 2016).

In neurodegenerative disease, there is a strong interrelationship between ROS/RNS production and the induction of proinflammatory cytokines, which results in enhanced cell damage and thus aggravates neurodegeneration (Fischer and Maier, 2015). In the AD brain, chronic activation of microglia by Aβ plaques causes the release of ROS and cytokines which disturbs neuronal functions and produces cellular damage (Suzumura, 2013, Solito and Sastre, 2012). Furthermore, severely damaged neuron mitochondria can elicit and potentiate inflammatory responses through mitochondrial ROS production and the release of mitochondrial damage-associated molecular patterns (DAMPs) ultimately leading to a perilous vicious cycle (Missiroli *et al.*, 2020). Mitochondrial defects have been demonstrated in the brain of AD patients

(Swerdlow, 2018) and a common mechanism that leads to defective mitochondria that contribute to neuron cell death, is excessive ROS production and mitochondrial membrane permeabilisation. ROS and mitochondrial membrane permeabilisation induces loss of ΔΨM, which can initiate both apoptosis and necrosis (Galluzzi *et al.*, 2009).

Another feature perceived in AD patients is deficiency of ACh, a neurotransmitter in the synapses of the cerebral cortex. AChE can promulgate the assembly of Aβ into fibrils (Carvajal and Inestrosa, 2011). Therefore, AChE inhibitors could be an effective natural therapeutic strategy for AD by increasing ACh-mediated neuron to neuron transmission (Damuka *et al.*, 2020). AChE inhibitors work by preserving the presence of ACh in the synaptic cleft by inhibiting AChE that breakdowns ACh into acetate and choline, thus allowing greater diffusion and half-life of ACh which results in improved cholinergic neurotransmission (Wong *et al.*, 2018).

This chapter focuses on the potential antioxidant activity and neuroprotective effect of 7-aca, aca and bala against oxidative stress-induced neuroblastoma SHSY-5Y cell death as well as drug discovery of a potential AChE inhibitor. Human neuroblastoma SHYSY-5Y cells have been used widely as an *in vitro* model to study neurodegenerative diseases, including analysis of neuronal differentiation, metabolism, and function related to neurodegenerative processes, neurotoxicity, and neuroprotection (Yang *et al.*, 2016b). Although this cell line is widely used as model of neurons since the early 1980's as these cells possess many biochemical and functional properties of neurons, the use of undifferentiated SH-SY5Y cells as neurodegenerative model involves some disadvantages (Xie *et al.*, 2010). For example, due to SH-SY5Y cells are a continuously dividing cell line, the number of

undifferentiated SH-SY5Y cells increases during the course of the experiment, so it is difficult to distinguish whether neuroprotective or neurotoxic agents influence the proliferation rate or the rate of cell death (Datki *et al.*, 2003). An important thing to be noted is that SH-SY5Y cells lose its characteristic morphology and growth profile as they are cultured for long. Therefore, it is recommended not to be used after passage 20. Several assays such DPPH, GSH, AChE inhibitor activity, DCFH-DA, TMRE and caspase-3/7, used in chapter 3, were conducted as described below.

5.1.1. Antioxidant assays

5.1.1.1. 2,2-Diphenyl-1-picrylhydrazyl (DPPH) Assay

The DPPH assay is an antioxidant assay that is widely used in natural product research due to its simplicity and sensitivity (Aqil *et al.*, 2012). The DPPH free radical (DPPH●) is a stable free radical that is available commercially. The basic principle of the assay is that DPPH● (purple) is reduced to a stable form (yellow) when it accepts an electron or hydrogen atom from an electron or hydrogen donor substance such as antioxidants (Kedare and Singh, 2011) (Figure 5.1). DPPH shows a strong absorption band at 517 nm and therefore the antioxidant activity can be detected using OD at 517nm wavelength (Santos and Silva, 2020).

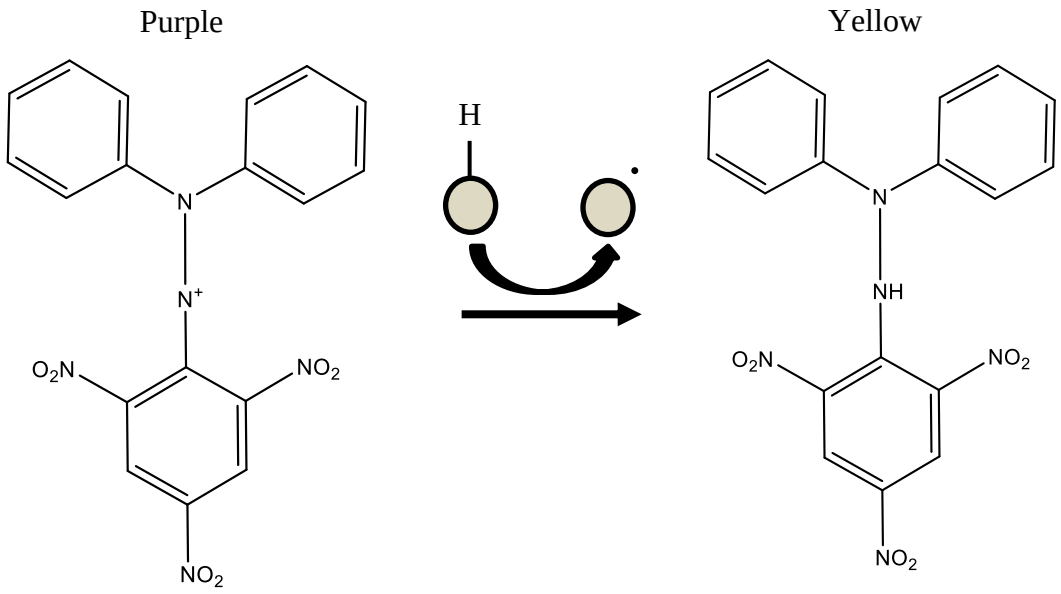

Figure 5.1 Unstable purple DPPH is reduced by antioxidant agents to yield a yellow DPPH colour.

5.1.2.Glutathione (GSH)

GSH is a tripeptide molecule comprised of three amino acids: glutamic acid, cysteine, and glycine that is present in most mammalian tissues (Gad, 2014). Intracellular GSH performs an important role in maintaining the proper ratio of oxidised to reduced forms of metabolically important thiols such as coenzyme A. It also provides reducing equivalents that detoxify ROS (Dietzen, 2018). GSH exists in two forms, the oxidised form (GSSG) and the reduced form (GSH) (Forman *et al.*, 2009). GSH enzymatically reduces redox-generated H_2O_2 to harmless H_2O via glutathione peroxidase (GPx). Glutathione reductase (GSR) is the enzyme responsible for converting GSSG to GSH in the presence of nicotinamide adenine dinucleotide phosphate (NADPH) (Figure 5.2) (Lushchak, 2012). The GSH-Glo™ Assay is a luminescent-based assay for the detection and quantification of GSH in cells or in various biological samples. The assay is based on the conversion of a luciferin derivative into luciferin in the presence

of GSH. The reaction is catalyzed by a glutathione S-transferase (GST) enzyme supplied in the kit. The luciferin formed is detected in a coupled reaction using Ultra-Glo™ Recombinant Luciferase that generates a glow type luminescence that is proportional to the amount of glutathione present in cells.

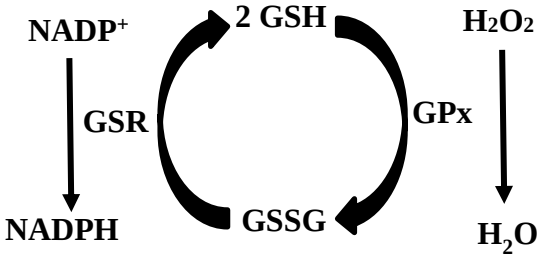

Figure 5.2 Redox states of GSH

5.1.3. Cholinesterase enzyme inhibitory activities

5.1.3.1. AChE inhibitor assay

Cholinesterase is a family of enzymes that catalyses the hydrolysis of the neurotransmitter ACh into choline and acetic acid. The Acetylcholinesterase Assay uses 10-acetyl-3, 7-dihydroxyphenoxazine (Amplex® Red) reagent that provides a fluorescence method to monitor AChE activity. Amplex® Red is a colourless and nonfluorescent compound that, when oxidised by H_2O_2, in the presence of horseradish peroxidase (HRP), produces resorufin, which is a highly fluorescent product (Kalyanaraman *et al.*, 2012). Firstly, AChE converts the ACh substrate to choline which is then oxidised by choline oxidase to betaine and H_2O_2. In the presence of HRP, the latter reacts with the colourless Amplex® Red reagent in a 1:1 stoichiometry to generate the highly fluorescent product resorufin (pink) (Figure 5.3). Resorufin has

absorption and fluorescence emission maxima of approximately 571 nm and 585 nm, respectively (Miao *et al.*, 2010). In the presence of AChE inhibitor or anti-cholinesterases, breakdown of Ach is inhibited; therefore, resorufin is not generated (colourless).

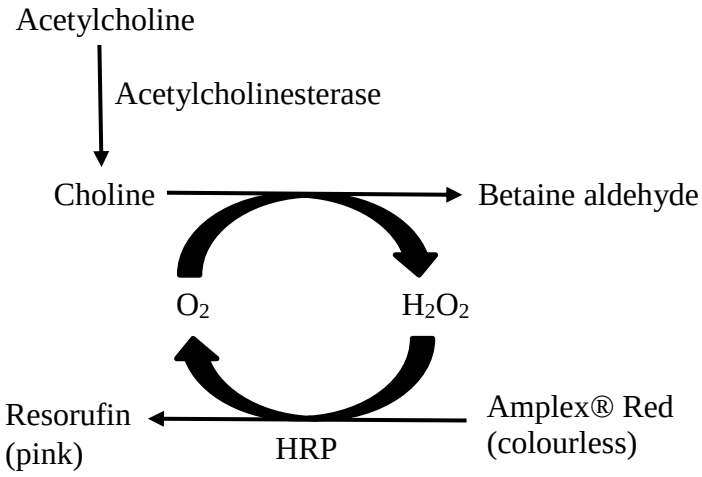

Figure 5.3 Amplex Red assay scheme for measuring AChE activity

5.2. Aims and objectives

This chapter aims to evaluate the cytoprotective effects on SH-SY5Y cells of 7-aca and bala and antioxidant activity that may contribute to their protective effects. The specific aims were:

1. To test the ability of the isolated compounds to inhibit tert-Butyl hydroperoxide (TBPH)-induced neuronal cell death in SH-SY5Y cells by measuring the cell viability using alamarBlue®.
2. To evaluate the radical scavenging activity of the compounds using DPPH assay.

3. To test the effects of the compounds on GSH levels in the SH-SY5Y cell line using GSH-Glo™.
4. To test the ability of the compounds to inhibit TBPH-induced ROS in SH-SY5Y cells using a DCFH-DA assay.
5. To test the ability of the compounds to inhibit TBPH-induced mitochondrial damage in SH-SY5Y cells using a TMRE assay.
6. To test the ability of the compounds to inhibit TBPH-induced activation of caspase-3/7 levels in in SH-SY5Y cells using a Caspase-Glo 3/7 assay.
7. To evaluate the inhibitory activities of the compounds towards AChE using Amplex® Red AChE inhibitory assay

5.3. Methods

5.3.1. Cell viability using an alamarBlue® assay

Cytotoxicity assays were carried out to ensure that the compounds were not cytotoxic to the cell line and to determine 50% toxic concentrations of TBPH. SH-SY5Y neurons were cultured in DMEM medium supplemented with penicillin/streptomycin and 10% (v/v) FBS. SH-SY5Y cells were seeded at a density of 1×10^5 cells/ml in 96-well plates and incubated for 48 h. Then the cells were treated with a range of concentrations of compounds (0.003, 0.001, 0.03, 0.1, 0.3, 1, 3 µM) or TBPH (1.56, 3.13, 6.25, 12.5, 25, 50, 100, 200 µM) for 24 h. Compounds and TBPH were dissolve using DMSO before preparing the range of concentrations. A cell viability assay was carried out as per section 3.3.2.

To investigate the protective effect of the compounds in TBHP-induced cell death, alamarBlue® was used to measure the percentage of viable SH-SY5Y cells. Cells were

pre-treated with non-toxic concentrations of the compounds. Compounds were prepared 2X the final concentration as they would be diluted 1:1 with cells and give a final concentration of 0.3, 1 and 3 µM of 7-aca and aca, and 1, 3 and 10 µM of bala in the well. Fifty µl medium was removed from each well and 50 µl of compound was added in the corresponding wells, whereas 50 µl of medium was added to the control wells. The plate was incubated for 24 h, then the medium was removed before adding TBPH (200 µM) to the wells and further incubated for a further 24 h.

5.3.2. DPPH assay

The assay was performed in a 96-well half-area clear flat bottom plate. Ascorbic acid was used as a positive control. The displacement curve of ascorbic acid was obtained using a range of ascorbic acid concentrations from 30 nM to 100 µM. A range of concentrations (0.003-10 µM) of 7-aca, aca and bala were prepared. A DPPH stock concentration of 10 mM was made by dissolving 7.98 mg of DPPH in 2 ml ethanol. DPPH was stored at 4°C until used. The working DPPH solution concentration was 200 µM and therefore the solution was prepared at 400µM as it was diluted twice in the assay plate.

In the assay plate, 20 µl of ascorbic acid or 20 µl of compounds were added to wells. Then, 20 µl of DPPH was added to all wells and the plate was covered with foil and incubated for 20 min at room temperature. OD was read at a wavelength of 512 nm on a M5 Spectramax Plate Reader using Softmax Pro software. The percent inhibition of DPPH was calculated as follows:

$$\%\ DPPH\ inhibition = \frac{(OD\ sample - OD\ control)}{OD\ control} \times 100$$

GraphPad Prism for Windows (version 8.00, GraphPad Software, San Diego, CA, USA) was used to obtain dose–response curves and mean inhibitory concentration (IC50) values. Data were normalized so that all curves begin at 0% and plateau at 100% and then fit into a sigmoidal dose-response curve with Bottom is set to equal zero, and Top is set to equal 100.

5.3.3. Measurement of cellular antioxidant enzyme GSH

The assay was carried out as per the manufacturer's instructions. SH-SY5Y cells were seeded in half-area black 96-well plates (clear bottom) at $1.5x10^5$ cells/well (50µl/well) and were allowed to attach overnight in an incubator at 37°C with 5% CO_2. Then, compounds were prepared 2X the final concentration as they would be diluted 1:1 with cells to give a final concentration of 0.3, 1, 3 µM for 7-aca and aca and a final concentration of 1, 3, 10 µM for bala in the well. The next day, the compounds were incubated with the cells for a further 6 h. As the SH-SY5Y cells were plated using DMEM which contains serum and phenol red that can interfere with the assays, the medium had to be completely removed before the next step. Then, 50 µl of GSH-Glo™ reagent was added to all wells. The plate was incubated at room temperature for 30 min after being shaken for 1 min using a plate-shaker. Fifty µl of Luciferin Detection Reagent was added to all wells. The plate was incubated at room temperature for 15 min after being shaken for 1 min using a plate-shaker. Luminescence with an integration time of 0.5 seconds/well was read on a M5 Spectramax Plate Reader using Softmax Pro software.

5.3.4. Estimation of Intracellular ROS levels using DCFH-DA probe

SH-SY5Y cells were seeded at 1 x 10^5 cells/well (25µl/well) in a 96-well half area black plate with a clear bottom. Cells were treated with compounds at a range of

concentrations of 0.3, 1, 3µM for 7-aca and aca and a final concentration of 1, 3, 10 µM for bala for 24 h, whereas the controls were treated with medium only. After 24 h, TBPH (200µM) was added and the cells were incubated for 1.5 h at 37°C with 5% CO_2. DCFH-DA dye was prepared, and the assay carried out as per section 3.3.3.

5.3.5. ΔΨM assessment

Cells were seeded and treated as per section 5.3.4. TMRE dye was prepared and the assay carried out as per section 3.3.4.

5.3.6. Measurement of Caspase 3/7

Cells were seeded and treated as per section 5.3.4. A Caspase-Glo 3/7 assay was carried out as per section 3.3.5.

5.3.7. Amplex® Red AChE inhibitory assay

AChE inhibitory activities of the compounds were determined using an Amplex® red detection system. In a half area 96-well plate, 10 µl of 50mM Tris HCL (pH 8.0), 10 µl of 7-aca (0.001-3µM), aca (0.001-3µM) or bala (0.003-10µM) and 10 µl of 0.4 U/ml of AChE from electric eel were added. The mixture was incubated for 30 min at room temperature. Thereafter, 20 µl of working solution consisting of 50mM Tris HCL, 90 µM acetylcholine chloride, 0.2 U/ml choline oxidase, 2 U/ml HRP and 100 µM Amplex® Red reagent was added to the wells. The mixture was incubated for 20 min at room temperature. Tacrine (0.03-10µM) served as a positive control. The fluorescence was measured with a fluorescence microplate reader using excitation in the range of 530–560 nm. The percentage of AChE inhibition was calculated using the formula:

$$Percentage\ of\ AChE\ inhibition = \frac{control - sample}{control}\ x\ 100$$

GraphPad Prism for Windows (version 8.00, GraphPad Software, San Diego, CA, USA) was used to obtain dose–response curves and mean inhibitory concentration (IC50) values. Data were normalized so that all curves begin at 0% and plateau at 100% and then fit into a sigmoidal dose-response curve with Bottom is set to equal zero, and Top is set to equal 100.

5.4. Results

5.4.1. Protective effect of compounds in TBPH-induced cytotoxicity using an alamarBlue® assay

Cytotoxicity testing using an alamarBlue® cell viability assay was carried out using 7-aca, aca and bala prior to performing the DCFH-DA, TMRE and GSH-Glo^{TM} assay in SH-SY5Y cells. Bala showed no toxicity to the cells at the tested concentrations (0.03-10 μM, Figure 5.4A). Although not significant ($P<0.01$), 7-aca and aca showed slight decreased cell viability to 90% at 10μM. To obtain an appropriate concentration of TBHP, which exhibits approximately 50% of cell death, SH-SY5Y cells were treated with a range of concentrations of TBHP for 24 h, and cell viability was determined using an alamarBlue® cell viability assay. Concentration-dependent cell death was observed with TBHP treatment (Figure 5.4B) and 200 μM TBHP, which exhibited approximately 50% cell death, was chosen in the following experiments.

Next, in order to assess the protective effects of the compounds, cells were pre-treated with increasing concentrations of 7-aca and aca at 0.3, 1 and 3μM and bala at 1, 3 and 10 μM before treating with 200 μM of TBHP. As illustrated in Figure 5.5, pre-treatment with 7-aca (3 μM), aca (3 μM) and bala (10 μM) significantly ($P<0.01$)

prevented cell death, restoring cell survival to 87%, 88.6% and 92.3%, respectively. Microscopy-assisted evaluation of cell viability confirmed that 7-aca, aca and bala was protective against TBHP (Figure 5.6). Untreated cells showed the characteristic elongated shape of healthy SH-SY5Y cells. Once stressed with TBPH for 24 h, the morphology of the cells changed to a rounded conformation. Pre-treatment with 7-aca (3 µM), aca (3 µM) and bala (10 µM) prevented the cell death induced by TBPH; the cells looked healthier maintaining their original shape while showing only fewer rounded shaped cells when compared to the TBPH control.

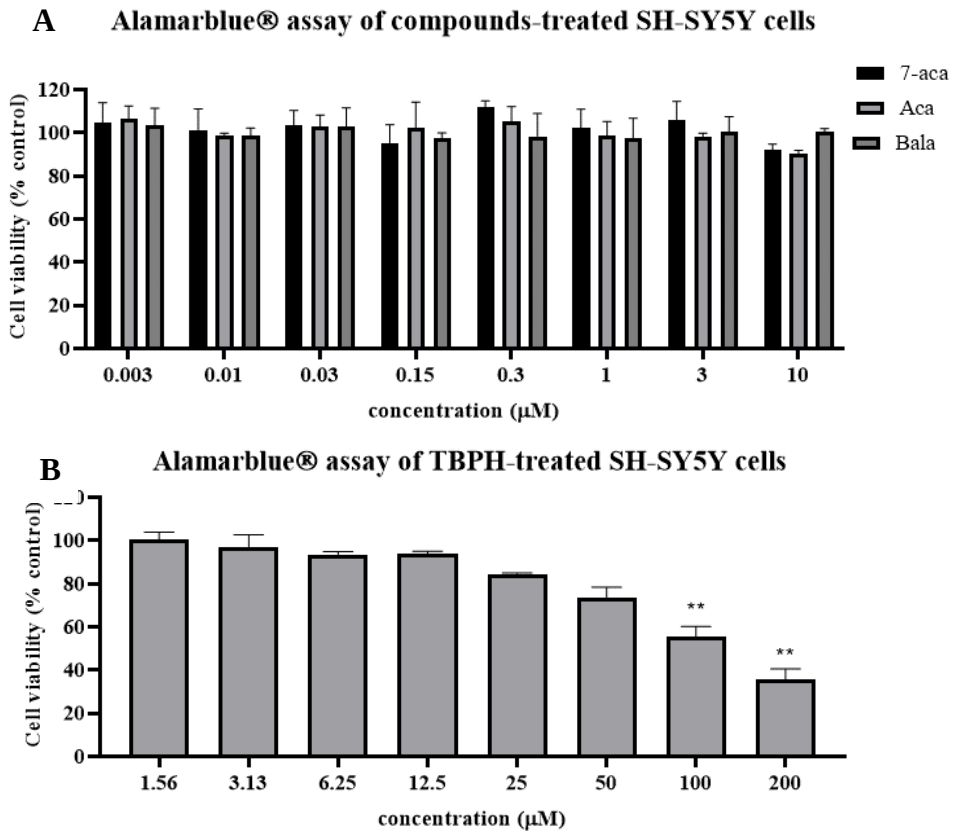

Figure 5.4 Concentration-dependent effects of A) 7-aca, aca and bala on cell survival in SH-SY5Y cells and B) TBHP on cell survival in SH-SY5Y cells. Cells were exposed to different concentrations of compounds or TBHP for 24 h. Cell viability was assessed using an alamarBlue® assay. Data was analysed using One-Way ANOVA with a Bonferroni multiple comparison test. Data represents the mean of triplicate readings ± SEM, n=3. **P<0.01 represents a significant decrease in cell viability vs untreated cells (control).

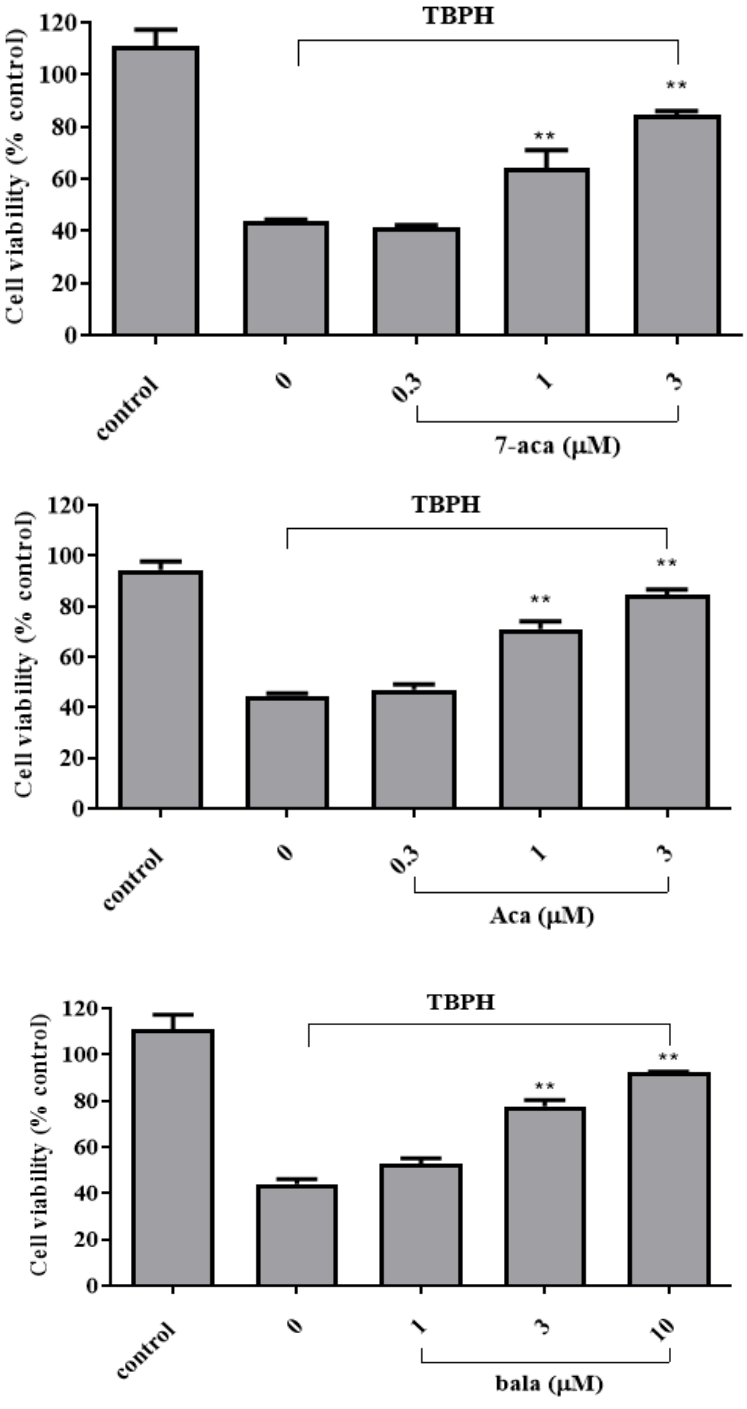

Figure 5.5 Protective effect of 7-aca, aca and bala on TBHP-induced neuronal cell death in SH-SY5Y human neuroblastoma cells. Cell viability at 200µM TBHP was measured using alamarBlue®. Data was analysed using One-Way ANOVA with

Bonferroni multiple comparison test. Data represents mean ± SEM, n=3. **P<0.01 represents significant increase in cell viability vs to TBHP alone (control).

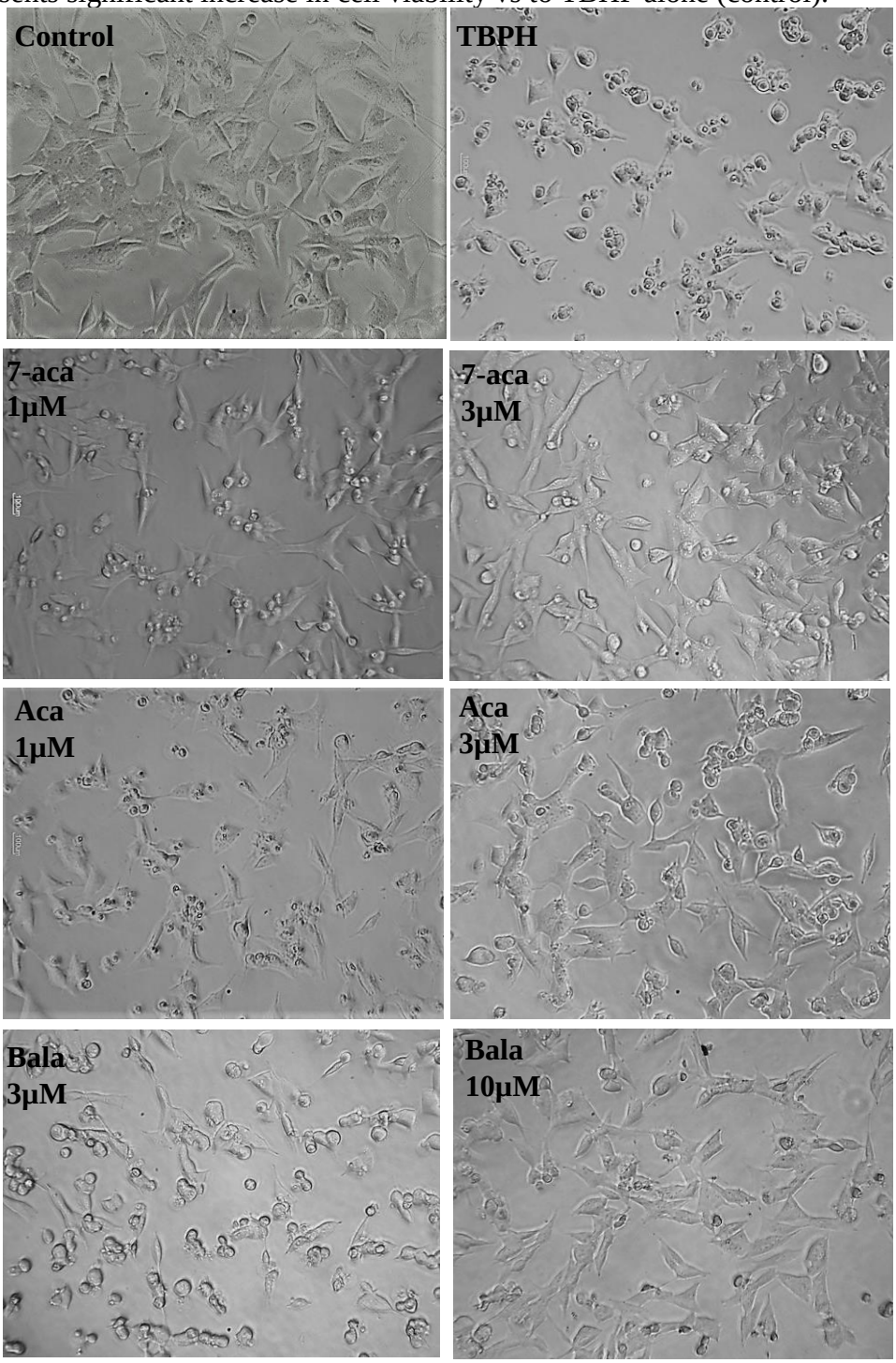

Figure 5.6 Microscopy images of SH-SY5Y cells pre-treated with compounds (24 h) and further treated 200µM TBPH (24 h), 200µM TBPH alone (24 h) or untreated cells (control). Objective lens x10.

5.4.2. DPPH

The compounds were investigated for their ability to scavenge DPPH activity. Ascorbic acid, a known antioxidant, was used as a positive control and tested at a range of concentrations where 100μM was the highest. Ascorbic acid significantly ($P < 0.01$) scavenged the DPPH activity in a concentration dependent manner with an IC_{50} value of 12.4 μM as shown in Figure 5.7. Inhibition of DPPH radicals by all the compounds tested was generally dose-dependent, with the highest concentration of the extracts showing the highest antioxidant activity (Figure 5.7). At a concentration of 10μM, 7-aca, aca, and bala inhibited DPPH radicals significantly ($P<0.01$) to 39%, 42% and 69.5% respectively. Bala showed the most potent antioxidant activity with an IC_{50} of 6.2μM.

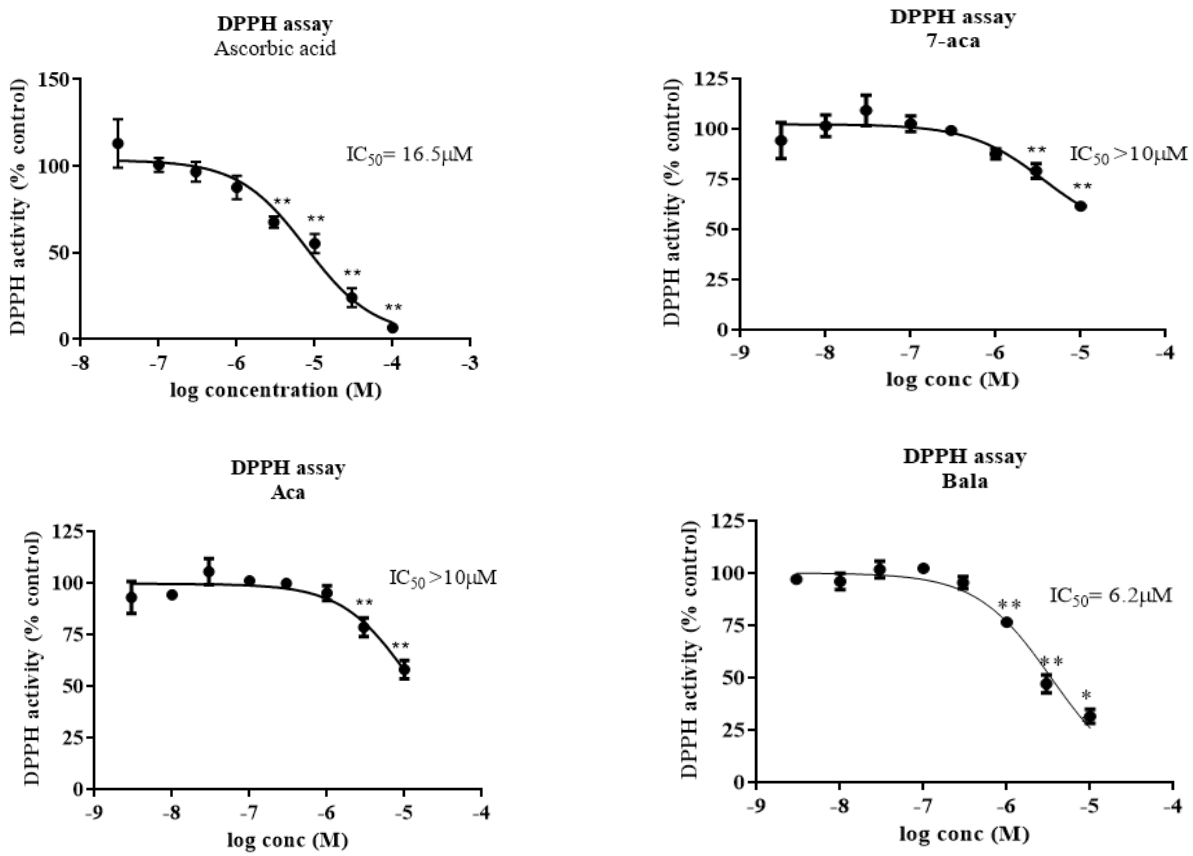

Figure 5.7 The percentage inhibition of DPPH by compounds and ascorbic acid (standard). Data represents mean ± SEM, n=4. Data was analysed using One-Way ANOVA with Bonferroni multiple comparison test. **P<0.01 is significant decrease in DPPH activity vs control.

5.4.3. GSH

GSH standard was used to ensure the GSH-Glo™ assay is at optimum performance. At a range of concentrations (0-5 μM) a curve was generated with a R^2 of 0.9967 which indicates a good curve fit as shown in Figure 5.8. After TBPH treatment, GSH decreased significantly (P<0.01) in SH-SY5Y cells. However, pre-treatment of 7-aca, aca and bala increased GSH levels significantly (P<0.01) in a dose-dependent manner (Figure 5.9). Pre-treatment of 7-aca and aca at 3μM and bala at 10 μM showed a significant (P < 0.01) increase in GSH levels by 60%, 61.9% and 66.1%, respectively in SH-SY5Y cells compared to TBPH alone.

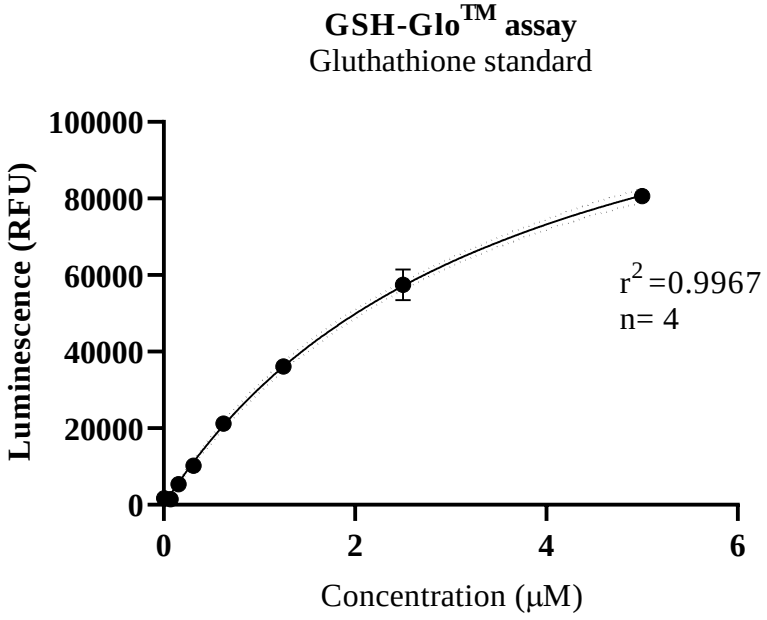

Figure 5.8 GSH standard curve generated from the GSH-Glo™ Assay. Data represents mean ± SEM, n=4.

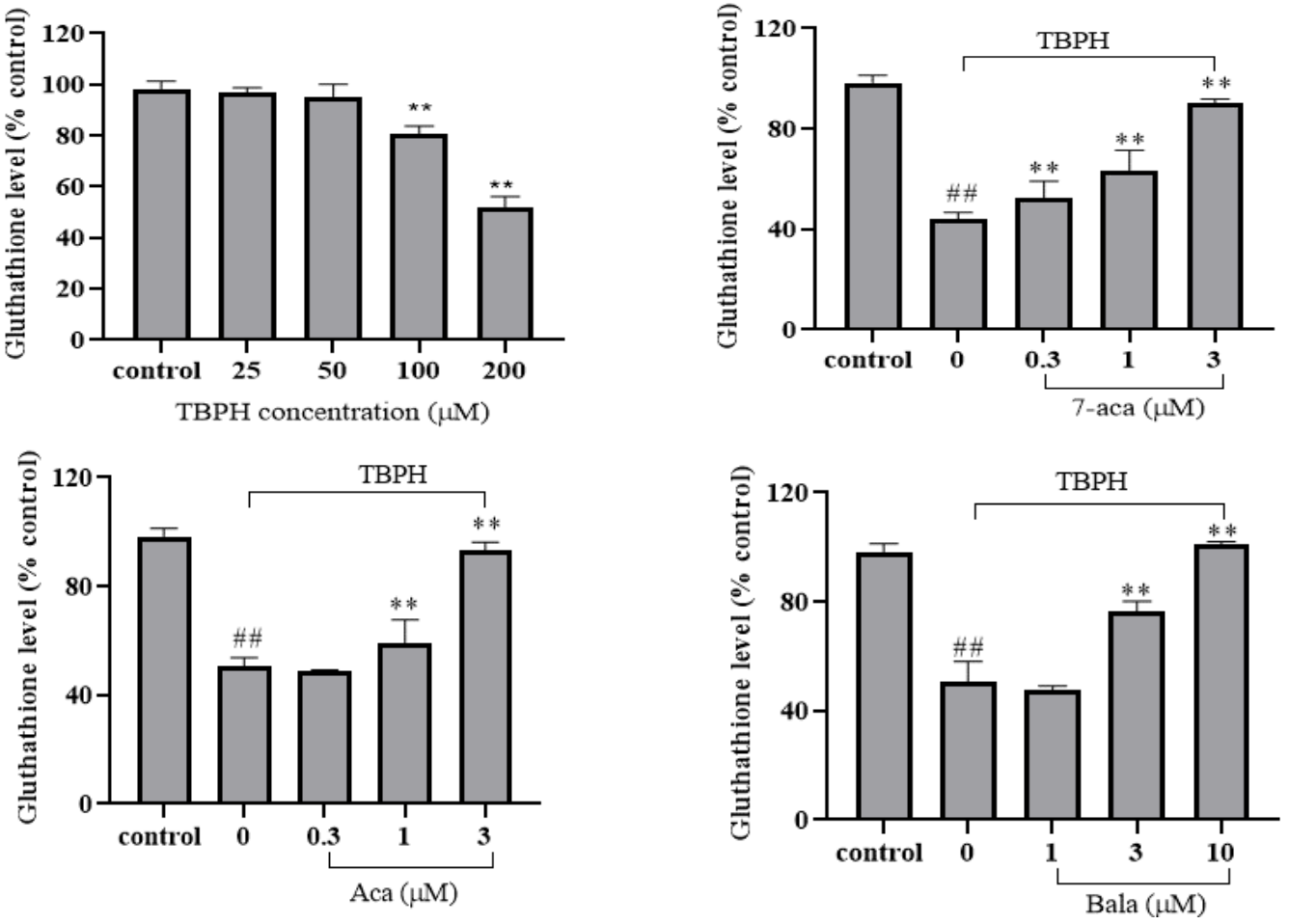

Figure 5.9 GSH levels on TBPH alone or compounds in TBPH-treated SH-SH5Y cells. Data represents mean ± SEM. Data was analysed using One-Way ANOVA with a Bonferroni multiple comparison test. The data are means ± SD of three independent experiments. ## P< 0.01 indicates significant decrease from the control group. ** P< 0.01 indicates significant increase from the TBHP treatment group.

5.4.4. DCFH-DA assay

The effects of 7-aca, aca and bala treatment on TBPH-induced endogenous ROS in SH-SY5Y cells were evaluated by measuring the levels of intracellular ROS in TBPH-treated SH-SY5Y cells. Fluorescent dye DCFH-Da was used in this experiment, that is oxidised to fluorescent DCF by ROS. TBPH treatment caused a marked concentration-dependent increase of intracellular ROS generation (1.56-200µM) (Figure 5.10). However, 1 and 3µM of 7-aca, aca and 3 and 10 µM bala pre-treatment significantly ($P < 0.01$) reduced ROS production (Figure 5.11). 7-aca decreased ROS levels by more than three times in comparison with TBPH alone, whereas aca and bala decreased ROS level by more than two times. Pre-treatment with 7-aca and aca at 3µM and bala at 10µM decreased ROS levels by about 54%, 55% and 69%, respectively, when compared to TBPH treatment alone Therefore, the compounds showed protection against TBPH-induced oxidative stress.

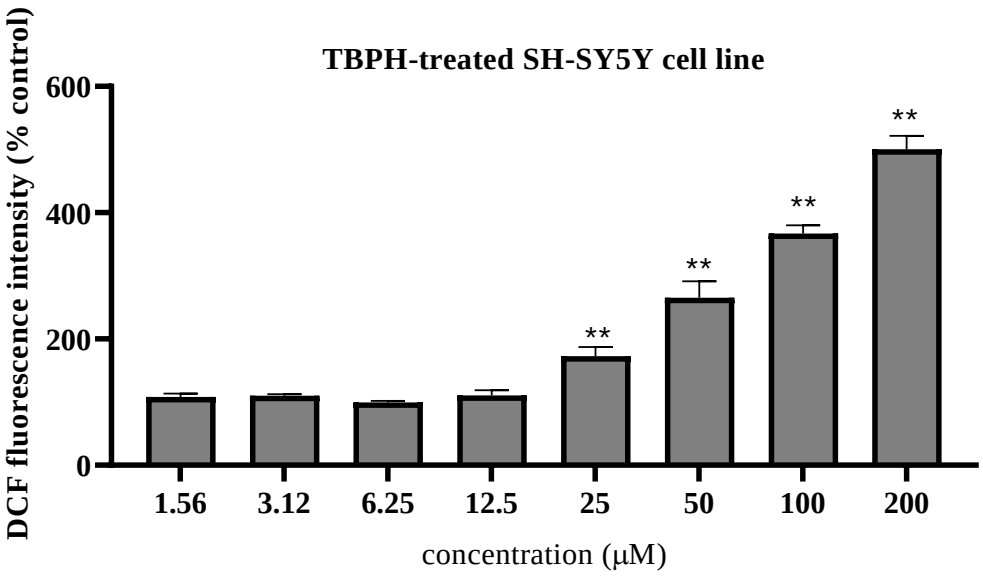

Figure 5.10 ROS production measurement using DCFH-DA assay in SH-SY5Y cells after various concentrations of TBHP stimulation for 1.5 h. Data was analysed using One-Way ANOVA with Bonferroni multiple comparison test. Data represents mean ± SEM, n=3. **P<0.01 represents a significant increase in ROS generation vs untreated cells (control).

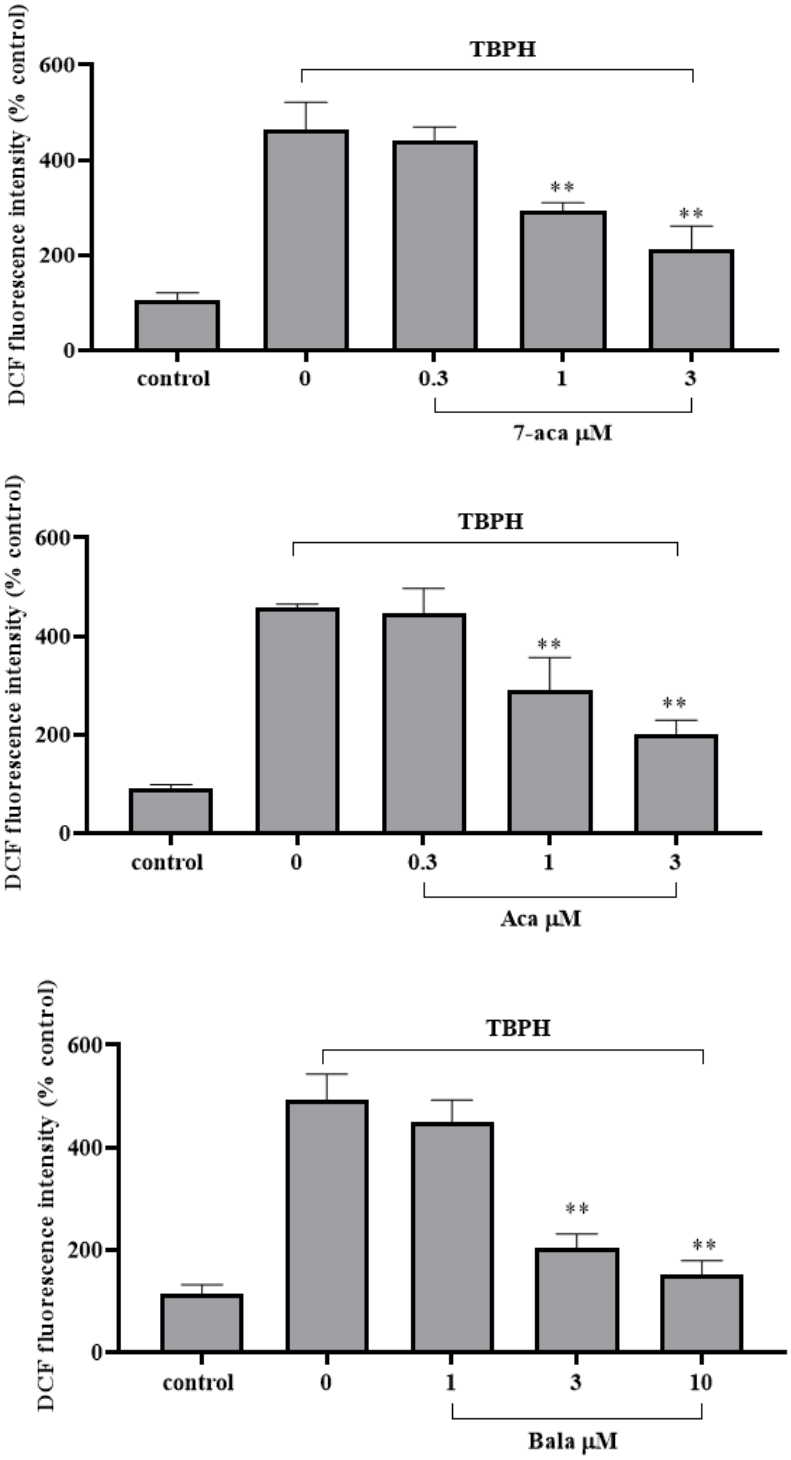

Figure 5.11 ROS production measurement using DCFH-DA solution in SH-SY5Y cells after stimulation with test samples with or without 200 µM TBPH for 1.5 h. Data was analysed using One-Way ANOVA with Bonferroni multiple comparison test. **P<0.01 represents significant decrease in ROS generation vs TBPH treated cells alone.

5.4.5. TMRE assay

The effects of 7-aca, aca and bala treatment on TBPH-induced disruption of ΔΨM in SH-SY5Y cells was evaluated using TMRE dye. Intact mitochondria are indicated by an increase in fluorescence intensity. TBPH-treated cells showed a significant ($P<0.01$) concentration-dependent decrease in fluorescence intensity, indicating loss of ΔΨM (Figure 5.12). However, 7-aca, aca and bala pre-treatment prevented the loss of ΔΨM under TBPH-induced neurotoxic conditions (Figure 5.13). In particular, 3 µM of 7-aca, 3 µM of aca and 10 µM of bala pre-treatment resulted in more than two times increase of ΔΨM. These results suggest that the neuroprotective effects of 7-aca, aca and bala against TBPH-induced cell injury occurred via inhibition of ΔΨM loss and oxidative stress.

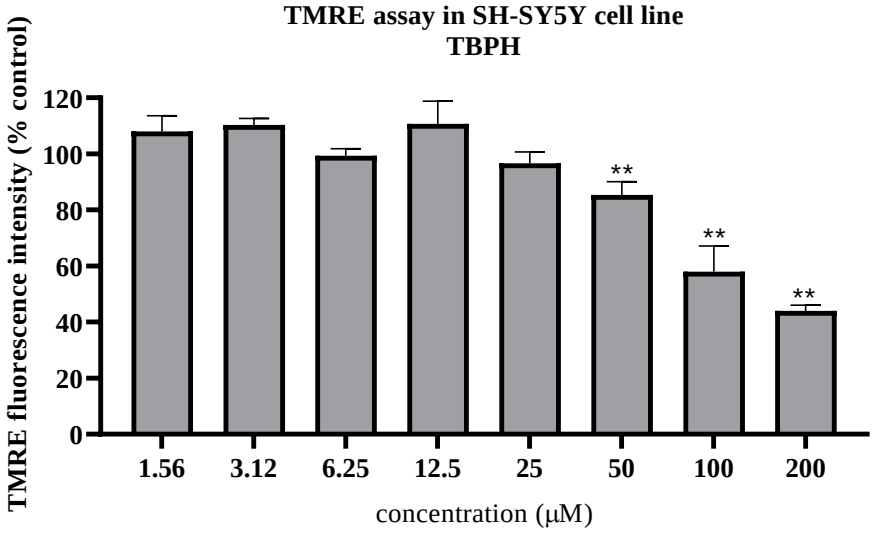

Figure 5.12 ΔΨM measurement using TMRE dye in SH-SY5Y cells after various concentrations of TBHP stimulation for 1.5 h. Data was analysed using One-Way ANOVA with Bonferroni multiple comparison test. Data represents mean ± SEM, n=3. **P<0.01 represents a significant decrease in ΔΨM vs untreated cells (control).

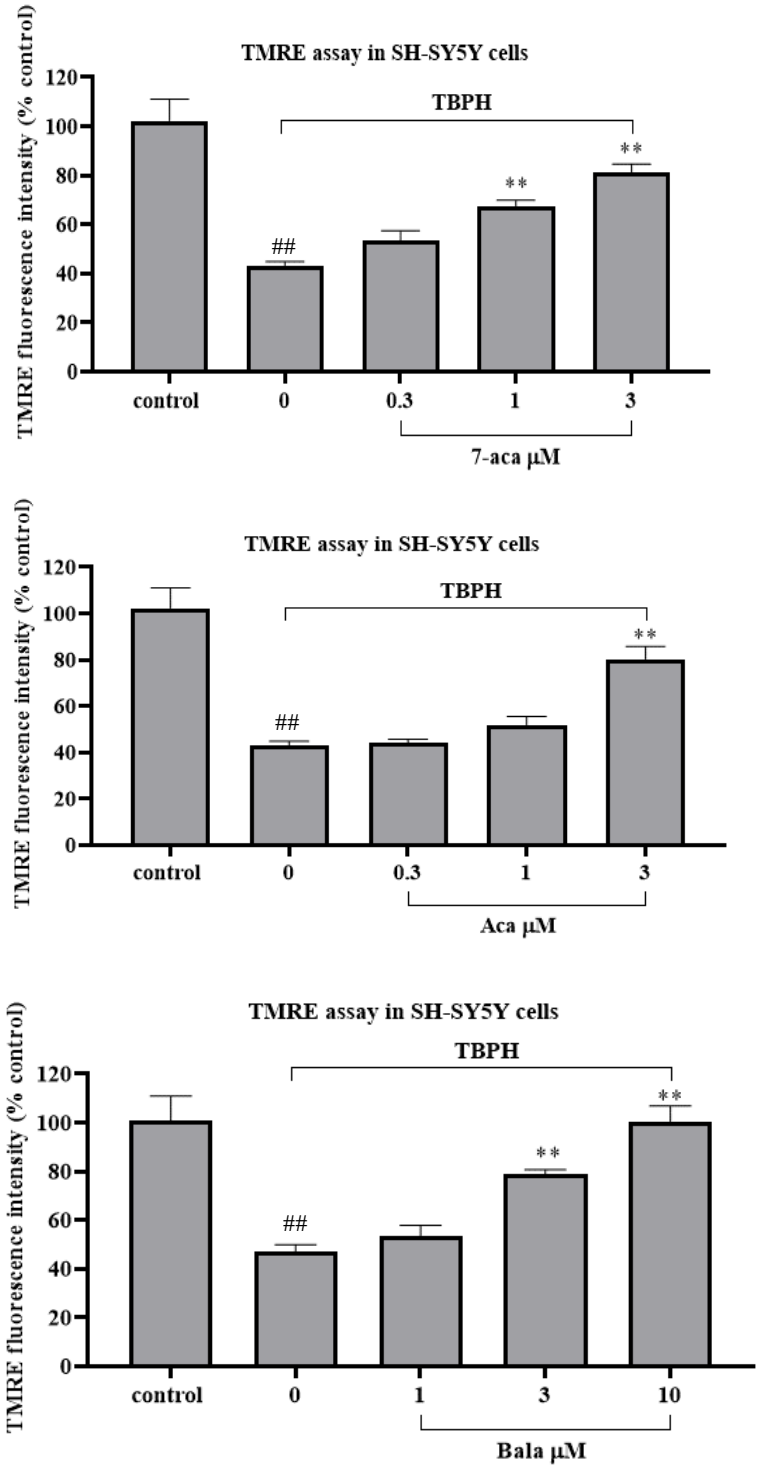

Figure 5.13 ΔΨM measurement using TMRE dye in SH-SY5Y cells after stimulation with test samples with or without 200 µM TBPH for 1.5 h. Data was analysed using One-Way ANOVA with Bonferroni multiple comparison test. ## P< 0.01 indicates significant differences from the control group. **P<0.01 represents significant increase in ΔΨM vs TBPH treated cells alone.

5.4.6. Caspase-3/7

The effectiveness of 7-aca, aca and bala as a neuroprotective agent was further evaluated by determining the mechanism of apoptosis through caspase activation. The Caspase-Glo 3/7 assay is a luminescent assay that measures caspase-3 and -7 activities. Figure 5.14 shows the comparison of caspase-3/7 activity in the various treatment groups, all of which show significant increases in caspase-3/7 activity when exposed to 200μM TBPH ($P<0.01$ compared with the untreated cells). Cells pre-treated with all compounds showed a significant ($P < 0.01$) decrease in caspase-3/7 activity in a dose-dependent manner indicating potential neuroprotective activity. Three μM of 7-aca, 3μM of aca and 10μM of bala resulted in a significant ($P < 0.01$) decrease in caspase-3/7 activity by 32.3%, 39.8% and 48.5%, respectively.

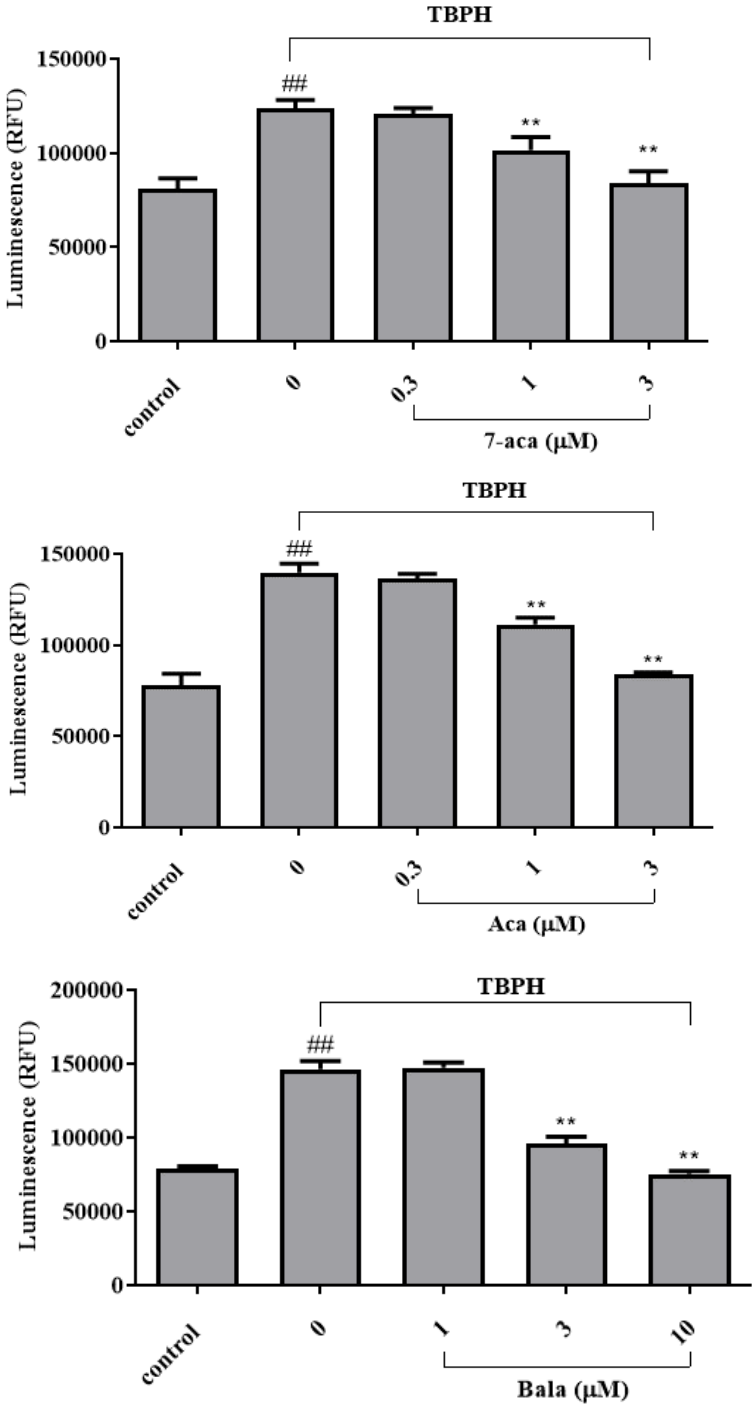

Figure 5.14 Neuroprotective effect of different concentrations of 7-aca, aca, and bala on caspases-3/7 level in SH-SY5Y cells after stimulation with test samples with or without 200 µM TBPH for 1.5 h. Data was analysed using One-Way ANOVA with Bonferroni multiple comparison test. ## P< 0.01 indicates significant differences from the control group. **P<0.01 represents a significant decrease in caspase 3/7 vs TBPH treated cells (control).

5.4.7. AChE

The AChE inhibitory potential of 7-aca, aca and bala is shown in Figure 5.16. AChE inhibitory assays were determined using Amplex® Red. The results revealed that the compounds inhibited AChE activity in a dose-dependent manner with an IC_{50} of 2.1µM for 7-aca and 2.8µM for aca and 2.7µM for bala.

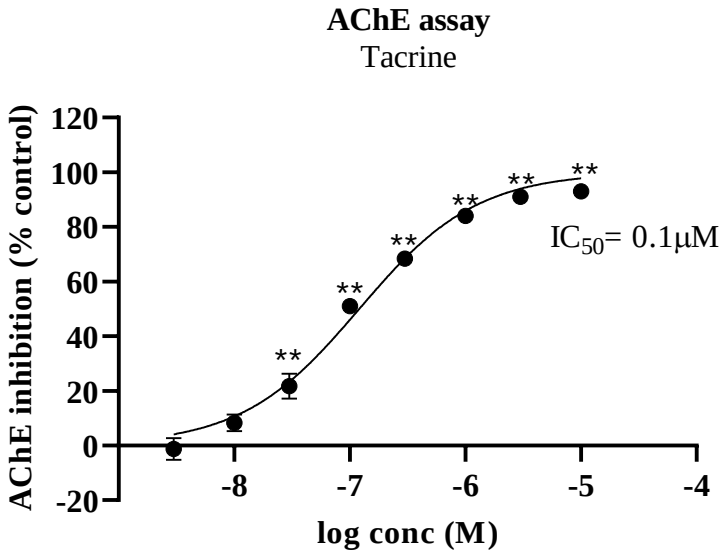

Figure 5.15 AChE inhibition activity of tacrine (standard) at a range of concentrations (0.003-10µM). Values represent mean ± SEM. Data was analysed using One-Way ANOVA with Bonferroni multiple comparison test. ** P< 0.01 indicates a significant increase from the control group (without tacrine).

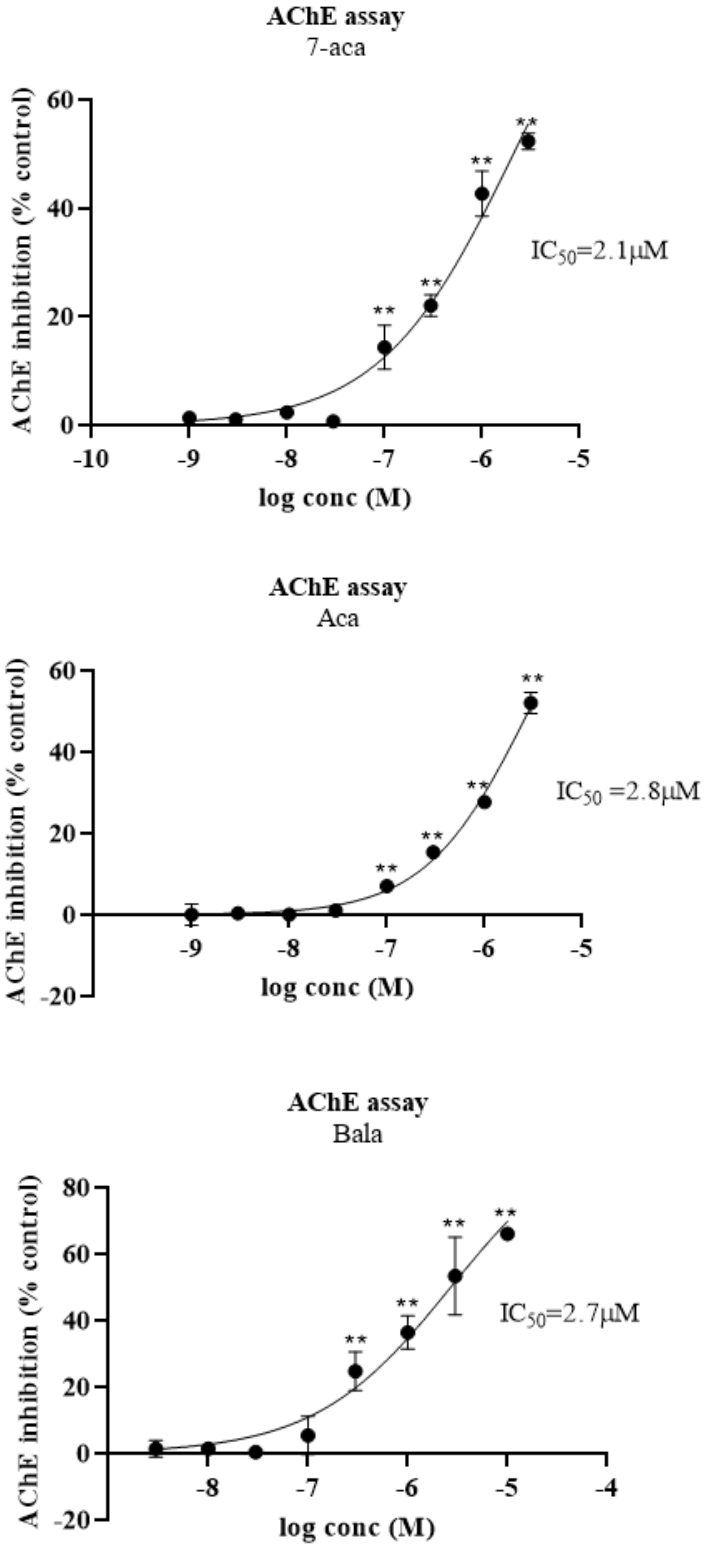

Figure 5.16 AChE inhibition activity of 7-aca (0.001-3μM), aca (0.001-3μM) and bala (0.003-10μM). Values represent mean ± SEM. Data was analysed using One-Way ANOVA with Bonferroni multiple comparison test. ** P< 0.01 indicates significant differences from the control group (without compounds).

5.5. Discussion and conclusion

In Chapter 3, a high concentration of 7-aca (30 µM), aca (30 µM) and bala (150 µM) showed cytotoxic effects and promoted apoptosis of cancer cells A2780 and ZR-75-1. However, at lower concentrations, 7-aca (3µM), aca (3µM) and bala (10µM) showed anti-inflammatory effects on LPS-stimulated THP-1 differentiated cells as described in Chapter 4. The link between chronic inflammation and oxidative damage that leads to neuronal death are important features of the brain pathology of AD. Thus, it was pertinent to investigate the protective effect of these compounds against neuronal cell death. Therefore, this chapter explored the potential use of 7-aca, aca and bala as a protective agent against neurotoxicity caused by oxidative stress.

Protective effects of the compounds were assessed in *in vitro* assays using the human neuroblastoma SH-SY5Y cell line which is widely used as a model cell system for studying neuronal cell death induced by oxidative stress (Martínez *et al.*, 2020). Non-cytotoxic concentrations of the compounds were selected using an alamarBlue® cell viability assay in order to determine safe working concentrations. TBHP is a membrane-permeant pro-oxidant agent frequently used for assessment of mechanisms involved in oxidative stress in biological systems and cellular function (Kučera *et al.*, 2014, Lu *et al.*, 2015b, Sardão *et al.*, 2007). In this study, TBHP was used as an oxidative agent that mimics oxidative cell injury by Aβ. Cell death was induced by incubating SH-SY5Y cells with TBHP (200 µM) for 24 h. At this TBPH concentration ~50% of cell death was observed. To assess the protective effect of 7-aca, aca and bala from TBPH-induced toxicity, cells were pre-treated with compounds for 12 h before the treatment of TBPH for 24 h. The data in this study determined that pre-treatment of neuron cells with 7-aca, aca and bala prevented TBPH-induced cell death

(> 80% viable cells) and inhibited morphological changes. Incubation of SH-SY5Y cells with TBPH for 24 h caused cell shrinkage and a decrease in the cell number, which is a sign of apoptotic morphological changes (Saraste and Pulkki, 2000). However, pre-treatment with 7-aca (3µM), aca (3µM) and bala (10 µM) showed very little to no apoptotic morphological changes.

Following the protection studies against cell death by TBPH, the role of redox regulation in the protective effect of 7-aca, aca and bala against TBPH–induced oxidative damage was investigated. This was carried out by measuring the free radical scavenging ability, intracellular oxidative stress and cellular antioxidant defence in SH-SY5Y cells. These parameters were selected as oxidative stress plays an important role in the early stages of AD manifestation. For example, several studies have shown an increase of ROS and RNS mediated injuries in AD brain along with increased levels of oxidised biomolecules (proteins, nucleic acids and lipids). Altered regulation of antioxidant enzymes was also observed in AD patients (Mecocci and Polidori, 2012, Rosini *et al.*, 2014). A DPPH assay was used to assess the ability of samples to scavenge ROS. Ascorbic acid was used in this assay as a positive control due to its known antioxidant activity. Ascorbic acid inhibited DPPH with an IC_{50} of 12.4 µM. 7-aca and aca showed a moderate DPPH radical scavenging activity and this finding is concordant with a published study by (Hu *et al.*, 2017). However, bala was able to scavenge DPPH radical more than 50% (IC_{50} =6.2 µM) and this potent activity was reported by (Ge *et al.*, 2009). In DCFH-DA-loaded SH-SY5Y cells, the fluorescence intensity increased after treatment with 200 µM TBPH for 1.5 h, suggesting an increase in the generation of intracellular ROS. The oxidant burden of SH-SY5Y neuroblastoma cells after exposure to TBPH decreased significantly in the presence of

7-aca, aca and bala in a concentration-dependent manner ($P < 0.01$). Pre-treatment with 7-aca and aca at 3µM and bala at 10µM decreased ROS levels by about 54%, 55% and 69%, respectively, when compared to TBPH treatment alone. This result indicates that the protective effects of the compounds against TBPH–induced oxidative damage could be mediated by their antioxidant ability. Incubation with 200 µM TBPH decreased GSH levels to approximately 50% in SH-SY5Y cells compared to untreated cells. GSH is an important co-substrate for several key cellular antioxidative enzymes intracellular antioxidant and it has the ability to scavenge both singlet oxygen and hydroxyl radicals and provides a first line of defence that targets intracellular ROS (Chetty *et al.,* 2005). In AD patients, GSH is depleted compared to healthy age-matched controls (Cristalli *et al.*, 2012, Padurariu *et al.*, 2010, Calabrese *et al.*, 2006). In *in vitro* studies carried out using neuron cells, the decrease in GSH levels and the onset of oxidative damage could possibly contribute to the activation of signalling events that leads to apoptotic cell death (Chetty *et al.,* 2005, Kern and Kehrer, 2005). TBPH has been reported to reduce GSH levels in cells numerous times (Liang *et al.*, 2018, Wang *et al.*, 2018c, Ko and Lam, 2002, Lim *et al.*, 2018). Pre-treatment of 7-aca and aca at 3µM and bala at 10 µM restored GSH levels by 60%, 61.9% increase and 66.1% increase, respectively in SH-SY5Y cells compared to TBPH alone. A well-known antioxidant drug, N-Acetylcysteine (NAC), has been proven to be a precursor for GSH production which is a protective approach against AD progression. In an *in vivo* study, mice pre-treated with NAC prior to intracerebroventricular injection of Aβ showed an increase in GSH content that resulted in decreased protein and lipid oxidation compared to control (Fu *et al.*, 2006). In *in vitro* studies, the protective effects of NAC of SH-SY5Y cells has been proven to be due to the activation of the

GSH redox-cycling pathway that leads to ROS suppression (Cheng *et al.*, 2016, Chandramani Shivalingappa *et al.*, 2012, Alboni *et al.*, 2013). Hence in this study it is suggested that the mechanism behind the compounds' protective effects against TBPH–induced oxidative damage could be via an increase in cellular antioxidant enzymes, specifically GSH.

Oxidative stress affects mitochondrial processes which causes mitochondrial dysfunction and thus disruption in brain function (Jordán *et al.*, 2003). Caspase-3 activation executes apoptosis. The effectors of apoptosis are responsible for the breakdown of the cellular cytoskeleton, mitochondrial DNA and DNA-associated proteins leading to neuronal cell death via mitochondrial-mediated apoptotic pathways (Tatton *et al.*, 2003). In response to treatment of TBPH in this study, decreased ΔΨM and increased caspase-3/7 compared to untreated cells was observed. This suggests that apoptotic cell death induced by TBPH was associated with ΔΨM depolarisation and an increase in caspase levels which was attenuated by the compounds. Results obtained by TMRE fluorescent sensitive probes showed that ΔΨM loss induced by TBPH was significantly ($P<0.01$) reversed by pre-treatment with 3 µM 7-aca (81.3%), 3 µM aca (80.3%) and 10 µM bala (91.5%). Furthermore, it was confirmed that activation of caspase-3/7 induced by TBPH was inhibited by pre-treatment with 7-aca (3µM), aca (3µM) and bala (10 µM) by 32.3%, 39.8% and 48.5, respectively.

Aca protection against cell death has been shown in a number of publications, but this is the first report of the protection effect of 7-aca. Kim *et al.* (2017) demonstrated that treatment of aca inhibited 6-hydroxy-dopamine (6-OHDA)-induced neuronal cell death in SH-SY5Y cells through reduction of ROS level and ΔΨM dysfunction. Aca also acted on key molecules in apoptotic cell death pathways such as reducing

phosphorylation of JNK, MAPK, (PI3K)/Akt, and glycogen synthase kinase-3beta (GSK-3b) (Kim *et al.*, 2017). Another study showed that the treatment of aca on inhibition of kainic acid-induced neuronal cell death in a rat model through the inhibition of glutamate release from hippocampal synaptosomes by attenuating voltage-dependent Ca2+ entry (Lin *et al.*, 2014). Furthermore, aca also showed cardioprotection in primary cultured neonatal rat cardiomyocytes and H9C2 cardiomyoblasts cells (Wu *et al.*, 2018). Aca (0.3–3 μM) significantly decreased apoptosis and ROS production induced by hypoxia/reoxygenation injury via reducing BAX and cleaved-caspase-3 and increasing the anti-apoptotic protein, BCL-2 (Wu *et al.*, 2018). Furthermore, aca has been reported to exhibit its neuroprotective effects through other mechanisms such as by interfering with human Aβ cleaving enzyme (BACE-1) activity and amyloid precursor protein (APP) synthesis which results in reduced Aβ production in a *Drosophila melanogaster* AD models (Wang *et al.*, 2015c). All the above points support the protective effect of 7-aca and aca in this study through the inhibition of the apoptotic cell death pathways.

Currently, there are no published reports on the protective effects of bala. However, resveratrol is known for its antioxidant properties and neuroprotection effects. At 5 μM, resveratrol protected SH-SY5Y cells against the cytotoxicity induced by dopamine through rescuing the loss of ΔΨM, causing a decrease in cleavage of PARP, an increase in BCL-2 protein, and inhibition of caspase-3 (Lee *et al.*, 2007a). Similarly, primary cortical neuron cultures treated with resveratrol showed protection against N-methyl-D-aspartate (NMDA)-induced neuronal cell death by inhibiting the elevation of intracellular calcium and ROS (Ban *et al.*, 2008, Zhang *et al.*, 2008). Another study showed that resveratrol protected the hippocampal neuronal HT22 cell line from high

exposure to glutamate, by reducing mitochondrial oxidative stress and damage through induction of the expression of mitochondrial superoxide dismutase 2 (SOD2) (Fukui *et al.*, 2010). Furthermore, other studies have demonstrated the neuroprotective effects of resveratrol through other mechanisms such as activation of Sirtuin-1 (SIRT1) in rat hippocampus and SH-SY5Y cells which is essential for synaptic plasticity and normal cognitive functions (Capiralla *et al.*, 2012, Wang *et al.*, 2017, Guida *et al.*, 2015). Resveratrol is also effective at preventing blood-brain barrier (BBB) impairment and inhibiting Aβ1–42 from crossing the BBB and accumulating in the hippocampus (Zhao *et al.*, 2015).

In this current study, 7-aca, aca and bala showed AChE inhibitory effect with an IC_{50} of 2.1µM for 7-aca, 2.8µM for aca and 2.7µM for bala. The major role of AChE is to breakdown ACh which is an important neuromodulator in the brain that plays a role in the enhancement of alertness on waking up, in sustaining attention and in learning and memory (Picciotto *et al.*, 2012). Therefore, the pathogenesis of AD has been linked to a deficiency in the brain neurotransmitter ACh. Aca has previously been reported to exhibit a potent anti-cholinesterase activity (IC_{50}: 50.33µM ± 0.87) (Nugroho *et al.*, 2019). However, an *in vivo* study on AChE inhibitory activity using $AlCl_3$-induced AD in rats showed that aca had weak activity (El-Sawi *et al.*, 2019). There are no published reports on the AChE inhibitory effect of bala, however resveratrol and its oligomers have been proven in a number of *in vitro* studies to be potent AChE inhibitors and butyrylcholinesterase (BChE) inhibitors (Jang *et al.*, 2008, Ślusarczyk *et al.*, 2019, Giri and Roy, 2015). BChE is another hydrolytic enzyme that acts on ACh to terminate its actions in the synaptic cleft, however the conversion rate of ACh by BChE is lower than the conversion by AChE (Zhao *et al.*, 2013a). Nevertheless, BChE

can still substitute AChE for the breakdown of the neurotransmitter (Pohanka, 2011, Karlsson *et al.*, 2012). An *in vivo* study by Schmatz *et al.* (2009) showed that treatment with resveratrol significantly prevented an increase in AChE activity in the cerebral cortex and hippocampus of adult male Wistar rats (Schmatz *et al.*, 2009).

Collectively, the data supports the neuroprotective effects of 7-aca, aca and bala against TBHP-induced cell death in SH-SY5Y cells. The possible mechanism that could be involved in the neuroprotective effect of the compounds is through elevation of intracellular GSH levels and the ability to modulate ROS levels. Furthermore, 7-aca and bala also showed AChE inhibition. Therefore, these findings support the potential of 7-aca and bala as treatments to prevent neuronal dysfunction and/or death associated with age or age-associated diseases such as AD wherein oxidative stress plays an important role.

Chapter 6 Summary, Future work and Conclusions

6.1 Summary

The current study provided some promising results on the bioactivity of isolated compounds from two Malaysian plants. As indicated in Chapter 1, the objective of this research was to evaluate the anti-cancer, anti-inflammatory and neuroprotective activities of *A. malaccensis* twigs and *H. dryobalanoides* bark extracts with focus on pure, isolated compounds.

Firstly, selected extracts underwent phytochemical investigation to identify and isolate potential bioactive compounds. Based on the cytotoxicity studies on cancer cells (A2780, HepG2, U2OS and ZR-75-1), the hexane and methanol extracts of *A. malaccensis* and the ethyl acetate extract of *H. dryobalanoides* showed strongest cytotoxicity against A2780 and ZR-75-1 cells. Therefore, these extracts were chosen for phytochemical investigation using chromatography techniques. Fractionation of *A. malaccensis* hexane and ethyl acetate extracts led to the isolation of 7-aca and Q/A (mixture of two compounds named quercitrin and afzelin), respectively. Fractionation of *H. dryobalanoides* ethyl acetate extract led to the isolation of bala and heimiol A.

6.1.1 Anti-cancer

In Chapter 3,7-aca, aca, Q/A and bala were tested for their anti-cancer activity on A2780 and ZR 75-1 cells. Due to limited published material on the anti-cancer effect of 7-aca, a similar compound called acacetin (aca) which is known to have potent anti-cancer effect was purchased (Chien *et al.*, 2011, Hsu *et al.*, 2004, Kim *et al.*, 2013). Preliminary testing of the cytotoxicity of 7-aca, aca, Q/A and bala on A2780 and ZR-75-1 cells suggests that these compounds could possess potential anti-cancer activity. Heimiol A did not show any cytotoxicity against both cancer cell lines. Amongst all

the compounds 7-aca was shown to have the strongest cytotoxicity effect against A2780 and ZR-75-1 cells with an IC_{50} of 6.5μM and 6.7 μM, respectively. Therefore, further investigation of the mechanism of action behind the cytotoxic effect of the compounds was carried out by measuring the ROS levels (DCFH-DA assay), the ΔΨM (TMRE assay) and the caspase-3/7 levels (Caspase-Glo assay). 7-aca, aca, Q/A and bala were able to increase ROS levels, reduce the ΔΨM and increase caspase 3/7 levels in A2780 and ZR-75-1 cells. Cancer and apoptosis are known as antagonistic processes and, therefore, stimulation of apoptosis is the main strategy in cancer therapy. Evidence suggests that malignant cells in most cancers, have increased levels of ROS compared to normal cells (Gonçalves *et al.*, 2015, Schumacker, 2006). A delicate balance of ROS levels is essential for normal cell growth and survival since a moderate increase in ROS can promote cell proliferation while excessively high concentrations of ROS leads to cell death (Boonstra and Post, 2004). Since cancer cells are already in a state of increased oxidative stress, they could be more susceptible to agents that further increase ROS generation (Pelicano *et al.*, 2004, Schumacker, 2006). Hence, a further increase in ROS is likely to push cancer cells, but not normal cells, beyond the toxic threshold. Excessive increases in ROS in cancer cells disrupts the mitochondrial membrane and opens the mitochondrial permeability transition pore (PTP), and thus interferes with the mitochondrial ETC and induces the release of cytochrome-c leading to the activation of effectors such as caspase-3, that results in the cleavage of cellular proteins and leads to apoptotic cell death (Giorgio *et al.*, 2005, Simon *et al.*, 2000, Redza-Dutordoir and Averill-Bates, 2016). Based on this theory, this suggests that 7-aca, aca, Q/A and bala exhibited apoptotic cell death on A2780 and ZR-5-1 cells by the induction of oxidative stress through the elevation of ROS, disruption of the ΔΨM

and an increase in caspase-3/7 levels. Furthermore, 7-aca, aca and bala showed anti-metastatic activity by inhibiting adhesion of A2780 and ZR-75-1 cells on fibronectin in the ECM and inhibited their migration and invasion. MMP inhibition has been known to be one of the strategies for blocking migration and tumour metastasis. Inhibition of MMP-2 and MMP-9 by chemotherapeutic agents has been reported to suppress A2780 and MCF-7 cell migration and invasion ability (Gao *et al.*, 2017, Jamialahmadi *et al.*, 2018, Majumder *et al.*, 2019).

Based on the results, 7-aca showed to have a significantly ($P<0.05$) stronger anti-cancer and anti-metastatic activity compared to aca. Therefore, 7-aca was selected for further study on the effect of these compounds on A2780 and ZR-75-1 cells through metabolomic profiling in order to achieve a deeper understanding of the mechanism of action and to identify potential new biomarker metabolites. Aca was also chosen to undergo metabolomics study in order to further compare these two compounds. The data obtained revealed that 7-aca and aca affected several metabolic pathways of A2780 and ZR-75-1 such as amino acid, energy, and carbohydrate metabolism. OXPHOS is preferentially stimulated in some cancer cells such as breast and ovarian (Lucantoni *et al.*, 2018, Guppy *et al.*, 2002, Jose *et al.*, 2011). Mitochondria are best known for their role in ATP production, which is performed via OXPHOS. The mitochondrial OXPHOS system is embedded in the mitochondrial inner membrane (MIM) and represents the final step in the conversion of nutrients to energy by catalysing the generation of ATP (Shahruzaman *et al.*, 2018). In this study, a clear inhibition of mitochondria OXPHOS was observed through the depletion of ATP and NAD+ levels in both A2780 and ZR-75-1 cells treated with 7-aca and aca. ATP and NAD+ levels were lower in cells treated with 7-aca compared to aca. Several studies

have demonstrated a decrease in ATP levels through the depletion of ΔΨM could initiate apoptosis (Zorova *et al.*, 2018). A well-known mitochondrial uncoupler, FCCP, inhibits ΔΨM by dissipating the proton gradient in mitochondria which causes the reduction of ATP synthesis from the mitochondria (Losano *et al.*, 2017). Another study showed that the combination treatment of gossypol with phenformin cause inhibition of mitochondrial complex I and ATP depletion, which efficiently induced cell death in non-small-cell lung cancer cells (NSCLC) (Kang *et al.*, 2016). Furthermore, in the current study, both A2780 and ZR-75-1 cells showed reduction of metabolites such as G6PD, GSSG and NADPH in the pentose phosphate pathway (PPP) after treatment with 7-aca and aca. Again, these metabolites were lower in 7-aca treated cells compared to aca-treated cells. NADPH, which is generated by G6PD in the PPP, plays a role in detoxifying intracellular ROS through reducing GSSG to GSH (Korge *et al.*, 2015). These metabolites are involved in the PPP which is a major antioxidant defence system in cancer to balance high ROS levels in order to maintain cell homeostasis and the inhibition of these metabolites are known to cause the build-up of ROS (Fang *et al.*, 2016, Miran *et al.*, 2018, Hong *et al.*, 2015, Yang *et al.*, 2019). Moreover, G6PD deficiency has been associated with lower cancer risk through downregulation of PPP and consequent shortage of NADPH needed by rapidly proliferating cancer cells to synthesise DNA (Patra and Hay, 2014, Pes *et al.*, 2019). Studies on cervical cancer and breast cancer cells have shown that inhibition of G6PD activity resulted in decreased cancer cell migration and proliferation ability as well as impairment of NADPH production, causing ROS-mediated stress that leads to cell shrinkage (apoptosis) (Fang *et al.*, 2016, Mele *et al.*, 2018). This suggests that 7-aca and aca caused an impaired antioxidant defence in the PPP which resulted in the build-

up of ROS and oxidative stress. Oxidative stress causes mitochondria damage. At the same time, the compounds also caused a decrease in ΔΨM that leads to decrease of ATP levels which triggers apoptosis.

Overall results in this study suggest that 7-aca is a more potent anti-cancer activity towards A2780 and ZR-75-1 cells compared to aca. 7-Aca contains 2 methoxylated carbons at position 7 and 4' as well as a hydroxyl group at C5 whereas aca has only 1 methoxylated carbon at 4' in B ring and a hydroxyl group at C5. Several studies has suggested that the presence of methoxy group or insertion of methoxy group at different positions in the compound could cause a stronger cytotoxic and anti-metastatic activity of the compound (Liew *et al.*, 2020, Tseng *et al.*, 2015, Wu *et al.*, 2017, Massi *et al.*, 2017). However, further investigation needs to be carried out to determine the structural-activity relationships analysis of different functional groups in 7-aca and aca with their anti-cancer activity.

6.1.2 Anti-inflammatory

The main objectives of the present study in Chapter 4 were to investigate the anti-inflammatory properties of 7-aca, aca, Q/A and bala in inhibiting the production of pro-inflammatory cytokines in LPS stimulated PMA-differentiated THP-1 cells. In this study, ELISAs confirmed that LPS treatment triggered the production of a significant amount of pro-inflammatory cytokines TNF-α, IL-1β and IL-6, as expected. In comparison, 7-aca, aca and bala pre-treatment inhibited LPS stimulation production of TNF-α, IL-1β and IL-6. Bala at 10μM showed the strongest inhibition of TNF-α, IL-1β and IL-6 by 75%, 68% and 67.28%, respectively. 7-aca and aca showed similar activity by causing approximately 40-50% inhibition of all the cytokines. *In vitro* and *in vivo* studies in the literature have reported that inhibition of

pro-inflammatory cytokines such as TNF-α, IL-1β and IL-6 are effective in treating chronic inflammation diseases such as RA, diabetes, IBD, Crohn's disease and AD (Mori *et al.*, 2011, Popko *et al.*, 2010, Sanchez-Munoz *et al.*, 2008, Pizarro *et al.*, 2006, McAlpine *et al.*, 2009). Prolonged activation of macrophages that results in the overproduction of cytokines in the TME has been reported to contribute to cancer progression (Kim *et al.*, 2009, Stoimenov and Helleday, 2009).

Following the more potent anti-inflammatory activity shown by bala compared to 7-aca and aca, bala was chosen to carry out a retrospective investigation into gene changes using RNA-Seq on RNA extracted from THP-1 macrophages following stimulation with LPS, with and without bala. RNA-Seq data analysed by Cytoscape ClueGo showed that the cytokine-cytokine receptor interaction pathway was most affected in both groups. The treatment of LPS and LPS/bala on THP-1 macrophage cells caused up-regulation of 47 and 22 genes associated with the cytokine-cytokine receptor interaction pathway, respectively, when compared to the no treatment control group. However, when LPS/bala treatment was compared to LPS alone, down-regulation of 27 genes associated with the cytokine-cytokine receptor interaction pathway was observed. Treatment with LPS/bala showed the down-regulation of *TNF-α* and *IL-6* genes compared to LPS alone, which reflects the data shown in the ELISA. However, the *IL-1β* gene was not significantly ($P>0.05$) altered by LPS alone or LPS/bala treatment. Two most significantly enriched pathways were suggested by the Pathview software: TNF signalling and JAK/STAT signalling pathways. Genes such as *TNF-α, BIRC3, MMP9, PTGS2* and *IL-6* were shown to be significantly ($P<0.05$) down-regulated after treatment with LPS/bala compared to LPS treatment alone. Activation of TNF family signalling is associated with the activation of a NF-κB-

dependent response (Hayden and Ghosh, 2014) that causes the release of pro-inflammatory cytokines such as TNF-α and IL-6 (Wu and Zhou, 2010b, Germano *et al.*, 2008). Studies on breast cancer cells (such as MCF-7 and MDA-MB-468) have demonstrated that TNF-α promotes self-renewal capacity in human breast cancer cell lines through the activation of non-canonical and canonical NF-κB pathway (Storci *et al.*, 2010, Liu *et al.*, 2020). NF-κB is a key regulator of macrophage activation pathways and is critical for macrophage activation responses to inflammatory stimuli including TLR ligands (Stout *et al.*, 2005). Activation of NF-κB in macrophages has been shown to be required for the onset of tumour development in several inflammation-induced cancer models through the release of TNFα, IL-6 and IL-1β (Mantovani *et al.*, 2013, Lewis and Pollard, 2006, Sica and Bronte, 2007, Maeda *et al.*, 2005, Hallam *et al.*, 2009). Inhibition of NF-κB has been linked to the reduction of pro-inflammatory cytokine release (Crinelli *et al.*, 2000, Karlsen *et al.*, 2007).

TNF-α has been reported to be an inducer of MMPs including MMP-9 in macrophages NF-κB, MAPK and JNK signalling pathways (Shubayev *et al.*, 2006, Zhang *et al.*, 2017a, Lee *et al.*, 2009b) and inhibition of these signalling pathways have been reported to cause the inhibition of *MMP-2* and *MMP-9* gene transcription in THP-1 macrophage cells (Kim *et al.*, 2015b). Moreover, TNF-α has been reported to induced production of MMP-9 which is associated with invasion/migration of various cancer cells such as breast, lung and prostate (Weiler *et al.*, 2018, Lee *et al.*, 2010a, Dilshara *et al.*, 2015). A study by (Hagemann *et al.*, 2004) demonstrated that co-cultivation of breast cancer cells (MCF-7, SK-BR-3) with macrophages leads to enhanced invasiveness of the malignant cells due to TNF-a dependent MMP-2 and -9 induction in the macrophages. In this study, *STAT3* and *STAT4* genes were significantly ($P<0.05$)

down regulated in the JAK/STAT signalling pathway after treatment with LPS/bala compared to LPS treatment alone. STAT3 has close association with chronic inflammation which is subsequently linked with tumour initiation due to a mutation in the genetic makeup of malignant cells (Ernst *et al.*, 2008, Gao *et al.*, 2007). IL-6 that is encoded by NF-κB target genes are known to be critical activators of STAT3 (Lee *et al.*, 2009a, Bollrath *et al.*, 2009, Grivennikov *et al.*, 2009). A considerable amount of literature presented that the activation of IL-6/STAT3 signalling pathway played an important role in cancer (Lu *et al.*, 2015a, Slattery *et al.*, 2013, Gyamfi *et al.*, 2018). Furthermore, a study showed that IL-6 released by macrophages exerted a promotive effect on migration and invasion of colon cancer cells via the IL-6/STAT3/ERK signalling pathway (Gao *et al.*, 2018). Therefore, this suggests that TNF/NF-κB and the JAK/STAT signalling pathway could be involved in the inhibition of TNFα and IL-6 by bala.

6.1.3 Neuroprotection

The main objectives of Chapter 5 were to investigate the neuroprotective effect of 7-aca, aca and bala in TBPH-induced cytotoxicity on SHSY-5Y cells. In Chapter 4, 7-aca, aca and bala had been shown to inhibit inflammation by supressing the production of pro-inflammatory cytokines such as TNF-α, IL-1β and IL-6, which is commonly believed to be a culprit in AD pathogenesis (Weninger and Yankner, 2001). Studies have shown that secretion of pro-inflammatory cytokines from activated human microglia or THP-1 cells cause toxic effects against SHSY-5Y cells (Jordán *et al.*, 2003, Little *et al.*, 2015, Klegeris and McGeer, 2001, Klegeris and McGeer, 2003). Oxidative stress also plays an important role in AD manifestation through an increase

of ROS and RNS and altered regulation of antioxidant enzymes (Mecocci and Polidori, 2012, Rosini *et al.*, 2014).

In this study, all compounds showed protective effects against TBPH-induced toxicity against SHSY-5Y cells through an increase in ΔΨM and a decrease in caspase-3/7. Furthermore, the compounds also showed a protective effect against oxidative stress through inhibition of TBPH-generated ROS by approximately 54% (7-aca), 55% (aca) and 69% (bala). Similarly to cancer cells, oxidative stress-induced neuronal cell death is associated with the mitochondria-related apoptotic pathway in H_2O_2-induced SH-SY5Y cells and is an important mechanism in neurodegenerative diseases. The overproduction of ROS leads to increased permeability of the mitochondrial membrane and loss of ΔΨM, thus resulting in release of cytochrome C which activates pro-apoptosis factors, such as caspase-3, eventually inducing cell death (Hu *et al.*, 2015b, Kim *et al.*, 2018). In this study, the protective effect of the compounds from the increase in ROS level could be due to the antioxidant activity of the compounds. Bala showed the most potent antioxidant activity by scavenging DPPH radicals (IC_{50} =2.4 μM) and increasing GSH levels by 66.1%. It has been reported in many studies that antioxidants with potent free radical scavenging properties (DPPH assay) and the ability to restore GSH levels are able to protect neurons from oxidative stress (Pruccoli *et al.*, 2020, Tarozzi *et al.*, 2012, Ali *et al.*, 2013, Sereia *et al.*, 2019). 7-aca and bala also showed significant ($P<0.01$) AChE inhibitory effects with an IC_{50} of 2.4μM and 1.9μM, respectively. The critical role of cholinesterase in neural transmission makes them a key target of a large number of cholinesterase-inhibiting drugs relevant to the treatment of neurodegenerative disorders, including AD (Ali Reza *et al.*, 2018). Furthermore, there is evidence showing that ACh exerts anti-inflammatory effects

through the inhibition of cytokine secretion from macrophages and rat microglial cultures (De Simone *et al.,* 2005, Yang *et al.*, 2015). Another report demonstrated that treatment of LPS-induced adult male Wistar rat with AChE inhibitors decrease the expression of IL-1β through the activation of the "cholinergic anti-inflammatory pathway" which in turn protects against neurodegeneration (Kalb *et al.,* 2013). The "cholinergic anti-inflammatory pathway" mediated by ACh acts by inhibiting the production of pro-inflammatory cytokines and chemokines, suppresses the activation of NF-kβ expression and oxidative system (Pavlov and Tracey, 2005). (Reale *et al.,* 2004) found that AChE inhibitors taken orally reduces expression and secretion of the pro-inflammatory cytokines IL-1β, IL-6 and TNF-α in peripheral blood mononuclear cells in AD patients.

At higher concentrations of 7-aca (30µM) and bala (150µM), toxic effects towards cancer cells and pro-oxidant activity by increasing ROS levels were shown. However, at lower concentration of 7-aca (3 µM) and bala (10 µM), the compounds showed protective effects towards cells such as SHSY-5Y and THP-1 macrophages as well as antioxidant effects by reducing ROS levels. Polyphenols are known to be "double edged swords" in the cellular redox state and pro-oxidant or antioxidant activity intimately depends on their concentration (Eghbaliferiz and Iranshahi, 2016, Bouayed and Bohn, 2010). Vitamin C or ascorbic acid, a powerful antioxidant, has been reported to exhibit pro-oxidant properties and cause cancer cell death at a high concentration (Chen *et al.*, 2008, Kondakçı *et al.,* 2013, Lim *et al.,* 2016). Many studies have also demonstrated that antioxidants such as resveratrol, curcumin, quercetin and epigallocatechin-3-gallate exhibit pro-oxidative activity at a high concentration (Robaszkiewicz *et al.*, 2007, de la Lastra and Villegas, 2007). Similarly,

in this study, 7-aca, aca and bala were demonstrated to possess antioxidant activity at low concentrations by increasing GSH levels and inhibiting production of ROS levels in TBPH-induced SHSY-5Y cells and demonstrated pro-oxidant activity at high concentrations by effecting the glutathione redox ratio (GSH/GSSG) and causing increasing ROS levels in A2780 and ZR-75-1 cancer cells.

6.2 Future work

The most significant issue in this study was the impact on the work of limited quantities of the compounds isolated due to the lack of fresh plant material. Therefore, if further work is to be carried out, larger quantities of fresh plant material would be required for an in-depth study. At a high concentration of bala (150μM) promising anti-cancer results towards A2780 and ZR-75-1 cells by activating the apoptosis pathway as discussed in Chapter 3 were obtained. Hence, further investigation of the anti-cancer effect of bala through metabolomics studies should be carried out to achieve a deeper understanding of the mechanism of action and to identify which metabolites are affected. Examination of the effects of 7-aca and bala on the metabolomes of different cell lines and *in vivo* models should also be performed to obtain a broader assessment of the affected metabolites.

In Chapter 4, 7-aca showed anti-inflammatory activity through inhibition of pro-inflammatory cytokines. Further investigation of anti-inflammatory effects of 7-aca on LPS-stimulated THP-1 macrophage cells by RNA-Seq and polymerase chain reaction (PCR) experiments as well as quantitative PCR experiments on the key genes highlighted from the RNA-Seq analysis of bala treatment should be carried out.

The results obtained from this study (Chapter 5) shows that 7-aca and bala could be potential anti-Alzheimer drugs that protect neuron cells from oxidative stress induced-cell death which initiates the progression of the disease. Further *in vivo* experiments using a suitable rodent experimental model such as several transgenic AβPP animal models for AD treated with compounds should be carried out to examine their clinical significance.

6.3 Conclusion

The main findings of the study were:

- For the first time, 7-aca, quercitrin and afzelin were isolated from the twigs of *A. malaccensis*. Bala and heimiol A were isolated from the bark of *H. dryobalanoides*.
- 7-aca, aca, Q/A and bala showed anticancer activity through cytotoxicity, increase in ROS levels, a decrease in ΔΨM and an increase in caspase-3/7 levels.
- 7-aca, aca and bala showed anti-metastatic activity through inhibition of cell adhesion, migration and invasion.
- Metabolomics study of 7-aca and aca on A2780 and ZR-75-1 cells showed that the PPP and OXPHOS pathways were affected.
- 7-aca, aca and bala shown anti-inflammatory activity through inhibition of TNFα, IL-6 and IL-1β in LPS-stimulated THP-1 macrophages.
- RNA-Seq analysis of LPS/bala treatment showed that the cytokine-cytokine receptor interaction pathway, TNF/NF-κB signalling pathway and JAK/STAT signalling pathway were affected.

- 7-aca, aca and bala showed neuroprotective effects on TBPH-induced toxicity in SHSY-5Y cells by inhibiting ROS production, an increase in GSH level, an increase in ΔΨM, a decrease in caspase-3/7 levels and inhibition of AChE.
- 7-aca showed a greater anti-cancer and anti-metastatic activity against A2780 and ZR-75-1 cells however showed similar anti-inflammatory and neuroprotective activity.

A summary of the results (anticancer, anti-inflammatory and neuroprotective activities) are presented in Table 6.1. Based on these results, the potential mechanisms of action of the isolated compounds mainly, 7-aca and bala are shown. This research produced findings that show how 7-aca and bala could potentially be used to combat cancer because they cause apoptotic cell death on cancer cells by raising the ROS levels and causing disruption in the ΔΨM. Moreover, 7-aca and bala showed potential anti-metastatic effects by inhibition of cell adhesion, migration and invasion. Potential anti-inflammatory activities of 7-aca and bala were also demonstrated by inhibition of pro-inflammatory cytokines in LPS-stimulated macrophage cells. While the RNA seq study suggests that TNF/NF-κB signalling and JAK/STAT signalling pathways could have been involved in the anti-inflammatory effect of bala. Furthermore, 7 aca and bala showed neuroprotective effects against TBPH-induced SHSY-5Y cell death through enhancing GSH synthesis, inhibiting ROS, rescuing the ΔΨM and inhibiting AChE. Overall, these results reveal that compounds isolated from natural products such as *A. malaccensis* and *H. dryobalanoides* have potential as a source of natural anticancer, anti-inflammatory and neuroprotective agents.

Table 6.1 Summary of the anticancer, anti-inflammatory and neuroprotective effects of compounds in this study.

Experiment	**7-aca**	**aca**	**Q/A**	**Bala**
Anti-cancer (A2780 / ZR-75-1 cells)				
alamarBlue®	IC_{50}= 7.9µM / 8.5µM	IC_{50}= 19.5µM / 17.5µM	IC_{50}= 22.7µg/ml / >30µg/ml	IC_{50}= 64.1µM / 134.4µM
DCFH-DA (ROS)	5.3 / 4.1-fold increase	4.1 / 3.3-fold increase	2.8/ 2.4-fold increase	3.5 / 2.6-fold increase
TMRE (ΔΨM)	72.2% / 70.1% decrease	63.4% / 60.1% decrease	49% / 49.3% decrease	55% / 37.3% decrease
Caspase-Glo (12 h)	8.8/ 7.2-fold increase	8.6 / 6.9 -fold increase	6.6 /5.4-fold increase	7.1 /6.8-fold increase
Cell adhesion	70.3% / 61.7% decrease	63% / 46% decrease	-	50.7% / 30% decrease
Cell migration	56.7% / 42.3 % decrease	40.7% / 32.2% decrease	-	21.4% / 23.7% decrease
Cell invasion	54.8% / 56.3 % decrease	45% / 44% decrease	-	32.1% / 38.5% decrease
Anti-inflammatory (THP-1 cells)				
TNF-α	43.8% inhibition	49.5% inhibition	-	75.3% inhibition
IL-1β	50.2% inhibition	48.9% inhibition	-	68% inhibition
IL-6	55.2% inhibition	50.7% inhibition	-	67.3% inhibition

Neuroprotective (SHSY-5Y cells)				
alamarBlue®	31% increase	34.6% increase	-	42.3% increase
DPPH	IC_{50}>10µM	IC_{50}>10µM	-	IC_{50} =6.2µM
GSH	60% increase	61.9% increase	-	66.1% increase
DCFH-DA (ROS)	54% decrease	55% decrease	-	69% decrease
TMRE (ΔΨM)	81.3% increase	80.3% increase	-	90% increase
Caspase-Glo	32.3% decrease	39.8% decrease	-	48.5% decrease
AChE	IC_{50} =2.1µM	$IC_{50=}$2.8µM	-	IC_{50} =2.7µM

REFERENCES

ABBAS, P., HASHIM, Y., AMID, A., SALLEH, H., JAMAL, P. & JASWIR, I. 2014. Anti-cancer Potential of Agarwood Distillate. *Journal of Pure and Applied Microbiology,* 8.
ABDELKADER, B., BELKACEM, N. & AMRANI, I. 2017. Health Benefits of Phenolic Compounds Against Cancers.
ABOU EL-SOUD, N. 2010. Herbal medicine in ancient Egypt. *Journal of Medicinal Plants Research,* 4**,** 82-86.
ADAMS, J. M. & CORY, S. 2007. The Bcl-2 apoptotic switch in cancer development and therapy. *Oncogene,* 26**,** 1324-37.
ADELINA, N., HARUM, F., SCHMIDT, L. H. & JØKER, D. 2004. Aquilaria malaccensis Lam.: Seed Leaflet.
ADI, A. S. D. I. 2015. *Dementia statistics* [Online]. Available: https://www.alz.co.uk/research/statistics [Accessed April 2020].
AFIFFUDDEN, S. K. N., ALWI, H. & HAMID, K. H. K. 2015. Determination of 4'-Hydroxyacetanilide in Leaves Extract of Aquilaria malaccencis by High Pressure Liquid Chromatograph. *Procedia - Social and Behavioral Sciences,* 195**,** 2726-2733.
AGGARWAL, V., TULI, H. S., VAROL, A., THAKRAL, F., YERER, M. B., SAK, K., VAROL, M., JAIN, A., KHAN, M. A. & SETHI, G. 2019. Role of Reactive Oxygen Species in Cancer Progression: Molecular Mechanisms and Recent Advancements. *Biomolecules,* 9**,** 735.
AJETI, V., LARA-SANTIAGO, J., ALKMIN, S. & CAMPAGNOLA, P. J. 2017. Ovarian and Breast Cancer Migration Dynamics on Laminin and Fibronectin Bidirectional Gradient Fibers Fabricated via Multiphoton Excited Photochemistry. *Cell Mol Bioeng,* 10**,** 295-311.
AKSENOVA, M. V., AKSENOV, M. Y., MACTUTUS, C. F. & BOOZE, R. M. 2005. Cell culture models of oxidative stress and injury in the central nervous system. *Curr Neurovasc Res,* 2**,** 73-89.
ALAEE, M., KHAGHANI, S., BEHROOZFAR, K., HESARI, Z., GHORBANHOSSEINI, S. S. & NOURBAKHSH, M. 2017. Inhibition of Nicotinamide Phosphoribosyltransferase Induces Apoptosis in Estrogen Receptor-Positive MCF-7 Breast Cancer Cells. *Journal of breast cancer,* 20**,** 20-26.
ALBANI, D., POLITO, L., BATELLI, S., DE MAURO, S., FRACASSO, C., MARTELLI, G., COLOMBO, L., MANZONI, C., SALMONA, M., CACCIA, S., NEGRO, A. & FORLONI, G. 2009. The SIRT1 activator resveratrol protects SK-N-BE cells from oxidative stress and against toxicity caused by alpha-synuclein or amyloid-beta (1-42) peptide. *J Neurochem.* England.
ALBONI, S., GIBELLINI, L., MONTANARI, C., BENATTI, C., BENATTI, S., TASCEDDA, F., BRUNELLO, N., COSSARIZZA, A. & PARIANTE, C. M. 2013. N-acetyl-cysteine prevents toxic oxidative effects induced by IFN-α in human neurons. *International Journal of Neuropsychopharmacology,* 16**,** 1849-1865.
ALDOSSARY, S. 2019. Review on Pharmacology of Cisplatin: Clinical Use, Toxicity and Mechanism of Resistance of Cisplatin. *Biomedical and Pharmacology Journal,* 11**,** 07-15.
ALHAJJ, M. & FARHANA, A. 2020. *Enzyme Linked Immunosorbent Assay (ELISA)*, StatPearls Publishing, Treasure Island (FL).
ALI REZA, A. S. M., HOSSAIN, M. S., AKHTER, S., RAHMAN, M. R., NASRIN, M. S., UDDIN, M. J., SADIK, G. & KHURSHID ALAM, A. H. M. 2018. In vitro antioxidant and cholinesterase inhibitory activities of Elatostema papillosum leaves and correlation with their phytochemical profiles: a study relevant to the treatment of Alzheimer's disease. *BMC complementary and alternative medicine,* 18**,** 123-123.

ALI, S. K., HAMED, A. R., SOLTAN, M. M., HEGAZY, U. M., ELGORASHI, E. E., EL-GARF, I. A. & HUSSEIN, A. A. 2013. In-vitro evaluation of selected Egyptian traditional herbal medicines for treatment of Alzheimer disease. *BMC Complement Altern Med,* 13**,** 121.
ALKHALAF, M., EL-MOWAFY, A., RENNO, W., RACHID, O., ALI, A. & AL-ATTYIAH, R. 2008. Resveratrol-induced apoptosis in human breast cancer cells is mediated primarily through the caspase-3-dependent pathway. *Arch Med Res.* United States.
ALLEN, T. D., ZHU, C. Q., JONES, K. D., YANAGAWA, N., TSAO, M. S. & BISHOP, J. M. 2011. Interaction between MYC and MCL1 in the genesis and outcome of non-small-cell lung cancer. *Cancer Res,* 71**,** 2212-21.
ALMTORP, G. T., HAZELL, A. C. & TORSSELL, K. B. G. 1991. A lignan and pyrone and other constituents from Hyptis capitata. *Phytochemistry,* 30**,** 2753-2756.
ALRAWAIQ, N. & ABDULLAH, A. 2014. A Review of Flavonoid Quercetin: Metabolism, Bioactivity and Antioxidant Properties. *International Journal of PharmTech Research,* 6**,** 933-941.
AMARO, H. M., FERNANDES, F., VALENTÃO, P., ANDRADE, P. B., SOUSA-PINTO, I., MALCATA, F. X. & GUEDES, A. C. 2015. Effect of Solvent System on Extractability of Lipidic Components of Scenedesmus obliquus (M2-1) and Gloeothece sp. on Antioxidant Scavenging Capacity Thereof. *Marine drugs,* 13**,** 6453-6471.
AMIGO, I., DA CUNHA, F. M., FORNI, M. F., GARCIA-NETO, W., KAKIMOTO, P. A., LUEVANO-MARTINEZ, L. A., MACEDO, F., MENEZES-FILHO, S. L., PELOGGIA, J. & KOWALTOWSKI, A. J. 2016. Mitochondrial form, function and signalling in aging. *Biochem J.* England: 2016 The Author(s); published by Portland Press Limited on behalf of the Biochemical Society.
AMINZADEH-GOHARI, S., WEBER, D. D., VIDALI, S., CATALANO, L., KOFLER, B. & FEICHTINGER, R. G. 2020. From old to new — Repurposing drugs to target mitochondrial energy metabolism in cancer. *Seminars in Cell & Developmental Biology,* 98**,** 211-223.
ANAND DAVID, A. V., ARULMOLI, R. & PARASURAMAN, S. 2016. Overviews of Biological Importance of Quercetin: A Bioactive Flavonoid. *Pharmacognosy reviews,* 10**,** 84-89.
ANDERSON, J. M. 2013. Chapter II.2.2 - Inflammation, Wound Healing, and the Foreign-Body Response. *In:* RATNER, B. D., HOFFMAN, A. S., SCHOEN, F. J. & LEMONS, J. E. (eds.) *Biomaterials Science (Third Edition).* Academic Press.
ANDO, Y., IWASA, S., TAKAHASHI, S., SAKA, H., KAKIZUME, T., NATSUME, K., SUENAGA, N., QUADT, C. & YAMADA, Y. 2019. Phase I study of alpelisib (BYL719), an α-specific PI3K inhibitor, in Japanese patients with advanced solid tumors. *Cancer science,* 110**,** 1021-1031.
ANISIMOVA, N. Y., KISELEVSKY, M. V., SOSNOV, A. V., SADOVNIKOV, S. V., STANKOV, I. N. & GAKH, A. A. 2011. Trans-, cis-, and dihydro-resveratrol: a comparative study. *Chemistry Central journal,* 5**,** 88-88.
ANNABI, B., LORD-DUFOUR, S., VÉZINA, A. & BÉLIVEAU, R. 2012. Resveratrol Targeting of Carcinogen-Induced Brain Endothelial Cell Inflammation Biomarkers MMP-9 and COX-2 is Sirt1-Independent. *Drug Target Insights,* 6**,** 1-11.
ANSTEY, K. J., ASHBY-MITCHELL, K. & PETERS, R. 2017. Updating the Evidence on the Association between Serum Cholesterol and Risk of Late-Life Dementia: Review and Meta-Analysis. *Journal of Alzheimer's disease : JAD,* 56**,** 215-228.
APARNA SUDHAKARAN, V., PANWAR, H., CHAUHAN, R., DUARY, R. K., RATHORE, R. K., BATISH, V. K. & GROVER, S. 2013. Modulation of anti-inflammatory response in lipopolysaccharide stimulated human THP-1 cell line and mouse model at gene expression level with indigenous putative probiotic lactobacilli. *Genes & nutrition,* 8**,** 637-648.
AQIL, F., GUPTA, A., MUNAGALA, R., JEYABALAN, J., KAUSAR, H., SHARMA, R. J., SINGH, I. P. & GUPTA, R. C. 2012. Antioxidant and antiproliferative activities of anthocyanin/ellagitannin-enriched extracts from Syzygium cumini L. (Jamun, the Indian Blackberry). *Nutr Cancer,* 64**,** 428-38.

ARMSTRONG, J. S., STEINAUER, K. K., HORNUNG, B., IRISH, J. M., LECANE, P., BIRRELL, G. W., PEEHL, D. M. & KNOX, S. J. 2002. Role of glutathione depletion and reactive oxygen species generation in apoptotic signaling in a human B lymphoma cell line. *Cell Death & Differentiation,* 9**,** 252-263.
ARUK, A. S. R. U. 2014. *Dementia statistics* [Online]. Available: https://www.dementiastatistics.org/statistics-about-dementia/prevalence/ [Accessed April 2020].
ARUK, A. S. R. U. 2018. *Deaths due to dementia* [Online]. Available: https://www.dementiastatistics.org/statistics/deaths-due-to-dementia/ [Accessed April 2020].
ARVIDSSON, Y., ANDERSSON, E., BERGSTRÖM, A., ANDERSSON, M. K., ALTIPARMAK, G., ILLERSKOG, A. C., AHLMAN, H., LAMAZHAPOVA, D. & NILSSON, O. 2008. Amyloid precursor-like protein 1 is differentially upregulated in neuroendocrine tumours of the gastrointestinal tract. *Endocr Relat Cancer.* England.
ATRI, A., MOLINUEVO, J. L., LEMMING, O., WIRTH, Y., PULTE, I. & WILKINSON, D. 2013. Memantine in patients with Alzheimer's disease receiving donepezil: new analyses of efficacy and safety for combination therapy. *Alzheimers Res Ther,* 5**,** 6.
ATRI, C., GUERFALI, F. Z. & LAOUINI, D. 2018. Role of Human Macrophage Polarization in Inflammation during Infectious Diseases. *Int J Mol Sci,* 19.
ATUN, S. 2006. Activity of Oligoresveratrols from Stem Bark of Hopea mengarawan (Dipterocarpaceae) as Hydroxyl Radical Scavenger. *HAYATI Journal of Biosciences,* 13.
ATUN, S., AZNAM, N. & ARIANINGRUM, R. 2012. Oligoresveratrol Isolated from Stem Bark of Hopea Odorata as

Antioxidant and Cytotoxicity againt Human Cancer Cell Line. *International Conference on Chemistry and Chemical Engineering,* 38**,** 6-10.
ATUN, S., AZNAM, N., ARIANINGRUM, R. & NIWA, M. 2006. *BALANOCARPOL AND HEIMIOL A, TWO RESVERATROLS DIMER FROM STEM BARK Hopea mengarawan (Dipterocarpaceae)*.
ATUN, S., NURFINA, A., RETNO, A., TAKAYA, Y. & NIWA, M. 2008. Resveratrol Derivatives from Stem Bark of Hopea and Their Biological Activity Test. Journal of Physical Science.
AULD, D. S., KORNECOOK, T. J., BASTIANETTO, S. & QUIRION, R. 2002. Alzheimer's disease and the basal forebrain cholinergic system: relations to beta-amyloid peptides, cognition, and treatment strategies. *Prog Neurobiol.* England: 2002 Elsevier Science Ltd.
AWANTU, A. F., LENTA, B. N., DONFACK, E. V., WANSI, J. D., NEUMANN, B., STAMMLER, H.-G., NOUNGOUE, D. T., TSAMO, E. & SEWALD, N. 2011. Flavonoids and other constituents of Hymenostegia afzelii (Caesalpiniaceae). *Phytochemistry Letters,* 4**,** 315-319.
AZIZ, N., KIM, M.-Y. & CHO, J. Y. 2018. Anti-inflammatory effects of luteolin: A review of in vitro, in vivo, and in silico studies. *Journal of Ethnopharmacology,* 225**,** 342-358.
BACHELOT, T., RAY-COQUARD, I., MENETRIER-CAUX, C., RASTKHA, M., DUC, A. & BLAY, J. Y. 2003. Prognostic value of serum levels of interleukin 6 and of serum and plasma levels of vascular endothelial growth factor in hormone-refractory metastatic breast cancer patients. *British Journal of Cancer,* 88**,** 1721-1726.
BAGLI, E., GOUSSIA, A., MOSCHOS, M. M., AGNANTIS, N. & KITSOS, G. 2016. Natural Compounds and Neuroprotection: Mechanisms of Action and Novel Delivery Systems. *In Vivo.* Greece.
BAHRANI, H., MOHAMAD, J., PAYDAR, M. & ROTHAN, H. 2014. Isolation and Characterisation of Acetylcholinesterase Inhibitors from Aquilaria subintegra for the Treatment of Alzheimer's Disease (AD). *Current Alzheimer research,* 11.
BAN, J. Y., CHO, S. O., CHOI, S.-H., JU, H. S., KIM, J. Y., BAE, K., SONG, K.-S. & SEONG, Y. H. 2008. Neuroprotective Effect of Smilacis chinae Rhizome on NMDA-Induced Neurotoxicity

In Vitro and Focal Cerebral Ischemia In Vivo. *Journal of Pharmacological Sciences,* 106**,** 68-77.
BARIBEAU, S., CHAUDHRY, P., PARENT, S. & ASSELIN, É. 2014. Resveratrol inhibits cisplatin-induced epithelial-to-mesenchymal transition in ovarian cancer cell lines. *PloS one,* 9**,** e86987-e86987.
BARROS, M., MOTA DA SILVA, L., BOEING, T., SOMENSI, L. B., CURY, B. J., BURCI, L., SANTIN, J. R., ANDRADE, S. F., MONACHE, F. D. & CECHINEL-FILHO, V. 2016. Pharmacological reports about gastroprotective effects of methanolic extract from leaves of Solidago chilensis (Brazilian arnica) and its components quercitrin and afzelin in rodents.(Report). *Naunyn-Schmiedeberg's Archives of Pharmacology,* 389**,** 403.
BARTOSCH, B. 2010. Hepatitis B and C viruses and hepatocellular carcinoma. *Viruses,* 2**,** 1504-1509.
BARTUS, R. T., DEAN, R. L., 3RD, BEER, B. & LIPPA, A. S. 1982. The cholinergic hypothesis of geriatric memory dysfunction. *Science,* 217**,** 408-14.
BASTOS, D. & ANTONARAKIS, E. 2019. Darolutamide For Castration-Resistant Prostate Cancer. *OncoTargets and Therapy,* Volume 12**,** 8769-8777.
BASU, A., DAS, A. S., SHARMA, M., PATHAK, M. P., CHATTOPADHYAY, P., BISWAS, K. & MUKHOPADHYAY, R. 2017. STAT3 and NF-κB are common targets for kaempferol-mediated attenuation of COX-2 expression in IL-6-induced macrophages and carrageenan-induced mouse paw edema. *Biochemistry and Biophysics Reports,* 12**,** 54-61.
BATAI, K., IMLER, E., PANGILINAN, J., BELL, R., LWIN, A., PRICE, E., MILINIC, T., ARORA, A., ELLIS, N. A., BRACAMONTE, E., SELIGMANN, B. & LEE, B. R. 2018. Whole-transcriptome sequencing identified gene expression signatures associated with aggressive clear cell renal cell carcinoma. *Genes Cancer,* 9**,** 247-256.
BAUD, V. & KARIN, M. 2001. Signal transduction by tumor necrosis factor and its relatives. *Trends in Cell Biology,* 11**,** 372-377.
BAYER, S. V., GRITHER, W. R., BRENOT, A., HWANG, P. Y., BARCUS, C. E., ERNST, M., PENCE, P., WALTER, C., PATHAK, A. & LONGMORE, G. D. 2019. DDR2 controls breast tumor stiffness and metastasis by regulating integrin mediated mechanotransduction in CAFs. *Elife,* 8.
BEHRENS, M. I., LENDON, C. & ROE, C. M. 2009. A common biological mechanism in cancer and Alzheimer's disease? *Current Alzheimer research,* 6**,** 196-204.
BEN-NERIAH, Y. & KARIN, M. 2011. Inflammation meets cancer, with NF-κB as the matchmaker. *Nature Immunology,* 12**,** 715-723.
BERNDT, C., LILLIG, C. H. & HOLMGREN, A. 2007. Thiol-based mechanisms of the thioredoxin and glutaredoxin systems: implications for diseases in the cardiovascular system. *Am J Physiol Heart Circ Physiol.* United States.
BEYDOUN, M. A., KAUFMAN, J. S., SATIA, J. A., ROSAMOND, W. & FOLSOM, A. R. 2007. Plasma n−3 fatty acids and the risk of cognitive decline in older adults: the Atherosclerosis Risk in Communities Study. *The American Journal of Clinical Nutrition,* 85**,** 1103-1111.
BHALLA, S., SINGH, A. T. K., PRACHAND, S., HALLORAN, T. V., WINTER, J. N., SCHUMACKER, P. T., PLATANIAS, L. C., GORDON, L. I. & EVENS, A. M. 2008. Arsenic Trioxide (As2O3) acts through redox pathways to induce apoptosis in Hodgkin Lymphoma (HL) and Non-Hodgkin Lymphoma cell lines: activation of JNK signaling by glutathione depletion. *Cancer Research,* 68**,** 5523.
BHAT, T., NAMBIAR, D., TAILOR, D., PAL, A., AGARWAL, R. & SINGH, R. 2013. Acacetin Inhibits In Vitro and In Vivo Angiogenesis and Downregulates Stat Signaling and VEGF Expression. *Cancer prevention research (Philadelphia, Pa.),* 6.
BHUI, K., PRASAD, S., GEORGE, J. & SHUKLA, Y. 2009. Bromelain inhibits COX-2 expression by blocking the activation of MAPK regulated NF-kappa B against skin tumor-initiation triggering mitochondrial death pathway. *Cancer Letters,* 282**,** 167-176.

BIASIBETTI, R., TRAMONTINA, A. C., COSTA, A. P., DUTRA, M. F., QUINCOZES-SANTOS, A., NARDIN, P., BERNARDI, C. L., WARTCHOW, K. M., LUNARDI, P. S. & GONCALVES, C. A. 2013. Green tea (-)epigallocatechin-3-gallate reverses oxidative stress and reduces acetylcholinesterase activity in a streptozotocin-induced model of dementia. *Behav Brain Res.* Netherlands: 2012 Elsevier B.V.
BIRBEN, E., SAHINER, U. M., SACKESEN, C., ERZURUM, S. & KALAYCI, O. 2012. Oxidative stress and antioxidant defense. *World Allergy Organ J,* 5**,** 9-19.
BIRKENMEIER, K., DROSE, S., WITTIG, I., WINKELMANN, R., KAFER, V., DORING, C., HARTMANN, S., WENZ, T., REICHERT, A. S., BRANDT, U. & HANSMANN, M. L. 2016. Hodgkin and Reed-Sternberg cells of classical Hodgkin lymphoma are highly dependent on oxidative phosphorylation. *Int J Cancer,* 138**,** 2231-46.
BIRKS, J. 2006. Cholinesterase inhibitors for Alzheimer's disease. *Cochrane Database Syst Rev***,** CD005593.
BISWAS, S. K. & MANTOVANI, A. 2010. Macrophage plasticity and interaction with lymphocyte subsets: cancer as a paradigm. *Nat Immunol,* 11**,** 889-96.
BITZINGER, D. I., GRUBER, M., TUMMLER, S., MALSY, M., SEYFRIED, T., WEBER, F., REDEL, A., GRAF, B. M. & ZAUSIG, Y. A. 2019. In Vivo Effects of Neostigmine and Physostigmine on Neutrophil Functions and Evaluation of Acetylcholinesterase and Butyrylcholinesterase as Inflammatory Markers during Experimental Sepsis in Rats. *Mediators Inflamm,* 2019**,** 8274903.
BLANQUER-ROSSELLÓ, M. D. M., HERNÁNDEZ-LÓPEZ, R., ROCA, P., OLIVER, J. & VALLE, A. 2017. Resveratrol induces mitochondrial respiration and apoptosis in SW620 colon cancer cells. *Biochimica et Biophysica Acta (BBA) - General Subjects,* 1861**,** 431-440.
BOLLRATH, J., PHESSE, T. J., VON BURSTIN, V. A., PUTOCZKI, T., BENNECKE, M., BATEMAN, T., NEBELSIEK, T., LUNDGREN-MAY, T., CANLI, O., SCHWITALLA, S., MATTHEWS, V., SCHMID, R. M., KIRCHNER, T., ARKAN, M. C., ERNST, M. & GRETEN, F. R. 2009. gp130-mediated Stat3 activation in enterocytes regulates cell survival and cell-cycle progression during colitis-associated tumorigenesis. *Cancer Cell,* 15**,** 91-102.
BONDA, D. J., WANG, X., LEE, H. G., SMITH, M. A., PERRY, G. & ZHU, X. 2014. Neuronal failure in Alzheimer's disease: a view through the oxidative stress looking-glass. *Neurosci Bull,* 30**,** 243-52.
BOONSTRA, J. & POST, J. A. 2004. Molecular events associated with reactive oxygen species and cell cycle progression in mammalian cells. *Gene,* 337**,** 1-13.
BOUAYED, J. & BOHN, T. 2010. Exogenous antioxidants--Double-edged swords in cellular redox state: Health beneficial effects at physiologic doses versus deleterious effects at high doses. *Oxidative medicine and cellular longevity,* 3**,** 228-237.
BOWLING, T., MERCER, L., DON, R., JACOBS, R. & NARE, B. 2012. Application of a resazurin-based high-throughput screening assay for the identification and progression of new treatments for human African trypanosomiasis. *International journal for parasitology. Drugs and drug resistance,* 2**,** 262-270.
BRAND, M. D. 2010. The sites and topology of mitochondrial superoxide production. *Exp Gerontol,* 45**,** 466-72.
BRATTON, S. B., WALKER, G., SRINIVASULA, S. M., SUN, X. M., BUTTERWORTH, M., ALNEMRI, E. S. & COHEN, G. M. 2001. Recruitment, activation and retention of caspases-9 and -3 by Apaf-1 apoptosome and associated XIAP complexes. *EMBO J,* 20**,** 998-1009.
BRAY, F., FERLAY, J., SOERJOMATARAM, I., SIEGEL, R. L., TORRE, L. A. & JEMAL, A. 2018. Global cancer statistics 2018: GLOBOCAN estimates of incidence and mortality worldwide for 36 cancers in 185 countries. *CA Cancer J Clin,* 68**,** 394-424.

BRIGGS, M. A., PETERSEN, K. S. & KRIS-ETHERTON, P. M. 2017. Saturated Fatty Acids and Cardiovascular Disease: Replacements for Saturated Fat to Reduce Cardiovascular Risk. *Healthcare (Basel, Switzerland),* 5**,** 29.
BROWNING, L., PATEL, M. R., HORVATH, E. B., TAWARA, K. & JORCYK, C. L. 2018. IL-6 and ovarian cancer: inflammatory cytokines in promotion of metastasis. *Cancer management and research,* 10**,** 6685-6693.
BU, G. 2009. Apolipoprotein E and its receptors in Alzheimer's disease: pathways, pathogenesis and therapy. *Nat Rev Neurosci,* 10**,** 333-44.
BU, J., SHI, S., WANG, H.-Q., NIU, X.-S., ZHAO, Z.-F., WU, W.-D., ZHANG, X.-L., MA, Z., ZHANG, Y.-J., ZHANG, H. & ZHU, Y. 2019. Acacetin protects against cerebral ischemia-reperfusion injury via the NLRP3 signaling pathway. *Neural regeneration research,* 14**,** 605-612.
BULLOCK, R., TOUCHON, J., BERGMAN, H., GAMBINA, G., HE, Y., RAPATZ, G., NAGEL, J. & LANE, R. 2005. Rivastigmine and donepezil treatment in moderate to moderately-severe Alzheimer's disease over a 2-year period. *Curr Med Res Opin,* 21**,** 1317-27.
BUREAU, G., LONGPRE, F. & MARTINOLI, M. G. 2008. Resveratrol and quercetin, two natural polyphenols, reduce apoptotic neuronal cell death induced by neuroinflammation. *J Neurosci Res,* 86**,** 403-10.
BUTLER, M. S. 2004. The role of natural product chemistry in drug discovery. *J Nat Prod,* 67**,** 2141-53.
CACABELOS, R. 2007. Donepezil in Alzheimer's disease: From conventional trials to pharmacogenetics. *Neuropsychiatr Dis Treat,* 3**,** 303-33.
CAIN, K., BRATTON, S. B., LANGLAIS, C., WALKER, G., BROWN, D. G., SUN, X. M. & COHEN, G. M. 2000. Apaf-1 oligomerizes into biologically active approximately 700-kDa and inactive approximately 1.4-MDa apoptosome complexes. *J Biol Chem,* 275**,** 6067-70.
CALABRESE, V., SULTANA, R., SCAPAGNINI, G., GUAGLIANO, E., SAPIENZA, M., BELLA, R., KANSKI, J., PENNISI, G., MANCUSO, C., STELLA, A. M. & BUTTERFIELD, D. A. 2006. Nitrosative stress, cellular stress response, and thiol homeostasis in patients with Alzheimer's disease. *Antioxid Redox Signal,* 8**,** 1975-86.
CALDERÓN-MONTAÑO, J. M., BURGOS-MORÓN, E., ORTA, M. L., MALDONADO-NAVAS, D., GARCÍA-DOMÍNGUEZ, I. & LÓPEZ-LÁZARO, M. 2014. Evaluating the cancer therapeutic potential of cardiac glycosides. *BioMed research international,* 2014**,** 794930-794930.
CAPIRALLA, H., VINGTDEUX, V., ZHAO, H., SANKOWSKI, R., AL-ABED, Y., DAVIES, P. & MARAMBAUD, P. 2012. Resveratrol mitigates lipopolysaccharide- and Aβ-mediated microglial inflammation by inhibiting the TLR4/NF-κB/STAT signaling cascade. *Journal of Neurochemistry,* 120**,** 461-472.
CARBALLO-VILLALOBOS, A. I., GONZALEZ-TRUJANO, M. E. & LOPEZ-MUNOZ, F. J. 2014. Evidence of mechanism of action of anti-inflammatory/antinociceptive activities of acacetin. *Eur J Pain,* 18**,** 396-405.
CARDOSO, S. M., PROENCA, M. T., SANTOS, S., SANTANA, I. & OLIVEIRA, C. R. 2004. Cytochrome c oxidase is decreased in Alzheimer's disease platelets. *Neurobiol Aging.* United States.
CARO, P., KISHAN, A. U., NORBERG, E., STANLEY, I. A., CHAPUY, B., FICARRO, S. B., POLAK, K., TONDERA, D., GOUNARIDES, J., YIN, H., ZHOU, F., GREEN, M. R., CHEN, L., MONTI, S., MARTO, J. A., SHIPP, M. A. & DANIAL, N. N. 2012. Metabolic signatures uncover distinct targets in molecular subsets of diffuse large B cell lymphoma. *Cancer Cell,* 22**,** 547-60.
CAROTHERS, A. M., DAVIDS, J. S., DAMAS, B. C. & BERTAGNOLLI, M. M. 2010. Persistent Cyclooxygenase-2 Inhibition Downregulates NF-κB, Resulting in Chronic Intestinal Inflammation in the Min/+ Mouse Model of Colon Tumorigenesis. *Cancer Research,* 70**,** 4433.

CARUANA, M., CAUCHI, R. & VASSALLO, N. 2016. Putative Role of Red Wine Polyphenols against Brain Pathology in Alzheimer's and Parkinson's Disease. *Frontiers in nutrition,* 3**,** 31-31.
CARVAJAL, F. J. & INESTROSA, N. C. 2011. Interactions of AChE with Aβ Aggregates in Alzheimer's Brain: Therapeutic Relevance of IDN 5706. *Frontiers in molecular neuroscience,* 4**,** 19-19.
CENINI, G. & VOOS, W. 2019. Mitochondria as Potential Targets in Alzheimer Disease Therapy: An Update. *Frontiers in Pharmacology,* 10.
CERELLA, C., SOBOLEWSKI, C., DICATO, M. & DIEDERICH, M. 2010. Targeting COX-2 expression by natural compounds: a promising alternative strategy to synthetic COX-2 inhibitors for cancer chemoprevention and therapy. *Biochem Pharmacol,* 80**,** 1801-15.
CHA, J.-D., CHOI, S.-M. & PARK, J. 2014. Combination of Acacetin with Antibiotics against Methicillin Resistant Staphylococcus aureus Isolated from Clinical Specimens. *Advances in Bioscience and Biotechnology,* 05**,** 398-408.
CHAHAR, M. K., SHARMA, N., DOBHAL, M. P. & JOSHI, Y. C. 2011. Flavonoids: A versatile source of anticancer drugs. *Pharmacognosy reviews,* 5**,** 1-12.
CHAITANYA, G. V., STEVEN, A. J. & BABU, P. P. 2010. PARP-1 cleavage fragments: signatures of cell-death proteases in neurodegeneration. *Cell communication and signaling : CCS,* 8**,** 31-31.
CHANDRAMANI SHIVALINGAPPA, P., JIN, H., ANANTHARAM, V. & KANTHASAMY, A. 2012. N-Acetyl Cysteine Protects against Methamphetamine-Induced Dopaminergic Neurodegeneration via Modulation of Redox Status and Autophagy in Dopaminergic Cells. *Parkinsons Dis,* 2012**,** 424285.
CHANG, C. H., CHEN, H. X., YU, G., PENG, C. C. & PENG, R. Y. 2014. Curcumin-Protected PC12 Cells Against Glutamate-Induced Oxidative Toxicity. *Food Technol Biotechnol,* 52**,** 468-478.
CHATTERJEE, S. 2016. Chapter Two - Oxidative Stress, Inflammation, and Disease. *In:* DZIUBLA, T. & BUTTERFIELD, D. A. (eds.) *Oxidative Stress and Biomaterials.* Academic Press.
CHAUDHRY, H., ZHOU, J., ZHONG, Y., ALI, M. M., MCGUIRE, F., NAGARKATTI, P. S. & NAGARKATTI, M. 2013. Role of cytokines as a double-edged sword in sepsis. *In vivo (Athens, Greece),* 27**,** 669-684.
CHAURASIYA, N. D., GOGINENI, V., ELOKELY, K. M., LEON, F., NUNEZ, M. J., KLEIN, M. L., WALKER, L. A., CUTLER, S. J. & TEKWANI, B. L. 2016. Isolation of Acacetin from Calea urticifolia with Inhibitory Properties against Human Monoamine Oxidase-A and -B. *J Nat Prod,* 79**,** 2538-2544.
CHEN, A. Y. & CHEN, Y. C. 2013. A review of the dietary flavonoid, kaempferol on human health and cancer chemoprevention. *Food chemistry,* 138**,** 2099-2107.
CHEN, C. Y., TSAI, Y. S., CHEN, C. T., YEH, H. C. & LI, H. T. 2019a. Flavonoids from the Flowers of Aquilaria agallocha. *Chemistry of Natural Compounds,* 55**,** 722-723.
CHEN, D., BI, D., SONG, Y.-L. & TU, P.-F. 2012. Flavanoids from the stems of Aquilaria sinensis. *Chinese Journal of Natural Medicines,* 10**,** 287-291.
CHEN, L., DENG, H., CUI, H., FANG, J., ZUO, Z., DENG, J., LI, Y., WANG, X. & ZHAO, L. 2017. Inflammatory responses and inflammation-associated diseases in organs. *Oncotarget,* 9**,** 7204-7218.
CHEN, Q., ESPEY, M. G., SUN, A. Y., POOPUT, C., KIRK, K. L., KRISHNA, M. C., KHOSH, D. B., DRISKO, J. & LEVINE, M. 2008. Pharmacologic doses of ascorbate act as a prooxidant and decrease growth of aggressive tumor xenografts in mice. *Proc Natl Acad Sci U S A,* 105**,** 11105-9.

CHEN, Q., VAZQUEZ, E. J., MOGHADDAS, S., HOPPEL, C. L. & LESNEFSKY, E. J. 2003. Production of reactive oxygen species by mitochondria: central role of complex III. *J Biol Chem.* United States.
CHEN, W.-P., YANG, Z.-G., HU, P.-F., BAO, J.-P. & WU, L.-D. 2015. Acacetin inhibits expression of matrix metalloproteinases via a MAPK-dependent mechanism in fibroblast-like synoviocytes. *Journal of cellular and molecular medicine,* 19**,** 1910-1915.
CHEN, Y., SONG, Y., DU, W., GONG, L., CHANG, H. & ZOU, Z. 2019b. Tumor-associated macrophages: an accomplice in solid tumor progression. *Journal of Biomedical Science,* 26**,** 78.
CHENG, B., ANAND, P., KUANG, A., AKHTAR, F. & SCOFIELD, V. L. 2016. N-Acetylcysteine in Combination with IGF-1 Enhances Neuroprotection against Proteasome Dysfunction-Induced Neurotoxicity in SH-SY5Y Cells. *Parkinson's disease,* 2016**,** 6564212-6564212.
CHENG, E. H., WEI, M. C., WEILER, S., FLAVELL, R. A., MAK, T. W., LINDSTEN, T. & KORSMEYER, S. J. 2001. BCL-2, BCL-X(L) sequester BH3 domain-only molecules preventing BAX- and BAK-mediated mitochondrial apoptosis. *Mol Cell.* United States.
CHENG, J. T., HAN, Y. Q., HE, J., DE WU, X., DONG, L. B., PENG, L. Y., LI, Y. & ZHAO, Q. S. 2013. Two new tirucallane triterpenoids from the leaves of Aquilaria sinensis. *Arch Pharm Res,* 36**,** 1084-9.
CHENG, L., YAN, B., CHEN, K., JIANG, Z., ZHOU, C., CAO, J., QIAN, W., LI, J., SUN, L., MA, J., MA, Q. & SHA, H. 2018. Resveratrol-Induced Downregulation of NAF-1 Enhances the Sensitivity of Pancreatic Cancer Cells to Gemcitabine via the ROS/Nrf2 Signaling Pathways. *Oxidative Medicine and Cellular Longevity,* 2018**,** 9482018.
CHENG, M.-L., HO, H.-Y., WU, Y.-H. & CHIU, D. T.-Y. 2004. Glucose-6-phosphate dehydrogenase-deficient cells show an increased propensity for oxidant-induced senescence. *Free Radical Biology and Medicine,* 36**,** 580-591.
CHENG, M. H., HUANG, H. L., LIN, Y. Y., TSUI, K. H., CHEN, P. C., CHENG, S. Y., CHONG, I. W., SUNG, P. J., TAI, M. H., WEN, Z. H., CHEN, N. F. & KUO, H. M. 2019. BA6 Induces Apoptosis via Stimulation of Reactive Oxygen Species and Inhibition of Oxidative Phosphorylation in Human Lung Cancer Cells. *Oxid Med Cell Longev,* 2019**,** 6342104.
CHETTY, C., VEMURI, M., CAMPBELL, K. & CHALLA, S. 2005. Lead-induced cell death of human neuroblastoma cells involves GSH deprivation. *Cellular & molecular biology letters,* 10**,** 413-23.
CHIEN, S.-T., LIN, S.-S., WANG, C.-K., LEE, Y.-B., CHEN, K.-S., FONG, Y. & SHIH, Y.-W. 2011. Acacetin inhibits the invasion and migration of human non-small cell lung cancer A549 cells by suppressing the p38α MAPK signaling pathway. *Molecular and Cellular Biochemistry,* 350**,** 135-148.
CHISTIAKOV, D. A., SOBENIN, I. A., REVIN, V. V., OREKHOV, A. N. & BOBRYSHEV, Y. V. 2014. Mitochondrial aging and age-related dysfunction of mitochondria. *Biomed Res Int,* 2014**,** 238463.
CHISWICK, E. L., DUFFY, E., JAPP, B. & REMICK, D. 2012. Detection and quantification of cytokines and other biomarkers. *Methods in molecular biology (Clifton, N.J.),* 844**,** 15-30.
CHIU, F. L. & LIN, J. K. 2008. Tomatidine inhibits iNOS and COX-2 through suppression of NF-kappaB and JNK pathways in LPS-stimulated mouse macrophages. *FEBS Lett.* England.
CHO, A., HOWELL, V. M. & COLVIN, E. K. 2015. The Extracellular Matrix in Epithelial Ovarian Cancer - A Piece of a Puzzle. *Frontiers in oncology,* 5**,** 245-245.
CHOI, Y. J., RHO, J. K., LEE, S. J., JANG, W. S., LEE, S. S., KIM, C. H. & LEE, J. C. 2009. HIF-1alpha modulation by topoisomerase inhibitors in non-small cell lung cancer cell lines. *J Cancer Res Clin Oncol,* 135**,** 1047-53.
CHUAKUL, W. 2005. *Medicinal plants in the Khok Pho District, Pattani Province (Thailand)*.

CHUNG, E. Y., ROH, E., KWAK, J. A., LEE, H. S., LEE, S. H., LEE, C. K., HAN, S. B. & KIM, Y. 2010. alpha-Viniferin suppresses the signal transducer and activation of transcription-1 (STAT-1)-inducible inflammatory genes in interferon-gamma-stimulated macrophages. *J Pharmacol Sci.* Japan.
CICHEWICZ, R. H. & KOUZI, S. A. 2002. Resveratrol oligomers: Structure, chemistry, and biological activity. *In:* ATTA UR, R. (ed.) *Studies in Natural Products Chemistry.* Elsevier.
CODY, V. 1988. Crystal and molecular structures of flavonoids. *Prog Clin Biol Res,* 280**,** 29-44.
COGGON, P., JANES, N. F., KING, F. E., KING, T. J., MOLYNEUX, R. J., MORGAN, J. W. W. & SELLARS, K. 1965. 61. Hopeaphenol, an extractive of the heartwood of Hopea odorata and Balanocarpus heimii. *Journal of the Chemical Society (Resumed)***,** 406-409.
COGGON, P., MCPHAIL, A. T. & WALLWORK, S. C. 1970. Structure of hopeaphenol: X-ray analysis of the benzene solvate of dibromodeca-O-methylhopeaphenol. *Journal of the Chemical Society B: Physical Organic***,** 884-897.
COLANGELO, C., SHICHKOVA, P., KELLER, D., MARKRAM, H. & RAMASWAMY, S. 2019. Cellular, Synaptic and Network Effects of Acetylcholine in the Neocortex. *Frontiers in neural circuits,* 13**,** 24-24.
COLOVIĆ, M. B., KRSTIĆ, D. Z., LAZAREVIĆ-PAŠTI, T. D., BONDŽIĆ, A. M. & VASIĆ, V. M. 2013. Acetylcholinesterase inhibitors: pharmacology and toxicology. *Current neuropharmacology,* 11**,** 315-335.
CONWAY, E. M., PIKOR, L. A., KUNG, S. H., HAMILTON, M. J., LAM, S., LAM, W. L. & BENNEWITH, K. L. 2016. Macrophages, Inflammation, and Lung Cancer. *Am J Respir Crit Care Med,* 193**,** 116-30.
CORLISS, B. A., AZIMI, M. S., MUNSON, J. M., PEIRCE, S. M. & MURFEE, W. L. 2016. Macrophages: An Inflammatory Link Between Angiogenesis and Lymphangiogenesis. *Microcirculation (New York, N.Y. : 1994),* 23**,** 95-121.
COSKUN, O. 2016. Separation techniques: Chromatography. *Northern clinics of Istanbul,* 3**,** 156-160.
COX, A. G., WINTERBOURN, C. C. & HAMPTON, M. B. 2009. Mitochondrial peroxiredoxin involvement in antioxidant defence and redox signalling. *Biochem J.* England.
CRAGG, G. M. & NEWMAN, D. J. 2005. Plants as a source of anti-cancer agents. *Journal of Ethnopharmacology,* 100**,** 72-79.
CRAGG GORDON, M. & NEWMAN DAVID, J. 2005. Biodiversity: A continuing source of novel drug leads. *Pure and Applied Chemistry.*
CREGAN, S. P., DAWSON, V. L. & SLACK, R. S. 2004. Role of AIF in caspase-dependent and caspase-independent cell death. *Oncogene,* 23**,** 2785-2796.
CRINELLI, R., ANTONELLI, A., BIANCHI, M., GENTILINI, L., SCARAMUCCI, S. & MAGNANI, M. 2000. Selective inhibition of NF-kB activation and TNF-alpha production in macrophages by red blood cell-mediated delivery of dexamethasone. *Blood Cells Mol Dis,* 26**,** 211-22.
CRISTALLI, D. O., ARNAL, N., MARRA, F. A., DE ALANIZ, M. J. & MARRA, C. A. 2012. Peripheral markers in neurodegenerative patients and their first-degree relatives. *J Neurol Sci.* Netherlands: © 2011 Elsevier B.V.
CROWLEY, L., CHRISTENSEN, M. & WATERHOUSE, N. 2016. Measuring Mitochondrial Transmembrane Potential by TMRE Staining. *Cold Spring Harbor Protocols,* 2016**,** pdb.prot087361.
CRUK. 2017a. *Breast cancer diagnosis and treatment statistics* [Online]. Available: https://www.cancerresearchuk.org/health-professional/cancer-statistics/statistics-by-cancer-type/breast-cancer/diagnosis-and-treatment#heading-Three [Accessed April 2020].

CRUK. 2017b. *Cancer Incidence Statistics* [Online]. Available: https://www.cancerresearchuk.org/health-professional/cancer-statistics/incidence [Accessed May 2020].
CRUK. 2017c. *Ovarian cancer diagnosis and treatment statistics* [Online]. Available: https://www.cancerresearchuk.org/health-professional/cancer-statistics/statistics-by-cancer-type/ovarian-cancer/diagnosis-and-treatment#heading-Four [Accessed April 2020].
CSISZAR, A. 2011. Anti-inflammatory effects of resveratrol: possible role in prevention of age-related cardiovascular disease. *Annals of the New York Academy of Sciences,* 1215**,** 117-122.
CVEJIC, J. M., DJEKIC, S. V., PETROVIC, A. V., ATANACKOVIC, M. T., JOVIC, S. M., BRCESKI, I. D. & GOJKOVIC-BUKARICA, L. C. 2010. Determination of trans- and cis-resveratrol in Serbian commercial wines. *J Chromatogr Sci,* 48**,** 229-34.
D'ORAZIO, J., JARRETT, S., AMARO-ORTIZ, A. & SCOTT, T. 2013. UV radiation and the skin. *International journal of molecular sciences,* 14**,** 12222-12248.
DABEEK, W. M. & MARRA, M. V. 2019. Dietary Quercetin and Kaempferol: Bioavailability and Potential Cardiovascular-Related Bioactivity in Humans. *Nutrients,* 11.
DAHHAM, S., TABANA, Y., SANDAI, D., AHMED, M. & ABDUL MAJID, A. M. S. 2016a. In Vitro Anti-Cancer and Anti-Angiogenic Activity of Essential Oils Extracts from Agarwood (Aquilaria crassna. *Medicinal & Aromatic Plants,* 5**,** 2167-0412.
DAHHAM, S. S., HASSAN, L. E. A., AHAMED, M. B. K., MAJID, A. S. A., MAJID, A. M. S. A. & ZULKEPLI, N. N. 2016b. In vivo toxicity and antitumor activity of essential oils extract from agarwood (Aquilaria crassna). *BMC complementary and alternative medicine,* 16**,** 236-236.
DAHHAM, S. S., TABANA, Y. M., AHMED HASSAN, L. E., KHADEER AHAMED, M. B., ABDUL MAJID, A. S. & ABDUL MAJID, A. M. S. 2016c. In vitro antimetastatic activity of Agarwood (Aquilaria crassna) essential oils against pancreatic cancer cells. *Alexandria Journal of Medicine,* 52**,** 141-150.
DAHHAM, S. S., TABANA, Y. M., IQBAL, M. A., AHAMED, M. B., EZZAT, M. O., MAJID, A. S. & MAJID, A. M. 2015. The Anticancer, Antioxidant and Antimicrobial Properties of the Sesquiterpene beta-Caryophyllene from the Essential Oil of Aquilaria crassna. *Molecules,* 20**,** 11808-29.
DAI, J. R., HALLOCK, Y. F., CARDELLINA, J. H., 2ND & BOYD, M. R. 1998. HIV-inhibitory and cytotoxic oligostilbenes from the leaves of Hopea malibato. *J Nat Prod.* United States.
DAMUKA, N., KAMMARI, K., POTSHANGBAM, A. M., RATHORE, R. S., KONDAPI, A. K. & VINDAL, V. 2020. Discovery of dual cation-π inhibitors of acetylcholinesterase: design, synthesis and biological evaluation. *Pharmacological Reports,* 72**,** 705-718.
DANG, T. O., OGUNNIYI, A., BARBEE, M. S. & DRILON, A. 2016. Pembrolizumab for the treatment of PD-L1 positive advanced or metastatic non-small cell lung cancer. *Expert review of anticancer therapy,* 16**,** 13-20.
DANI, S. U. 2010. Arsenic for the fool: an exponential connection. *Sci Total Environ.* Netherlands.
DAR, S., CHHINA, J., MERT, I., CHITALE, D., BUEKERS, T., KAUR, H., GIRI, S., MUNKARAH, A. & RATTAN, R. 2017. Bioenergetic Adaptations in Chemoresistant Ovarian Cancer Cells. *Scientific Reports,* 7.
DE ALMEIDA CARVALHO, L. M., DE OLIVEIRA SAPORI AVELAR, S., HASLAM, A., GILL, J. & PRASAD, V. 2019. Estimation of Percentage of Patients With Fibroblast Growth Factor Receptor Alterations Eligible for Off-label Use of Erdafitinib. *JAMA network open,* 2**,** e1916091-e1916091.
DE SIMONE, R., AJMONE-CAT, M. A., CARNEVALE, D. & MINGHETTI, L. 2005. Activation of alpha7 nicotinic acetylcholine receptor by nicotine selectively up-regulates cyclooxygenase-2 and prostaglandin E2 in rat microglial cultures. *Journal of neuroinflammation,* 2**,** 4-4.

DE SÁ COUTINHO, D., PACHECO, M. T., FROZZA, R. L. & BERNARDI, A. 2018. Anti-Inflammatory Effects of Resveratrol: Mechanistic Insights. *International journal of molecular sciences,* 19**,** 1812.
DEEKS, E. 2019. Polatuzumab Vedotin: First Global Approval. *Drugs,* 79.
DEIDDA, M., PIRAS, C., BASSAREO, P. P., CADEDDU DESSALVI, C. & MERCURO, G. 2015. Metabolomics, a promising approach to translational research in cardiology. *IJC Metabolic & Endocrine,* 9**,** 31-38.
DELL'AGLI, M., FAGNANI, R., GALLI, G. V., MASCHI, O., GILARDI, F., BELLOSTA, S., CRESTANI, M., BOSISIO, E., DE FABIANI, E. & CARUSO, D. 2010. Olive Oil Phenols Modulate the Expression of Metalloproteinase 9 in THP-1 Cells by Acting on Nuclear Factor-κB Signaling. *Journal of Agricultural and Food Chemistry,* 58**,** 2246-2252.
DENG, H. & MI, M. T. 2016. Resveratrol Attenuates Abeta25-35 Caused Neurotoxicity by Inducing Autophagy Through the TyrRS-PARP1-SIRT1 Signaling Pathway. *Neurochem Res.* United States.
DENISENKO, T. V., GORBUNOVA, A. S. & ZHIVOTOVSKY, B. 2019. Mitochondrial Involvement in Migration, Invasion and Metastasis. *Frontiers in cell and developmental biology,* 7**,** 355-355.
DETTMER, K., ARONOV, P. A. & HAMMOCK, B. D. 2007. Mass spectrometry-based metabolomics. *Mass Spectrom Rev,* 26**,** 51-78.
DEVORE, E. E., STAMPFER, M. J., BRETELER, M. M. B., ROSNER, B., HEE KANG, J., OKEREKE, O., HU, F. B. & GRODSTEIN, F. 2009. Dietary Fat Intake and Cognitive Decline in Women With Type 2 Diabetes. *Diabetes Care,* 32**,** 635.
DE LA LASTRA, C. A. & VILLEGAS, I. 2007. Resveratrol as an antioxidant and pro-oxidant agent: mechanisms and clinical implications. *Biochemical Society Transactions,* 35**,** 1156-1160.
DIANTINI, A., SUBARNAS, A., LESTARI, K., HALIMAH, E., SUSILAWATI, Y., SUPRIYATNA, JULAEHA, E., ACHMAD, T., SURADJI, E., YAMAZAKI KOBAYASHI, C., KOBAYASHI, K., KOYAMA, H. & ABDULAH, R. 2012a. Kaempferol-3-O-rhamnoside isolated from the leaves of Schima wallichii Korth. Inhibits MCF-7 breast cancer cell proliferation through activation of the caspase cascade pathway. *Oncology letters,* 3**,** 1069-1072.
DIANTINI, A., SUBARNAS, A., LESTARI, K., HALIMAH, E., SUSILAWATI, Y., SUPRIYATNA, JULAEHA, E., ACHMAD, T. H., SURADJI, E. W., YAMAZAKI, C., KOBAYASHI, K., KOYAMA, H. & ABDULAH, R. 2012b. Kaempferol-3-O-rhamnoside isolated from the leaves of Schima wallichii Korth. inhibits MCF-7 breast cancer cell proliferation through activation of the caspase cascade pathway. *Oncology letters,* 3**,** 1069-1072.
DIAS, D. A., URBAN, S. & ROESSNER, U. 2012. A historical overview of natural products in drug discovery. *Metabolites,* 2**,** 303-336.
DICATO, M. A. 2013. *Side Effects of Medical Cancer Therapy [internet resource] : Prevention and Treatment*, London : Springer London.
DIETZEN, D. J. 2018. 13 - Amino Acids, Peptides, and Proteins. *In:* RIFAI, N., HORVATH, A. R. & WITTWER, C. T. (eds.) *Principles and Applications of Molecular Diagnostics.* Elsevier.
DILSHARA, M. G., KANG, C.-H., CHOI, Y. H. & KIM, G.-Y. 2015. Mangiferin inhibits tumor necrosis factor-α-induced matrix metalloproteinase-9 expression and cellular invasion by suppressing nuclear factor-κB activity. *BMB reports,* 48**,** 559-564.
DILSHARA, M. G., LEE, K. T., KIM, H. J., LEE, H. J., CHOI, Y. H., LEE, C. M., KIM, L. K. & KIM, G. Y. 2014. Anti-inflammatory mechanism of alpha-viniferin regulates lipopolysaccharide-induced release of proinflammatory mediators in BV2 microglial cells. *Cell Immunol.* Netherlands: 2014 Elsevier Inc.
DIYASENA, M. N. C., SOTHEESWARAN, S., SURENDRAKUMAR, S., BALASUBRAMANIAN, S., BOKEL, M. & KRAUS, W. 1985. Balanocarpol, a new polyphenol from Balanocarpus

zeylanicus(trimen) and Hopea jucunda(Thw.)(Dipterocarpaceae). *Journal of the Chemical Society, Perkin Transactions 1*, 1807-1809.
DOLLOFF, N. G., REYES, L., SMITH, B., LANGENHEIM, J. F. & MANEVICH, Y. 2015. Targeting Redox Overcomes Proteasome Inhibitor Resistance in Multiple Myeloma. *Blood,* 126, 1819-1819.
DRAGICEVIC, N., SMITH, A., LIN, X., YUAN, F., COPES, N., DELIC, V., TAN, J., CAO, C., SHYTLE, R. D. & BRADSHAW, P. C. 2011. Green tea epigallocatechin-3-gallate (EGCG) and other flavonoids reduce Alzheimer's amyloid-induced mitochondrial dysfunction. *J Alzheimers Dis.* Netherlands.
DU, H., GUO, L., YAN, S., SOSUNOV, A. A., MCKHANN, G. M. & YAN, S. S. 2010. Early deficits in synaptic mitochondria in an Alzheimer's disease mouse model. *Proc Natl Acad Sci U S A,* 107, 18670-5.
DU, L. & PERTSEMLIDIS, A. 2011. Cancer and neurodegenerative disorders: pathogenic convergence through microRNA regulation. *Journal of molecular cell biology,* 3, 176-180.
DUNN, N. R., PEARCE, G. L. & SHAKIR, S. A. 2000. Adverse effects associated with the use of donepezil in general practice in England. *J Psychopharmacol,* 14, 406-8.
DUONG, S., PATEL, T. & CHANG, F. 2017. Dementia: What pharmacists need to know. *Canadian pharmacists journal : CPJ = Revue des pharmaciens du Canada : RPC,* 150, 118-129.
DUPUY, F., TABARIES, S., ANDRZEJEWSKI, S., DONG, Z., BLAGIH, J., ANNIS, M. G., OMEROGLU, A., GAO, D., LEUNG, S., AMIR, E., CLEMONS, M., AGUILAR-MAHECHA, A., BASIK, M., VINCENT, E. E., ST-PIERRE, J., JONES, R. G. & SIEGEL, P. M. 2015. PDK1-Dependent Metabolic Reprogramming Dictates Metastatic Potential in Breast Cancer. *Cell Metab.* United States: 2015 Elsevier Inc.
DURAZZO, T. C., MATTSSON, N. & WEINER, M. W. 2014. Smoking and increased Alzheimer's disease risk: a review of potential mechanisms. *Alzheimers Dement,* 10, S122-45.
DYRMOSE, A.-M., TURREIRA-GARCÍA, N., THEILADE, I. & MEILBY, H. 2017. Economic importance of oleoresin (Dipterocarpus. alatus) to forest-adjacent households in Cambodia. *The Journal of the Siam Society,* 62, 67-84.
ECKERT, A., KEIL, U., SCHERPING, I., HAUPTMANN, S. & MULLER, W. E. 2005. Stabilization of mitochondrial membrane potential and improvement of neuronal energy metabolism by Ginkgo biloba extract EGb 761. *Ann N Y Acad Sci.* United States.
EDILOVA, M. I., ABDUL-SATER, A. A. & WATTS, T. H. 2018. TRAF1 Signaling in Human Health and Disease. *Frontiers in Immunology,* 9.
EGHBALIFERIZ, S. & IRANSHAHI, M. 2016. Prooxidant Activity of Polyphenols, Flavonoids, Anthocyanins and Carotenoids: Updated Review of Mechanisms and Catalyzing Metals: Prooxidant Activity of Polyphenols and Carotenoids. *Phytotherapy Research,* 30.
EGUCHI, R., ONO, N., HIRAI MORITA, A., KATSURAGI, T., NAKAMURA, S., HUANG, M., ALTAF-UL-AMIN, M. & KANAYA, S. 2019. Classification of alkaloids according to the starting substances of their biosynthetic pathways using graph convolutional neural networks. *BMC bioinformatics,* 20, 380-380.
EISSA, L. A., KENAWY, H. I., EL-KAREF, A., ELSHERBINY, N. M. & EL-MIHI, K. A. 2018. Antioxidant and anti-inflammatory activities of berberine attenuate hepatic fibrosis induced by thioacetamide injection in rats. *Chemico-Biological Interactions,* 294, 91-100.
EISSA, M., HASHIM, H. Y., EL-KERSH, D., SARIPAH, S., SALLEH, H., LOKMAN, M., ISA, M., MALIA, N. & WARIF, A. 2020. Metabolite Profiling of Aquilaria malaccensis Leaf Extract Using Liquid Chromatography-Q-TOF-Mass Spectrometry and Investigation of Its Potential Antilipoxygenase Activity In-Vitro. *Processes,* 8, 1-22.

EL-SAWI, S. A., EZZAT, S. M., ALY, H. F., MERGHANY, R. M. & MESELHY, M. R. 2019. Neuroprotective effect of Salvia splendens extract and its constituents against AlCl3-induced Alzheimer's disease in rats. *Advances in Traditional Medicine*.
ELIAS, M. F., IBRAHIM, H. & WAN MAHAMOD, W. R. 2017. A Review on the Malaysian Aquilaria species in Karas Plantation and Agarwood Production. International Journal of Academic Research in Business and Social Sciences , Human Resource Management Academic Research Society, International Journal of Academic Research in Business and Social Sciences.
ELRAYESS, R. & NAGEH, H. 2019. Anticancer Natural Products: A Review. 5**,** 14-25.
ENDALE, M., KIM, T. H., KWAK, Y. S., KIM, N. M., KIM, S. H., CHO, J. Y., YUN, B. S. & RHEE, M. H. 2017. Torilin Inhibits Inflammation by Limiting TAK1-Mediated MAP Kinase and NF-κB Activation. *Mediators Inflamm,* 2017**,** 7250968.
ENDALE, M., PARK, S. C., KIM, S., KIM, S. H., YANG, Y., CHO, J. Y. & RHEE, M. H. 2013. Quercetin disrupts tyrosine-phosphorylated phosphatidylinositol 3-kinase and myeloid differentiation factor-88 association, and inhibits MAPK/AP-1 and IKK/NF-kappaB-induced inflammatory mediators production in RAW 264.7 cells. *Immunobiology.* Netherlands: 2013 Elsevier GmbH.
ENGELKE, L. H., HAMACHER, A., PROKSCH, P. & KASSACK, M. U. 2016. Ellagic Acid and Resveratrol Prevent the Development of Cisplatin Resistance in the Epithelial Ovarian Cancer Cell Line A2780. *J Cancer,* 7**,** 353-63.
ERNST, M., NAJDOVSKA, M., GRAIL, D., LUNDGREN-MAY, T., BUCHERT, M., TYE, H., MATTHEWS, V. B., ARMES, J., BHATHAL, P. S., HUGHES, N. R., MARCUSSON, E. G., KARRAS, J. G., NA, S., SEDGWICK, J. D., HERTZOG, P. J. & JENKINS, B. J. 2008. STAT3 and STAT1 mediate IL-11-dependent and inflammation-associated gastric tumorigenesis in gp130 receptor mutant mice. *J Clin Invest,* 118**,** 1727-38.
ESKELINEN, M. H., NGANDU, T., HELKALA, E.-L., TUOMILEHTO, J., NISSINEN, A., SOININEN, H. & KIVIPELTO, M. 2008. Fat intake at midlife and cognitive impairment later in life: a population-based CAIDE study. *International Journal of Geriatric Psychiatry,* 23**,** 741-747.
ESPINOZA, J. A., BIZAMA, C., GARCÍA, P., FERRECCIO, C., JAVLE, M., MIQUEL, J. F., KOSHIOL, J. & ROA, J. C. 2016. The inflammatory inception of gallbladder cancer. *Biochimica et biophysica acta,* 1865**,** 245-254.
FAIZAL, A., ESYANTI, R. R., AULIANISA, E. N., IRIAWATI, SANTOSO, E. & TURJAMAN, M. 2017. Formation of agarwood from Aquilaria malaccensis in response to inoculation of local strains of Fusarium solani. *Trees,* 31**,** 189-197.
FAN, C., ZHENG, W., FU, X., LI, X., WONG, Y. S. & CHEN, T. 2014. Enhancement of auranofin-induced lung cancer cell apoptosis by selenocystine, a natural inhibitor of TrxR1 in vitro and in vivo. *Cell Death Dis,* 5**,** e1191.
FANG, Z., JIANG, C., FENG, Y., CHEN, R., LIN, X., ZHANG, Z., HAN, L., CHEN, X., LI, H., GUO, Y. & JIANG, W. 2016. Effects of G6PD activity inhibition on the viability, ROS generation and mechanical properties of cervical cancer cells. *Biochim Biophys Acta.* Netherlands: © 2016 Elsevier B.V.
FARAHMAND, L., DARVISHI, B. & MAJIDZADEH-A, K. 2017. Suppression of chronic inflammation with engineered nanomaterials delivering nuclear factor κB transcription factor decoy oligodeoxynucleotides. *Drug Delivery,* 24**,** 1249-1261.
FARES, J., FARES, M. Y., KHACHFE, H. H., SALHAB, H. A. & FARES, Y. 2020. Molecular principles of metastasis: a hallmark of cancer revisited. *Signal Transduction and Targeted Therapy,* 5**,** 28.
FARGE, T., SALAND, E., DE TONI, F., AROUA, N., HOSSEINI, M., PERRY, R., BOSC, C., SUGITA, M., STUANI, L., FRAISSE, M., SCOTLAND, S., LARRUE, C., BOUTZEN, H., FELIU, V., NICOLAU-TRAVERS, M. L., CASSANT-SOURDY, S., BROIN, N., DAVID, M., SERHAN, N., SARRY, A.,

TAVITIAN, S., KAOMA, T., VALLAR, L., IACOVONI, J., LINARES, L. K., MONTERSINO, C., CASTELLANO, R., GRIESSINGER, E., COLLETTE, Y., DUCHAMP, O., BARREIRA, Y., HIRSCH, P., PALAMA, T., GALES, L., DELHOMMEAU, F., GARMY-SUSINI, B. H., PORTAIS, J. C., VERGEZ, F., SELAK, M., DANET-DESNOYERS, G., CARROLL, M., RECHER, C. & SARRY, J. E. 2017. Chemotherapy-Resistant Human Acute Myeloid Leukemia Cells Are Not Enriched for Leukemic Stem Cells but Require Oxidative Metabolism. *Cancer Discov,* 7**,** 716-735.
FENG, J. & YANG, X. 2012. [Constituents from the leaves of Aquilaria sinensis]. *Zhongguo Zhong Yao Za Zhi,* 37**,** 230-4.
FERNALD, K. & KUROKAWA, M. 2013. Evading apoptosis in cancer. *Trends in cell biology,* 23**,** 620-633.
FERNANDEZ, M. A., DE LAS HERAS, B., GARCIA, M. D., SAENZ, M. T. & VILLAR, A. 2001. New insights into the mechanism of action of the anti-inflammatory triterpene lupeol. *J Pharm Pharmacol,* 53**,** 1533-9.
FERREIRA, A. K., MENEGUELO, R., PEREIRA, A., MENDONÇA FILHO, O., CHIERICE, G. O. & MARIA, D. A. 2012. Anticancer effects of synthetic phosphoethanolamine on Ehrlich ascites tumor: an experimental study. *Anticancer Res.* Greece.
FILOMENI, G., GRAZIANI, I., ROTILIO, G. & CIRIOLO, M. R. 2007. trans-Resveratrol induces apoptosis in human breast cancer cells MCF-7 by the activation of MAP kinases pathways. *Genes & nutrition,* 2**,** 295-305.
FIORELLA, S., DAVID, M., VICTOR, J. A. & ANTONIO MIRALLES AND SUSANA, E. 2017. Effects of Resveratrol and Other Polyphenols on the Most Common Brain Age-Related Diseases. *Current Medicinal Chemistry,* 24**,** 4245-4266.
FISAR, Z., HROUDOVA, J., HANSIKOVA, H., SPACILOVA, J., LELKOVA, P., WENCHICH, L., JIRAK, R., ZVEROVA, M., ZEMAN, J., MARTASEK, P. & RABOCH, J. 2016. Mitochondrial Respiration in the Platelets of Patients with Alzheimer's Disease. *Curr Alzheimer Res.* United Arab Emirates.
FISCHER, C., SPETH, V., FLEIG-EBERENZ, S. & NEUHAUS, G. 1997. Induction of Zygotic Polyembryos in Wheat: Influence of Auxin Polar Transport. *The Plant Cell,* 9**,** 1767.
FISCHER, R. & MAIER, O. 2015. Interrelation of Oxidative Stress and Inflammation in Neurodegenerative Disease: Role of TNF. *Oxidative Medicine and Cellular Longevity,* 2015**,** 610813.
FOGUER, K., BRAGA, M. D. S., PERON, J. P. S., BORTOLUCI, K. R. & BELLINI, M. H. 2016. Endostatin gene therapy inhibits intratumoral macrophage M2 polarization. *Biomedicine & Pharmacotherapy,* 79**,** 102-111.
FORKINK, M., BASIT, F., TEIXEIRA, J., SWARTS, H. G., KOOPMAN, W. J. H. & WILLEMS, P. H. G. M. 2015. Complex I and complex III inhibition specifically increase cytosolic hydrogen peroxide levels without inducing oxidative stress in HEK293 cells. *Redox biology,* 6**,** 607-616.
FORMAN, H. J., ZHANG, H. & RINNA, A. 2009. Glutathione: overview of its protective roles, measurement, and biosynthesis. *Molecular aspects of medicine,* 30**,** 1-12.
FORTIN, A., CREGAN, S. P., MACLAURIN, J. G., KUSHWAHA, N., HICKMAN, E. S., THOMPSON, C. S., HAKIM, A., ALBERT, P. R., CECCONI, F., HELIN, K., PARK, D. S. & SLACK, R. S. 2001. APAF1 is a key transcriptional target for p53 in the regulation of neuronal cell death. *J Cell Biol,* 155**,** 207-16.
FU, A. L., DONG, Z. H. & SUN, M. J. 2006. Protective effect of N-acetyl-L-cysteine on amyloid beta-peptide-induced learning and memory deficits in mice. *Brain Res.* Netherlands.
FU, Y., LIU, S., YIN, S., NIU, W., XIONG, W., TAN, M., LI, G. & ZHOU, M. 2017. The reverse Warburg effect is likely to be an Achilles' heel of cancer that can be exploited for cancer therapy. *Oncotarget,* 8.

FUKUI, M., CHOI, H. J. & ZHU, B. T. 2010. Mechanism for the protective effect of resveratrol against oxidative stress-induced neuronal death. *Free radical biology & medicine,* 49**,** 800-813.
FULDA, S. & DEBATIN, K. M. 2006. Extrinsic versus intrinsic apoptosis pathways in anticancer chemotherapy. *Oncogene,* 25**,** 4798-4811.
GABALLAH, H. H., ZAKARIA, S. S., ELBATSH, M. M. & TAHOON, N. M. 2016. Modulatory effects of resveratrol on endoplasmic reticulum stress-associated apoptosis and oxido-inflammatory markers in a rat model of rotenone-induced Parkinson's disease. *Chem Biol Interact.* Ireland: 2016 Elsevier Ireland Ltd.
GAD, S. C. 2014. Glutathione. *In:* WEXLER, P. (ed.) *Encyclopedia of Toxicology (Third Edition).* Oxford: Academic Press.
GALLUZZI, L., BLOMGREN, K. & KROEMER, G. 2009. Mitochondrial membrane permeabilization in neuronal injury. *Nature Reviews Neuroscience,* 10**,** 481-494.
GANDHI, S. & ABRAMOV, A. Y. 2012. Mechanism of oxidative stress in neurodegeneration. *Oxid Med Cell Longev,* 2012**,** 428010.
GAO, C., ZHOU, Y., LI, H., CONG, X., JIANG, Z., WANG, X., CAO, R. & TIAN, W. 2017. Antitumor effects of baicalin on ovarian cancer cells through induction of cell apoptosis and inhibition of cell migration in vitro. *Mol Med Rep,* 16**,** 8729-8734.
GAO, L.-P., CHENG, M.-L., CHOU, H.-J., YANG, Y.-H., HO, H.-Y. & TSUN-YEE CHIU, D. 2009. Ineffective GSH regeneration enhances G6PD-knockdown Hep G2 cell sensitivity to diamide-induced oxidative damage. *Free Radical Biology and Medicine,* 47**,** 529-535.
GAO, S., HU, J., WU, X. & LIANG, Z. 2018. PMA treated THP-1-derived-IL-6 promotes EMT of SW48 through STAT3/ERK-dependent activation of Wnt/β-catenin signaling pathway. *Biomedicine & Pharmacotherapy,* 108**,** 618-624.
GAO, S. P., MARK, K. G., LESLIE, K., PAO, W., MOTOI, N., GERALD, W. L., TRAVIS, W. D., BORNMANN, W., VEACH, D., CLARKSON, B. & BROMBERG, J. F. 2007. Mutations in the EGFR kinase domain mediate STAT3 activation via IL-6 production in human lung adenocarcinomas. *J Clin Invest,* 117**,** 3846-56.
GAO, X., WANG, B., WEI, X., MEN, K., ZHENG, F., ZHOU, Y., ZHENG, Y., GOU, M., HUANG, M., GUO, G., HUANG, N., QIAN, Z. & WEI, Y. 2012. Anticancer effect and mechanism of polymer micelle-encapsulated quercetin on ovarian cancer. *Nanoscale,* 4**,** 7021-30.
GAO, X., XIE, M., LIU, S., GUO, X., CHEN, X., ZHONG, Z., WANG, L. & ZHANG, W. 2014. Chromatographic fingerprint analysis of metabolites in natural and artificial agarwood using gas chromatography-mass spectrometry combined with chemometric methods. *J Chromatogr B Analyt Technol Biomed Life Sci.* Netherlands: 2014 Elsevier B.V.
GAO, Y. & HE, C. 2017. Anti-proliferative and anti-metastasis effects of ten oligostilbenes from the seeds of Paeonia suffruticosa on human cancer cells. *Oncology letters,* 13**,** 4371-4377.
GARRIDO, C., GALLUZZI, L., BRUNET, M., PUIG, P. E., DIDELOT, C. & KROEMER, G. 2006. Mechanisms of cytochrome c release from mitochondria. *Cell Death & Differentiation,* 13**,** 1423-1433.
GAUTHIER, S. & MOLINUEVO, J. 2012. Benefits of combined cholinesterase inhibitor and memantine treatment in moderate-severe Alzheimer's disease. *Alzheimer's & dementia : the journal of the Alzheimer's Association,* 9.
GAZIT, N., VERTKIN, I., SHAPIRA, I., HELM, M., SLOMOWITZ, E., SHEIBA, M., MOR, Y., RIZZOLI, S. & SLUTSKY, I. 2016. IGF-1 Receptor Differentially Regulates Spontaneous and Evoked Transmission via Mitochondria at Hippocampal Synapses. *Neuron,* 89**,** 583-97.
GE, H.-M., YANG, W.-H., ZHANG, J. & TAN, R.-X. 2009. Antioxidant Oligostilbenoids from the Stem Wood of Hopea hainanensis. *Journal of Agricultural and Food Chemistry,* 57**,** 5756-5761.

GENIN, M., CLEMENT, F., FATTACCIOLI, A., RAES, M. & MICHIELS, C. 2015. M1 and M2 macrophages derived from THP-1 cells differentially modulate the response of cancer cells to etoposide. *BMC Cancer,* 15**,** 577.
GEORGIEVA, E., IVANOVA, D., ZHELEV, Z., BAKALOVA, R., GULUBOVA, M. & AOKI, I. 2017. Mitochondrial Dysfunction and Redox Imbalance as a Diagnostic Marker of "Free Radical Diseases". *Anticancer Res.* Greece: 2017, International Institute of Anticancer Research (Dr. George J. Delinasios),.
GERAETS, L., MOONEN, H. J., BRAUERS, K., WOUTERS, E. F., BAST, A. & HAGEMAN, G. J. 2007. Dietary flavones and flavonoles are inhibitors of poly(ADP-ribose)polymerase-1 in pulmonary epithelial cells. *J Nutr.* United States.
GERMANO, G., ALLAVENA, P. & MANTOVANI, A. 2008. Cytokines as a key component of cancer-related inflammation. *Cytokine,* 43**,** 374-379.
GIACOBINI, E. 2004. Cholinesterase inhibitors: new roles and therapeutic alternatives. *Pharmacol Res.* Netherlands.
GIBSON, G. E. & SHI, Q. 2010. A mitocentric view of Alzheimer's disease suggests multi-faceted treatments. *J Alzheimers Dis,* 20 Suppl 2**,** S591-607.
GIORGIO, M., MIGLIACCIO, E., ORSINI, F., PAOLUCCI, D., MORONI, M., CONTURSI, C., PELLICCIA, G., LUZI, L., MINUCCI, S., MARCACCIO, M., PINTON, P., RIZZUTO, R., BERNARDI, P., PAOLUCCI, F. & PELICCI, P. G. 2005. Electron transfer between cytochrome c and p66Shc generates reactive oxygen species that trigger mitochondrial apoptosis. *Cell,* 122**,** 221-33.
GIRI, B. R. & ROY, B. 2015. Resveratrol- and α-viniferin-induced alterations of acetylcholinesterase and nitric oxide synthase in Raillietina echinobothrida. *Parasitol Res,* 114**,** 3775-81.
GODOY, J. A., LINDSAY, C. B., QUINTANILLA, R. A., CARVAJAL, F. J., CERPA, W. & INESTROSA, N. C. 2017. Quercetin Exerts Differential Neuroprotective Effects Against H2O2 and Abeta Aggregates in Hippocampal Neurons: the Role of Mitochondria. *Mol Neurobiol.* United States.
GOLDBERG, E. L. & DIXIT, V. D. 2015. Drivers of age-related inflammation and strategies for healthspan extension. *Immunological Reviews,* 265**,** 63-74.
GONZALEZ-SARRIAS, A., GROMEK, S., NIESEN, D., SEERAM, N. P. & HENRY, G. E. 2011. Resveratrol oligomers isolated from Carex species inhibit growth of human colon tumorigenic cells mediated by cell cycle arrest. *J Agric Food Chem,* 59**,** 8632-8.
GONÇALVES, A. C., CORTESÃO, E., OLIVEIROS, B., ALVES, V., ESPADANA, A. I., RITO, L., MAGALHÃES, E., LOBÃO, M. J., PEREIRA, A., NASCIMENTO COSTA, J. M., MOTA-VIEIRA, L. & SARMENTO-RIBEIRO, A. B. 2015. Oxidative stress and mitochondrial dysfunction play a role in myelodysplastic syndrome development, diagnosis, and prognosis: A pilot study. *Free Radic Res,* 49**,** 1081-94.
GOODWIN, C. M., ROSSANESE, O. W., OLEJNICZAK, E. T. & FESIK, S. W. 2015. Myeloid cell leukemia-1 is an important apoptotic survival factor in triple-negative breast cancer. *Cell Death Differ,* 22**,** 2098-106.
GORDZIEL, C., BRATSCH, J., MORIGGL, R., KNÖSEL, T. & FRIEDRICH, K. 2013. Both STAT1 and STAT3 are favourable prognostic determinants in colorectal carcinoma. *Br J Cancer,* 109**,** 138-46.
GORINI, S., DE ANGELIS, A., BERRINO, L., MALARA, N., ROSANO, G. & FERRARO, E. 2018. Chemotherapeutic Drugs and Mitochondrial Dysfunction: Focus on Doxorubicin, Trastuzumab, and Sunitinib. *Oxid Med Cell Longev,* 2018**,** 7582730.
GRAY, N. E., ZWEIG, J. A., CARUSO, M., ZHU, J. Y., WRIGHT, K. M., QUINN, J. F. & SOUMYANATH, A. 2018. Centella asiatica attenuates hippocampal mitochondrial dysfunction and improves memory and executive function in beta-amyloid overexpressing mice. *Mol Cell Neurosci,* 93**,** 1-9.

GREENWELL, M. & RAHMAN, P. K. S. M. 2015. Medicinal Plants: Their Use in Anticancer Treatment. *International journal of pharmaceutical sciences and research,* 6**,** 4103-4112.
GRETEN, F. R., ECKMANN, L., GRETEN, T. F., PARK, J. M., LI, Z. W., EGAN, L. J., KAGNOFF, M. F. & KARIN, M. 2004. IKKbeta links inflammation and tumorigenesis in a mouse model of colitis-associated cancer. *Cell,* 118**,** 285-96.
GRIGUER, C. E., OLIVA, C. R. & GILLESPIE, G. Y. 2005. Glucose metabolism heterogeneity in human and mouse malignant glioma cell lines. *J Neurooncol,* 74**,** 123-33.
GRIVENNIKOV, S., KARIN, E., TERZIC, J., MUCIDA, D., YU, G.-Y., VALLABHAPURAPU, S., SCHELLER, J., ROSE-JOHN, S., CHEROUTRE, H., ECKMANN, L. & KARIN, M. 2009. IL-6 and Stat3 Are Required for Survival of Intestinal Epithelial Cells and Development of Colitis-Associated Cancer. *Cancer Cell,* 15**,** 103-113.
GUENGERICH, F. P. 2001. Common and Uncommon Cytochrome P450 Reactions Related to Metabolism and Chemical Toxicity. *Chemical Research in Toxicology,* 14**,** 611-650.
GUIDA, N., LAUDATI, G., ANZILOTTI, S., SECONDO, A., MONTUORI, P., DI RENZO, G., CANZONIERO, L. M. T. & FORMISANO, L. 2015. Resveratrol via sirtuin-1 downregulates RE1-silencing transcription factor (REST) expression preventing PCB-95-induced neuronal cell death. *Toxicology and Applied Pharmacology,* 288**,** 387-398.
GUNASEKERA, S. P., KINGHORN, A. D., CORDELL, G. A. & FARNSWORTH, N. R. 1981. Plant anticancer agents. XIX Constituents of Aquilaria malaccensis. *J Nat Prod,* 44**,** 569-72.
GUPPY, M., LEEDMAN, P., ZU, X. & RUSSELL, V. 2002. Contribution by different fuels and metabolic pathways to the total ATP turnover of proliferating MCF-7 breast cancer cells. *Biochemical Journal,* 364**,** 309-315.
GUPTA, R. B., HARPAZ, N., ITZKOWITZ, S., HOSSAIN, S., MATULA, S., KORNBLUTH, A., BODIAN, C. & ULLMAN, T. 2007. Histologic inflammation is a risk factor for progression to colorectal neoplasia in ulcerative colitis: a cohort study. *Gastroenterology,* 133**,** 1099-105; quiz 1340-1.
GYAMFI, J., LEE, Y.-H., EOM, M. & CHOI, J. 2018. Interleukin-6/STAT3 signalling regulates adipocyte induced epithelial-mesenchymal transition in breast cancer cells. *Scientific Reports,* 8**,** 8859.
GYÖRFFY, B., LANCZKY, A., EKLUND, A. C., DENKERT, C., BUDCZIES, J., LI, Q. & SZALLASI, Z. 2010. An online survival analysis tool to rapidly assess the effect of 22,277 genes on breast cancer prognosis using microarray data of 1,809 patients. *Breast Cancer Research and Treatment,* 123**,** 725-731.
GÜLÇIN, İ. 2010. Antioxidant properties of resveratrol: A structure–activity insight. *Innovative Food Science & Emerging Technologies,* 11**,** 210-218.
HA, S. K., MOON, E., LEE, P., RYU, J. H., OH, M. S. & KIM, S. Y. 2012. Acacetin attenuates neuroinflammation via regulation the response to LPS stimuli in vitro and in vivo. *Neurochem Res,* 37**,** 1560-7.
HAGEMANN, T., ROBINSON, S. C., SCHULZ, M., TRÜMPER, L., BALKWILL, F. R. & BINDER, C. 2004. Enhanced invasiveness of breast cancer cell lines upon co-cultivation with macrophages is due to TNF-alpha dependent up-regulation of matrix metalloproteases. *Carcinogenesis,* 25**,** 1543-1549.
HAGEMANN, T., WILSON, J., KULBE, H., LI, N. F., LEINSTER, D. A., CHARLES, K., KLEMM, F., PUKROP, T., BINDER, C. & BALKWILL, F. R. 2005. Macrophages Induce Invasiveness of Epithelial Cancer Cells Via NF-κB and JNK. *The Journal of Immunology,* 175**,** 1197.
HAGL, S., HEINRICH, M., KOCHER, A., SCHIBORR, C., FRANK, J. & ECKERT, G. P. 2014. Curcumin Micelles Improve Mitochondrial Function in a Mouse Model of Alzheimer's Disease. *J Prev Alzheimers Dis,* 1**,** 80-83.

HAHM, E.-R., MOURA, M. B., KELLEY, E. E., VAN HOUTEN, B., SHIVA, S. & SINGH, S. V. 2011. Withaferin A-Induced Apoptosis in Human Breast Cancer Cells Is Mediated by Reactive Oxygen Species. *PLOS ONE,* 6**,** e23354.
HAKKINEN, S. H., KARENLAMPI, S. O., HEINONEN, I. M., MYKKANEN, H. M. & TORRONEN, A. R. 1999. Content of the flavonols quercetin, myricetin, and kaempferol in 25 edible berries. *J Agric Food Chem.* United States.
HALIMAH, E., DIANTINI, A., DESTIANI, D. P., PRADIPTA, I. S., SASTRAMIHARDJA, H. S., LESTARI, K., SUBARNAS, A., ABDULAH, R. & KOYAMA, H. 2015. Induction of caspase cascade pathway by kaempferol-3-O-rhamnoside in LNCaP prostate cancer cell lines. *Biomed Rep,* 3**,** 115-117.
HALLAM, S., ESCORCIO-CORREIA, M., SOPER, R., SCHULTHEISS, A. & HAGEMANN, T. 2009. Activated macrophages in the tumour microenvironment-dancing to the tune of TLR and NF-kappaB. *The Journal of pathology,* 219**,** 143-152.
HAMILTON, V. 2018. *Mabberley's Plant-Book: A Portable Dictionary of Plants, their Classification and Uses (4th edition)RR 2018/114 Mabberley's Plant-Book: A Portable Dictionary of Plants, their Classification and Uses (4th edition) David J. Mabberley Cambridge University Press Cambridge2017xix + 1102 pp. ISBN 978 1 107 11502 6 £59.99 $74.99*.
HAN, C. P., TSAO, Y. P., SUN, C. A., NG, H. T. & CHEN, S. L. 1997. Human papillomavirus, cytomegalovirus and herpes simplex virus infections for cervical cancer in Taiwan. *Cancer Lett.* Ireland.
HANDY, D. E. & LOSCALZO, J. 2012. Redox regulation of mitochondrial function. *Antioxid Redox Signal,* 16**,** 1323-67.
HANSEL, D. E., RAHMAN, A., WEHNER, S., HERZOG, V., YEO, C. J. & MAITRA, A. 2003. Increased expression and processing of the Alzheimer amyloid precursor protein in pancreatic cancer may influence cellular proliferation. *Cancer Res,* 63**,** 7032-7.
HARKINS, L., VOLK, A. L., SAMANTA, M., MIKOLAENKO, I., BRITT, W. J., BLAND, K. I. & COBBS, C. S. 2002. Specific localisation of human cytomegalovirus nucleic acids and proteins in human colorectal cancer. *Lancet.* England.
HASHIM, Y., KERR, P., ABBAS, P. & SALLEH, H. 2016. Aquilaria spp. (agarwood) as source of health beneficial compounds: A review of traditional use, phytochemistry and pharmacology. *Journal of Ethnopharmacology,* 189.
HASHIM, Y., SALLEH, H. & ABBAS, P. 2018. Uninfected agarwood branch extract possess cytotoxic and inhibitory effects on MCF-7 breast cancer cells. *Journal of Research in Pharmacy,* 23**,** 120-129.
HASHIM, Y. Z. H.-Y., PHIRDAOUS, A. & AZURA, A. 2014. Screening of anticancer activity from agarwood essential oil. *Pharmacognosy research,* 6**,** 191-194.
HAYDEN, M. S. & GHOSH, S. 2008. Shared Principles in NF-κB Signaling. *Cell,* 132**,** 344-362.
HAYDEN, M. S. & GHOSH, S. 2014. Regulation of NF-κB by TNF family cytokines. *Seminars in immunology,* 26**,** 253-266.
HE, F., LI, D., WANG, D. & DENG, M. 2016. Extraction and Purification of Quercitrin, Hyperoside, Rutin, and Afzelin from Zanthoxylum Bungeanum Maxim Leaves Using an Aqueous Two-Phase System. *J Food Sci,* 81**,** C1593-602.
HE, W., LI, X. & XIA, S. 2018. Lupeol triterpene exhibits potent antitumor effects in A427 human lung carcinoma cells via mitochondrial mediated apoptosis, ROS generation, loss of mitochondrial membrane potential and downregulation of m-TOR/PI3Ksol;AKT signalling pathway. *J BUON,* 23**,** 635-640.
HEINRICH, P. C., BEHRMANN, I., HAAN, S., HERMANNS, H. M., MÜLLER-NEWEN, G. & SCHAPER, F. 2003. Principles of interleukin (IL)-6-type cytokine signalling and its regulation. *Biochem J,* 374**,** 1-20.

HENGARTNER, M. O. 2000. The biochemistry of apoptosis. *Nature,* 407**,** 770-776.
HERRUP, K. 2015. The case for rejecting the amyloid cascade hypothesis. *Nature Neuroscience,* 18**,** 794-799.
HIPPIUS, H. & NEUNDÖRFER, G. 2003. The discovery of Alzheimer's disease. *Dialogues in clinical neuroscience,* 5**,** 101-108.
HIRPARA, J., EU, J. Q., TAN, J. K. M., WONG, A. L., CLEMENT, M. V., KONG, L. R., OHI, N., TSUNODA, T., QU, J., GOH, B. C. & PERVAIZ, S. Metabolic reprogramming of oncogene-addicted cancer cells to OXPHOS as a mechanism of drug resistance.
HO, H.-Y., CHENG, M.-L., LU, F.-J., CHOU, Y.-H., STERN, A., LIANG, C.-M. & CHIU, D. T.-Y. 2000. Enhanced oxidative stress and accelerated cellular senescence in glucose-6-phosphate dehydrogenase (G6PD)-deficient human fibroblasts. *Free Radical Biology and Medicine,* 29**,** 156-169.
HONDA, T., COPPOLA, S., GHIBELLI, L., CHO, S. H., KAGAWA, S., SPURGERS, K. B., BRISBAY, S. M., ROTH, J. A., MEYN, R. E., FANG, B. & MCDONNELL, T. J. 2004. GSH depletion enhances adenoviral bax-induced apoptosis in lung cancer cells. *Cancer Gene Therapy,* 11**,** 249-255.
HONE, E., MARTINS, I. J., JEOUNG, M., JI, T. H., GANDY, S. E. & MARTINS, R. N. 2005. Alzheimer's disease amyloid-beta peptide modulates apolipoprotein E isoform specific receptor binding. *J Alzheimers Dis,* 7**,** 303-14.
HONG, C. O., LEE, H. A., RHEE, C. H., CHOUNG, S. Y. & LEE, K. W. 2013. Separation of the antioxidant compound quercitrin from Lindera obtusiloba Blume and its antimelanogenic effect on B16F10 melanoma cells. *Biosci Biotechnol Biochem.* England.
HONG, Y.-H., UDDIN, M. H., JO, U., KIM, B., SONG, J., SUH, D. H., KIM, H. S. & SONG, Y. S. 2015. ROS Accumulation by PEITC Selectively Kills Ovarian Cancer Cells via UPR-Mediated Apoptosis. *Frontiers in oncology,* 5**,** 167-167.
HORDYJEWSKA, A., OSTAPIUK, A., HORECKA, A. & KURZEPA, J. 2019. Betulin and betulinic acid: triterpenoids derivatives with a powerful biological potential. *Phytochemistry Reviews*.
HOU, Z., FALCONE, D. J., SUBBARAMAIAH, K. & DANNENBERG, A. J. 2011. Macrophages induce COX-2 expression in breast cancer cells: role of IL-1β autoamplification. *Carcinogenesis,* 32**,** 695-702.
HSU, Y. L., KUO, P. L., LIU, C. F. & LIN, C. C. 2004. Acacetin-induced cell cycle arrest and apoptosis in human non-small cell lung cancer A549 cells. *Cancer Lett.* Ireland.
HU, J., MA, W., LI, N. & WANG, K.-J. 2017. Antioxidant and Anti-Inflammatory Flavonoids from the Flowers of Chuju, a Medical Cultivar of Chrysanthemum Morifolim Ramat. *Journal of the Mexican Chemical Society,* 61**,** 282-289.
HU, X.-T., DING, C., ZHOU, N. & XU, C. 2015a. Quercetin protects gastric epithelial cell from oxidative damage in vitro and in vivo. *European Journal of Pharmacology,* 754**,** 115-124.
HU, X. L., NIU, Y. X., ZHANG, Q., TIAN, X., GAO, L. Y., GUO, L. P., MENG, W. H. & ZHAO, Q. C. 2015b. Neuroprotective effects of Kukoamine B against hydrogen peroxide-induced apoptosis and potential mechanisms in SH-SY5Y cells. *Environ Toxicol Pharmacol,* 40**,** 230-40.
HUANG, D., YANG, S., DAI, Z., LI, W. & WANG, R. 2017a. Cytotoxicity of Kaempferol-3-O-rhamnoside against nasopharyngeal cancer via inhibition of EGFR-TK. *International Journal of Clinical and Experimental Pathology,* 10**,** 5462-5470.
HUANG, D.-S., YU, Y.-C., WU, C.-H. & LIN, J.-Y. 2017b. Protective Effects of Wogonin against Alzheimer's Disease by Inhibition of Amyloidogenic Pathway. *Evidence-Based Complementary and Alternative Medicine,* 2017**,** 3545169.
HUANG, Q., LI, F., LIU, X., LI, W., SHI, W., LIU, F.-F., O'SULLIVAN, B., HE, Z., PENG, Y., TAN, A.-C., ZHOU, L., SHEN, J., HAN, G., WANG, X.-J., THORBURN, J., THORBURN, A., JIMENO, A., RABEN, D., BEDFORD, J. S. & LI, C.-Y. 2011. Caspase 3-mediated stimulation of tumor cell repopulation during cancer radiotherapy. *Nature medicine,* 17**,** 860-866.

HUANG, W. J., ZHANG, X. & CHEN, W. W. 2016a. Role of oxidative stress in Alzheimer's disease. *Biomed Rep,* 4**,** 519-522.
HUANG, Y., CHEN, R. & ZHOU, J. 2016b. E2F1 and NF-κB: Key Mediators of Inflammation-associated Cancers and Potential Therapeutic Targets. *Curr Cancer Drug Targets.* Netherlands.
HUSSAIN, G., RASUL, A., ANWAR, H., AZIZ, N., RAZZAQ, A., WEI, W., ALI, M., LI, J. & LI, X. 2018. Role of Plant Derived Alkaloids and Their Mechanism in Neurodegenerative Disorders. *International journal of biological sciences,* 14**,** 341-357.
HUSSEIN, A., HASHIM, Y., ZAINURIN, N., SALLEH, H. & ABDULLAH, N. 2019. Anticancer potential and chemical profile of agarwood hydrosol. 15**,** 761-766.
HWANG, B., LEE, J. H. & BANG, D. 2018. Single-cell RNA sequencing technologies and bioinformatics pipelines. *Experimental & Molecular Medicine,* 50**,** 96.
HWANG, J. R., JO, K., LEE, Y., SUNG, B. J., PARK, Y. W. & LEE, J. H. 2012. Upregulation of CD9 in ovarian cancer is related to the induction of TNF-α gene expression and constitutive NF-κB activation. *Carcinogenesis.* England.
IBRAHIM, A. H., AL-RAWI, S. S., MAJID, A. M. S. A., RAHMAN, N. N. A., SALAH, K. M. A. & KADIR, M. O. A. 2011. Separation and Fractionation of Aquilaria Malaccensis Oil Using Supercritical Fluid Extraction and tThe Cytotoxic Properties of the Extracted Oil. *Procedia Food Science,* 1**,** 1953-1959.
IMRAN, M., SALEHI, B., SHARIFI-RAD, J., ASLAM GONDAL, T., SAEED, F., IMRAN, A., SHAHBAZ, M., TSOUH FOKOU, P. V., UMAIR ARSHAD, M., KHAN, H., GUERREIRO, S. G., MARTINS, N. & ESTEVINHO, L. M. 2019. Kaempferol: A Key Emphasis to Its Anticancer Potential. *Molecules (Basel, Switzerland),* 24**,** 2277.
INSUA-RODRÍGUEZ, J. & OSKARSSON, T. 2016. The extracellular matrix in breast cancer. *Adv Drug Deliv Rev.* Netherlands: © 2015 Elsevier B.V.
IQBAL, J., ABBASI, B. A., MAHMOOD, T., KANWAL, S., ALI, B., SHAH, S. A. & KHALIL, A. T. 2017. Plant-derived anticancer agents: A green anticancer approach. *Asian Pacific Journal of Tropical Biomedicine,* 7**,** 1129-1150.
ISAH, T. 2019. Stress and defense responses in plant secondary metabolites production. *Biological Research,* 52**,** 39.
ISMAIL, N., MOHAMAD ALI, N. A., JAMIL, M., FAZALUL RAHIMAN, M. H., TAJUDDIN, S. N. & TAIB, M. N. 2014. A Review Study of Agarwood Oil and Its Quality Analysis. *Jurnal Teknologi,* 68.
ITO, T., AKAO, Y., YI, H., OHGUCHI, K., MATSUMOTO, K., TANAKA, T., IINUMA, M. & NOZAWA, Y. 2003. Antitumor effect of resveratrol oligomers against human cancer cell lines and the molecular mechanism of apoptosis induced by vaticanol C. *Carcinogenesis,* 24**,** 1489-97.
IUGA, C., ALVAREZ-IDABOY, J. R. & RUSSO, N. 2012. Antioxidant Activity of trans-Resveratrol toward Hydroxyl and Hydroperoxyl Radicals: A Quantum Chemical and Computational Kinetics Study. *The Journal of Organic Chemistry,* 77**,** 3868-3877.
IZYUMOV, D. S., AVETISYAN, A. V., PLETJUSHKINA, O. Y., SAKHAROV, D. V., WIRTZ, K. W., CHERNYAK, B. V. & SKULACHEV, V. P. 2004. "Wages of fear": transient threefold decrease in intracellular ATP level imposes apoptosis. *Biochim Biophys Acta.* Netherlands.
JABŁOŃSKA-TRYPUĆ, A., MATEJCZYK, M. & ROSOCHACKI, S. 2016. Matrix metalloproteinases (MMPs), the main extracellular matrix (ECM) enzymes in collagen degradation, as a target for anticancer drugs. *Journal of Enzyme Inhibition and Medicinal Chemistry,* 31**,** 177-183.
JABŁOŃSKA-TRYPUĆ, A., WYDRO, U., WOŁEJKO, E., RODZIEWICZ, J. & BUTAREWICZ, A. 2020. Possible Protective Effects of TA on the Cancerous Effect of Mesotrione. *Nutrients,* 12.

JACKMAN, L. M. 1969. PREFACE TO THE 1st EDITION. *In:* JACKMAN, L. M. & STERNHELL, S. (eds.) *Applications of Nuclear Magnetic Resonance Spectroscopy in Organic Chemistry (Second Edition).* Pergamon.
JAHN, H. 2013. Memory loss in Alzheimer's disease. *Dialogues in clinical neuroscience,* 15**,** 445-454.
JAMIALAHMADI, K., SALARI, S., ALAMOLHODAEI, N. S., AVAN, A., GHOLAMI, L. & KARIMI, G. 2018. Auraptene Inhibits Migration and Invasion of Cervical and Ovarian Cancer Cells by Repression of Matrix Metalloproteinasas 2 and 9 Activity. *Journal of pharmacopuncture,* 21**,** 177-184.
JANG, M. H., PIAO, X. L., KIM, J. M., KWON, S. W. & PARK, J. H. 2008. Inhibition of cholinesterase and amyloid-beta aggregation by resveratrol oligomers from Vitis amurensis. *Phytother Res,* 22**,** 544-9.
JANTAN, I., BUKHARI, A. P. D. S. N. A., MOHAMED, M., LAM, D. & MESAIK, A. 2015. The Evolving Role of Natural Products From the Tropical Rainforests as a Replenishable Source of New Drug Leads.
JENA, M. K. & JANJANAM, J. 2018. Role of extracellular matrix in breast cancer development: a brief update. *F1000Research,* 7**,** 274-274.
JESS, T., LOFTUS, E. V., VELAYOS, F. S., HARMSEN, W. S., ZINSMEISTER, A. R., SMYRK, T. C., SCHLECK, C. D., TREMAINE, W. J., MELTON, L. J., MUNKHOLM, P. & SANDBORN, W. J. 2006. Risk of Intestinal Cancer in Inflammatory Bowel Disease: A Population-Based Study From Olmsted County, Minnesota. *Gastroenterology,* 130**,** 1039-1046.
JIANG, W. G., SANDERS, A. J., KATOH, M., UNGEFROREN, H., GIESELER, F., PRINCE, M., THOMPSON, S. K., ZOLLO, M., SPANO, D., DHAWAN, P., SLIVA, D., SUBBARAYAN, P. R., SARKAR, M., HONOKI, K., FUJII, H., GEORGAKILAS, A. G., AMEDEI, A., NICCOLAI, E., AMIN, A., ASHRAF, S. S., YE, L., HELFERICH, W. G., YANG, X., BOOSANI, C. S., GUHA, G., CIRIOLO, M. R., AQUILANO, K., CHEN, S., AZMI, A. S., KEITH, W. N., BILSLAND, A., BHAKTA, D., HALICKA, D., NOWSHEEN, S., PANTANO, F. & SANTINI, D. 2015. Tissue invasion and metastasis: Molecular, biological and clinical perspectives. *Seminars in Cancer Biology,* 35**,** S244-S275.
JIANG, Z., KEMPINSKI, C. & CHAPPELL, J. 2016. Extraction and Analysis of Terpenes/Terpenoids. *Current protocols in plant biology,* 1**,** 345-358.
JONES, R. A., ROBINSON, T. J., LIU, J. C., SHRESTHA, M., VOISIN, V., JU, Y., CHUNG, P. E., PELLECCHIA, G., FELL, V. L., BAE, S., MUTHUSWAMY, L., DATTI, A., EGAN, S. E., JIANG, Z., LEONE, G., BADER, G. D., SCHIMMER, A. & ZACKSENHAUS, E. 2016. RB1 deficiency in triple-negative breast cancer induces mitochondrial protein translation. *J Clin Invest,* 126**,** 3739-3757.
JORDÁN, J., CEÑA, V. & PREHN, J. H. 2003. Mitochondrial control of neuron death and its role in neurodegenerative disorders. *J Physiol Biochem,* 59**,** 129-41.
JOSE, C., BELLANCE, N. & ROSSIGNOL, R. 2011. Choosing between glycolysis and oxidative phosphorylation: a tumor's dilemma? *Biochim Biophys Acta,* 1807**,** 552-61.
JOSHI, D. C. & BAKOWSKA, J. C. 2011. Determination of mitochondrial membrane potential and reactive oxygen species in live rat cortical neurons. *J Vis Exp*.
JUNG, W. W. 2014. Protective effect of apigenin against oxidative stress-induced damage in osteoblastic cells. *Int J Mol Med,* 33**,** 1327-34.
KADIOGLU, O., NASS, J., SAEED, M. E., SCHULER, B. & EFFERTH, T. 2015. Kaempferol Is an Anti-Inflammatory Compound with Activity towards NF-kappaB Pathway Proteins. *Anticancer Res.* Greece: 2015 International Institute of Anticancer Research (Dr. John G. Delinassios),.
KADIYALA, G., KRISHNAN, A., R, K., JAYANTHI, S., VISHWANATH, B. S. & JAYARAMAN, G. 2016. Quercetin-3-O-rhamnoside from Euphorbia hirta protects against snake Venom induced toxicity. *Biochimica et Biophysica Acta (BBA) - General Subjects,* 1860.

KALB, A., VON HAEFEN, C., SIFRINGER, M., TEGETHOFF, A., PAESCHKE, N., KOSTOVA, M., FELDHEISER, A. & SPIES, C. D. 2013. Acetylcholinesterase Inhibitors Reduce Neuroinflammation and -Degeneration in the Cortex and Hippocampus of a Surgery Stress Rat Model. *PLOS ONE,* 8**,** e62679.
KALRA, R. & KAUSHIK, N. 2017. A review of chemistry, quality and analysis of infected agarwood tree (Aquilaria sp.). *Phytochemistry Reviews,* 16**,** 1045-1079.
KALYANARAMAN, B., DARLEY-USMAR, V., DAVIES, K. J. A., DENNERY, P. A., FORMAN, H. J., GRISHAM, M. B., MANN, G. E., MOORE, K., ROBERTS, L. J., 2ND & ISCHIROPOULOS, H. 2012. Measuring reactive oxygen and nitrogen species with fluorescent probes: challenges and limitations. *Free radical biology & medicine,* 52**,** 1-6.
KAMAL, M. A., GREIG, N. H., ALHOMIDA, A. S. & AL-JAFARI, A. A. 2000. Kinetics of human acetylcholinesterase inhibition by the novel experimental Alzheimer therapeutic agent, tolserine. *Biochem Pharmacol.* England.
KANG, J. H., LEE, S.-H., LEE, J.-S., NAM, B., SEONG, T. W., SON, J., JANG, H., HONG, K. M., LEE, C. & KIM, S.-Y. 2016. Aldehyde dehydrogenase inhibition combined with phenformin treatment reversed NSCLC through ATP depletion. *Oncotarget,* 7**,** 49397-49410.
KAPLANOV, I., CARMI, Y., KORNETSKY, R., SHEMESH, A., SHURIN, G. V., SHURIN, M. R., DINARELLO, C. A., VORONOV, E. & APTE, R. N. 2019. Blocking IL-1β reverses the immunosuppression in mouse breast cancer and synergizes with anti–PD-1 for tumor abrogation. *Proceedings of the National Academy of Sciences,* 116**,** 1361.
KARIN, M. & GRETEN, F. R. 2005. NF-kappaB: linking inflammation and immunity to cancer development and progression. *Nat Rev Immunol,* 5**,** 749-59.
KARLSEN, A., RETTERSTØL, L., LAAKE, P., PAUR, I., BØHN, S. K., SANDVIK, L. & BLOMHOFF, R. 2007. Anthocyanins inhibit nuclear factor-kappaB activation in monocytes and reduce plasma concentrations of pro-inflammatory mediators in healthy adults. *J Nutr,* 137**,** 1951-4.
KARLSSON, D., FALLARERO, A., BRUNHOFER, G., MAYER, C., PRAKASH, O., MOHAN, G., VUORELA, P. & ERKER, T. 2012. The exploration of thienothiazines as selective butyrylcholinesterase inhibitors. *European journal of pharmaceutical sciences : official journal of the European Federation for Pharmaceutical Sciences,* 47**,** 190-205.
KEDARE, S. B. & SINGH, R. P. 2011. Genesis and development of DPPH method of antioxidant assay. *Journal of food science and technology,* 48**,** 412-422.
KELEG, S., BÜCHLER, P., LUDWIG, R., BÜCHLER, M. W. & FRIESS, H. 2003. Invasion and metastasis in pancreatic cancer. *Molecular cancer,* 2**,** 14-14.
KENDALL, J., LIU, Q., BAKLEH, A., KRASNITZ, A., NGUYEN, K. C., LAKSHMI, B., GERALD, W. L., POWERS, S. & MU, D. 2007. Oncogenic cooperation and coamplification of developmental transcription factor genes in lung cancer. *Proc Natl Acad Sci U S A,* 104**,** 16663-8.
KENNY, H. A., KAUR, S., COUSSENS, L. M. & LENGYEL, E. 2008. The initial steps of ovarian cancer cell metastasis are mediated by MMP-2 cleavage of vitronectin and fibronectin. *J Clin Invest,* 118**,** 1367-79.
KERN, J. C. & KEHRER, J. P. 2005. Free radicals and apoptosis: relationships with glutathione, thioredoxin, and the BCL family of proteins. *Front Biosci.* United States.
KHAN, R. S., FONSECA-KELLY, Z., CALLINAN, C., ZUO, L., SACHDEVA, M. M. & SHINDLER, K. S. 2012. SIRT1 activating compounds reduce oxidative stress and prevent cell death in neuronal cells. *Front Cell Neurosci,* 6**,** 63.
KHANSARI, N., SHAKIBA, Y. & MAHMOUDI, M. 2009. Chronic inflammation and oxidative stress as a major cause of age-related diseases and cancer. *Recent Pat Inflamm Allergy Drug Discov,* 3**,** 73-80.
KIM, E. K. & CHOI, E. J. 2015. Compromised MAPK signaling in human diseases: an update. *Arch Toxicol,* 89**,** 867-82.

KIM, G. H., KIM, J. E., RHIE, S. J. & YOON, S.
KIM, G. H., KIM, J. E., RHIE, S. J. & YOON, S. 2015a. The Role of Oxidative Stress in Neurodegenerative Diseases. *Experimental neurobiology,* 24**,** 325-340.
KIM, H., PARK, C. & JUNG, J.-Y. 2013. Acacetin (5,7-dihydroxy-4'-methoxyflavone) exhibits in vitro and in vivo anticancer activity through the suppression of NF-?B/Akt signaling in prostate cancer cells. *International journal of molecular medicine,* 33.
KIM, H. P., MANI, I., IVERSEN, L. & ZIBOH, V. A. 1998. Effects of naturally-occurring flavonoids and biflavonoids on epidermal cyclooxygenase and lipoxygenase from guinea-pigs. *Prostaglandins Leukot Essent Fatty Acids,* 58**,** 17-24.
KIM, J. H., LEE, S. & CHO, E. J. 2018. Acer okamotoanum protects SH-SY5Y neuronal cells against hydrogen peroxide-induced oxidative stress. *Food science and biotechnology,* 28**,** 191-200.
KIM, S., PARK, Y. J., SHIN, M.-S., KIM, H.-R., KIM, M. J., SANG HUN, L., YUN, S. P. & KWON, S.-H. 2017. Acacetin inhibits neuronal cell death induced by 6-hydroxydopamine in cellular Parkinson's disease model. *Bioorganic & Medicinal Chemistry Letters,* 27.
KIM, S., TAKAHASHI, H., LIN, W. W., DESCARGUES, P., GRIVENNIKOV, S., KIM, Y., LUO, J. L. & KARIN, M. 2009. Carcinoma-produced factors activate myeloid cells through TLR2 to stimulate metastasis. *Nature,* 457**,** 102-6.
KIM, Y. I., PARK, S. W., YOON, Y. K., LEE, K. W., LEE, J. H., WOO, H. J. & KIM, Y. 2015b. Orostachys japonicus inhibits the expression of MMP-2 and MMP-9 mRNA and modulates the expression of iNOS and COX-2 genes in human PMA-differentiated THP-1 cells via inhibition of NF-κB and MAPK activation. *Mol Med Rep,* 12**,** 657-662.
KINGHORN, A. D., CHIN, Y. W. & SWANSON, S. M. 2009. Discovery of natural product anticancer agents from biodiverse organisms. *Curr Opin Drug Discov Devel,* 12**,** 189-96.
KIRWAN, G. M., JOHANSSON, E., KLEEMANN, R., VERHEIJ, E. R., WHEELOCK Å, M., GOTO, S., TRYGG, J. & WHEELOCK, C. E. 2012. Building multivariate systems biology models. *Anal Chem,* 84**,** 7064-71.
KLEGERIS, A. & MCGEER, P. L. 2001. Inflammatory cytokine levels are influenced by interactions between THP-1 monocytic, U-373 MG astrocytic, and SH-SY5Y neuronal cell lines of human origin. *Neuroscience Letters,* 313**,** 41-44.
KLEGERIS, A. & MCGEER, P. L. 2003. Toxicity of human monocytic THP-1 cells and microglia toward SH-SY5Y neuroblastoma cells is reduced by inhibitors of 5-lipoxygenase and its activating protein FLAP. *Journal of Leukocyte Biology,* 73**,** 369-378.
KO, K.-M. & LAM, B. 2002. Schisandrin B protects against tert-butylhydroperoxide induced cerebral toxicity by enhancing glutathione antioxidant status in mouse brain. *Molecular and cellular biochemistry,* 238**,** 181-6.
KO, S. Y., LIN, S. C., CHANG, K. W., WONG, Y. K., LIU, C. J., CHI, C. W. & LIU, T. Y. 2004. Increased expression of amyloid precursor protein in oral squamous cell carcinoma. *Int J Cancer,* 111**,** 727-32.
KOMATSU, N., NAKAGAWA, M., ODA, T. & MURAMATSU, T. 2000. Depletion of Intracellular NAD+ and ATP Levels during Ricin-Induced Apoptosis through the Specific Ribosomal Inactivation Results in the Cytolysis of U937 Cells. *Journal of biochemistry,* 128**,** 463-70.
KONDAKÇI, E., ÖZYÜREK, M., GÜÇLÜ, K. & APAK, R. 2013. Novel pro-oxidant activity assay for polyphenols, vitamins C and E using a modified CUPRAC method. *Talanta,* 115**,** 583-9.
KONG, L., ZHOU, Y., BU, H., LV, T., SHI, Y. & YANG, J. 2016. Deletion of interleukin-6 in monocytes/macrophages suppresses the initiation of hepatocellular carcinoma in mice. *J Exp Clin Cancer Res,* 35**,** 131.
KONYALIOGLU, S., ARMAGAN, G., YALCIN, A., ATALAYIN, C. & DAGCI, T. 2013. Effects of resveratrol on hydrogen peroxide-induced oxidative stress in embryonic neural stem cells. *Neural regeneration research,* 8**,** 485-495.

KORGE, P., CALMETTES, G. & WEISS, J. N. 2015. Increased reactive oxygen species production during reductive stress: The roles of mitochondrial glutathione and thioredoxin reductases. *Biochimica et biophysica acta,* 1847**,** 514-525.
KORINEK, M., WAGH, V. D., LO, I. W., HSU, Y. M., HSU, H. Y., HWANG, T. L., WU, Y. C., CHENG, Y. B., CHEN, B. H. & CHANG, F. R. 2016. Antiallergic Phorbol Ester from the Seeds of Aquilaria malaccensis. *Int J Mol Sci,* 17**,** 398.
KOWALTOWSKI, A. J., DE SOUZA-PINTO, N. C., CASTILHO, R. F. & VERCESI, A. E. 2009. Mitochondria and reactive oxygen species. *Free Radic Biol Med.* United States.
KRAUSE, K., KARGER, S., SHEU, S. Y., AIGNER, T., KURSAWE, R., GIMM, O., SCHMID, K. W., DRALLE, H. & FUHRER, D. 2008. Evidence for a role of the amyloid precursor protein in thyroid carcinogenesis. *J Endocrinol.* England.
KRIEGER JOHN, N., RILEY DONALD, E., VESELLA ROBERT, L., MINER DAVID, C., ROSS SUSAN, O. & LANGE PAUL, H. 2000. BACTERIAL DNA SEQUENCES IN PROSTATE TISSUE FROM PATIENTS WITH PROSTATE CANCER AND CHRONIC PROSTATITIS. *Journal of Urology,* 164**,** 1221-1228.
KRISHNA, M. S., JOY, B. & SUNDARESAN, A. 2015. Effect on oxidative stress, glucose uptake level and lipid droplet content by Apigenin 7, 4'-dimethyl ether isolated from Piper longum L. *Journal of food science and technology,* 52**,** 3561-3570.
KRISTANTI, A. N., TANJUNG, M. & AMINAH, N. S. 2018. Review: Secondary Metabolites of Aquilaria, a Thymelaeaceae Genus. *Mini-reviews in organic chemistry,* 15**,** 36-55.
KUMAR, P. 2019. Chapter 12 - Role of Food and Nutrition in Cancer. *In:* SINGH, R. B., WATSON, R. R. & TAKAHASHI, T. (eds.) *The Role of Functional Food Security in Global Health.* Academic Press.
KUMAR, S. & PANDEY, A. K. 2013. Chemistry and biological activities of flavonoids: an overview. *ScientificWorldJournal,* 2013**,** 162750.
KUMARI, S., BADANA, A. K., G, M. M., G, S. & MALLA, R. 2018. Reactive Oxygen Species: A Key Constituent in Cancer Survival. *Biomarker insights,* 13**,** 1177271918755391-1177271918755391.
KURMI, K., HITOSUGI, S., YU, J., BOAKYE-AGYEMAN, F., WIESE, E. K., LARSON, T. R., DAI, Q., MACHIDA, Y. J., LOU, Z., WANG, L., BOUGHEY, J. C., KAUFMANN, S. H., GOETZ, M. P., KARNITZ, L. M. & HITOSUGI, T. 2018. Tyrosine Phosphorylation of Mitochondrial Creatine Kinase 1 Enhances a Druggable Tumor Energy Shuttle Pathway. *Cell metabolism,* 28**,** 833-847.e8.
KURŠVIETIENĖ, L., STANEVIČIENĖ, I., MONGIRDIENĖ, A. & BERNATONIENĖ, J. 2016. Multiplicity of effects and health benefits of resveratrol. *Medicina,* 52**,** 148-155.
KUČERA, O., ENDLICHER, R., ROUŠAR, T., LOTKOVÁ, H., GARNOL, T., DRAHOTA, Z. & ČERVINKOVÁ, Z. 2014. The Effect of tert-Butyl Hydroperoxide-Induced Oxidative Stress on Lean and Steatotic Rat Hepatocytes In Vitro. *Oxidative Medicine and Cellular Longevity,* 2014**,** 752506.
LAFERLA, F. M., GREEN, K. N. & ODDO, S. 2007. Intracellular amyloid-beta in Alzheimer's disease. *Nat Rev Neurosci.* England.
LAHLOU, M. 2013. The Success of Natural Products in Drug Discovery. *Pharmacology & Pharmacy,* 04**,** 17-31.
LAI, C.-S., LI, S., CHAI, C.-Y., LO, C.-Y., HO, C.-T., WANG, Y.-J. & PAN, M.-H. 2007. Inhibitory effect of citrus 5-hydroxy-3,6,7,8,3',4'-hexamethoxyflavone on 12- O -tetradecanoylphorbol 13-acetate-induced skin inflammation and tumor promotion in mice. *Carcinogenesis,* 28**,** 2581-2588.
LAI, W. W., HSU, S. C., CHUEH, F. S., CHEN, Y. Y., YANG, J. S., LIN, J. P., LIEN, J. C., TSAI, C. H. & CHUNG, J. G. 2013. Quercetin inhibits migration and invasion of SAS human oral cancer

cells through inhibition of NF-κB and matrix metalloproteinase-2/-9 signaling pathways. *Anticancer Res.* Greece.
LAITINEN, M. H., NGANDU, T., ROVIO, S., HELKALA, E. L., UUSITALO, U., VIITANEN, M., NISSINEN, A., TUOMILEHTO, J., SOININEN, H. & KIVIPELTO, M. 2006. Fat intake at midlife and risk of dementia and Alzheimer's disease: a population-based study. *Dement Geriatr Cogn Disord.* Switzerland.
LAKHANI, S. A., MASUD, A., KUIDA, K., PORTER, G. A., JR., BOOTH, C. J., MEHAL, W. Z., INAYAT, I. & FLAVELL, R. A. 2006. Caspases 3 and 7: key mediators of mitochondrial events of apoptosis. *Science (New York, N.Y.),* 311**,** 847-851.
LANDSKRON, G., DE LA FUENTE, M., THUWAJIT, P., THUWAJIT, C. & HERMOSO, M. A. 2014. Chronic inflammation and cytokines in the tumor microenvironment. *Journal of immunology research,* 2014**,** 149185-149185.
LANE, R. M., POTKIN, S. G. & ENZ, A. 2006. Targeting acetylcholinesterase and butyrylcholinesterase in dementia. *Int J Neuropsychopharmacol.* England.
LANGCAKE, P. & PRYCE, R. J. 1977. A new class of phytoalexins from grapevines. *Experientia,* 33**,** 151-2.
LAPPAS, M., PERMEZEL, M. & RICE, G. E. 2003. N-Acetyl-cysteine inhibits phospholipid metabolism, proinflammatory cytokine release, protease activity, and nuclear factor-kappaB deoxyribonucleic acid-binding activity in human fetal membranes in vitro. *J Clin Endocrinol Metab,* 88**,** 1723-9.
LARSEN, K. 1998. PROSEA. Plant resources of South-East Asia 5(1–3). 1. 1993. I. Soerianegara & R. H. M. J. Lemmens (eds). Timber trees: Major commercial timbers. *Nordic Journal of Botany,* 18**,** 146-146.
LAWRENCE, T. 2009. The nuclear factor NF-kappaB pathway in inflammation. *Cold Spring Harbor perspectives in biology,* 1**,** a001651-a001651.
LEE, D. W., OBERBAUER, S. F., KRISHNAPILAY, B., MANSOR, M., MOHAMAD, H. & YAP, S. K. 1997. Effects of irradiance and spectral quality on seedling development of two Southeast Asian Hopea species. *Oecologia,* 110**,** 1-9.
LEE, H., HERRMANN, A., DENG, J.-H., KUJAWSKI, M., NIU, G., LI, Z., FORMAN, S., JOVE, R., PARDOLL, D. M. & YU, H. 2009a. Persistently Activated Stat3 Maintains Constitutive NF-κB Activity in Tumors. *Cancer Cell,* 15**,** 283-293.
LEE, I. T., LIN, C. C., WU, Y. C. & YANG, C. M. 2010a. TNF-alpha induces matrix metalloproteinase-9 expression in A549 cells: role of TNFR1/TRAF2/PKCalpha-dependent signaling pathways. *J Cell Physiol,* 224**,** 454-64.
LEE, K. M., HWANG, M. K., LEE, D. E., LEE, K. W. & LEE, H. J. 2010b. Protective effect of quercetin against arsenite-induced COX-2 expression by targeting PI3K in rat liver epithelial cells. *J Agric Food Chem,* 58**,** 5815-20.
LEE, M. K., KANG, S. J., PONCZ, M., SONG, K.-J. & PARK, K. S. 2007a. Resveratrol protects SH-SY5Y neuroblastoma cells from apoptosis induced by dopamine. *Experimental & Molecular Medicine,* 39**,** 376-384.
LEE, M. K., KANG, S. J., PONCZ, M., SONG, K. J. & PARK, K. S. 2007b. Resveratrol protects SH-SY5Y neuroblastoma cells from apoptosis induced by dopamine. *Exp Mol Med.* United States.
LEE, S. Y., SO, Y.-J., SHIN, M. S., CHO, J. Y. & LEE, J. 2014a. Antibacterial effects of afzelin isolated from Cornus macrophylla on Pseudomonas aeruginosa, a leading cause of illness in immunocompromised individuals. *Molecules (Basel, Switzerland),* 19**,** 3173-3180.
LEE, S. Y., SO, Y. J., SHIN, M. S., CHO, J. Y. & LEE, J. 2014b. Antibacterial effects of afzelin isolated from Cornus macrophylla on Pseudomonas aeruginosa, a leading cause of illness in immunocompromised individuals. *Molecules,* 19**,** 3173-80.

LEE, Y.-S., LAN TRAN, H. T. & VAN TA, Q. 2009b. Regulation of expression of matrix metalloproteinase-9 by JNK in Raw 264.7 cells: presence of inhibitory factor(s) suppressing MMP-9 induction in serum and conditioned media. *Experimental & Molecular Medicine,* 41**,** 259-268.
LEMARIE, A. & GRIMM, S. 2011. Mitochondrial respiratory chain complexes: apoptosis sensors mutated in cancer? *Oncogene.* England.
LEMARIE, A., HUC, L., PAZARENTZOS, E., MAHUL-MELLIER, A. L. & GRIMM, S. 2011. Specific disintegration of complex II succinate:ubiquinone oxidoreductase links pH changes to oxidative stress for apoptosis induction. *Cell death and differentiation,* 18**,** 338-349.
LEOPOLDINI, M., RUSSO, N. & TOSCANO, M. 2011. The molecular basis of working mechanism of natural polyphenolic antioxidants. *Food Chemistry,* 125**,** 288-306.
LETAI, A., BASSIK, M. C., WALENSKY, L. D., SORCINELLI, M. D., WEILER, S. & KORSMEYER, S. J. 2002. Distinct BH3 domains either sensitize or activate mitochondrial apoptosis, serving as prototype cancer therapeutics. *Cancer Cell.* United States.
LEUNER, K., SCHULZ, K., SCHÜTT, T., PANTEL, J., PRVULOVIC, D., RHEIN, V., SAVASKAN, E., CZECH, C., ECKERT, A. & MÜLLER, W. E. 2012. Peripheral Mitochondrial Dysfunction in Alzheimer's Disease: Focus on Lymphocytes. *Molecular Neurobiology,* 46**,** 194-204.
LEWIS, C. E. & POLLARD, J. W. 2006. Distinct role of macrophages in different tumor microenvironments. *Cancer Res,* 66**,** 605-12.
LEWIS, J. E., SINGH, N., HOLMILA, R. J., SUMER, B. D., WILLIAMS, N. S., FURDUI, C. M., KEMP, M. L. & BOOTHMAN, D. A. 2019. Targeting NAD(+) Metabolism to Enhance Radiation Therapy Responses. *Seminars in radiation oncology,* 29**,** 6-15.
LI, C., ZHANG, C., ZHOU, H., FENG, Y., TANG, F., HOI, M. P. M., HE, C., MA, D., ZHAO, C. & LEE, S. M. Y. 2018. Inhibitory Effects of Betulinic Acid on LPS-Induced Neuroinflammation Involve M2 Microglial Polarization via CaMKKbeta-Dependent AMPK Activation. *Front Mol Neurosci,* 11**,** 98.
LI, C., ZHAO, Y., YANG, D., YU, Y., GUO, H., ZHAO, Z., ZHANG, B. & YIN, X. 2015. Inhibitory effects of kaempferol on the invasion of human breast carcinoma cells by downregulating the expression and activity of matrix metalloproteinase-9. *Biochem Cell Biol,* 93**,** 16-27.
LI, F., JIANG, T., LI, Q. & LING, X. 2017. Camptothecin (CPT) and its derivatives are known to target topoisomerase I (Top1) as their mechanism of action: did we miss something in CPT analogue molecular targets for treating human disease such as cancer? *American journal of cancer research,* 7**,** 2350-2394.
LI, H., JIA, Z., LI, A., JENKINS, G., YANG, X., HU, J. & GUO, W. 2013. Resveratrol repressed viability of U251 cells by miR-21 inhibiting of NF-κB pathway. *Mol Cell Biochem,* 382**,** 137-43.
LI, J., FENG, L., XING, Y., WANG, Y., DU, L., XU, C., CAO, J., WANG, Q., FAN, S., LIU, Q. & FAN, F. 2014a. Radioprotective and antioxidant effect of resveratrol in hippocampus by activating Sirt1. *Int J Mol Sci,* 15**,** 5928-39.
LI, W., CAI, C. H., DONG, W. H., GUO, Z. K., WANG, H., MEI, W. L. & DAI, H. F. 2014b. 2-(2-phenylethyl)chromone derivatives from Chinese agarwood induced by artificial holing. *Fitoterapia.* Netherlands: 2014 Elsevier B.V.
LI, W.-Y., CHAN, S.-W., GUO, D.-J. & YU, P. 2008. Correlation Between Antioxidative Power and Anticancer Activity in Herbs from Traditional Chinese Medicine Formulae with Anticancer Therapeutic Effect. *Pharmaceutical Biology,* 45**,** 541-546.
LI, Y., YAO, J., HAN, C., YANG, J., CHAUDHRY, M. T., WANG, S., LIU, H. & YIN, Y. 2016. Quercetin, Inflammation and Immunity. *Nutrients,* 8**,** 167-167.
LI, Z., GENG, Y.-N., JIANG, J.-D. & KONG, W.-J. 2014c. Antioxidant and anti-inflammatory activities of berberine in the treatment of diabetes mellitus. *Evidence-based complementary and alternative medicine : eCAM,* 2014**,** 289264-289264.

LIANG, F., FANG, Y., CAO, W., ZHANG, Z., PAN, S. & XU, X. 2018. Attenuation of tert-Butyl Hydroperoxide (t-BHP)-Induced Oxidative Damage in HepG2 Cells by Tangeretin: Relevance of the Nrf2–ARE and MAPK Signaling Pathways. *Journal of Agricultural and Food Chemistry,* 66**,** 6317-6325.
LIAO, H., BAO, X., ZHU, J., QU, J., SUN, Y., MA, X., WANG, E., GUO, X., KANG, Q. & ZHEN, Y. 2015. O-Alkylated derivatives of quercetin induce apoptosis of MCF-7 cells via a caspase-independent mitochondrial pathway. *Chem Biol Interact.* Ireland: 2015 Elsevier Ireland Ltd.
LIBBY, P. 2007. Inflammatory mechanisms: the molecular basis of inflammation and disease. *Nutr Rev,* 65**,** S140-6.
LIEW, S. K., MALAGOBADAN, S., ARSHAD, N. M. & NAGOOR, N. H. 2020. A Review of the Structure-Activity Relationship of Natural and Synthetic Antimetastatic Compounds. *Biomolecules,* 10**,** 138.
LILIENFELD, S. 2002. Galantamine--a novel cholinergic drug with a unique dual mode of action for the treatment of patients with Alzheimer's disease. *CNS Drug Rev,* 8**,** 159-76.
LIM, J. Y., KIM, D., KIM, B. R., JUN, J. S., YEOM, J. S., PARK, J. S., SEO, J.-H., PARK, C. H., WOO, H. O., YOUN, H.-S., BAIK, S.-C., LEE, W.-K., CHO, M.-J. & RHEE, K.-H. 2016. Vitamin C induces apoptosis in AGS cells via production of ROS of mitochondria. *Oncology letters,* 12**,** 4270-4276.
LIM, K. G., GRAY, A. I., PYNE, S. & PYNE, N. J. 2012. Resveratrol dimers are novel sphingosine kinase 1 inhibitors and affect sphingosine kinase 1 expression and cancer cell growth and survival. *British journal of pharmacology,* 166**,** 1605-1616.
LIM, S., KWON, M., JOUNG, E.-J., SHIN, T., OH, C.-W., CHOI, J. S. & KIM, H.-R. 2018. Meroterpenoid-Rich Fraction of the Ethanolic Extract from Sargassum serratifolium Suppressed Oxidative Stress Induced by Tert-Butyl Hydroperoxide in HepG2 Cells. *Marine Drugs,* 16.
LIN, C.-W., CHEN, P.-N., CHEN, M.-K., YANG, W.-E., TANG, C.-H., YANG, S.-F. & HSIEH, Y.-S. 2013. Kaempferol reduces matrix metalloproteinase-2 expression by down-regulating ERK1/2 and the activator protein-1 signaling pathways in oral cancer cells. *PloS one,* 8**,** e80883-e80883.
LIN, L., YAN, L., LIU, Y., YUAN, F., LI, H. & NI, J. 2019a. Incidence and death in 29 cancer groups in 2017 and trend analysis from 1990 to 2017 from the Global Burden of Disease Study. *Journal of Hematology & Oncology,* 12**,** 96.
LIN, T.-Y., HUANG, W.-J., WU, C.-C., LU, C.-W. & WANG, S.-J. 2014. Acacetin inhibits glutamate release and prevents kainic acid-induced neurotoxicity in rats. *PloS one,* 9**,** e88644-e88644.
LIN, Y., XU, J. & LAN, H. 2019b. Tumor-associated macrophages in tumor metastasis: biological roles and clinical therapeutic applications. *Journal of Hematology & Oncology,* 12**,** 76.
LINS, A. P., RIBEIRO, M. N. D. S., GOTTLIEB, O. R. & GOTTLIEB, H. E. 1982. Gnetins: Resveratrol Oligomers From Gnetum Species. *Journal of Natural Products,* 45**,** 754-761.
LIOU, C.-J., WU, S.-J., CHEN, L.-C., YEH, K.-W., CHEN, C.-Y. & HUANG, W.-C. 2017. Acacetin from Traditionally Used Saussurea involucrata Kar. et Kir. Suppressed Adipogenesis in 3T3-L1 Adipocytes and Attenuated Lipid Accumulation in Obese Mice. *Frontiers in Pharmacology,* 8.
LITTLE, J., SIMTCHOUK, S., SCHINDLER, S., VILLANUEVA, E., GILL, N., WALKER, D., WOLTHERS, K. & KLEGERIS, A. 2015. Mitochondrial transcription.
LIU, C., PERNG, M. & CHEN, C. 2018a. The antioxidation and antiproliferation activity of flavonoids from Aquilaria agallocha and Aquilaria sinensis. *Biomedical Research,* 29.
LIU, C. W., SUNG, H. C., LIN, S. R., WU, C. W., LEE, C. W., LEE, I. T., YANG, Y. F., YU, I. S., LIN, S. W., CHIANG, M. H., LIANG, C. J. & CHEN, Y. L. 2017a. Resveratrol attenuates ICAM-1

expression and monocyte adhesiveness to TNF-α-treated endothelial cells: evidence for an anti-inflammatory cascade mediated by the miR-221/222/AMPK/p38/NF-κB pathway. *Sci Rep,* 7**,** 44689.
LIU, L.-Z., JING, Y., JIANG, L. L., JIANG, X.-E., JIANG, Y., ROJANASAKUL, Y. & JIANG, B.-H. 2011. Acacetin inhibits VEGF expression, tumor angiogenesis and growth through AKT/HIF-1α pathway. *Biochemical and biophysical research communications,* 413**,** 299-305.
LIU, T., ZHANG, L., JOO, D. & SUN, S.-C. 2017b. NF-κB signaling in inflammation. *Signal transduction and targeted therapy,* 2**,** 17023.
LIU, W., LU, X., SHI, P., YANG, G., ZHOU, Z., LI, W., MAO, X., JIANG, D. & CHEN, C. 2020. TNF-α increases breast cancer stem-like cells through up-regulating TAZ expression via the non-canonical NF-κB pathway. *Scientific Reports,* 10**,** 1804.
LIU, Y., TONG, L., LUO, Y., LI, X., CHEN, G. & WANG, Y. 2018b. Resveratrol inhibits the proliferation and induces the apoptosis in ovarian cancer cells via inhibiting glycolysis and targeting AMPK/mTOR signaling pathway. *Journal of Cellular Biochemistry,* 119**,** 6162-6172.
LOEF, M. & WALACH, H. 2012. Copper and iron in Alzheimer's disease: a systematic review and its dietary implications. *Br J Nutr.* England.
LOO, J. M., SCHERL, A., NGUYEN, A., MAN, F. Y., WEINBERG, E., ZENG, Z., SALTZ, L., PATY, P. B. & TAVAZOIE, S. F. 2015. Extracellular metabolic energetics can promote cancer progression. *Cell,* 160**,** 393-406.
LOPEZ-LAZARO, M. 2015. How many times should we screen a chemical library to discover an anticancer drug? *Drug Discov Today.* England.
LORENZO, J. M., MOUSAVI KHANEGHAH, A., GAVAHIAN, M., MARSZALEK, K., ES, I., MUNEKATA, P. E. S., FERREIRA, I. & BARBA, F. J. 2019. Understanding the potential benefits of thyme and its derived products for food industry and consumer health: From extraction of value-added compounds to the evaluation of bioaccessibility, bioavailability, anti-inflammatory, and antimicrobial activities. *Crit Rev Food Sci Nutr,* 59**,** 2879-2895.
LOSANO, J. D. A., PADÍN, J. F., MÉNDEZ-LÓPEZ, I., ANGRIMANI, D. S. R., GARCÍA, A. G., BARNABE, V. H. & NICHI, M. 2017. The Stimulated Glycolytic Pathway Is Able to Maintain ATP Levels and Kinetic Patterns of Bovine Epididymal Sperm Subjected to Mitochondrial Uncoupling. *Oxidative medicine and cellular longevity,* 2017**,** 1682393-1682393.
LOTIA, S., MONTOJO, J., DONG, Y., BADER, G. & PICO, A. 2013. Cytoscape App Store. *Bioinformatics (Oxford, England),* 29.
LOU, Y.-H., WANG, J.-S., DONG, G., GUO, P.-P., WEI, D.-D., XIE, S.-S., YANG, M.-H. & KONG, L.-Y. 2015. The acute hepatotoxicity of tacrine explained by 1H NMR based metabolomic profiling. *Toxicology Research,* 4**,** 1465-1478.
LU, C.-C., KUO, H.-C., WANG, F.-S., JOU, M.-H., LEE, K.-C. & CHUANG, J.-H. 2015a. Upregulation of TLRs and IL-6 as a Marker in Human Colorectal Cancer. *International Journal of Molecular Sciences,* 16.
LU, D., XU, A., MAI, H., ZHAO, J., ZHANG, C., QI, R., WANG, H., LU, D. & ZHU, L. 2015b. The Synergistic Effects of Heat Shock Protein 70 and Ginsenoside Rg1 against Tert-Butyl Hydroperoxide Damage Model In Vitro. *Oxidative Medicine and Cellular Longevity,* 2015**,** 437127.
LU, J., WANG, Z., LI, S., XIN, Q., YUAN, M., LI, H., SONG, X., GAO, H., PERVAIZ, N., SUN, X., LV, W., JING, T. & ZHU, Y. 2018. Quercetin Inhibits the Migration and Invasion of HCCLM3 Cells by Suppressing the Expression of p-Akt1, Matrix Metalloproteinase (MMP) MMP-2, and MMP-9. *Medical science monitor : international medical journal of experimental and clinical research,* 24**,** 2583-2589.
LU, L., SHI, W., DESHMUKH, R. R., LONG, J., CHENG, X., JI, W., ZENG, G., CHEN, X., ZHANG, Y. & DOU, Q. P. 2014. Tumor necrosis factor-α sensitizes breast cancer cells to natural products with proteasome-inhibitory activity leading to apoptosis. *PLoS One,* 9**,** e113783.

LU, Y.-C., YEH, W.-C. & OHASHI, P. S. 2008. LPS/TLR4 signal transduction pathway. *Cytokine,* 42**,** 145-151.
LUCANTONI, F., DUSSMANN, H. & PREHN, J. H. M. 2018. Metabolic Targeting of Breast Cancer Cells With the 2-Deoxy-D-Glucose and the Mitochondrial Bioenergetics Inhibitor MDIVI-1. *Frontiers in Cell and Developmental Biology,* 6.
LUCHSINGER, J. A., TANG, M. X., SHEA, S. & MAYEUX, R. 2002. Caloric intake and the risk of Alzheimer disease. *Arch Neurol.* United States.
LUEDDE, T., BERAZA, N., KOTSIKORIS, V., VAN LOO, G., NENCI, A., DE VOS, R., ROSKAMS, T., TRAUTWEIN, C. & PASPARAKIS, M. 2007. Deletion of NEMO/IKKgamma in liver parenchymal cells causes steatohepatitis and hepatocellular carcinoma. *Cancer Cell,* 11**,** 119-32.
LUO, H., JIANG, B. H., KING, S. M. & CHEN, Y. C. 2008. Inhibition of cell growth and VEGF expression in ovarian cancer cells by flavonoids. *Nutr Cancer.* United States.
LUO, W. & BROUWER, C. 2013. Pathview: an R/Bioconductor package for pathway-based data integration and visualization. *Bioinformatics,* 29**,** 1830-1831.
LUSHCHAK, V. 2012. Glutathione Homeostasis and Functions: Potential Targets for Medical Interventions. *Journal of amino acids,* 2012**,** 736837.
LÓPEZ-LÁZARO, M. 2015. Two preclinical tests to evaluate anticancer activity and to help validate drug candidates for clinical trials. *Oncoscience,* 2**,** 91-98.
MA, B., YANG, Y., LI, Z., ZHAO, D., ZHANG, W., JIANG, Y. & XUE, D. 2018. Modular bioinformatics analysis demonstrates that a Toll-like receptor signaling pathway is involved in the regulation of macrophage polarization. *Molecular medicine reports,* 18**,** 4313-4320.
MA, C., WANG, Y., DONG, L., LI, M. & CAI, W. 2015. Anti-inflammatory effect of resveratrol through the suppression of NF-κB and JAK/STAT signaling pathways. *Acta Biochimica et Biophysica Sinica,* 47**,** 207-213.
MAEDA, S., KAMATA, H., LUO, J. L., LEFFERT, H. & KARIN, M. 2005. IKKbeta couples hepatocyte death to cytokine-driven compensatory proliferation that promotes chemical hepatocarcinogenesis. *Cell,* 121**,** 977-90.
MAGDA, D. & MILLER, R. A. 2006. Motexafin gadolinium: a novel redox active drug for cancer therapy. *Semin Cancer Biol.* England.
MAJUMDER, M., DEBNATH, S., GAJBHIYE, R. L., SAIKIA, R., GOGOI, B., SAMANTA, S. K., DAS, D. K., BISWAS, K., JAISANKAR, P. & MUKHOPADHYAY, R. 2019. Ricinus communis L. fruit extract inhibits migration/invasion, induces apoptosis in breast cancer cells and arrests tumor progression in vivo. *Scientific Reports,* 9**,** 14493.
MALINS, D. C. 1965. Thin-layer chromatography: A laboratory handbook (Stahl, Egon). *Journal of Chemical Education,* 42**,** 692.
MALLA, J. A., UMESH, R. M., YOUSF, S., MANE, S., SHARMA, S., LAHIRI, M. & TALUKDAR, P. 2020. A Glutathione Activatable Ion Channel Induces Apoptosis in Cancer Cells by Depleting Intracellular Glutathione Levels. *Angewandte Chemie International Edition,* 59**,** 7944-7952.
MANDEL, S., AMIT, T., REZNICHENKO, L., WEINREB, O. & YOUDIM, M. B. 2006. Green tea catechins as brain-permeable, natural iron chelators-antioxidants for the treatment of neurodegenerative disorders. *Mol Nutr Food Res,* 50**,** 229-34.
MANGOYI, R., MIDIWO, J. & MUKANGANYAMA, S. 2015. Isolation and characterization of an antifungal compound 5-hydroxy-7,4'-dimethoxyflavone from Combretum zeyheri. *BMC Complementary and Alternative Medicine,* 15**,** 405.
MANI, S., SEKAR, S., BARATHIDASAN, R., MANIVASAGAM, T., THENMOZHI, A. J., SEVANAN, M., CHIDAMBARAM, S. B., ESSA, M. M., GUILLEMIN, G. J. & SAKHARKAR, M. K. 2018. Naringenin Decreases α-Synuclein Expression and Neuroinflammation in MPTP-Induced Parkinson's Disease Model in Mice. *Neurotoxicity Research,* 33**,** 656-670.
MANJEET, K. R. & GHOSH, B. 1999. Quercetin inhibits LPS-induced nitric oxide and tumor necrosis factor-alpha production in murine macrophages. *Int J Immunopharmacol.* England.

MANN, J. F., GOERIG, M., BRUNE, K. & LUFT, F. C. 1993. Ibuprofen as an over-the-counter drug: is there a risk for renal injury? *Clinical nephrology,* 39**,** 1-6.
MANOOCHEHRI, M., KARBASI, A., BANDEHPOUR, M. & KAZEMI, B. 2014. Down-regulation of BAX gene during carcinogenesis and acquisition of resistance to 5-FU in colorectal cancer. *Pathol Oncol Res,* 20**,** 301-7.
MANOUCHEHRI, J. M., KALAFATIS, M. & LINDNER, D. 2016. Abstract 1295: Evaluation of the efficacy of TRAIL plus quercetin as a potential breast carcinoma therapeutic. *Cancer Research,* 76**,** 1295.
MANSANO-SCHLOSSER, T. C. & CEOLIM, M. F. 2012. Qualidade de vida de pacientes com câncer no período de quimioterapia. *Texto & Contexto - Enfermagem,* 21**,** 600-607.
MANTOVANI, A. 2010. Molecular pathways linking inflammation and cancer. *Curr Mol Med.* Netherlands.
MANTOVANI, A., BISWAS, S. K., GALDIERO, M. R., SICA, A. & LOCATI, M. 2013. Macrophage plasticity and polarization in tissue repair and remodelling. *J Pathol,* 229**,** 176-85.
MARBANIANG, C. & KMA, L. 2018. Dysregulation of Glucose Metabolism by Oncogenes and Tumor Suppressors in Cancer Cells. *Asian Pacific journal of cancer prevention : APJCP,* 19**,** 2377-2390.
MARKOVIĆ, Z. 2016. Study of the mechanisms of antioxidative action of different antioxidants. *Journal of Serbian Society for Computational Mechanics,* 10**,** 135-150.
MARSTON, A. 2011. Thin-layer chromatography with biological detection in phytochemistry. *J Chromatogr A.* Netherlands: 2010 Elsevier B.V.
MARTIN, D. S., BERTINO, J. R. & KOUTCHER, J. A. 2000. ATP Depletion + Pyrimidine Depletion Can Markedly Enhance Cancer Therapy: Fresh Insight for a New Approach. *Cancer Research,* 60**,** 6776.
MARTIN, T., YE, L., AJ, S., LANE, J. & JIANG, W. 2013. Cancer Invasion andMetastasis: Molecular and Cellular perspective.
MARTÍNEZ, M.-A., RODRÍGUEZ, J.-L., LOPEZ-TORRES, B., MARTÍNEZ, M., MARTÍNEZ-LARRAÑAGA, M.-R., MAXIMILIANO, J.-E., ANADÓN, A. & ARES, I. 2020. Use of human neuroblastoma SH-SY5Y cells to evaluate glyphosate-induced effects on oxidative stress, neuronal development and cell death signaling pathways. *Environment International,* 135**,** 105414.
MARZANO, C., GANDIN, V., FOLDA, A., SCUTARI, G., BINDOLI, A. & RIGOBELLO, M. P. 2007. Inhibition of thioredoxin reductase by auranofin induces apoptosis in cisplatin-resistant human ovarian cancer cells. *Free Radical Biology and Medicine,* 42**,** 872-881.
MASJEDI, A., HASHEMI, V., HOJJAT-FARSANGI, M., GHALAMFARSA, G., AZIZI, G., YOUSEFI, M. & JADIDI-NIARAGH, F. 2018. The significant role of interleukin-6 and its signaling pathway in the immunopathogenesis and treatment of breast cancer. *Biomedicine & Pharmacotherapy,* 108**,** 1415-1424.
MASSI, A., BORTOLINI, O., RAGNO, D., BERNARDI, T., SACCHETTI, G., TACCHINI, M. & DE RISI, C. 2017. Research Progress in the Modification of Quercetin Leading to Anticancer Agents. *Molecules (Basel, Switzerland),* 22**,** 1270.
MAT, N. A. A. R. S. A. N. N. A. K. M. A. A. R. N. A. R. K. 2012. Growth and Mineral Nutrition of Aquilaria Malaccensis (Karas) In Two Habitats As Affected By Different Cultural Practices. 9**,** 6-16.
MATTSON, M. P. 2000. Apoptosis in neurodegenerative disorders. *Nat Rev Mol Cell Biol,* 1**,** 120-9.
MAURER, I., ZIERZ, S. & MÖLLER, H. J. 2000. A selective defect of cytochrome c oxidase is present in brain of Alzheimer disease patients. *Neurobiology of Aging,* 21**,** 455-462.
MCALPINE, F. E., LEE, J.-K., HARMS, A. S., RUHN, K. A., BLURTON-JONES, M., HONG, J., DAS, P., GOLDE, T. E., LAFERLA, F. M., ODDO, S., BLESCH, A. & TANSEY, M. G. 2009. Inhibition of

soluble TNF signaling in a mouse model of Alzheimer's disease prevents pre-plaque amyloid-associated neuropathology. *Neurobiology of disease,* 34**,** 163-177.
MCFARLAND, B. C., HONG, S. W., RAJBHANDARI, R., TWITTY, G. B., JR., GRAY, G. K., YU, H., BENVENISTE, E. N. & NOZELL, S. E. 2013. NF-κB-Induced IL-6 Ensures STAT3 Activation and Tumor Aggressiveness in Glioblastoma. *PLOS ONE,* 8**,** e78728.
MECOCCI, P. & POLIDORI, M. C. 2012. Antioxidant clinical trials in mild cognitive impairment and Alzheimer's disease. *Biochim Biophys Acta.* Netherlands: Â© 2011 Elsevier B.V.
MELE, L., PAINO, F., PAPACCIO, F., REGAD, T., BOOCOCK, D., STIUSO, P., LOMBARDI, A., LICCARDO, D., AQUINO, G., BARBIERI, A., ARRA, C., COVENEY, C., LA NOCE, M., PAPACCIO, G., CARAGLIA, M., TIRINO, V. & DESIDERIO, V. 2018. A new inhibitor of glucose-6-phosphate dehydrogenase blocks pentose phosphate pathway and suppresses malignant proliferation and metastasis in vivo. *Cell Death & Disease,* 9**,** 572.
MENG, Y., CHEN, C.-W., YUNG, M. M. H., SUN, W., SUN, J., LI, Z., LI, J., LI, Z., ZHOU, W., LIU, S. S., CHEUNG, A. N. Y., NGAN, H. Y. S., BRAISTED, J. C., KAI, Y., PENG, W., TZATSOS, A., LI, Y., DAI, Z., ZHENG, W., CHAN, D. W. & ZHU, W. 2018. DUOXA1-mediated ROS production promotes cisplatin resistance by activating ATR-Chk1 pathway in ovarian cancer. *Cancer Letters,* 428**,** 104-116.
MIAO, Y., HE, N. & ZHU, J.-J. 2010. History and New Developments of Assays for Cholinesterase Activity and Inhibition. *Chemical Reviews,* 110**,** 5216-5234.
MILLS, C. D., LENZ, L. L. & HARRIS, R. A. 2016. A Breakthrough: Macrophage-Directed Cancer Immunotherapy. *Cancer Res,* 76**,** 513-6.
MINIOTI, K. S. & GEORGIOU, C. A. 2010. Comparison of different tests used in mapping the Greek virgin olive oil production for the determination of its total antioxidant capacity. *Grasas y Aceites,* 61**,** 45-51.
MIRAN, T., VOGG, A. T. J., DRUDE, N., MOTTAGHY, F. M. & MORGENROTH, A. 2018. Modulation of glutathione promotes apoptosis in triple-negative breast cancer cells. *The FASEB Journal,* 32**,** 2803-2813.
MIRZAPUR, P., KHAZAEI, M. R., MORADI, M. T. & KHAZAEI, M. 2018. Apoptosis induction in human breast cancer cell lines by synergic effect of raloxifene and resveratrol through increasing proapoptotic genes. *Life Sciences,* 205**,** 45-53.
MISHRA, B. B. & TIWARI, V. K. 2011. Natural products: an evolving role in future drug discovery. *Eur J Med Chem,* 46**,** 4769-807.
MISSIROLI, S., GENOVESE, I., PERRONE, M., VEZZANI, B., VITTO, V. A. M. & GIORGI, C. 2020. The Role of Mitochondria in Inflammation: From Cancer to Neurodegenerative Disorders. *Journal of clinical medicine,* 9**,** 740.
MITRA, A. K., SAWADA, K., TIWARI, P., MUI, K., GWIN, K. & LENGYEL, E. 2011. Ligand-independent activation of c-Met by fibronectin and α(5)β(1)-integrin regulates ovarian cancer invasion and metastasis. *Oncogene,* 30**,** 1566-76.
MODUGNO, F., NESS, R. B., CHEN, C. & WEISS, N. S. 2005. Inflammation and endometrial cancer: a hypothesis. *Cancer Epidemiol Biomarkers Prev.* United States.
MOHAMAD ALI, N. A., SAID, A., JALIL, M., SAIDATUL, J. & YASMIN, N. 2008. Comparison of chemical profile of selected gaharu oils from Peninsular Malaysia. *Malays J Anal Sci,* 12.
MONTINARI, M. R., MINELLI, S. & CATERINA, R. 2018. The first 3500 years of aspirin history from its roots – A concise summary. *Vascular Pharmacology*.
MORI, T., MIYAMOTO, T., YOSHIDA, H., ASAKAWA, M., KAWASUMI, M., KOBAYASHI, T., MORIOKA, H., CHIBA, K., TOYAMA, Y. & YOSHIMURA, A. 2011. IL-1β and TNFα-initiated IL-6-STAT3 pathway is critical in mediating inflammatory cytokines and RANKL expression in inflammatory arthritis. *Int Immunol,* 23**,** 701-12.
MORIYAMA, H., MORIYAMA, M., NINOMIYA, K., MORIKAWA, T. & HAYAKAWA, T. 2016. Inhibitory Effects of Oligostilbenoids from the Bark of Shorea roxburghii on Malignant

Melanoma Cell Growth: Implications for Novel Topical Anticancer Candidates. *Biol Pharm Bull,* 39**,** 1675-1682.
MORRIS, G. & BERK, M. 2016. The Putative Use of Lithium in Alzheimer's Disease. *Curr Alzheimer Res.* United Arab Emirates.
MORRIS, L. G., VEERIAH, S. & CHAN, T. A. 2010. Genetic determinants at the interface of cancer and neurodegenerative disease. *Oncogene,* 29**,** 3453-64.
MOUDI, M., GO, R., YIEN, C. Y. S. & NAZRE, M. 2013. Vinca alkaloids. *International journal of preventive medicine,* 4**,** 1231-1235.
MUHTADI, HAKIM, E. H., JULIAWATY, L. D., SYAH, Y. M., ACHMAD, S. A., LATIP, J. & GHISALBERTI, E. L. 2006. Cytotoxic resveratrol oligomers from the tree bark of Dipterocarpus hasseltii. *Fitoterapia,* 77**,** 550-555.
MUKHERJEE, A. K., SAVIOLA, A. J., BURNS, P. D. & MACKESSY, S. P. 2015. Apoptosis induction in human breast cancer (MCF-7) cells by a novel venom l-amino acid oxidase (Rusvinoxidase) is independent of its enzymatic activity and is accompanied by caspase-7 activation and reactive oxygen species production. *Apoptosis,* 20**,** 1358-1372.
MUKHERJEE, S., DUDLEY, J. & DAS, D. 2010. Dose-Dependency of Resveratrol in Providing Health Benefits. *Dose-response : a publication of International Hormesis Society,* 8**,** 478-500.
MURIAS, M., MIKSITS, M., AUST, S., SPATZENEGGER, M., THALHAMMER, T., SZEKERES, T. & JAEGER, W. 2008. Metabolism of resveratrol in breast cancer cell lines: Impact of sulfotransferase 1A1 expression on cell growth inhibition. *Cancer Letters,* 261**,** 172-182.
MURPHY, M. P. 2009. How mitochondria produce reactive oxygen species. *Biochem J,* 417**,** 1-13.
NAEF, R. 2011. The volatile and semi-volatile constituents of agarwood, the infected heartwood of Aquilaria species: a review. *Flavour and Fragrance Journal,* 26**,** 73-87.
NEAG, M. A., MOCAN, A., ECHEVERRÍA, J., POP, R. M., BOCSAN, C. I., CRIŞAN, G. & BUZOIANU, A. D. 2018. Berberine: Botanical Occurrence, Traditional Uses, Extraction Methods, and Relevance in Cardiovascular, Metabolic, Hepatic, and Renal Disorders. *Frontiers in pharmacology,* 9**,** 557-557.
NGUYEN, L. T., LEE, Y.-H., SHARMA, A. R., PARK, J.-B., JAGGA, S., SHARMA, G., LEE, S.-S. & NAM, J.-S. 2017a. Quercetin induces apoptosis and cell cycle arrest in triple-negative breast cancer cells through modulation of Foxo3a activity. *The Korean journal of physiology & pharmacology : official journal of the Korean Physiological Society and the Korean Society of Pharmacology,* 21**,** 205-213.
NGUYEN, S. T., HUYNH, K. L., NGUYEN, H. L., NGUYEN THI THANH, M., NGUYEN TRUNG, N., NGUYEN XUAN, H., NGOC, K. P., TRUONG DINH, K. & PHAM, P. V. 2017b. Hopea odorata extract inhibits hepatocellular carcinoma via induction of caspase-dependent apoptosis. *Onco Targets Ther,* 10**,** 5765-5774.
NIKOLIC, V. D., SAVIC, I. M., SAVIC, I. M., NIKOLIC, L. B., STANKOVIC, M. Z. & MARINKOVIC, V. D. 2011. Paclitaxel as an anticancer agent: isolation, activity, synthesis and stability. *Central European Journal of Medicine,* 6**,** 527.
NING, C., LI, Y. Y., WANG, Y., HAN, G. C., WANG, R. X., XIAO, H., LI, X. Y., HOU, C. M., MA, Y. F., SHENG, D. S., SHEN, B. F., FENG, J. N., GUO, R. F., LI, Y. & CHEN, G. J. 2015. Complement activation promotes colitis-associated carcinogenesis through activating intestinal IL-1β/IL-17A axis. *Mucosal Immunol,* 8**,** 1275-84.
NIZARI, S., CARARE, R. O. & HAWKES, C. A. 2016. Increased Aβ pathology in aged Tg2576 mice born to mothers fed a high fat diet. *Scientific Reports,* 6**,** 21981.
NOWAK, J. Z. 2013. Oxidative stress, polyunsaturated fatty acids-derived oxidation products and bisretinoids as potential inducers of CNS diseases: focus on age-related macular degeneration. *Pharmacol Rep.* Switzerland.

NOY, R. & POLLARD, JEFFREY W. 2014. Tumor-Associated Macrophages: From Mechanisms to Therapy. *Immunity,* 41**,** 49-61.
NUGROHO, A., PARK, J.-H., CHOI, J. S., PARK, K.-S., HONG, J.-P. & PARK, H.-J. 2019. Structure determination and quantification of a new flavone glycoside with anti-acetylcholinesterase activity from the herbs of Elsholtzia ciliata. *Natural Product Research,* 33**,** 814-821.
O'MAHONY, F., RAZANDI, M., PEDRAM, A., HARVEY, B. J. & LEVIN, E. R. 2012. Estrogen modulates metabolic pathway adaptation to available glucose in breast cancer cells. *Molecular endocrinology (Baltimore, Md.),* 26**,** 2058-2070.
O'SULLIVAN, K. E., PHELAN, J. J., O'HANLON, C., LYSAGHT, J., O'SULLIVAN, J. N. & REYNOLDS, J. V. 2014. The role of inflammation in cancer of the esophagus. *Expert Rev Gastroenterol Hepatol,* 8**,** 749-60.
OBUOBI, S., KARATAYEV, S., CHAI, C. L. L., EE, P. L. R. & MÁTYUS, P. 2016. The role of modulation of antioxidant enzyme systems in the treatment of neurodegenerative diseases. *Journal of Enzyme Inhibition and Medicinal Chemistry,* 31**,** 194-204.
ODA, E., OHKI, R., MURASAWA, H., NEMOTO, J., SHIBUE, T., YAMASHITA, T., TOKINO, T., TANIGUCHI, T. & TANAKA, N. 2000. Noxa, a BH3-only member of the Bcl-2 family and candidate mediator of p53-induced apoptosis. *Science.* United States.
OHYAMA, M., TANAKA, T., ITO, T., IINUMA, M., BASTOW, K. F. & LEE, K. H. 1999. Antitumor agents 200. Cytotoxicity of naturally occurring resveratrol oligomers and their acetate derivatives. *Bioorg Med Chem Lett.* England.
OIKAWA, S., YAMADA, K., YAMASHITA, N., TADA-OIKAWA, S. & KAWANISHI, S. 1999. N-acetylcysteine, a cancer chemopreventive agent, causes oxidative damage to cellular and isolated DNA. *Carcinogenesis,* 20**,** 1485-90.
OKEREKE, O. I., ROSNER, B. A., KIM, D. H., KANG, J. H., COOK, N. R., MANSON, J. E., BURING, J. E., WILLETT, W. C. & GRODSTEIN, F. 2012. Dietary fat types and 4-year cognitive change in community-dwelling older women. *Ann Neurol,* 72**,** 124-34.
OLDFIELD, S., LUSTY, C. & MACKINVEN, A. 1998. The Word List of Threatened Trees. . World Conservation Press, Cambridge.
ONNIS, B., RAPISARDA, A. & MELILLO, G. 2009. Development of HIF-1 inhibitors for cancer therapy. *Journal of cellular and molecular medicine,* 13**,** 2780-2786.
ORR, A. L., ASHOK, D., SARANTOS, M. R., SHI, T., HUGHES, R. E. & BRAND, M. D. 2013. Inhibitors of ROS production by the ubiquinone-binding site of mitochondrial complex I identified by chemical screening. *Free radical biology & medicine,* 65**,** 1047-1059.
PADURARIU, M., CIOBICA, A., HRITCU, L., STOICA, B., BILD, W. & STEFANESCU, C. 2010. Changes of some oxidative stress markers in the serum of patients with mild cognitive impairment and Alzheimer's disease. *Neurosci Lett.* Ireland: 2009 Elsevier Ireland Ltd.
PAN, H., KIM, E., RANKIN, O. G., ROJANASAKUL, Y., TU, Y. & CHEN, C. Y. 2018. Theaflavin-3,3'-Digallate Enhances the Inhibitory Effect of Cisplatin by Regulating the Copper Transporter 1 and Glutathione in Human Ovarian Cancer Cells. *International Journal of Molecular Sciences,* 19.
PAN, M.-H., LAI, C.-S., HSU, P.-C. & WANG, Y.-J. 2005. Acacetin Induces Apoptosis in Human Gastric Carcinoma Cells Accompanied by Activation of Caspase Cascades and Production of Reactive Oxygen Species. *Journal of Agricultural and Food Chemistry,* 53**,** 620-630.
PAN, M. H., LAI, C. S., WANG, Y. J. & HO, C. T. 2006. Acacetin suppressed LPS-induced up-expression of iNOS and COX-2 in murine macrophages and TPA-induced tumor promotion in mice. *Biochem Pharmacol.* England.
PANDEY, P., SLIKER, B., PETERS, H. L., TULI, A., HERSKOVITZ, J., SMITS, K., PUROHIT, A., SINGH, R. K., DONG, J., BATRA, S. K., COULTER, D. W. & SOLHEIM, J. C. 2016. Amyloid precursor protein and amyloid precursor-like protein 2 in cancer. *Oncotarget,* 7**,** 19430-19444.

PARAMESWARAN, N. & PATIAL, S. 2010. Tumor necrosis factor-α signaling in macrophages. *Critical reviews in eukaryotic gene expression,* 20**,** 87-103.
PATRA, K. C. & HAY, N. 2014. The pentose phosphate pathway and cancer. *Trends Biochem Sci,* 39**,** 347-54.
PATTEN, D. A., GERMAIN, M., KELLY, M. A. & SLACK, R. S. 2010. Reactive oxygen species: stuck in the middle of neurodegeneration. *J Alzheimers Dis.* Netherlands.
PAUL, A., SHOIBE, M., ISLAM, M., AWAL, M., HOQ, M., RAHMAN, M., MAMUR, A., HOQUE, M., CHOWDHURY, T. & KABIR, M. 2016. ANTICANCER POTENTIAL OF ISOLATED PHYTOCHEMICALS FROM HOPEA ODORATA AGAINST BREAST CANCER: IN SILICO MOLECULAR DOCKING APPROACH. *World Journal of Pharmaceutical Research,* 5**,** 1162-1169.
PAVLOV, V. A. & TRACEY, K. J. 2005. The cholinergic anti-inflammatory pathway. *Brain Behav Immun,* 19**,** 493-9.
PELICANO, H., CARNEY, D. & HUANG, P. 2004. ROS stress in cancer cells and therapeutic implications. *Drug Resist Updat,* 7**,** 97-110.
PERVEEN, S. 2018. Introductory Chapter: Terpenes and Terpenoids.
PES, G. M., ERRIGO, A., SORO, S., LONGO, N. P. & DORE, M. P. 2019. Glucose-6-phosphate dehydrogenase deficiency reduces susceptibility to cancer of endodermal origin. *Acta Oncol,* 58**,** 1205-1211.
PETERS, S., REID, A., FRITSCHI, L., DE KLERK, N. & MUSK, A. W. 2013. Long-term effects of aluminium dust inhalation. *Occup Environ Med.* England.
PICCIOTTO, M. R., HIGLEY, M. J. & MINEUR, Y. S. 2012. Acetylcholine as a neuromodulator: cholinergic signaling shapes nervous system function and behavior. *Neuron,* 76**,** 116-129.
PIKARSKY, E., PORAT, R. M., STEIN, I., ABRAMOVITCH, R., AMIT, S., KASEM, S., GUTKOVICH-PYEST, E., URIELI-SHOVAL, S., GALUN, E. & BEN-NERIAH, Y. 2004. NF-kappaB functions as a tumour promoter in inflammation-associated cancer. *Nature.* England.
PITCHAI, A., RAJARETINAM, R. K. & FREEMAN, J. L. 2019. Zebrafish as an Emerging Model for Bioassay-Guided Natural Product Drug Discovery for Neurological Disorders. *Medicines (Basel),* 6.
PIZARRO, T. T., DE LA RUE, S. A. & COMINELLI, F. 2006. Role of interleukin 6 in a murine model of Crohn's ileitis: are cytokine/anticytokine strategies the future for IBD therapies? *Gut,* 55**,** 1226-1227.
POH, A. R. & ERNST, M. 2018. Targeting Macrophages in Cancer: From Bench to Bedside. *Frontiers in oncology,* 8**,** 49-49.
POHANKA, M. 2011. Cholinesterases, a target of pharmacology and toxicology. *Biomed Pap Med Fac Univ Palacky Olomouc Czech Repub,* 155**,** 219-29.
POLLARD, J. W. 2004. Tumour-educated macrophages promote tumour progression and metastasis. *Nat Rev Cancer.* England.
POPIVANOVA, B. K., KITAMURA, K., WU, Y., KONDO, T., KAGAYA, T., KANEKO, S., OSHIMA, M., FUJII, C. & MUKAIDA, N. 2008. Blocking TNF-alpha in mice reduces colorectal carcinogenesis associated with chronic colitis. *J Clin Invest,* 118**,** 560-70.
POPKO, K., GORSKA, E., STELMASZCZYK-EMMEL, A., PLYWACZEWSKI, R., STOKLOSA, A., GORECKA, D., PYRZAK, B. & DEMKOW, U. 2010. Proinflammatory cytokines Il-6 and TNF-α and the development of inflammation in obese subjects. *European journal of medical research,* 15 Suppl 2**,** 120-122.
PORQUET, D., GRINAN-FERRE, C., FERRER, I., CAMINS, A., SANFELIU, C., DEL VALLE, J. & PALLAS, M. 2014. Neuroprotective role of trans-resveratrol in a murine model of familial Alzheimer's disease. *J Alzheimers Dis.* Netherlands.
PRASAD, P. R., REDDY, C. S., RAZA, S. H. & DUTT, C. B. 2008. Folklore medicinal plants of North Andaman Islands, India. *Fitoterapia,* 79**,** 458-64.

PRUCCOLI, L., MORRONI, F., SITA, G., HRELIA, P. & TAROZZI, A. 2020. Esculetin as a Bifunctional Antioxidant Prevents and Counteracts the Oxidative Stress and Neuronal Death Induced by Amyloid Protein in SH-SY5Y Cells. *Antioxidants (Basel, Switzerland),* 9**,** 551.
PUNIA, R., RAINA, K., AGARWAL, R. & SINGH, R. P. 2017. Acacetin enhances the therapeutic efficacy of doxorubicin in non-small-cell lung carcinoma cells. *PloS one,* 12**,** e0182870-e0182870.
QI, J., LU, J. J., LIU, J. H. & YU, B. Y. 2009. Flavonoid and a rare benzophenone glycoside from the leaves of Aquilaria sinensis. *Chem Pharm Bull (Tokyo).* Japan.
QIAN, B.-Z. & POLLARD, J. W. 2010a. Macrophage diversity enhances tumor progression and metastasis. *Cell,* 141**,** 39-51.
QIAN, B. Z. & POLLARD, J. W. 2010b. Macrophage diversity enhances tumor progression and metastasis. *Cell,* 141**,** 39-51.
QU, X., TANG, Y. & HUA, S. 2018. Immunological Approaches Towards Cancer and Inflammation: A Cross Talk. *Front Immunol,* 9**,** 563.
QUAIL, D. F. & JOYCE, J. A. 2013. Microenvironmental regulation of tumor progression and metastasis. *Nature Medicine,* 19**,** 1423-1437.
QUINLAN, C. L., TREBERG, J. R., PEREVOSHCHIKOVA, I. V., ORR, A. L. & BRAND, M. D. 2012. Native rates of superoxide production from multiple sites in isolated mitochondria measured using endogenous reporters. *Free Radic Biol Med,* 53**,** 1807-17.
RAFFA, D., MAGGIO, B., RAIMONDI, M. V., PLESCIA, F. & DAIDONE, G. 2017. Recent discoveries of anticancer flavonoids. *European Journal of Medicinal Chemistry,* 142**,** 213-228.
RAGER, J. E. 2015. Chapter 8 - The Role of Apoptosis-Associated Pathways as Responders to Contaminants and in Disease Progression. *In:* FRY, R. C. (ed.) *Systems Biology in Toxicology and Environmental Health.* Boston: Academic Press.
RAGHAVENDRA, G. M., VARAPRASAD, K. & JAYARAMUDU, T. 2015. Chapter 2 - Biomaterials: Design, Development and Biomedical Applications. *In:* THOMAS, S., GROHENS, Y. & NINAN, N. (eds.) *Nanotechnology Applications for Tissue Engineering.* Oxford: William Andrew Publishing.
RAMPAL, G., KHANNA, N., THIND, T. S., ARORA, S. & VIG, A. 2020. Role of isothiocyanates as anticancer agents and their contributing molecular and cellular mechanisms.
RAMPERSAD, S. N. 2012. Multiple Applications of Alamar Blue as an Indicator of Metabolic Function and Cellular Health in Cell Viability Bioassays. *Sensors (Basel, Switzerland),* 12**,** 12347-12360.
RANGANATHAN, S., HALAGOWDER, D. & SIVASITHAMBARAM, N. D. 2015. Quercetin Suppresses Twist to Induce Apoptosis in MCF-7 Breast Cancer Cells. *PLoS One,* 10**,** e0141370.
RAYAN, A., RAIYN, J. & FALAH, M. 2017. Nature is the best source of anticancer drugs: Indexing natural products for their anticancer bioactivity. *PLoS ONE,* 12**,** e0187925.
REALE, M., IARLORI, C., GAMBI, F., FELICIANI, C., SALONE, A., TOMA, L., DELUCA, G., SALVATORE, M., CONTI, P. & GAMBI, D. 2004. Treatment with an acetylcholinesterase inhibitor in Alzheimer patients modulates the expression and production of the pro-inflammatory and anti-inflammatory cytokines. *J Neuroimmunol,* 148**,** 162-71.
RECZEK, C. & CHANDEL, N. 2017. The Two Faces of Reactive Oxygen Species in Cancer. *Annual Review of Cancer Biology,* 1.
REDZA-DUTORDOIR, M. & AVERILL-BATES, D. A. 2016. Activation of apoptosis signalling pathways by reactive oxygen species. *Biochim Biophys Acta,* 1863**,** 2977-2992.
REITZ, C. & MAYEUX, R. 2014. Alzheimer disease: epidemiology, diagnostic criteria, risk factors and biomarkers. *Biochemical pharmacology,* 88**,** 640-651.

REN, H., MA, J., SI, L., REN, B., CHEN, X., WANG, D., HAO, W., TANG, X., LI, D. & ZHENG, Q. 2018. Low Dose of Acacetin Promotes Breast Cancer MCF-7 Cells Proliferation Through the Activation of ERK/ PI3K /AKT and Cyclin Signaling Pathway. *Recent Pat Anticancer Drug Discov.* United Arab Emirates: Bentham Science Publishers; For any queries, please email at epub@benthamscience.org.
REYNOSO, M., GEDDIS, A., MITROPHANOV, A., MATHENY JR, R. W. & HOBBS, S. 2017. NFkB activation and cytokine output in LPS-treated RAW 264.7 macrophages. *The FASEB Journal,* 31**,** lb146-lb146.
RHEE, J. W., LEE, K. W., KIM, D., LEE, Y., JEON, O. H., KWON, H. J. & KIM, D. S. 2007. NF-kappaB-dependent regulation of matrix metalloproteinase-9 gene expression by lipopolysaccharide in a macrophage cell line RAW 264.7. *J Biochem Mol Biol,* 40**,** 88-94.
RHEE, S. G., WOO, H. A., KIL, I. S. & BAE, S. H. 2012. Peroxiredoxin functions as a peroxidase and a regulator and sensor of local peroxides. *J Biol Chem,* 287**,** 4403-10.
RHEIN, V., GIESE, M., BAYSANG, G., MEIER, F., RAO, S., SCHULZ, K. L., HAMBURGER, M. & ECKERT, A. 2010. Ginkgo biloba extract ameliorates oxidative phosphorylation performance and rescues abeta-induced failure. *PLoS One,* 5**,** e12359.
RICCI, J. E., MUÑOZ-PINEDO, C., FITZGERALD, P., BAILLY-MAITRE, B., PERKINS, G. A., YADAVA, N., SCHEFFLER, I. E., ELLISMAN, M. H. & GREEN, D. R. 2004. Disruption of mitochondrial function during apoptosis is mediated by caspase cleavage of the p75 subunit of complex I of the electron transport chain. *Cell.* United States.
RICCIARDELLI, C. & RODGERS, R. J. 2006. Extracellular matrix of ovarian tumors. *Semin Reprod Med,* 24**,** 270-82.
RICHARDSON, A. K., CURRIE, M. J., ROBINSON, B. A., MORRIN, H., PHUNG, Y., PEARSON, J. F., ANDERSON, T. P., POTTER, J. D. & WALKER, L. C. 2015. Cytomegalovirus and Epstein-Barr virus in breast cancer. *PLoS One,* 10**,** e0118989.
RIDDELL, J. R., WANG, X. Y., MINDERMAN, H. & GOLLNICK, S. O. 2010. Peroxiredoxin 1 stimulates secretion of proinflammatory cytokines by binding to TLR4. *J Immunol,* 184**,** 1022-30.
RINGNÉR, M., FREDLUND, E., HÄKKINEN, J., BORG, Å. & STAAF, J. 2011. GOBO: Gene Expression-Based Outcome for Breast Cancer Online. *PLOS ONE,* 6**,** e17911.
ROBASZKIEWICZ, A., BALCERCZYK, A. & BARTOSZ, G. 2007. Antioxidative and prooxidative effects of quercetin on A549 cells. *Cell Biol Int,* 31**,** 1245-50.
ROBINSON, R. & VENKATARAMAN, K. 1926. CCCXI.—A synthesis of acacetin and certain other derivatives of flavone. *Journal of the Chemical Society (Resumed),* 129**,** 2344-2348.
ROHLENA, J., DONG, L., RALPH, S. & NEUZIL, J. 2011. Anticancer Drugs Targeting the Mitochondrial Electron Transport Chain. *Antioxidants & redox signaling,* 15**,** 2951-74.
ROMANOVA, D., VACHALKOVA, A., CIPAK, L., OVESNA, Z. & RAUKO, P. 2001. Study of antioxidant effect of apigenin, luteolin and quercetin by DNA protective method. *Neoplasma,* 48**,** 104-7.
RONDEAU, V., JACQMIN-GADDA, H., COMMENGES, D., HELMER, C. & DARTIGUES, J. F. 2009. Aluminum and silica in drinking water and the risk of Alzheimer's disease or cognitive decline: findings from 15-year follow-up of the PAQUID cohort. *Am J Epidemiol,* 169**,** 489-96.
ROSINI, M., SIMONI, E., MILELLI, A., MINARINI, A. & MELCHIORRE, C. 2014. Oxidative stress in Alzheimer's disease: are we connecting the dots? *J Med Chem,* 57**,** 2821-31.
ROSSI, M., CARUSO, F., ANTONIOLETTI, R., VIGLIANTI, A., TRAVERSI, G., LEONE, S., BASSO, E. & COZZI, R. 2013. Scavenging of hydroxyl radical by resveratrol and related natural stilbenes after hydrogen peroxide attack on DNA. *Chem Biol Interact.* Ireland: 2013 Elsevier Ireland Ltd.

ROTUNDO, R. L. 2009. Neuromuscular Junction (NMJ): Acetylcholinesterases. *In:* SQUIRE, L. R. (ed.) *Encyclopedia of Neuroscience.* Oxford: Academic Press.
ROVELET-LECRUX, A., HANNEQUIN, D., RAUX, G., LE MEUR, N., LAQUERRIÈRE, A., VITAL, A., DUMANCHIN, C., FEUILLETTE, S., BRICE, A., VERCELLETTO, M., DUBAS, F., FREBOURG, T. & CAMPION, D. 2006. APP locus duplication causes autosomal dominant early-onset Alzheimer disease with cerebral amyloid angiopathy. *Nat Genet.* United States.
SAELENS, X., FESTJENS, N., VANDE WALLE, L., VAN GURP, M., VAN LOO, G. & VANDENABEELE, P. 2004. Toxic proteins released from mitochondria in cell death. *Oncogene.* England.
SAHARAN, S. & MANDAL, P. 2014. The Emerging Role of Glutathione in Alzheimer's Disease. *Journal of Alzheimer's disease : JAD,* 40.
SAHIDIN, S., HAKIM, E., JULIAWATY, L., SYAH, Y., DIN, L., GHISALBERTI, E., LATIP, J., SAID, I. & ACHMAD, S. 2005. *Cytotoxic Properties of Oligostilbenoids from the Tree Barks of Hopea dryobalanoides*.
SALEEM, M. 2009. Lupeol, a novel anti-inflammatory and anti-cancer dietary triterpene. *Cancer letters,* 285**,** 109-115.
SALIH, M., AHMED, W., GARELNABI, E., OSMAN, Z., OSMAN, B., KHALID, H. & MOHAMED, M. 2014. Secondary metabolites as anti-inflammatory agents. *The Journal of Phytopharmacology,* 3**,** 275-285.
SALIMI, A., ROUDKENAR, M. H., SADEGHI, L., MOHSENI, A., SEYDI, E., PIRAHMADI, N. & POURAHMAD, J. 2016. Selective Anticancer Activity of Acacetin Against Chronic Lymphocytic Leukemia Using Both In Vivo and In Vitro Methods: Key Role of Oxidative Stress and Cancerous Mitochondria. *Nutrition and Cancer,* 68**,** 1404-1416.
SALMINEN, A., LEHTONEN, M., SUURONEN, T., KAARNIRANTA, K. & HUUSKONEN, J. 2008. Terpenoids: Natural inhibitors of NF-κB signaling with anti-inflammatory and anticancer potential. *Cellular and molecular life sciences : CMLS,* 65**,** 2979-99.
SAMANTA, A., DAS, G. & DAS, S. 2011. Roles of flavonoids in Plants. *International Journal of pharmaceutical science and technology,* 6**,** 12-35.
SAMANTA, M., HARKINS, L., KLEMM, K., BRITT, W. J. & COBBS, C. S. 2003. High prevalence of human cytomegalovirus in prostatic intraepithelial neoplasia and prostatic carcinoma. *J Urol.* United States.
SAMPATH, D., ZABKA, T. S., MISNER, D. L., O'BRIEN, T. & DRAGOVICH, P. S. 2015. Inhibition of nicotinamide phosphoribosyltransferase (NAMPT) as a therapeutic strategy in cancer. *Pharmacology & Therapeutics,* 151**,** 16-31.
SAN HIPOLITO-LUENGO, A., ALCAIDE, A., RAMOS-GONZALEZ, M., CERCAS, E., VALLEJO, S., ROMERO, A., TALERO, E., SANCHEZ-FERRER, C. F., MOTILVA, V. & PEIRO, C. 2017. Dual Effects of Resveratrol on Cell Death and Proliferation of Colon Cancer Cells. *Nutr Cancer,* 69**,** 1019-1027.
SANCHEZ-MUNOZ, F., DOMINGUEZ-LOPEZ, A. & YAMAMOTO-FURUSHO, J.-K. 2008. Role of cytokines in inflammatory bowel disease. *World journal of gastroenterology,* 14**,** 4280-4288.
SANTOS, C. M. M. & SILVA, A. M. S. 2020. The Antioxidant Activity of Prenylflavonoids. *Molecules,* 25.
SANTOS, C. Y., SNYDER, P. J., WU, W.-C., ZHANG, M., ECHEVERRIA, A. & ALBER, J. 2017. Pathophysiologic relationship between Alzheimer's disease, cerebrovascular disease, and cardiovascular risk: A review and synthesis. *Alzheimer's & Dementia: Diagnosis, Assessment & Disease Monitoring,* 7**,** 69-87.
SARASTE, A. & PULKKI, K. 2000. Morphologic and biochemical hallmarks of apoptosis. *Cardiovascular Research,* 45**,** 528-537.

SARDÃO, V. A., OLIVEIRA, P. J., HOLY, J., OLIVEIRA, C. R. & WALLACE, K. B. 2007. Vital imaging of H9c2 myoblasts exposed to tert-butylhydroperoxide – characterization of morphological features of cell death. *BMC Cell Biology,* 8**,** 11.
SARKHOSH-INANLOU, R., MOLAPARAST, M., MOHAMMADZADEH, A. & SHAFIEI-IRANNEJAD, V. 2020. Sanguinarine enhances cisplatin sensitivity via glutathione depletion in cisplatin-resistant ovarian cancer (A2780) cells. *Chemical Biology & Drug Design,* 95**,** 215-223.
SASIDHARAN, S., CHEN, Y., SARAVANAN, D., SUNDRAM, K. M. & YOGA LATHA, L. 2011. Extraction, isolation and characterization of bioactive compounds from plants' extracts. *African journal of traditional, complementary, and alternative medicines : AJTCAM,* 8**,** 1-10.
SASIKUMAR, P., LEKSHMY, K., SINI, S., PRABHA, B., KUMAR, N. A., SIVAN, V. V., JITHIN, M. M., JAYAMURTHY, P., SHIBI, I. G. & RADHAKRISHNAN, K. V. 2019. Isolation and characterization of resveratrol oligomers from the stem bark of Hopea ponga (Dennst.) Mabb. And their antidiabetic effect by modulation of digestive enzymes, protein glycation and glucose uptake in L6 myocytes. *J Ethnopharmacol.* Ireland: © 2019 Elsevier B.V.
SCADUTO, R. C. & GROTYOHANN, L. W. 1999. Measurement of Mitochondrial Membrane Potential Using Fluorescent Rhodamine Derivatives. *Biophysical Journal,* 76**,** 469-477.
SCHIEBER, M. & CHANDEL, N. S. 2014. ROS function in redox signaling and oxidative stress. *Current biology : CB,* 24**,** R453-R462.
SCHMATZ, R., MAZZANTI, C. M., SPANEVELLO, R., STEFANELLO, N., GUTIERRES, J., CORRÊA, M., DA ROSA, M. M., RUBIN, M. A., CHITOLINA SCHETINGER, M. R. & MORSCH, V. M. 2009. Resveratrol prevents memory deficits and the increase in acetylcholinesterase activity in streptozotocin-induced diabetic rats. *European Journal of Pharmacology,* 610**,** 42-48.
SCHMID, P., ADAMS, S., RUGO, H. S., SCHNEEWEISS, A., BARRIOS, C. H., IWATA, H., DIÉRAS, V., HEGG, R., IM, S.-A., SHAW WRIGHT, G., HENSCHEL, V., MOLINERO, L., CHUI, S. Y., FUNKE, R., HUSAIN, A., WINER, E. P., LOI, S. & EMENS, L. A. 2018. Atezolizumab and Nab-Paclitaxel in Advanced Triple-Negative Breast Cancer. *New England Journal of Medicine,* 379**,** 2108-2121.
SCHULTZE, J. L., SCHMIEDER, A. & GOERDT, S. 2015. Macrophage activation in human diseases. *Semin Immunol.* England: © 2015 Elsevier Ltd.
SCHUMACKER, P. T. 2006. Reactive oxygen species in cancer cells: live by the sword, die by the sword. *Cancer Cell,* 10**,** 175-6.
SECA, A. M. L. & PINTO, D. C. G. A. 2018. Plant Secondary Metabolites as Anticancer Agents: Successes in Clinical Trials and Therapeutic Application. *International journal of molecular sciences,* 19**,** 263.
SEO, H. S., KU, J. M., CHOI, H. S., CHOI, Y. K., WOO, J. K., KIM, M., KIM, I., NA, C. H., HUR, H., JANG, B. H., SHIN, Y. C. & KO, S. G. 2016. Quercetin induces caspase-dependent extrinsic apoptosis through inhibition of signal transducer and activator of transcription 3 signaling in HER2-overexpressing BT-474 breast cancer cells. *Oncol Rep,* 36**,** 31-42.
SEREIA, A. L., DE OLIVEIRA, M. T., BARANOSKI, A., MARQUES, L. L. M., RIBEIRO, F. M., ISOLANI, R. G., DE MEDEIROS, D. C., CHIERRITO, D., LAZARIN-BIDÓIA, D., ZIELINSKI, A. A. F., NOVELLO, C. R., NAKAMURA, C. V., MANTOVANI, M. S. & MELLO, J. C. P. D. 2019. In vitro evaluation of the protective effects of plant extracts against amyloid-beta peptide-induced toxicity in human neuroblastoma SH-SY5Y cells. *PloS one,* 14**,** e0212089-e0212089.
SHAH, U., SHAH, R., ACHARYA, S. & ACHARYA, N. 2013. Novel anticancer agents from plant sources. *Chinese Journal of Natural Medicines,* 11**,** 16-23.
SHAHRUZAMAN, S. H., FAKURAZI, S. & MANIAM, S. 2018. Targeting energy metabolism to eliminate cancer cells. *Cancer management and research,* 10**,** 2325-2335.
SHAMSIZADEH, A., ROOHBAKHSH, A., AYOOBI, F. & MOGHADDAMAHMADI, A. 2017. Chapter 25 - The Role of Natural Products in the Prevention and Treatment of Multiple

Sclerosis. *In:* WATSON, R. R. & KILLGORE, W. D. S. (eds.) *Nutrition and Lifestyle in Neurological Autoimmune Diseases.* Academic Press.
SHANKAR, G. M. & WALSH, D. M. 2009. Alzheimer's disease: synaptic dysfunction and Abeta. *Mol Neurodegener,* 4**,** 48.
SHANNON, P., MARKIEL, A., OZIER, O., BALIGA, N. S., WANG, J. T., RAMAGE, D., AMIN, N., SCHWIKOWSKI, B. & IDEKER, T. 2003. Cytoscape: a software environment for integrated models of biomolecular interaction networks. *Genome Res,* 13**,** 2498-504.
SHARIF, M. K., ZAHID, A. & SHAH, F.-U.-H. 2018. Chapter 15 - Role of Food Product Development in Increased Food Consumption and Value Addition. *In:* GRUMEZESCU, A. M. & HOLBAN, A. M. (eds.) *Food Processing for Increased Quality and Consumption.* Academic Press.
SHARMA, D. R., WANI, W. Y., SUNKARIA, A., KANDIMALLA, R. J., SHARMA, R. K., VERMA, D., BAL, A. & GILL, K. D. 2016. Quercetin attenuates neuronal death against aluminum-induced neurodegeneration in the rat hippocampus. *Neuroscience.* United States: 2016 IBRO. Published by Elsevier Ltd.
SHAULOV-ROTEM, Y., MERQUIOL, E., SADAN, T., MOSHEL, O., SALPETER, S., SHABAT, D., KASCHANI, F., KAISER, M. & BLUM, G. 2015. A Novel Quenched Fluorescent Activity-Based Probe Reveals Caspase-3 Activity in the Endoplasmic Reticulum During Apoptosis. *Chem. Sci.,* 7.
SHEN, K. H., HUNG, S. H., YIN, L. T., HUANG, C. S., CHAO, C. H., LIU, C. L. & SHIH, Y. W. 2010. Acacetin, a flavonoid, inhibits the invasion and migration of human prostate cancer DU145 cells via inactivation of the p38 MAPK signaling pathway. *Mol Cell Biochem,* 333**,** 279-91.
SHEN, X. L., YU, J. H., ZHANG, D. F., XIE, J. X. & JIANG, H. 2014. Positive relationship between mortality from Alzheimer's disease and soil metal concentration in mainland China. *J Alzheimers Dis.* Netherlands.
SHIM, H. Y., PARK, J. H., PAIK, H. D., NAH, S. Y., KIM, D. S. & HAN, Y. S. 2007. Acacetin-induced apoptosis of human breast cancer MCF-7 cells involves caspase cascade, mitochondria-mediated death signaling and SAPK/JNK1/2-c-Jun activation. *Mol Cells.* Korea South.
SHIN, S. W., JUNG, E., KIM, S., KIM, J. H., KIM, E. G., LEE, J. & PARK, D. 2013. Antagonizing effects and mechanisms of afzelin against UVB-induced cell damage. *PLoS One,* 8**,** e61971.
SHUBAYEV, V. I., ANGERT, M., DOLKAS, J., CAMPANA, W. M., PALENSCAR, K. & MYERS, R. R. 2006. TNFalpha-induced MMP-9 promotes macrophage recruitment into injured peripheral nerve. *Molecular and cellular neurosciences,* 31**,** 407-415.
SICA, A. & BRONTE, V. 2007. Altered macrophage differentiation and immune dysfunction in tumor development. *J Clin Invest,* 117**,** 1155-66.
SIDORYK-WEGRZYNOWICZ, M., WEGRZYNOWICZ, M., LEE, E., BOWMAN, A. B. & ASCHNER, M. 2011. Role of astrocytes in brain function and disease. *Toxicol Pathol,* 39**,** 115-23.
SIMON, H. U., HAJ-YEHIA, A. & LEVI-SCHAFFER, F. 2000. Role of reactive oxygen species (ROS) in apoptosis induction. *Apoptosis,* 5**,** 415-8.
SIMON, P., SARGENT, R. & RABSON, A. 2007. Inhibitor of apoptosis protein BIRC3 (API2, cIAP2, AIP1) is upregulated by the non-canonical NFKB pathway. *Cancer Research,* 67**,** 5327.
SINGH, M., CHAUDHRY, P., FABI, F. & ASSELIN, E. 2013. Cisplatin-induced caspase activation mediates PTEN cleavage in ovarian cancer cells: a potential mechanism of chemoresistance. *BMC cancer,* 13**,** 233-233.
SIQUEIRA, E., DE OLIVEIRA, D. M., JOHANN, S., CISALPINO, P., COTA, B., RABELLO, A., ALVES, T. & ZANI, C. 2011. Bioactivity of the compounds isolated from Blepharocalyx salicifolius. *Revista Brasileira de Farmacognosia,* 21**,** 645-651.

SLATTERY, M. L., LUNDGREEN, A., KADLUBAR, S. A., BONDURANT, K. L. & WOLFF, R. K. 2013. JAK/STAT/SOCS-signaling pathway and colon and rectal cancer. *Molecular Carcinogenesis,* 52**,** 155-166.
SOARES, R., AZEVEDO, I., SAWATZKY, D. A. & ROSSI, A. G. 2006. Apigenin: Is It a Pro- or Anti-Inflammatory Agent? *The American Journal of Pathology,* 168**,** 1762-1763.
SOINI, Y., PAAKKO, P. & LEHTO, V. P. 1998. Histopathological evaluation of apoptosis in cancer. *Am J Pathol,* 153**,** 1041-53.
SOLINAS, G., GERMANO, G., MANTOVANI, A. & ALLAVENA, P. 2009. Tumor-associated macrophages (TAM) as major players of the cancer-related inflammation. *J Leukoc Biol,* 86**,** 1065-73.
SOLITO, E. & SASTRE, M. 2012. Microglia function in Alzheimer's disease. *Front Pharmacol,* 3**,** 14.
SOLOMON, A., KIVIPELTO, M., WOLOZIN, B., ZHOU, J. & WHITMER, R. A. 2009. Midlife serum cholesterol and increased risk of Alzheimer's and vascular dementia three decades later. *Dement Geriatr Cogn Disord,* 28**,** 75-80.
SONG, J., JUN, M., AHN, M.-R. & KIM, O. 2016. Involvement of miR-Let7A in inflammatory response and cell survival/apoptosis regulated by resveratrol in THP-1 macrophage. *Nutrition Research and Practice,* 10**,** 377.
SONG, W., MAZZIERI, R., YANG, T. & GOBE, G. C. 2017. Translational Significance for Tumor Metastasis of Tumor-Associated Macrophages and Epithelial–Mesenchymal Transition. *Frontiers in Immunology,* 8.
SOOD, P. K., NAHAR, U. & NEHRU, B. 2011. Curcumin attenuates aluminum-induced oxidative stress and mitochondrial dysfunction in rat brain. *Neurotox Res,* 20**,** 351-61.
SOUKUP, R. 2019. On the occasion of the 100th anniversary: Ernst Späth and his mescaline synthesis of 1919. *Monatshefte für Chemie - Chemical Monthly*.
SREEKANTH, D., SYED, A., SARKAR, S., SANTHAKUMARI, B., AHMAD, A. & KHAN, I. 2009. Production, Purification, and Characterization of Taxol and 10-DABIII from a new Endophytic Fungus Gliocladium sp Isolated from the Indian Yew Tree, Taxus baccata. *Journal of microbiology and biotechnology,* 19**,** 1342-7.
STANTON, P. 2004. Gel Filtration Chromatography. *In:* AGUILAR, M.-I. (ed.) *HPLC of Peptides and Proteins: Methods and Protocols.* Totowa, NJ: Springer New York.
STERVBO, U., VANG, O. & BONNESEN, C. 2007. Time- and concentration-dependent effects of resveratrol in HL-60 and HepG2 cells. *Cell proliferation,* 39**,** 479-93.
STIVALA, L. A., SAVIO, M., CARAFOLI, F., PERUCCA, P., BIANCHI, L., MAGA, G., FORTI, L., PAGNONI, U. M., ALBINI, A., PROSPERI, E. & VANNINI, V. 2001. Specific structural determinants are responsible for the antioxidant activity and the cell cycle effects of resveratrol. *J Biol Chem.* United States.
STOIMENOV, I. & HELLEDAY, T. 2009. PCNA on the crossroad of cancer. *Biochemical Society Transactions,* 37**,** 605-613.
STORCI, G., SANSONE, P., MARI, S., D'UVA, G., TAVOLARI, S., GUARNIERI, T., TAFFURELLI, M., CECCARELLI, C., SANTINI, D., CHIECO, P., MARCU, K. B. & BONAFÈ, M. 2010. TNFalpha up-regulates SLUG via the NF-kappaB/HIF1alpha axis, which imparts breast cancer cells with a stem cell-like phenotype. *J Cell Physiol,* 225**,** 682-91.
STOUT, R. D., JIANG, C., MATTA, B., TIETZEL, I., WATKINS, S. K. & SUTTLES, J. 2005. Macrophages sequentially change their functional phenotype in response to changes in microenvironmental influences. *J Immunol,* 175**,** 342-9.
SU, Z., YANG, Z., XU, Y., CHEN, Y. & YU, Q. 2015. Apoptosis, autophagy, necroptosis, and cancer metastasis. *Molecular cancer,* 14**,** 48-48.
SUBHASH, V., YEO, M., WANG, L.-Z., TAN, S. H., WONG, F., THUYA, W., TAN, W., PEETHALA, P., SOE, M., TAN, D., PADMANABHAN, N., BALOGLU, E., SHACHAM, S., TAN, P., KOEFFLER,

H. & YONG, W. 2018. Anti-tumor efficacy of Selinexor (KPT-330) in gastric cancer is dependent on nuclear accumulation of p53 tumor suppressor. *Scientific Reports,* 8.
SUBRAMANIAN, R., RAJ, V., MANIGANDAN, K. & ELANGOVAN, N. 2015. Antioxidant activity of hopeaphenol isolated from Shorea roxburghii stem bark extract. *Journal of Taibah University for Science,* 9**,** 237-244.
SULLIVAN, WILLIAM J. & CHRISTOFK, HEATHER R. 2015. The Metabolic Milieu of Metastases. *Cell,* 160**,** 363-364.
SUN, L.-C., ZHANG, H.-B., GU, C.-D., GUO, S.-D., LI, G., LIAN, R., YAO, Y. & ZHANG, G.-Q. 2018. Protective effect of acacetin on sepsis-induced acute lung injury via its anti-inflammatory and antioxidative activity. *Archives of pharmacal research,* 41**,** 1199-1210.
SUN, S., HAN, Y., LIU, J., FANG, Y., TIAN, Y., ZHOU, J., MA, D. & WU, P. 2014. Trichostatin A Targets the Mitochondrial Respiratory Chain, Increasing Mitochondrial Reactive Oxygen Species Production to Trigger Apoptosis in Human Breast Cancer Cells. *PLOS ONE,* 9**,** e91610.
SUN, Y., ZHOU, Q.-M., LU, Y.-Y., ZHANG, H., CHEN, Q.-L., ZHAO, M. & SU, S.-B. 2019. Resveratrol Inhibits the Migration and Metastasis of MDA-MB-231 Human Breast Cancer by Reversing TGF-β1-Induced Epithelial-Mesenchymal Transition. *Molecules (Basel, Switzerland),* 24**,** 1131.
SUNG, S. H., KANG, S. Y., LEE, K. Y., PARK, M. J., KIM, J. H., PARK, J. H., KIM, Y. C. & KIM, J. 2002. (+)-Alpha-viniferin, a stilbene trimer from Caragana chamlague, inhibits acetylcholinesterase. *Biol Pharm Bull,* 25**,** 125-7.
SUZUMURA, A. 2013. Neuron-microglia interaction in neuroinflammation. *Curr Protein Pept Sci.* United Arab Emirates.
SWEE, L. & CHUA, L. 2008. AGARWOOD (AQUILARIA MALACCENSIS) IN MALAYSIA.
SWERDLOW, R. H. 2018. Mitochondria and Mitochondrial Cascades in Alzheimer's Disease. *J Alzheimers Dis,* 62**,** 1403-1416.
SYED ALWI, S. S., CAVELL, B. E., DONLEVY, A. & PACKHAM, G. 2012. Differential induction of apoptosis in human breast cancer cell lines by phenethyl isothiocyanate, a glutathione depleting agent. *Cell stress & chaperones,* 17**,** 529-538.
SYNG-AI, C., KUMARI, A. L. & KHAR, A. 2004. Effect of curcumin on normal and tumor cells: Role of glutathione and bcl-2. *Molecular Cancer Therapeutics,* 3**,** 1101.
SZEKERES, T., FRITZER-SZEKERES, M., SAIKO, P. & JAGER, W. 2010. Resveratrol and resveratrol analogues--structure-activity relationship. *Pharm Res,* 27**,** 1042-8.
SZENDE, B., TYIHAK, E. & KIRALY-VEGHELY, Z. 2000. Dose-dependent effect of resveratrol on proliferation and apoptosis in endothelial and tumor cell cultures. *Exp Mol Med,* 32**,** 88-92.
SZLOSAREK, P., CHARLES, K. A. & BALKWILL, F. R. 2006. Tumour necrosis factor-α as a tumour promoter. *European Journal of Cancer,* 42**,** 745-750.
TAI, L. M., BILOUSOVA, T., JUNGBAUER, L., ROESKE, S. K., YOUMANS, K. L., YU, C., POON, W. W., CORNWELL, L. B., MILLER, C. A., VINTERS, H. V., VAN ELDIK, L. J., FARDO, D. W., ESTUS, S., BU, G., GYLYS, K. H. & LADU, M. J. 2013. Levels of soluble apolipoprotein E/amyloid-β (Aβ) complex are reduced and oligomeric Aβ increased with APOE4 and Alzheimer disease in a transgenic mouse model and human samples. *The Journal of biological chemistry,* 288**,** 5914-5926.
TAKAOKA, M. 1939. The Phenolic Substances of white Hellebore (Veratrum Grandiflorum Loes fil.) II

Oxyresveratrol. *NIPPON KAGAKU KAISHI,* 60**,** 1261-1264.
TAM, C. S., TROTMAN, J., OPAT, S., BURGER, J. A., CULL, G., GOTTLIEB, D., HARRUP, R., JOHNSTON, P. B., MARLTON, P., MUNOZ, J., SEYMOUR, J. F., SIMPSON, D., TEDESCHI, A., ELSTROM, R., YU, Y., TANG, Z., HAN, L., HUANG, J., NOVOTNY, W., WANG, L. & ROBERTS, A.

W. 2019. Phase 1 study of the selective BTK inhibitor zanubrutinib in B-cell malignancies and safety and efficacy evaluation in CLL. *Blood,* 134**,** 851-859.
TAM, L., MCGLYNN, L. M., TRAYNOR, P., MUKHERJEE, R., BARTLETT, J. M. S. & EDWARDS, J. 2007. Expression levels of the JAK/STAT pathway in the transition from hormone-sensitive to hormone-refractory prostate cancer. *British Journal of Cancer,* 97**,** 378-383.
TAN, B., DONG, S., SHEPARD, R. L., KAYS, L., ROTH, K. D., GEEGANAGE, S., KUO, M. S. & ZHAO, G. 2015. Inhibition of Nicotinamide Phosphoribosyltransferase (NAMPT), an Enzyme Essential for NAD+ Biosynthesis, Leads to Altered Carbohydrate Metabolism in Cancer Cells. *J Biol Chem,* 290**,** 15812-24.
TAN, B. M., ZAMMIT, N. W., YAM, A. O., SLATTERY, R., WALTERS, S. N., MALLE, E. & GREY, S. T. 2013. Baculoviral inhibitors of apoptosis repeat containing (BIRC) proteins fine-tune TNF-induced nuclear factor κB and c-Jun N-terminal kinase signalling in mouse pancreatic beta cells. *Diabetologia,* 56**,** 520-532.
TANAKA, T., ITO, T., IDO, Y., SON, T. K., NAKAYA, K., IINUMA, M., OHYAMA, M. & CHELLADURAI, V. 2000. Stilbenoids in the stem bark of Hopea parviflora. *Phytochemistry,* 53**,** 1015-1019.
TANG, D., TAO, D., FANG, Y., DENG, C., XU, Q. & ZHOU, J. 2017. TNF-Alpha Promotes Invasion and Metastasis via NF-Kappa B Pathway in Oral Squamous Cell Carcinoma. *Medical science monitor basic research,* 23**,** 141-149.
TANG, F. Y., SU, Y. C., CHEN, N. C., HSIEH, H. S. & CHEN, K. S. 2008. Resveratrol inhibits migration and invasion of human breast-cancer cells. *Mol Nutr Food Res,* 52**,** 683-91.
TANIGAWA, N., HAGIWARA, M., TADA, H., KOMATSU, T., SUGIURA, S., KOBAYASHI, K., KATO, Y., ISHIDA, N., NISHIDA, K., NINOMIYA, M., KOKETSU, M. & MATSUSHITA, K. 2013. Acacetin inhibits expression of E-selectin on endothelial cells through regulation of the MAP kinase signaling pathway and activation of NF-κB. *Immunopharmacology and Immunotoxicology,* 35**,** 471-477.
TANNE, J. 2006. Paracetamol causes most liver failure in UK and US. *BMJ : British Medical Journal,* 332**,** 628-628.
TARIOT, P. N., FARLOW, M. R., GROSSBERG, G. T., GRAHAM, S. M., MCDONALD, S. & GERGEL, I. 2004. Memantine treatment in patients with moderate to severe Alzheimer disease already receiving donepezil: a randomized controlled trial. *JAMA.* United States.
TAROZZI, A., MORRONI, F., BOLONDI, C., SITA, G., HRELIA, P., DJEMIL, A. & CANTELLI-FORTI, G. 2012. Neuroprotective effects of erucin against 6-hydroxydopamine-induced oxidative damage in a dopaminergic-like neuroblastoma cell line. *International journal of molecular sciences,* 13**,** 10899-10910.
TATTON, W. G., CHALMERS-REDMAN, R., BROWN, D. & TATTON, N. 2003. Apoptosis in Parkinson's disease: Signals for neuronal degradation. *Annals of Neurology,* 53**,** S61-S72.
TEEKARAMAN, D., ELAYAPILLAI, S. P., VISWANATHAN, M. P. & JAGADEESAN, A. 2019. Quercetin inhibits human metastatic ovarian cancer cell growth and modulates components of the intrinsic apoptotic pathway in PA-1cell line. *Chem Biol Interact.* Ireland: 2019 Elsevier B.V.
THEUNS, J., BROUWERS, N., ENGELBORGHS, S., SLEEGERS, K., BOGAERTS, V., CORSMIT, E., DE POOTER, T., VAN DUIJN, C. M., DE DEYN, P. P. & VAN BROECKHOVEN, C. 2006. Promoter mutations that increase amyloid precursor-protein expression are associated with Alzheimer disease. *Am J Hum Genet,* 78**,** 936-46.
TIAN, X., ZHANG, L., WANG, J., DAI, J., SHEN, S., YANG, L. & HUANG, P. 2013. The protective effect of hyperbaric oxygen and Ginkgo biloba extract on Abeta25-35-induced oxidative stress and neuronal apoptosis in rats. *Behav Brain Res.* Netherlands: 2012 Elsevier B.V.

TINO, A. B., CHITCHOLTAN, K., SYKES, P. H. & GARRILL, A. 2016. Resveratrol and acetyl-resveratrol modulate activity of VEGF and IL-8 in ovarian cancer cell aggregates via attenuation of the NF-κB protein. *J Ovarian Res,* 9**,** 84.
TISONCIK, J. R., KORTH, M. J., SIMMONS, C. P., FARRAR, J., MARTIN, T. R. & KATZE, M. G. 2012. Into the eye of the cytokine storm. *Microbiology and molecular biology reviews : MMBR,* 76**,** 16-32.
TO, W. S. & MIDWOOD, K. S. 2011. Plasma and cellular fibronectin: distinct and independent functions during tissue repair. *Fibrogenesis Tissue Repair,* 4**,** 21.
TONON, G., WONG, K. K., MAULIK, G., BRENNAN, C., FENG, B., ZHANG, Y., KHATRY, D. B., PROTOPOPOV, A., YOU, M. J., AGUIRRE, A. J., MARTIN, E. S., YANG, Z., JI, H., CHIN, L. & DEPINHO, R. A. 2005. High-resolution genomic profiles of human lung cancer. *Proc Natl Acad Sci U S A,* 102**,** 9625-30.
TORRES-NARANJO, M., SUAREZ, A. I., GILARDONI, G., CARTUCHE, L., FLORES, P. & MOROCHO, V. 2016. Chemical Constituents of Muehlenbeckia tamnifolia (Kunth) Meisn (Polygonaceae) and Its In Vitro α-Amilase and α-Glucosidase Inhibitory Activities. *Molecules,* 21**,** 1461.
TRABER, M. G., VAN DER VLIET, A., REZNICK, A. Z. & CROSS, C. E. 2000. Tobacco-related diseases. Is there a role for antioxidant micronutrient supplementation? *Clin Chest Med.* United States.
TRACHOOTHAM, D., ALEXANDRE, J. & HUANG, P. 2009. Targeting cancer cells by ROS-mediated mechanisms: a radical therapeutic approach? *Nat Rev Drug Discov.* England.
TRAMUTOLA, A., ABATE, G., LANZILLOTTA, C., TRIANI, F., BARONE, E., IAVARONE, F., VINCENZONI, F., CASTAGNOLA, M., MARZIANO, M., MEMO, M., GARRAFA, E., BUTTERFIELD, D. A., PERLUIGI, M., DI DOMENICO, F. & UBERTI, D. 2018. Protein nitration profile of CD3+ lymphocytes from Alzheimer disease patients: Novel hints on immunosenescence and biomarker detection. *Free Radical Biology and Medicine,* 129**,** 430-439.
TRIPATHI, P. & AGGARWAL, A. 2006. NF-kB transcription factor: A key player in the generation of immune response. *Current Science,* 90.
TSAI, C.-L., CHEN, W.-C., HSIEH, H.-L., CHI, P.-L., HSIAO, L.-D. & YANG, C.-M. 2014. TNF-α induces matrix metalloproteinase-9-dependent soluble intercellular adhesion molecule-1 release via TRAF2-mediated MAPKs and NF-κB activation in osteoblast-like MC3T3-E1 cells. *Journal of biomedical science,* 21**,** 12-12.
TSAI, J.-H., HSU, L.-S., LIN, C.-L., HONG, H.-M., PAN, M.-H., WAY, T.-D. & CHEN, W.-J. 2013. 3,5,4′-Trimethoxystilbene, a natural methoxylated analog of resveratrol, inhibits breast cancer cell invasiveness by downregulation of PI3K/Akt and Wnt/β-catenin signaling cascades and reversal of epithelial–mesenchymal transition. *Toxicology and Applied Pharmacology,* 272**,** 746-756.
TSENG, C. H., TZENG, C. C., CHIU, C. C., HSU, C. Y., CHOU, C. K. & CHEN, Y. L. 2015. Discovery of 2-[2-(5-nitrofuran-2-yl)vinyl]quinoline derivatives as a novel type of antimetastatic agents. *Bioorg Med Chem,* 23**,** 141-8.
TUMIATTI, V., MINARINI, A., BOLOGNESI, M. L., MILELLI, A., ROSINI, M. & MELCHIORRE, C. 2010. Tacrine derivatives and Alzheimer's disease. *Curr Med Chem.* United Arab Emirates.
TUN, M. K. M. & HERZON, S. B. 2012. The pharmacology and therapeutic potential of (-)-huperzine A. *Journal of experimental pharmacology,* 4**,** 113-123.
TUORKEY, M. J. 2016. Molecular targets of luteolin in cancer. *European journal of cancer prevention : the official journal of the European Cancer Prevention Organisation (ECP),* 25**,** 65-76.
UEDA, J. Y., IMAMURA, L., TEZUKA, Y., TRAN, Q. L., TSUDA, M. & KADOTA, S. 2006. New sesquiterpene from Vietnamese agarwood and its induction effect on brain-derived neurotrophic factor mRNA expression in vitro. *Bioorg Med Chem.* England.

VAINIO, H. & BOFFETTA, P. 1994. Mechanisms of the combined effect of asbestos and smoking in the etiology of lung cancer. *Scandinavian Journal of Work, Environment & Health,* 20**,** 235-242.
VALLA, J., SCHNEIDER, L., NIEDZIELKO, T., COON, K. D., CASELLI, R., SABBAGH, M. N., AHERN, G. L., BAXTER, L., ALEXANDER, G., WALKER, D. G. & REIMAN, E. M. 2006. Impaired platelet mitochondrial activity in Alzheimer's disease and mild cognitive impairment. *Mitochondrion,* 6**,** 323-30.
VAN DEN BERG, R. A., HOEFSLOOT, H. C., WESTERHUIS, J. A., SMILDE, A. K. & VAN DER WERF, M. J. 2006. Centering, scaling, and transformations: improving the biological information content of metabolomics data. *BMC Genomics,* 7**,** 142.
VASCONCELOS, J. F., TEIXEIRA, M. M., BARBOSA-FILHO, J. M., LUCIO, A. S., ALMEIDA, J. R., DE QUEIROZ, L. P., RIBEIRO-DOS-SANTOS, R. & SOARES, M. B. 2008. The triterpenoid lupeol attenuates allergic airway inflammation in a murine model. *Int Immunopharmacol.* Netherlands.
VEERESHAM, C. 2012. Natural products derived from plants as a source of drugs. *Journal of advanced pharmaceutical technology & research,* 3**,** 200-201.
VENKATADRI, R., MUNI, T., IYER, A. K. V., YAKISICH, J. S. & AZAD, N. 2016. Role of apoptosis-related miRNAs in resveratrol-induced breast cancer cell death. *Cell death & disease,* 7**,** e2104-e2104.
VERMEERSCH, K. A. & STYCZYNSKI, M. P. 2013. Applications of metabolomics in cancer research. *J Carcinog,* 12**,** 9.
VERSTREKEN, P., LY, C. V., VENKEN, K. J., KOH, T. W., ZHOU, Y. & BELLEN, H. J. 2005. Synaptic mitochondria are critical for mobilization of reserve pool vesicles at Drosophila neuromuscular junctions. *Neuron.* United States.
VIALE, A., CORTI, D. & DRAETTA, G. F. 2015. Tumors and mitochondrial respiration: a neglected connection. *Cancer Res.* United States.
VIALE, A., PETTAZZONI, P., LYSSIOTIS, C. A., YING, H., SÁNCHEZ, N., MARCHESINI, M., CARUGO, A., GREEN, T., SETH, S., GIULIANI, V., KOST-ALIMOVA, M., MULLER, F., COLLA, S., NEZI, L., GENOVESE, G., DEEM, A. K., KAPOOR, A., YAO, W., BRUNETTO, E., KANG, Y., YUAN, M., ASARA, J. M., WANG, Y. A., HEFFERNAN, T. P., KIMMELMAN, A. C., WANG, H., FLEMING, J. B., CANTLEY, L. C., DEPINHO, R. A. & DRAETTA, G. F. 2014. Oncogene ablation-resistant pancreatic cancer cells depend on mitochondrial function. *Nature,* 514**,** 628-32.
VO, T.-T. & LETAI, A. 2010. BH3-only proteins and their effects on cancer. *Advances in experimental medicine and biology,* 687**,** 49-63.
WAGH, V. D., KORINEK, M., LO, I. W., HSU, Y. M., CHEN, S. L., HSU, H. Y., HWANG, T. L., WU, Y. C., CHEN, B. H., CHENG, Y. B. & CHANG, F. R. 2017. Inflammation Modulatory Phorbol Esters from the Seeds of Aquilaria malaccensis. *J Nat Prod,* 80**,** 1421-1427.
WALKER, J., SCHUELLER, K., SCHAEFER, L.-M., PIGNITTER, M., ESEFELDER, L. & SOMOZA, V. 2014. Resveratrol and its metabolites inhibit pro-inflammatory effects of lipopolysaccharides in U-937 macrophages in plasma-representative concentrations. *Food & Function,* 5**,** 74-84.
WALLIMANN, T., TOKARSKA-SCHLATTNER, M. & SCHLATTNER, U. 2011. The creatine kinase system and pleiotropic effects of creatine. *Amino acids,* 40**,** 1271-1296.
WALTON, J. R. 2014. Chronic aluminum intake causes Alzheimer's disease: applying Sir Austin Bradford Hill's causality criteria. *J Alzheimers Dis.* Netherlands.
WANG, D. M., LI, S. Q., WU, W. L., ZHU, X. Y., WANG, Y. & YUAN, H. Y. 2014a. Effects of long-term treatment with quercetin on cognition and mitochondrial function in a mouse model of Alzheimer's disease. *Neurochem Res,* 39**,** 1533-43.

WANG, H., JIANG, T., LI, W., GAO, N. & ZHANG, T. 2018a. Resveratrol attenuates oxidative damage through activating mitophagy in an in vitro model of Alzheimer's disease. *Toxicol Lett.* Netherlands: 2017 Elsevier B.V.
WANG, J., FANG, X., GE, L., CAO, F., ZHAO, L., WANG, Z. & XIAO, W. 2018b. Antitumor, antioxidant and anti-inflammatory activities of kaempferol and its corresponding glycosides and the enzymatic preparation of kaempferol. *PLOS ONE,* 13**,** e0197563.
WANG, J., HU, D., HOU, J., LI, S., WANG, W., LI, J. & BAI, J. 2018c. Ethyl Acetate Fraction of Hemerocallis citrina Baroni Decreases Tert-butyl Hydroperoxide-Induced Oxidative Stress Damage in BRL-3A Cells. *Oxidative Medicine and Cellular Longevity,* 2018**,** 1526125.
WANG, L., GUO, L., LU, L., SUN, H., SHAO, M., BECK, S. J., LI, L., RAMACHANDRAN, J., DU, Y. & DU, H. 2016a. Synaptosomal Mitochondrial Dysfunction in 5xFAD Mouse Model of Alzheimer's Disease. *PLOS ONE,* 11**,** e0150441.
WANG, P., QIU, W., DUDGEON, C., LIU, H., HUANG, C., ZAMBETTI, G. P., YU, J. & ZHANG, L. 2009. PUMA is directly activated by NF-κB and contributes to TNF-α-induced apoptosis. *Cell Death & Differentiation,* 16**,** 1192-1202.
WANG, Q., HE, Y., SHEN, Y., ZHANG, Q., CHEN, D., ZUO, C., QIN, J., WANG, H., WANG, J. & YU, Y. 2014b. Vitamin D inhibits COX-2 expression and inflammatory response by targeting thioesterase superfamily member 4. *The Journal of biological chemistry,* 289**,** 11681-11694.
WANG, R., ZHANG, Y., LI, J. & ZHANG, C. 2017. Resveratrol ameliorates spatial learning memory impairment induced by Aβ1–42 in rats. *Neuroscience,* 344**,** 39-47.
WANG, S., YU, Z., WANG, C., WU, C., GUO, P. & WEI, J. 2018d. Chemical Constituents and Pharmacological Activity of Agarwood and Aquilaria Plants. *Molecules (Basel, Switzerland),* 23**,** 342.
WANG, S.-W. & SUN, Y.-M. 2014. The IL-6/JAK/STAT3 pathway: Potential therapeutic strategies in treating colorectal cancer (Review). *Int J Oncol,* 44**,** 1032-1040.
WANG, S. L., HWANG, T. L., CHUNG, M. I., SUNG, P. J., SHU, C. W., CHENG, M. J. & CHEN, J. J. 2015a. New Flavones, a 2-(2-Phenylethyl)-4H-chromen-4-one Derivative, and Anti-Inflammatory Constituents from the Stem Barks of Aquilaria sinensis. *Molecules,* 20**,** 20912-25.
WANG, T. J., LARSON, M. G., VASAN, R. S., CHENG, S., RHEE, E. P., MCCABE, E., LEWIS, G. D., FOX, C. S., JACQUES, P. F., FERNANDEZ, C., O'DONNELL, C. J., CARR, S. A., MOOTHA, V. K., FLOREZ, J. C., SOUZA, A., MELANDER, O., CLISH, C. B. & GERSZTEN, R. E. 2011. Metabolite profiles and the risk of developing diabetes. *Nature medicine,* 17**,** 448-453.
WANG, X., LI, X., ZHANG, X., FAN, R., GU, H., SHI, Y. & LIU, H. 2015b. Glucose-6-phosphate dehydrogenase expression is correlated with poor clinical prognosis in esophageal squamous cell carcinoma. *Eur J Surg Oncol.* England: © 2015 Elsevier Ltd.
WANG, X., PERUMALSAMY, H., KWON, H. W., NA, Y.-E. & AHN, Y.-J. 2015c. Effects and possible mechanisms of action of acacetin on the behavior and eye morphology of Drosophila models of Alzheimer's disease. *Scientific reports,* 5**,** 16127-16127.
WANG, X., WANG, W., LI, L., PERRY, G., LEE, H. G. & ZHU, X. 2014c. Oxidative stress and mitochondrial dysfunction in Alzheimer's disease. *Biochim Biophys Acta,* 1842**,** 1240-7.
WANG, Y., HONG, D., QIAN, Y., TU, X., WANG, K., YANG, X., SHAO, S., KONG, X., LOU, Z. & JIN, L. 2018e. Lupeol inhibits growth and migration in two human colorectal cancer cell lines by suppression of Wnt-β-catenin pathway. *OncoTargets and therapy,* 11**,** 7987-7999.
WANG, Y., WANG, K., HAN, G. C., WANG, R. X., XIAO, H., HOU, C. M., GUO, R. F., DOU, Y., SHEN, B. F., LI, Y. & CHEN, G. J. 2014d. Neutrophil infiltration favors colitis-associated tumorigenesis by activating the interleukin-1 (IL-1)/IL-6 axis. *Mucosal Immunol,* 7**,** 1106-15.
WANG, Z., WEI, X., YANG, J., SUO, J., CHEN, J., LIU, X. & ZHAO, X. 2016b. Chronic exposure to aluminum and risk of Alzheimer's disease: A meta-analysis. *Neurosci Lett.* Ireland: 2015 Elsevier Ireland Ltd.

WATANABE, K., KANNO, S., TOMIZAWA, A., YOMOGIDA, S. & ISHIKAWA, M. 2012. Acacetin induces apoptosis in human T cell leukemia Jurkat cells via activation of a caspase cascade. *Oncol Rep,* 27**,** 204-9.
WATKINS, P., ZIMMERMAN, H., KNAPP, M. J., GRACON, S. & LEWIS, K. W. 1994. Hepatotoxic effects of tacrine administration in patients with Alzheimer's disease. *JAMA,* 271 13**,** 992-8.
WATSON, D. G., TONELLI, F., ALOSSAIMI, M., WILLIAMSON, L., CHAN, E., GORSHKOVA, I., BERDYSHEV, E., BITTMAN, R., PYNE, N. J. & PYNE, S. 2013. The roles of sphingosine kinases 1 and 2 in regulating the Warburg effect in prostate cancer cells. *Cellular signalling,* 25**,** 1011-1017.
WEBER, J.-F. F., WAHAB, I. A., MARZUKI, A., THOMAS, N. F., KADIR, A. A., HADI, A. H. A., AWANG, K., LATIFF, A. A., RICHOMME, P. & DELAUNAY, J. 2001. Heimiol A, a new dimeric stilbenoid from Neobalanocarpus heimii. *Tetrahedron Letters,* 42**,** 4895-4897.
WEILER, J., MOHR, M., ZÄNKER, K. S. & DITTMAR, T. 2018. Matrix metalloproteinase-9 (MMP9) is involved in the TNF-α-induced fusion of human M13SV1-Cre breast epithelial cells and human MDA-MB-435-pFDR1 cancer cells. *Cell Communication and Signaling,* 16**,** 14.
WEINBERG, F., RAMNATH, N. & NAGRATH, D. 2019. Reactive Oxygen Species in the Tumor Microenvironment: An Overview. *Cancers,* 11.
WENINGER, S. C. & YANKNER, B. A. 2001. Inflammation and Alzheimer disease: The good, the bad, and the ugly. *Nature Medicine,* 7**,** 527-528.
WHITAKER-MENEZES, D., MARTINEZ-OUTSCHOORN, U. E., FLOMENBERG, N., BIRBE, R. C., WITKIEWICZ, A. K., HOWELL, A., PAVLIDES, S., TSIRIGOS, A., ERTEL, A., PESTELL, R. G., BRODA, P., MINETTI, C., LISANTI, M. P. & SOTGIA, F. 2011. Hyperactivation of oxidative mitochondrial metabolism in epithelial cancer cells in situ: visualizing the therapeutic effects of metformin in tumor tissue. *Cell cycle (Georgetown, Tex.),* 10**,** 4047-4064.
WHO, W. H. O. 2019. *Dementia* [Online]. Available: https://www.who.int/news-room/fact-sheets/detail/dementia [Accessed April 2020].
WIBOWO, A., AHMAT, N., HAMZAH, A. S., SUFIAN, A. S., ISMAIL, N. H., AHMAD, R., JAAFAR, F. M. & TAKAYAMA, H. 2011. Malaysianol A, a new trimer resveratrol oligomer from the stem bark of Dryobalanops aromatica. *Fitoterapia.* Netherlands: 2011 Elsevier B.V.
WICK, W. & PLATTEN, M. 2014. CMV infection and glioma, a highly controversial concept struggling in the clinical arena. *Neuro Oncol,* 16**,** 332-3.
WILLCOTT, M. R. 2009. MestRe Nova. *Journal of the American Chemical Society,* 131**,** 13180-13180.
WILLIAMS, C. B., YEH, E. S. & SOLOFF, A. C. 2016. Tumor-associated macrophages: unwitting accomplices in breast cancer malignancy. *npj Breast Cancer,* 2**,** 15025.
WILLIAMSON, G. & MANACH, C. 2005. Bioavailability and bioefficacy of polyphenols in humans. II. Review of 93 intervention studies. *Am J Clin Nutr.* United States.
WIYAKRUTTA, S., SRIUBOLMAS, N., PANPHUT, W., THONGON, N., DANWISETKANJANA, K., RUANGRUNGSI, N. & MEEVOOTISOM, V. 2004. Endophytic fungi with anti-microbial, anti-cancer and anti-malarial activities isolated from Thai medicinal plants. *World Journal of Microbiology and Biotechnology,* 20**,** 265-272.
WOJSIAT, J., PRANDELLI, C., LASKOWSKA-KASZUB, K., MARTIN-REQUERO, A. & WOJDA, U. 2015. Oxidative Stress and Aberrant Cell Cycle in Alzheimer's Disease Lymphocytes: Diagnostic Prospects. *J Alzheimers Dis.* Netherlands.
WOJTALA, A., BONORA, M., MALINSKA, D., PINTON, P., DUSZYNSKI, J. & WIECKOWSKI, M. R. 2014. Methods to monitor ROS production by fluorescence microscopy and fluorometry. *Methods Enzymol.* United States: © 2014 Elsevier Inc.
WOLLENWEBER, E. & MANN, K. 1984. Flavonoid aglycones in the leaf resin of some Cistus species. *Z. Naturforsch.,* 39**,** 303-306.

WONG, C. H., GAN, S. Y., TAN, S. C., GANY, S. A., YING, T., GRAY, A. I., IGOLI, J., CHAN, E. W. L. & PHANG, S. M. 2018. Fucosterol inhibits the cholinesterase activities and reduces the release of pro-inflammatory mediators in lipopolysaccharide and amyloid-induced microglial cells. *Journal of Applied Phycology,* 30**,** 3261-3270.
WONGCHANA, W. & PALAGA, T. 2012. Direct regulation of interleukin-6 expression by Notch signaling in macrophages. *Cellular & molecular immunology,* 9**,** 155-162.
WOOD, Z. A., SCHRODER, E., ROBIN HARRIS, J. & POOLE, L. B. 2003. Structure, mechanism and regulation of peroxiredoxins. *Trends Biochem Sci.* England.
WU, J., WU, S., SHI, L., ZHANG, S., REN, J., YAO, S., YUN, D., HUANG, L., WANG, J., LI, W., WU, X., QIU, P. & LIANG, G. 2017. Design, synthesis, and evaluation of asymmetric EF24 analogues as potential anti-cancer agents for lung cancer. *Eur J Med Chem,* 125**,** 1321-1331.
WU, W.-Y., LI, Y.-D., CUI, Y.-K., WU, C., HONG, Y.-X., LI, G., WU, Y., JIE, L.-J., WANG, Y. & LI, G.-R. 2018. The Natural Flavone Acacetin Confers Cardiomyocyte Protection Against Hypoxia/Reoxygenation Injury via AMPK-Mediated Activation of Nrf2 Signaling Pathway. *Frontiers in pharmacology,* 9**,** 497-497.
WU, X., CHEN, S. & LU, C. 2020. Amyloid precursor protein promotes the migration and invasion of breast cancer cells by regulating the MAPK signaling pathway. *Int J Mol Med,* 45**,** 162-174.
WU, Y. & ZHOU, B. P. 2010a. TNF-alpha/NF-kappaB/Snail pathway in cancer cell migration and invasion. *Br J Cancer,* 102**,** 639-44.
WU, Y. & ZHOU, B. P. 2010b. TNF-alpha/NF-kappaB/Snail pathway in cancer cell migration and invasion. *British journal of cancer,* 102**,** 639-644.
WU, Z., LI, D., MENG, J. & WANG, H. 2010. Introduction to SIMCA-P and Its Application. *In:* ESPOSITO VINZI, V., CHIN, W. W., HENSELER, J. & WANG, H. (eds.) *Handbook of Partial Least Squares: Concepts, Methods and Applications.* Berlin, Heidelberg: Springer Berlin Heidelberg.
WYNN, T. A., CHAWLA, A. & POLLARD, J. W. 2013. Macrophage biology in development, homeostasis and disease. *Nature,* 496**,** 445-55.
XIA, J., SINELNIKOV, I., HAN, B. & WISHART, D. 2015. MetaboAnalyst 3.0—Making metabolomics more meaningful. *Nucleic acids research,* 43.
XIE, X., YANG, M., DING, Y. & CHEN, J. 2017. Microbial infection, inflammation and epithelial ovarian cancer (Review). *Oncol Lett,* 14**,** 1911-1919.
XU, X., YE, J., HUANG, C., YAN, Y. & LI, J. 2019. M2 macrophage-derived IL6 mediates resistance of breast cancer cells to hedgehog inhibition. *Toxicol Appl Pharmacol.* United States: © 2018. Published by Elsevier Inc.
XUE, Y.-Q., DI, J.-M., LUO, Y., CHENG, K.-J., WEI, X. & SHI, Z. 2014. Resveratrol Oligomers for the Prevention and Treatment of Cancers. *Oxidative Medicine and Cellular Longevity,* 2014**,** 9.
YAKU, K., OKABE, K., HIKOSAKA, K. & NAKAGAWA, T. 2018. NAD Metabolism in Cancer Therapeutics. *Frontiers in oncology,* 8**,** 622-622.
YAMATO, A., SODA, M., UENO, T., KOJIMA, S., SONEHARA, K., KAWAZU, M., SAI, E., YAMASHITA, Y., NAGASE, T. & MANO, H. 2015. Oncogenic activity of BIRC2 and BIRC3 mutants independent of nuclear factor-κB-activating potential. *Cancer science,* 106**,** 1137-1142.
YAN, D., WANG, H. W., BOWMAN, R. L. & JOYCE, J. A. 2016. STAT3 and STAT6 Signaling Pathways Synergize to Promote Cathepsin Secretion from Macrophages via IRE1α Activation. *Cell Rep,* 16**,** 2914-2927.
YAN, T., WANG, T., WEI, W., JIANG, N., QIN, Y. H., TAN, R. X. & GE, H. M. 2012. Polyphenolic acetylcholinesterase inhibitors from Hopea chinensis. *Planta Med,* 78**,** 1015-9.

YAN, X., QI, M., LI, P., ZHAN, Y. & SHAO, H. 2017. Apigenin in cancer therapy: anti-cancer effects and mechanisms of action. *Cell & bioscience,* 7**,** 50-50.
YANG, D. L., WANG, H., GUO, Z. K., DONG, W. H., MEI, W. L. & DAI, H. F. 2014a. A new 2-(2-phenylethyl)chromone derivative in Chinese agarwood 'Qi-Nan' from Aquilaria sinensis. *J Asian Nat Prod Res,* 16**,** 770-6.
YANG, H.-C., WU, Y.-H., YEN, W.-C., LIU, H.-Y., HWANG, T.-L., STERN, A. & CHIU, D. T.-Y. 2019. The Redox Role of G6PD in Cell Growth, Cell Death, and Cancer. *Cells,* 8**,** 1055.
YANG, L., GUO, H., LI, Y., MENG, X., YAN, L., DAN, Z., WU, S., ZHOU, H., PENG, L., XIE, Q. & JIN, X. 2016a. Oleoylethanolamide exerts anti-inflammatory effects on LPS-induced THP-1 cells by enhancing PPARα signaling and inhibiting the NF-κB and ERK1/2/AP-1/STAT3 pathways. *Scientific Reports,* 6**,** 34611.
YANG, M.-H., CHEN, K.-C., CHIANG, P.-W., CHUNG, T.-W., CHEN, W.-J., CHU, P.-Y., CHEN, S. C.-J., LU, Y.-S., YUAN, C.-H., WANG, M.-C., LIN, C.-Y., HUANG, Y.-F., JONG, S.-B., LIN, P.-C. & TYAN, Y.-C. 2016b. Proteomic Profiling of Neuroblastoma Cells Adhesion on Hyaluronic Acid-Based Surface for Neural Tissue Engineering. *BioMed Research International,* 2016**,** 1917394.
YANG, M. X., LIANG, Y. G., CHEN, H. R., HUANG, Y. F., GONG, H. G., ZHANG, T. Y. & ITO, Y. 2018. Isolation of Flavonoids From Wild Aquilaria sinensis Leaves by an Improved Preparative High-Speed Counter-Current Chromatography Apparatus. *J Chromatogr Sci,* 56**,** 18-24.
YANG, S., ZHOU, Q. & YANG, X. 2007. Caspase-3 status is a determinant of the differential responses to genistein between MDA-MB-231 and MCF-7 breast cancer cells. *Biochimica et Biophysica Acta (BBA) - Molecular Cell Research,* 1773**,** 903-911.
YANG, W.-J., LIU, C., GU, Z.-Y., ZHANG, X.-Y., CHENG, B., MAO, Y. & XUE, G.-P. 2014b. Protective effects of acacetin isolated from Ziziphora clinopodioides Lam. (Xintahua) on neonatal rat cardiomyocytes. *Chinese Medicine,* 9**,** 28.
YANG, Y., LI, S., YANG, Q., SHI, Y., ZHENG, M., LIU, Y., CHEN, F., SONG, G., XU, H., WAN, T., HE, J. & CHEN, Z. 2014c. Resveratrol Reduces the Proinflammatory Effects and Lipopolysaccharide- Induced Expression of HMGB1 and TLR4 in RAW264.7 Cells. *Cellular Physiology and Biochemistry,* 33**,** 1283-1292.
YANG, Y., YU, T., GYU LEE, Y., SEOK YANG, W., OH, J., JEONG, D., LEE, S., WOONG KIM, T., CHUL PARK, Y., SUNG, G.-H. & YOUL CHO, J. 2013. Methanol extract of Hopea odorata suppresses inflammatory responses via the direct inhibition of multiple kinases. *Journal of Ethnopharmacology,* 145**,** 598-607.
YANG, Y. H., LI, D. L., BI, X. Y., SUN, L., YU, X. J., FANG, H. L., MIAO, Y., ZHAO, M., HE, X., LIU, J. J. & ZANG, W. J. 2015. Acetylcholine Inhibits LPS-Induced MMP-9 Production and Cell Migration via the a7 nAChR-JAK2/STAT3 Pathway in RAW264.7 Cells. *Cellular Physiology and Biochemistry,* 36**,** 2025-2038.
YIN, Y., YAO, S., HU, Y., FENG, Y., LI, M., BIAN, Z., ZHANG, J., QIN, Y., QI, X., ZHOU, L., FEI, B., ZOU, J., HUA, D. & HUANG, Z. 2017. The Immune-microenvironment Confers Chemoresistance of Colorectal Cancer through Macrophage-Derived IL6. *Clin Cancer Res.* United States: ©2017 American Association for Cancer Research.
YIP, K. W. & REED, J. C. 2008. Bcl-2 family proteins and cancer. *Oncogene.* England.
YIP, L. Y., AW, C. C., LEE, S. H., HONG, Y. S., KU, H. C., XU, W. H., CHAN, J. M. X., CHEONG, E. J. Y., CHNG, K. R., NG, A. H. Q., NAGARAJAN, N., MAHENDRAN, R., LEE, Y. K., BROWNE, E. R. & CHAN, E. C. Y. 2018. The liver–gut microbiota axis modulates hepatotoxicity of tacrine in the rat. *Hepatology,* 67**,** 282-295.
YOON, S., WOO, S. U., KANG, J. H., KIM, K., SHIN, H. J., GWAK, H. S., PARK, S. & CHWAE, Y. J. 2012. NF-κB and STAT3 cooperatively induce IL6 in starved cancer cells. *Oncogene,* 31**,** 3467-3481.

YOSHIDA, T., KATO, J., INOUE, I., YOSHIMURA, N., DEGUCHI, H., MUKOUBAYASHI, C., OKA, M., WATANABE, M., ENOMOTO, S., NIWA, T., MAEKITA, T., IGUCHI, M., TAMAI, H., UTSUNOMIYA, H., YAMAMICHI, N., FUJISHIRO, M., IWANE, M., TAKESHITA, T., USHIJIMA, T. & ICHINOSE, M. 2014. Cancer development based on chronic active gastritis and resulting gastric atrophy as assessed by serum levels of pepsinogen and Helicobacter pylori antibody titer. *International Journal of Cancer,* 134**,** 1445-1457.
YOUSEF, M., VLACHOGIANNIS, I. A. & TSIANI, E. 2017. Effects of Resveratrol against Lung Cancer: In Vitro and In Vivo Studies. *Nutrients,* 9**,** 1231.
YOUSIF, N. G. 2014. Fibronectin promotes migration and invasion of ovarian cancer cells through up-regulation of FAK-PI3K/Akt pathway. *Cell Biol Int,* 38**,** 85-91.
YU, J., ZHANG, L., HWANG, P. M., KINZLER, K. W. & VOGELSTEIN, B. 2001. PUMA induces the rapid apoptosis of colorectal cancer cells. *Mol Cell.* United States.
YU, L., CHEN, X., SUN, X., WANG, L. & CHEN, S. 2017. The Glycolytic Switch in Tumors: How Many Players Are Involved? *Journal of Cancer,* 8**,** 3430-3440.
YUAN, C.-J., MANDAL, A. K., ZHANG, Z. & MUKHERJEE, A. B. 2000. Transcriptional Regulation of Cyclooxygenase-2 Gene Expression: Novel Effects of Nonsteroidal Anti-Inflammatory Drugs. *Cancer Research,* 60**,** 1084.
YUAN, J. & YANKNER, B. A. 2000. Apoptosis in the nervous system. *Nature,* 407**,** 802-9.
YUAN, Z., LONG, C., JUNMING, T., QIHUAN, L., YOUSHUN, Z. & CHAN, Z. 2012. Quercetin-induced apoptosis of HL-60 cells by reducing PI3K/Akt. *Molecular Biology Reports,* 39**,** 7785-7793.
YUNOS, N., MOHAMAD ALI, N. A., ABDULLAH, Z., HUMERIAH, A., SYARIFAH, M. M. & HAYATI, A. 2017. In vitro anticancer activity and high-performance liquid chromatography profiles of Aquilaria subintegra fruit and seed extracts. *Journal of Tropical Forest Science,* 29**,** 208-214.
ZABRON, A., EDWARDS, R. J. & KHAN, S. A. 2013. The challenge of cholangiocarcinoma: dissecting the molecular mechanisms of an insidious cancer. *Disease Models & Mechanisms,* 6**,** 281.
ZACKSENHAUS, E., SHRESTHA, M., LIU, J. C., VOROBIEVA, I., CHUNG, P. E. D., JU, Y., NIR, U. & JIANG, Z. 2017. Mitochondrial OXPHOS Induced by RB1 Deficiency in Breast Cancer: Implications for Anabolic Metabolism, Stemness, and Metastasis. *Trends in Cancer,* 3**,** 768-779.
ZENG, W., ZHANG, C., CHENG, H., WU, Y.-L., LIU, J., CHEN, Z., JIAN-GANG, H., ERICKSEN, R., CHEN, L., ZHANG, H., WONG, A., ZHANG, X.-K., HAN, W. & ZENG, J.-Z. 2017. Targeting to the non-genomic activity of retinoic acid receptor-gamma by acacetin in hepatocellular carcinoma. *Scientific Reports,* 7.
ZERIN, T., KIM, Y. S., HONG, S. Y. & SONG, H. Y. 2013. Quercetin reduces oxidative damage induced by paraquat via modulating expression of antioxidant genes in A549 cells. *J Appl Toxicol,* 33**,** 1460-7.
ZHANG, A., SUN, H., XU, H., QIU, S. & WANG, X. 2013. Cell metabolomics. *Omics : a journal of integrative biology,* 17**,** 495-501.
ZHANG, H., SCHOOLS, G., LEI, T., WANG, W., KIMELBERG, H. & ZHOU, M. 2008. Resveratrol attenuates early pyramidal neuron excitability impairment and death in acute rat hippocampal slices caused by oxygen-glucose deprivation. *Experimental neurology,* 212**,** 44-52.
ZHANG, P., WU, C., HUANG, X. H., SHEN, C. L., LI, L., ZHANG, W. & YAO, C. Z. 2017a. Aspirin suppresses TNF-α-induced MMP-9 expression via NF-κB and MAPK signaling pathways in RAW264.7 cells. *Exp Ther Med,* 14**,** 5597-5604.
ZHANG, Q.-W., LIN, L.-G. & YE, W.-C. 2018. Techniques for extraction and isolation of natural products: a comprehensive review. *Chinese medicine,* 13**,** 20-20.

ZHANG, R., LIU, Q., PENG, J., WANG, M., GAO, X., LIAO, Q. & ZHAO, Y. 2019. Pancreatic cancer-educated macrophages protect cancer cells from complement-dependent cytotoxicity by up-regulation of CD59. *Cell Death & Disease,* 10**,** 836.
ZHANG, Z. X., LI, Y. B. & ZHAO, R. P. 2017b. Epigallocatechin Gallate Attenuates beta-Amyloid Generation and Oxidative Stress Involvement of PPARgamma in N2a/APP695 Cells. *Neurochem Res.* United States.
ZHAO, H. F., LI, N., WANG, Q., CHENG, X. J., LI, X. M. & LIU, T. T. 2015. Resveratrol decreases the insoluble Aβ1–42 level in hippocampus and protects the integrity of the blood–brain barrier in AD rats. *Neuroscience,* 310**,** 641-649.
ZHAO, J., LI, R., PAWLAK, A., HENKLEWSKA, M., SYSAK, A., WEN, L., YI, J.-E. & OBMIŃSKA-MRUKOWICZ, B. 2018. Antitumor Activity of Betulinic Acid and Betulin in Canine Cancer Cell Lines. *In vivo (Athens, Greece),* 32**,** 1081-1088.
ZHAO, P., MAO, J.-M., ZHANG, S.-Y., ZHOU, Z.-Q., TAN, Y. & ZHANG, Y. 2014. Quercetin induces HepG2 cell apoptosis by inhibiting fatty acid biosynthesis. *Oncology letters,* 8**,** 765-769.
ZHAO, T., DING, K.-M., ZHANG, L., CHENG, X.-M., WANG, C.-H. & WANG, Z.-T. 2013a. Acetylcholinesterase and Butyrylcholinesterase Inhibitory Activities of β-Carboline and Quinoline Alkaloids Derivatives from the Plants of Genus Peganum. *Journal of Chemistry,* 2013**,** 717232.
ZHAO, Y., BUTLER, E. B. & TAN, M. 2013b. Targeting cellular metabolism to improve cancer therapeutics. *Cell death & disease,* 4**,** e532-e532.
ZHAO, Y.-F., ZHANG, C. & SUO, Y.-R. 2012. MMPT as a reactive oxygen species generator induces apoptosis via the depletion of intracellular GSH contents in A549 cells. *European Journal of Pharmacology,* 688**,** 6-13.
ZHENG, C. Y., LAM, S. K., LI, Y. Y. & HO, J. C. 2015. Arsenic trioxide-induced cytotoxicity in small cell lung cancer via altered redox homeostasis and mitochondrial integrity. *Int J Oncol,* 46**,** 1067-78.
ZHOU, J., GONG, J., DING, C. & CHEN, G. 2015. Quercetin induces the apoptosis of human ovarian carcinoma cells by upregulating the expression of microRNA-145. *Mol Med Rep,* 12**,** 3127-31.
ZHOU, M., WANG, H., SUOLANGJIBA, KOU, J. & YU, B. 2008. Antinociceptive and anti-inflammatory activities of Aquilaria sinensis (Lour.) Gilg. Leaves extract. *J Ethnopharmacol.* Ireland.
ZHOU, Y., HONG, Y. & HUANG, H. 2016. Triptolide Attenuates Inflammatory Response in Membranous Glomerulo-Nephritis Rat via Downregulation of NF-κB Signaling Pathway. *Kidney Blood Press Res.* Switzerland: © 2016 The Author(s) Published by S. Karger AG, Basel.
ZHOU, Y., XIA, L., LIU, Q., WANG, H., LIN, J., OYANG, L., CHEN, X., LUO, X., TAN, S., TIAN, Y., SU, M., WANG, Y., CHEN, P., WU, Y. & LIAO, Q. 2018. Induction of Pro-Inflammatory Response via Activated Macrophage-Mediated NF-κB and STAT3 Pathways in Gastric Cancer Cells. *Cellular Physiology and Biochemistry,* 47**,** 1399-1410.
ZHU, L. & CHEN, L. 2019. Progress in research on paclitaxel and tumor immunotherapy. *Cellular & molecular biology letters,* 24**,** 40-40.
ZHU, X., LI, N., WANG, Y., DING, L., CHEN, H., YU, Y. & SHI, X. 2017a. Protective effects of quercetin on UVB irradiationinduced cytotoxicity through ROS clearance in keratinocyte cells. *Oncol Rep,* 37**,** 209-218.
ZHU, X., SHEN, H., YIN, X., LONG, L., CHEN, X., FENG, F., LIU, Y., ZHAO, P., XU, Y., LI, M., XU, W. & LI, Y. 2017b. IL-6R/STAT3/miR-204 feedback loop contributes to cisplatin resistance of epithelial ovarian cancer cells. *Oncotarget,* 8**,** 39154-39166.

ZIELIŃSKA, K., KWAŚNIAK, K., TABARKIEWICZ, J. & KARCZMAREK-BOROWSKA, B. 2018. The role of pro-inflammatory cytokines in the pathogenesis and progression of neoplasms. *Postępy Higieny i Medycyny Doświadczalnej,* 72**,** 896-905.
ZONG, Y., SUN, L., LIU, B., DENG, Y.-S., ZHAN, D., CHEN, Y.-L., HE, Y., LIU, J., ZHANG, Z.-J., SUN, J. & LU, D. 2012. Resveratrol inhibits LPS-induced MAPKs activation via activation of the phosphatidylinositol 3-kinase pathway in murine RAW 264.7 macrophage cells. *PloS one,* 7**,** e44107-e44107.
ZOROVA, L. D., POPKOV, V. A., PLOTNIKOV, E. Y., SILACHEV, D. N., PEVZNER, I. B., JANKAUSKAS, S. S., BABENKO, V. A., ZOROV, S. D., BALAKIREVA, A. V., JUHASZOVA, M., SOLLOTT, S. J. & ZOROV, D. B. 2018. Mitochondrial membrane potential. *Analytical biochemistry,* 552**,** 50-59.
ZUHAIDI, A. 2016. GROWTH AND MANAGEMENT OF AQUILARIA MALACCENSIS FOR AGARWOOD

-A NEW DOMESTICATION PERSPECTIVE. *International Journal of Agriculture, Forestry and Plantation,* 3**,** 55-60.
ČOKIĆ, V. P., MITROVIĆ-AJTIĆ, O., BELESLIN-ČOKIĆ, B. B., MARKOVIĆ, D., BUAČ, M., DIKLIĆ, M., KRAGULJAC-KURTOVIĆ, N., DAMJANOVIĆ, S., MILENKOVIĆ, P., GOTIĆ, M. & RAJ, P. K. 2015. Proinflammatory Cytokine IL-6 and JAK-STAT Signaling Pathway in Myeloproliferative Neoplasms. *Mediators of inflammation,* 2015**,** 453020-453020.
ŚLUSARCZYK, S., SENOL DENIZ, F. S., WOŹNIAK, D., PECIO, Ł., PÉREZ-SÁNCHEZ, H., CERÓN-CARRASCO, J. P., STOCHMAL, A., DEN-HAAN ALONSO, H., MATKOWSKI, A. & ORHAN, I. E. 2019. Selective in vitro and in silico cholinesterase inhibitory activity of isoflavones and stilbenes from Belamcandae chinensis rhizoma. *Phytochemistry Letters,* 30**,** 261-272.
ŠALAMON, Š., KRAMAR, B., MAROLT, T. P., POLJŠAK, B. & MILISAV, I. 2019. Medical and Dietary Uses of N-Acetylcysteine. *Antioxidants (Basel, Switzerland),* 8**,** 111.

Appendix 1: Isolated compounds mass spec

7-aca

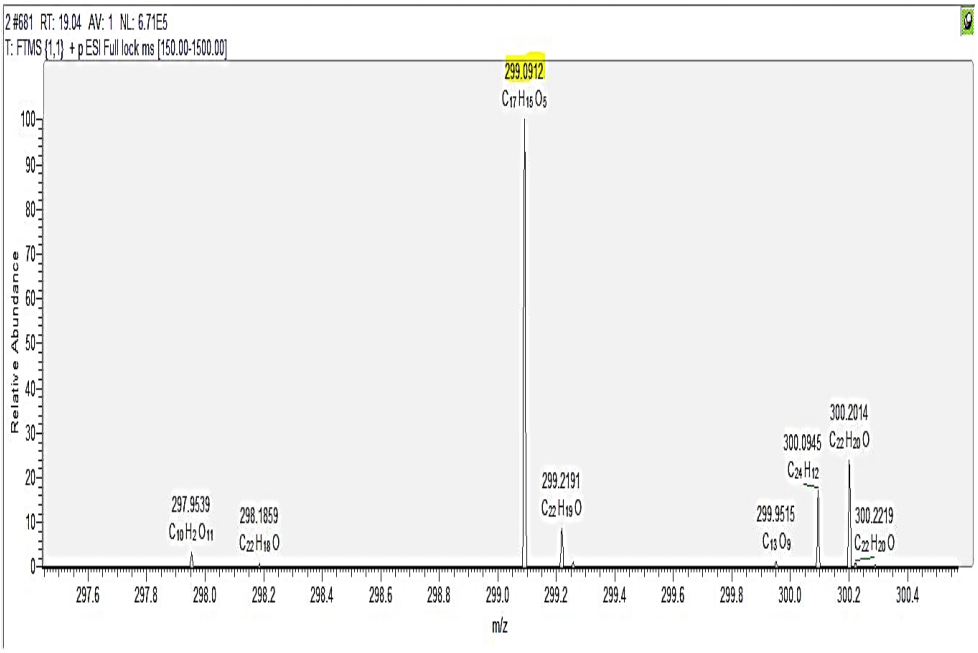

Bala

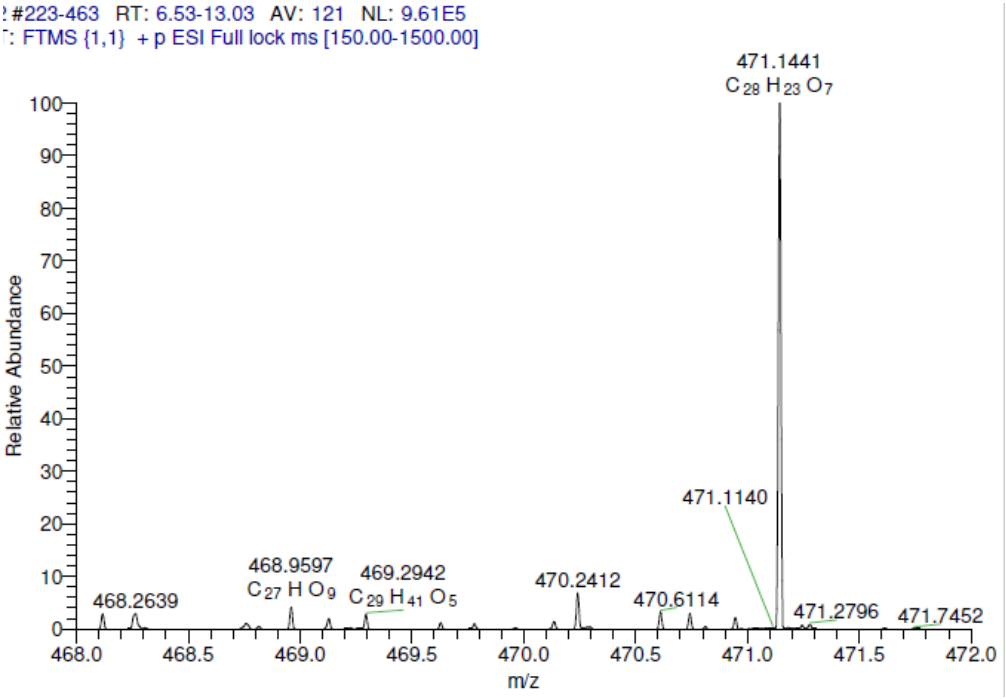

Q/A

Quercitrin

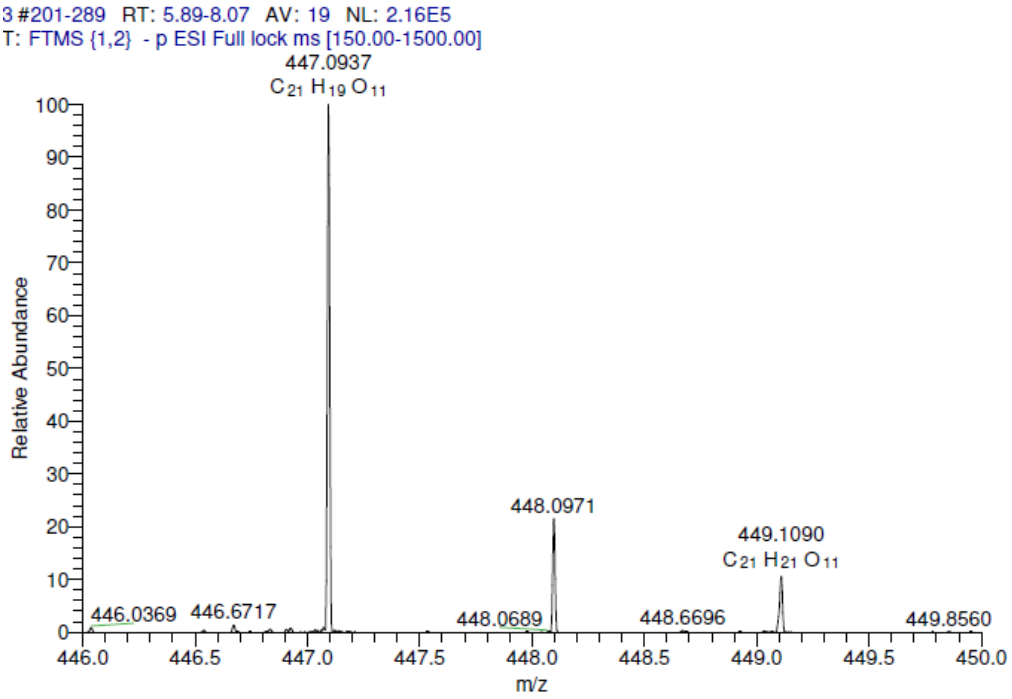

Afzelin

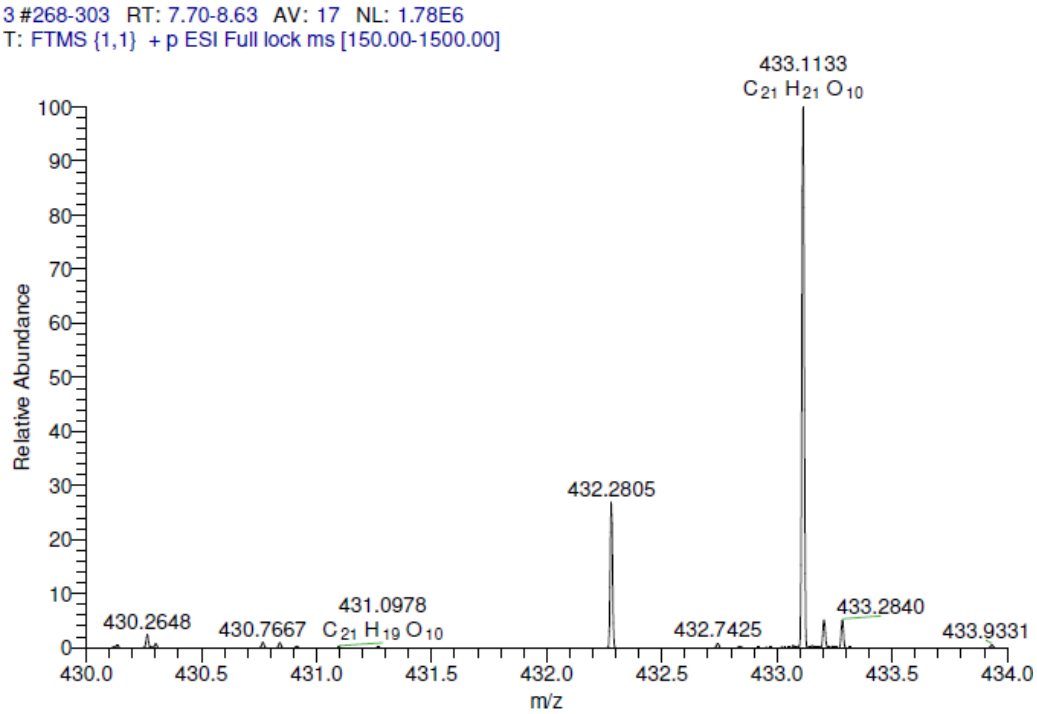

Appendix 2, Cytotoxicity assay

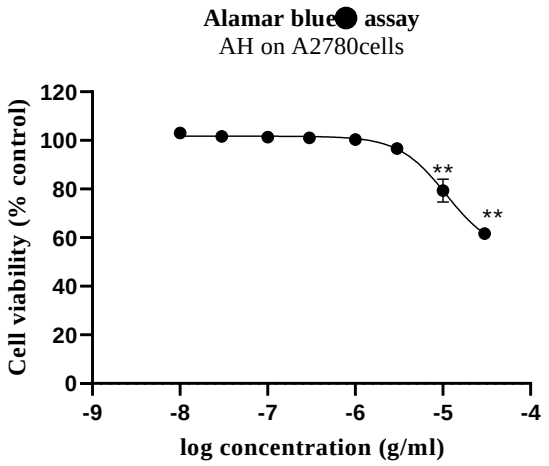

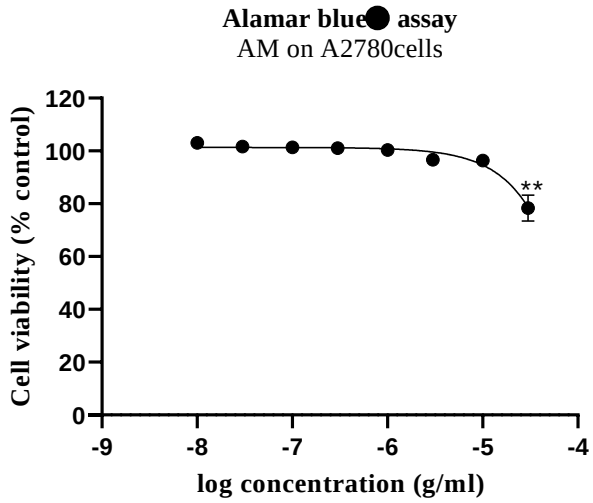

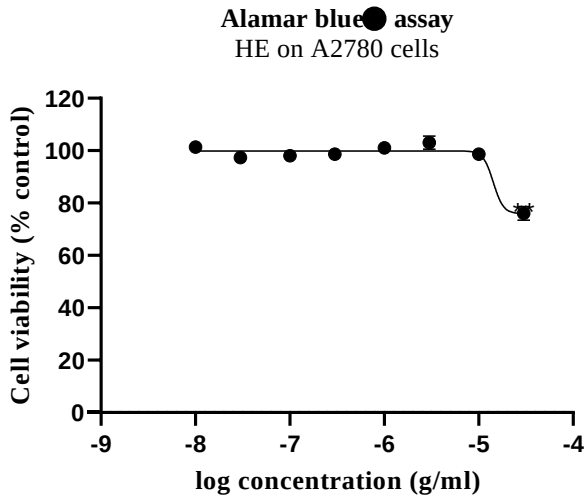

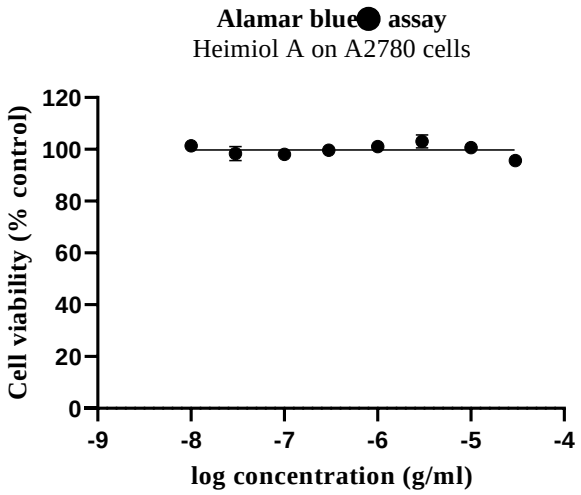
Alamar blue® assay
Heimiol A on A2780 cells
Cell viability (% control)
120
100
80
60
40
20
0
-9
-8
-7
-6
-5
-4
log concentration (g/ml)

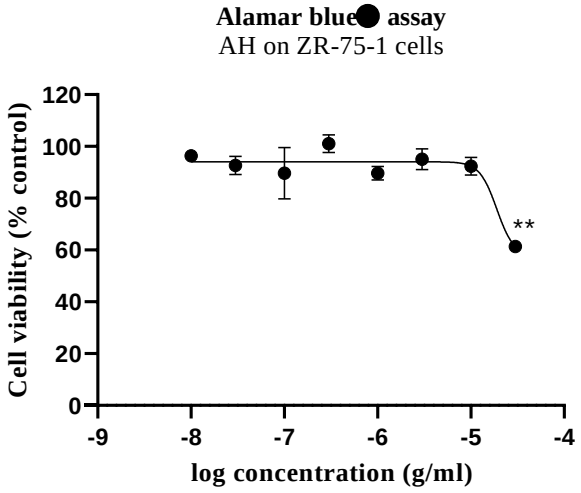
Alamar blue® assay
AH on ZR-75-1 cells
Cell viability (% control)
120
100
80
60
40
20
0
**
-9
-8
-7
-6
-5
-4
log concentration (g/ml)

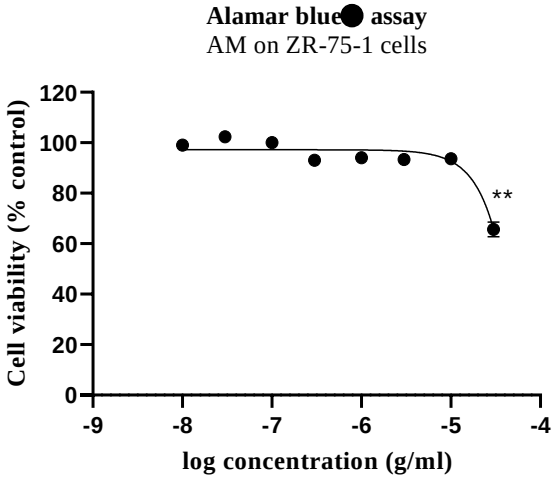
Alamar blue® assay
AM on ZR-75-1 cells
Cell viability (% control)
120
100
80
60
40
20
0
**
-9
-8
-7
-6
-5
-4
log concentration (g/ml)

Alamar blue® assay
HE on ZR-75-1 cells

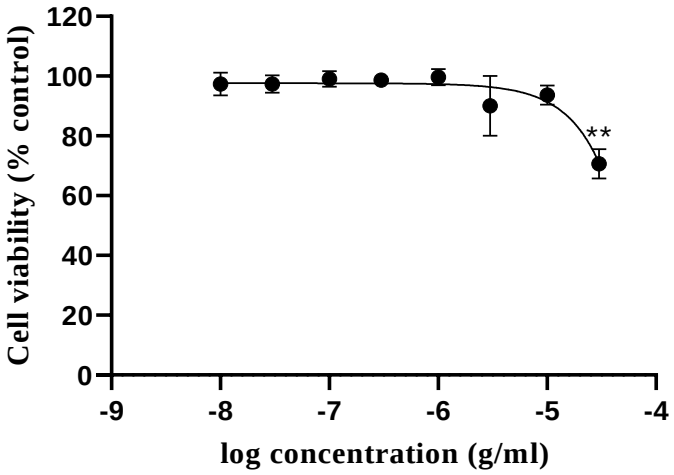

Alamar blue® assay
Heimiol A on ZR-75-1 cells

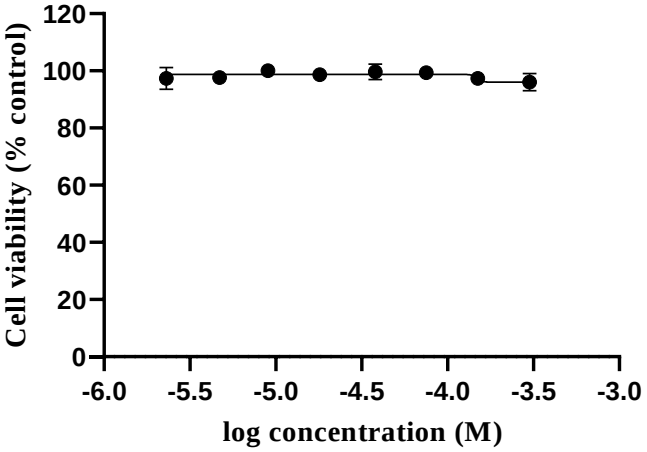

Appendix 3, Nano drop curves

Nanodrop curves for isolated RNA samples from THP-1 cells

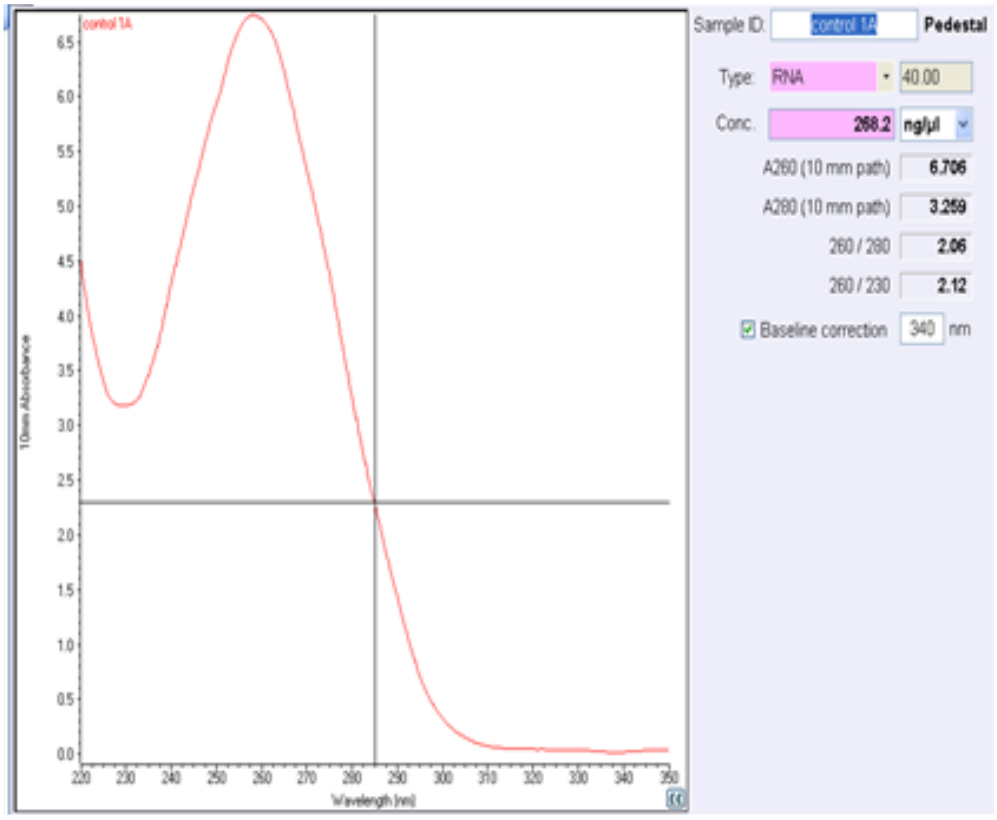

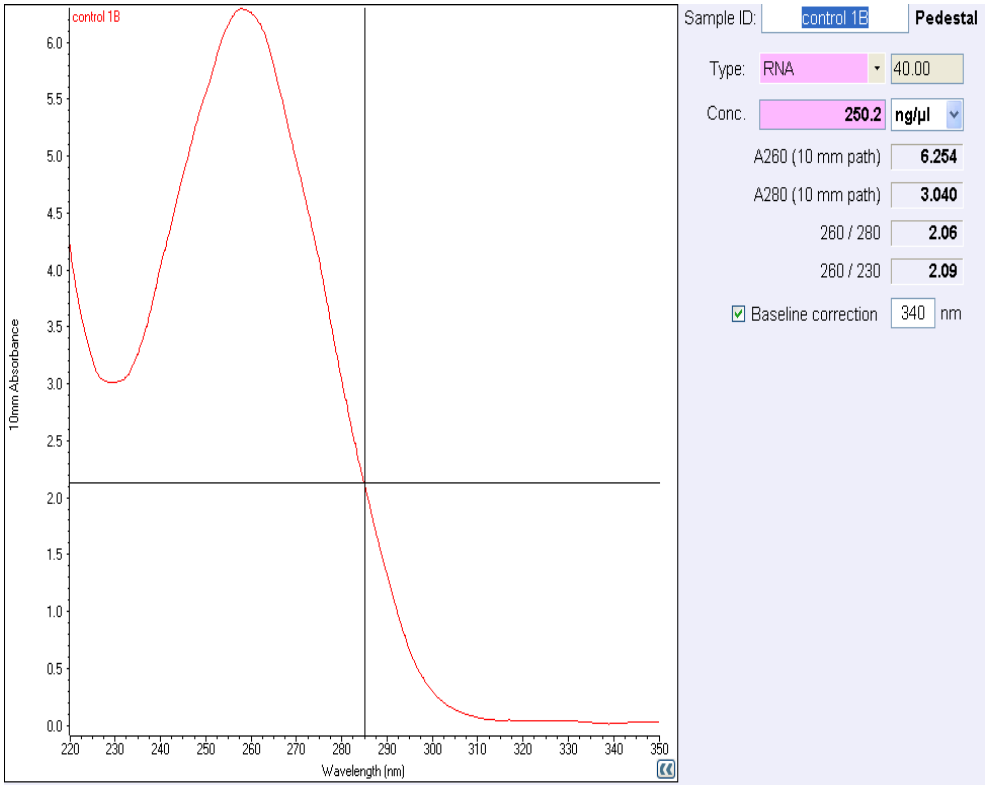

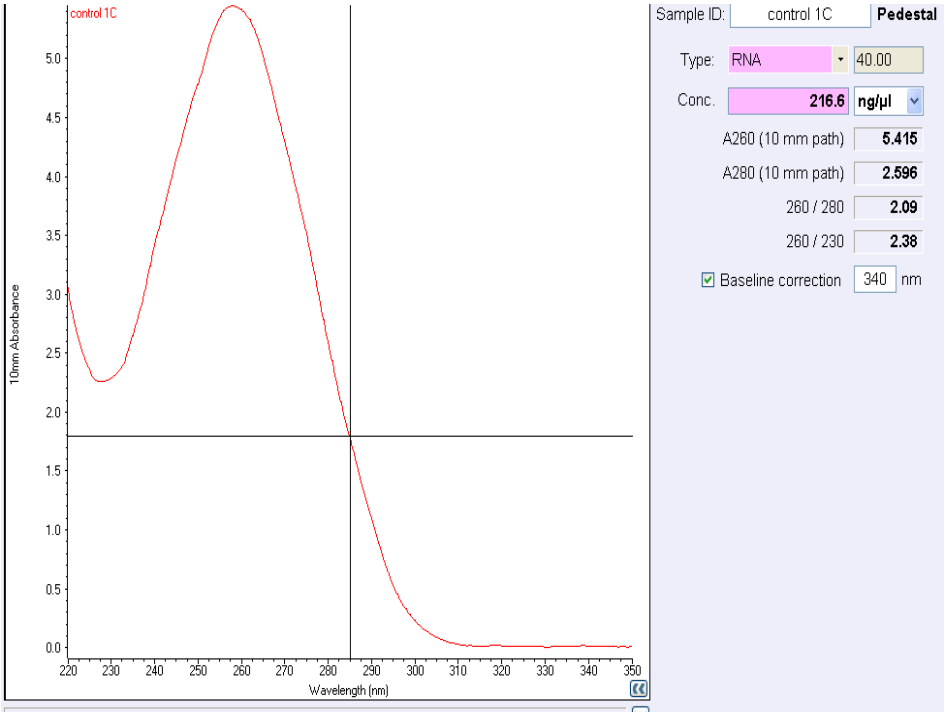
control 1C
10mm Absorbance
Wavelength (nm)
Sample ID: control 1C
Pedestal
Type: RNA
40.00
Conc. 216.6 ng/µl
A260 (10 mm path) 5.415
A280 (10 mm path) 2.596
260 / 280 2.09
260 / 230 2.38
Baseline correction 340 nm

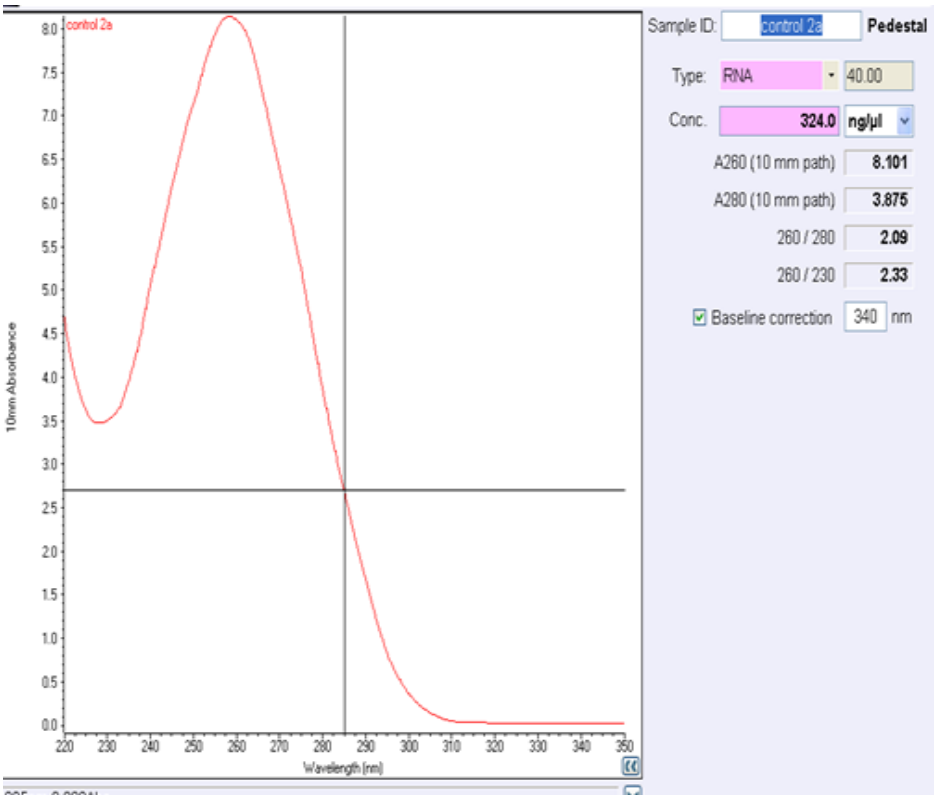
control 2a
10mm Absorbance
Wavelength (nm)
Sample ID: control 2a
Pedestal
Type: RNA
40.00
Conc. 324.0 ng/µl
A260 (10 mm path) 8.101
A280 (10 mm path) 3.875
260 / 280 2.09
260 / 230 2.33
Baseline correction 340 nm

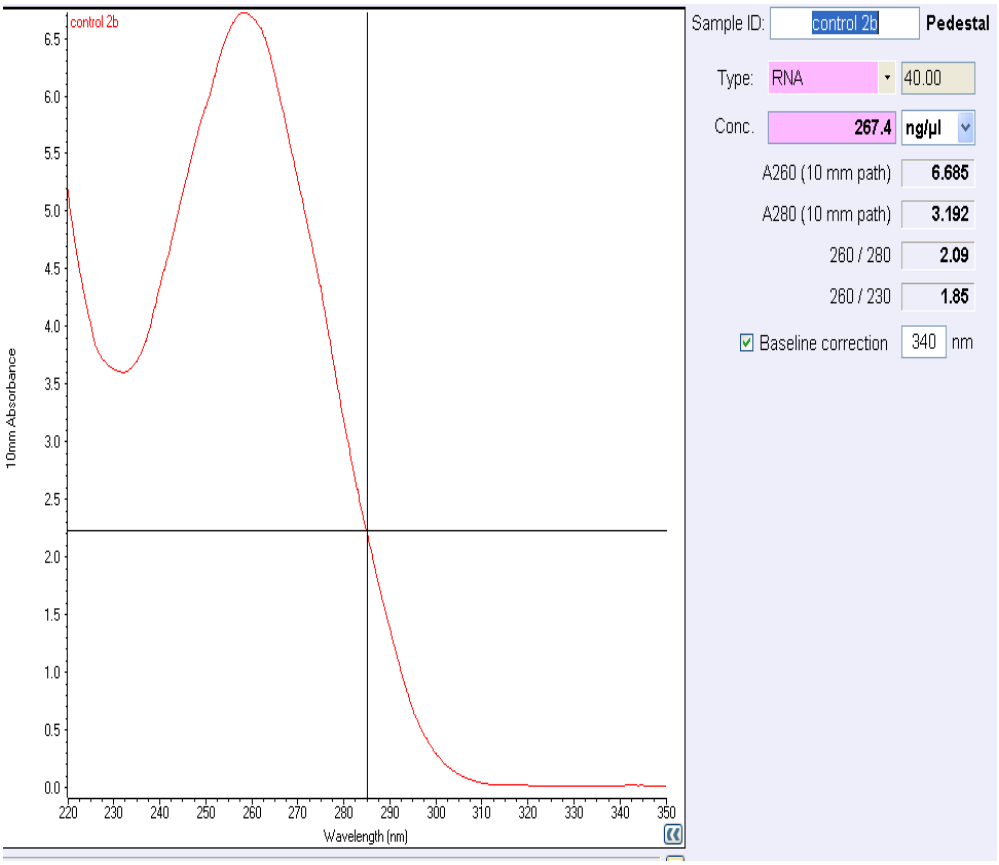
control 2b
10mm Absorbance
Wavelength (nm)
Sample ID: control 2b
Pedestal
Type: RNA
40.00
Conc. 267.4 ng/µl
A260 (10 mm path) 6.685
A280 (10 mm path) 3.192
260 / 280 2.09
260 / 230 1.85
Baseline correction 340 nm

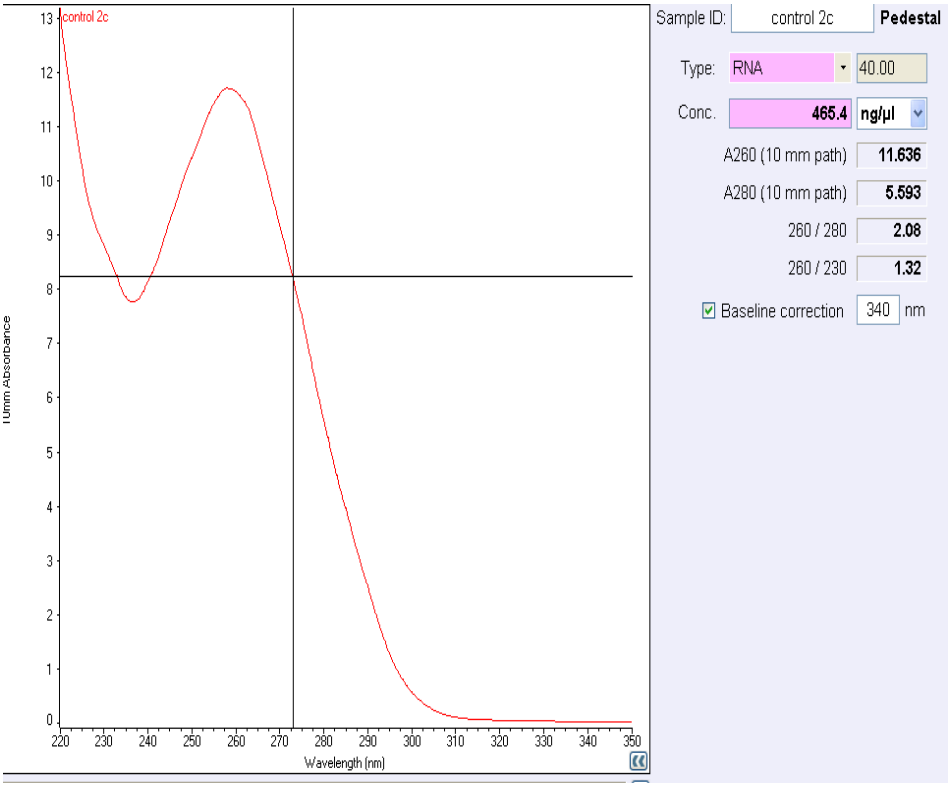
control 2c
10mm Absorbance
Wavelength (nm)
Sample ID: control 2c
Pedestal
Type: RNA
40.00
Conc. 465.4 ng/µl
A260 (10 mm path) 11.636
A280 (10 mm path) 5.593
260 / 280 2.08
260 / 230 1.32
Baseline correction 340 nm

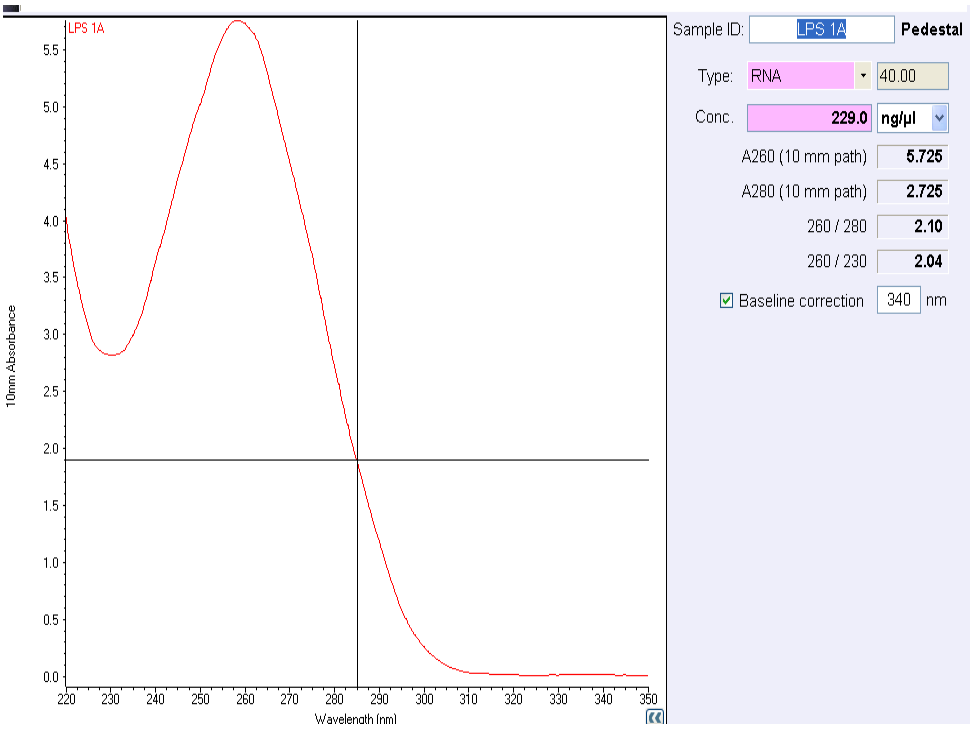
LPS 1A
10mm Absorbance
Wavelength (nm)
Sample ID: LPS 1A
Pedestal
Type: RNA
40.00
Conc. 229.0 ng/µl
A260 (10 mm path) 5.725
A280 (10 mm path) 2.725
260 / 280 2.10
260 / 230 2.04
Baseline correction 340 nm

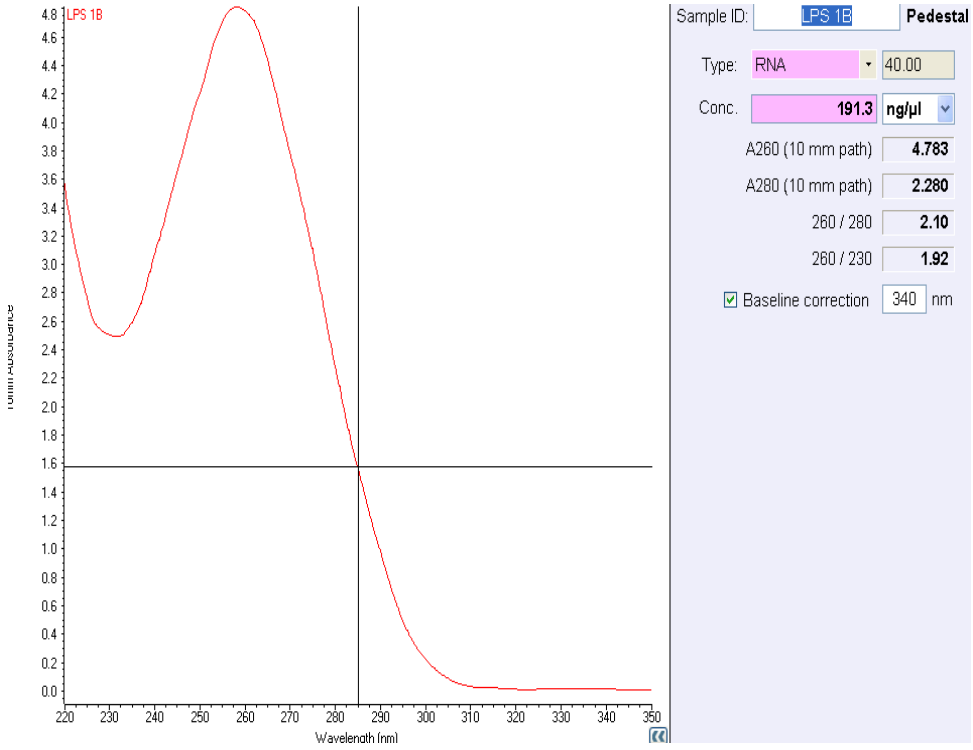
LPS 1B
Wavelength (nm)
Sample ID: LPS 1B
Pedestal
Type: RNA
40.00
Conc. 191.3 ng/µl
A260 (10 mm path) 4.783
A280 (10 mm path) 2.280
260 / 280 2.10
260 / 230 1.92
Baseline correction 340 nm

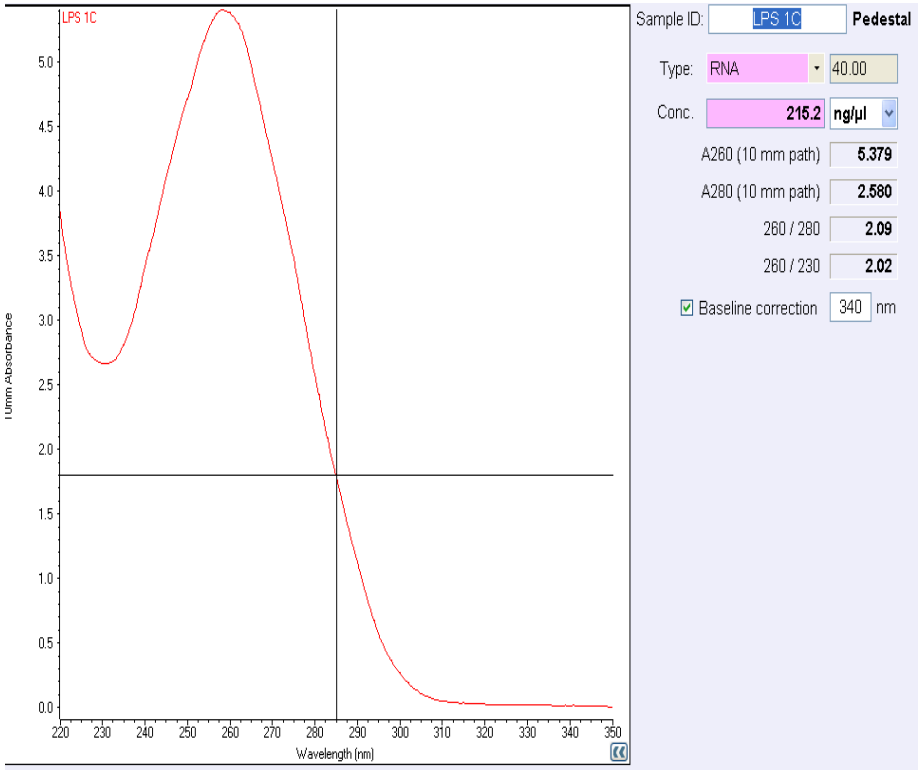
LPS 1C
10mm Absorbance
Wavelength (nm)
Sample ID: LPS 1C
Pedestal
Type: RNA
40.00
Conc. 215.2 ng/µl
A260 (10 mm path) 5.379
A280 (10 mm path) 2.580
260 / 280 2.09
260 / 230 2.02
Baseline correction 340 nm

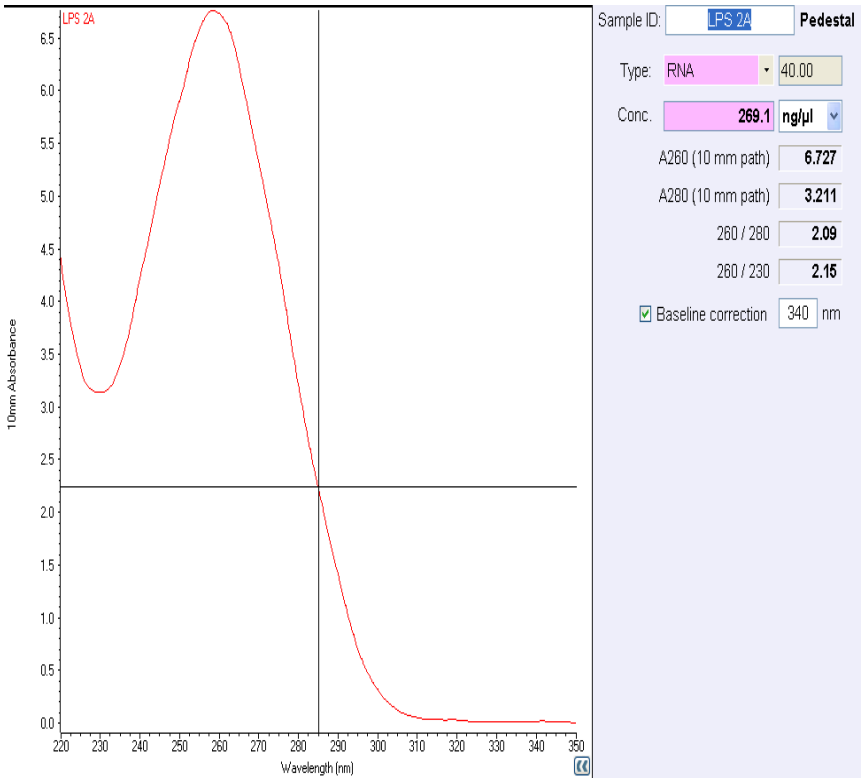
LPS 2A
10mm Absorbance
Wavelength (nm)
Sample ID: LPS 2A
Pedestal
Type: RNA
40.00
Conc. 269.1 ng/µl
A260 (10 mm path) 6.727
A280 (10 mm path) 3.211
260 / 280 2.09
260 / 230 2.15
Baseline correction 340 nm

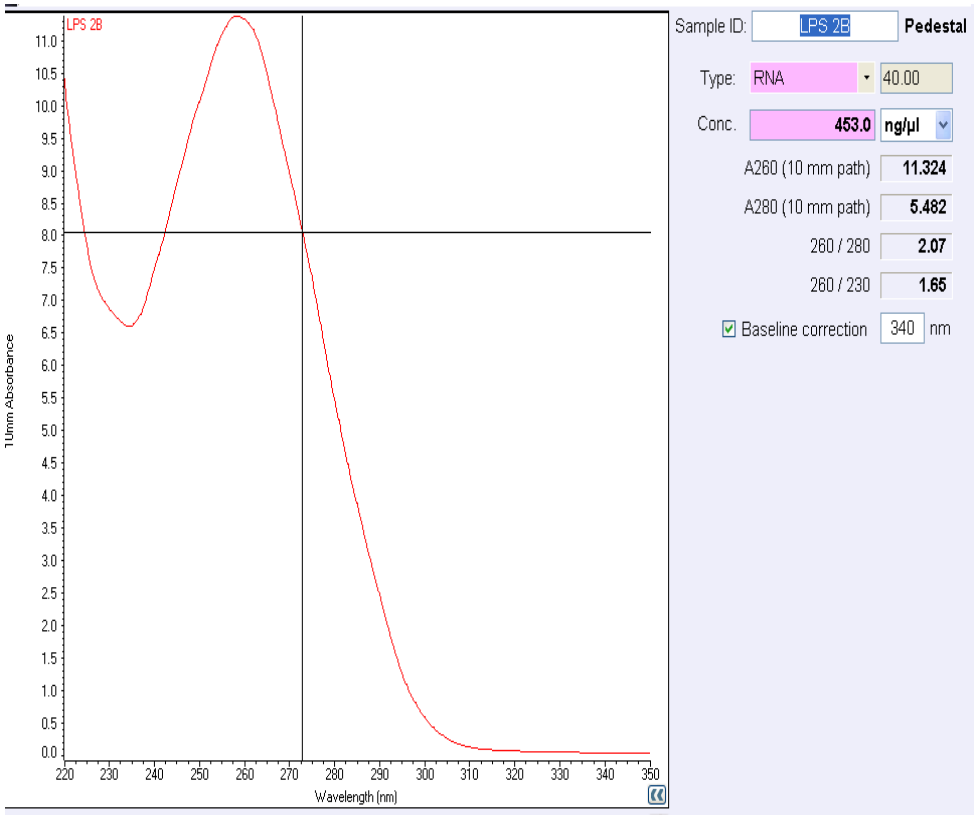
LPS 2B
10mm Absorbance
Wavelength (nm)
Sample ID: LPS 2B
Pedestal
Type: RNA
40.00
Conc. 453.0 ng/µl
A260 (10 mm path) 11.324
A280 (10 mm path) 5.482
260 / 280 2.07
260 / 230 1.65
Baseline correction 340 nm

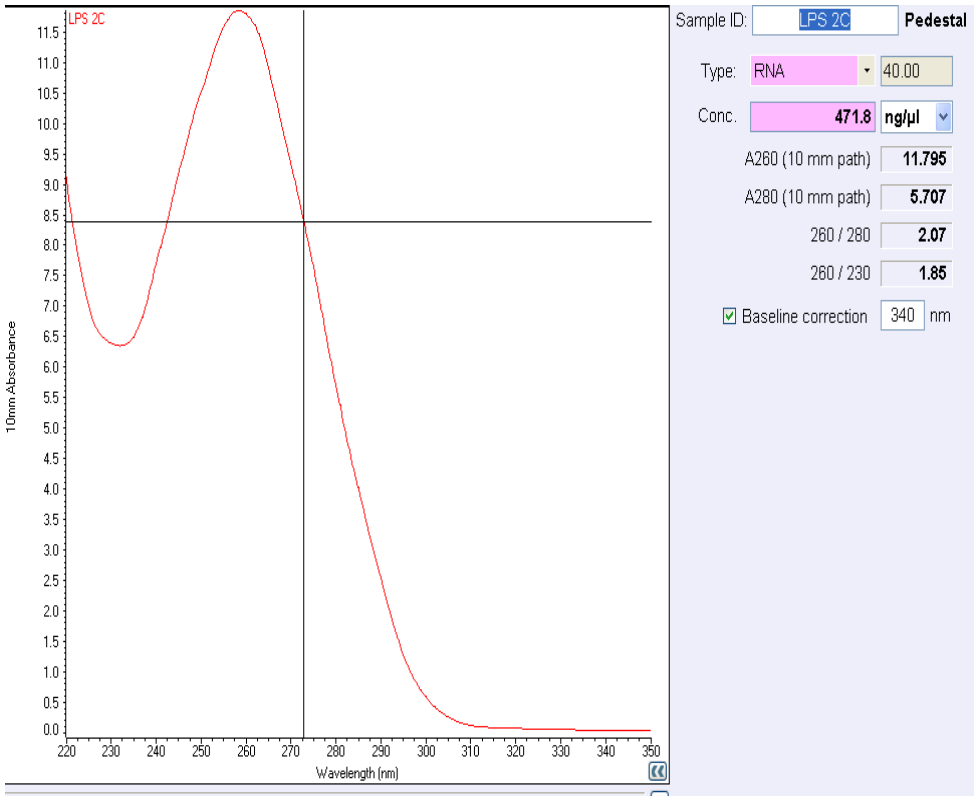
LPS 2C
10mm Absorbance
Wavelength (nm)
Sample ID: LPS 2C
Pedestal
Type: RNA
40.00
Conc. 471.8 ng/µl
A260 (10 mm path) 11.795
A280 (10 mm path) 5.707
260 / 280 2.07
260 / 230 1.85
Baseline correction 340 nm

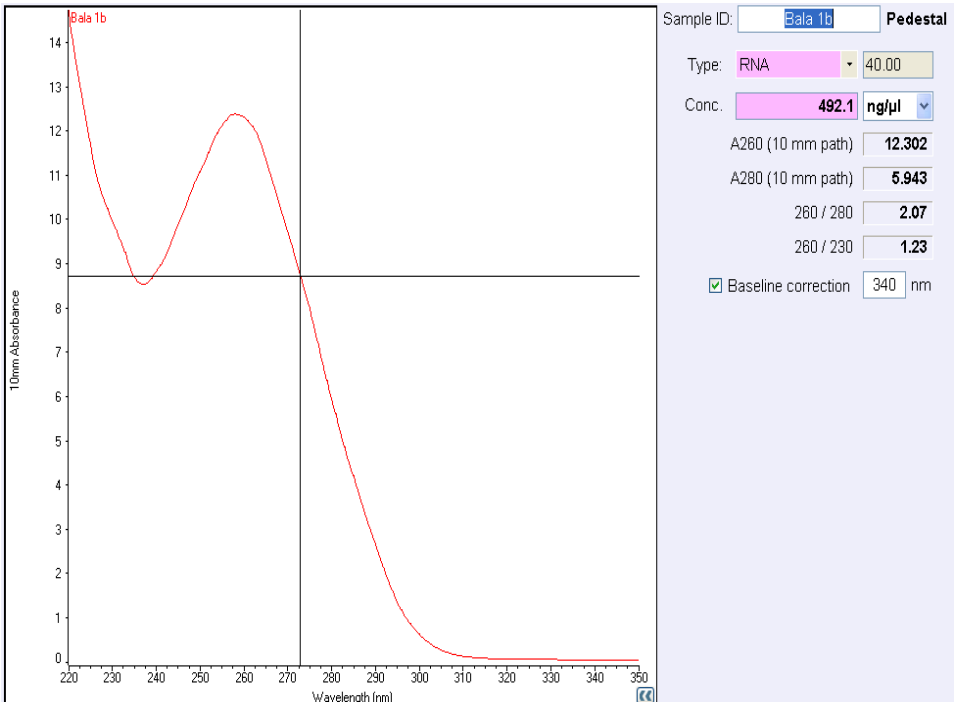
Bala 1b
10mm Absorbance
Wavelength (nm)
Sample ID: Bala 1b
Pedestal
Type: RNA
40.00
Conc. 492.1 ng/µl
A260 (10 mm path) 12.302
A280 (10 mm path) 5.943
260 / 280 2.07
260 / 230 1.23
Baseline correction 340 nm

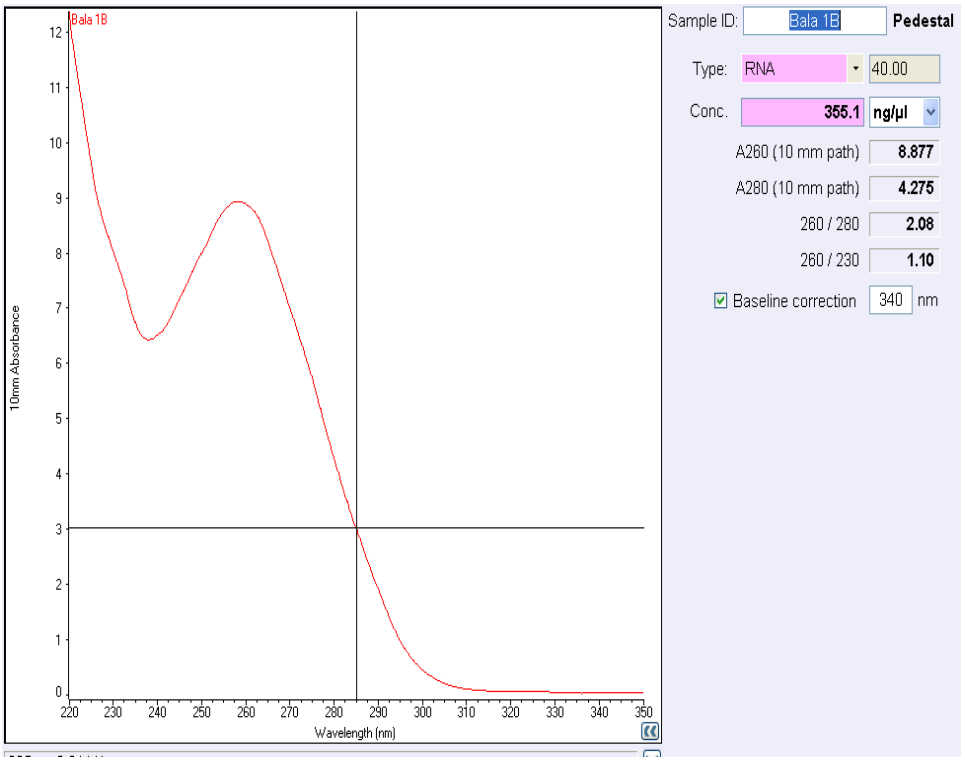
Bala 1B
10mm Absorbance
Wavelength (nm)
Sample ID: Bala 1B
Pedestal
Type: RNA
40.00
Conc. 355.1 ng/µl
A260 (10 mm path) 8.877
A280 (10 mm path) 4.275
260 / 280 2.08
260 / 230 1.10
Baseline correction 340 nm

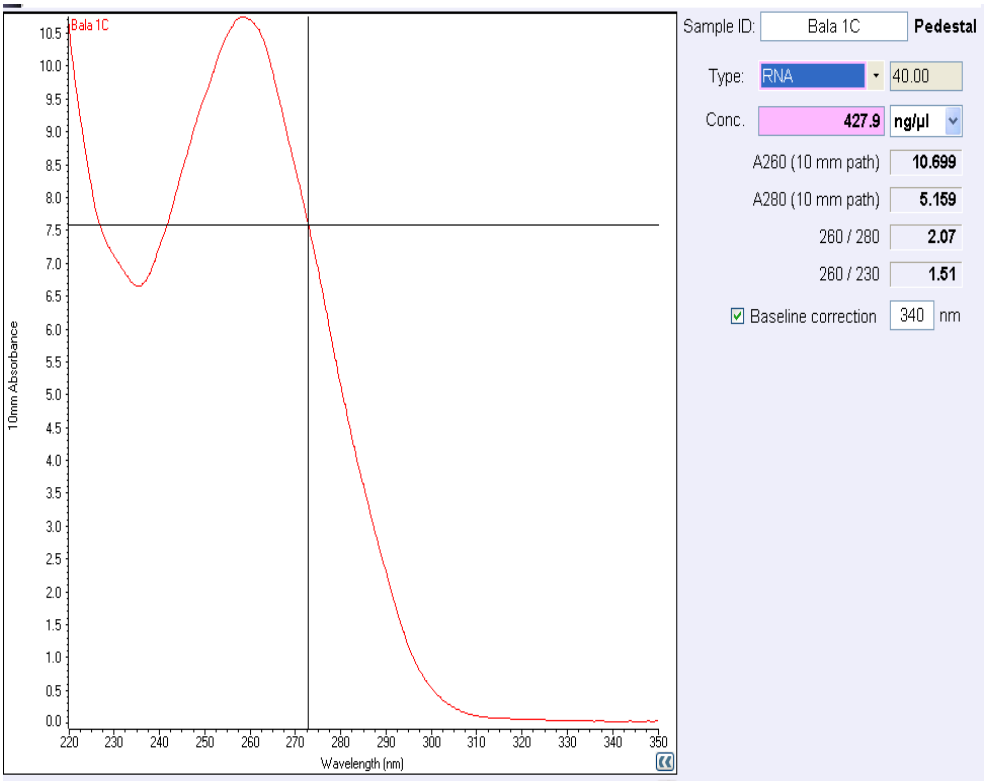
Bala 1C
10mm Absorbance
Wavelength (nm)
Sample ID: Bala 1C
Pedestal
Type: RNA
40.00
Conc. 427.9 ng/µl
A260 (10 mm path) 10.699
A280 (10 mm path) 5.159
260 / 280 2.07
260 / 230 1.51
Baseline correction 340 nm

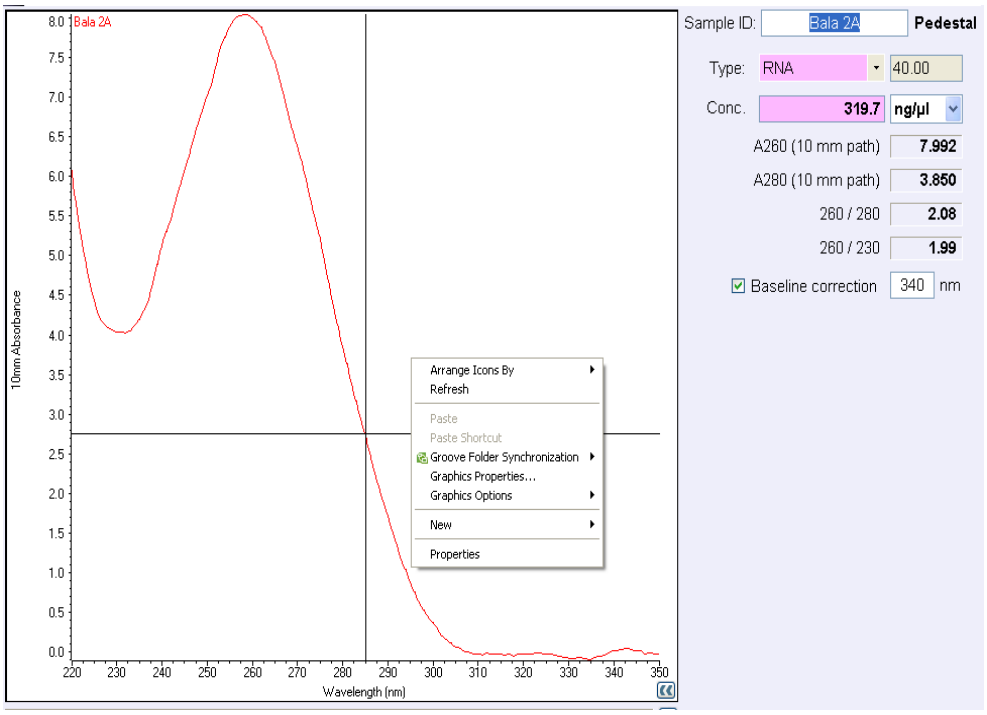
Bala 2A
10mm Absorbance
Wavelength (nm)
Arrange Icons By
Refresh
Paste
Paste Shortcut
Groove Folder Synchronization
Graphics Properties...
Graphics Options
New
Properties
Sample ID: Bala 2A
Pedestal
Type: RNA
40.00
Conc. 319.7 ng/µl
A260 (10 mm path) 7.992
A280 (10 mm path) 3.850
260 / 280 2.08
260 / 230 1.99
Baseline correction 340 nm

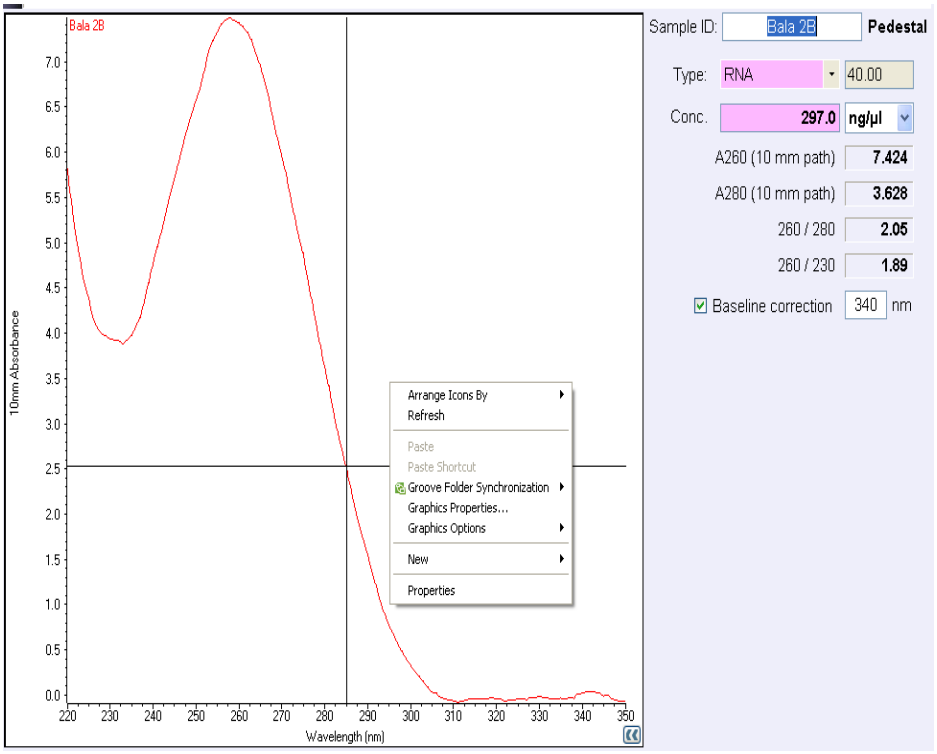
Bala 2B
10mm Absorbance
Wavelength (nm)
Arrange Icons By
Refresh
Paste
Paste Shortcut
Groove Folder Synchronization
Graphics Properties...
Graphics Options
New
Properties
Sample ID: Bala 2B
Pedestal
Type: RNA 40.00
Conc. 297.0 ng/µl
A260 (10 mm path) 7.424
A280 (10 mm path) 3.628
260 / 280 2.05
260 / 230 1.89
Baseline correction 340 nm

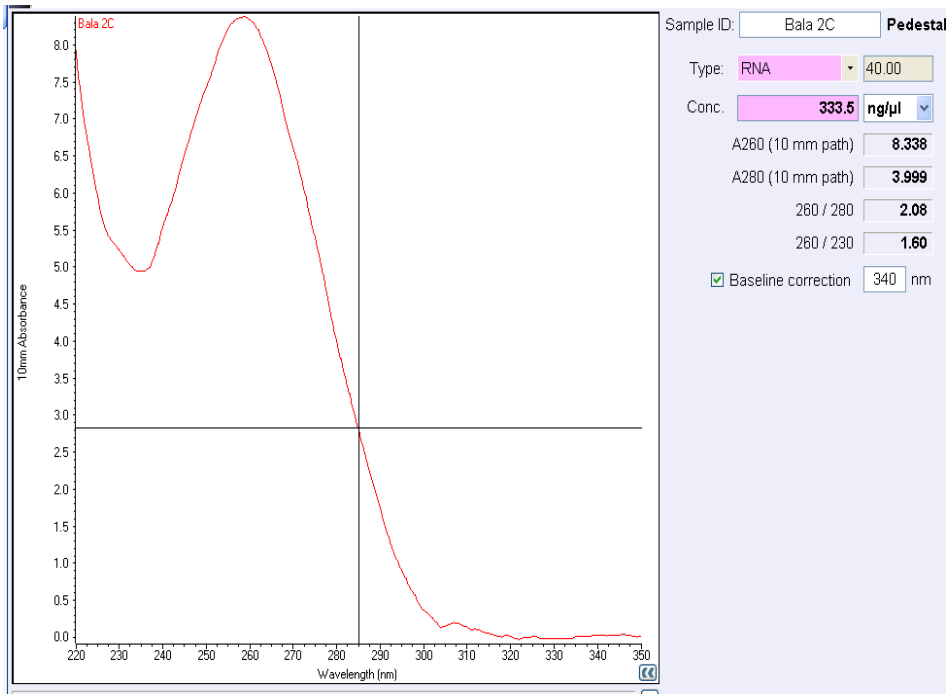
Bala 2C
10mm Absorbance
Wavelength (nm)
Sample ID: Bala 2C
Pedestal
Type: RNA 40.00
Conc. 333.5 ng/µl
A260 (10 mm path) 8.338
A280 (10 mm path) 3.999
260 / 280 2.08
260 / 230 1.60
Baseline correction 340 nm